Synthesis and Characterisation of Polymeric Materials via RAFT Polymerisation

IAIN JOSEPH JOHNSON

Synthesis and Characterisation of Polymeric Materials *via* RAFT Polymerisation

A thesis submitted for the degree of

Doctor of Philosophy

by

Iain Joseph Johnson

Department of Chemistry

University of Durham

England

September 2013

Abstract

Well-defined polymeric materials incorporating N-vinylpyrrolidone (NVP), vinyl acetate (VAc) and / or N-vinylcaprolactam (NVCL) were synthesised using reversible addition fragmentation chain transfer (RAFT) polymerisation.

Chapter 1 is a general introduction on controlled / living radical polymerisation methods, in addition to a brief background on poly(N-vinylpyrrolidone) (PNVP), poly(vinyl acetate) (PVAc) and poly(N-vinylcaprolactam) (PNVCL).

Chapter 2 describes the synthesis of RAFT agents (RAFT agents 1-7) used within this study comprising either a dithiocarbamate (RAFT agent 1) or xanthate (RAFT agents 2-7) structure. Several novel RAFT agents with pyrrolidone functionality and based on xanthates (RAFT agents 4-7) were synthesised to improve the RAFT polymerisation of "less activated" monomers (LAMs). Furthermore, multi-armed RAFT agents (RAFT agents 9-11) based on xanthates were also synthesised with the aim of generating star-like polymeric structures incorporating LAMs. ^{1}H and ^{13}C nuclear magnetic resonance (NMR) spectroscopy methods were used to characterise the RAFT agents synthesised.

Chapter 3 involves the use of RAFT agents 1-8, to mediate the polymerisation of NVP, VAc and NVCL in order to synthesise linear homopolymers with controlled molecular weight and narrow PDI. The kinetics of NVP RAFT mediated polymerisations using novel RAFT agents 5-7 were also investigated and showed that the polymerisations had controlled / living characteristics. Furthermore, the effect of having either primary, secondary or tertiary R groups was explored, for the controlled polymerisation of NVP. RAFT agent 4 which incorporates a primary R group was found to be ineffective in controlling the polymerisation of NVP, whereas RAFT agents with a secondary or tertiary R groups were found to be effective. The resulting polymers were characterised by ^{1}H NMR spectroscopy and size exclusion chromatography (SEC).

Chapter 4 focuses on the synthesis of linear block and novel random copolymers incorporating various combinations of PNVP, PVAc and PNVCL. PNVP macroCTA's (12-14) were used to synthesise PNVP-*block*-PVAc and PNVP-*block*-PNVCL, whereas PVAc macroCTA's (15-17) were used to synthesise PVAc-*block*-PNVP and PVAc-*block*-PNVCL. Bimodal molecular weight distributions were observed in all the block copolymers synthesised. Novel linear PNVP-*ran*-PVAc, PNVCL-*ran*-PVAc and

PNVP-*ran*-PNVCL were also synthesised in the presence of RAFT agent 5, with monomodal molecular weight distributions and narrow PDI's.

Chapter 5 describes the synthesis of more complex polymeric structures using multi-armed RAFT agents prepared in Chapter 2 (RAFT agents 9-11). A "core first" R group approach was implemented instead of a "core first" Z group approach to synthesise the polymeric stars, in order to maintain the integrity of the star structure. NVP, VAc and NVCL were polymerised *via* RAFT in the presence of RAFT agents 9-11, to synthesise Star 1-6. PNVP and PVAc three and four armed stars (Star 1-4) were found to exhibit monomodal molecular weight distributions and low PDI. However, PNVCL three and four armed stars (Star 5 and 6) were found to show bimodal molecular weight distributions. Star 3 (4 arm star of PNVP) and Star 4 (4 arm star of PVAc) were then subsequently used as star macroCTA's and chain extended with NVP, VAc and NVCL to synthesise novel Star-block 1-4. Star block copolymers were found to either have broad or bimodal molecular weight distributions. In addition, novel three and four armed star random copolymers (Star-random 1-6) were also synthesised *via* RAFT using RAFT agents 9 and 11, respectively. All Star-random copolymers were observed to have monomodal molecular weight distributions and narrow PDI.

Chapter 6 investigates the temperature responsive behaviour of polymeric materials containing NVCL using UV-Visible spectroscopy and optical microscopy. PNVCL synthesised *via* conventional free radical polymerisation, with a M_n of 9.97 x 10^4 $gmol^{-1}$, was found to exhibit an LCST at 33°C. In comparison, linear PNVCL samples prepared *via* RAFT polymerisation, with M_n ranging from 1.02 x 10^4 to 2.62 x 10^4 $gmol^{-1}$ were observed to exhibit higher LCST's in the region of 38-40°C. This suggests that the LCST of PNVCL is dependent on the polymer chain length; i.e. "classical" (Type 1) Flory-Huggins behaviour. Furthermore, PNVCL synthesised using RAFT agents 2-5 exhibited LCST's in the region of 39-40°C, which is known as fever temperature. Novel linear PNVCL-*ran*-PNVP, PNVCL-*ran*-PVAc and Star-random 2, 3, 5-6 were also analysed to determine their temperature responsive behaviour. The introduction of a hydrophobic (PVAc) and hydrophilic (PNVP) entities into PNVCL is shown to significantly decrease and increase the LCST, respectively. Comparison of the LCST transition range for PNVCL-*ran*-PVAc synthesised *via* RAFT and conventional FRP, indicated that the former showed a much narrower transition. Novel Star-random 5 and 6 (four armed random copolymers) were found to have a lower LCST compared to Star-random 2 and 3 (three armed random copolymers) despite

having similar monomer compositions. A thermal hysteresis was found to be present in all polymer samples, which was attributed to the possibility of weak cross-linking interactions between water molecules and PNVCL carbonyl groups.

Chapter 7 is a general conclusion of the work discussed in Chapters 1-6 and future work.

Acknowledgements

Fore mostly, I wish to thank my supervisor, Dr. Ezat Khosravi for his advice and guidance throughout my PhD studies, which has been invaluable. I would also like to thank my industrial supervisor Dr. Osama Musa, for his contribution and discussions regarding my research. For matters regarding SEC analysis I would like to thank Dr. Lian Hutchings and for NMR experiments thanks go to Dr. Alan Kenwright, Catherine Heffernan and Ian Mckeag. For other related technical help I would also wish to thank Dr. Richard Thompson and Doug Carswell. I am very grateful for the help I have received from the mechanical / electrical workshops, Chem-IT department, technicians from the stores and laboratory attendants.

From when I first started my studies, thanks go to Dr. Yulia Rogan and Dr. Ahmed Eissa for my integration into Dr. Ezat Khosravi's group. Thanks also go to Dr. David Johnson, Dr. William Bergius and Dr. Barry Dean for many enlightening and amusing discussions as well as their advice on work issues. I would also like to thank David Cole, Peter King, Paul Brooks, Serena Agostini, Tatiana Lovato, Rose Simnett, Alex Hudson, Shenghui Hou, Richard Delley and many other members and affiliates of CG156 and CG165 both past and present who have helped me.

My time in Durham has not always been easy and I would like to thank the people who know this the most. Firstly of all I wish to thank my mother, Allison, whose support and drive has been an inspiration for getting me where I am today and secondly, I would like to thank my partner, Lindsay, for her patience, devotion and support.

Memorandum

The work reported in this thesis was carried out in the Department of Chemistry, University of Durham, between October 2008 and December 2011. This work has not been submitted for any other degree in Durham or elsewhere and is the original work of the author except where acknowledged by means of appropriate reference.

Signed:_____ Date:_____

Statement of Copyright

Financial Support

I gratefully acknowledge International Specialty Products Inc., now part of Ashland Inc. for their funding of this research.

Contents

Chapter 3 – RAFT homopolymerisation of N-vinylpyrrolidone, vinyl acetate and N-vinylcaprolactam

Chapter 6 – Temperature responsive polymers

Abbreviation List

ACS	American chemical society
ACVA	4,4'-azobis(4-cyanovaleric acid)
AIBN	2,2'-azobisisobutyronitrile
AGET	Activator generated by electron transfer
ARGET	Activator regenerated by electron transfer
ATRA	Atom transfer radical addition
ATRP	Atom transfer radical polymerisation
BA	Butyl acrylate
t-BA	*tert*-butyl acrylate
BIPY	2, 2-bipyidine
CCTP	Catalytic chain transfer polymerisation
CMRP	Cobalt mediated radical polymerisation
CRP	Controlled radical polymerisation
CS_2	Carbon disulphide
CSIRO	Commonwealth scientific and industrial research organisation
CTA	Chain transfer agent
d	Doublet
DCM	Dichloromethane
DIP	Isopropylxanthic disulphide
DMF	Dimethylformamide
DMSO	Dimethylsulfoxide
$\overline{DP}$	Degree of polymerisation
DPCM	Diphenyldithiocarbamate of diethylmalonate
DT	Degenerative transfer
eATRP	Electrochemically mediated atom transfer radical polymerisation
e.g.	*exempli gratia*

Et	Ethyl
et al.	*et alii, et alia*
EVA	Ethylene vinyl acetate
f	Initiator efficiency
FRP	Free radical polymerisation
g	Gram(s)
GPC	Gel permeation chromatography
GTP	Group transfer polymerisation
h	Hour(s)
HEP	Hydroxyethylpyrrolidone
I	Initiator
ICAR	Initiators for continuous activator regeneration
i.e.	*id est*
k_i	Rate constant of initiation
k_p	Rate constant of propagation
k_t	Rate constant of termination
LAMs	Less activated monomers
LCST	Lower critical solution temperature
LDPE	Low density polyethylene
LRP	Living radical polymerisation
[M]	Monomer concentration
MA	Methyl acrylate
MADIX	Macromolecular design *via* interchange of xanthate
MAMs	More activated monomers
Me	Methyl
MeOH	Methanol
Me_6TREN	Tris[2-(dimethylamino)ethyl]amine
mg	Milligram(s)

min	Minute(s)
mL	Millilitre(s)
MMA	Methyl methacrylate
mmol	Millimole(s)
M_n	Number average molecular weight
mol	Mole(s)
MS	Mass spectroscopy
M_w	Weight average molecular weight
NMP	Nitroxide mediate polymerisation
NMR	Nuclear magnetic resonance
NVC	N-vinylcarbazole
NVCL	N-vinylcaprolactam
NVP	N-vinylpyrrolidone
OSET	Outer-sphere electron transfer
[P•]	Radical concentration
PDI	Polydispersity Index
PDMAEMA	Poly(dimethylaminoethylmethacrylate
PEG	Poly(ethylene glycol)
Ph	Phenyl
PMDETA	N,N,N′,N″,N″-Pentamethyldiethylenetriamine
PNIPAAm	Poly(N-isopropylacrylamide)
PNVC	Poly(N-vinylcarbazole)
PNVCL	Poly(N-vinylcaprolactam)
PNVP	Poly(N-vinylpyrrolidone)
ppm	Parts per million
PRE	Persistent radical effect
Pr	Propyl
PS	Polystyrene

PVAc	Poly(vinyl acetate)
q	Quartet
R_d	Rate of decomposition
R_i	Rate of initiation
RAFT	Reversible addition fragmentation chain transfer
ROMP	Ring opening metathesis polymerisation
ROP	Ring opening polymerisation
R_p	Rate of propagation
R_t	Rate of termination
s	Singlet
SARA	Supplemental activators and reducing agents
SEC	Size exclusion chromatography
SET-LRP	Single electron transfer – living radical polymerisation
SPS	Solvent Purification System
SR&NI	Simultaneous reverse & normal
t	Triplet
TCDI	1,1-thiocarbonyl diimidazole
TEMPO	2, 2, 6, 6-tetramethylpiperidinyloxy
theor.	Theoretical
THF	Tetrahydrofuran
TIBA	Triisobutylaluminium
TREN	Tris(2-aminoethyl)amine
VAc	Vinyl acetate
vs.	*verses*

Chapter 1

General Introduction

1.1. Free radical polymerisation

Free radical polymerisation (FRP) is the most widely used pathway to synthesise polymers from vinyl monomers in industry or the laboratory and accounts for approximately 50% of polymers produced worldwide.[1, 2] FRP is an example of a chain growth polymerisation technique, where monomer concentration decreases steadily as the polymerisation evolves and higher molecular weights can be achieved at low conversions. FRP can be used for a broad range of vinyl monomers and is versatile with respect to different functional groups. The method is tolerant of impurities and unlike ionic or coordination polymerisations, FRP can be carried out over a wide temperature range (-80 to 250°C)[3] and can be conducted in bulk, solution (organic or aqueous media), suspension or in an emulsion. The active species in the reaction are organic (free) radicals which are highly reactive and high molecular weight polymer can be produced using short reaction times, with the lifetime of a propagating chain in FRP being approximately one second.[4] However, the highly reactive nature of the radicals is also a disadvantage, as there is a distinct lack of control over the molecular weight and polydispersity of the resulting polymer, as well as an inability to control the architecture.[5] A conventional FRP process has three main elementary steps; namely initiation, propagation and termination.

Initiation involves the attack of a free radical on the C=C bond of a vinyl monomer, to generate a propagating radical capable of then attacking further monomer, Scheme 1.1.

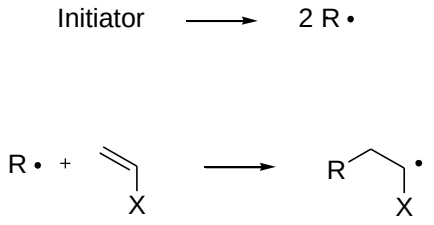

Scheme 1.1. Initiation in a free radical polymerisation

The sources of the free radical initiating species are commonly generated from the thermal decomposition of an azo or peroxide compound. These compounds can also fragment to give a radical species when irradiated with electromagnetic radiation. Other methods used for initiation step in FRP include ionizing radiation (α, β, γ, x-rays), redox initiation and also initiation *via* electrolysis.

The rate of decomposition of radical initiator (R_d) is the rate controlling step in FRP:

$$I \xrightarrow{k_d} 2R\cdot \qquad \text{Equation 1.1}$$

$$R_d = \frac{-d[I]}{dt} = k_d[I] \qquad \text{Equation 1.2}$$

The rate of initiation (R_i) can be described as: -

$$R_i = \frac{d[RM\cdot]}{dt} = k_i[R\cdot][M] \qquad \text{Equation 1.3}$$

and: -

$$R_i = 2k_d f[I] \qquad \text{Equation 1.4}$$

Where f is the intiator efficiency, i.e. the ratio of number of chains initiated: number of radicals produced. Ideally, this value would be 1.0, however in practice the value is typically between 0.3 – 0.8.[6] This is due to side reactions involving the free radicals generated from the initiating compound. Free radicals can be terminated *via* primary recombination (i.e. cage effect) or induced decomposition, where a free radical attacks an unreacted initiating compound, generating dead species.

Propagation is a bimolecular reaction which involves the newly formed propagating radical attacking a further monomer unit, which in turn then adds more monomer units, to generate a polymeric chain (Scheme 1.2).

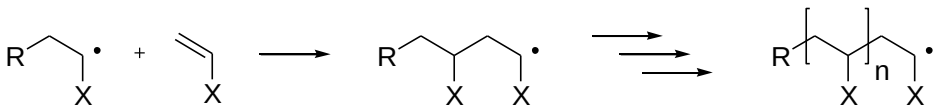

Scheme 1.2. Propagation in a free radical polymerisation

The propagation rate constant is generally considered to be independent of chain length. Therefore, the rate of polymerisation (R_p) can be written as:-

$$R_p = \frac{-d[M]}{dt} = k_p[M][M\cdot] \qquad \text{Equation 1.5}$$

[M ·] is difficult to attain experimentally so R_p can be described by: -

$$R_p = k'[M][I]^{1/2} \qquad \text{Equation 1.6}$$

Where $k' = (k_p^2 k_d f/k_t)^{1/2}$. Therefore, the rate of polymerisation is proportional to the concentration of monomer and to the square root of the concentration of the initiator. In FRP, head-to-tail arrangements are generally observed.

There are two routes in which termination can occur in FRP. The first route is recombination. In ionic polymerisations, recombination does not occur due to the repulsive behaviour of the reacting species. However, in FRP it is likely that when the active propagating chains are in close proximity to each other they will react to form a new bond and create a dead polymer chain (Scheme 1.3). This creates a head-to-head configuration where the two polymer chains meet.

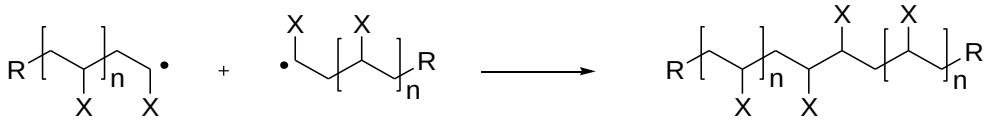

Scheme 1.3. Termination *via* recombination

The rate of termination (R_t) due to coupling of polymer chains is given by:-

$$R_t = \frac{-d[M\cdot]}{dt} = 2k_t[M\cdot][M\cdot] = 2k_t[M\cdot]^2 \qquad \text{Equation 1.7}$$

Termination in FRP can also occur through disproportionation. This involves the abstraction of a hydrogen atom from one active chain end to another, giving two dead polymer chains, one of which is unsaturated (Scheme 1.4).

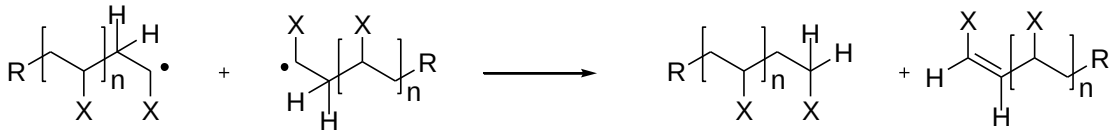

Scheme 1.4. Termination *via* disproportionation

The rate of termination (R_{td}) due to disproportionation is given by:-

$$R_{td} = 2k_{td}[M\cdot]^2 \qquad \text{Equation 1.8}$$

The overall rate of termination is given by:-

$$R_T = 2k_d f[I] \qquad \text{Equation 1.9}$$

Therefore, the overall the rate of termination is proportional to the concentration of the initiator.

Radical species are highly reactive and can attack polymer chains, abstracting hydrogen atoms. When the abstraction of hydrogen takes place on the polymer chain away from the chain end, this results in branching. Short chain branching is a result of "back biting" through intramolecular hydrogen abstraction (Scheme 1.5). An example of this is in the production of low density polyethylene (LDPE).[7]

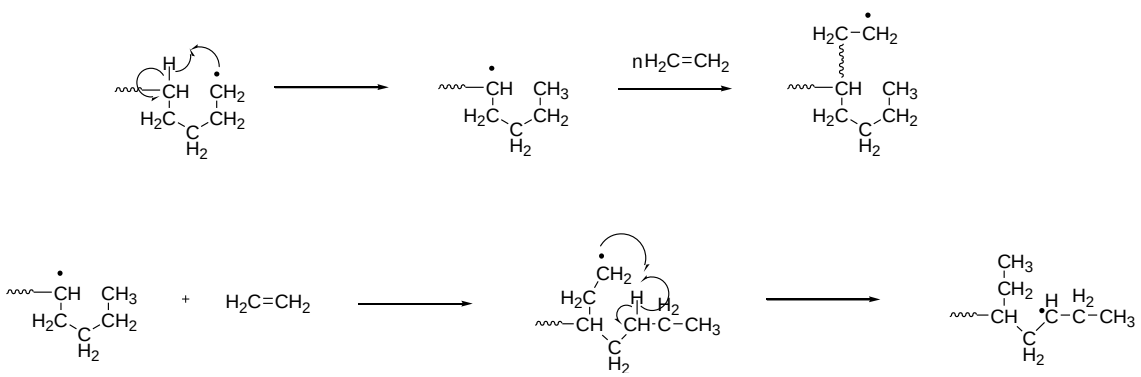

Scheme 1.5. Intramolecular "back biting"

Long chain branching takes place through the hydrogen abstraction from intermolecular reactions between polymer chains, Scheme 1.6.[8] A radical from one chain abstracts a hydrogen atom from another polymer chain to form dead polymer and a new radical, consequently forming long branches. An example is in the radical polymerisation of (meth) acrylates, where chain transfer to polymer is *via* hydrogen abstraction from the tertiary carbon in the backbone chain. This is due to the tertiary carbon being more stable than the secondary carbon.

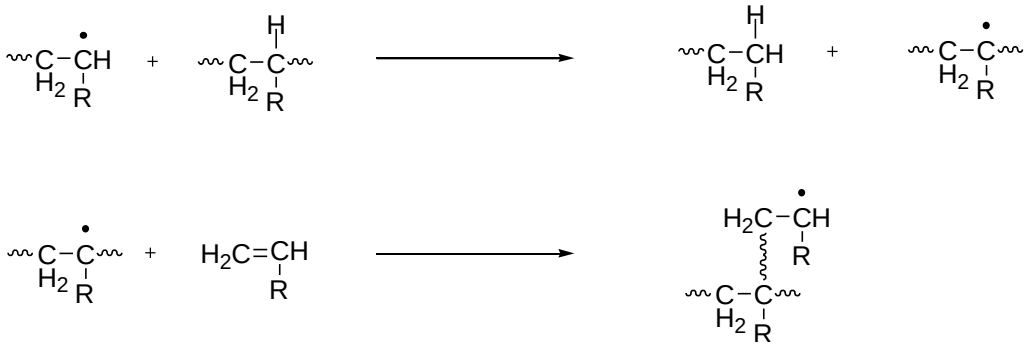

Scheme 1.6. Intermolecular chain transfer to polymer

For poly(vinyl acetate) (PVAc), chain transfer to polymer is *via* hydrogen abstraction from the primary carbon present in the side group. This is due the CH_3 in the monomer unit being adjacent to the C=O and being stabilised through the electron delocalisation with the carbonyl π-bond. The tertiary carbon on the backbone chain does not have this stabilization effect, therefore chain transfer to polymer occurs on the side groups (Scheme 1.7).[8]

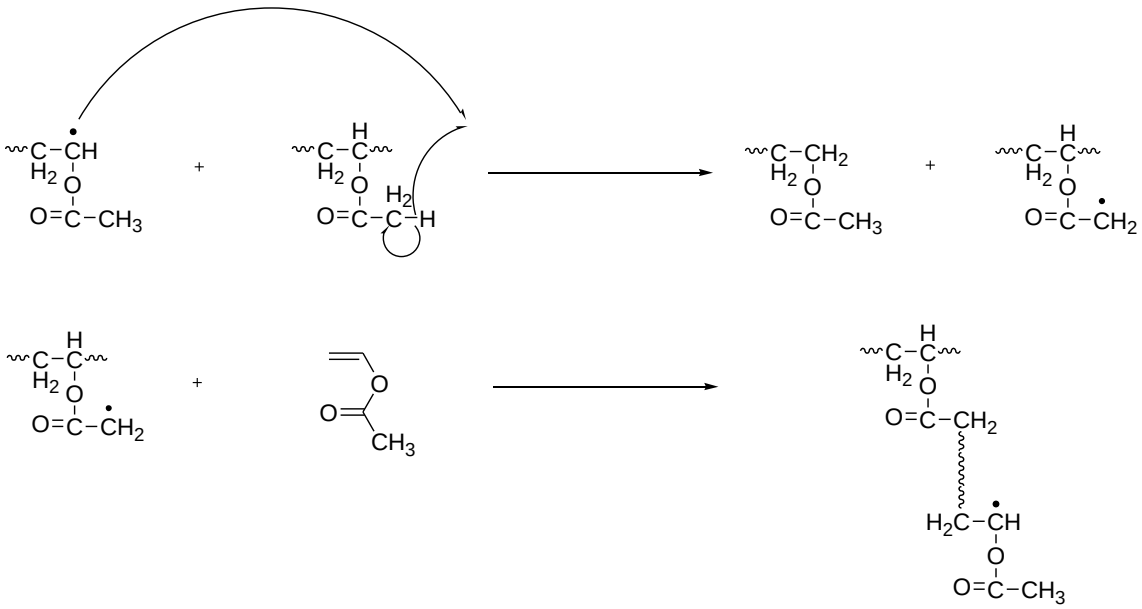

Scheme 1.7. Intermolecular chain transfer to polymer in PVAc

Additives such as thiols can be added to the polymerisation medium to increase the amount of chain transfer reactions and reduce the overall molecular weight. The solvent used in the polymerisation can also take part in chain transfer reactions, which can reduce the length of the polymeric chains.

When the polymerisation is carried out in bulk, a gel or Trommsdorff – Norrish effect is observed.[9] At higher conversions, the viscosity of the polymerisation medium is increased leading to termination events being diffusion controlled and thus the rate of termination is decreased. This means that the concentration of active propagating radicals is increased and with a large amount of monomer still present the rate of propagation is also increased. Propagation is an exothermic reaction; therefore there is a large increase in temperature which causes an increase in initiator decomposition, generating more propagating radicals. This run away reaction is known as autoacceleration and can potentially cause explosions. This effect can be avoided by using an emulsion, suspension or solution polymerisation to dissipate the heat generated from propagation.

1.2. Controlled / living polymerisation

A "controlled / living polymerisation" is where by the active species are able to propagate without any termination or transfer reactions occurring. Polymerisation will therefore continue until all the monomer has been consumed and will restart when more monomer is added to the chain end. Mono disperse polymers can be synthesised when the rate of initiation (R_i) is much faster than that of the rate of propagation (R_p). This means that the polymeric chains are initiated at the same time and have an equal probability of adding more monomer and grow at a constant rate. A distinction needs to be made between a "controlled" and "living" polymerisation. A controlled polymerisation is where molecular weight can be pre-determined / controlled and polydispersity is low so that all the polymeric chains are of a similar length. A polymerisation can still be classed as controlled in the presence of termination and transfer reactions but a rapid initiation stage and transfer between an active and dormant species is essential. In contrast, a living polymerisation is where there are no termination or transfer reactions. The living polymerisation continues until all monomer is consumed, with the retention of the active chain end. This is then capable of reacting with further monomer or co-monomer, giving rise to multi-block copolymers.

The first published work on "living polymers" was reported in 1956 by Szwarc *et al*,[10, 11] for the polymerisation of styrene using sodium naphthalenide in tetrahydrofuran (THF). However, anion chain carriers are extremely sensitive to

moisture and oxygen and the polymerisations must be carried out under controlled conditions.[10]

Since the discovery of living anionic polymerisations, other controlled / living polymerisation methods have also been developed, such as cationic polymerisation,[12] ring-opening polymerisation (ROP),[13] ring opening metathesis polymerisation (ROMP),[14] group transfer polymerisation (GTP)[15] and also living radical polymerisation (LRP) - which will be discussed further in this chapter.

1.3. Controlled / living radical polymerisation

The development of controlled / living radical polymerisation techniques using several different approaches enables the ability to control the molecular weight, polydispersity and architecture of a polymer, with the retention of an active chain end. For a controlled polymerisation it is required that there is fast initiation and an absence of termination reactions, which directly conflicts with conventional free radical polymerisation, where slow initiation and random termination are inherent within the free radical process. However, as with any radical reaction, termination and transfer processes cannot be fully eliminated therefore controlled / living radical polymerisations are not expected to be fully "living".

Having a dynamic equilibrium between propagating radicals and a dormant species is essential for a controlled radical polymerisation.[16, 17] There have been two routes explored in order to achieve this. Radicals can be reversibly trapped in a deactivation / activation process (Scheme 1.8), or the radicals can be involved in a reversible transfer, degenerate exchange process (Scheme 1.9).[4]

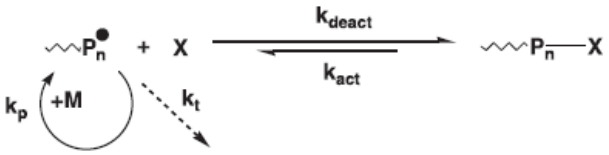

Scheme 1.8. Radicals reversibly trapped in a deactivation / activation process

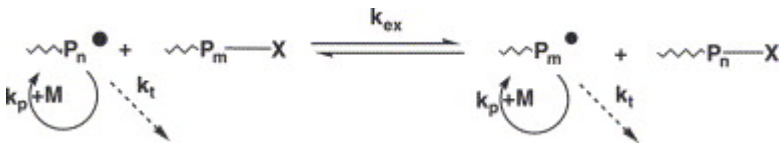

Scheme 1.9. Radicals involved in a reversible transfer, degenerative exchange process

In both cases the equilibrium between the dormant and active species is shifted strongly to the dormant species, in order to reduce the active radical concentration and avoid termination reactions. As shown in Equation 1.5 the rate of polymerisation is proportional to the concentration of propagating radicals and in Equations 1.7 and 1.8 that the rate of termination in proportional to the square root of the concentration of propagating radicals. Therefore, reducing the concentration of radicals in the polymerisation will contribute greatly to the suppression of termination reactions.

For a controlled / living radical polymerisation to be classed as successful, a number of criteria need to be met:[18]

(i) First order kinetics in terms of monomer concentration *vs*. time
(ii) Molecular weight increases as a linear function with increasing conversion of monomer to polymer
(iii) Narrow polydispersity indices
(iv) Polymers should have their chain ends end capped with active species and ability to synthesise block copolymers
(v) Molecular weight is controlled in relation to the stoichiometry of the reaction
(vi) Polymerisation continues until all monomer is consumed

1.4. Atom transfer radical polymerisation (ATRP)

ATRP originates from the organic synthesis reaction of atomic transfer radical addition (ATRA).[19, 20, 21] Kharasch *et al*. discovered that halogenated methanes could be directly added to olefinic bonds in the presence of radical initiators or light.[22] High yields of monoadduct could be obtained, e.g. from the reaction of CBr_4 with α – olefins. However, with more reactive monomers such as styrene, the yield is significantly decreased due to radical – radical coupling reactions and the addition of more than one monomer unit, producing oligomers. The reasoning behind this is that the chain transfer constant is low enough so more than one monomer unit can add to the active radical. Complexes of Cu, Fe, Ru and Ni were seen to be more effective in the transfer of halogen rather than alkyl halides, which was developed into ATRA.[23] In ATRA, a transition metal complex undergoes an inner-sphere oxidation *via* abstraction of a halogen atom from an alkyl halide, to generate an organic radical and an oxidized

transition metal complex. The organic radical is then capable of reacting with an alkene.

An extension of the ATRA process known as atom transfer radical polymerisation (ATRP) was reported by several groups in the mid 1990's.[24, 25] In ATRP the propagating radicals can be activated and deactivated in a dynamic equilibrium using a transition metal complex (commonly a copper complex with nitrogen based ligands).[26] This approach relies on the persistent radical effect (PRE),[27] where the propagating radicals are rapidly trapped and deactivated into a dormant state by a stable radical species (persistent radical), such as an organometallic complex in ATRP. The persistent radical cannot generally recombine due to steric hindrance or electronic effects. However, they can reversibly react with the reactive propagating radicals. Activation of the dormant species can occur by the introduction of external stimuli such as, heat / light or presence of a catalyst - as in ATRP. The concentration of the persistent radical is observed to increase over time, shifting the equilibrium towards the dormant species. A steady state of growing polymeric chains is due to the activation – deactivation from the dormant state, as opposed to the initiation – termination in conventional FRP. In ATRP, only a catalytic amount of the organometallic species is needed.

The mechanism of ATRP is shown in Scheme 1.10.[23] The transition metal complex undergoes oxidation by abstracting a halogen atom (**X**) from an alkyl halide, thus generating an alkyl radical (**R•**). **X** is either a chlorine or bromine atom. The alkyl radical is then able to attack a monomer unit and initiate the polymerisation. If the reactivity of the radical species before and after the addition of monomer is comparable, then this favours a continual activation – addition – deactivation cycle and polymerisation will continue until all monomer is consumed. Due to the reactive nature of the radicals in ATRP, termination reactions due to disproportionation or radical coupling are still inherent. The presence of these termination events generally accounts for the termination of no more than 5% of the total polymer chains, but does reduce the concentration of active radicals. Therefore, the persistent radicals (oxidized transition metal complexes) increase in concentration and the equilibrium between dormant and active species shifts to the dormant species. As the polymerisation continues and termination reactions are less prevalent, the PDI of the polymer gradually decreases.

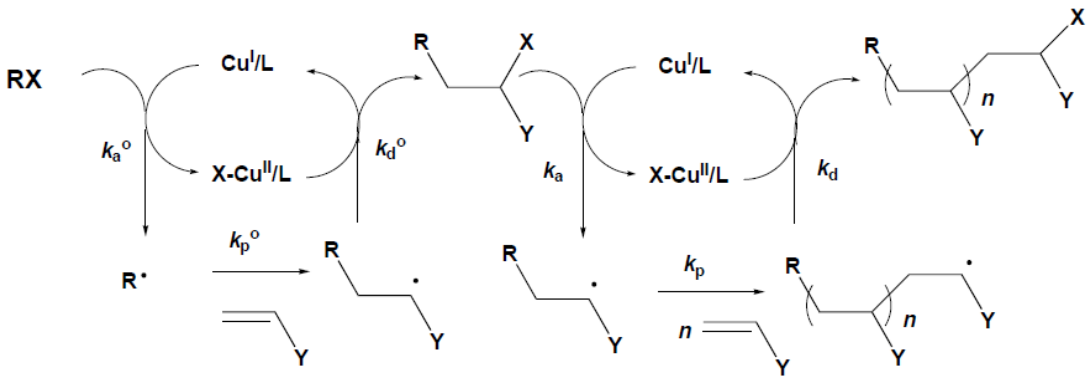

Scheme 1.10. Mechanism for ATRP

ATRP is applicable to wide range of monomers such as styrenics, (meth)acrylates and (meth)acrylamides. In an ATRP system, there are generally five components to consider, namely monomer, alkyl halide initiator, transition metal, ligand and solvent. A number of transition metals have been used in ATRP catalysts; however Cu(I) complexes are most commonly used. The main disadvantage of ATRP is the presence of residual copper in the final polymer product. More advanced ATRP methods such as Initiators for Continuous Activator Regeneration (ICAR),[28, 29] Activators ReGenerated by Electron Transfer (ARGET),[30, 31] Supplemental Activators and Reducing Agents (SARA)[32, 33] and electrochemically mediated ATRP (eATRP)[34] have been employed to reduce the amount of catalyst used.[35] Other ATRP methods developed include, "reverse" ATRP,[36] Simultaneous Reverse & Normal (SR&NI) ATRP[37] and Activator Generated by Electron Transfer (AGET) ATRP.[38, 39]

1.5. Single electron transfer - living radical polymerisation (SET-LRP)

SET-LRP was first reported in 2006 by Percec *et al*.[40] and is closely related to ATRP, as both controlled polymerisation methods generally use the same initiators and ligands. The main difference is that Cu(0) is used as the activating species in SET-LRP rather than Cu(I) complexes. In SET-LRP, the balance between active and dormant species is mediated by an outer-sphere electron transfer (OSET) activation process, where polymeric chains are activated by Cu(0) and deactivated by a Cu(II) complexes.[41] The proposed mechanism for SET-LRP and its comparison with ATRP is shown in Scheme 1.11.[42]

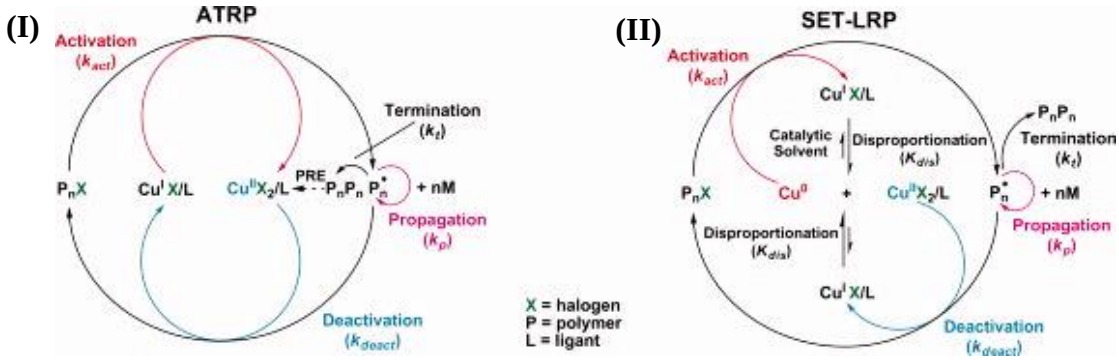

Scheme 1.11. Comparison of mechanisms for (I) ATRP and (II) proposed mechanism for SET-LRP

In SET-LRP, initiation occurs when a dormant species (**P_nX**) reacts with Cu(0) and the carbon – halide bond dissociates, to leave an active radical species (**P_n•**). The propagating chain can then either react with monomer and propagate, undergo termination or become deactivated *via* halogen exchange with a Cu(II) complex. The single electron transfer processes involved in activation and deactivation generates a Cu(I) species *in situ*. For a successful SET-LRP polymerisation the Cu(I) species needs to undergo disproportionation rapidly to give the Cu(0) and Cu(II) species to activate and deactivate the polymer chains. This can generally be done by using water, other polar solvents (e.g. DMSO, alcohols, and acetone) or a mixture of solvents with water. The use of appropriate ligands such as, Tris[2-(dimethylamino)ethyl]amine (Me_6TREN), Tris(2-aminoethyl)amine (TREN), N,N,N′,N″,N″-Pentamethyldiethylenetriamine (PMDETA) can also improve disproportionation.[41] Cu(0) is often present in the form of copper wire and as such can be easily removed from the polymerisation medium, thus reducing the contamination of copper. Contrary to ATRP, it is reported that SET-LRP does not obey PRE and control over the polymerisation is governed by disproportionation and therefore SET-LRP is not reliant on termination reactions and is able to maximize chain end functionality.[40, 43, 44]

1.6. Nitroxide mediated polymerisation (NMP)

NMP was first developed in the mid 1980's by CSIRO.[45, 46] Nitroxides were used as radical scavengers to trap carbon radicals and form alkoxyamines. It was reported that under certain conditions, the trapping of the radicals by the nitroxide moiety could be

reversed. Propagating radicals were trapped using 2, 2, 6, 6-tetramethylpiperidinyloxy (TEMPO) as the nitroxide. At 40 – 60°C the active radicals reacted with TEMPO to give an alkoxyamine, which could not react further. However, as the temperature was increased to 80 - 100°C, oligomers of (meth)acrylates were formed. At these temperatures the polymerisation method was not controlled or living.

In 1993, NMP based polymerisations gained more interest from the work by Georges *et al.*[47] This was the first successful controlled radical polymerisation using NMP. Styrene was polymerised in a controlled / living manner using TEMPO as the nitroxide mediating agent and benzoyl peroxide as the initiator. The temperature used in these polymerisations was 130°C. At this temperature the NO–C bond of the alkoxyamine becomes unstable and releases the nitroxide. At temperatures < 130°C, the nitroxide moiety acts as a radical trap.

In NMP either, a bimolecular or unimolecular initiator system can be used. In a bimolecular system a conventional initiating species such as benzoyl peroxide is combined with a nitroxide such as TEMPO and the alkoxyamine is made *in situ*. The disadvantage of using a bimolecular system is that the initiating species is poorly defined in structure and concentration. In a unimolecular system, an alkoxyamine is thermally initiated giving the initiating radical and the nitroxide. The nitroxide radical should not combine or react with monomer to initiate the polymerisation.

The control in NMP is attained by the transfer between the dormant chains (alkoxyamines) and the active propagating chains. The success of the polymerisation method relies on PRE and the nitroxide (persistent radical) reversibly caps the polymer chain end, transferring it from an active to dormant state.[48]

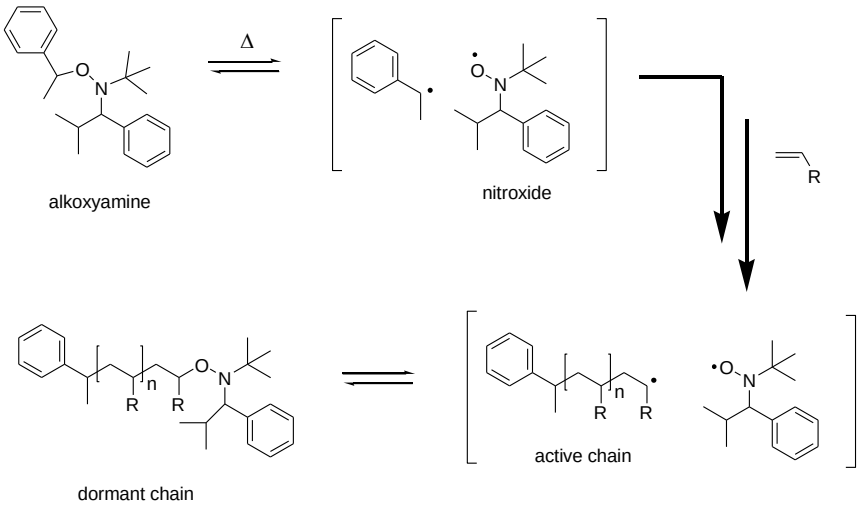

Scheme 1.12. Polymerisation of a vinyl monomer *via* NMP

As it is shown in Scheme 1.12, at the start of the reaction, the alkoxyamine thermally decomposes into the nitroxide species and the initiating radical. At this point, the initiating radicals may couple together, however the nitroxide radicals cannot combine to form inactive species. This means there is an overall increase in the concentration of the nitroxide relative to the initiating radical and therefore, there is a greater chance for the formation of the dormant chain. As the equilibrium is shifted towards the dormant state, then the active species is at a lower concentration and chain termination is limited. In this polymerisation technique only organic compounds need to be used and there are no metal complexes that need to be disposed of (as in ATRP). Also in contrast relation to ATRP, NMP is able to control the polymerisation of acidic monomers.

Disadvantages of NMP are the necessity of relatively high temperatures and difficulty of introducing end functionality into the polymer chain. Furthermore, a stoichiometric amount of mediating compound is needed in relation to polymer chains.

1.7. Cobalt mediated radical polymerisation (CMRP)

Organocobalt (III) compounds have often been of interest due to the ease of the homolytic cleavage of the Co – C bond, under mild conditions to form radicals. The first CMRP was reported in 1994 by Wayland *et al*.,[49] in which they reported the synthesis of homopolymers and block copolymers of acrylates using a cobalt porphyrin. It is generally accepted that a Co(II) complex can react with a propagating radical to form an alkyl-Co(III) complex (PRE), or alternatively can undergo hydrogen abstraction to give a polymer chain with an unsaturated end group. Vinyl monomers without α - methyl groups, such as acrylics and vinyl esters, are less prone to hydrogen abstraction by cobalt complexes and can undergo CMRP. Other monomers, such as methacrylates and α-methylstyrene which have a α-methyl group favour a catalytic chain transfer polymerisation (CCTP) (Scheme 1.13).[50]

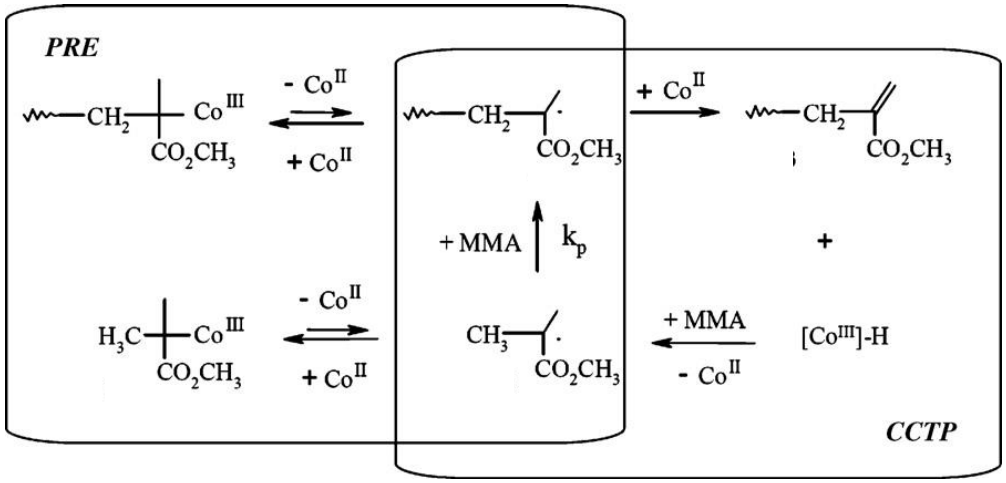

Scheme 1.13. Role of PRE and CCTP in polymerisations in the presence of cobalt complexes

The general mechanism for CMRP is shown in Scheme 1.14.[50] The Co – C bond of the cobalt complex is broken photolytically or thermally, generating an alkyl radical (**R•**) and a Co(II) complex (persistent radical). **R•** then attacks the double bond of the vinyl monomer and initiates the polymerisation. The propagating chain is then end capped with the cobalt complex and the chains are now dormant, but can be reactivated due to the low strength of the Co – C bond. There is then a chain of activation – deactivation processes until the monomer is consumed. The concentration of the active radicals (in accordance with PRE) should be continuously low so that termination reactions are limited.

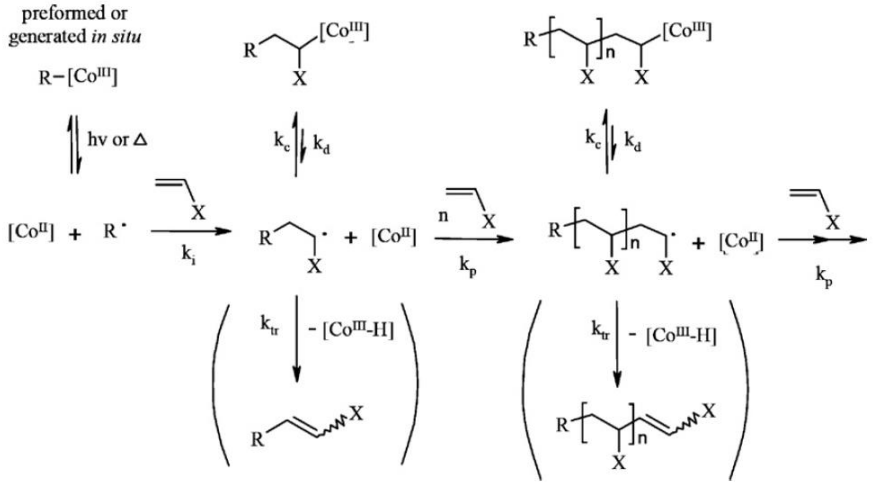

Scheme 1.14. General mechanism for CMRP

1.8. Reversible addition fragmentation chain transfer (RAFT) polymerisation

RAFT polymerisation is an example of a process where radicals are involved in a reversible transfer, degenerative exchange process, Scheme 1.9.[51, 52] This approach does not employ PRE and follows the same kinetics as a conventional free radical polymerisation, i.e. slow initiation and fast termination. The RAFT agent present in the polymerisation mixture degeneratively transfers the propagating radicals to a dormant species. Rapid chain transfer between the dormant and active moieties is essential in order to obtain low polydispersities and a controlled molecular weight. As with FRP the lifetime of an active propagating chain may be in the region of one second, however the overall reaction time will be far greater due to the polymeric chains largely being in a dormant state before re-activation.

RAFT has its origins in the radical addition reactions of the 1970s and 1980s, where a radical process for deoxygenating secondary alcohols was reported, *via* their corresponding xanthates using a stannyl radical as the reactive species.[53] After a dispute over the mechanism on how the xanthate fragments, it was concluded that a fast and reversible transfer involving a radical intermediate take place, which fragments through the C-S rather than through the C-O bond.[54, 55]

The addition of a carbon centered radical (R′•) the addition to xanthate leads to a radical intermediate which can either fragment to the original xanthate or can fragment to give R• (Scheme 1.15).[54]

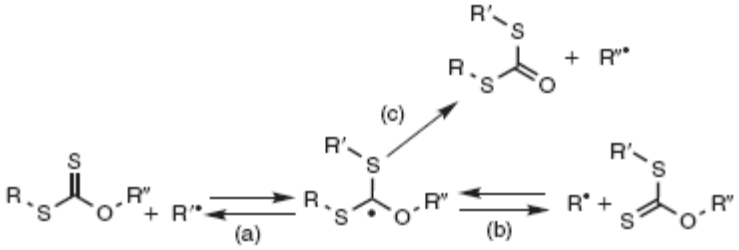

Scheme 1.15. Xanthate fragmentation pathways

The pathway which is prevalent will depend on the relative stabilities of R and R′, respectively. Both these pathways are reversible; however the third pathway in which there is scission of the C-O is irreversible. If R″ is either a methyl, ethyl or another possible high energy radical then this pathway is no longer possible. Therefore, if R′• is less stable than R•, then attack on the thiocarbonyl group from R′• would result in the fragmentation of the intermediate radical to give R• through a reversible addition

– fragmentation pathway on the thiocarbonyl group, with the pathway forming a C=O bond forbidden. This process was extended for use in polymer synthesis in 1998.[56] The Rhodia research group, in collaboration with Samir Z. Zard produced polymers with controlled / living characteristics. They named the radical polymer process MADIX (MAcromolecular Design *via* Interchange of Xanthate).

Also in 1998 (at a similar time to the Rhodia group), the CSIRO group discovered that when using a thiocarbonyl-thio group, polymers with controllable molecular weights and low polydispersities are produced.[57] In addition, the end groups of the polymer were still active upon the addition of a monomer or co-monomer, giving a control / living radical polymerisation technique. The group named this technique Reversible Addition Fragmentation chain Transfer (RAFT) polymerisation. RAFT polymerisations can be performed with the addition of a RAFT chain transfer agent (CTA), to a conventional FRP system. RAFT agents can be divided into four different groups, all of which are based on a thiocarbonyl thio structure (Figure 1.1).[58]

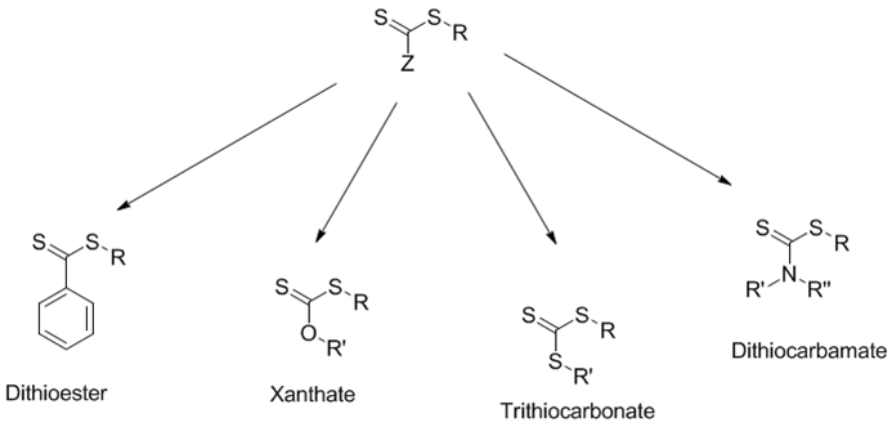

Figure 1.1. RAFT agent structures

A wide variety of RAFT agents have been developed to control the polymerisation of conjugated and unconjugated monomers. R and Z groups are found to be monomer specific. The R group of the RAFT agent needs to be a good leaving group compared to that of the propagating radical. It is also requisite that the R group is a good re-initiating species to continue the polymerisation. Figure 1.2 shows the variation of R groups and control over different monomers.[59]

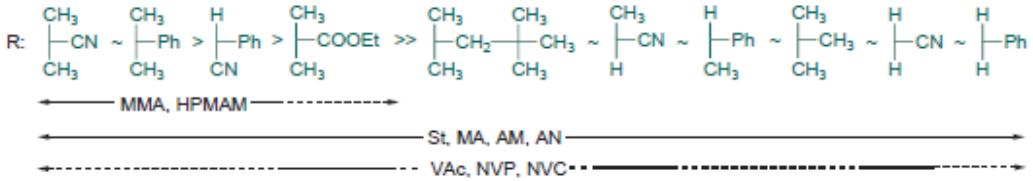

Figure 1.2. R group guidelines (Fragmentation rates decrease from left to right). Dashed line indicates limited control

The role of the Z group in the RAFT agent, is to control the reactivity of the C=S bond and influence the rates of addition. In addition, the Z group influences the stability of the intermediate radical. In general, reactivity transfer coefficients decrease in the order of dithiobenzoates > trithiocarbonates ≈ dithioalkanoates > xanthates > dithiocarbamates.[58] The "more activated" monomers (MAMs) such as styrene and methyl acrylate which have a conjugated structure are controlled by Z groups which stabilise the intermediate radical. These Z groups are namely dithioesters and trithiocarbonates, as they have strong stabilizing groups and therefore increase the reactivity of the C=S towards radical addition. For "less activated" monomers (LAMs) such as vinyl acetate and N-vinylpyrrolidone where a non-conjugated structure is present, Z groups with electron withdrawing moieties are most effective in controlling the polymerisation, Figure 1.3.[59]

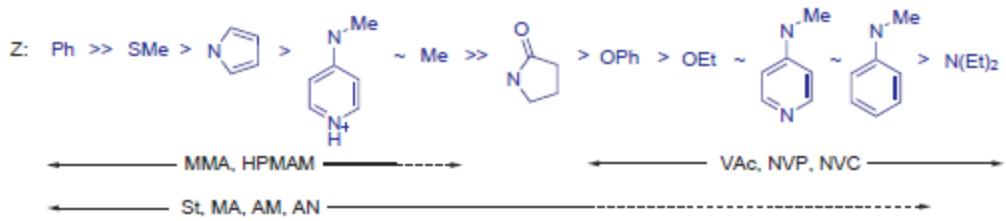

Figure 1.3. Z group guidelines (addition rates and transfer constants decrease and fragmentation rates increase from left to right**).** Dashed line indicates limited control

The RAFT mechanism is shown in Scheme 1.16.[60] Initiation occurs in RAFT polymerisation as in conventional free radical polymerisation (Scheme 1.16, i), typically through the thermal decomposition of an azo or peroxide compound which then reacts with monomer, to generate a propagating polymer chain (Scheme 1.16, ii). This then reacts with the thiocarbonylthio double bond of the RAFT agent to give an intermediate radical (Scheme 1.16, iii). The intermediate radical is part of the "pre-equilibrium" and

can either fragment to give the original RAFT agent or alternatively can fragment to expel **R•**. The expelled R group radical can then attack monomer to generate another propagating polymer chain $\mathbf{P_n}$• (Scheme 1.16, iv). $\mathbf{P_n}$• can then either react with RAFT agent or polymer end-capped with the thiocarbonylthio species (macroCTA). Once the initial RAFT agent has been consumed then only polymeric macroCTA remains. If $\mathbf{P_n}$• reacts with macroCTA then this forms a new radical intermediate in the "main equilibrium" which can fragment to give either $\mathbf{P_m}$• or $\mathbf{P_n}$• (Scheme 1.16, v). The termination reactions of radical coupling and disproportionation are still present as with conventional FRP and can only be suppressed by using a low concentration of radicals (Scheme 1.16, vi).

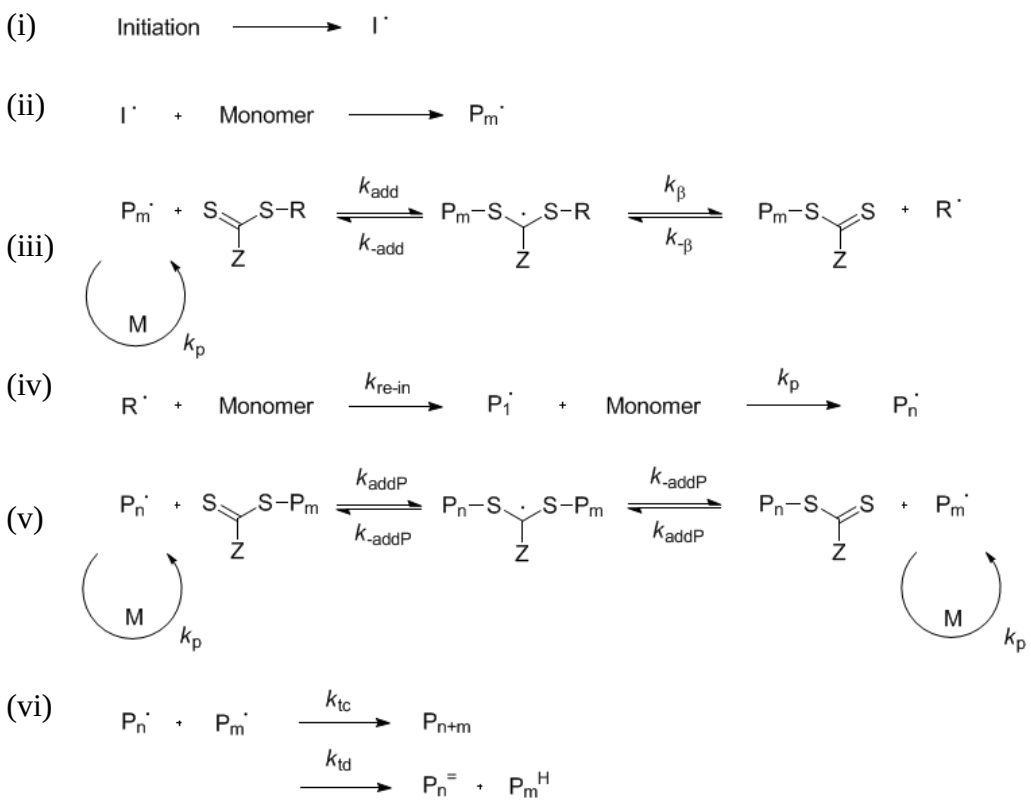

Scheme 1.16. RAFT mechanism (i) initiation, (ii) propagation, (iii) pre-equilibrium, (iv) re-initiation, (v) main equilibrium and (vi) termination

RAFT polymerisations do have some disadvantages in that the RAFT agents need to be synthesised and purification is often by column chromatography. RAFT agents are generally quite odorous and the final polymer products maybe coloured (e.g. pink or yellow). Also the polymerisation times can be significantly longer than in a conventional FRP.

1.9. Poly(N-vinylpyrrolidone) (PNVP)

PNVP was first synthesised in 1939 by Fickentscher and Herrle, through the conventional free radical polymerisation of NVP in aqueous solution using H_2O_2 and NH_3 as initiating species.[61, 62] PNVP comprises a highly polar pyrrolidone ring connected through the nitrogen atom to a non-polar hydrocarbon backbone chain. Hence, the polymer is soluble in both organic solvents and water.[63] PNVP is biocompatible, non-toxic, temperature and pH-stable, however, due to the hydrocarbon backbone chain it is non-biodegradable.[64] During the second world war, PNVP was used a substitute for blood plasma[65] and has since found many more applications in various fields,[66] such as a binder[67, 68] and to film coat pharmaceutical tablets.[69] PNVP-iodine has disinfectant properties and is used in liquid soaps, surgical scrubs, and ointments.[70, 71, 72] It is also a food additive (E1201, E1202) and is used to stabilise beer.[73] It has been used in personal care products,[74] adhesives[75] and as a cosmetic excipient.[74] In addition, PNVP has been seen as a replacement for poly(ethylene glycol) (PEG).[76-78]

NVP has been polymerised using radical methods in bulk, aqueous solution and in organic solvents. The use of hydrogen peroxide as initiating species gave PNVP with low molecular weight.[61, 62] The use of benzoyl peroxide also gave similar results.[61, 62] Beritenbach *et al*. were the first to use AIBN as the initiating species in bulk.[79] As NVP is polar and capable of hydrogen bonding due to the amide functionality, the rate of polymerisation can be influenced by the solvent, such as water.[80]

The polymerisation of NVP has been performed using a number of controlled radical polymerisation methods, most commonly, RAFT. This will be discussed further in Chapter 3. The polymerisation of NVP has also been performed using ATRP[81, 82] and CMRP.[83-86]

1.10. Poly(N-vinylcaprolactam) (PNVCL)

Poly(N-vinylcaprolactam) (PNVCL) is a non-ionic, non-toxic and biocompatible polymer[87, 88] with a hydrocarbon backbone chain, rendering it non-biodegradable. Upon hydrolysis of PNVCL, polymeric carboxylic acid is produced without the formation of any small toxic amide compounds.[87, 89] PNVCL is a water soluble polymer, however also undergoes phase transition (generally between 32 - 35°C) upon heating. This is further discussed in Chapter 6.

The radical polymerisation of NVCL has not been as extensively studied as for NVP. Solomon *et al*. reported the polymerisation of NVCL in bulk using a number of radical initiators, at temperatures ranging from 60 - 120°C.[90] AIBN was found to give high conversion of monomer to polymer in the temperature range of 60 - 80°C, whereas benzoyl and lauroyl peroxides were reported to be inefficient initiators and no polymerisation was observed. The same group also reported the radical polymerisation of NVCL in a number of solvents.[91] When toluene, 1, 4 dioxane or chlorobenzene were used as the polymerisation solvent, polymer was obtained using either AIBN or tert-butyl perbenzoate as the radical initiator. No polymer was obtained when either dimethylformamide or ethylene carbonate were used as solvent.

Eisele *et al*. reported the radical polymerisation of NVCL in benzene using AIBN as the radical initiator, with the found M_n ranging from 3.7×10^4 $gmol^{-1}$ to 6.3×10^5 $gmol^{-1}$.[92] NVCL is only partially soluble in water (approximately 1% NVCL in H_2O),[63] therefore the monomer cannot be polymerised in aqueous solution without the addition of an emulsifying agent[92] or co-solvent.[93] The polymerisation of NVCL has been performed in water in the presence of sodium 1, 2-bis(2-ethylhexyloxycarbonyl)-1-ethanesulphonate as emulsifier and AIBN, $NaHSO_2$ / tert-butyl peroxide or NH_3 / H_2O_2 as the initiating species. The found M_n was observed to range from 2.0×10^4 $gmol^{-1}$ to 2.7×10^5 $gmol^{-1}$ and polydispersity indices were in the range of 3.5 – 4.3.[92]

PNVCL was reported to be synthesised *via* the radiation polymerisation of NVCL, using γ-radiation in aqueous solution.[88] It was shown that using a radiation dose beyond 2.0 kGy and a dose rate range between 2-14 Gy/min produced PNVCL in yields over 90%.

PNVCL is used widely in hair-care and cosmetics products in a terpolymer of PNVCL/PNVP/PDMAEMA (poly(dimethylaminoethylmethacrylate)), to function as a film former / hair-fixative resin.[74] Due to its non-toxic and biocompatible nature, it is also an important polymer in biomedical applications such as in the stabilisation of proteases,[94] controlled drug delivery[95] and drug release.[96] PNVCL is also as an effective material used for gas hydrate inhibition (LUVICAP® EG).[97-99]

The controlled radical polymerisation of NVCL has been achieved using various methods. The most studied controlled radical polymerisation method is RAFT and this is discussed further in Chapter 3. The polymerisation of NVCL has also been performed by ATRP[100] and CMRP.[101]

1.11. Poly(vinyl acetate) (PVAc)

Poly(vinyl acetate) (PVAc) is synthesised *via* the free radical polymerisation of VAc and is an industrially important polymer which is used in water-based paints and adhesives such as wood glue. Ethylene vinyl acetate (EVA) copolymer is used in paper coatings. One of the main uses of PVAc is the modification to poly(vinyl alcohol) (PVA), patented by Herrmann *et al*. in 1924.[102]

The controlled / living radical polymerisation of VAc has been hard to achieve due to the monomer lacking a conjugated system needed to stabilise the propagating radical. This makes the VAc propagating radical reactive and hence increasing the rate of propagation. Therefore, VAc is susceptible to chain transfer and also termination. The first report of controlled / living radical polymerisation of VAc was reported in 1994.[103] Aluminium alkyls of the type R_nAlCl_{3-n} (triisobutylaluminium (TIBA)) complexed with 2, 2 – bipyridine (BIPY) and stable nitroxide radicals (TEMPO), initiated the homo and copolymerisation of VAc. It was thought that addition of TEMPO to TIBA/BIPY improved the control of the polymerisation by the reversible addition of the propagating chain with the aluminium complex, producing a persistent hexa-coordinated aluminium radical as a dormant species. However, a further study on this system, several years later, confirmed that the polymerisation did not follow a controlled / living radical mechanism.[104]

Further attempts to control the radical polymerisation of VAc were conducted using ATRP.[105] CCl_4 was used as the initiating species in the presence of a copper or iron complex. In the presence of copper complexes, no PVAc was produced and in the presence of iron complexes, the polymerisation was not greatly controlled, as the PDI of the polymers produced was in the range of 1.8 - 2.0. It was reported that ATRP was not the polymerisation process involved but that a redox initiated telomerisation of VAc had occurred.**[105]**

Controlled radical polymerisation of VAc by ATRP is problematic, because the carbon – halogen bond of the PVAc dormant chain is not easily broken by ATRP catalysts (K_{act} is low). Therefore, the propagating chain cannot be reactivated for monomer addition. The equilibrium constant K_{eq} (K_{act} / K_{deact}) is very low and the equilibrium lies firmly on the dormant side (Scheme 1.17).[106]

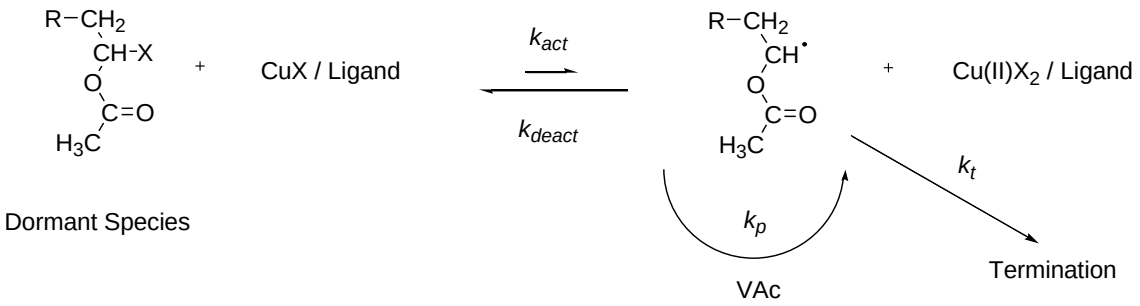

Scheme 1.17. ATRP equilibrium in VAc

Within the last decade great progress has been made in controlling the polymerisation of VAc. RAFT has been found to be the most common method used to control the radical polymerisation of VAc, as it is discussed in Chapter 3. CMRP has also been successful in controlling the polymerisation of VAc.[50, 107, 108]

1.12. Random copolymers incorporating PNVP, PVAc or PNVCL

PNVP-*ran*-PVAc is a commercially available linear random copolymer performed *via* FRP, which is soluble in alcohols, esters and ketones.[109] Industrially prepared random copolymers of PNVP and PVAc have broad polydispersity indices and there is little control over their molecular weight. The solubility of the copolymer in water is dependent on the PNVP content, e.g. soluble when PNVP > 30%. The random copolymer is used in the cosmetic and pharmaceutical industries as well as being an effective adhesive (Plasdone® S-630 copovidone from Ashland).[74, 110-112]

PNVP-*ran*-PNVCL and PNVP-*ran*-PNVCL-*ran*-PDMAEMA are commercially available random copolymers as Inhibex® 501 and Inhibex® 713, from Ashland respectively. Both copolymers are used in the area of gas hydrate inhibition[97, 98, 113-116] and furthermore VC-713® is also used in the cosmetic industry as a film former in hair styling products.[74] Industrially prepared random copolymers of PNVP and PNVCL have broad polydispersity indices and like PNVP-*ran*-PVAc there is little control over the molecular weight.

The reactivity ratios of the monomers play an important role on their compositions within the copolymer chain. This is governed by the steric and electronic properties of the monomers in question. Consequently, both the monomer feed and copolymer composition will drift with conversion. Thus, conventional copolymers are not homogenous in composition, at the molecular level.[60] In RAFT polymerisation all

chains grow throughout the polymerisation and hence have similar compositions, leading to the formation of gradient or tapered copolymers. The composition of the copolymer is captured between the chain ends.[60]

1.13. Size Exclusion Chromatography (SEC) / Gel Permeation Chromatography (GPC)

Size Exclusion Chromatography (SEC) also known as Gel Permeation Chromatography (GPC) is a liquid chromatography (LC) analytical technique used to determine the molecular weight and molecular weight distribution of natural and synthetic polymeric samples. The principle method of separation in SEC is based on the sample molecules hydrodynamic volume (size) in solution.[117] The stationary phase packing in the SEC column is a porous material; typically cross-linked polystyrene beads. The polymer sample is dissolved in the mobile phase and will take a coil conformation, with the size of the coil dependent on the polymers molecular weight. The dissolved polymer molecules are injected into the SEC system and flow through the column at a constant flow rate. If a particular polymer molecule is too large to enter the pores of the stationary phase then it will pass through the column in a shorter elution time in comparison to smaller polymer molecules which can penetrate through the pores. Figure 1.4 shows the mechanism by which SEC works.[118]

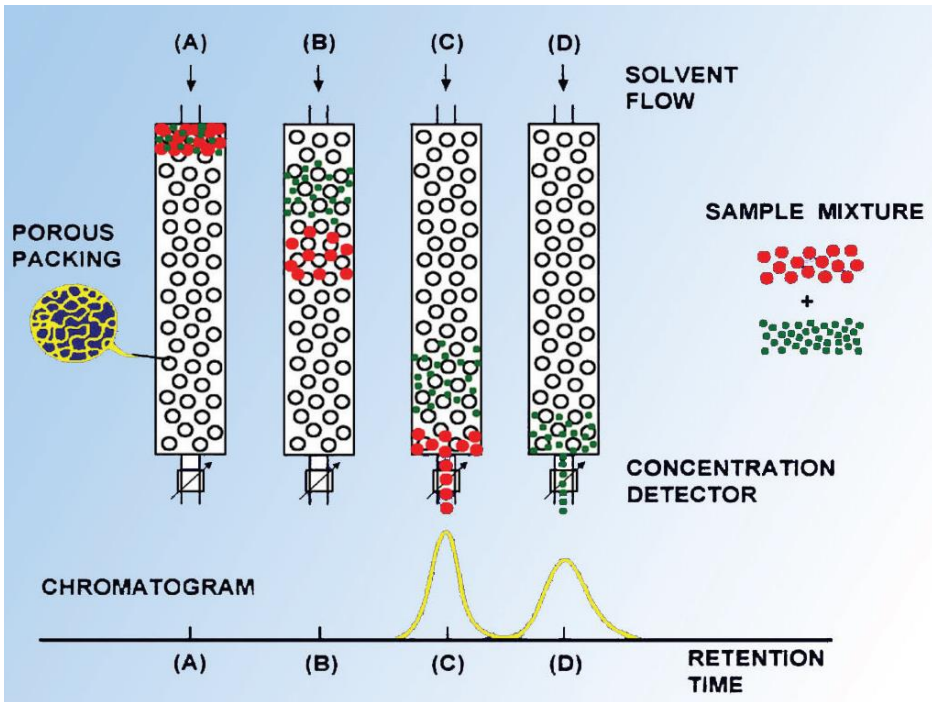

Figure 1.4. Separation mechanism in SEC

Therefore, larger molecules are eluted first and smaller molecules are eluted later. As the sample elutes from the column it is passed through various detectors and analysed using a data processing system. The simplest SEC technique involves using a single concentration detector, normally a differential refractive index detector, where a beam of light is passed through a dual compartment flow cell and its deflection is measured. One side of the compartment contains the reference solvent of refractive index n_0 and the other side contains the polymer sample eluent with refractive index n. The refractive index is proportional to concentration of the polymer solution and is also sample dependent. The sample dependent parameter is called the refractive index increment (dn/dc). General equation for the RI detector is given by:-

$$RI.Signal = \frac{RI.Cal}{n_0} \cdot C \cdot \frac{dn}{dc} \qquad \text{Equation 1.10}$$

Where:

$$\frac{dn}{dc} = \frac{n - n_0}{C} \qquad \text{Equation 1.11}$$

The refractive index detector is a concentration detector and as such can be used to generate a conventional calibration with a number of standards of known molecular weight and low PDI. A calibration curve can be constructed where log (MW) is plotted against elution volume (Figure 1.5).[119]

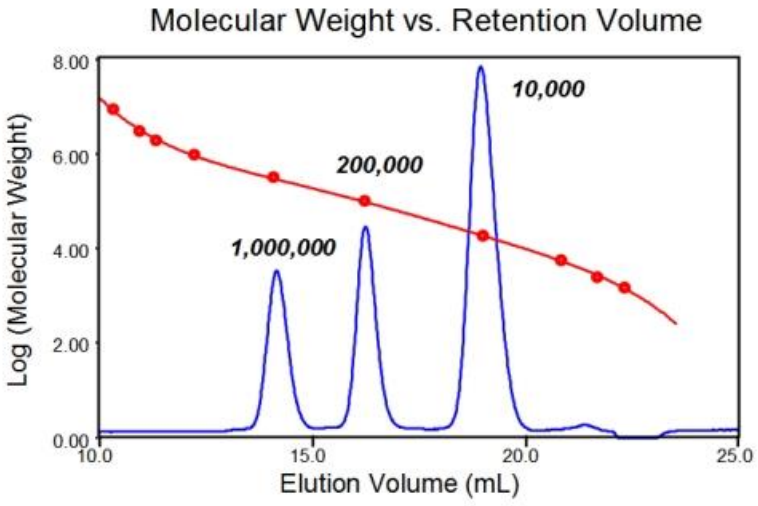

Figure 1.5. Conventional calibration

An unknown sample can then be analysed and it's molecular weight can be determined by relating the retention volume of the unknown sample to the calibration curve (Figure 1.6).[119]

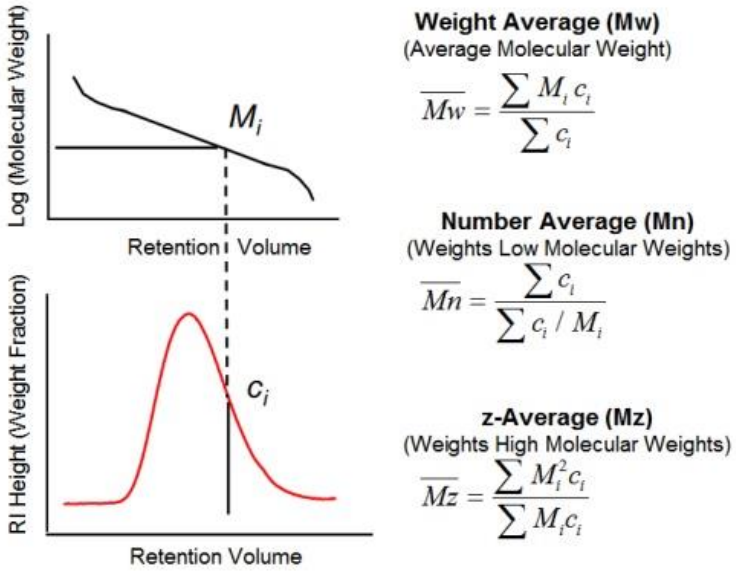

Figure 1.6. Determination of molecular weight using a conventional calibration.

Conventional calibration has severe limitations as the standard used is most likely not the same as the sample. There will be a difference in hydrodynamic volume between the sample and standard, so therefore the molecular weight determined can only be relative to the standard used. Hence, conventional calibration is only a comparative technique. A more accurate method to measure the molecular weight is to construct a calibration curve where the y-axis is proportional to hydrodynamic volume. A viscometer detector enables this to be achieved by measuring the solution viscosity of the sample as it elutes and comparing it to the viscosity of the mobile phase. The viscometer detector measures the intrinsic viscosity $[\eta]$, which can be related to hydrodynamic volume and molecular weight (Equation 1.12).

$$Hydrodynamic\ volume = k\ x\ MW\ x\ [\eta] \qquad \text{Equation 1.12}$$

Where k is a constant. Therefore, plotting log $([\eta]\ x\ MW)$ against retention time is equivalent to plotting log size against retention time and allows a universal calibration to be generated (Figure 1.7).[120]

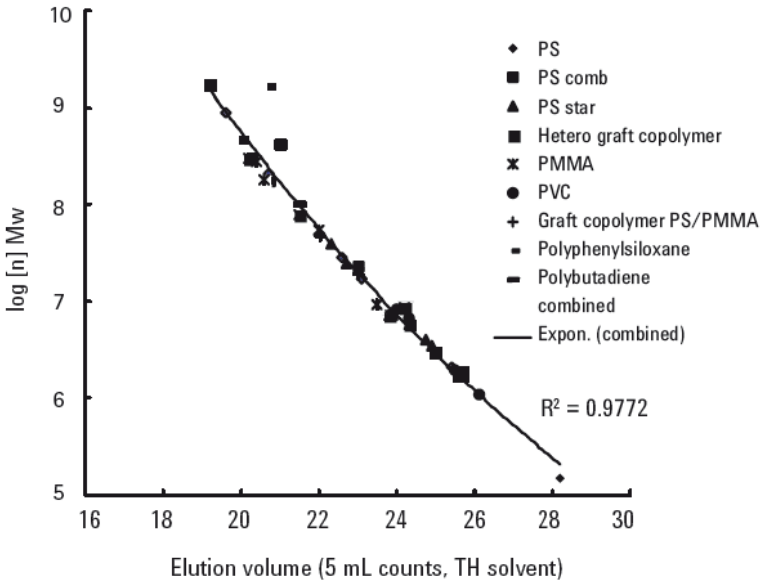

Figure 1.7. Universal calibration for SEC

Molecular weight of the polymer sample can then be determined by taking a the data point and relating it to the universal calibration to get log ($[\eta]\, x\, MW$) (Figure 1.8).[121]

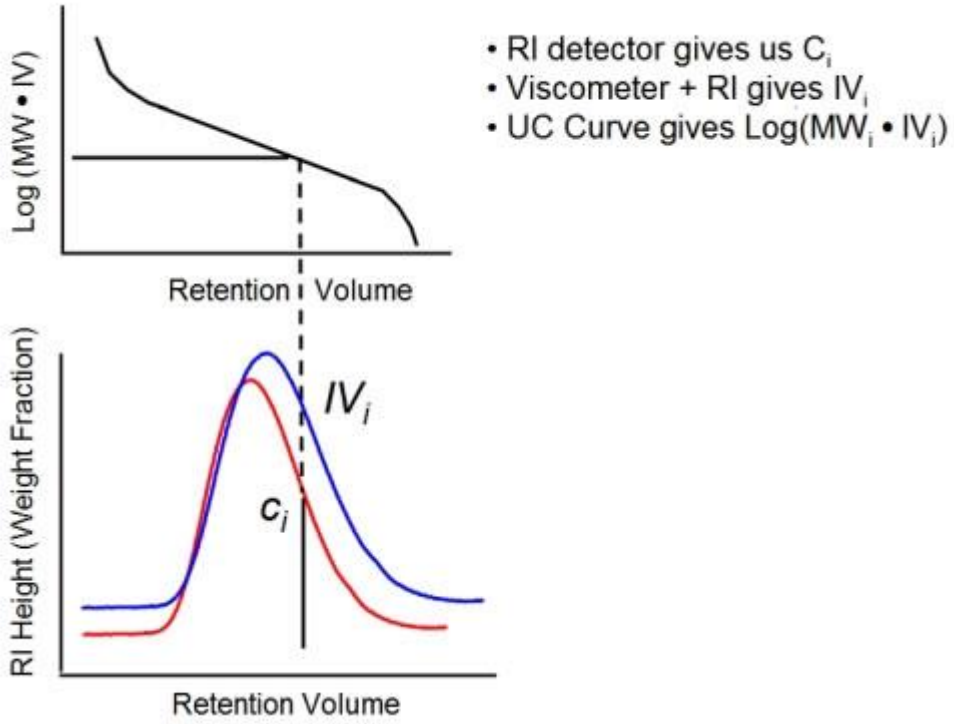

Figure 1.8. Determination of molecular weight using a universal calibration.

Using a viscometer detector on the SEC system also allows a Mark-Houwink plot to be generated. The Mark-Houwink plot is the relationship between molecular weight and intrinsic viscosity:-

$$[\eta] = KM^{\alpha} \qquad \text{Equation 1.13}$$

Where K and α are constants for a given solvent. The latter constant can give information about the dynamic behaviour of the polymer molecules in solution. Rearranging Equation 1.13 into log form gives:-

$$\log[\eta] = \log K + \alpha \log M \qquad \text{Equation 1.14}$$

Plotting logM against log[η] gives a straight line with intercept of logK and slope of α (Figure 1.9).[120]

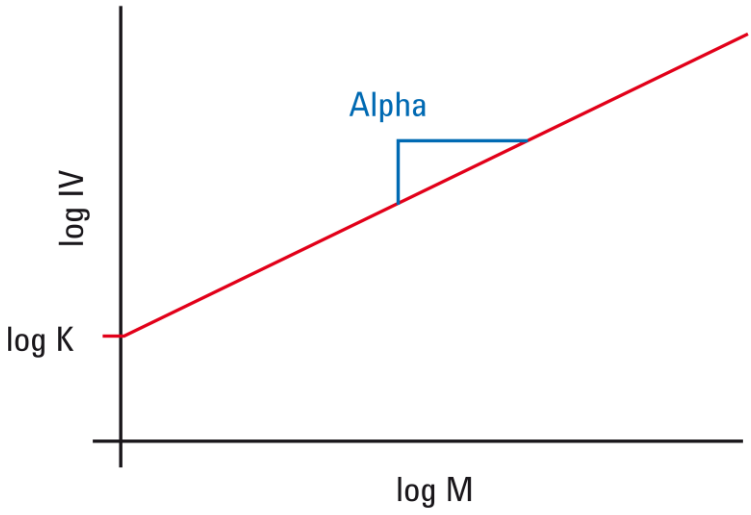

α = <0.5 for 'hard sphere'
α = 0.7 for random coil in good solvent
α = ~2.0 for 'rigid rod'

Figure 1.9. Mark-Houwink plot

A static light scattering detector is also used to determine the absolute molecular weight of a polymer sample. A beam of light interacts with a polymer solution and is scattered at different angles. This is known as Raleigh scattering. The intensity of scattered light (Raleigh ratio - RΘ) is proportional to the molecular weight of the

polymer. The fundamental equation relating to the scattering of light from a polymer solution is given by:-

$$\frac{K^*C}{R_\Theta} = \left(\frac{1}{M_w P_\Theta}\right) + 2A_2C + \Lambda \qquad \text{Equation 1.15}$$

Where C is the polymer solution concentration, M_w is the weight average molecular weight, R_Θ is the excess Rayleigh scattering ratio measured at angle Θ with respect to the incident beam and A_2 is the second virial coefficient. P_Θ is the particle scattering factor and describes the scattered lights angular dependence. K* is an optical constant defined by: -

$$K* = \frac{4\pi^2\ n_0^2(\frac{dn}{dc})^2}{\lambda_0^4 N_A} \qquad \text{Equation 1.16}$$

Under dilute conditions often observed for SEC the virial coefficient can be considered zero and for molecules under 10nm, P_Θ is equal to one. Therefore, Equation 1.15 can be simplified to:-

$$R_\Theta = M_w K * C \qquad \text{Equation 1.17}$$

Where $K^* = (dn/dc)^2K$. By measuring R_Θ using the light scattering detector, and knowing K, dn/dc and C, the weight average molecular weight can be determined. Low molecular weight polymers or those with low dn/dc values in a particular solvent will result in poor light scattering responses.

A limitation is that the intensity of the scattered light may not be equal in all directions. The true intensity can only be obtained at zero angle; however, this is not able to be measured due to being at the same angle as the incident laser beam which has not been scattered by the polymer molecule. At molecular sizes above 10nm there is dissymmetric scattering; there is a reduction in the amount of scattered light at higher angles. A low angle light scattering (LALS) light detector may be used, which can give an accurate result by measuring the scattered light at an angle as close to zero as possible. However, the precision may be affected by the incident beam as well as light scattered by dust particles. An alternative is to use a light scattering detector at an angle of 90°C (right angle light scattering – RALS). This can give a more precise result due

to not being effected by the incident laser beam. However, this method relies on having molecule sizes < 10nm so that the effect of dissymmetry is reduced and the intensity of light is equal in all directions. At large molecule sizes the molecular weight of the polymer sample can be underestimated.

In this study, the method used was triple detection with refractive index (concentration), viscosity and a RALS detector. The refractive index detector is necessary for the determination of both molecular weight and refractive index, the viscometer detector enables the determination on intrinsic viscosity and molecular size, conformation and structure. In triple detection the light scattering detector provides the direct measurement of molecular weight.

1.14. Aims and objectives of the work presented here

Currently Ashland Inc. produces linear random copolymers containing either PNVP, PNVCL or PVAc. The polymeric materials are available in powder form, or in solution; i.e. in polymerisation solvent (water, methanol, ethanol, 2-propanol, 2-butoxyethanol). These copolymers have a wide range of applications including, hair-styling products, tablet-coatings, adhesives, shampoos, paper coatings and gas hydrate inhibitors.

The main aim of this research was to use controlled / living radical polymerisation to synthesise well-defined block copolymers containing PNVP, PNVCL or PVAc with high conversion / yield, using reasonable reaction times and to a high degree of purity. RAFT polymerisation was thought to be the most effective technique to mediate the polymerisation of LAMs and ATRP was avoided, due to concerns over the contamination of copper. In addition, the ATRP of NVP and VAc has been shown to be problematic, due to the deactivation of catalyst (copper) *via* chelation with PNVP and low ATRP equilibrium constants with both monomers. As part of the objectives, novel RAFT agents were to be synthesised with the aim of improving the controlled polymerisation of LAMs. Moreover, the synthesis of polymeric materials with more complex structures containing LAMs was also of great interest, particularly for their temperature responsive behaviour.

1.15. References

1. Matyjaszewski, K., In *Advances in Controlled / Living Radical Polymerization*, Matyjaszewski, K., Ed. ACS: 2003; Vol. 854, p 2.
2. Braun, D. *International Journal of Polymer Science* **2009,** 2009, 1-10.
3. Sandler, S. R.; Karo, W., In *Polymer Syntheses*, 1st ed.; Academic Press: London, 1974; Vol. I, p 3.
4. Braunecker, W. A.; Matyjaszewski, K. *Progress in Polymer Science* **2007,** 32, (1), 93-146.
5. Wang, J. S.; Matyjaszewski, K. *Journal of the American Chemical Society* **1995,** 117, (20), 5614-5615.
6. Young, R. J.; Lovell, P. A., In *Introduction to Polymers*, 3rd ed.; CRC Press: 2011; p 73.
7. Young, R. J.; Lovell, P. A., In *Introduction to Polymers*, 3rd edition ed.; CRC Press: 2011; p 69.
8. Young, R. J.; Lovell, P. A., In *Introduction to Polymers*, 3rd ed.; CRC Press: 2011; p 70.
9. Matyjaszewski, K.; Davis, T. P., In *Handbook of Radical Polymerization*, John Wiley and Sons, Inc.: 2002; p 214.
10. Szwarc, M. *Nature* **1956,** 178, (4543), 1168-1169.
11. Szwarc, M.; Levy, M.; Milkovich, R. *Journal of the American Chemical Society* **1956,** 78, (11), 2656-2657.
12. Kennedy, J. P. *Journal of Polymer Science Part a-Polymer Chemistry* **1999,** 37, (14), 2285-2293.
13. Brunelle, D. J., In *Ring-opening polymerization: mechanisms, catalysis, structure, utility*, Hanser: New York, 1993.
14. Bielawski, C. W.; Grubbs, R. H. *Progress in Polymer Science* **2007,** 32, (1), 1-29.
15. Webster, O. W. *Journal of Polymer Science Part a-Polymer Chemistry* **2000,** 38, (16), 2855-2860.
16. Goto, A.; Fukuda, T. *Progress in Polymer Science* **2004,** 29, (4), 329-385.
17. Greszta, D.; Mardare, D.; Matyjaszewski, K. *Macromolecules* **1994,** 27, (3), 638-644.
18. Matyjaszewski, K.; Davis, T. P., Handbook of Radical Polymerization. John Wiley and Sons, Inc.: 2002; p 364.

19. Matyjaszewski, K. *Current Organic Chemistry* **2002,** 6, (2), 67-82.
20. Kharasch, M. S.; Jensen, E. V.; Urry, W. H. *Science* **1945,** 102, (2640), 128-128.
21. Kharasch, M. S.; Urry, W. H.; Jensen, E. V. *Journal of the American Chemical Society* **1945,** 67, (9), 1626-1626.
22. Pintauer, T.; Matyjaszewski, K. *Chemical Society Reviews* **2008,** 37, (6), 1087-1097.
23. Matyjaszewski, K. *Chemistry-a European Journal* **1999,** 5, (11), 3095-3102.
24. Wang, J. S.; Matyjaszewski, K. *Macromolecules* **1995,** 28, (23), 7901-7910.
25. Kato, M.; Kamigaito, M.; Sawamoto, M.; Higashimura, T. *Macromolecules* **1995,** 28, (5), 1721-1723.
26. Matyjaszewski, K. *Israel Journal of Chemistry* **2012,** 52, (3-4), 206-220.
27. Fischer, H. *Chemical Reviews* **2001,** 101, (12), 3581-3610.
28. Jakubowski, W.; Matyjaszewski, K. *Angewandte Chemie-International Edition* **2006,** 45, (27), 4482-4486.
29. Konkolewicz, D.; Magenau, A. J. D.; Averick, S. E.; Simakova, A.; He, H. K.; Matyjaszewski, K. *Macromolecules* **2012,** 45, (11), 4461-4468.
30. Jakubowski, W.; Min, K.; Matyjaszewski, K. *Macromolecules* **2006,** 39, (1), 39-45.
31. Min, K.; Gao, H. F.; Matyjaszewski, K. *Macromolecules* **2007,** 40, (6), 1789-1791.
32. Zhang, Y. Z.; Wang, Y.; Matyjaszewski, K. *Macromolecules* **2011,** 44, (4), 683-685.
33. Mendonca, P. V.; Serra, A. C.; Coelho, J. F. J.; Popov, A. V.; Guliashvili, T. *European Polymer Journal* **2011,** 47, (7), 1460-1466.
34. Magenau, A. J. D.; Strandwitz, N. C.; Gennaro, A.; Matyjaszewski, K. *Science* **2011,** 332, (6025), 81-84.
35. Matyjaszewski, K. *Macromolecules* **2012,** 45, (10), 4015-4039.
36. Wang, J. S.; Matyjaszewski, K. *Macromolecules* **1995,** 28, (22), 7572-7573.
37. Gromada, J.; Matyjaszewski, K. *Macromolecules* **2001,** 34, (22), 7664-7671.
38. Jakubowski, W.; Matyjaszewski, K. *Macromolecules* **2005,** 38, (10), 4139-4146.
39. Min, K.; Jakubowski, W.; Matyjaszewski, K. *Macromolecular Rapid Communications* **2006,** 27, (8), 594-598.

40. Percec, V.; Guliashvili, T.; Ladislaw, J. S.; Wistrand, A.; Stjerndahl, A.; Sienkowska, M. J.; Monteiro, M. J.; Sahoo, S. *Journal of the American Chemical Society* **2006,** 128, (43), 14156-14165.
41. Rosen, B. M.; Percec, V. *Chemical Reviews* **2009,** 109, (11), 5069-5119.
42. Guliashvili, T.; Percec, V. *Journal of Polymer Science Part a-Polymer Chemistry* **2007,** 45, (9), 1607-1618.
43. Lligadas, G.; Percec, V. *Journal of Polymer Science Part a-Polymer Chemistry* **2007,** 45, (20), 4684-4695.
44. Lligadas, G.; Percec, V. *Journal of Polymer Science Part a-Polymer Chemistry* **2008,** 46, (20), 6880-6895.
45. Solomon, D. H.; Rizzardo, E.; Cacioli, P. US 4581429. 1986.
46. Hawker, C. J.; Bosman, A. W.; Harth, E. *Chemical Reviews* **2001,** 101, (12), 3661-3688.
47. Georges, M. K.; Veregin, R. P. N.; Kazmaier, P. M.; Hamer, G. K. *Macromolecules* **1993,** 26, (11), 2987-2988.
48. Ruehl, J.; Nilsen, A.; Born, S.; Thoniyot, P.; Xu, L.-P.; Chen, S.; Braslau, R. *Polymer* **2007,** 48, (9), 2564-2571.
49. Wayland, B. B.; Poszmik, G.; Mukerjee, S. L.; Fryd, M. *Journal of the American Chemical Society* **1994,** 116, (17), 7943-7944.
50. Debuigne, A.; Poli, R.; Jerome, C.; Jerome, R.; Detrembleur, C. *Progress in Polymer Science* **2009,** 34, (3), 211-239.
51. Moad, G.; Rizzardo, E.; Thang, S. H. *Australian Journal of Chemistry* **2006,** 59, (10), 669-692.
52. Moad, G.; Rizzardo, E.; Thang, S. H. *Australian Journal of Chemistry* **2009,** 62, (11), 1402-1472.
53. Barton, D. H. R.; McCombie, S. W. *Journal of the Chemical Society-Perkin Transactions 1* **1975**, (16), 1574-1585.
54. Zard, S. Z. *Australian Journal of Chemistry* **2006,** 59, (10), 663-668.
55. Barker, P. J.; Beckwith, A. L. J. *Journal of the Chemical Society-Chemical Communications* **1984**, (11), 683-684.
56. Corpart, P.; Charmot, D.; Biadatti, T.; Zard, S. Z.; Michelet, D. WO 98/58974. 1998.
57. Chiefari, J.; Chong, Y. K.; Ercole, F.; Krstina, J.; Jeffery, J.; Le, T. P. T.; Mayadunne, R. T. A.; Meijs, G. F.; Moad, C. L.; Moad, G.; Rizzardo, E.; Thang, S. H. *Macromolecules* **1998,** 31, (16), 5559-5562.

58. Perrier, S.; Takolpuckdee, P. *Journal of Polymer Science Part a-Polymer Chemistry* **2005,** 43, (22), 5347-5393.

59. Moad, G.; Rizzardo, E.; Thang, S. H. *Australian Journal of Chemistry* **2012,** 65, (8), 985-1076.

60. *Handbook of RAFT Polymerization*. Wiley-VCH: 2008.

61. Schuster, C.; Sauerbier, K.; Fikentscher, H. 1943.

62. Fikentscher, H.; Herrle, K. *Modern Plastics* **1945,** 23, 157-163.

63. Kirsh, Y. E., *Water Soluble Poly-N-Vinylamides. Synthesis and Physicochemical Properties*. 1998.

64. Nair, B. *International Journal of Toxicology* **1998,** 17, (4), 95-130.

65. Ravin, H. A.; Seligman, A. M.; Fine, J. *New England Journal of Medicine* **1952,** 247, (24), 921-929.

66. Ko, J. H., Poly(N-vinylpyrrolidone). In *Polymer Data Handbook,* Mark, J. E., Ed. Oxford University Press, Inc.: New York, 1999; p 962.

67. Davies, W. L.; Gloor, W. T. *Journal of Pharmaceutical Sciences* **1972,** 61, (4), 618-622.

68. Lee, J. *Macromolecular Bioscience* **2005,** 5, (11), 1085-1093.

69. Florence, A. T.; Attwood, D., *Physicochemical Principles of Pharmacy*. 4th ed.; Pharmaceutical Press: London, 2006.

70. Williams, P. A., *Handbook of Industrial Water Soluble Polymers*. Blackwell Publishing Ltd.: 2008.

71. Banwell, H. *Dermatology* **2006,** 212, 66-76.

72. Ignatova, M.; Stoilova, O.; Manolova, N.; Markova, N.; Rashkov, I. *Macromolecular Bioscience* **2010,** 10, (8), 944-954.

73. McMurrough, I. *Cerevesia* **1998,** 23, 27-34.

74. *Principles of Polymer Science and Technology in Cosmetics and Personal Care*. Marcel Dekker: New York, 1999; p 570.

75. Haaf, F.; Sanner, A.; Straub, F. *Polymer Journal* **1985,** 17, (1), 143-152.

76. Pound, G.; Aguesse, F.; McLeary, J.; Lange, R.; Klumperman, B. *Macromolecules* **2007,** 40, (25), 8861-8871.

77. Pound, G.; McLeary, J.; McKenzie, J.; Lange, R.; Klumperman, B. *Macromolecules* **2006,** 39, (23), 7796-7797.

78. Baldoli, C.; Oldani, C.; Maiorana, S.; Ferruti, P.; Ranucci, E.; Bencini, M.; Contini, A. *Journal of Polymer Science Part a-Polymer Chemistry* **2008,** 46, (5), 1683-1698.

79. Senogles, E.; Thomas, R. *Journal of Polymer Science Part C-Polymer Symposium* **1975**, (49), 203-210.

80. Senogles, E.; Thomas, R. A. *Journal of Polymer Science Part C-Polymer Letters* **1978,** 16, (11), 555-562.

81. Lu, X.; Gong, S.; Meng, L.; Li, C.; Yang, S.; Zhang, L. *Polymer* **2007,** 48, (10), 2835-2842.

82. Liu, X. L.; Sun, K.; Wu, Z. Q.; Lu, J. H.; Song, B.; Tong, W. F.; Shi, X. J.; Chen, H. *Langmuir* **2012,** 28, (25), 9451-9459.

83. Debuigne, A.; Willet, N.; Jerome, R.; Detrembleur, C. *Macromolecules* **2007,** 40, (20), 7111-7118.

84. Jeon, H. J.; You, Y. C.; Youk, J. H. *Journal of Polymer Science Part a-Polymer Chemistry* **2009,** 47, (12), 3078-3085.

85. Debuigne, A.; Poli, R.; De Winter, J.; Laurent, P.; Gerbaux, P.; Wathelet, J.-P.; Jerome, C.; Detrembleur, C. *Macromolecules* **2010,** 43, (6), 2801-2813.

86. Debuigne, A.; Schoumacher, M.; Willet, N.; Riva, R.; Zhu, X.; Rutten, S.; Jerome, C.; Detrembleur, C. *Chemical Communications* **2011,** 47, (47), 12703-12705.

87. Lau, A. C. W.; Wu, C. *Macromolecules* **1999,** 32, (3), 581-584.

88. Cheng, S. C.; Feng, W.; Pashikin, II; Yuan, L. H.; Deng, H. C.; Zhou, Y. *Radiation Physics and Chemistry* **2002,** 63, (3-6), 517-519.

89. Maeda, Y.; Nakamura, T.; Ikeda, I. *Macromolecules* **2002,** 35, (1), 217-222.

90. Solomon, O. F.; Corciove.M; Boghina, C. *Journal of Applied Polymer Science* **1968,** 12, (8), 1843-1851.

91. Solomon, O. F.; Vasilesc.Ds; Tararesc.V. *Journal of Applied Polymer Science* **1969,** 13, (1), 1-7.

92. Eisele, M.; Burchard, W. *Makromolekulare Chemie-Macromolecular Chemistry and Physics* **1990,** 191, (1), 169-184.

93. Lozinsky, V. I.; Simenel, I. A.; Kurskaya, E. A.; Kulakova, V. K.; Galaev, I. Y.; Mattiasson, B.; Grinberg, V. Y.; Grinberg, N. V.; Khokhlov, A. R. *Polymer* **2000,** 41, (17), 6507-6518.

94. Peng, S. F.; Wu, C. *Macromolecular Symposia* **2000,** 159, (1), 179-186.

95. Markvicheva, E. A.; Tkachuk, N. E.; Kuptsova, S. V.; Dugina, T. N.; Strukova, S. M.; Kirsh, Y. E.; Zubov, V. P.; Rumsh, L. D. *Applied Biochemistry and Biotechnology* **1996,** 61, (1-2), 75-84.

96. Vihola, H.; Laukkanen, A.; Hirvonen, J.; Tenhu, H. *European Journal of Pharmaceutical Sciences* **2002,** 16, (1-2), 69-74.

97. Lederhos, J. P.; Long, J. P.; Sum, A.; Christiansen, R. L.; Sloan, E. D. *Chemical Engineering Science* **1996,** 51, (8), 1221-1229.

98. Del Villano, L.; Kommedal, R.; Fijten, M. W. M.; Schubert, U. S.; Hoogenboom, R.; Kelland, M. A. *Energy & Fuels* **2009,** 23, (7), 3665-3673.

99. Duchateau, C.; Glenat, P.; Pou, T. E.; Hidalgo, M.; Dicharry, C. *Energy & Fuels* **2010,** 24, 616-623.

100. Singh, P.; Srivastava, A.; Kumar, R. *Journal of Polymer Science Part a-Polymer Chemistry* **2012,** 50, (8), 1503-1514.

101. Hurtgen, M.; Liu, J.; Debuigne, A.; Jerome, C.; Detrembleur, C. *Journal of Polymer Science Part a-Polymer Chemistry* **2012,** 50, (2), 400-408.

102. Herrmann, W. O.; Haehnel, W. DRP 450 286. 1924.

103. Mardare, D.; Matyjaszewski, K. *Macromolecules* **1994,** 27, (3), 645-649.

104. Granel, C.; Jerome, R.; Teyssie, P.; Jasieczek, C. B.; Shooter, A. J.; Haddleton, D. M.; Hastings, J. J.; Gigmes, D.; Grimaldi, S.; Tordo, P.; Greszta, D.; Matyjaszewski, K. *Macromolecules* **1998,** 31, (21), 7133-7141.

105. Xia, J. H.; Paik, H. J.; Matyjaszewski, K. *Macromolecules* **1999,** 32, (25), 8310-8314.

106. Tang, H. D.; Radosz, M.; Shen, Y. Q. *Aiche Journal* **2009,** 55, (3), 737-746.

107. Debuigne, A.; Caille, J. R.; Jerome, R. *Angewandte Chemie-International Edition* **2005,** 44, (7), 1101-1104.

108. Debuigne, A.; Caille, J. R.; Jerome, R. *Macromolecules* **2005,** 38, (13), 5452-5458.

109. BASF, PVP and more... LUVITEC, LUVICROSS and COLLACRAL VAL. 2009.

110. Cheng, G. L.; Cullen, J.; Wu, C. S. *Journal of Chromatography A* **2011,** 1218, (2), 237-241.

111. Flick, E. W., *Cosmetics Additives: An Industrial Guide*. Noyes Publications: New Jersey, 1991.

112. Buhler, V., Polyvinylpyrrolidone excipients for the pharmaceutical industry. 9th ed.; BASF, Ed. Ludwigshafen, Germany, 2008.

113. Al-Adel, S.; Dick, J. A. G.; El-Ghafari, R.; Servio, P. *Fluid Phase Equilibria* **2008,** 267, (1), 92-98.

114. Duchateau, C.; Pou, T. E.; Hidalgo, M.; Glenat, P.; Dicharry, C. *Chemical Engineering Science* **2012,** 71, 220-225.

115. Del Villano, L.; Kommedal, R.; Kelland, M. A. *Energy & Fuels* **2008,** 22, (5), 3143-3149.

116. Del Villano, L.; Kelland, M. A. *Chemical Engineering Science* **2011,** 66, (9), 1973-1985.

117. An Introduction to Gel Permeation Chromatography and Size Exclusion Chromatography. Agilent Technologies: 2011.

118. Complete Guide for GPC / SEC / GFC Instrumentation and Detection Technologies. Viscotek: 2006.

119. Malvern GPC/SEC Theory: Conventional Calibration. http://www.malvern.com/labeng/technology/gel_permeation_chromatography_theory/conventional_calibration_gpc_theory.htm

120. A guide to multi-detector gel permeation chromatography. Agilent Technologies: 2012.

121. Malvern GPC / SEC Theory: Universal Calibration. http://www.malvern.com/labeng/technology/gel_permeation_chromatography_theory/universal_calibration_gpc_theo

Chapter 2
Synthesis and characterisation of RAFT agents

2.1. Introduction

The work in this chapter focuses on the synthesis of RAFT agents with the ability of controlling the polymerisation of "less activated" monomers (LAMs). Initially, RAFT agents which were already known in the literature, were synthesised to evaluate their ability to control the polymerisation of LAMs. The study then moved to making RAFT agents which have a novel element within their structures. RAFT agents that are able to give more complex structures; such as stars, have also been synthesised in order to produce novel (co)polymer products.

RAFT agents made during the course of this study have been based around a central xanthate or dithiocarbamate core. These classes of RAFT agent have been found to be the most useful in controlling the polymerisation of LAMs such as N-vinylpyrrolidone (NVP) and vinyl acetate (VAc). Xanthates (dithiocarbonates) are compounds which possess a thiocarbonylthio centre where the Z-group is an alkoxy (Figure 2.1 A). Dithiocarbamates have a similar structure to xanthates, however the alkoxy group is replaced with an amine group (Figure 2.1 B).

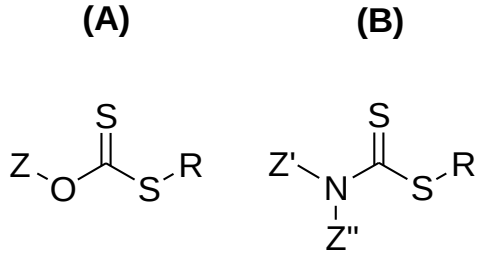

Figure 2.1. (A) xanthate, (B) dithiocarbamate

Xanthates have been widely studied in the area of radical reactions, in particular organic synthesis with its origins dating back to 1975 and the Barton-McCombie deoxygenation reaction of secondary alcohols with tributylstannane.[1] The ability of non-activated alkenes to take part in intermolecular C-C bond formation is relatively remote. The rate of addition to non-activated alkenes is too low compared with other competitive pathways. The addition of a xanthate to an alkene under radical conditions can help overcome this problem as it forces a degenerate process to give the desired product (Scheme 2.1).[2, 3]

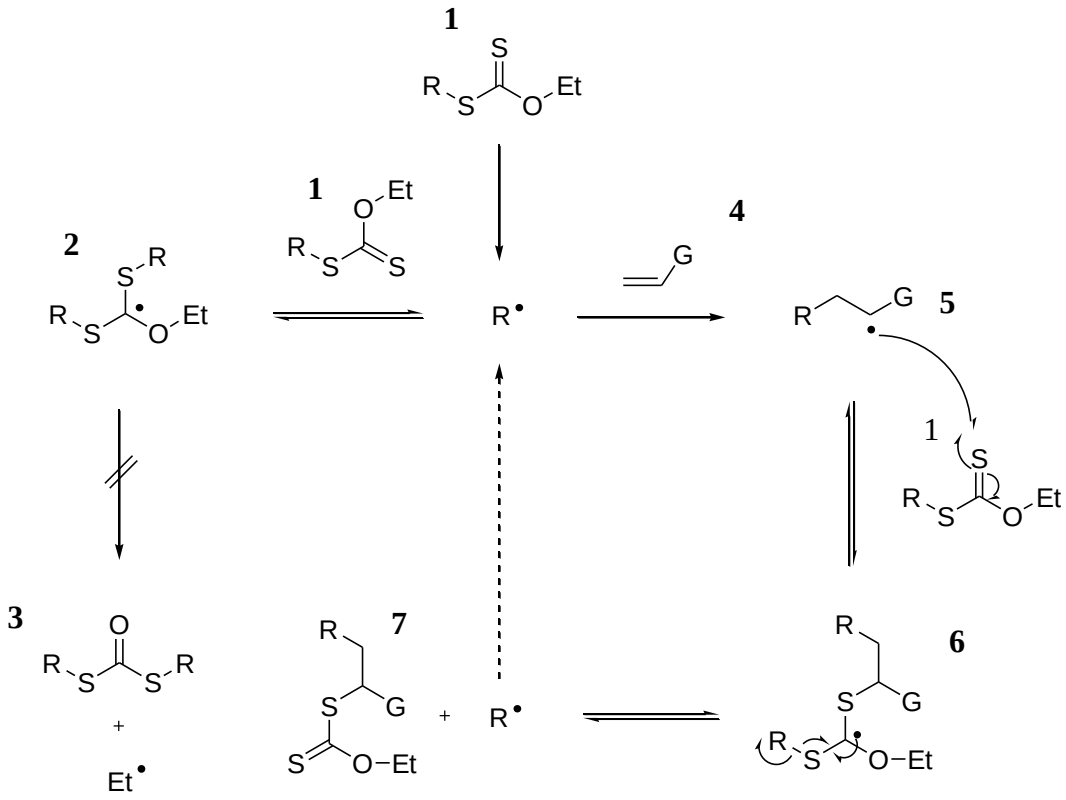

Scheme 2.1. Radical addition of a xanthate to an alkene

Initiation occurs by the fragmentation of xanthate **1** to give the radical species R•. This then reacts with another xanthate **1** to give the radical intermediate **2**. At this point, the intermediate has the possibility of fragmenting either to give an ethyl radical and a symmetrical dithiocarbonate (**3**) or return to the original xanthate **1** and R•. In reality, the O-Et bond is very strong and would generate a high energy ethyl radical, therefore the reformation of the starting xanthate **1** is preferred. This is the key reversible and degenerate step. Addition of an alkene **4** gives the product **5**. This is then able to reversibly react with the starting xanthate **1** to give the radical intermediate **6**. Like the radical intermediate **2**, **6** fragments to give the final desired product **7** and reproduce R•, which is free to react further with alkene. Using this mechanism even non-activated alkenes can be involved in the radical addition to xanthates in high yields to give the final adduct. Mild reactions conditions can be used and numerous functional groups on the alkene can be tolerated. When a vinylic monomer is used, the mechanism is effectively the RAFT or more appropriately MADIX (Macromolecular Design *via* Interchange of Xanthate) mechanism.

Within the structure of the RAFT agent, the non-bonded electron pair on the heteroatom for xanthates (oxygen atom) and dithiocarbamates (nitrogen atom) is delocalised with the C=S double bond (Figure 2.2). This reduces the reactivity of the

C=S bond towards radical addition. For "more activated" monomers (MAMs), this means that the rate of addition of the propagating radical on the sulphur atom is decreased. Therefore, this leads to poor control over the molecular weight and polydispersity of the resulting polymer. However, the propagating radicals of LAMs are highly reactive and readily add to the C=S double bond of a xanthate or dithiocarbamate. This is because of the destabilisation of the intermediate radical, in both the pre-equilibrium and main equilibrium. The fragmentation rates of these radical intermediates are much faster than more reactive RAFT agents, such as dithioesters, due to the delocalisation of the C=S (O or N).

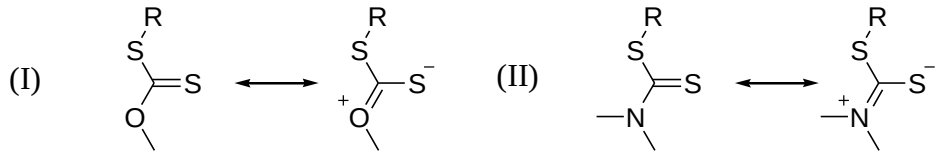

Figure 2.2. Delocalisation of (I) xanthate and (II) dithiocarbamate groups[3]

In the literature, there are several main methodologies in which xanthate RAFT agents have been synthesised[4]: -

i) Free radical pathway - free radical initiators (AIBN) can be reacted with a xanthogen disulphide to give tertiary R leaving groups.[5]

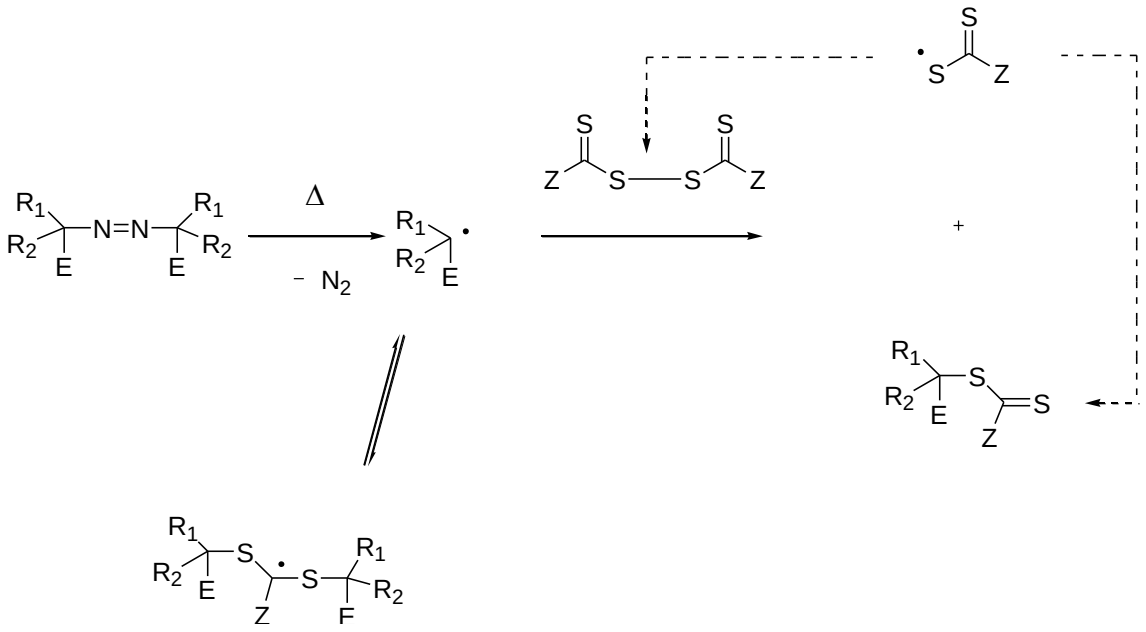

Scheme 2.2. Reaction of radicals with bis(thioacyl) disulphides

ii) TCDI (1,1-thiocarbonyl diimidazole) can be reacted with primary or secondary alcohols (thiols or amines) to give a wide range of RAFT agents.[6]

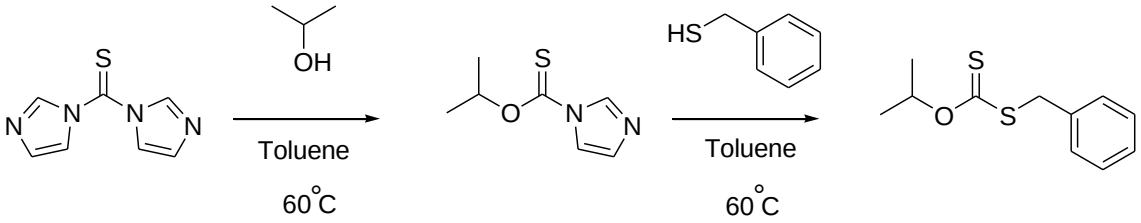

Scheme 2.3. Synthesis of xanthate from 1,1-thiocarbonyl diimidazole

iii) Carbon disulphide can be reacted with an alkoxide, followed by the addition of an alkyl halide.[7]

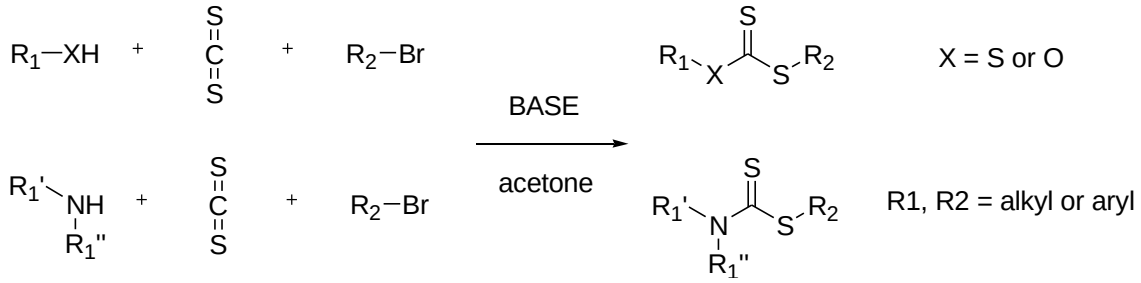

Scheme 2.4. Synthesis of RAFT agents using carbodithioate salts

The methodology that we used was based on the reaction of a carbodithioate salt with an alkylating agent (iii). RAFT agents based on xanthates take advantage from the commercially available and cheap carbodithioate salt - potassium *O*-ethyl xanthate. Alternative alkyl and aryl groups can replace the ethyl group attached to the oxygen atom (Z group). However, it needs to be able to generate a radical which is less stable than that of R• (Scheme 2.1). The same radical addition fragmentation mechanism applies for dithiocarbamates. The only requirements are that the substituents on the nitrogen atom are electron withdrawing. Potassium *O*-ethyl xanthate can be reacted with primary or secondary alkyl halides in a nucleophilic substitution reaction to give RAFT agents. Many ATRP initiators can be viewed as precursors for xanthate RAFT agents. We have utilised this method for the majority of the RAFT agents prepared in this study. The remaining RAFT agents have been prepared by synthesising the carbodithioate salt *in situ* then reacting further with an alkyl / aryl halide.

This chapter describes the synthesis of a number of RAFT agents in order to mediate the (co)polymerisation of LAMs (Figure 2.3). RAFT agents 1-3 were prepared

in accordance with literature methods. Several novel RAFT agents (RAFT 4-7) were prepared incorporating a pyrrolidone ring in both the R and Z groups of the CTA. Novel RAFT agents 4 – 6 incorporate the pyrrolidone ring as part of their R group, fragmenting from the CTA to give primary, secondary or tertiary radicals, respectively. Novel RAFT agent 7 incorporates the pyrrolidone ring as part of the Z group, fragmenting to give a secondary radical. The addition of a pyrrolidone ring at the chain end is anticipated to increase the homogeneity of NVP homopolymer. RAFT agent 8 (Cyanomethyl methyl(phenyl)carbamodithioate) was purchased from Sigma Aldrich and will not be discussed in this chapter. RAFT agents 9 – 11 were designed to control the polymerization of LAMs and to produce well defined star-like polymeric materials, with 3 (RAFT agent 9) and 4 (RAFT agents 10 – 11) armed architectures, respectively.

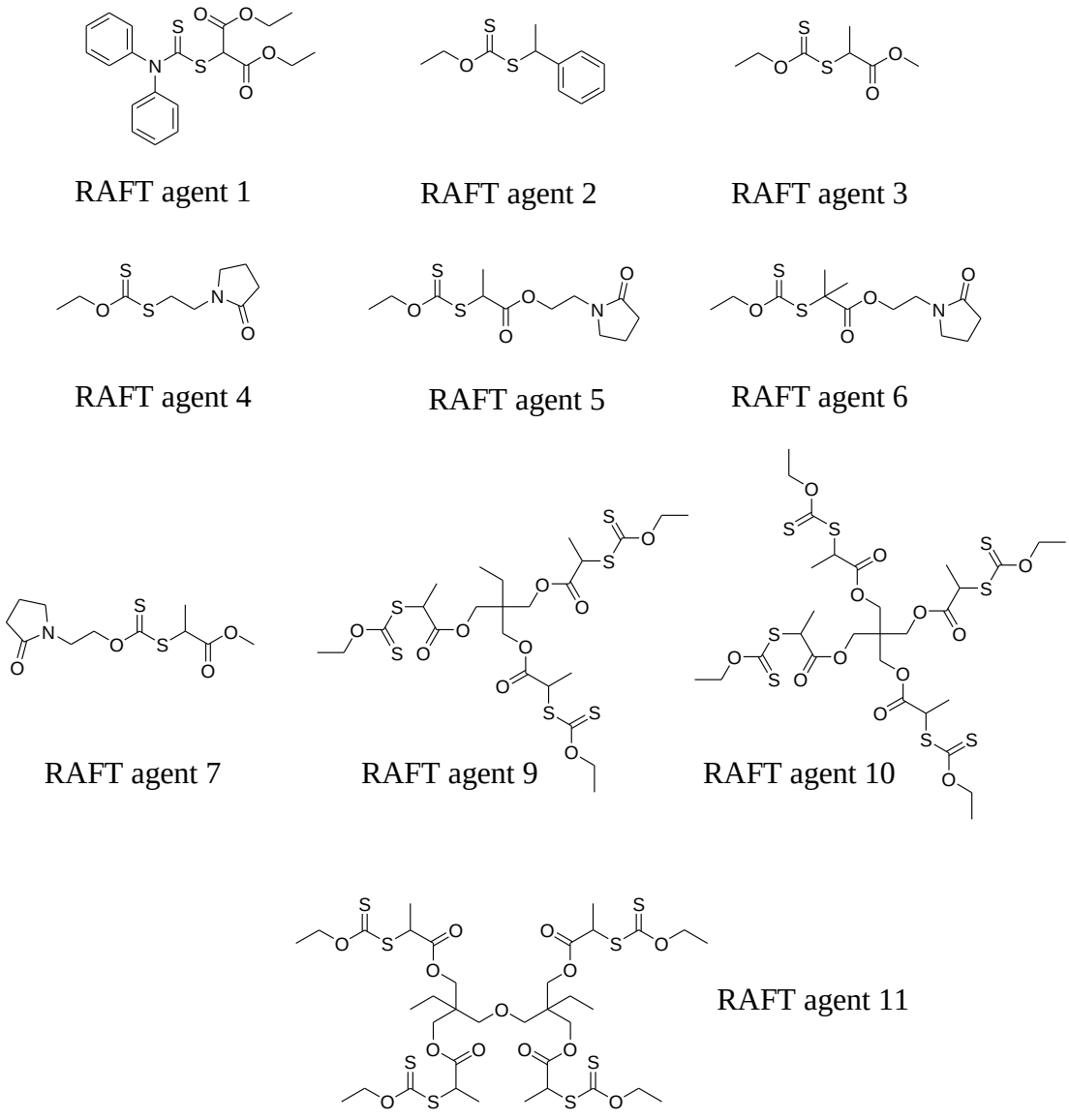

Figure 2.3. RAFT agents 1 – 11

2.2. Experimental

2.2.1. Materials

Potassium *O*-ethyl xanthate (96%), anhydrous magnesium sulphate, triethylamine (≥ 99.5%), 2-bromopropionyl bromide (97%), α-bromoisobutyryl bromide (98%), potassium phosphate tribasic (≥ 98%), carbon disulphide (99.9%), and methyl 2-bromopropionate (98%), 1,1,1-tris(hydroxymethyl)propane (98%), di(trimethylolpropane) (≥ 97.0%), pyridine (≥ 99.0%), sodium hydride (60% dispersion in mineral oil), diphenylamine (99.9%), 1-bromoethylbenzene (97%) phosphorus tribromide (99%) and pentaerythritol (98%) were purchased from Sigma Aldrich and used as received. N-hydroxyethylpyrrolidone supplied from ISP. All dry solvents were obtained from Durham University's Solvent Purification System (SPS) - Purification grade (HPLC) solvent was pushed from its storage container under low argon pressure through two stainless steel columns containing activated alumina or copper catalyst; depending on solvent used. Trace amounts of water were removed by the alumina, producing a dry solvent. In addition, deoxygenated solvent was achieved when it was suitable for a copper catalyst column to be used. Water content values - DCM < 25.1ppm, DMF < 735.1ppm, Toluene < 21.3ppm, THF < 35.7 ppm, Chloroform < 20.9ppm, Diethyl ether < 19.1ppm, Hexane < 7.6 ppm and Acetonitrile < 8.7ppm. All other solvents were analytical grade and used without any purification.

2.2.2. Characterisation Techniques

Nuclear Magnetic Resonance (NMR) Spectroscopy – ^{1}H NMR and ^{13}C NMR were performed on a Bruker Avance-400MHz, Varian iNova-500, 600 or VNMRS 700. ^{1}H NMR spectra were recorded at either 400, 500, 600 or 700 MHz. ^{13}C NMR spectra were recorded at either 101, 126, 151 or 176 MHz. Samples of RAFT / MADIX agents were analysed in deuterated chloroform ($CDCl_3$ - Sigma-Aldrich) or DCM (CD_2Cl_2 – Goss Scientific). The following abbreviations are used in listing NMR spectra: s = singlet, d = doublet, t = triplet, q = quartet, quin = quintet, m = multiplet, b = broad.

Infrared spectroscopy was performed on a PerkinElmer 1600 series FT-IR using an ATR accessory.

Low resolution MS were recorded using a Micromass LCT ToF- all recorded as ES^{+}.

2.2.3. Synthesis of RAFT agent 1 (Diphenyldithiocarbamate of Diethylmalonate (DPCM))

Sodium hydride (60% in mineral oil) (0.473 g, 11.8 mmol), was added to a 100 ml two-necked round bottomed flask fitted with a suba-seal, reflux condenser with nitrogen inlet and a magnetic stirrer bar. The flask was purged with nitrogen for 1 h and dry tetrahydrofuran (6 ml) was added to the flask *via* a syringe. The reaction mixture was cooled to 0°C using an ice bath. Diphenylamine (2.00 g, 11.8 mmol) in dimethyl sulfoxide (18 ml) was purged with nitrogen for 10 min, and was added *via* a syringe into reaction flask. A colour change from off-white to light green was observed. The reaction mixture was stirred for 1.5 h. Carbon disulphide (1.08 g, 14.2 mmol) was injected into the reaction flask giving a yellow colour and the mixture was stirred at 0°C for a further 30 min. Diethylchloromalonate (1.91 ml, 11.8 mmol) was added *via* a syringe and the reaction mixture was allowed to rise to ambient temperature. The reaction flask was placed into an oil bath and heated to gentle reflux (90°C) for 1.5 h. Reaction mixture was then allowed to cool to ambient temperature and deionised water (5 ml) was injected into the flask. Reaction mixture was then transferred to a separating funnel and deionised water (150 ml) was added. The reaction mixture was extracted with diethyl ether (100 ml x 3). Organic layer dried over $MgSO_4$, filtered and the solvent was removed using rotary evaporator. The oil residue was dried under reduced pressure to give 3.93 g of crude product. Crude product was purified through column chromatography (SiO_2) using toluene as the eluent to give RAFT agent 1, (3.07 g, 7.62 mmol 64 % yield). $C_{20}H_{21}NO_4S_2$ (403.09). ^{1}H NMR (400MHz, $CDCl_3$, δ, ppm: 1.30 (t, 6H, *J* = 7.1Hz, $CH_2C\boldsymbol{H}_3$), 4.25 (q, 4H, *J* = 7.1Hz, $C\boldsymbol{H}_2CH_3$), 5.76 (s, 1H, C***H***), 7.14-7.48 (m, 10H, Ar***H***). ^{13}C NMR (101MHz, $CDCl_3$, δ, ppm): 13.8 ($CH_2\boldsymbol{C}H_3$), 59.4 (***C***H), 62.6 ($\boldsymbol{C}H_2CH_3$), 125.5-129.8 (***Ar***H), 165.7 (***C***=O), 197.8 (***C***=S). MS: *m/z* ES$^+$, M + H$^+$ = 404.2, M + Na$^+$ = 426.2.

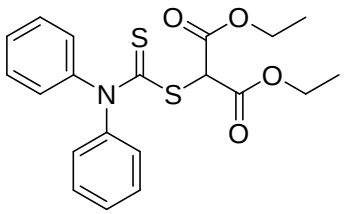

Figure 2.4. Structure of RAFT agent 1

2.2.4. Synthesis of RAFT agent 2 ([1-(*O*-ethylxanthyl)ethyl]benzene)

1-bromoethylbenzene (8.00 ml, 58.6 mmol), was added to ethanol (100 ml) in a 250 ml two-necked round-bottomed flask fitted with a suba-seal, nitrogen gas inlet and a magnetic stirrer bar. The flask was purged with nitrogen for 1 h and the reaction mixture was cooled to 0°C using an ice bath. Potassium *O*-ethyl xanthate (10.4 g, 64.7 mmol) was added to reaction mixture. A colour change from colourless to yellow was observed. The flask was covered with tin foil and the reaction mixture was left to stir at 0°C for 4.5 h under a flow of nitrogen. Reaction mixture was then transferred to a separating funnel and deionised water (100 ml) was added. The reaction mixture was extracted with pentane / diethyl ether (200 ml / 100 ml). Organic layer dried over $MgSO_4$, filtered and the solvent was removed using rotary evaporator. Crude product was purified by removal of starting materials by distillation to give yellow oil of RAFT agent 2, (8.90 g, 39.4 mmol, 67% yield). $C_{11}H_{14}OS_2$ (226.05). ^{1}H NMR (400MHz, $CDCl_3$, δ, ppm): 1.26 (t, 3H, *J* = 7.1Hz, C***H***$_3$CH$_2$), 1.61 (d, 3H, J = 7.2Hz, C***H***$_3$CH), 4.50 (q, 2H, *J* = 7.1Hz, CH$_3$C***H***$_2$), 4.79 (q, 1H, *J* = 7.2Hz, C***H***CH$_3$), 7.1-7.4 (m, 5H, Ar***H***). ^{13}C NMR (126MHz, $CDCl_3$, δ, ppm): 13.6 (CH$_2$***C***H$_3$), 21.6 (CH***C***H$_3$), 49.1 (***C***HCH$_3$), 69.6 (***C***H$_2$CH$_3$), 127.4-128.5 (***Ar***H), 141.6 (CH$_3$CHAr***C***), 213.2 (***C***=S). IR (cm-1): 1490.71, 1449.31, 1207.12, 1144.15, 1108.98, 1039.60, 763.05, 695.69. MS: *m/z* ES$^+$, M + H$^+$ = 227.096.

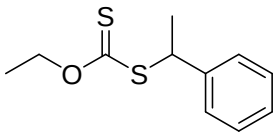

Figure 2.5. Structure of RAFT agent 2

2.2.5. Synthesis of RAFT agent 3 (*O*-ethyl-*S*-(1-ethyoxycarbonyl)ethyl dithiocarbonate)

Methyl 2-bromopropionate (6.80 ml, 61.4 mmol), was added to ethanol (100 ml) in a 250 ml two-necked round bottomed flask fitted with a suba-seal, nitrogen gas inlet and magnetic stirrer bar. The flask was purged with nitrogen for 0.5 h and the reaction mixture was cooled to 0°C using an ice bath. Potassium *O*-ethyl xanthate (10.8 g, 67.4 mmol) was added to the reaction mixture. The reaction mixture immediately turned cloudy and yellow. The flask was covered in tin foil and the reaction mixture was left

to stir at 0°C for 5 h under a flow of nitrogen. Reaction mixture was then transferred to a separating funnel and deionised water (100 ml) was added. The reaction mixture was extracted with pentane / diethyl ether (200 ml / 100 ml). Organic layer dried over $MgSO_4$, filtered and the solvent was removed using rotary evaporator to give a yellow oil of RAFT agent 3, (12.1 g, 58.1 mmol, 95% yield). $C_7H_{12}O_3S_2$ (208.02). ^{1}H NMR (400MHz, $CDCl_3$, δ, ppm): 1.39 (t, 3H, *J* = 7.1Hz, C***H***$_3$CH$_2$), 1.54 (d, 3H, *J* = 7.4Hz, C***H***$_3$CH), 3.73 (s, 3H, C***H***$_3$O), 4.37 (q, 1H, *J* = 7.4Hz, CH$_3$C***H***), 4.63 (qd, 2H, *J* = 1.7Hz, 7.1Hz, CH$_3$C***H***$_2$). ^{13}C NMR (101MHz, $CDCl_3$, δ, ppm): 13.7 (***C***H$_3$CH$_2$). 16.9 (***C***H$_3$CH), 47.0 (CH$_3$***C***H), 52.8 (***C***H$_3$O), 70.3 (CH$_3$***C***H$_2$), 171.9 (***C***=O), 212.0 (***C***=S). IR (cm^{-1}): 1735.98, 1450.93, 1318.90, 1211.04, 1163.03, 1110.35, 1039.05, 856.18. MS: *m/z* ES^+, M + Na^+ = 231.009.

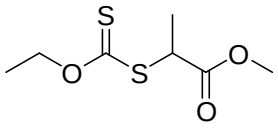

Figure 2.6. Structure of RAFT agent 3

2.2.6. Synthesis of N-bromoethylpyrrolidone

N-hydroxyethylpyrrolidone (12.9 g, 100 mmol), was added to a 100 ml multi-necked round bottomed flask fitted with a reflux condenser, nitrogen gas inlet and a magnetic stirrer bar. The flask was purged with nitrogen for 0.5 h. Dry toluene (20 ml) was added to the flask and the reaction mixture was cooled to 0°C using an ice bath. Phosphorus tribromide (9.10 g, 33.6 mmol) was added slowly drop-wise to the cooled mixture. After the addition of phosphorus tribromide the flask was removed from the ice bath and placed in an oil bath which was heated to 40°C. The reaction mixture was stirred at 40°C for 21 h under a flow of nitrogen. The reaction mixture was seen to become a viscous yellow gel. The solvent was decanted from reaction mixture and the residue was distilled (90-100^{0}C, 0.08 torr). A viscous colourless clear liquid product was collected of N-bromoethylpyrrolidone, (14.4 g, 75.2 mmol, 75% yield). $C_6H_{10}BrNO$ (190.99). ^{1}H NMR (400MHz, $CDCl_3$, δ, ppm): 2.09 (quin, 2H, *J* = 6.4 Hz, CH$_2$C***H***$_2$CH$_2$), 2.61 (t, 2H, *J* = 8.2Hz, CH$_2$C***H***$_2$C=O), 3.48 (t, 2H, *J* = 6.3Hz, BrC***H***$_2$), 3.59 (t, 2H, *J* = 7.2Hz, CH$_2$CH$_2$C***H***$_2$N), 3.73 (t, 2H, *J* = 6.3Hz, C***H***$_2$CH$_2$Br). ^{13}C NMR (126MHz, $CDCl_3$, δ, ppm): 18.3 (CH$_2$***C***H$_2$CH$_2$), 28.5 (Br***C***H$_2$), 31.1 (CH$_2$***C***H$_2$C=O), 45.4 (BrCH$_2$***C***H$_2$), 49.2 (CH$_2$CH$_2$***C***H$_2$N), 177.5 (***C***=O).

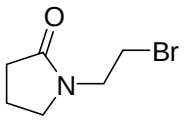

Figure 2.7. Structure of N-bromoethylpyrrolidone

2.2.7. Synthesis of RAFT agent 4 (*O*-ethyl *S*-(2-(2-oxopyrrolidin-1-yl)ethyl) carbonodithioate)

N-bromoethylpyrrolidone (10.0 g, 52.1 mmol), was added to a 250 ml multi-necked round bottomed flask fitted with a reflux condenser, nitrogen gas inlet and magnetic stirrer bar. The flask was purged with nitrogen for 0.5 h and dry tetrahydrofuran (100 ml) was added to flask *via* a syringe. The reaction mixture was cooled to 0°C using an ice bath. Potassium *O*-ethyl xanthate (9.30 g, 58.0 mmol) was added portion-wise to the reaction mixture which was left to stir for 12 h at ambient temperature. Solvent was removed using rotary evaporator to give a bright yellow residue. Dichloromethane (100 ml) was added to dissolve the residue and reaction mixture was washed with deionised water (3 x 50 ml). Organic layer was dried over $MgSO_4$, filtered and solvent removed by rotary evaporator to give a bright yellow / green clear viscous gel of RAFT agent 4, (10.2 g, 43.9 mmol, 84% yield). $C_9H_{15}NO_2S_2$ (233.05). ^{1}H NMR (400MHz, $CDCl_3$, δ, ppm): 1.38 (t, 3H, *J* = 7.1Hz, $OCH_2C\boldsymbol{H}_3$), 1.99 (quin, 2H, *J* = 6.4 Hz, $CH_2C\boldsymbol{H}_2CH_2$), 2.32 (t, 2H, *J* = 8.1Hz, $CH_2C\boldsymbol{H}_2C{=}O$), 3.26 (t, 2H, *J* = 7.1Hz, $SC\boldsymbol{H}_2$), 3.45 (t, 2H, *J* = 8.0Hz, $CH_2CH_2C\boldsymbol{H}_2N$), 3.51 (t, 2H, *J* = 8.0Hz, $SCH_2C\boldsymbol{H}_2N$), 4.60 (q, 2H, *J* = 7.1Hz, $C\boldsymbol{H}_2CH_3$). ^{13}C NMR (126MHz, $CDCl_3$, δ, ppm): 13.9 ($OCH_2\boldsymbol{C}H_3$), 18.2 ($CH_2\boldsymbol{C}H_2CH_2$), 30.9 ($CH_2\boldsymbol{C}H_2C{=}O$), 33.2 ($S\boldsymbol{C}H_2$), 41.3 ($SCH_2\boldsymbol{C}H_2N$), 47.9 ($CH_2CH_2\boldsymbol{C}H_2N$), 70.4 ($\boldsymbol{C}H_2CH_3$), 175.3 (**C**=O), 214.2 (***C***=S). IR (cm^{-1}): 1681.24, 1421.27, 1286.13, 1206.56, 1048.64. MS: *m/z* ES^+, $M + H^+ = 234.2$, $M + Na^+ = 256.2$.

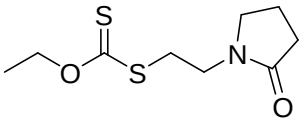

Figure 2.8. Structure of RAFT agent 4

2.2.8. Synthesis of RAFT agent 5 (2-(2-oxopyrrolidin-1-yl)ethyl 2-(ethoxycarbonothioylthio)propanoate)

2-(2-oxopyrrolidin-1-yl)ethyl 2-bromopropanoate. N-hydroxyethylpyrrolidone (15.0 g, 116 mmol), was dissolved in dry tetrahydrofuran (100 ml) and triethylamine (13.0 g, 129 mmol) in a 250 ml multi-necked flask fitted with a reflux condenser, N_2 inlet, magnetic stirrer bar and a pressure equalising dropping funnel. The flask was purged with nitrogen for 1 h and the reaction mixture was cooled to 0°C using an ice bath. 2-Bromopropionyl bromide (25.0 g, 116 mmol) in dry tetrahydrofuran (20 ml), was added drop-wise to the reaction mixture *via* the pressure equalising dropping funnel over a period of 30 mins. The reaction mixture was stirred at 0ºC for 5 h, then at ambient temperature for 20 h under a flow of nitrogen. The white suspension that formed was filtered through Celite and solvent was removed using rotary evaporator. The residue was dissolved in ethyl acetate (50 ml) and washed with deionised water (3 x 100ml). Organic layer dried over $MgSO_4$ and solvent removed under reduced pressure give a dark brown liquid (17.1 g, 64.6 mmol, 57% yield). Un-purified product used as the precursor for next step.

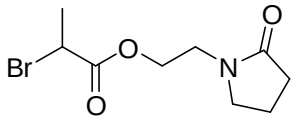

Figure 2.9. Structure of 2-(2-oxopyrrolidin-1-yl)ethyl 2-bromopropanoate

(2-(2-oxopyrrolidin-1-yl)ethyl 2-(ethoxycarbonothioylthio)propanoate). 2-(2-oxopyrrolidin-1-yl)ethyl 2-bromopropanoate (5.00 g, 18.9 mmol), was dissolved in dry acetonitrile (50 ml) in a 100 ml multi-necked flask fitted with a reflux condenser, N_2 inlet and magnetic stirrer bar. The flask was purged with nitrogen for 1 h and the reaction mixture was cooled to 0°C using an ice bath. Potassium *O*-ethyl xanthate (3.12 g, 19.5 mmol) was added to the reaction mixture over a period of 30 minutes. The reaction mixture stirred at 0ºC for 4 h then at ambient temperature for 48 h. The yellow suspension that formed was filtered and solvent was removed under reduced pressure. The residue was dissolved in ethyl acetate (50 ml) and washed with deionised water (3 x 50 ml). Organic layer dried over $MgSO_4$ and solvent removed under reduced pressure. Product purified by column chromatography (alumina, ethyl acetate 50:50 hexane) to give a viscous lime coloured oil of RAFT agent 5, (3.24 g, 10.6 mmol, 56% yield).

$C_{12}H_{19}NO_4S_2$ (305.08). ^{1}H NMR (400MHz, $CDCl_3$, δ, ppm) 4.58 (q, 2H, *J* = 7.2 Hz, C***H***$_2$CH$_3$), 4.33 (q, 1H, *J* = 7.6 Hz, C***H***CH$_3$), 4.23 (t, 2H, *J* = 5.6 Hz, OC***H***$_2$CH$_2$N), 3.51 (t, 2H, *J* = 5.6 Hz, OCH$_2$C***H***$_2$N), 3.43 (t, 2H, *J* = 7.6 Hz, NC***H***$_2$CH$_2$CH$_2$), 2.32 (t, 2H, *J* = 7.6 Hz, CH$_2$CH$_2$C***H***$_2$C=O), 1.98 (quin, 2H, *J* = 7.6 Hz, CH$_2$C***H***$_2$CH$_2$), 1.52 (d, 3H, *J* = 7.6 Hz, CHC***H***$_3$), 1.36 (t, 3H, *J* = 7.2 Hz, CH$_2$C***H***$_3$). ^{13}C NMR (101 MHz, $CDCl_3$, δ, ppm) 212.0 (***C***=S), 175.4 (N***C***=O), 171.0 (O***C***=O), 70.3 (O***C***H$_2$CH$_3$), 62.8 ((C=O)O***C***H$_2$), 47.9 (CH$_2$CH$_2$***C***H$_2$N), 46.9 (***C***HCH$_3$), 41.5 (OCH$_2$***C***H$_2$N), 30.7 (NC=O***C***H$_2$), 18.1 (CH$_2$***C***H$_2$CH$_2$), 16.7 (CH***C***H$_3$), 13.7 (***C***H$_3$CH$_2$). MS: *m/z* ES$^+$, M + H$^+$ = 234.2, M + Na$^+$ = 328.203.

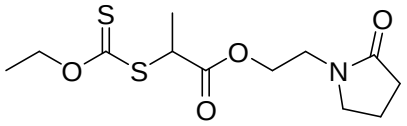

Figure 2.10. Structure of RAFT agent 5

2.2.9. Synthesis of RAFT agent 6 (2-(2-oxopyrrolidin-1-yl)ethyl 2-(ethoxycarbonothioylthio)-2-methylpropanoate)

2-Bromo-2-methyl-propionic acid 2-(2-oxo-pyrrolidin-1-yl)-ethyl ester. N-hydroxyethylpyrrolidone (12.3 g, 95.0 mmol), was dissolved in dry tetrahydrofuran (100 ml) and triethylamine (10.2 g, 100 mmol) in a 250 ml multi-necked flask fitted with a reflux condenser, N_2 inlet, magnetic stirrer bar and a pressure equalising dropping funnel. The flask was purged with nitrogen for 1 h and the reaction mixture was cooled to 0°C using an ice bath. α-Bromoisobutyryl bromide (20.0 g, 87.0 mmol) in dry tetrahydrofuran (20 ml), was added drop-wise to the reaction mixture *via* the pressure equalising dropping funnel over a period of 30 mins. The reaction mixture was stirred at 0ºC for 6 h, then at ambient temperature for 48 h under a flow of nitrogen. The white suspension that formed was filtered through Celite and solvent was removed under reduced pressure. The residue was dissolved in ethyl acetate (50 ml) and washed with deionised water (3 x 100 ml). Organic layer dried over $MgSO_4$ and solvent removed under reduced pressure to give a dark brown liquid (11.1 g, 39.8 mmol, 46% yield). Un-purified product used as the precursor for next step.

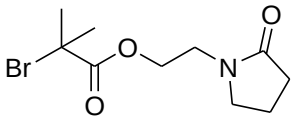

Figure 2.11. Structure of 2-Bromo-2-methyl-propionic acid 2-(2-oxo-pyrrolidin-1-yl)-ethyl ester

(2-(2-oxopyrrolidin-1-yl)ethyl 2-(ethoxycarbonothioylthio)-2-methylpropanoate). 2-Bromo-2-methyl-propionic acid 2-(2-oxo-pyrrolidin-1-yl)-ethyl ester (10.0 g, 36.0 mmol), was dissolved in ethanol (100 ml) in a 250 ml multi-necked flask fitted with a reflux condenser, N_2 inlet and magnetic stirrer bar. The flask was purged with nitrogen for 1 h and the reaction mixture was cooled to 0°C using an ice bath. Potassium *O*-ethyl xanthate (12.0 g, 74.9 mmol) was added over a period of 30 minutes. The reaction mixture stirred at 0ºC for 4 h then at ambient temperature for 48 h. The yellow suspension that formed was filtered and solvent removed under reduced pressure. The residue was dissolved in ethanol (50 ml) and potassium *O*-ethyl xanthate (6.00 g, 37.4 mmol) was added over 30 minutes. The reaction mixture was stirred at ambient temperature for 24 h. The yellow suspension was filtered and solvent removed under reduced pressure. The residue was dissolved in ethyl acetate (50 ml) and washed with deionised water (3 x 50 ml). Organic layer dried over $MgSO_4$ and solvent removed under reduced pressure. Crude product purified by column chromatography (neutral Al_2O_3, Hexane 50 : 50 Ethyl Acetate, RF = 0.26) to give a viscous lime coloured material of RAFT agent 6, (3.16 g, 9.90 mmol, 28% yield). $C_{13}H_{21}CO_4S_2$ (319.09). ^{1}H NMR (600 MHz, $CDCl_3$, δ, ppm) 4.56 (q, 2H, *J* = 7.2 Hz, $CH_3C\boldsymbol{H}_2$), 4.21 (t, 2H, *J* = 5.4 Hz, (C=O)OC$\boldsymbol{H}_2$), 3.52 (t, 2H, *J* = 5.4 Hz, $OCH_2C\boldsymbol{H}_2N$), 3.47 (t, 2H, *J* = 7.2 Hz, $CH_2CH_2C\boldsymbol{H}_2N$), 2.33 (t, 2H, *J* = 7.8 Hz, NC=OC$\boldsymbol{H}_2$), 1.99 (quin, 2H, *J* = 7.6 Hz, $CH_2C\boldsymbol{H}_2CH_2$), 1.58 (s, 6H, $C(C\boldsymbol{H}_3)_2$), 1.35 (t, 3H, *J* = 7.2 Hz, $C\boldsymbol{H}_3CH_2$). ^{13}C NMR (151 MHz, $CDCl_3$, δ, ppm) 210.8 (***C***=S), 175.3 (N***C***=O), 172.8 (O***C***=O), 69.9 ($CH_3\boldsymbol{C}H_2$), 63.7 ((C=O)OC$\boldsymbol{H}_2$), 54.0 ($\boldsymbol{C}(CH_3)_2$), 48.3 ($CH_2CH_2C\boldsymbol{H}_2N$), 41.6 ($OCH_2C\boldsymbol{H}_2N$), 30.7 (NC=OC$\mathbf{H}_2$), 25.7 ($\mathbf{C}H_3)_2$, 18.2 ($CH_2\boldsymbol{C}H_2CH_2$), 13.4 ($CH_2\boldsymbol{C}H_3$). IR ($cm^{-1}$): 1736.37, 1681.53, 1368.88, 1272.67, 1159.30, 1104.97. MS: *m/z* ES^+, M + Na^+ = 342.257.

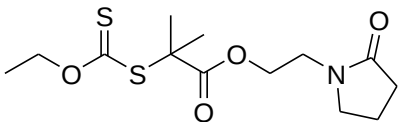

Figure 2.12. Structure of RAFT agent 6

2.2.10. Synthesis of RAFT agent 7 (methyl 2-((2-(2-oxopyrrolidin-1-yl)ethoxy)carbonothioylthio)propanoate)

N-hydroxyethylpyrrolidone (5.00 g, 38.7 mmol), was dissolved in dry tetrahydrofuran (50 ml) in a 250 ml multi-necked flask fitted with a reflux condenser, N_2 inlet and magnetic stirrer bar. The flask was purged with nitrogen for 1 h. Potassium phosphate tribasic (10.0 g, 47.0 mmol) was added to the reaction mixture which was stirred at ambient temperature for 4 h. Carbon disulphide (3.55 g, 45.0 mmol) was then added and the reaction mixture. An immediate colour change from off-white to bright yellow was observed. The reaction mixture was stirred at ambient temperature for 12 h. Methyl 2-bromopropionate (5.80 g, 34.7 mmol), was added drop-wise to reaction mixture which and subsequently stirred for 24 h. The reaction mixture was filtered and solvent removed under reduced pressure. The residue was dissolved in ethyl acetate (50 ml) and washed with water (3 x 50 ml). Organic layer was dried over $MgSO_4$ and solvent removed under reduced pressure to leave an orange residue. Crude product was purified by column chromatography (neutral Al_2O_3, Hexane 50 : 50 Ethyl Acetate, RF = 0.27), to give a viscous lime green oil of RAFT agent 7, (5.21 g, 17.9 mmol, 52% yield). $C_{11}H_{17}NO_4S_2$ (291.06). ^{1}H NMR (600 MHz, $CDCl_3$, δ, ppm) 4.66 (m, 2H), 4.36 (q, 1H, *J* = 7.2 Hz, C***H***CH_3), 3.68 (s, 3H, OC***H***$_3$), 3.62 (t, 2H, *J* = 5.4 Hz, NC***H***$_2CH_2O$), 3.42 (t, 2H, *J* = 7.2 Hz, CH_2CH_2C***H***$_2N$), 2.31 (t, 2H, *J* = 7.8 Hz, C=OC***H***$_2CH_2CH_2$), 1.99 (quin, 2H, *J* = 7.5 Hz, CH_2C***H***$_2CH_2$), 1.52 (d, 3H, *J* = 7.8 Hz, CHC***H***$_3$). ^{13}C NMR (151 MHz, $CDCl_3$, δ, ppm) 211.9 (**C**=S), 175.3 (N***C***=O), 171.6 (O***C***=O), 71.3 (NCH_2***C***H_2O), 52.8 (O***C***H_3), 48.2 (CH_2CH_2***C***H_2N), 47.4 (***C***HCH_3), 41.2 (N***C***H_2CH_2O), 30.6 (C=O***C***$H_2CH_2CH_2$), 18.1 (CH_2***C***H_2CH_2), 16.9 (CH***C***H_3). MS: *m/z* ES^+, M + Na^+ = 314.225.

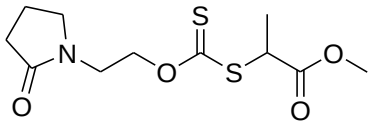

Figure 2.13. Structure of RAFT agent 7

2.2.11. Synthesis of RAFT agent 9 (2-((2-(ethoxycarbonothioylthio)propanoyloxy)methyl)-2-propylpropane-1, 3-diyl bis(2-(ethoxycarbonothioylthio)propanoate))

2-Bromo-propionic acid 2,2-bis-(2-bromo-propionyloxymethyl)-butyl ester. 1,1,1-Tris(hydroxymethyl)propane (2.68 g, 20.0 mmol), was dissolved in dry chloroform (50 ml) and pyridine (5 ml) in a 250 ml multi-necked round bottomed flask fitted with a reflux condenser, N_2 inlet, magnetic stirrer bar and pressure equalising dropping funnel. The flask was purged with nitrogen for 1 h. The reaction mixture was cooled to 0°C using an ice bath. 2-Bromopropionyl bromide (19.1 g, 90.0 mmol) was added drop-wise to the reaction mixture over a period of 1 h. The reaction mixture was allowed to reach ambient temperature and was subsequently stirred for 48 h. Dilute hydrochloric acid (10%) was added to the reaction mixture which was washed with $NaHCO_3$ (3 x 100 ml) (5 wt%). Organic layer dried over $MgSO_4$, filtered and solvent was removed under reduced pressure. Trifunctional bromide precursor was purified by column chromatography (SiO_2, DCM) to give an opaque colourless liquid, (7.40 g, 13.8 mmol, 69% yield). $C_{15}H_{23}Br_3O_6$. ^{1}H NMR (500 MHz, $CDCl_3$, δ, ppm) 4.35 (q, 3H, *J* = 7.0 Hz, C***H***CH_3), 4.13 (m, 6H, C(C***H***$_2$O)), 1.78 (d, 9H, *J* = 7.0 Hz, CHC***H***$_3$), 1.54 (q, 2H, *J* = 7.5 Hz, C***H***$_2CH_3$), 0.90 (t, 3H, ***J*** = 7.5 Hz, CH_2C***H***$_3$). ^{13}C NMR (126 MHz, $CDCl_3$, δ, ppm) 169.9 (***C***=O), 65.0 ((O***C***H_2)C), 41.8 (CH_3CH_2***C***), 39.9 (***C***HCH_3), 23.1 (CH_3***C***H_2), 21.8 (CH***C***H_3), 7.6 (***C***H_3CH_2).

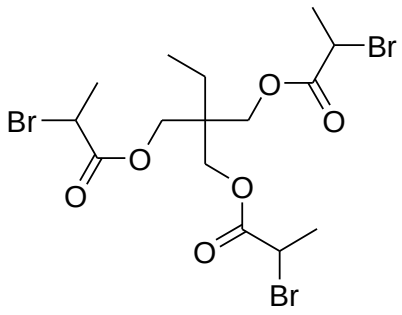

Figure 2.14. Structure of 2-bromo-propionic acid 2,2-bis-(2-bromo-propionyloxymethyl)-butyl ester

(2-((2-(ethoxycarbonothioylthio)propanoyloxy)methyl)-2-propylpropane-1,3-diyl bis(2-(ethoxycarbonothioylthio)propanoate)). 2-Bromo-propionic acid 2,2-bis-(2-bromo-propionyloxymethyl)-butyl ester (5.00 g, 9.30 mmol), re-dissolved in dry chloroform (50 ml) in a 100ml multi-necked flask fitted with a reflux condenser, N_2 inlet and magnetic stirrer bar. The flask was purged with nitrogen for 30 mins. Potassium *O*-ethyl xanthate (12.0 g, 74.5 mmol) was added portion-wise to solution over a period of 15 min at ambient temperature. Reaction mixture stirred for 48 h at ambient temperature The yellow suspension that formed was filtered to remove excess potassium *O*-ethyl xanthate and potassium bromide. The filtrate was washed deionised water (3 x 100ml). Organic layer was dried over $MgSO_4$, filtered and solvent was removed under reduced pressure to give a lime coloured viscous material of RAFT agent 9, (5.57 g, 8.40 mmol, 90% yield). $C_{24}H_{38}O_9S_6$ (662.08). ^{1}H NMR (500 MHz, $CDCl_3$, δ, ppm) 4.61 (q, 6H, *J* = 7.0 Hz, OC***H***$_2$CH$_3$), 4.38 (q, 3H, *J* = 7.5 Hz, CC***H***CH$_3$) 4.03 (m, 6H, C(C***H***$_2$O)), 1.54 (d, 9H, *J* = 7.5 Hz, CHC***H***$_3$), 1.47 (q, 2H, *J* = 7.5 Hz, CH$_3$C***H***$_2$), 1.39 (t, 9H, *J* = 7.0 Hz, OCH$_2$C***H***$_3$), 0.85 (t, 3H, *J* = 7.5 Hz, C***H***$_3$CH$_2$C). ^{13}C NMR (126 MHz, $CDCl_3$, δ, ppm) 212.2 (**C**=S), 171.2 (***C***=O), 70.7 (O***C***H$_2$CH$_3$), 64.8 (C(***C***H$_2$O), 47.4 (***C***HCH$_3$), 41.3 (***C***CH$_2$CH$_3$), 23.0 (CH$_3$***C***H$_2$C), 16.9 (CH***C***H$_3$), 14.0 (OCH$_2$***C***H$_3$), 7.5 (***C***H$_3$CH$_2$C). MS: *m/z* ES$^+$, M + Na$^+$ = 685.266.

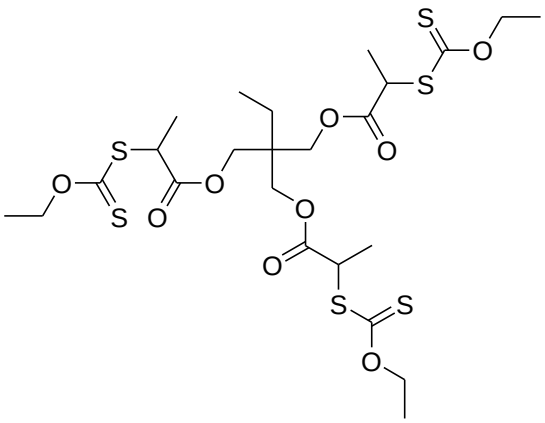

Figure 2.15. Structure of RAFT agent 9

2.2.12. Synthesis of RAFT agent 10 (2-Ethoxythiocarbonylsulfanyl-propionic acid 3-(2-ethoxythiocarbonylsulfanyl-propionyloxy)-2,2-bis-(2-ethoxythiocarbonylsulfanyl-propionyloxymethyl)-propyl ester)

2-bromo-propionic acid 3-(2-bromo-propionyloxy)-2,2-bis-(2-bromo-propionyloxymethyl)-propyl ester. Pentaerythritol (2.72 g, 20.0 mmol), was dissolved in dry chloroform (50 ml) and pyridine (5 ml) in a 250 ml multi-necked round bottomed flask fitted with a reflux condenser, N_2 inlet, magnetic stirrer bar and pressure equalising dropping funnel. The flask was purged with nitrogen for 1 h. The reaction mixture was cooled to 0°C using an ice bath. 2-Bromopropionyl bromide (19.1 g, 90.0 mmol) was added drop-wise to the reaction mixture *via* the pressure equalising dropping funnel over a period of 1 h. The reaction mixture was allowed to reach ambient temperature and subsequently stirred for 48 h. Dilute hydrochloric acid (10%) was added to the reaction mixture which was washed with $NaHCO_3$ (3 x 100 ml) (5 wt %). Organic layer dried over $MgSO_4$, filtered and solvent removed under reduced pressure. Tetrafunctional bromide precursor product purified by recrystallization to give white solid (11.0 g, 16.2 mmol, 81% yield). $C_{17}H_{24}Br_4O_8$. ^{1}H NMR (500 MHz, $CDCl_3$, δ, ppm) 4.38 (q, 4H, J = 6.5Hz, $CH_3C\boldsymbol{H}$) 4.35-4.19 (m, 8H, $C\boldsymbol{H}_2$), 1.82 (d, 12H, J = 6.5Hz, $C\boldsymbol{H}_3CH$). ^{13}C NMR (126 MHz, $CDCl_3$, δ, ppm) 21.6 ($\boldsymbol{C}H_3CH$), 39.5 ($CH_3\boldsymbol{C}H$), 43.3 ($OCH_2\boldsymbol{C}$), 63.1 ($\boldsymbol{C}H_2$), 169.6 ($\boldsymbol{C}$=O).

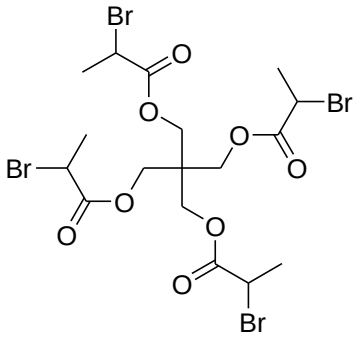

Figure 2.16. Structure of 2-bromo-propionic acid 3-(2-bromo-propionyloxy)-2,-bis-(2-bromo-propionyloxymethyl)-propyl ester

(2-Ethoxythiocarbonylsulfanyl-propionic acid 3-(2-ethoxythiocarbonylsulfanyl-propionyloxy)-2,2-bis-(2-ethoxythiocarbonylsulfanyl-propionyloxymethyl)-propyl ester). 2-bromo-propionic acid 3-(2-bromo-propionyloxy)-2,2-bis-(2-bromo-propionyloxymethyl)-propyl ester (5.00 g, 7.40 mmol), was re-dissolved in dry chloroform (50 ml) in a 100ml multi-necked flask fitted with a reflux condenser, N_2 inlet and magnetic stirrer bar. The flask was purged with nitrogen for 1 h. Potassium *O*-ethyl xanthate (12.0 g, 74.5 mmol) was added portion-wise to solution over a period of 15 minutes at ambient temperature. Reaction mixture stirred for 48 h at ambient temperature. The yellow suspension that formed was filtered to remove excess potassium *O*-ethyl xanthate and potassium bromide. The filtrate was washed with deionised water (3 x 100 ml). Organic layer dried over $MgSO_4$, filtered and solvent was removed under reduced pressure to give a lime coloured viscous oil of RAFT agent 10, (3.95 g, 4.70 mmol, 64% yield). $C_{29}H_{44}O_{12}S_8$ (840.06). ^{1}H NMR (500 MHz, $CDCl_3$, δ, ppm) 4.63 (q, 8H, *J* = 7.0 Hz, OC***H***$_2$CH$_3$) 4.41 (q, 4H, *J* = 7.5Hz, C***H***CH$_3$), 4.13 (m, 8H, CC***H***$_2$O), 1.56 (d, 12H, *J* = 7.0Hz, CHC***H***$_3$), 1.41 (t, 12H, *J* = 7.5Hz, OCH$_2$C***H***$_3$). ^{13}C NMR (126 MHz, $CDCl_3$, δ, ppm) 13.9 (OCH$_2$***C***H$_3$), 16.7 (CH***C***H$_3$), 42.5 (OCH$_2$***C***), 47.2 (***C***HCH$_3$), 63.0 (C***C***H$_2$O), 70.8 (O***C***H$_2$CH$_3$), 170.9 (***C***=O), 212.1 (***C***=S). MS: *m/z* ES$^+$, M + Na$^+$ = 863.235.

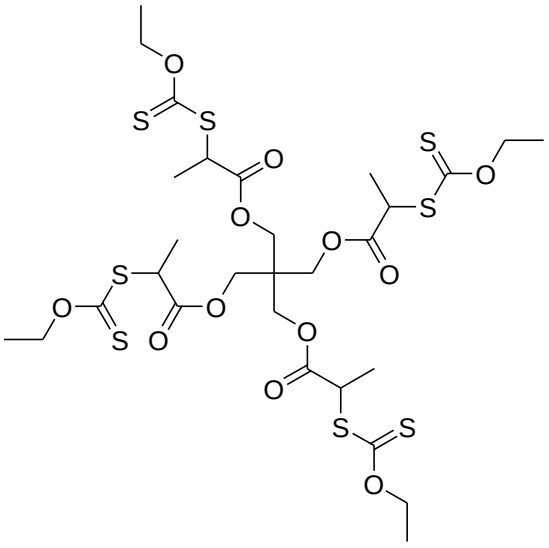

Figure 2.17. Structure of RAFT agent 10

2.2.13. Synthesis of RAFT agent 11 (2,2'-oxybis(methylene)bis(2-ethylpropane-3,2,1-triyl) tetrakis(2-(ethoxycarbonothioylthio)propanoate))

2-Bromo-propionic acid 2-[2,2-bis-(2-bromo-propionyloxymethyl)-butoxymethyl]-2-(2-bromo-propionyloxymethyl)-butyl ester. Di(trimethylolpropane) (5.00 g, 20.0 mmol) was dissolved in dry chloroform (50 ml) and pyridine (5 ml) in a 250 ml multi-necked round bottomed flask fitted with a reflux condenser, N_2 inlet, magnetic stirrer bar and pressure equalising dropping funnel. The flask was purged with nitrogen for 1 h and the reaction mixture was cooled to 0°C using an ice bath. 2-Bromopropionyl bromide (19.1 g, 90.0 mmol) was added drop-wise to the reaction mixture over a period of 1 h. The reaction mixture was allowed to reach ambient temperature and subsequently stirred for 48 h. Dilute hydrochloric acid (10%) was added to the reaction mixture which was washed with 3 x 100ml $NaHCO_3$ (5 wt%). Organic layer dried over $MgSO_4$, filtered and solvent removed under reduced pressure. Tetrafunctional bromide precursor product purified by column chromatography (SiO_2, Ethyl Acetate 5% : 95% DCM) to give an opaque colourless liquid, (8.29 g, 10.5 mmol, 53% yield). $C_{24}H_{38}Br_4O_9$. ^{1}H NMR (500 MHz, $CDCl_3$, δ, ppm) 4.37 (q, 4H, *J* = 7.0 Hz, C***H***CH_3), 4.20-3.99 (m, 8H, C=OOC***H***$_2$C), 3.32 (s, 4H, C***H***$_2$OC***H***$_2$) 1.80 (d, 12H, *J* = 7.0 Hz, CHC***H***$_3$), 1.48 (q, 4H, *J* = 7.5 Hz, CC***H***$_2$$CH_3$), 0.87 (t, 6H, *J* = 7.5 Hz, CCH_2C***H***$_3$). ^{13}C NMR (126 MHz, $CDCl_3$, δ, ppm) 170.0 (***C***=O), 70.7 (***C***H_2O***C***H_2), 65.4 (C=OO***C***H_2C), 42.5 (***C***HCH_3), 40.2 (***C***CH_2CH_3), 23.1 (C***C***H_2CH_3), 21.8 (CH***C***H_3), 7.7 (CCH_2***C***H_3).

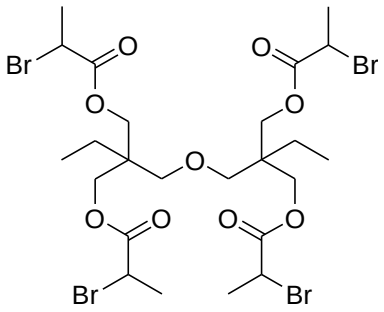

Figure 2.18. Structure of 2-bromo-propionic acid 2-[2,2-bis-(2-bromo-propionyloxymethyl)-butoxymethyl]-2-(2-bromo-propionyloxymethyl)-butyl ester

(2,2'-oxybis(methylene)bis(2-ethylpropane-3,2,1-triyl) tetrakis(2-(ethoxycarbonothioylthio)propanoate)). 2-Bromo-propionic acid 2-[2,2-bis-(2-bromo-propionyloxymethyl)-butoxymethyl]-2-(2-bromo-propionyloxymethyl)-butyl ester (5.00 g, 6.30 mmol), was re-dissolved in dry chloroform (50 ml) in a 100 ml multi-necked flask fitted with a reflux condenser, N_2 inlet and magnetic stirrer bar. The flask was purged with nitrogen for 1 h. Potassium *O*-ethyl xanthate (12.0 g, 74.5 mmol) added portion-wise to solution over a period of 15 minutes at ambient temperature. The reaction mixture was stirred for 48 h at ambient temperature The yellow suspension that formed was filtered to remove excess potassium *O*-ethyl xanthate and potassium bromide. The filtrate was washed with deionised water (3 x 100 ml). Organic layer dried over $MgSO_4$, filtered and solvent removed under reduced pressure to give a lime coloured viscous oil of RAFT agent 11, (4.64 g, 4.90 mmol, 78% yield). $C_{36}H_{58}O_{13}S_8$ (954.16). ^{1}H NMR (500 MHz, $CDCl_3$, δ, ppm) 4.63 (q, 8H, *J* = 7.0 Hz, OC***H***$_2$CH$_3$), 4.40 (q, 4H, *J* = 7.5 Hz, C***H***CH$_3$) 4.01 (m, 8H, C=OOC***H***$_2$C), 3.26 (s, 4H, C***H***$_2$OC***H***$_2$) 1.56 (d, 12H, *J* = 7.5 Hz, C***H***$_3$CH), 1.47-1.36 (m, 16H, CC***H***$_2$CH$_3$ and OCH$_2$C***H***$_3$), 0.83 (t, 6H, *J* = 7.5 Hz, C***H***$_3$CH$_2$C). ^{13}C NMR (126 MHz, $CDCl_3$, δ, ppm) 212.3 (***C***=S), 171.2 (***C***=O), 70.8 (***C***H$_2$O***C***H$_2$), 70.6 (O***C***H$_2$CH$_3$), 65.4 (C=OO***C***H$_2$C), 47.4 (***C***HCH$_3$), 42.2 (***C***CH$_2$CH$_3$), 23.1 (C***C***H$_2$CH$_3$), 17.1 (OCH$_2$***C***H$_3$), 14.0 (CH***C***H$_3$), 7.7 (CCH$_2$***C***H$_3$). MS: *m/z* ES$^+$, M + Na$^+$ = 977.357.

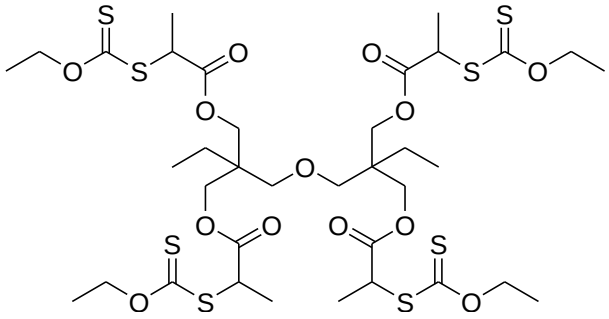

Figure 2.19. Structure of RAFT agent 11

2.3. Results and Discussion

2.3.1. Synthesis of RAFT agent 1 (Diphenyldithiocarbamate of Diethylmalonate - DPCM)

RAFT agent 1 (DPCM) has previously been used to control the polymerisation of N-vinylpyrrolidone (NVP) and vinyl acetate (VAc).[8, 9] For this reason, DPCM was seen as a good RAFT agent to synthesise as a starting point for this study. It was prepared in a three step process (Scheme 2.5) similar to that previously reported.[10] Firstly, diphenylamine was deprotonated using a strong base - sodium hydride (NaH), then carbon disulphide (CS_2) was added to the intermediate to give an orange / yellow sodium salt of diphenyldithiocarbamate. This precursor is then used as a nucleophile for the substitution reaction with diethylchloromalonate, giving the final product of DPCM in a relatively good yield of 64%.

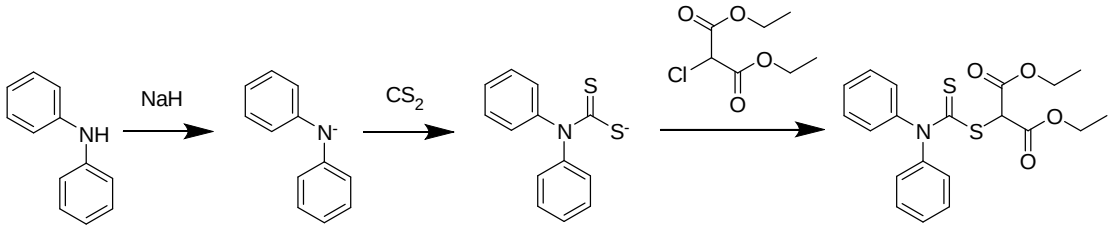

Scheme 2.5. Synthesis of RAFT agent 1

The synthesis of RAFT agent 1 has previously been poorly discussed and characterised. We have therefore chosen to discuss the synthesis and characterisation of RAFT agent 1. Comparison of ^{1}H NMR spectra of diphenylamine (Figure 2.20-I) and DPCM (Figure 2.20-III) shows the appearance of the peaks in the spectrum of DPCM at 7.48-7.14 ppm due to the resonances of the aromatic protons. It also shows the total disappearance of the NH at 5.73 ppm in the spectrum of diphenylamine. Comparing the spectra of diethylchloromalonate (Figure 2.20-II) to DPCM shows the presence of the resonances due to the diethyl malonate groups (**A**, **B** and **C**). The resonance due to CH (**C**) at 4.82 ppm in diethylchloromalonate spectrum is shifted to a higher value of 5.76 ppm in the DPCM spectrum and no resonance due to residual diethylchloromalonate is observed. Furthermore, the ^{1}H NMR spectrum of DPCM (Figure 2.20-III) revealed an integration ratio of 10:6 for the aromatic protons : CH_3 protons (**A**) of the diethylmalonate group, as expected. The small peaks in the spectrum at 7.20 ppm and

2.36 ppm are due to the resonances of the aromatic and methyl groups, respectively, of toluene impurity.

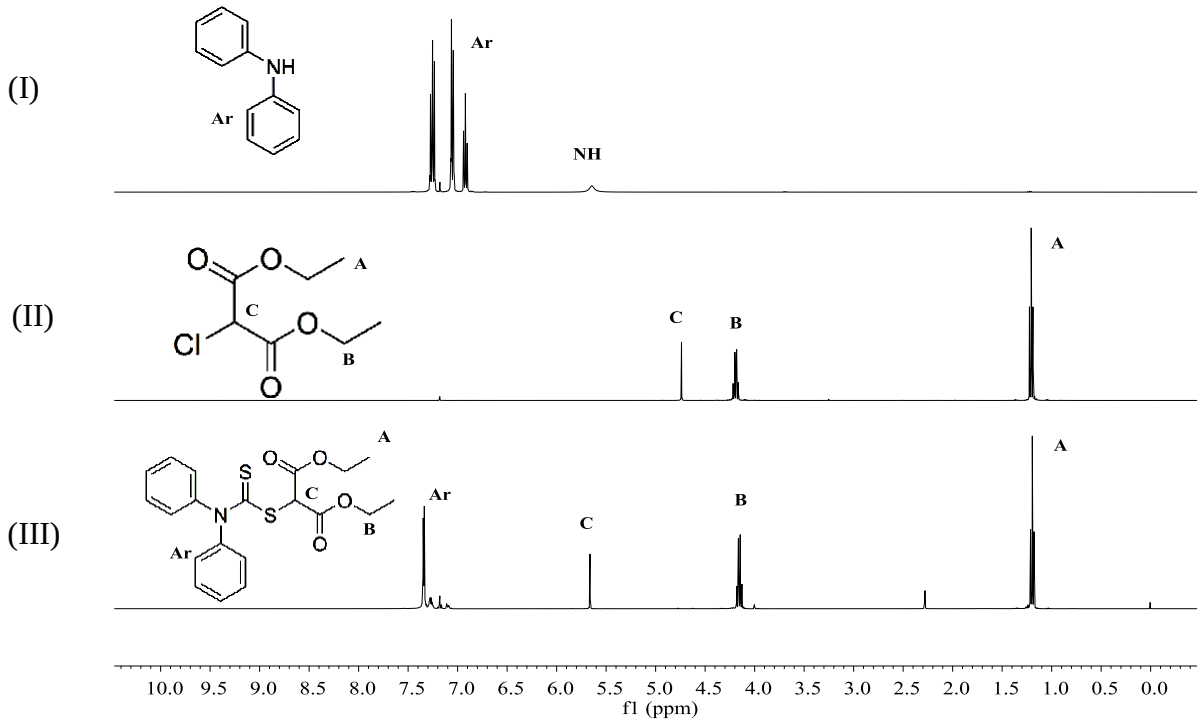

Figure 2.20. 400 MHz-^{1}H NMR spectra of (I) diphenylamine, (II) diethylchloromalonate, (III) DPCM in $CDCl_3$

^{13}C NMR spectra of the starting materials (I-II) and final product (III) are compared in Figure 2.21. Figure 2.21-III shows the presence of the resonances due to the aromatic carbons of the diphenylamine moiety at 125-130 ppm. The resonance due to CH_2 carbon (**3**) and CH_3 carbon (**4**) of the diethylmalonate moiety are also present in the spectrum at 62.6 ppm and 13.8 ppm, respectively. The resonance due to CH of the diethylmalonate moiety (**1**) is shifted from 55.5 ppm in diethylchloromalonate (Figure 2.21-II) to a higher value of 59.4 ppm in DPCM (Figure 2.21-III). This suggests that the diethylmalonate group is now attached to the thiocarbonylthio core. The resonances due to carbonyl (**2**) of the diethylmalonate and C=S (**5**) are also present at 166 ppm and 198 ppm, respectively.

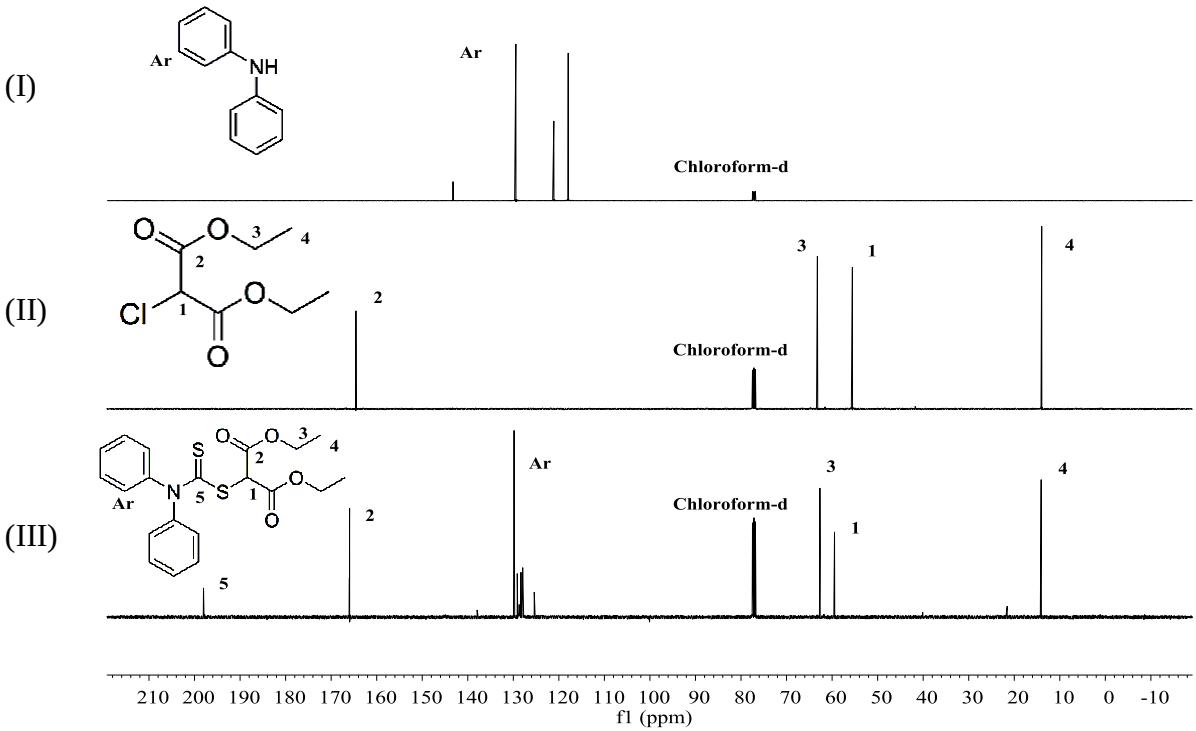

Figure 2.21. 101 MHz-^{13}C NMR spectra of (I) diphenylamine, (II) diethylchloromalonate, (III) DPCM in $CDCl_3$

2.3.2. Synthesis of RAFT agent 2 ([1-(*O*-ethylxanthyl)ethyl]benzene)

CS_2 is highly toxic, flammable and volatile, pure NaH can ignite in air. Therefore, on an industrial scale these materials would be extremely hazardous. Due to these reasons other alternative RAFT agents were explored, which involved milder reactions conditions and starting materials.

[1-(*O*-ethylxanthyl)ethyl]benzene has previously been used to control the polymerisation of NVCL[11] and NVP.[12, 13] RAFT agent 2 was synthesised in a one pot method using potassium *O*-ethyl xanthate as a nucleophile for the substitution reaction with alkyl halides, Scheme 2.6.

Potassium *O*-ethyl xanthate was added to 1-bromoethylbenzene in ethanol. RAFT agent 2 was purified by distilling off any residual starting material, 1-bromoethylbenzene. This method gave a relatively good yield of 67%.

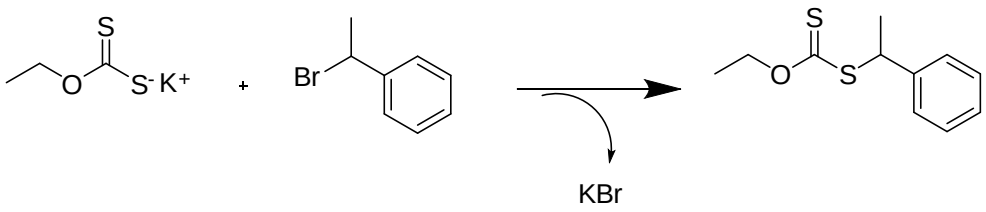

Scheme 2.6. Synthesis of RAFT agent 2

RAFT agent 2 has been synthesised previously, however its structure has not been discussed in detail. We have therefore chosen to discuss it's characterisation in detail. Comparison of ^{1}H NMR spectra of 1-bromoethylbenzene (Figure 2.22-I) and RAFT agent 2 (Figure 2.22-II) shows the appearance of the peaks in the spectrum of RAFT agent 2 at 7.4 - 7.1 ppm due to the resonances of the aromatic protons. The resonance due to CH_3 (**A**) in 1-bromoethylbenzene at 1.97 ppm is shifted to a lower value of 1.61 ppm in RAFT agent 2 and no resonance to any residual 1-bromoethylbenzene is observed. The resonance of the CH (**B**) in 1-bromoethylbenzene at 5.13 ppm is also shifted to a lower value of 4.79 ppm. The resonances of CH_3 (**D**) and CH_2 (**C**) of the ethyl group from potassium *O*-ethyl xanthate are distinguishable at 1.26 ppm and 4.50 ppm, respectively. ^{1}H NMR spectrum of RAFT agent 2 (Figure 2.22-II) revealed the integration ratio of 1:1 for the CH_3 protons (**A**) of the 1-bromoethylbenzene to the CH_3 protons (**D**) of the *O*-ethyl moiety, as expected.

The ^{13}C NMR of 1-bromoethylbenzene (I) and RAFT agent 2 (II) are compared in Figure 2.23. Figure 2.23-II shows the peaks due to the resonances of the aromatic carbons of the 1-bromoethylbenzene moiety at 127 - 142 ppm. The resonance CH_3 (**1**) and CH (**2**) carbons of the 1-bromoethylbezene moiety are also present in the spectrum at 21.6 ppm and 49.1 ppm, respectively. This shift suggests that the ethylbenzene group is now attached to the xanthate moiety. The resonance due to the C=S (**4**) carbon is also present at 213.2 ppm.

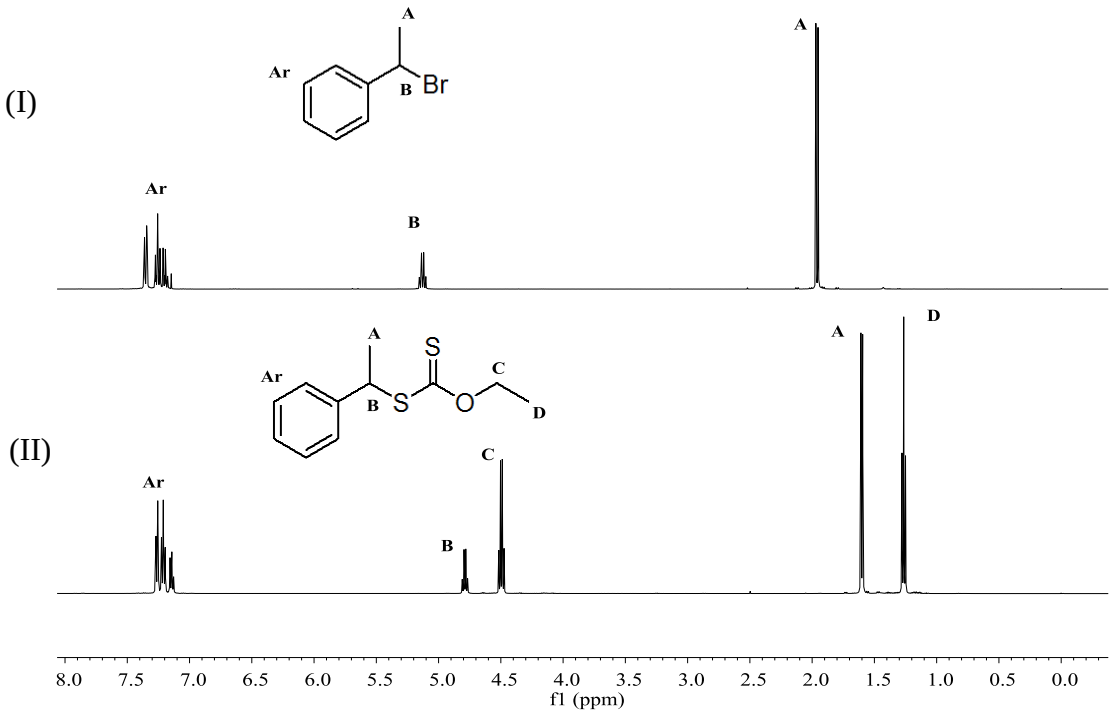

Figure 2.22. 500 MHz-^{1}H NMR of (I) 1-bromoethylbenzene, (II) RAFT agent 2 in $CDCl_3$

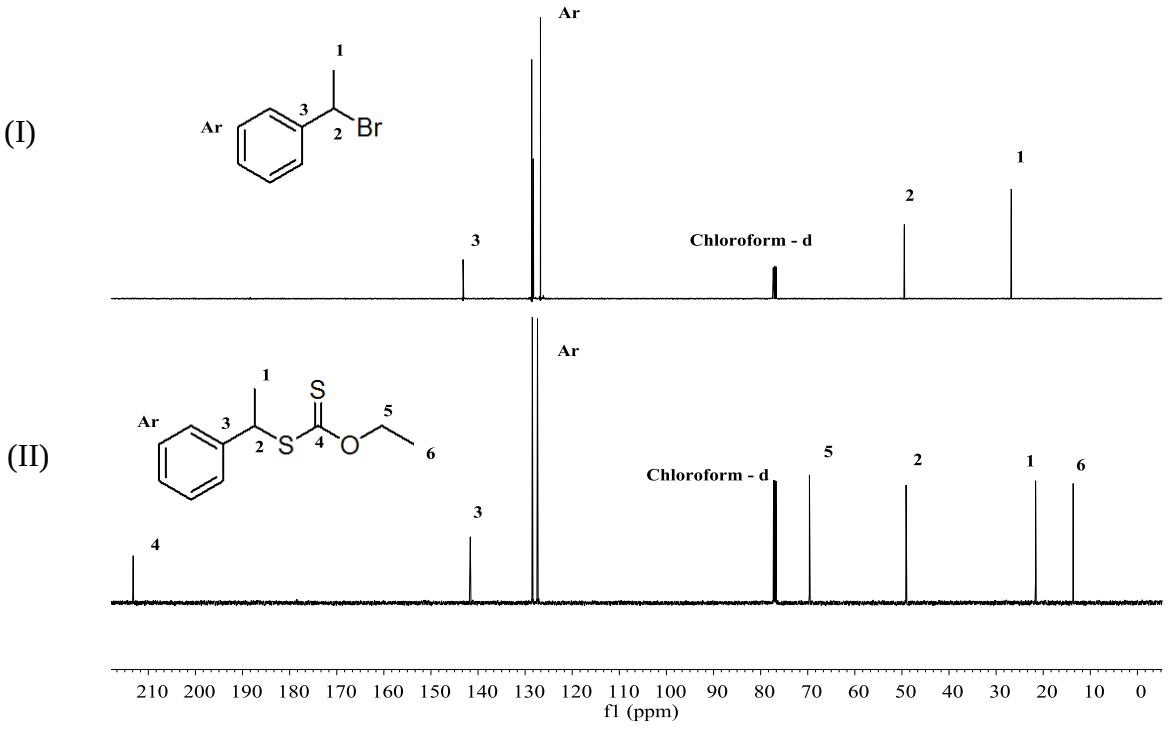

Figure 2.23. 126 MHz-^{13}C NMR of (I) 1-bromoethylbenzene, (II) RAFT agent 2 in $CDCl_3$

2.3.3. Synthesis of RAFT agent 3 (*O*-ethyl-*S*-(1-ethyoxycarbonyl)ethyl dithiocarbonate)

RAFT agent 3 (Rhodixan A1 ®) and structurally similar *S*-(2-ethyl propionate)-*O*-ethyl xanthate, have been widely used in the literature to control the polymerisation of NVP, VAc and NVCL.[7, 14-22] RAFT agent 3 was synthesised using the same reaction strategy as that for RAFT agent 2. In this case methyl 2-bromopropionate was used to react with potassium *O*-ethyl xanthate, (Scheme 2.7). No further purification stages were needed to obtain a pure product with a high yield of 95%.

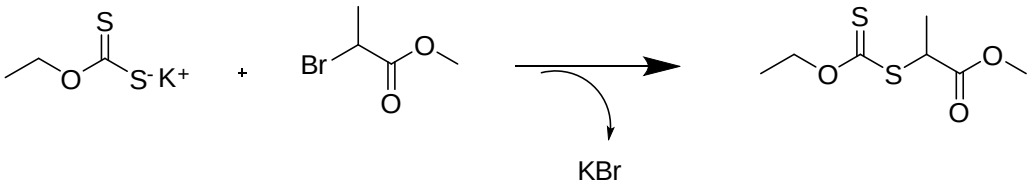

Scheme 2.7. Synthesis of RAFT agent 3

RAFT agent 3 has previously been prepared, however its structure has not been discussed in detail. We have therefore chosen to discuss it's characterisation in detail. Comparison of ^{1}H NMR spectra of methyl 2-bromopropionate (Figure 2.24-I) and RAFT agent 3 (Figure 2.24-II) shows the appearance of the singlet in the spectra of RAFT agent 3 at 3.73 ppm due to the resonance of the protons of the CH_3 (**A**) adjacent to the carbonyl group. The resonance in the spectrum of RAFT agent 3, at 4.37 ppm are due to the CH (**B**) proton of methyl 2-bromopropionate. The resonances corresponding to the *O*-ethyl group are present at 1.39 ppm (CH_3 - **E**) and 4.63 ppm (CH_2 - **D**). The resonance due to CH_3 (**C**) protons in the methyl 2-bromopropionate spectrum at 1.81 ppm is shifted to a lower value of 1.54 ppm in the RAFT agent 3 spectrum and no resonance due to residual methyl 2-bromopropionate is observed. Furthermore, ^{1}H NMR spectrum of RAFT agent 3 revealed an integration ratio of 1:1 for the CH_3 (**A**) protons in methyl 2-bromopropionate to the CH_3 (**E**) protons in the *O*-ethyl group, as expected.

^{13}C NMR spectra of methyl 2-bromopropionate (I) and RAFT agent 3 (II) are compared in Figure 2.25. Figure 2.25-II shows the presence of the carbonyl (**2**) and thiocarbonyl (**5**) groups at 171.9 ppm and 212.0 ppm, respectively. The resonances due to CH_3 carbons (**1** and **4**) of the methyl propionate moiety are present in the spectrum at 52.8 ppm and 16.9 ppm, respectively. The resonance due to CH of the methyl

propionate moiety (**3**) has shifted from 39.7 ppm in methyl 2-bromopropionate (Figure 2.25-I) to a higher value of 47.0 ppm in RAFT agent 3 (Figure 2.25-II). This suggests that the methyl propionate group is now attached to the thiocarbonylthio core.

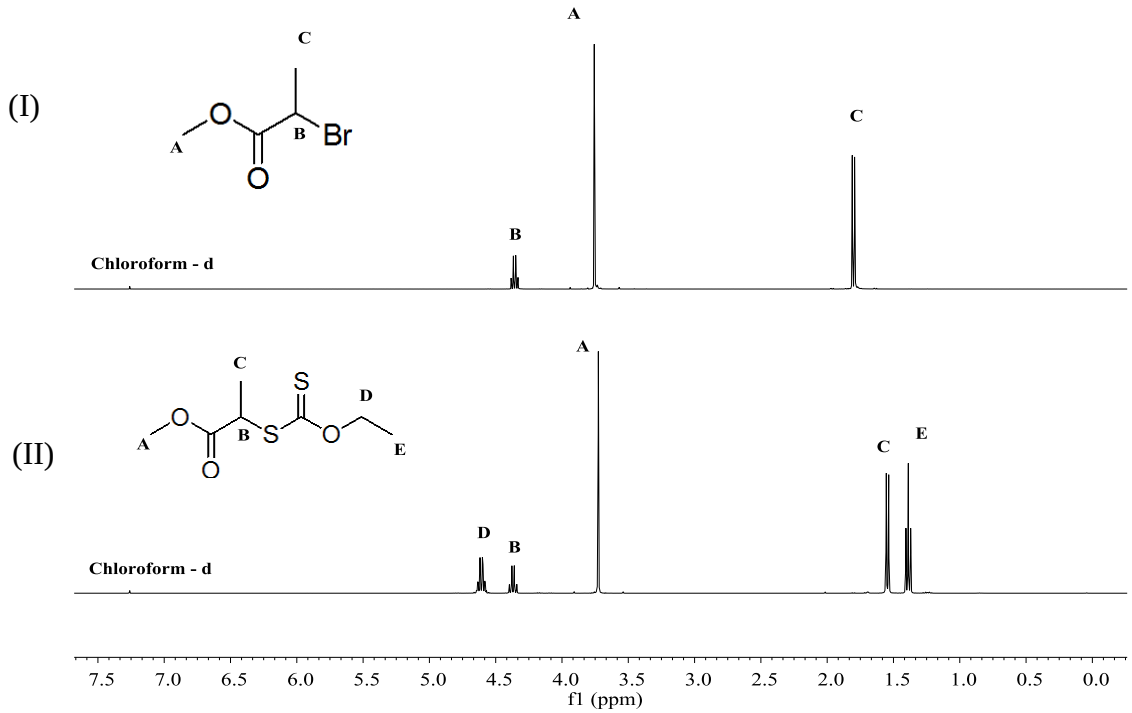

Figure 2.24. 400 MHz-^{1}H NMR of (I) methyl 2-bromopropionate, (II) RAFT agent 3 in $CDCl_3$

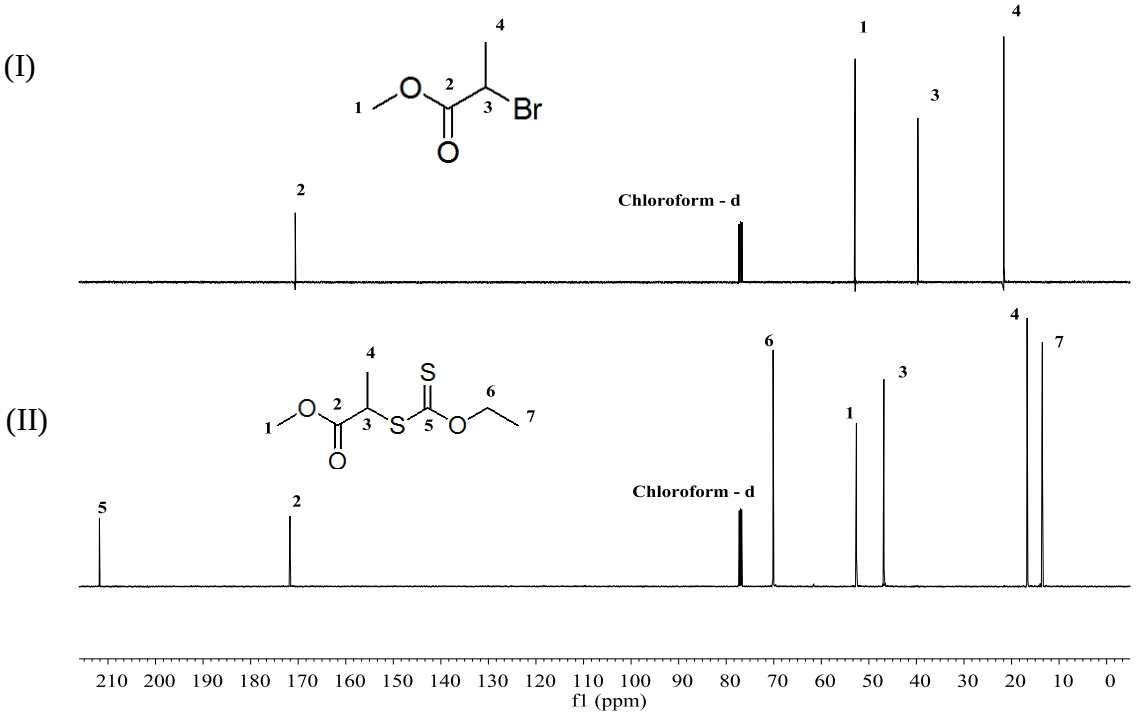

Figure 2.25. 126 MHz-^{13}C NMR of (I) methyl 2-bromopropionate, (II) RAFT agent 3 in $CDCl_3$

2.3.4. Synthesis of RAFT agent 4 (*O*-ethyl *S*-(2-(2-oxopyrrolidin-1-yl)ethyl) carbonodithioate)

RAFT agent 4 was prepared through the reaction between N-bromoethylpyrrolidone and potassium *O*-ethyl xanthate. Initially, the N-bromoethylpyrrolidone was synthesised in high yield (75%) through the bromination of N-hydroxyethylpyrrolidone (HEP), using PBr_3 as the brominating reagent, Scheme 2.8.[23]

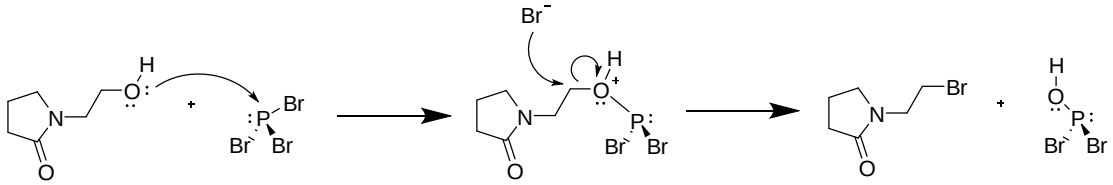

Scheme 2.8. Bromination of N-hydroxyethylpyrrolidone

Comparison of ^{1}H NMR spectra of N-hydroxyethylpyrrolidone (Figure 2.26-I) and N-bromoethylpyrrolidone (Figure 2.26-II) shows the total disappearance of the OH resonance at 4.13 ppm in the spectrum of N-hydroxyethylpyrrolidone. No resonance of any residual N-hydroxyethylpyrrolidone is observed. The resonance due to CH_2 (**A**) protons in N-hydroxyethylpyrrolidone present at 2.29 ppm is shifted to a higher value of 2.61 ppm. The resonances due to the CH_2 protons of N-hydroxyethylpyrrolidone (**D** and **E**) have shifted from 3.29 ppm and 3.62 ppm to 3.73 ppm and 3.48 ppm respectively.

^{13}C NMR spectra of N-hydroxyethylpyrrolidone (I) and N-bromoethylpyrrolidone (II) are compared in Figure 2.27. The resonance due to CH_2 carbon (**6**) adjacent to either OH or Br is the main peak of interest. The resonance due to the carbon at **6** is shifted from 61 ppm in N-hydroxyethylpyrrolidone (Figure 2.27-I) to a lower value of 28 ppm in N-bromoethylpyrrolidone (Figure 2.27-II). This suggests that the OH has been fully replaced by Br. There are no residual peaks due to N-hydroxyethylpyrrolidone.

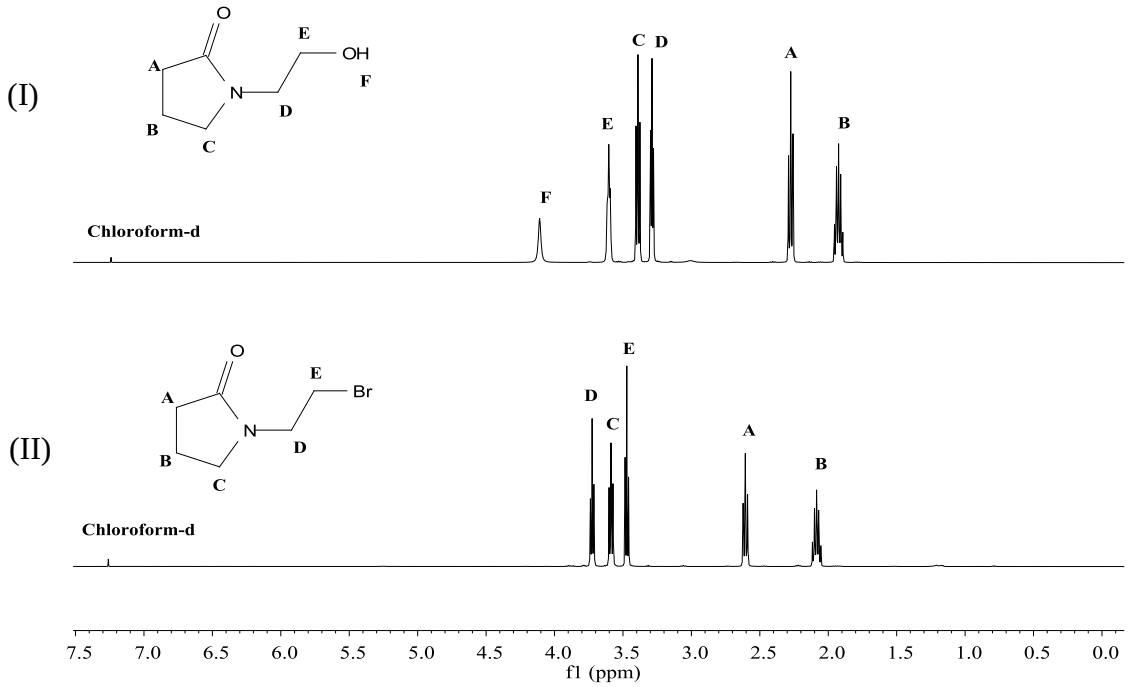

Figure 2.26. 500 MHz-^{1}H NMR spectra of (I) N-hydroxyethylpyrrolidone, (II) N-bromoethylpyrrolidone in $CDCl_3$

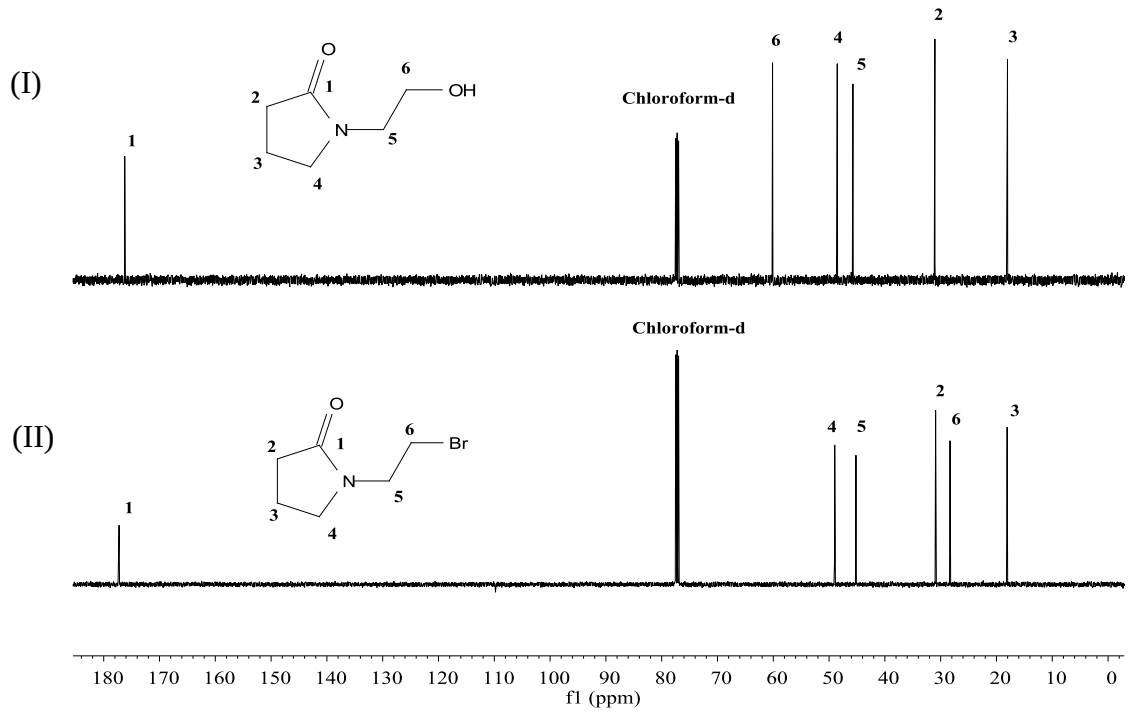

Figure 2.27. 126MHz-^{13}C NMR spectra of (I) N-hydroxyethylpyrrolidone, (II) N-bromoethylpyrrolidone in $CDCl_3$

N-bromoethylpyrrolidone was then reacted with potassium *O*-ethyl xanthate in a nucleophilic substitution reaction (Scheme 2.9), giving RAFT agent 4 in good yield (84%).

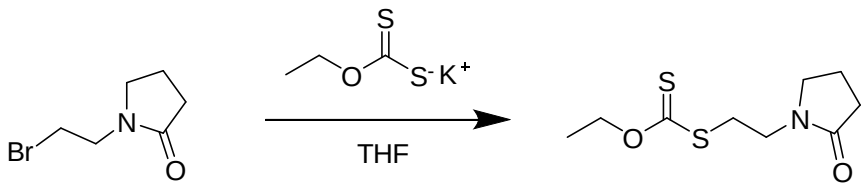

Scheme 2.9. Synthetic route for RAFT agent 4

The product was characterised by ^{1}H and ^{13}C NMR spectroscopy. Comparison of ^{1}H NMR spectra of N-bromoethylpyrrolidone (Figure 2.28-I) and RAFT agent 4 (Figure 2.28-II) shows the resonances due to the ethyl pyrrolidone ring (**A - E**) in the spectrum of RAFT agent 4 between 1.99 ppm and 3.51 ppm. The resonance due CH_2 (**A**) of the pyrrolidone ring at 2.61 ppm in N-bromoethylpyrrolidone spectrum is shifted to a lower value of 2.32 ppm in RAFT agent 4 spectrum. The resonance due to the CH_2 (**E**) adjacent to Br in N-bromoethylpyrrolidone spectrum at 3.47 ppm is shifted to a lower value of 3.26 ppm in RAFT agent 4 spectrum. The resonances due to the *O*-ethyl CH_2 (**F**) and CH_3 (**G**) protons are present in the spectrum of RAFT agent 4 at 4.60 ppm and 1.38 ppm, respectively. No resonance due to residual N-bromoethylpyrrolidone is observed. Furthermore, ^{1}H NMR spectrum of RAFT agent 4 revealed an integration ratio 1:1 for the CH_2 (**E**) protons, to the CH_2 (**F**) protons, as expected.

^{13}C NMR spectra of N-bromoethylpyrrolidone (I) and RAFT agent 4 (II) are compared in Figure 2.29. Figure 2.29-II shows the resonances of the carbonyl (**1**) and thiocarbonyl (**7**) groups at 175.3 ppm and 214.2 ppm, respectively. The ethyl pyrrolidone carbons (**2** – **6**) are also present in the spectrum (Figure 2.29-II) between 18.2 ppm and 47.9 ppm. The resonance due to CH_2 (**6**) carbon adjacent to Br in N-bromoethylpyrrolidone has shifted from 28.1 ppm to a higher value of 33.2 ppm in RAFT agent 4 (Figure 2.29-II). This suggests that the ethyl pyrrolidone moiety is attached to the thiocarbonylthio core.

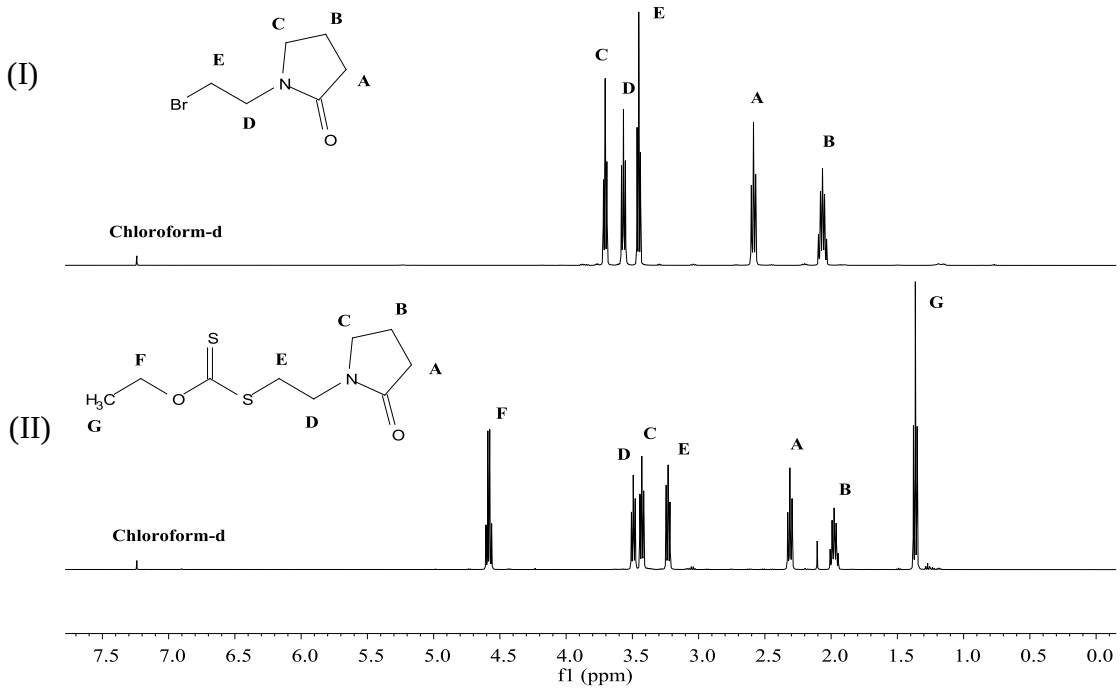

Figure 2.28. 500 MHz-^{1}H NMR spectra of (I) N-bromoethylpyrrolidone, (II) *O*-ethyl *S*-(2-(2-oxopyrrolidin-1-yl)ethyl) carbonodithioate in $CDCl_3$

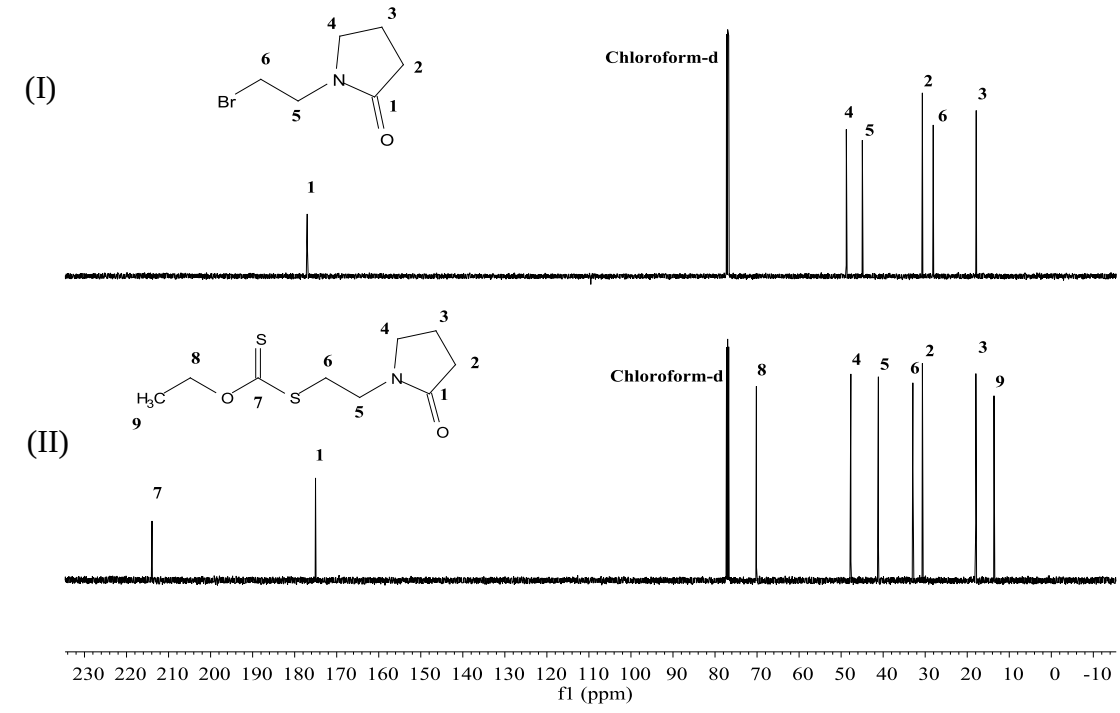

Figure 2.29. 126 MHz-^{13}C NMR spectra of (I) N-bromoethylpyrrolidone, (II) *O*-ethyl *S*-(2-(2-oxopyrrolidin-1-yl)ethyl) carbonodithioate in $CDCl_3$

2.3.5. Synthesis of RAFT agent 5 (2-(2-oxopyrrolidin-1-yl)ethyl 2-(ethoxycarbonothioylthio)propanoate)

RAFT agent 5 was prepared in two steps. The first step involves the synthesis of a brominated intermediate; 2-(2-oxopyrrolidin-1-yl)ethyl 2-bromopropanoate (Scheme 2.10) through the reaction between N-hydroxyethylpyrrolidone and 2-bromopropionyl bromide. The product was characterised by ^{1}H and ^{13}C NMR spectroscopy.

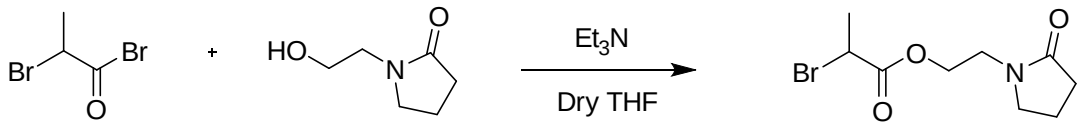

Scheme 2.10. Synthesis of 2-(2-oxopyrrolidin-1-yl)ethyl 2-bromopropanoate

Comparison of ^{1}H NMR spectra of N-hydroxyethylpyrrolidone (Figure 2.30-I) and the intermediate product (Figure 2.30-III) shows the resonances of the protons in the spectrum in Figure 2.30-III of the ethyl pyrrolidone moiety (**A** – **E**) between 1.94 ppm and 4.26 ppm. It also shows the total disappearance of the OH resonance at 4.13 ppm in the spectrum of N-hydroxyethylpyrrolidone. In addition, the resonances due to CH (**F**) and CH_3 (**G**) protons are present in the spectrum (Figure 2.30-III) at 4.32 ppm and 1.76 ppm, respectively. The resonance due to CH (**F**) in the intermediate product is shifted from a higher value of 4.68 ppm in the 2-bromopropionyl bromide spectrum, (Figure 2.30-II). The resonance due to CH_2 (**E**) at 3.62 ppm in N-hydroxyethylpyrrolidone spectrum (Figure 2.30-I) is shifted to a higher value of 4.26 ppm in the spectrum of the intermediate product (Figure 2.30-III) and no resonance due to residual N-hydroxyethylpyrrolidone was observed.

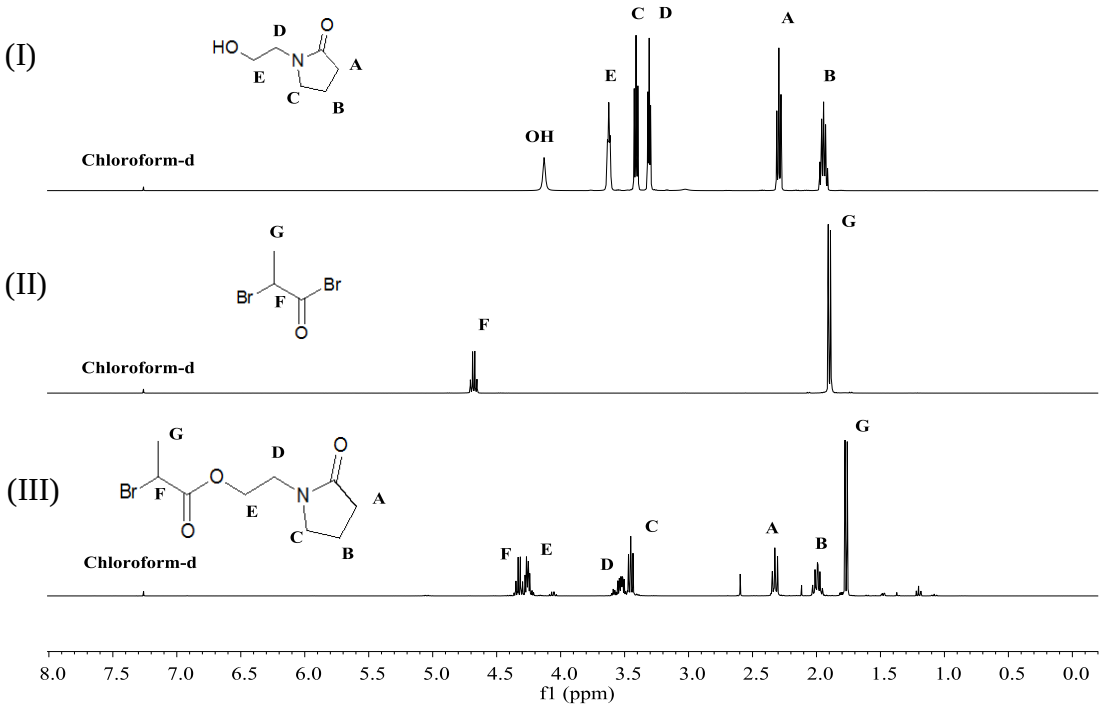

Figure 2.30. 400 MHz-^{1}H NMR spectra of (I) N-hydroxyethylpyrrolidone, (II) 2-bromopropionyl bromide, (III) 2-(2-oxopyrrolidin-1-yl)ethyl 2-bromopropanoate in $CDCl_3$

^{13}C NMR spectra of the starting materials (I-II) and the intermediate product (III) are compared in Figure 2.31. Figure 2.31-III shows the resonances of the carbonyl group carbons (**1** and **7**) at 175.4 ppm and 169.9 ppm, respectively. The resonance due to the CH (**8**) of the 2-bromopropionyl moiety has shifted from 52.7 ppm in 2-bromopropionyl bromide (Figure 2.31-II) to a lower value of 39.8 ppm in the intermediate product (Figure 2.31-III). This suggests that the ethyl pyrrolidone group is now attached to the 2-bromopropionyl moiety. The crude yield was 57%.

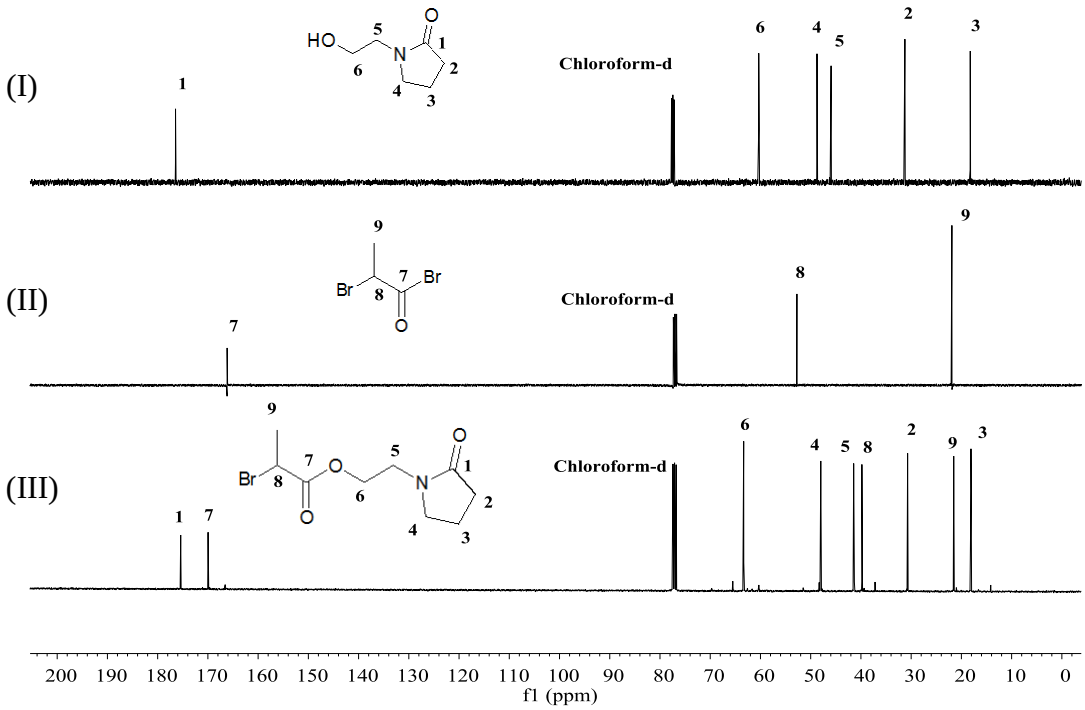

Figure 2.31. 400 MHz-^{13}C NMR of (I) N-hydroxyethylpyrrolidone, (II) 2-bromopropionyl bromide, (III) 2-(2-oxopyrrolidin-1-yl)ethyl 2-bromopropanoate in $CDCl_3$

The next step to synthesise RAFT agent 5 involved the reaction between the intermediate product and potassium *O*-ethyl xanthate in a nucleophilic substitution reaction (Scheme 2.11) in 56% yield.

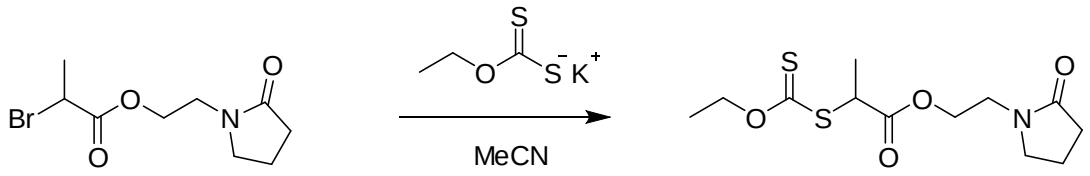

Scheme 2.11. Synthesis of 2-(2-oxopyrrolidin-1-yl)ethyl 2-bromopropanoate

Comparison of ^{1}H NMR spectra of the intermediate product (Figure 2.32-I) and RAFT agent 5 (Figure 2.32-II) shows the appearance of the resonances due to the CH_2 (**H**) and CH_3 (**I**) protons in the spectrum of RAFT agent 5 at 4.58 ppm and 1.36 ppm, respectively. The resonance due to the CH_3 (**G**) in the spectrum of the intermediate product at 1.78 ppm is shifted to a lower value of 1.52 ppm in spectrum of RAFT agent 5 and no resonance due to residual brominated intermediate is observed. Furthermore, ^{1}H NMR spectrum of RAFT

agent 5 (Figure 2.32-II) revealed an integration ratio of 1:1 for the CH_3 protons at 1.52 ppm (**G**) and 1.36 ppm (**I**), as expected.

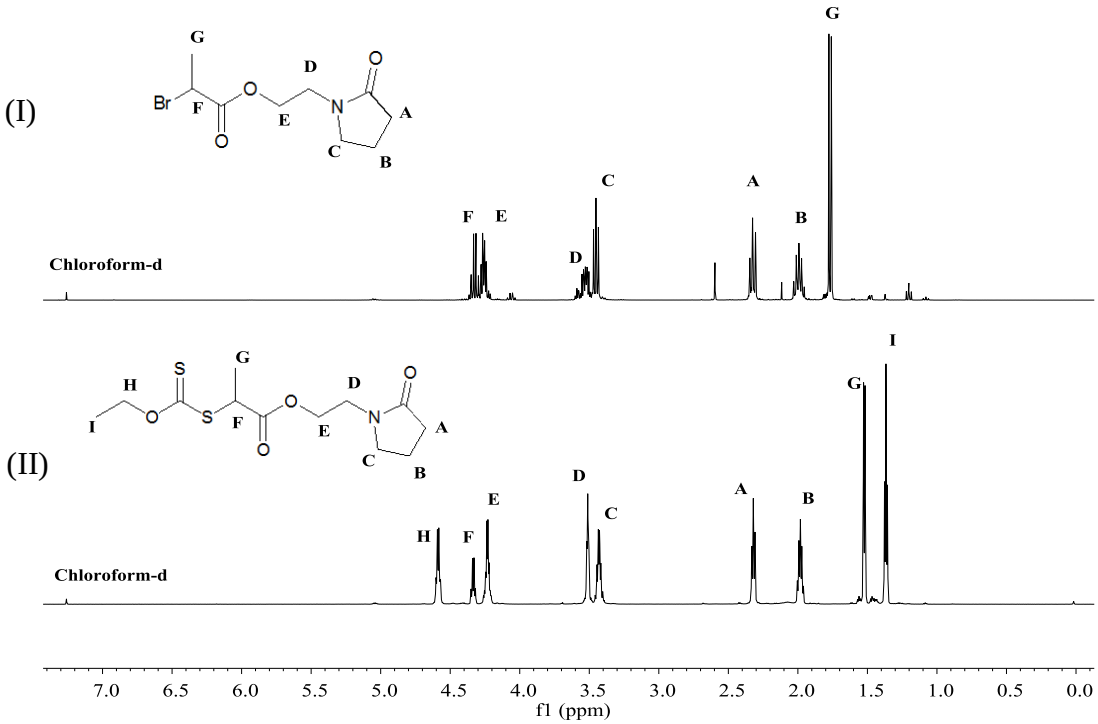

Figure 2.32. 700 MHz-^{1}H NMR spectra of (I) 2-(2-oxopyrrolidin-1-yl)ethyl 2-bromopropanoate, (II) 2-(2-oxopyrrolidin-1-yl)ethyl 2(ethoxycarbonothioylthio)propanoate in $CDCl_3$

^{13}C NMR spectra of the intermediate product (I) and RAFT agent 5 (II) are compared in Figure 2.33. Figure 2.33-II shows the presence of the resonances due to the thiocarbonylthio group (**10**) at 212.0 ppm and the carbonyl groups (**1** and **7**) at 175.4 ppm and 171.0 ppm, respectively. The resonances due to CH_2 (**11**) and CH_3 (**12**) carbons of the *O*-ethyl moiety are also present at 70.3 ppm and 13.6 ppm, respectively. The CH (**8**) of the intermediate product is shifted from 39.8 ppm to a higher value of 47.0 ppm in RAFT agent 5. This suggests that the intermediate product is now attached to the thiocarbonylthio core.

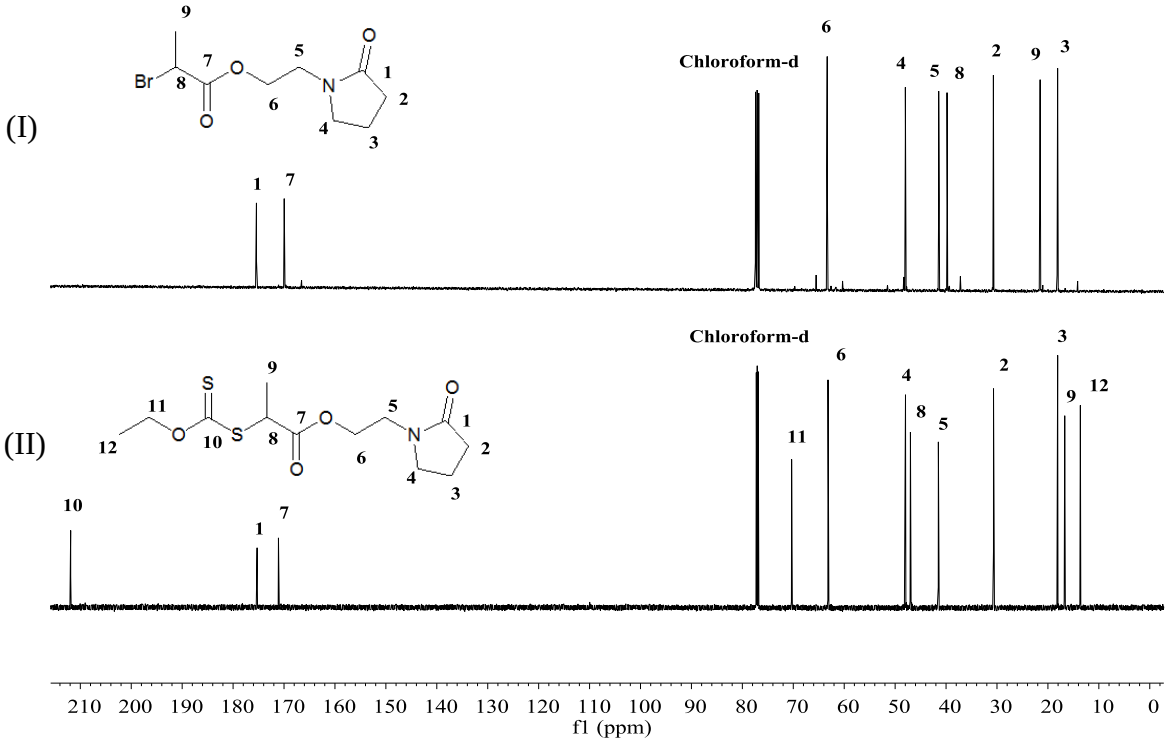

Figure 2.33. 176 MHz-^{13}C NMR spectra of (I) 2-(2-oxopyrrolidin-1-yl)ethyl 2-bromopropanoate, (II) 2-(2-oxopyrrolidin-1-yl)ethyl 2(ethoxycarbonothioylthio)propanoate in $CDCl_3$

2.3.6. Synthesis of RAFT agent 6 ((2-(2-oxopyrrolidin-1-yl)ethyl 2-(ethoxycarbonothioylthio)-2-methylpropanoate)

A two-step synthetic route used for RAFT agent 5 was utilized for the preparation of RAFT agent 6, (Scheme 2.12). In the first step, N-hydroxyethylpyrrolidone was reacted with 2-bromoisobutyryl bromide in dry THF and 2-bromo-2-methyl-propionic acid 2-(2-oxopyrrolidin-1-yl)-ethyl ester intermediate was prepared in 46% yield.

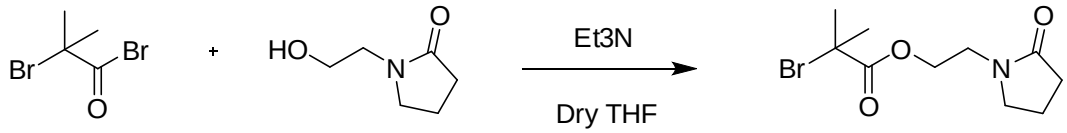

Scheme 2.12. Synthesis of 2-bromo-2-methyl-propionic acid 2-(2-oxopyrrolidin-1-yl)-ethyl ester

The intermediate product was analysed and characterised by ^{1}H NMR and ^{13}C NMR spectroscopy. Comparison of ^{1}H NMR spectra of N-hydroxyethylpyrrolidone (Figure 2.34-I), 2-bromoisobutyryl bromide (Figure 2.34-II) and the intermediate product (Figure 2.34-III) shows the total disappearance of the OH at 4.13 ppm in the spectrum of N-hydroxyethylpyrrolidone. The spectrum of the intermediate product shows the resonances due to the ethyl pyrrolidone moiety (**A** – **E**) between 1.95 ppm and 4.27 ppm. The resonance due to the CH_3 (**F**) protons in 2-bromoisobutyryl bromide at 1.99 ppm is shifted to a lower value of 1.87 ppm in the spectrum of the intermediate product and no resonance due to residual 2-bromoisobutyryl bromide is observed. Furthermore, ^{1}H NMR spectrum of the intermediate product (Figure 2.34-III) revealed an integration ratio of 3:1 for the CH_3 (**F**) protons to the CH_2 (**E**) protons, as expected.

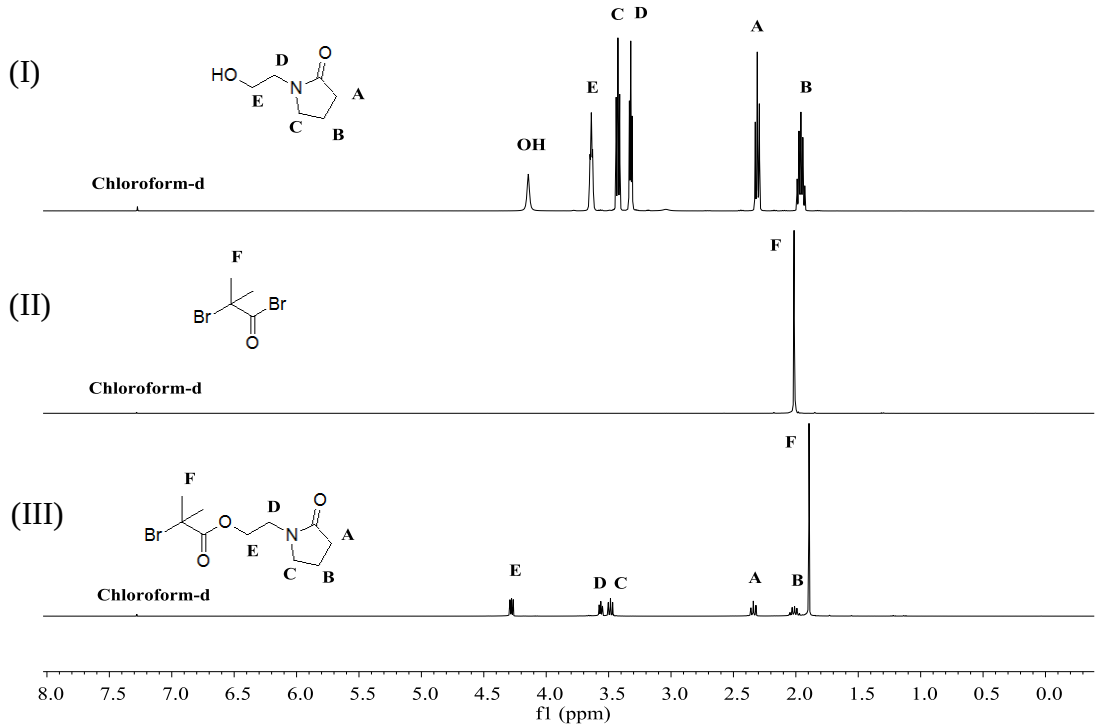

Figure 2.34. 400 MHz-^{1}H NMR spectra of (I) N-hydroxyethylpyrrolidone, (II) 2-bromoisobutyryl bromide, (III) 2-bromo-2-methyl-propionic acid 2-(2-oxopyrrolidin-1-yl)-ethyl ester in $CDCl_3$

^{13}C NMR spectra of the starting materials (I-II) and the intermediate product (III) are compared in Figure 2.35. Figure 2.35-III shows the resonances of both carbonyl groups (**1**) and (**7**) at 175.4 ppm and 171.4 ppm, respectively.

The resonance due to the carbon at 65.7 ppm (**8**) in the spectrum of 2-bromoisobutyryl bromide (Figure 2.35-II) is shifted to a lower value of 55.6 ppm in the spectrum of the intermediate product (Figure 2.35-III). This suggests that the ethyl pyrrolidone group is now attached to the 2-bromoisobutyryl moiety.

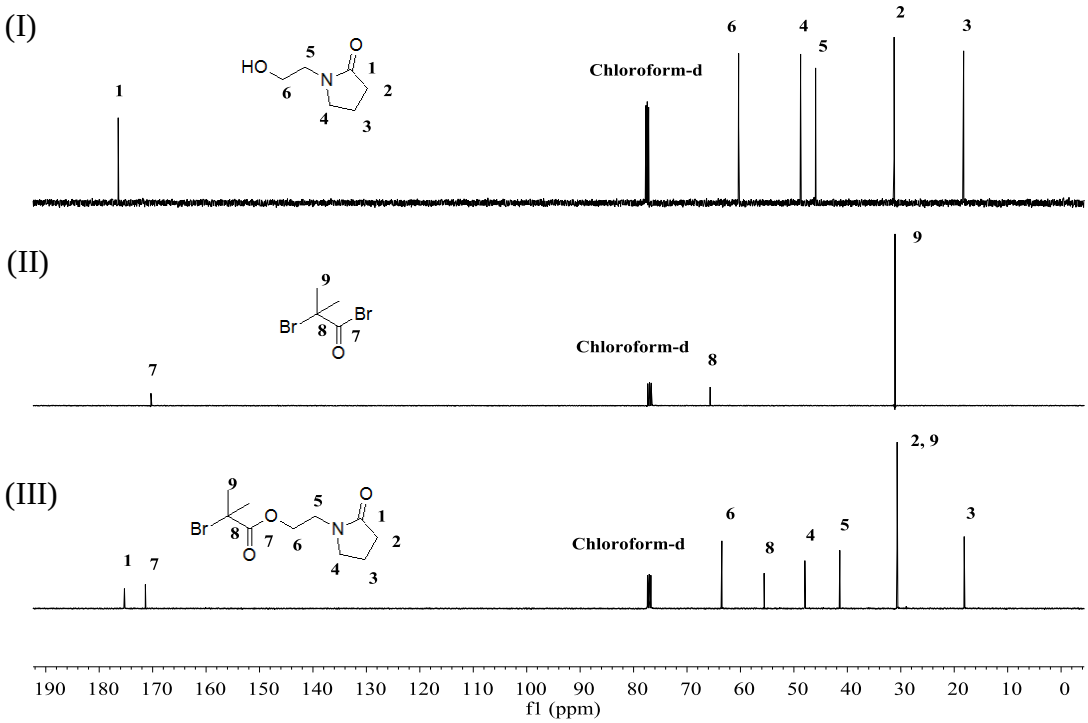

Figure 2.35. 101 MHz-^{13}C NMR spectra of (I) N-hydroxyethylpyrrolidone, (II) 2-bromoisobutyryl bromide, (III) 2-bromo-2-methyl-propionic acid 2-(2-oxopyrrolidin-1-yl)-ethyl ester in $CDCl_3$

The second step in the synthesis of RAFT agent 6 involved the nucleophilic substitution reaction between potassium *O*-ethyl xanthate and the intermediate product (Scheme 2.13). The resulting product, RAFT agent 6 with a yield of 28% was analysed by ^{1}H and ^{13}C NMR spectroscopy.

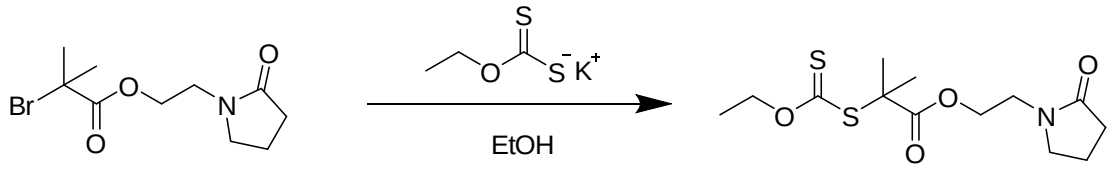

Scheme 2.13. Synthesis of 2-(2-oxopyrrolidin-1-yl)ethyl 2-(ethoxycarbonothioylthio)-2-methylpropanoate.

Comparison of ^{1}H NMR spectra of the intermediate product (Figure 2.36-I) and RAFT agent 6 (Figure 2.36-II) shows the appearance of the resonances due to the CH_2 (**G**) and CH_3 (**H**) protons in the spectrum of RAFT agent 6 at 4.56 ppm and 1.35 ppm, respectively. The resonance due to CH_3 (**F**) at 1.87 ppm in the intermediate product is shifted to a lower value of 1.58 ppm in RAFT agent 6 spectrum and no resonance due to the residual intermediate product is observed. Furthermore, ^{1}H NMR spectrum of RAFT agent 6 (Figure 2.36-II) revealed an integration ratio of 2:1 for the CH_3 (**F**) protons to the CH_3 (**H**) protons of the *O*-ethyl moiety, as expected.

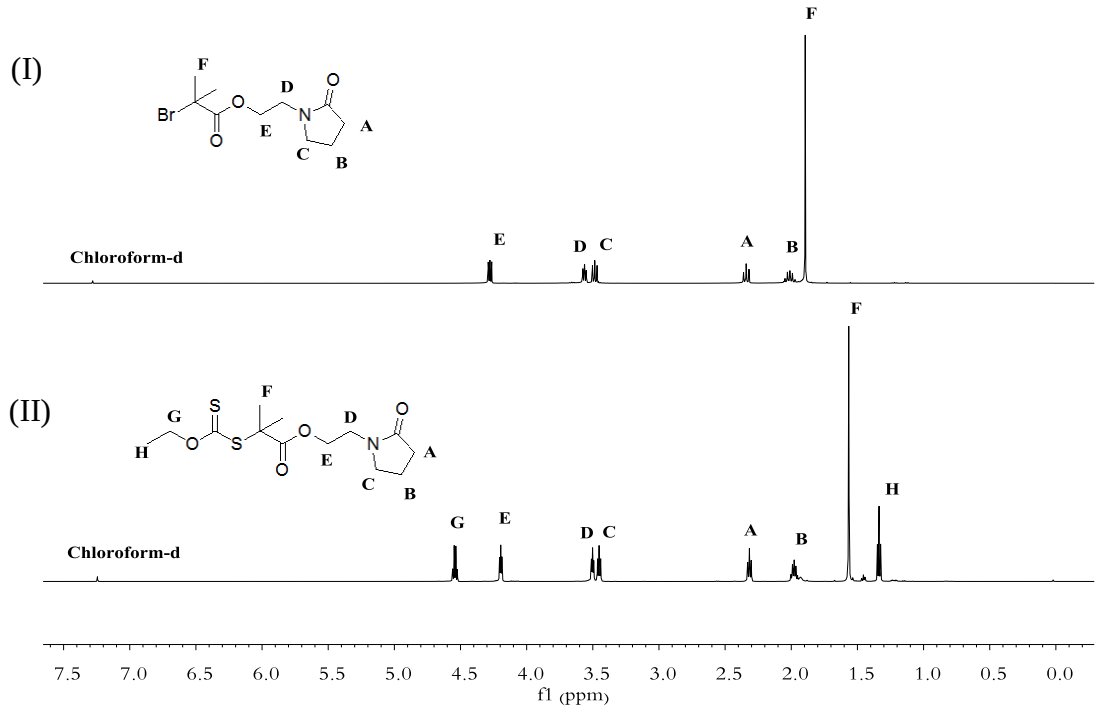

Figure 2.36. 600 MHz-^{1}H NMR spectra of (I) 2-bromo-2-methyl-propionic acid 2-(2-oxopyrrolidin-1-yl)-ethyl ester, (II) 2-(2-oxopyrrolidin-1-yl)ethyl 2-(ethoxycarbonothioylthio)-2-methylpropanoate in $CDCl_3$

^{13}C NMR spectra of the intermediate product (I) and RAFT agent 6 (II) are compared in Figure 2.37. Figure 2.37-II shows the resonances due to the thiocarbonylthio group (**10**) at 210.8 ppm and carbonyl groups (**1**) and (**7**) at 175.3 ppm and 172.8 ppm, respectively. The resonances due to CH_2 (**11**) and CH_3 (**12**) carbons of the *O*-ethyl moiety are present at 69.9 ppm and 13.4 ppm, respectively. The resonance due to CH_3 (**9**) carbon of the intermediate product is shifted from

30.6 ppm to a lower value of 25.7 ppm in RAFT agent 6. This suggests that the intermediate product is now attached to the thiocarbonylthio core.

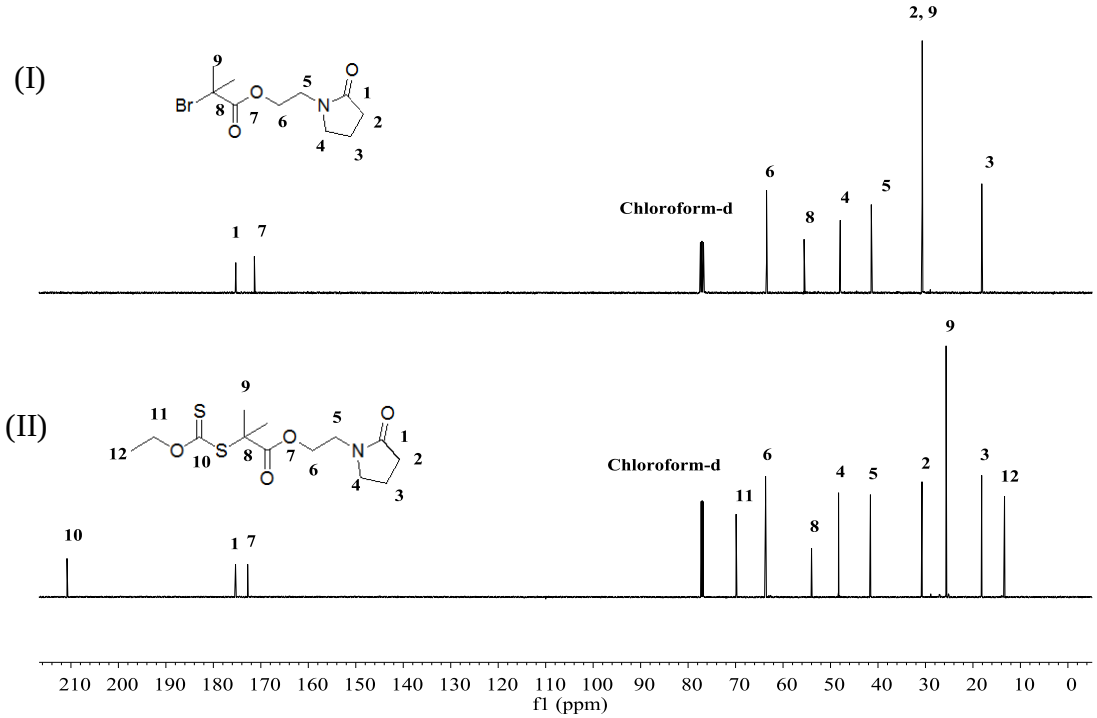

Figure 2.37. 151 MHz-^{13}C NMR spectra of (I) 2-bromo-2-methyl-propionic acid 2-(2-oxopyrrolidin-1-yl)-ethyl ester (II) 2-(2-oxopyrrolidin-1-yl)ethyl 2-(ethoxycarbonothioylthio)-2-methylpropanoate in $CDCl_3$

2.3.7. Synthesis of RAFT agent 7 (methyl 2-((2-(2-oxopyrrolidin-1-yl)ethoxy)carbonothioylthio)propanoate)

Methyl 2-((2-(2-oxopyrrolidin-1-yl)ethoxy)carbonothioylthio)propanoate was prepared in a "one pot" synthesis (Scheme 2.14) in a yield of 52%.

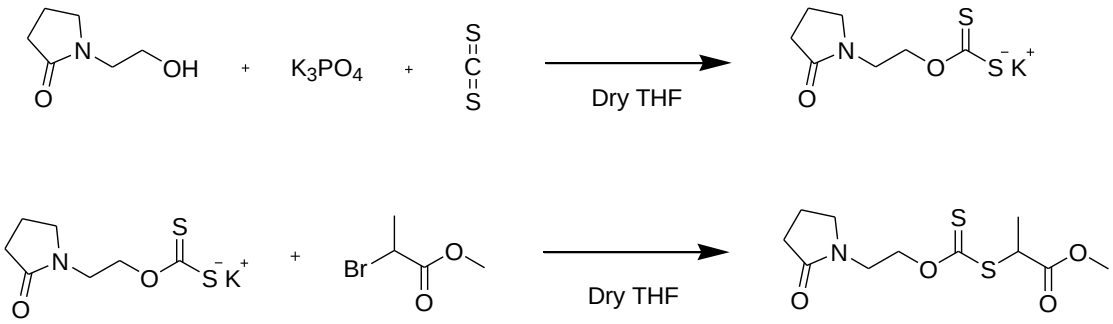

Scheme 2.14. Synthesis RAFT agent 7

Initially, N-hydroxyethylpyrrolidone was reacted with tribasic potassium phosphate (K_3PO_4) and then subsequently with carbon disulphide to give a potassium *O*-ethylpyrrolidone xanthate intermediate. Then methyl 2-bromopropionate was added slowly to the reaction mixture to give the final RAFT agent product. RAFT agent 7 was characterised by ^{1}H and ^{13}C NMR spectroscopy.

Comparison of ^{1}H NMR spectra of N-hydroxyethylpyrrolidone (Figure 2.37-I), methyl 2-bromopropionate (Figure 2.37-II) and RAFT agent 7 (Figure 2.37-III) shows the total disappearance of the resonance due to OH in the spectrum of N-hydroxyethylpyrrolidone at 4.13 ppm. Comparison of the spectra of methyl 2-bromopropionate (Figure 2.38-II) to RAFT agent 7 (Figure 2.38-III) shows the resonances due to the CH (**F**), CH_3 (**H)** and CH_3 (**G**) at 4.36, 3.68 and 1.52 ppm, respectively in the spectrum of RAFT agent 7 (Figure 2.38-III). The resonance due to CH_3 (**G**) at 1.79 ppm in methyl 2-bromopropionate spectrum is shifted to a lower value of 1.52 ppm in RAFT agent 7 spectrum and no resonance due to residual methyl 2-bromopropionate is observed. The resonance due to the CH_2 (**E**) adjacent to the OH in N-hydroxyethylpyrrolidone spectrum at 3.62 ppm is shifted to a higher value of 4.66 ppm in RAFT agent 7 spectrum. Furthermore, ^{1}H NMR spectrum of RAFT agent 7 (Figure 2.37-III) revealed an integration ratio of 3:2 for the CH_3 (**G**) of the methyl propionate group to the CH_2 (**E**) adjacent to the thiocarbonyl thio core, as expected.

^{13}C NMR spectra of the starting materials (I-II) and RAFT agent 7 (III) are compared in Figure 2.39. Figure 2.39-III shows the appearance of the resonances due to both carbonyl groups (**1**) and (**10**) at 175.3 ppm and 171.6 ppm, respectively. The thiocarbonyl carbon (**7**) is also present at 211.9 ppm. The resonances due to the CH (**8**), CH_3 (**9)** and CH_3 (**11**) of the methyl propionate moiety are also present in the spectrum (Figure 2.39-III) at 47.4 ppm, 16.9 ppm and 52.8 ppm, respectively. The resonance due to CH (**8**) carbon of the methyl propionate moiety has shifted from 39.7 ppm in the methyl 2-bromopriopionate spectrum to a higher value of 47.4 ppm in RAFT agent 7 spectrum. This suggests that the methyl propionate moiety is attached to the thiocarbonylthio core. The CH_2 (**6**) adjacent to the OH in the N-hydroxyethylpyrrolidone spectrum at 61 ppm is shifted to a higher value of 71.3 ppm in RAFT agent 7 spectrum. This suggests that the ethyl pyrrolidone group is attached to the thiocarbonylthio core.

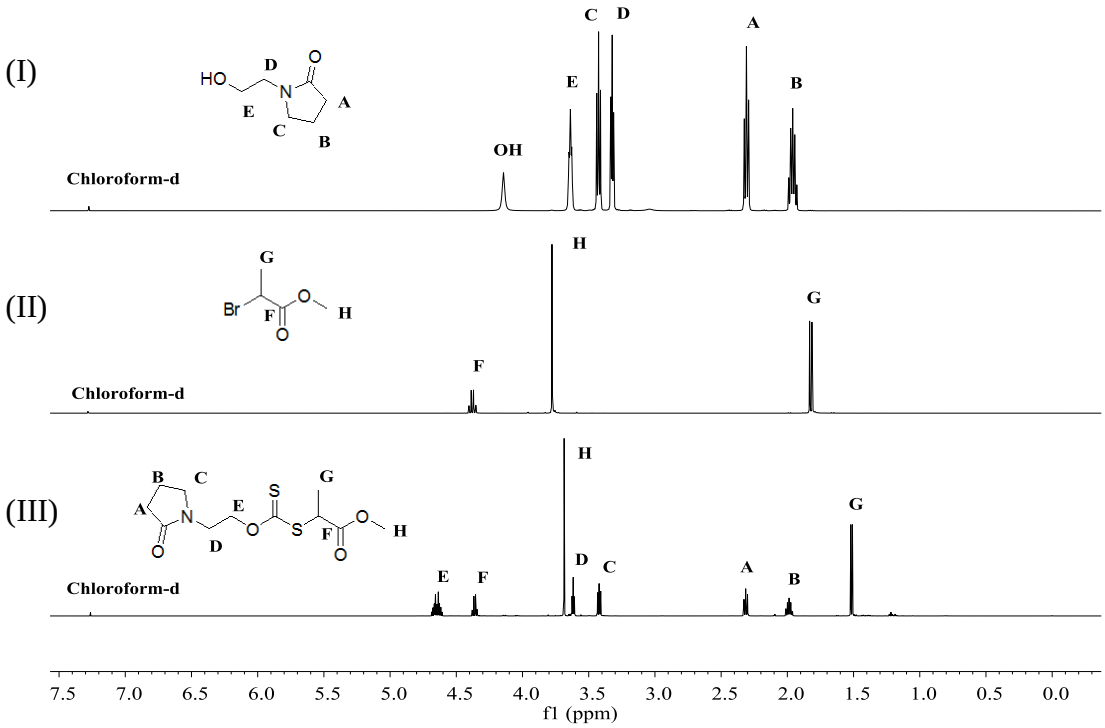

Figure 2.38. 600 MHz-^{1}H NMR spectra of (I) N-hydroxyethylpyrrolidone, (II) methyl 2-bromopropionate, (III) methyl 2-((2-(2-oxopyrrolidin-1-yl)ethoxy)carbonothioylthio)propanoate in $CDCl_3$

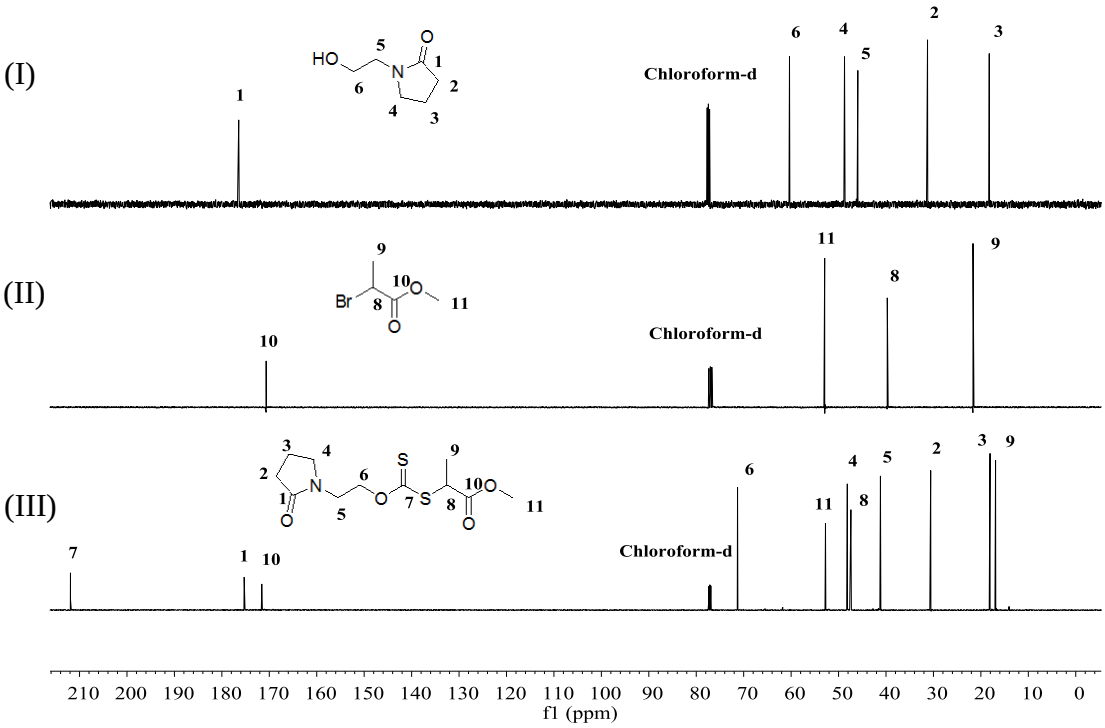

Figure 2.39. 151 MHz-^{13}C NMR spectra of (I) N-hydroxyethylpyrrolidone, (II) methyl 2-bromopropionate, (III) methyl 2-((2-(2-oxopyrrolidin-1-yl)ethoxy)carbonothioylthio)propanoate in $CDCl_3$

2.3.8. Synthesis of RAFT agent 9 ((2-((2-(ethoxycarbonothioylthio)propanoyloxy)methyl)-2-propylpropane-1,3-diyl bis(2-(ethoxycarbonothioylthio)propanoate))

RAFT agent 9 is a three armed star RAFT agent that is synthesised in a two-step process (Scheme 2.15). Firstly, 1,1,1-tris(hydroxymethyl)propane was reacted with 2-bromopropionyl bromide to make a trifunctional precursor. The yield of the reaction was 69% and previous work from Bernard *et al.*[24] recorded a yield of 70% using 1,1,1-tris(hydroxymethyl)ethane as a starting material to prepare a similar trifunctional RAFT agent.

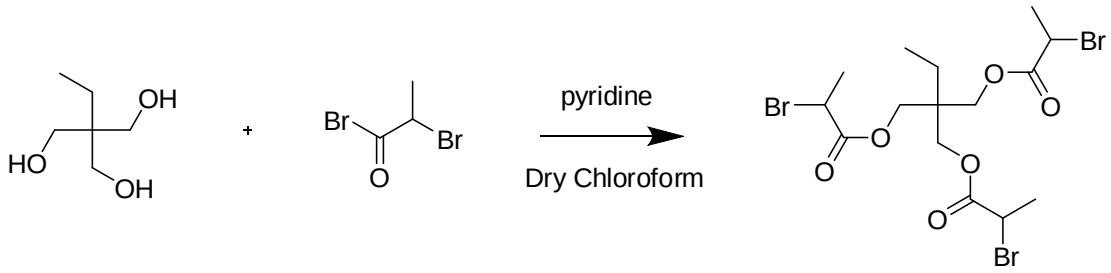

Scheme 2.15. Synthesis of 2-bromo-propionic acid 2,2-bis-(2-bromo-propionyloxymethyl)-butyl ester

2-bromo-propionic acid 2,2-bis-(2-bromo-propionyloxymethyl)-butyl ester, trifunctional bromide precursor, was characterised by ^{1}H and ^{13}C NMR spectroscopy. Comparison of ^{1}H NMR spectra of 2-bromopropionyl bromide (Figure 2.40-I) and the trifunctional bromide precursor (Figure 2.40-II) shows the appearance of the resonances due to CH_3 (**A**), CH_2 (**B**) and CH_2 (**C**) of the central core in the spectrum of the trifunctional bromide precursor at 0.90 ppm, 1.54 ppm and 4.05 - 4.35 ppm, respectively. The 1, 1, 1-tris(hydroxymethyl)propane starting material was insoluble in $CDCl_3$. The resonance due to CH (**E**) at 4.69 ppm in 2-bromopropionyl bromide spectrum is shifted to a lower value of 4.38 ppm in the trifunctional bromide precursor spectrum (Figure 2.40-II) and no resonance due to the residual 2-bromopropionly bromide is observed. Furthermore, ^{1}H NMR spectrum of the trifunctional bromide precursor (Figure 2.40-II) revealed an integration ratio of 1:3 for the CH_3 (**A**) protons of the core to the CH_3 (**D**) protons of the arms, as expected.

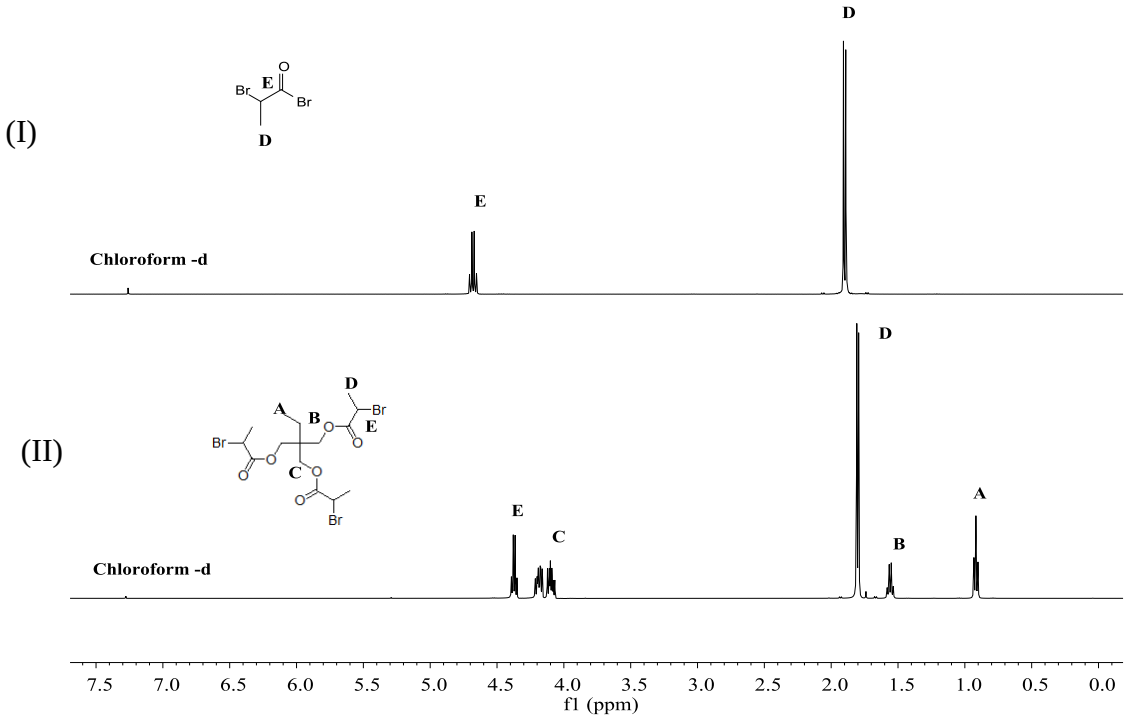

Figure 2.40. 500 MHz-^{1}H NMR spectra of (I) 2-bromopropionyl bromide, (II) 2-bromo-propionic acid 2,2-bis-(2-bromo-propionyloxymethyl)-butyl ester in $CDCl_3$

^{13}C NMR spectra of 2-bromopropionyl bromide (I) and the trifunctional bromide precursor (II) are compared in Figure 2.41. Figure 2.41-II shows the presence of the carbonyl group (**6**) of the methyl propionate at 169.9 ppm. The resonance due to the CH_3 (**1**) of the core is present at 7.6 ppm, the CH_2 (**2**) and CH_2 (**4**) of the core are present at 23.1 ppm and 65.0 ppm, respectively. The resonance due to CH (**3**) and CH_3 (**5**) carbons of the methyl propionate moiety are also present in the spectrum (Figure 2.41-II) at 39.9 ppm and 21.8 ppm, respectively. The resonance due to CH (**3**) of the methyl propionate moiety is shifted from 52.7 ppm to a lower value of 39.9 ppm in the trifunctional bromide precursor (Figure 2.41-II). This suggests that the methyl propionate moiety is attached to the core structure.

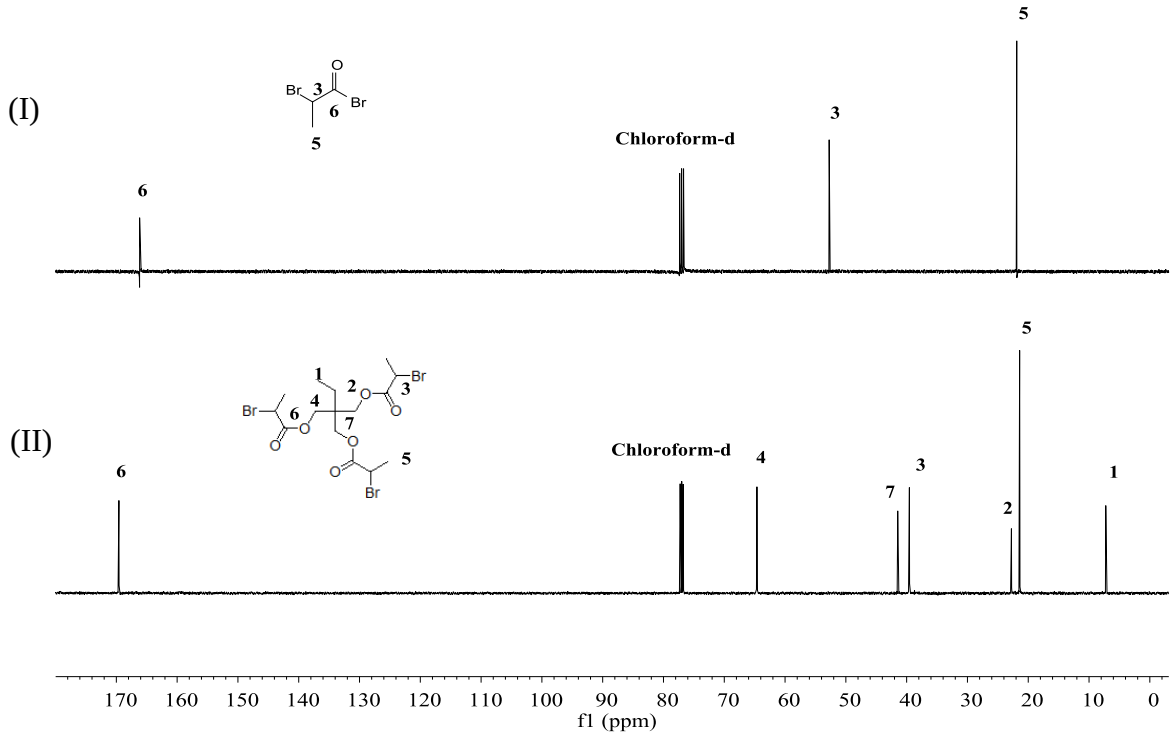

Figure 2.41. 126 MHz-^{13}C NMR spectra of (I) 2-bromopropionyl bromide, (II) 2-bromo-propionic acid 2,2-bis-(2-bromo-propionyloxymethyl)-butyl ester in $CDCl_3$

2-bromo-propionic acid 2,2-bis-(2-bromo-propionyloxymethyl)-butyl ester was then reacted with potassium *O*-ethyl xanthate in a nucleophilic substitution reaction to give RAFT agent 9 (Scheme 2.16). No further purification was necessary. The RAFT agent prepared can be described as being an R-group designed chain transfer agent. Bernard *et al.*[24] found that using an R-group designed RAFT agent gave narrowly polydisperse polymers without any evidence of linear or coupled side products. In addition, under hydrolytic conditions the architecture was unaffected and no linear chains were broken off. The yield of the reaction 90%. This is in comparison to the 40% yield quoted for the similar trifunctional RAFT agent synthesised by Bernard *et al.*[24]

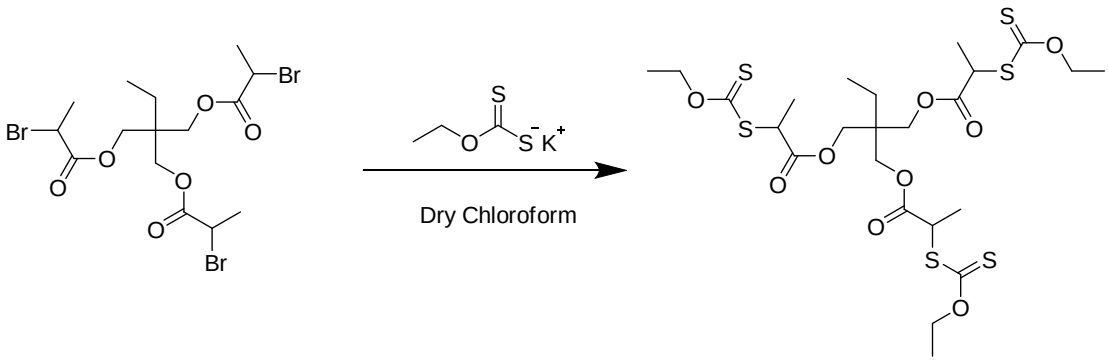

Scheme 2.16. Synthesis of 2-((2-(ethoxycarbonothioylthio)propanoyloxy)methyl)-2-propylpropane-1,3-diyl bis(2-(ethoxycarbonothioylthio)propanoate)

Comparison of ^{1}H NMR spectra of the trifunctional bromide precursor (Figure 2.42-I) and RAFT agent 9 (Figure 2.42-II) shows the appearance of the resonances due to the CH_2 (**F**) and CH_3 (**G**) protons of the *O*-ethyl moiety in the spectrum of RAFT agent 9 at 4.61 ppm and 1.39 ppm, respectively. The peaks of the trifunctional bromide precursor are also present in the spectrum of RAFT agent 9 (**A** – **E**). The resonance due to CH_3 (**D**) in trifunctional bromide precursor spectrum at 1.79 ppm is shifted to a lower value of 1.54 ppm in RAFT agent 9 spectrum and no resonance due to residual trifunctional bromide precursor is observed. Furthermore, ^{1}H NMR spectrum of RAFT agent 9 (Figure 2.42-II) revealed an integration ratio of 3:1 for the CH_3 (**G**) of the *O*-ethyl moiety to the CH_3 (**A**) of the core structure, as expected. This indicates that three arms are present within the structure.

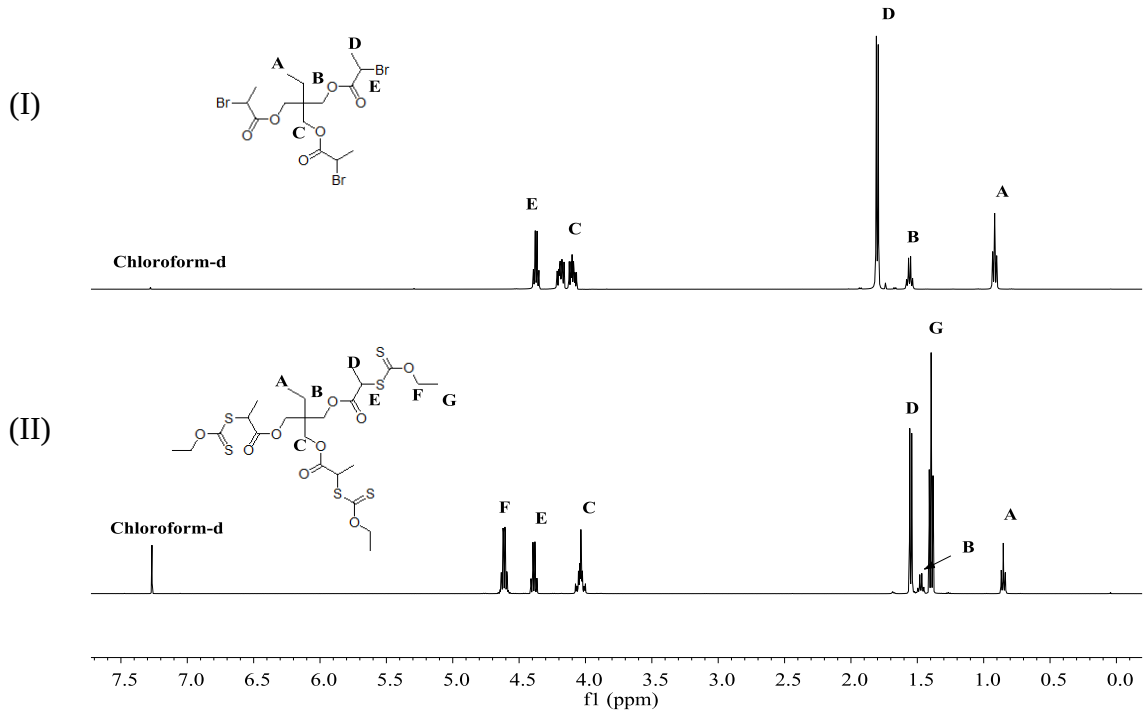

Figure 2.42. 500 MHz-^{1}H NMR spectra of (I) 2-bromo-propionic acid 2,2-bis-(2-bromo-propionyloxymethyl)-butyl ester, (II) 2-((2-(ethoxycarbonothioylthio)propanoyloxy)methyl)-2-propylpropane-1,3-diyl bis(2-(ethoxycarbonothioylthio)propanoate) in $CDCl_3$

^{13}C NMR spectra of the trifunctional bromide precursor (I) and RAFT agent 9 (II) are compared in Figure 2.43. Figure 2.43-II shows the resonances of the carbonyl (**6**) group and the thiocarbonyl (**8**) group at 171.2 ppm and 212.2 ppm, respectively. The resonances due to the carbons of the trifunctional bromide precursor are also present in the spectrum of RAFT agent 9 (**1** – **7**). The resonance due to CH_2 (**9**) and CH_3 (**10**) carbons of the *O*-ethyl moiety are present in the spectrum of RAFT agent 9 at 70.7 ppm and 14.0 ppm, respectively. The resonance due to CH (**3**) carbon of the methyl propionate moiety is shifted from 39.9 ppm to a higher value of 47.4 ppm in the spectrum of RAFT agent 9. This suggests that the xanthate functionality is attached to the core structure.

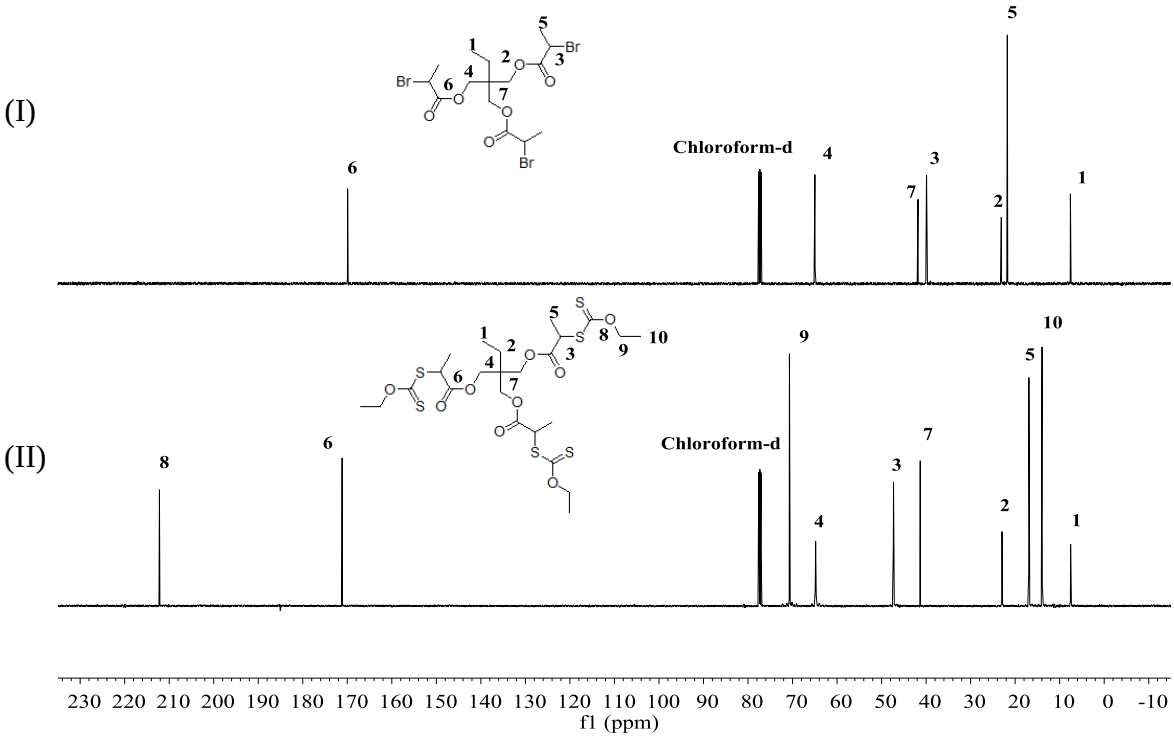

Figure 2.43. 126 MHz-^{13}C NMR spectra of (I) 2-bromo-propionic acid 2,2-bis-(2-bromo-propionyloxymethyl)-butyl ester, (II) 2-((2-(ethoxycarbonothioylthio)propanoyloxy)methyl)-2-propylpropane-1,3-diyl bis(2-(ethoxycarbonothioylthio)propanoate) in $CDCl_3$

2.3.9. Synthesis of RAFT agent 10 (2-ethoxthiocarbonylsulfanyl-propionic acid 3-(2-ethoxythiocarbonylsulfanyl-propionyloxy)-2,2-bis-(2-ethoxythiocarbonylsulfanyl-propionyloxymethyl)-propyl ester)

RAFT agent 10 is a four armed star RAFT agent and is synthesised in a two-step process (Scheme 2.17). It has previously been made by Bernard *et al.*[24] Firstly, pentaerythritol was reacted with 2-bromopropionyl bromide to make a tetrafunctional precursor. The yield of the reaction was 81%. This is in comparison to the 70% yield quoted for the similar tetrafunctional bromide precursor synthesised by Bernard *et al.*[24]

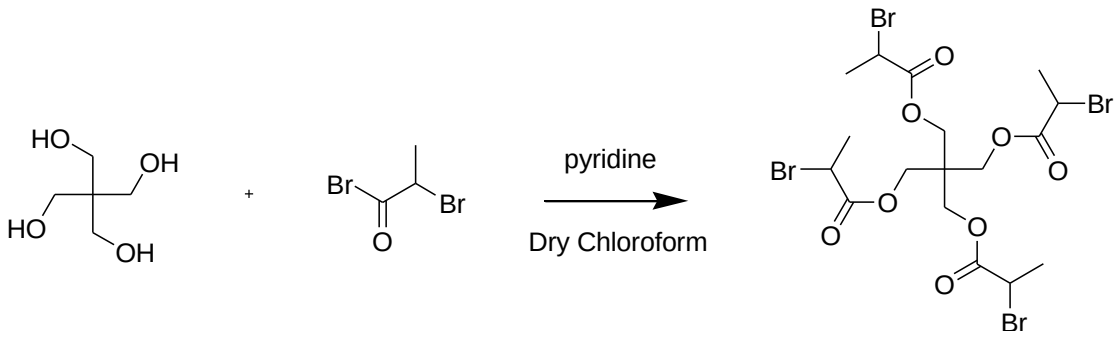

Scheme 2.17. Synthesis of 2-bromopropionic acid 3-(2-bromo-propionyloxy)-2,2-bis-(2-bromo-propionyloxymethyl)-propyl ester

The tetrafunctional bromide precursor to the RAFT agent 10 was characterised by ^{1}H and ^{13}C NMR. Comparison of ^{1}H NMR spectra of 2-bromopropionyl bromide (Figure 2.44-I) and the tetrafunctional bromide precursor (Figure 2.44-II) shows the resonances of the CH_2 (**C**) of the central core in the spectrum of the tetrafunctional bromide precursor between 4.19 ppm and 4.35 ppm. Pentaerythritol is insoluble in $CDCl_3$. The resonance due to the CH (**A**) in the 2-bromopropionyl bromide spectrum at 4.69 ppm is shifted to a lower value of 4.38 ppm in the tetrafunctional bromide precursor spectrum and no resonance due to the residual 2-bromopropionyl bromide is observed. Furthermore, ^{1}H NMR spectrum of the tetrafunctional bromide precursor (Figure 2.44-II) revealed an integration ratio of 2:3 for the CH_2 (**C**) protons of the core to the CH_3 (**B**) protons of the arms, as expected.

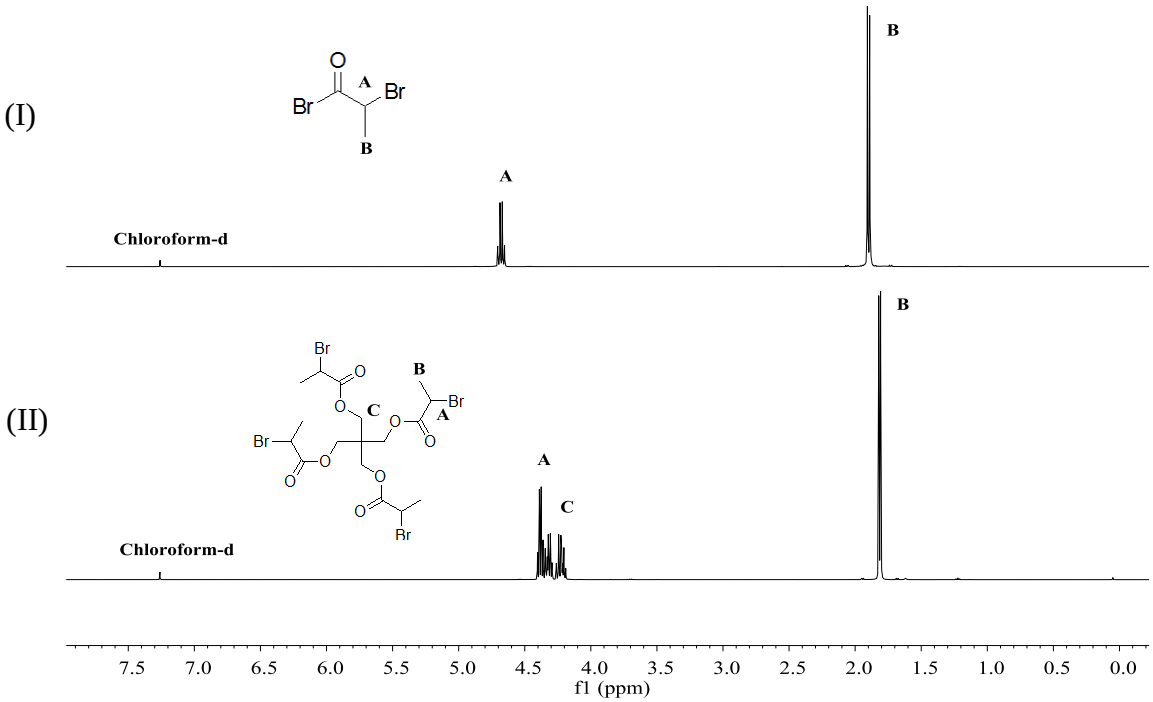

Figure 2.44. 500 MHz-^{1}H NMR spectra of (I) 2-bromopropionyl bromide, (II) 2-bromopropionic acid 3-(2-bromo-propionyloxy)-2,2-bis-(2-bromo-propionyloxymethyl)-propyl ester in $CDCl_3$

^{13}C NMR spectra of 2-bromopropionyl bromide (I) and the tetrafunctional bromide precursor (II) are compared in Figure 2.45. Figure 2.45-II shows the resonances of the carbonyl group (**1**) of the methyl propionate at 169.6 ppm. The resonance due to CH_2 (**4**) of the core is present at 63.1 ppm and the carbon at the centre (**5**) is present at 43.3 ppm. The resonances due to CH (**3**) and CH_3 (**2**) carbons of the methyl propionate moiety are also present in the spectrum (Figure 2.45-II) at 39.5 ppm and 21.6 ppm, respectively. The resonance due to CH (**3**) of the methyl propionate moiety is shifted from 52.7 ppm to a lower value of 39.5 ppm in the tetrafunctional bromide precursor (Figure 2.45-II). This suggests that the methyl propionate moiety is attached to the core structure.

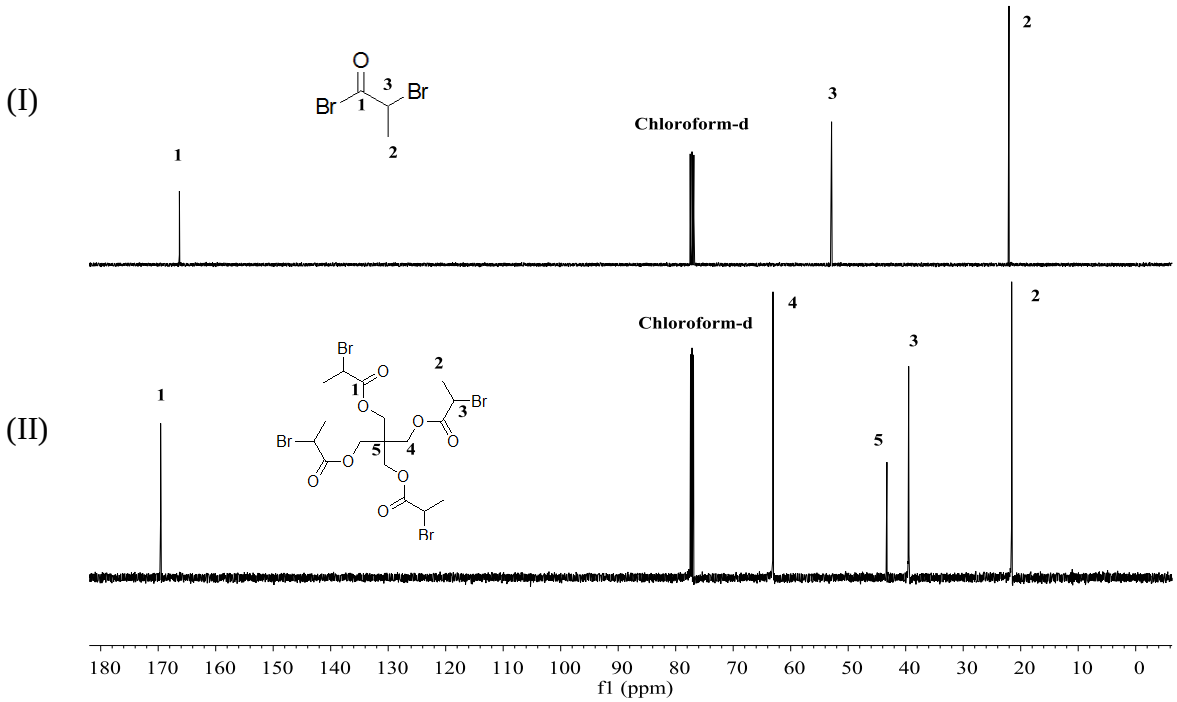

Figure 2.45. 126 MHz-^{13}C NMR spectra of (I) 2-bromopropionyl bromide, (II) 2-bromopropionic acid 3-(2-bromo-propionyloxy)-2,2-bis-(2-bromo-propionyloxymethyl)-propyl ester in $CDCl_3$

The tetrafunctional bromide precursor was then reacted with potassium *O*-ethyl xanthate in a nucleophilic substitution reaction to give the final product (RAFT agent 10) (Scheme 2.18). The yield of the reaction was 64%. This is in comparison to the 40% yield quoted for the similar tetrafunctional RAFT agent synthesised by Bernard *et al.*[24]

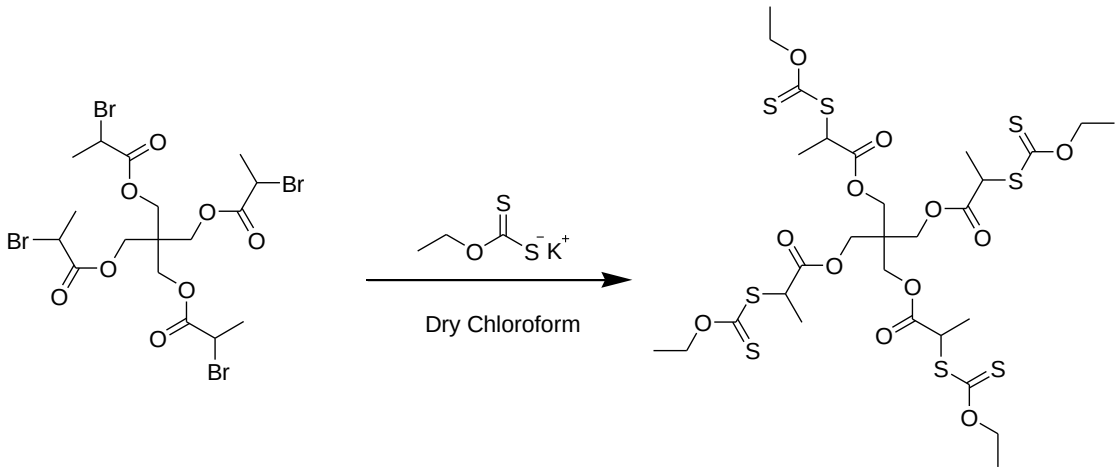

Scheme 2.18. Synthesis of RAFT agent 10

Comparison of ^{1}H NMR spectra of the tetrafunctional bromide precursor (Figure 2.46-I) and RAFT agent 10 (Figure 2.46-II) shows the appearance of the resonances due to the CH_2 (**D**) and CH_3 (**E**) protons of the *O*-ethyl moiety in the spectrum of RAFT agent 10 at 4.63 ppm and 1.41 ppm, respectively. The resonances due to the tetrafunctional bromide precursor are also present in the spectrum of RAFT agent 10 (**A** – **C**). The resonances due to CH_3 (**A**) in tetrafunctional bromide precursor spectrum at 1.79 ppm is shifted to a lower value of 1.56 ppm in RAFT agent 10 spectrum and no resonance due to residual tetrafunctional bromide precursor is observed. Furthermore, ^{1}H NMR spectrum of RAFT agent 10 (Figure 2.46-II) revealed an integration ratio of 1:1 for the CH_2 (**D**) of the *O*-ethyl moiety to the CH_2 (**C**) of the core structure, as expected. This indicates that four arms are present within the structure.

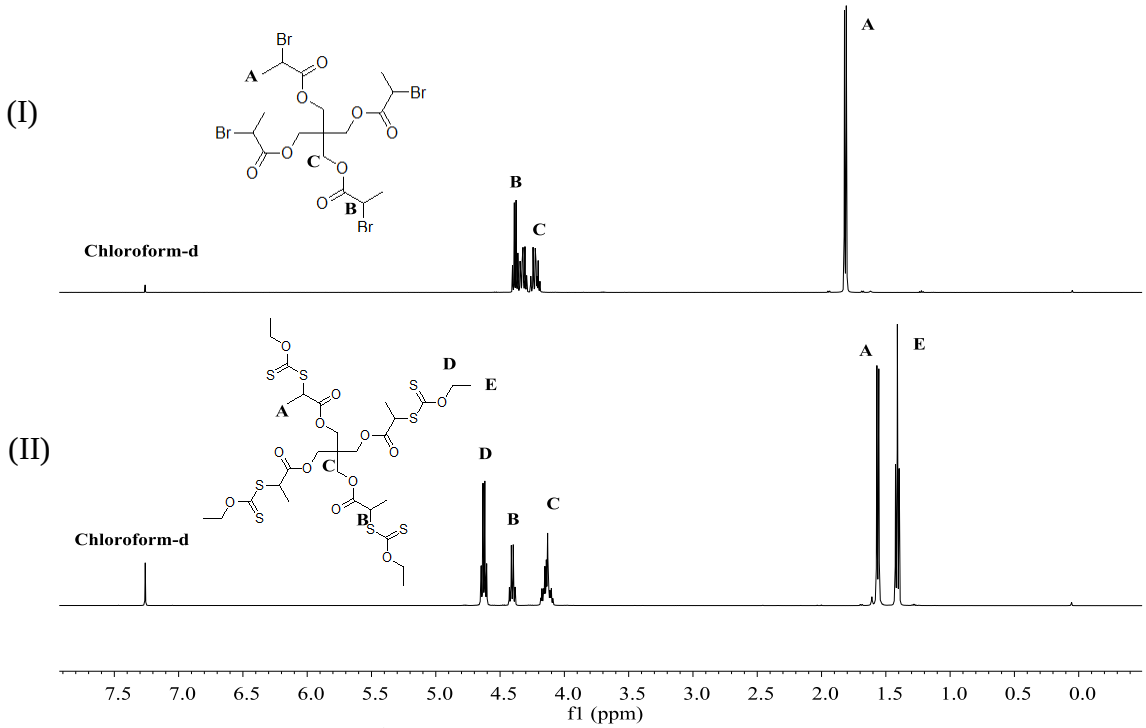

Figure 2.46. 500 MHz-^{1}H NMR spectra of (I) 2-bromopropionic acid 3-(2-bromo-propionyloxy)-2,2-bis-(2-bromo-propionyloxymethyl)-propyl ester, (II) (2-ethoxthiocarbonylsulfanyl-propionic acid 3-(2-ethoxythiocarbonylsulfanyl-propionyloxy)-2,2-bis-(2-ethoxythiocarbonylsulfanyl-propionyloxymethyl)-propyl ester) in $CDCl_3$

^{13}C NMR spectra of the tetrafunctional bromide precursor (I) and RAFT agent 10 (II) are compared in Figure 2.47. Figure 2.47-II shows the presence due to the resonances due to the carbonyl (**1**) group and the thiocarbonyl (**8**) group at 170.9 ppm and 212.1 ppm, respectively. The resonances due to the carbons of the tetrafunctional

bromide precursor are also present in the spectrum of RAFT agent 10 (**1** – **5**). The resonances due to CH_2 (**6**) and CH_3 (**7**) carbons of the *O*-ethyl moiety are present in the spectrum of RAFT agent 10 at 70.8 ppm and 13.9 ppm, respectively. The resonances due to CH (**3**) carbon of the methyl propionate moiety is shifted from 39.9 ppm to a higher value of 47.2 ppm in the spectrum of RAFT agent 10. This suggests that the xanthate functionality is attached to the core structure.

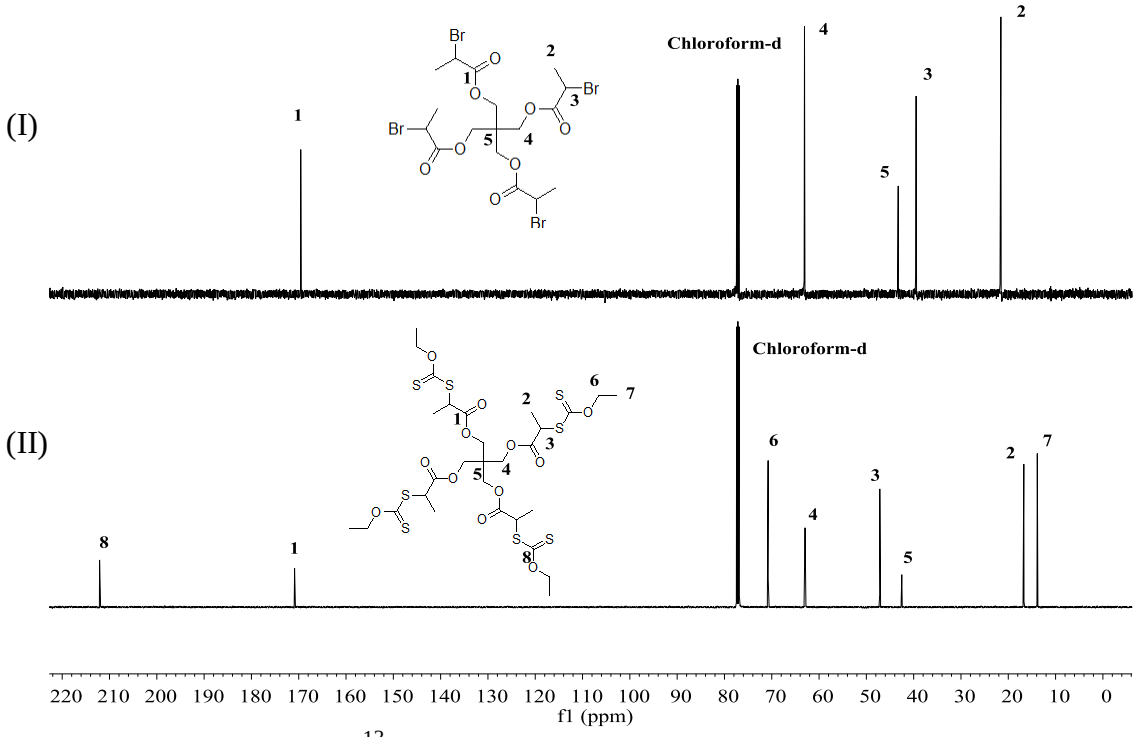

Figure 2.47. 126 MHz-^{13}C NMR spectra of (I) 2-bromopropionic acid 3-(2-bromo-propionyloxy)-2,2-bis-(2-bromo-propionyloxymethyl)-propyl ester, (II) (2-ethoxthiocarbonylsulfanyl-propionic acid 3-(2-ethoxythiocarbonylsulfanyl-propionyloxy)-2,2-bis-(2-ethoxythiocarbonylsulfanyl-propionyloxymethyl)-propyl ester) in $CDCl_3$

2.3.10. Synthesis of RAFT agent 11 (2,2'-oxybis(methylene)bis(2-ethylpropane-3,2,1-triyl) tetrakis(2-(ethoxycarbonothioylthio)propanoate))

RAFT agent 11 is a four armed RAFT agent with a central ether linkage and was also prepared in a two-step reaction. Initially Di(trimethylolpropane) was reacted with 2-bromopropionyl bromide to give a four armed bromide containing intermediate (Scheme 2.19). The intermediate product was synthesised in a yield of 53% and characterised by ^{1}H and ^{13}C NMR spectroscopy.

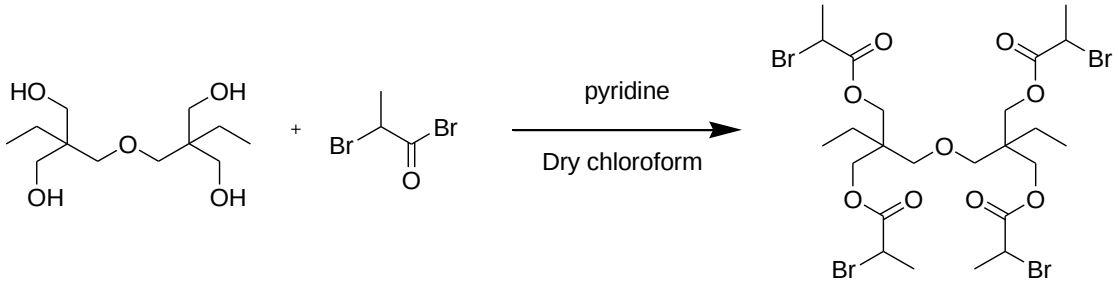

Scheme 2.19. Synthesis of 2-bromo-propionic acid 2-[2,2-bis-(2-bromo-propionyloxymethyl)-butoxymethyl]-2-(2-bromo-propionyloxymethyl)-butyl ester.

Comparison of ^{1}H NMR spectra of 2-bromopropionyl bromide (Figure 2.48-I) and tetrafunctional bromide precursor (Figure 2.48-II) shows the appearance of the resonances due to CH_2 (**C**), CH_2 (**E**), CH_2 (**F**) and CH_3 (**D**) of the central core in the spectrum of the tetrafunctional bromide precursor at 4.10, 1.48, 3.32 and 0.87 ppm, respectively. Di(trimethylolpropane) was insoluble in $CDCl_3$. The resonance due to the CH (**B**) in the 2-bromopropionyl bromide spectrum at 4.69 ppm is shifted to a lower value of 4.37 ppm in the tetrafunctional bromide precursor spectrum and no resonance due to the residual 2-bromopropionyl bromide is observed. Furthermore, ^{1}H NMR spectrum of the tetrafunctional bromide precursor (Figure 2.48-II) revealed an integration ratio of 1:2 for the CH_3 (**D**) protons of the core to the CH_3 (**A**) protons of the arms, as expected.

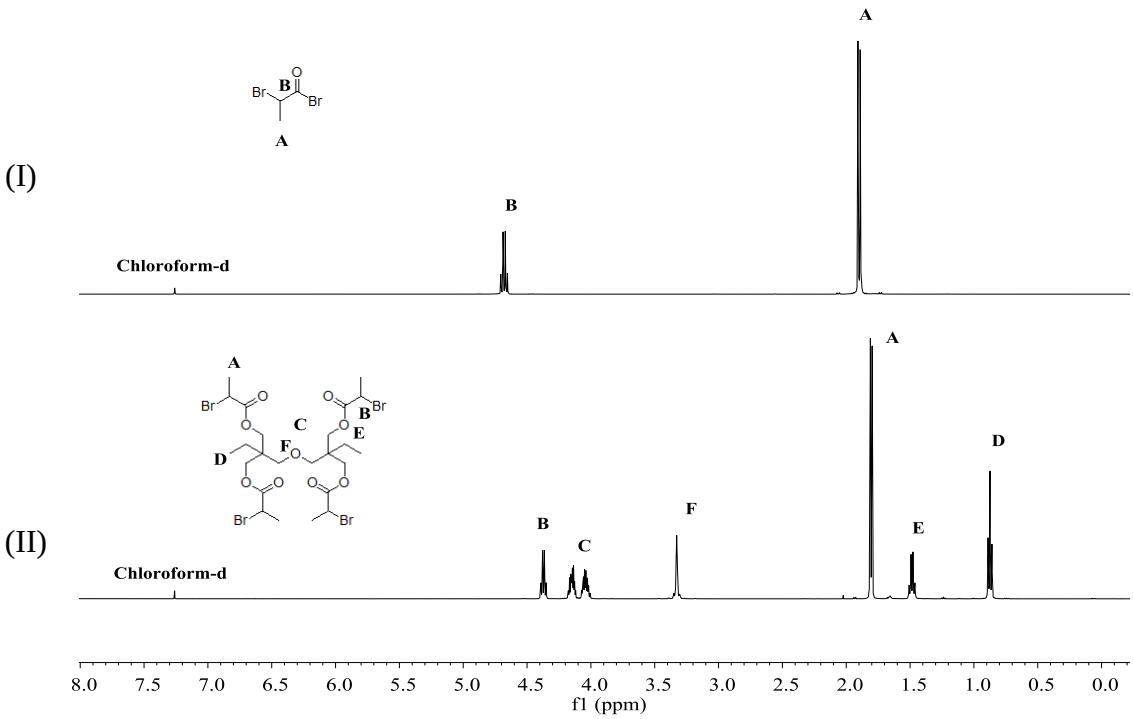

Figure 2.48. 500 MHz-^{1}H NMR spectra of (I) 2-bromopropionyl bromide, (II) 2-[2,2-bis-(2-bromo-propionyloxymethyl)-butoxymethyl]-2-(2-bromo-propionyloxymethyl)-butyl ester in $CDCl_3$

^{13}C NMR spectra of 2-bromopropionyl bromide (I) and the tetrafunctional bromide precursor (II) are compared in Figure 2.49. Figure 2.49-II shows the presence of the carbonyl group (**3**) of the methyl propionate at 170.0 ppm. The resonances due to the presence of CH_2 (**4**), CH_2 (**5**), CH_2 (**7**), CH_3 (**6**) and carbon (**8**) of the core in the spectrum of the tetrafunctional bromide precursor are present at 65.4, 23.1, 70.7, 7.7 and 40.2 ppm, respectively. The resonance due to the CH (**2**) and CH_3 (**1**) carbons of the methyl propionate moiety are also present in the spectrum at 42.5 ppm and 21.8 ppm, respectively. The resonance due to the CH (**2**) of the methyl propionate moiety is shifted from 52.7 ppm to a lower value of 42.5 ppm in the tetrafunctional bromide precursor (Figure 2.49-II). This suggests that the methyl propionate moiety is attached to the core structure.

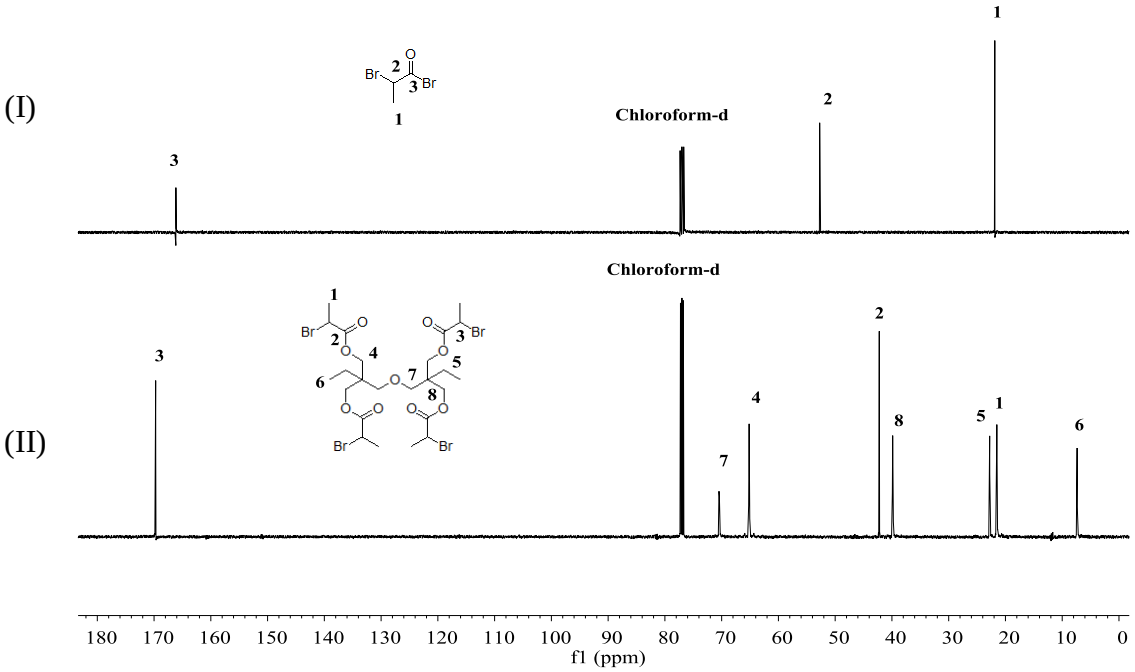

Figure 2.49. 126 MHz-^{13}C NMR spectra of (I) 2-bromopropionyl bromide, (II) 2-[2,2-bis-(2-bromo-propionyloxymethyl)-butoxymethyl]-2-(2-bromo-propionyloxymethyl)-butyl ester in $CDCl_3$

The second step in the synthesis of RAFT agent 11 was to react the tetrafunctional precursor with potassium *O*-ethyl xanthate (Scheme 2.20) to give the four armed RAFT agent in a yield of 78%. The final product was characterised by ^{1}H and ^{13}C NMR spectroscopy.

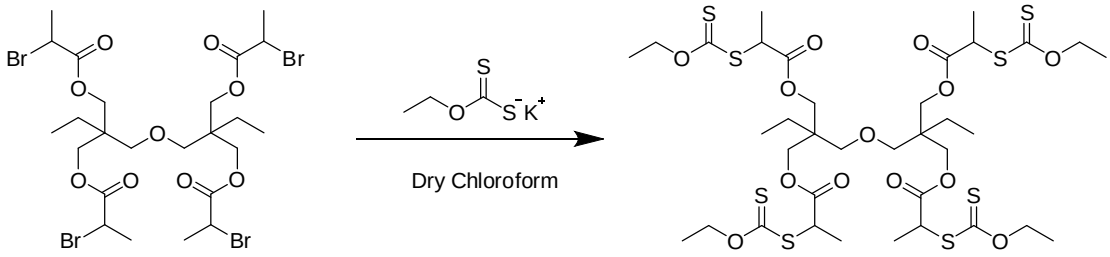

Scheme 2.20. Synthesis of 2,2'-oxybis(methylene)bis(2-ethylpropane-3,2,1-triyl) tetrakis(2-(ethoxycarbonothioylthio)propanoate).

Comparison of ^{1}H NMR spectra of the tetrafunctional bromide precursor (Figure 2.50-I) and RAFT agent 11 (Figure 2.50-II) shows the appearance of the resonances due to the CH_2 (**G**) and CH_3 (**H**) protons of the *O*-ethyl moiety in the spectrum of RAFT agent 11 at 4.63 ppm and 1.41 ppm, respectively. The resonances of the tetrafunctional

bromide precursor are also present in the spectrum of RAFT agent 11 (**A** – **F**). The resonances due to CH_3 (**A**) in tetrafunctional bromide precursor spectrum at 1.81 ppm is shifted to a lower value of 1.56 ppm in RAFT agent 11 spectrum and no resonance due to residual tetrafunctional bromide precursor is observed. Furthermore, ^{1}H NMR spectrum of RAFT agent 11 (Figure 2.49-II) revealed an integration ratio of 1:1 for the CH_2's (**G**) of the *O*-ethyl moiety to the CH_2 (**C**) of the core structure, as expected. This indicates that four arms are present within the structure.

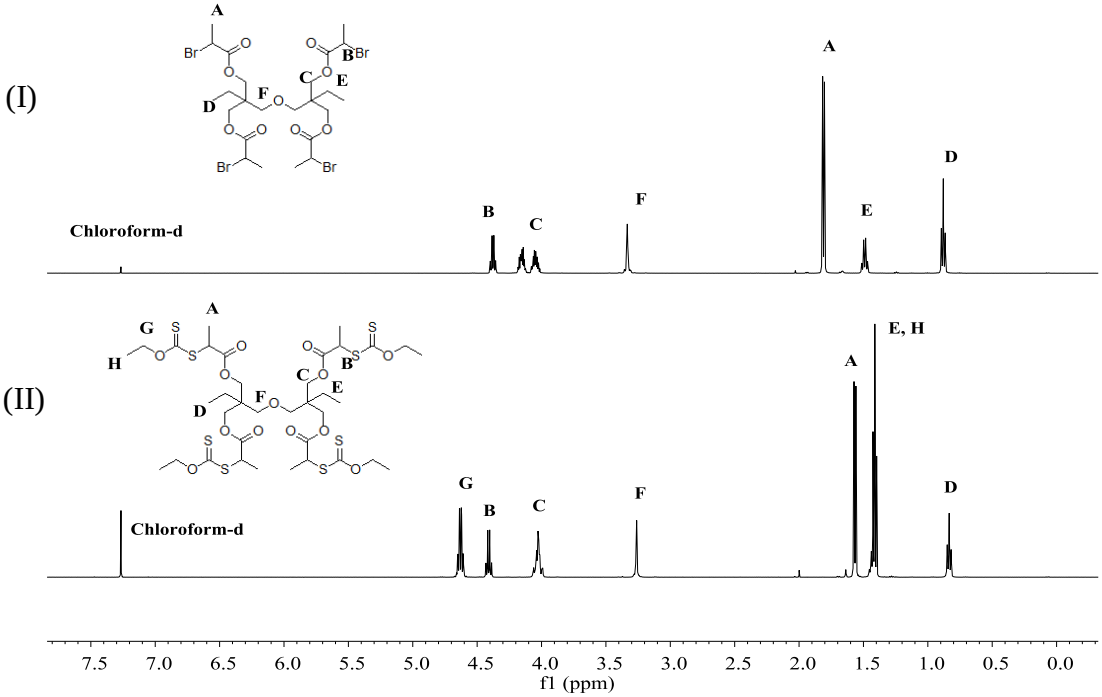

Figure 2.50. 500 MHz-^{1}H NMR spectra of (I) 2-[2,2-bis-(2-bromo-propionyloxymethyl)-butoxymethyl]-2-(2-bromo-propionyloxymethyl)-butyl ester, (II) 2,2'-oxybis(methylene)bis(2-ethylpropane-3,2,1-triyl) tetrakis(2-(ethoxycarbonothioylthio)propanoate) in $CDCl_3$

^{13}C NMR spectra of the tetrafunctional bromide precursor (I) and RAFT agent 11 (II) are compared in Figure 2.51. Figure 2.51-II shows the resonances of the carbonyl (**3**) group and the thiocarbonyl (**9**) group at 171.2 ppm and 212.3 ppm, respectively. The resonances due to the carbons of the trifunctional bromide precursor are also present in the spectrum of RAFT agent 11 (**1** – **8**). The resonances due to CH_2 (**10**) and CH_3 (**11**) carbons of the *O*-ethyl moiety are present in the spectrum of RAFT agent 11 at 70.6 ppm and 17.1 ppm, respectively. The CH (**2**) carbon of the methyl propionate moiety is shifted from 42.5 ppm to a higher value of 47.2 ppm in the

spectrum of RAFT agent 11. This suggests that the xanthate functionality is attached to the core structure.

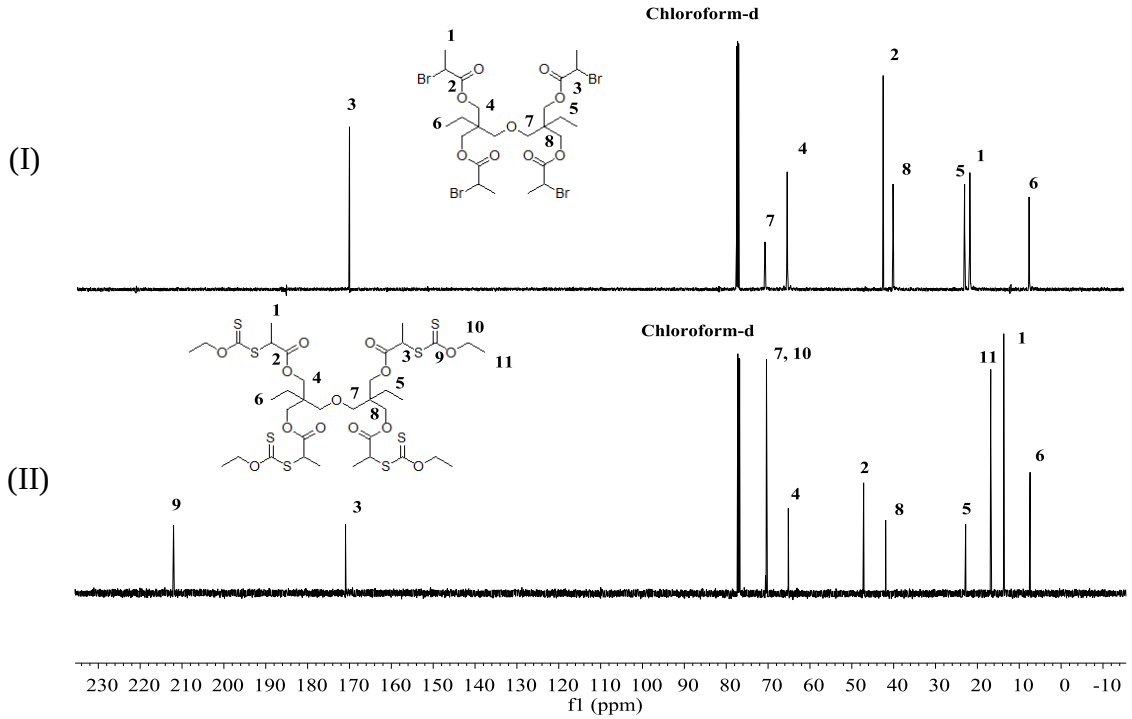

Figure 2.51. 151 MHz-^{1}H NMR spectra of (I) 2-[2,2-bis-(2-bromo-propionyloxymethyl)-butoxymethyl]-2-(2-bromo-propionyloxymethyl)-butyl ester, (II) 2,2'-oxybis(methylene)bis(2-ethylpropane-3,2,1-triyl) tetrakis(2-(ethoxycarbonothioylthio)propanoate) in $CDCl_3$

2.4. Summary

A number of RAFT agents have been prepared to control the polymerisation of "less activated" monomers. These CTA's will be used throughout this study. ^{1}H and ^{13}C NMR spectroscopy has been found useful to fully characterise the compounds made. All RAFT agents were prepared through nucleophilic substitution reactions to give pure compounds.

Several novel RAFT agents have been prepared in which a primary, secondary and tertiary radical will be produced upon fragmentation of the CTA. Each of the these RAFT agents incorporate a pyrrolidone ring in the structure of the leaving R group. In addition, a novel RAFT agent which forms a secondary radical upon fragmentation but where the Z group incorporates the pyrrolidone functionality has also been synthesised.

Three "star" RAFT agents have been synthesised with the aim of creating more complex polymer structures through the controlled polymerisation of LAMs. An R group approach has been used as this has been shown previously to tolerate hydrolytic conditions so that the architecture of the structure is not compromised.[24]

2.5. References

1. Barton, D. H. R.; McCombie, S. W. *Journal of the Chemical Society-Perkin Transactions 1* **1975**, (16), 1574-1585.
2. Quiclet-Sire, B.; Zard, S. Z. *Chemistry-a European Journal* **2006,** 12, (23), 6002-6016.
3. Perrier, S.; Takolpuckdee, P. *Journal of Polymer Science Part a-Polymer Chemistry* **2005,** 43, (22), 5347-5393.
4. Keddie, D. J.; Moad, G.; Rizzardo, E.; Thang, S. H. *Macromolecules* **2012,** 45, (13), 5321-5342.
5. Bouhadir, G.; Legrand, N.; Quiclet-Sire, B.; Zard, S. Z. *Tetrahedron Letters* **1999,** 40, (2), 277-280.
6. Wood, M. R.; Duncalf, D. J.; Rannard, S. P.; Perrier, S. *Organic Letters* **2006,** 8, (4), 553-556.
7. Skey, J.; O'Reilly, R. K. *Chemical Communications* **2008**, (35), 4183-4185.
8. Devasia, R.; Bindu, R.; Borsali, R.; Mougin, N.; Gnanou, Y. *Macromolecular Symposia* **2005,** 229, 8-17.
9. Destarac, M.; Charmot, D.; Franck, X.; Zard, S. Z. *Macromolecular Rapid Communications* **2000,** 21, (15), 1035-1039.
10. Mougin, N. Block ethylenic copolymers comprising a vinyllactam block, cosmetic or pharmaceutical compositions containing them and cosmetic use of these copolymers. 2006.
11. Wan, D. C.; Zhou, Q.; Pu, H. T.; Yang, G. J. *Journal of Polymer Science Part a-Polymer Chemistry* **2008,** 46, (11), 3756-3765.
12. Wan, D.; Satoh, K.; Kamigaito, M.; Okamoto, Y. *Macromolecules* **2005,** 38, (25), 10397-10405.
13. Nguyen, T.; Eagles, K.; Davis, T.; Barner-Kowollik, C.; Stenzel, M. *Journal of Polymer Science Part a-Polymer Chemistry* **2006,** 44, (15), 4372-4383.
14. Devasia, R.; Borsali, R.; Lecommandoux, S.; Bindu, R.; Mougin, N.; Gnanou, Y. *Abstracts of Papers of the American Chemical Society* **2005,** 230, U4231-U4232.
15. Gnanou, Y.; Devasia, R.; Bindu, R.; Mougin, N. *Abstracts of Papers of the American Chemical Society* **2005,** 230, U4144-U4145.
16. Pound, G.; Aguesse, F.; McLeary, J.; Lange, R.; Klumperman, B. *Macromolecules* **2007,** 40, (25), 8861-8871.

17. Pound, G.; Eksteen, Z.; Pfukwa, R.; McKenzie, J. M.; Lange, R. F. M.; Klumperman, B. *Journal of Polymer Science Part a-Polymer Chemistry* **2008,** 46, (19), 6575-6593.

18. Patel, V. K.; Mishra, A. K.; Vishwakarma, N. K.; Biswas, C. S.; Ray, B. *Polymer Bulletin* **2010,** 65, (2), 97-110.

19. Huang, C.; Yoon, J.; Matyjaszewski, K. *Canadian Journal of Chemistry-Revue Canadienne De Chimie* **2010,** 88, (3), 228-235.

20. Guinaudeau, A.; Mazieres, S.; Wilson, D. J.; Destarac, M. *Polymer Chemistry* **2012,** 3, (1), 81-84.

21. Brown, S. L.; Rayner, C. M.; Graham, S.; Cooper, A.; Rannard, S.; Perrier, S. *Chemical Communications* **2007**, (21), 2145-2147.

22. Lee, H.; Terry, E.; Zong, M.; Arrowsmith, N.; Perrier, S.; Thurecht, K.; Howdle, S. *Journal of the American Chemical Society* **2008,** 130, (37), 12242-12243.

23. Lisina, N.; Chernov, G.; Bizunov, Y.; Emelyanov, V.; Knunyants, I. *Khimiko-Farmatsevticheskii Zhurnal* **1988,** 22, (6), 705-710.

24. Bernard, J.; Favier, A.; Zhang, L.; Nilasaroya, A.; Davis, T. P.; Barner-Kowollik, C.; Stenzel, M. H. *Macromolecules* **2005,** 38, (13), 5475-5484.

Chapter 3
RAFT homopolymerisation of N-vinylpyrrolidone, vinyl acetate and N-vinylcaprolactam

3.1. Introduction

The work in this chapter focuses on the controlled homopolymerisation of "less activated" monomers (LAMs), in particular, N-vinylpyrrolidone (NVP), vinyl acetate (VAc) and N-vinylcaprolactam (NVCL). Until recently, the controlled polymerisation of these monomers has been reported to be difficult to achieve due to the lack of any conjugation in the structure of the monomers which allows the resonance stabilisation of the propagating radical. Hence, the propagating chains are highly reactive and prone to termination reactions. RAFT polymerisation using xanthates and dithiocarbamates as chain transfer agents (CTAs) has been employed to control the polymerisation of LAMs.[1-3]

In the work presented here, the RAFT agents synthesised in Chapter 2 were used for the polymerisation of NVP, VAc and NVCL to demonstrate control of the molecular weight and polydispersity of the resulting polymers. ^{1}H NMR spectroscopy and size exclusion chromatography (SEC) analysis were used to characterise the homopolymers produced.

3.1.1. Polymerisation of N-vinylpyrrolidone *via* RAFT

NVP can be considered as an unconjugated monomer as the π-electrons of the vinyl bond are not conjugated to the carbonyl group. The first report of a successful controlled polymerisation of NVP by RAFT showed that diphenyldithiocarbamate of diethylmalonate (DPCM) in 1, 4 dioxane at 80°C gave polymers with low PDI.[4] Using NVP:DPCM ratios of 50:1 – 400:1, molecular weights of 4.2 x 10^3 – 4.58 x 10^4 gmol^{-1} with PDI's of 1.2 – 1.4 were reported. Furthermore, the found molecular weights were found to be close to that of the theoretical M_n. The conversion of monomer to polymer was 61% after a polymerisation time of 24 h with a NVP:DPCM ratio of 50:1, which was found to increase to 85% after a polymerisation time of 37 h with a NVP:DPCM ratio of 200:1. However, the conversion of monomer to polymer was found to decrease to 75% after 49 h as the NVP:DPCM ratio was increased further to 400:1. In a separate communication, the same group also used *S*-(2-propionic acid methyl ester)-*O*-ethyl xanthate (Rhodixan® A1) as a RAFT agent and reported PNVP with molecular weights of 8.0 x 10^3 – 5.3 x 10^4 gmol^{-1} with PDI's of 1.3 - 1.7. The conversion of monomer to polymer ranged from 60 to 80%.[5]

A range of RAFT agents in fluoroalcohols have also been used to simultaneously control the tacticity and molecular weight distribution of PNVP.[6] It was reported that the dithioester, phenethyl dithiobenzoate inhibited the polymerisation of NVP (no polymerisation for at least 108 h), whereas *O*-ethyl xanthates, produced PNVP with low PDI (< 1.4). A greater control over the polymerisation was found at 60°C in bulk when the R group was a benzyl rather than a phenethyl moiety. The M_n of PNVP when the R group was a benzyl moiety was 1.69 x 10^4 $gmol^{-1}$ with a PDI of 1.26. The conversion of monomer to polymer was 80%. When a phenethyl moiety was used as the R group, the molecular weight was 1.24 x 10^4 $gmol^{-1}$ with a PDI of 1.47. The conversion of monomer to polymer was reported to be lower at 68%. The found molecular weights were reported to be in good agreement with the theoretical molecular weights.

Moad *et al*.[1] have reported that NVP could be polymerised in methanol at 60°C *via* RAFT using *O*-ethyl *S*-(cyanomethyl) xanthate giving PNVP with a PDI of 1.35 and a M_n of 1.7 x 10^4 $gmol^{-1}$. The monomer to polymer conversion was reported to be low at 53% after a reaction time of 8.5 h.

Dithioesters and trithiocarbonates have also been used as RAFT agents for the polymerisation of NVP at 80°C in bulk, DMF, THF and water.[7] The level of control over the polymerisation was found to be very poor and PDI's ranged from 1.5 to 2.3.

The synthesis of PNVP in bulk at 60°C using *O*-ethyl-*S*-(1-benzyl) dithiocarbonate as RAFT agent has been reported with PDI's less than 1.45.[8] It was reported that a benzyl R group gave polymers with higher molecular weights than expected at lower conversions, which was attributed to hybrid behaviour.

NVP has been polymerised using a phthalimidomethyl trithiocarbonate based RAFT agent in bulk at 60°C.[9] This resulted in an inhibition period, during which the reaction mixture was decolourised and oligomers were formed upto a reaction time of 8 h, suggesting the consumption of the RAFT agent during this time. When the ratio of NVP:RAFT agent was 151:1, the M_n was found to be 2.7 x 10^4 $gmol^{-1}$ with a PDI of 1.61. The found M_n was far greater to that of the theoretical of 9.4 x 10^3 $gmol^{-1}$. The monomer to polymer conversion was only 48% after 16 h. The inhibition period was attributed to the relative stability of the RAFT intermediate. The group has also used *S*-phthalimidomethyl *O*-ethyl xanthate as a RAFT agent in the polymerisation of NVP, which showed no apparent inhibition period in toluene at 60°C. When a ratio of NVP:RAFT agent of 71:1, the M_n of the resulting PNVP was found to be 8.6 x 10^3 $gmol^{-1}$ with a PDI of 1.16. The found M_n was close to that of the theoretical of 7.6 x

10^3 gmol^{-1}. The conversion of monomer to polymer was 98% after a reaction time of 24 h. However, when the ratio of NVP:RAFT agent was increased to 517:1 the M_n of the resulting PNVP was 1.85 x 10^4 gmol^{-1} with a PDI of 1.54. The found M_n was far lower to that of the theoretical of 3.05 x 10^4 gmol^{-1}. The conversion of monomer to polymer was only 53% after a reaction time of 24 h.

Pound *et al.*[10] compared the polymerisation of NVP using three *O*-ethyl xanthates with various R groups as RAFT agents. *In situ* ^{1}H NMR spectroscopy in C_6D_6 at 70°C was used to follow the concentration of monomer and xanthate throughout the polymerisation. The nature of the R group was reported to be the determining factor in the initialisation process of the polymerisation. When the R group of the xanthate RAFT agent was a cyanoisopropyl, during the first 275 min of reaction time, only a single monomer insertion was observed followed by the formation of higher molecular weight polymer. When a *tert*-butyl was used as the R group, simultaneous formation of oligomers was observed. This was attributed to the propagating monomer radicals being a better leaving group to that of the *tert*-butyl R group. However, when 2-carboxyethyl was used as the R group, significant side reactions were observed. The 2-carboxyethyl radicals were found to have similar reactivity to that of the propagating monomer radicals, indicating hybrid behaviour. The three RAFT agents were also used to polymerise NVP in bulk at 60°C for 6 h using a NVP:RAFT agent ratio of 450:1. In the cases when a cyanoisopropyl or 2-carboxyethyl R group was used, the conversions were low at 27% and 26%, respectively. The experimental molecular weights were found to be close to the theoretical M_n and PDI's were low at 1.32 - 1.34. However, when a *tert*-butyl R group was used, a broad PDI of 1.74 was reported with a conversion of monomer to polymer of 48% and M_n of 3.19 x 10^4 gmol^{-1} which was greater than the theoretical M_n of 2.42 x 10^4 gmol^{-1}.

The formation of side products during the RAFT polymerisation of NVP have been investigated in the presence of six *O*-ethyl xanthates.[11] A summary of the side products are summarised in Scheme 3.1. The side reactions involving NVP are shown in Scheme 3.1-i. Route (a) describes the hydrolysis of NVP to give 1-(1-hydroxy-ethyl)-pyrrolidone which further decomposes to give acetaldehyde and pyrrolidone which can react with NVP to form 1, 1-bis(N-pyrroldionyl)-ethane. The decomposition of 1-(1-hydroxy-ethyl)-pyrrolidone also gives a dimeric hydration product. *In situ* ^{1}H NMR spectroscopy experiments in C_6D_6 at 70°C were conducted in the presence of RAFT agents which either had carboxylic acid or hydroxyl functionalities and dimerisation of NVP was observed, with or without the presence of a

radical source (Scheme 3.1, b). Moreover, it was reported that alkyl halides also catalyse NVP dimerisation. Alkyl halides are generally used in the synthesis of xanthate RAFT agents and therefore any residual starting material can catalyse the dimerisation of NVP.

The side products generated during the RAFT polymerisation of NVP involving xanthate functionality are shown in Scheme 3.1-ii.[11] Route (a) describes the side products due to the elimination of the xanthate moiety from single monomer insertions or polymeric species. This resulted in the formation of unsaturated chain ends and it was reported that xanthic acid may form as a result of the labile C – S bond breaking at the chain end and eliminating the sulphur moiety. Route (b) shows the formation of a new xanthate species through the reaction of xanthic acid and NVP.

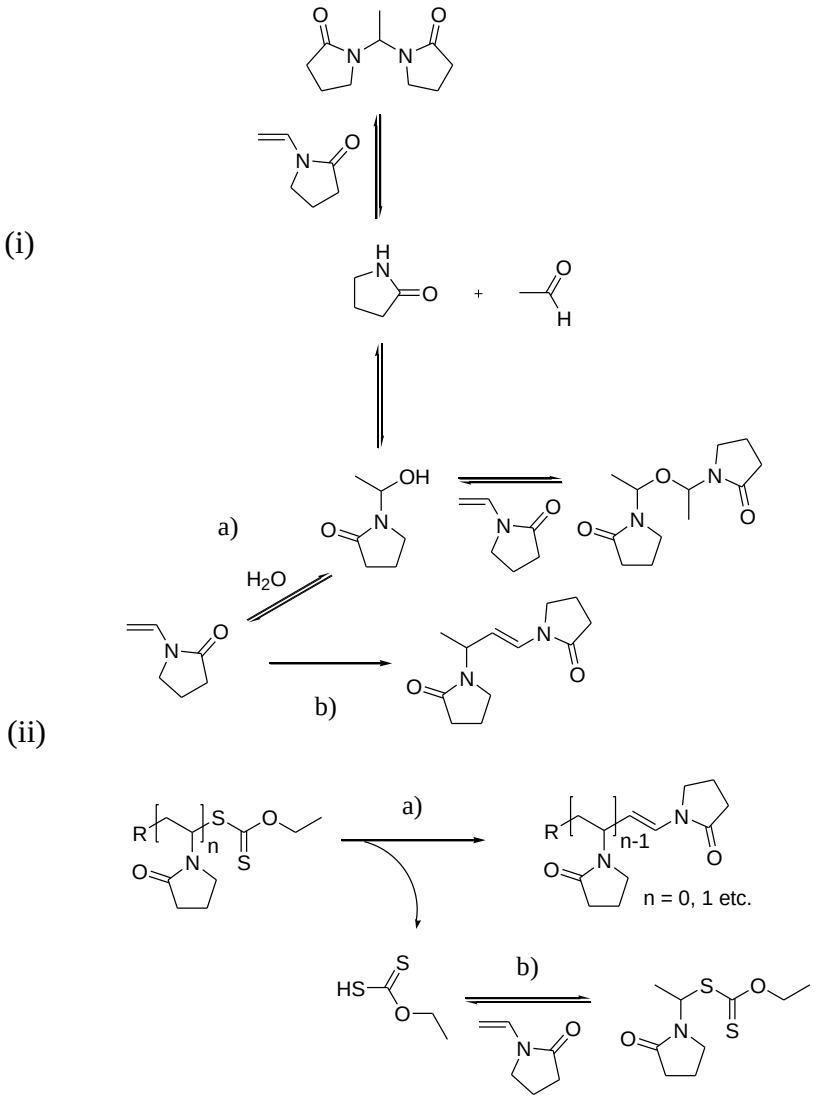

Scheme 3.1. Summary of side reaction products of, (i) NVP, (ii) PNVP-xanthate

Benaglia *et al.*[12] have reported the synthesis of a "universal (switchable) RAFT agent" which can control the polymerisation of both MAMs and LAMs. This was achieved by modifying the electronic properties of the dithiocarbamate nitrogen by protonation / deprotonation. The deprotonated RAFT agent was reported to control the polymerisation of NVP in acetonitrile at 60°C. When the ratio of NVP:RAFT agent was 374:1, the M_n by GPC was found to be 2.9 x 10^4 $gmol^{-1}$ with a PDI of 1.19. The found M_n was relatively close to that of the theoretical of 3.5 x 10^4 $gmol^{-1}$. The conversion of monomer to polymer was reported to be 83% after the polymerisation time of 16 h.

Commercially available isopropylxanthic disulfide (DIP), an example of a xanthogen disulphide, has been used as a RAFT agent precursor to mediate the polymerisations of NVP.[13] DIP reacts with azo initiator (AIBN) to form *S*-(cyano)isopropyl xanthate *in situ,* generating two RAFT agents. The polymerisation of NVP was conducted in 2-propanol at 60°C, 70°C and 80°C using a ratio of 400:1:2 (NVP:DIP:AIBN). Molecular weights of 7.8 x 10^3 – 1.28 x 10^4 $gmol^{-1}$ and PDI's of 1.22 – 1.28 were reported. The found molecular weights were close to those of the theoretical M_n, at all temperatures. The conversion of monomer to polymer ranged from 37% to 65%. Increasing the ratio of NVP:DIP to 800:1 at 80°C led to a M_n of 2.45 x 10^4 $gmol^{-1}$ and a broader PDI of 1.51. The found M_n was significantly lower to that of the theoretical M_n of 4.43 x 10^4 $gmol^{-1}$. The conversion of monomer to polymer was higher at 99.9% after a polymerisation time of 2 h.

More recently Guinaudeau *et al.*[14] have reported the polymerisation of NVP at ambient temperature by RAFT in aqueous solution. The polymerisation was initiated by the redox reaction consisting of *tert*-butyl hydroperoxide / ascorbic acid, using Rhodixan® A1 as the RAFT agent. When the ratio of NVP:RAFT agent was 33:1, the M_n by GPC was found to be 5.5 x 10^3 $gmol^{-1}$ and PDI of 1.15. The found M_n was close to that of the theoretical M_n of 3.6 x 10^3 $gmol^{-1}$. The conversion of monomer to polymer was reported to be 93% after a reaction time of 24 h. When the ratio of NVP:RAFT agent was increased to 89:1, the M_n was found to be 1.46 x 10^4 $gmol^{-1}$ and a broader PDI of 1.30. The found M_n was larger than that of the theoretical of 9.6 x 10^3 $gmol^{-1}$. The conversion of monomer to polymer was reported to be 97% after a reaction time of 24 h. As the ratio of NVP:RAFT agent was increased again to 177:1, the M_n by GPC was found to be 1.7 x 10^4 $gmol^{-1}$ and PDI of 1.25. The found M_n was close to that of the theoretical of 1.8 x 10^4 $gmol^{-1}$. The conversion of monomer to polymer was

reported to be 89% after 24 h. No side products were formed from the reactions between NVP and water.

3.1.2. Polymerisation of vinyl acetate *via* RAFT

VAc is also a "less activated" monomer as there is no conjugation with the double (vinyl) bond and carbonyl group. This makes the VAc propagating radical extremely reactive and the chain propagation rate is extremely fast. Therefore, the monomer is more susceptible to chain transfer and termination meaning controlling the polymerisation is harder to achieve. RAFT agents based around dithiocarbamates and xanthates have been reported to give the most successful results.

The first report of RAFT of VAc was published in 2000 by Rizzardo *et al.*[15] The polymerisation of VAc was reported to be inhibited in the presence of dithioesters and trithiocarbonates, whereas *O*-ethyl xanthates and dithiocarbamates were reported to control the polymerisation of VAc in either bulk or ethyl acetate at temperatures ranging from 60 to 100°C. When VAc was polymerised in the presence of an *O*-ethyl xanthate with a cyanomethyl R group at 80°C in bulk with a VAc:RAFT agent ratio of 670:1, the M_n was found to be 4.7 x 10^4 gmol^{-1} with a PDI of 1.62. The found M_n was in good agreement to that of the theoretical of 4.98 x 10^4 gmol^{-1}. The conversion of monomer to polymer was reported to be 88% after a reaction time of 18.5 h. An N-aryl, N-dialkyl dithiocarbamate with a cyanomethyl R group was used to mediate the polymerisation of VAc in ethyl acetate at 75°C. When the ratio of VAc:RAFT agent was 143:1, the M_n was found to be 1.34 x 10^4 gmol^{-1} with a PDI of 1.29. The found M_n was close to that of the theoretical of 1.14 x 10^4 gmol^{-1}. The conversion of monomer to polymer was reported to be 93% after a reaction time of 24 h. When, a similar VAc:RAFT agent ratio was used under the same conditions for an N, N-dialkyl dithiocarbamate RAFT agent, similar M_n was obtained but PDI was broader (PDI = 1.50), indicating that the N-aryl, N-alkyl dithiocarbamate provides better control than the N, N-dialkyl dithiocarbamate. This was attributed to the phenyl group reducing the electron density on the nitrogen atom. The conversion of monomer to polymer was reported to be 95% after a reaction time of 24 h. In addition, however, when a pyrrolidone ring was used as the Z group on the dithiocarbamate, there was inhibition in the polymerisation of VAc.

When VAc was polymerised in the presence of DPCM in bulk at 80°C, the M_n was found to be 4.9 x 10^3 gmol^{-1} with a PDI of 1.56.[16] The found M_n was in good agreement to that of the theoretical of 5.4 x 10^3 gmol^{-1}. The conversion of monomer to

polymer was 73% after a polymerisation time of 7.25 h. Under the same conditions, when the aromatic groups in the Z group were replaced with alkyl chains, similar M_n was observed, however the PDI was broader (PDI = 1.82). The conversion of monomer to polymer was 68% after a polymerisation time of 7.25 h.

Stenzel *et al.*[17] have mediated the controlled bulk polymerisation of VAc with a number of xanthates at 60°C. The R group was kept constant throughout the study and the Z group was systematically changed. All the RAFT agents studied showed inhibition periods and rate retardation. This was attributed to the slow fragmentation of the radical intermediate in the pre-equilibrium and main equilibrium. Methyl (4-methoxyphenoxy)-carbonothiosulfanyl acetate, methyl (methoxycarbonothioyl)sulfanyl acetate, methyl (ethoxycarbonothioyl)sulfanyl acetate and methyl (isopropoxycarbonothioyl)sulfanyl acetate were reported to give PNVP with low PDI (< 1.2) However, when methyl (*tert*-butoxycarbonothioyl)sulfanyl acetate was used as the RAFT agent there was total inhibition and no polymer was formed, even after 48 h.

VAc has also been polymerised in the presence of a xanthate with a phthalimidomethyl R group.[9] *S*-phthalimidomethyl *O*-ethyl xanthate was reported to give good control over the polymerisation of VAc in bulk at 60°C. When the ratio of VAc:RAFT agent was 109:1, the M_n was found to be 8.8 x 10^3 $gmol^{-1}$ with a PDI of 1.31. The found M_n was in relatively good agreement to that of the theoretical of 1.09 x 10^4 $gmol^{-1}$. The conversion of monomer to polymer was 77% after a reaction time of 16 h. When the temperature was increased to 100°C, after 16 h the conversion of monomer to polymer was increased to 88%, M_n increased to 1.1 x 10^4 $gmol^{-1}$ but a broader PDI of 1.65 was observed. Moreover, the M_n found was in good agreement to that of the theoretical of 1.25 x 10^4 $gmol^{-1}$.

Pound *et al.*[10] have reported the controlled polymerisation of VAc in the presence of three *O*-ethyl xanthates with various R groups. *In situ* ^{1}H NMR spectroscopy in C_6D_6 at 70°C was used to follow the concentration of monomer and xanthate throughout the polymerisation. When a cyanoisopropyl functionality was used as the R group there was total inhibition and no polymer was formed. This was attributed to the slow rate of addition of the cyanoisopropyl R group radicals towards VAc. When a *tert*-butyl moiety was used as the R group, oligomeric products were formed simultaneously with single monomer insertion products. This was attributed to the propagating monomer radicals have a better leaving group ability over the *tert*-butyl group. When a 2-carboxyethyl group was used as the R group it was observed that

during the first 25 min of reaction time only single monomer insertion products were formed, followed by higher molecular weight polymer. The three RAFT agents were also used to polymerise VAc in bulk at 60°C in a VAc:RAFT agent ratio of 450:1. In the case when a cyanoisopropyl moiety was used as R group the conversion of monomer to polymer was less than 1% after 22 h. When a *tert*-butyl R group was used, the M_n was found to be 2.15 x 10^4 $gmol^{-1}$ with a PDI of 1.43. The conversion of monomer to polymer was 54% after a reaction time of 3.5 h. When a 2-carboxyethyl R group was used, the M_n was 9.7 x 10^3 $gmol^{-1}$ with a PDI of 1.26. The conversion of monomer to polymer was 28% after a reaction time of 3.5 h. The found M_n was close to that of the theoretical M_n for PVAc obtained from RAFT agents containing *tert*-butyl or 2-carboxyethyl R groups.

The controlled polymerisation of VAc at 60°C in bulk using dithiocarbonic acid *S*-benzyl ester *O*-isopropyl ester has been reported.[18] When the ratio of VAc:RAFT agent was 100:1, the M_n was found to be 3.9 x 10^3 $gmol^{-1}$ with a PDI of 1.17. The found M_n was found to be very close to that of the theoretical of 3.85 x 10^3 $gmol^{-1}$. The conversion of monomer to polymer was reported to be 45% after 22 h. Skey *et al.*[19] have also used the same RAFT agent in bulk using the same VAc:RAFT agent ratio. However, the polymerisation was conducted at 80°C and the M_n was found to be 8.7 x 10^3 $gmol^{-1}$ with a PDI of 1.43. The found M_n was very close to that of the theoretical of 8.9 x 10^3 $gmol^{-1}$. The conversion of monomer to polymer was reported to be over 99% after a polymerisation time of 13 h. Therefore, the increase in temperature from 60°C to 80°C increased the conversion as well as broadening the PDI.

Benaglia *et al.*[12] have reported the synthesis of a "universal (switchable) RAFT agent" to control the polymerisation of VAc. When the ratio of VAc:RAFT agent was 138:1, the M_n was found to be 8.9 x 10^3 $gmol^{-1}$ and PDI of 1.24. The found M_n was greater than that of the theoretical M_n of 6.4 x 10^3 $gmol^{-1}$. The conversion of monomer to polymer was only 54% after a reaction time of 72 h, indicating a severe inhibition period.

Isopropylxanthic disulfide (DIP) has been used as a RAFT agent precursor to mediate the polymerisation of VAc.[13] As discussed in the previous section, DIP reacts with azo initiator (AIBN) to form *S*-(cyano)isopropyl xanthate *in situ*, generating two RAFT agents. The polymerisation of VAc was conducted in THF at 60°C, 70°C and 80°C using a ratio of 100:1:1 (VAc:DIP:AIBN). Molecular weights ranged from 3.1 x 10^3 to 7.6 x 10^3 $gmol^{-1}$ and PDI's broadened as temperature increased (1.30 – 1.55). The found molecular weights were reported to be greater than those of the theoretical

M_n. The conversion of monomer to polymer ranged from 25% to 83%. Increasing the ratio of VAc:DIP to 200:1 at 80°C led to a M_n of 4.7 x 10^3 $gmol^{-1}$ and a broader PDI of 1.82. The found M_n was reported to be lower to that of the theoretical of 6.2 x 10^3 $gmol^{-1}$. The conversion of monomer to polymer was 70% after a reaction time of 3.5 h.

Recently, Patel *et al.*[20] have reported the controlled polymerisation of VAc using two RAFT agents; (*S*)-2-(ethyl propionate)-(*O*-ethyl xanthate) and (*S*)-2-(ethyl isobutyrate)-(*O*-ethyl xanthate). For (*S*)-2-(ethyl propionate)-(*O*-ethyl xanthate) as RAFT agent, the ratio of VAc:RAFT agent of 100:1 at 60°C in bulk was used. The M_n was found to be 7.4 x 10^3 $gmol^{-1}$ with a PDI of 1.30 and the found M_n was lower than that of the theoretical of 1.35 x 10^4 $gmol^{-1}$. The conversion of monomer to polymer was reported to be 87% after a reaction time of 3 h. For (*S*)-2-(ethyl isobutyrate)-(*O*-ethyl xanthate) as RAFT agent under similar conditions, the M_n by GPC was found to be 1.36 x 10^3 $gmol^{-1}$ with a PDI of 1.35 and M_n was lower to that of the theoretical of 6.2 x 10^3 $gmol^{-1}$. The conversion of monomer to polymer was reported to be 67% after a reaction time of 4 h. As the VAc:RAFT agent ratio was increased for both RAFT agents the PDI also increased.

3.1.3. Polymerisation of N-vinylcaprolactam *via* RAFT

In comparison with NVP and VAc, NVCL has received little attention in relation to its controlled polymerisation by RAFT or by any other radical method. NVCL contains a lactam ring where the vinyl bond is connected through the nitrogen atom. Like NVP, NVCL is also "less activated" as the vinyl bond has no conjugation to the carbonyl group.

The first report of the controlled polymerisation of NVCL was published in 2005 by Devasia *et al*,[21] using Rhodixan® A1 as the RAFT agent in 1, 4 dioxane at 80°C. When the ratio of NVCL:RAFT was 100:1, the M_n was found to be 9.6 x 10^3 $gmol^{-1}$ and PDI of 1.31. The found M_n was in relatively good agreement with the theoretical of 1.16 x 10^4 $gmol^{-1}$. The conversion of monomer to polymer was 83% after a reaction time of 15 h. However, when the NVCL:RAFT agent ratio was increased to 350:1, the M_n was found to be 3.3 x 10^4 $gmol^{-1}$ and PDI increased to 1.65. The found M_n was lower than the theoretical M_n of 4.1 x 10^4 $gmol^{-1}$. The conversion of monomer to polymer was 84% after a reaction time of 12 h.

The controlled RAFT polymerisation of NVCL using several RAFT agents based on dithiocarbamates and xanthates has been reported.[22]

2-diphenylthiocarbamoylsulfanyl-2-methyl-propionic acid was used as RAFT agent to control the polymerisation of NVCL in bulk at 60°C. When the ratio of NVCL:RAFT agent was 150:1, the M_n was found to be 5.0 x 10^3 $gmol^{-1}$ with a PDI of 1.46. The found M_n was significantly lower to that of the theoretical of 1.05 x 10^4 $gmol^{-1}$. The conversion of monomer to polymer was only 50% after a reaction time of 48 h. Furthermore, ((*O*-ethylxanthyl)methyl)benzene was also used as RAFT agent to control the polymerisation of NVCL under the same conditions and the M_n was found to be 4.2 x 10^3 $gmol^{-1}$ with a PDI of 1.48. The found M_n was reported to be far lower than that of the theoretical of 1.11 x 10^4 $gmol^{-1}$. The conversion of monomer to polymer was 52% after a reaction time of 16 h. (1-(*O*-ethylxanthyl)ethyl)benzene was used to control the polymerisation of NVCL under the same conditions and NVCL:RAFT agent ratio. The M_n was found to be 4.1 x 10^3 $gmol^{-1}$ with a PDI of 1.34. The found M_n was reported to be far lower to that of the theoretical of 1.08 x 10^4 $gmol^{-1}$. The conversion of monomer to polymer was 51% after a reaction time of 16 h.

The controlled polymerisation of NVCL using Rhodixan® A1 as RAFT agent has been reported.[23] The polymerisation of NVCL was conducted in 1, 4 dioxane at 60°C for 20 h. Several various NVCL:RAFT agent ratios (137:1 – 1121:1) were used to produce different molecular weight PNVCL. Molecular weights ranged from 1.8 x 10^4 to 1.5 x 10^5 $gmol^{-1}$ and PDI remained low throughout (1.1 – 1.2). Theoretical molecular weights were observed to correlate well with the found molecular weights. Monomer to polymer conversions were reported to increase from 83 – 97%.

More recently the polymerisation of NVCL has been reported by Shao *et al*,[24] using a trithiocarbonate (*S*-benzyl-*S*-(benzyl propionate) trithiocarbonate) and a dithiocarbamate (*N*, *N*-diethyl-*S*-(α, α′-dimethyl-α″-actetic acid) dithiocarbamate) as RAFT agents in bulk at 70°C. For *S*-benzyl-*S*-(benzyl propionate) trithiocarbonate as RAFT agent using the ratio of NVCL:RAFT agent of 200:1, the M_n was found to be 2.06 x 10^4 $gmol^{-1}$ with a PDI of 1.33. The found M_n was relatively close to that of the theoretical of 1.83 x 10^4 $gmol^{-1}$. The conversion of monomer to polymer was 64% after a reaction time of 60 h. For *N*, *N*-diethyl-*S*-(α, α′-dimethyl-α″-actetic acid) dithiocarbamate as RAFT agent using the ratio of NVCL:RAFT agent of 100:1, the M_n was found to be 7.2 x 10^3 $gmol^{-1}$ with a PDI of 1.15. The found M_n was reported to be close to that of the theoretical of 6.8 x 10^3 $gmol^{-1}$. The conversion of monomer to polymer was low at 47% after a reaction time of 25 h.

3.2. Experimental

3.2.1. Materials

N-vinylpyrrolidone (ISP) and vinyl acetate (Sigma Aldrich, ≥99%) were distilled under reduced pressure and stored under nitrogen at -4°C. N-vinylcaprolactam (ISP) was recrystallised from either pentane or hexane then distilled under reduced pressure and stored under nitrogen at -4°C. 4,4'-Azobis(4-cyanovaleric acid) (ACVA) (Sigma Aldrich, ≥98%), 2, 2'-Azobis(isobutyonitrile) (AIBN) (Sigma Aldrich) was recrystallized from methanol. 1,4 dioxane was dried over calcium hydride and distilled under reduced pressure. All dry polymerisation solvents, such as acetonitrile, toluene, tetrahydrofuran and dimethylformamide were obtained from the departments solvent purification system (SPS) - Purification grade (HPLC) solvent was pushed from its storage container under low argon pressure through two stainless steel columns containing activated alumina or copper catalyst depending on solvent used. Trace amounts of water were removed by the alumina, producing a dry solvent. In addition, deoxygenated solvent was achieved when it was suitable for a copper catalyst column to be used. Water content values - DCM < 25.1ppm, DMF < 735.1ppm, Toluene < 21.3ppm, THF < 35.7 ppm, Chloroform < 20.9ppm, Diethyl ether < 19.1ppm, Hexane < 7.6 ppm and Acetonitrile < 8.7ppm. All other solvents were analytical grade and used without any purification.

3.2.2. Characterisation Techniques

Nuclear Magnetic Resonance (NMR) Spectroscopy – ^{1}H NMR was performed on a Bruker Avance-400MHz, Varian iNova-500 or VNMRS 700. ^{1}H NMR spectra were recorded at either 400, 500 or 700MHz. Samples of polymers were analysed in deuterated chloroform ($CDCl_3$ - Sigma-Aldrich) or DCM (CD_2Cl_2 – Goss Scientific). The following abbreviations are used in listing NMR spectra: s = singlet, d = doublet, t = triplet, q = quartet, quin = quintet, m = multiplet, b = broad.

Size exclusion chromatography (SEC) analysis on PNVP and PNVCL was carried out using a Viscotek TDA 302 with triple detection (refractive index, viscosity and light scattering), using 2 x 300ml PLgel 5μm C columns and DMF (containing 0.1% w/v LiBr) as the eluent at a flow rate of 1ml/min (70°C). The system was calibrated using polystyrene standards. A value of 0.099 mL/g was used for the dn/dc

of PNVP. SEC analysis on PVAc was carried out on a Viscotek TDA 302 with triple detection (refractive index, viscosity and light scattering), using 2 x 300ml PLgel 5µm C columns using THF as the eluent at a flow rate of 1ml/min (35°C). The system was calibrated with polystyrene standards. A value of 0.058 mL/g was used for the dn/dc of PVAc.

3.2.3. Calculating conversion of monomer to polymer using ^{1}H NMR spectroscopy

Conversion of NVP to PNVP was determined by calculating the amount of residual monomer left in the ^{1}H NMR spectrum of the polymerisation mixture. An example is shown in Figure 3.1.

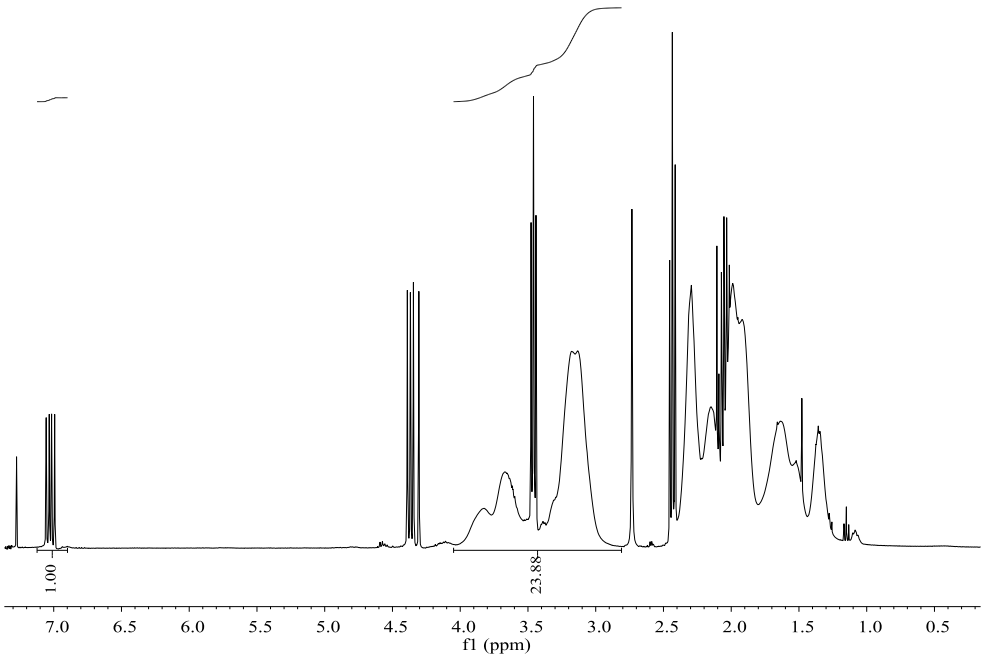

Figure 3.1. 400 MHz-^{1}H NMR of a typical PNVP polymerisation mixture

The amount of residual monomer in NVP RAFT polymerisations were obtained by integrating the resonance due to NVP at 7.0 ppm (C***H***=CHH), against the overlapping resonances due to NVP at 3.5 ppm (C***H***$_2$N) and PNVP between 2.8 – 4.0 ppm (C***H***$_2$NC***H***).[9] An alternative method also used, was to compare the integrals of the resonance due to NVP at 7.0 ppm (C***H***=CHH), against the resonance due to PNVP at 2.8 – 3.4 ppm (C***H***$_2$NCH) only.[25, 26]

3.2.4. RAFT polymerisation of N-vinylpyrrolidone using RAFT agent 1

3.2.4.1. In bulk

To a 50 ml Schlenk tube containing a magnetic stirrer bar, was added NVP (10.5 g, 10.0 ml, 94.5 mmol), RAFT agent 1 (240 mg, 5.95 x 10^{-1} mmol) and AIBN (20.0 mg, 1.22 x 10^{-1} mmol). The polymerisation mixture was thoroughly degassed by four freeze pump thaw cycles. The flask was back-filled with nitrogen gas, sealed, placed into an oil bath, heated to 80°C and stirred for 43 h. The flask was allowed to cool to ambient temperature. Dichloromethane (20 ml) was added to dissolve the reaction mixture and the resulting solution was added dropwise into diethyl ether. A white precipitate was immediately formed which was subsequently filtered and dried under reduced pressure at 40°C to give a white solid, (7.40 g). The yield was measured gravimetrically to be 71%. SEC: M_n = 1.37 x 10^4 gmol^{-1}, M_w = 1.61 x 10^4 gmol^{-1}, PDI = 1.17.

3.2.4.2. In 1, 4 dioxane

To a 50 ml Schlenk tube containing a magnetic stirrer bar, was added NVP (2.09 g, 2.00 ml, 18.8 mmol), RAFT agent 1 (70.0 mg, 1.74 x 10^{-1} mmol), AIBN (3.70 mg, 2.25 x 10^{-2} mmol) and 1, 4 dioxane (2 ml). The polymerisation mixture was thoroughly degassed by four freeze pump thaw cycles. The flask was back-filled with nitrogen gas, sealed, placed into an oil bath heated to 80°C and stirred for 39 h. The flask was removed from the oil bath and allowed to cool to ambient temperature. The mixture, a dark yellow viscous liquid, was added dropwise into diethyl ether to obtain a white precipitate. The product was purified by repeated precipitation from DCM / diethyl ether. The product was dried under reduced pressure at 40°C to give a white solid, (1.30 g). The yield was measured gravimetrically to be 62%. SEC: M_n = 5.32 x 10^3 gmol^{-1}, M_w = 6.64 x 10^3 gmol^{-1}, PDI = 1.25.

3.2.4.3. In toluene

To a 50 ml Schlenk tube containing a magnetic stirrer bar, was added NVP (2.09 g, 2.0 ml, 18.8 mmol), RAFT agent 1 (78.0 mg, 1.94 x 10^{-1} mmol), AIBN (4.80 mg, 2.92 x 10^{-2} mmol) and dry toluene (1 ml). The polymerisation mixture was thoroughly degassed by four freeze pump thaw cycles. The flask was back-filled with nitrogen gas,

sealed, placed into an oil bath, heated to 80°C and stirred for 44 h. The flask was removed from the oil bath and allowed to cool to ambient temperature. A clear viscous orange gel was formed. Dichloromethane was added to dilute the mixture which was subsequently added dropwise to diethyl ether. A precipitate was immediately formed which was filtered and dried under reduced pressure at 40°C to give an orange fine solid, (0.400 g) The yield was measured gravimetrically to be 19%. SEC: M_n = 3.84 x 10^3 gmol^{-1}, M_w = 4.96 x 10^3 gmol^{-1}, PDI = 1.16.

3.2.5. RAFT polymerisation of vinyl acetate using RAFT agent 1

3.2.5.1. In bulk

To a 50 ml Schlenk tube containing a magnetic stirrer bar, was added VAc (10.0 g, 10.7 ml, 116 mmol), RAFT agent 1 (0.310 g, 7.69 x 10^{-1} mmol) and AIBN (26.0 mg, 1.58 x 10^{-1} mmol). The polymerisation mixture was thoroughly degassed by four freeze pump thaw cycles. The flask was back-filled with nitrogen gas, sealed, placed in an oil bath, heated to 80°C and stirred for 39 h. The flask was removed from the oil bath and allowed to cool to ambient temperature. A solid yellow gel was formed. Tetrahydrofuran was added to dissolve the gel and the resulting solution was added dropwise into hexane. A yellow oil residue was formed, and volatiles were then removed under reduced pressure to give a yellow solid, (9.20 g). The yield was measured gravimetrically to be 92%. SEC: M_n = 1.58 x 10^4 gmol^{-1}, M_w = 2.30 x 10^4 gmol^{-1}, PDI = 1.46. ^{1}H NMR: 1.44 x 10^4 gmol^{-1}.

3.2.5.2. In 1, 4 dioxane

To a 50 ml Schlenk tube containing a magnetic stirrer bar, was added VAc (1.87 g, 2.00 ml, 21.7 mmol), RAFT agent 1 (87.0 mg, 2.16 x 10^{-1} mmol), AIBN (4.40 mg, 2.68 x 10^{-2} mmol) and 1, 4 dioxane (1 ml). The polymerisation mixture was thoroughly degassed by four freeze pump thaw cycles. The flask was back-filled with nitrogen gas, sealed, placed in an oil bath, heated to 80°C and stirred for 45 h. The flask was removed from the oil bath and allowed to cool to ambient temperature. A viscous yellow gel was formed. Dichloromethane was added to dilute the polymer product and the resulting solution was added dropwise into diethyl ether. A cloudy mixture was observed. Volatiles were removed under reduced pressure at 30°C to give a light

yellow solid, (1.68 g). The yield was measure gravimetrically to be 90%. SEC: M_n = 6.60 x 10^3 $gmol^{-1}$, M_w = 1.01 x 10^4 $gmol^{-1}$, PDI = 1.53. ^{1}H NMR: 9.57 x 10^3 $gmol^{-1}$.

3.2.5.3. In toluene

To a 50 ml Schlenk tube containing a magnetic stirrer bar, was added VAc (1.87 g, 2.00 ml, 21.7 mmol), RAFT agent 1 (87.0 mg, 2.16 x 10^{-1} mmol), AIBN (4.40 mg, 2.68 x 10^{-2} mmol) and dry toluene (1 ml). The polymerisation mixture was thoroughly degassed by four freeze pump thaw cycles. The flask was back-filled with nitrogen gas, sealed, placed in an oil bath, heated to 80°C and stirred for 44 h. The flask was removed from the oil bath and allowed to cool to ambient temperature. A viscous yellow gel was formed. Tetrahydrofuran was added to dilute the polymer product and the resulting solution was added dropwise to hexane. A yellow residue was formed and volatiles were removed under reduced pressure at 30°C to give a light yellow solid, (0.880 g). The yield was measured gravimetrically to be 47%. SEC: M_n = 6.03 x 10^3 $gmol^{-1}$, M_w = 7.77 x 10^3 $gmol^{-1}$, PDI = 1.29. ^{1}H NMR: 5.18 x 10^3 $gmol^{-1}$.

3.2.6. RAFT polymerisation of N-vinylpyrrolidone using RAFT agent 2

3.2.6.1. In bulk

To a 50ml Schlenk tube containing a magnetic stirrer bar, was added NVP (10.5 g, 10.0 ml, 94.0 mmol), RAFT agent 2 (0.150 g, 6.64 x 10^{-1} mmol) and AIBN (21.0 mg, 1.28 x 10^{-1} mmol). The polymerisation mixture was thoroughly degassed by four freeze pump thaw cycles. The flask was back-filled with nitrogen gas, sealed, placed in an oil bath, heated to 80°C and stirred for 40 h. The flask was removed from the oil bath and allowed to cool to ambient temperature. The product was a dark yellow gel like solid which was dissolved in dichloromethane. The solution was then added dropwise into diethyl ether and a precipitate was formed. The white solid was filtered and dried under reduced pressure at 40°C, (6.82 g). The yield was measured gravimetrically to be, 65%. SEC: M_n = 1.25 x 10^4 $gmol^{-1}$, M_w = 1.43 x 10^4 $gmol^{-1}$, PDI = 1.15. ^{1}H NMR: 1.20 x 10^4 $gmol^{-1}$.

3.2.6.2. In 1, 4 dioxane

To a 50 ml Schlenk tube containing a magnetic stirrer bar, was added NVP (4.18 g, 4.00 ml, 37.6 mmol), RAFT agent 2 (90.0 mg, 3.98 x 10^{-1} mmol), AIBN (7.80 mg, 4.75 x 10^{-2} mmol) and 1, 4 dioxane (4 ml). The polymerisation mixture was thoroughly degassed by four freeze pump thaw cycles. The flask was back-filled with nitrogen gas, sealed, placed in an oil bath, heated to 80°C and stirred for 51 h. The flask was removed from the oil bath and allowed to cool to ambient temperature. The product was a clear yellow viscous liquid. The solution was then directly added dropwise into diethyl ether and a yellow precipitate was formed. The yellow solid was filtered and dried under reduced pressure at 40°C, (2.10 g). The yield was measured gravimetrically to be 50%. SEC: M_n = 5.13 x 10^3 gmol^{-1}, M_w = 6.37 x 10^3 gmol^{-1}, PDI = 1.24. ^{1}H NMR: 4.68 x 10^3 gmol^{-1}.

3.2.7. RAFT polymerisation of N-vinylcaprolactam using RAFT agent 2

3.2.7.1. In bulk

To a 50 ml Schlenk tube containing a magnetic stirrer bar, was added NVCL (10.3 g, 10.0 ml, 74.0 mmol), RAFT agent 2 (0.109 g, 0.482 mmol) and AIBN (16.0 mg, 9.74 x 10^{-2} mmol). The flask was placed in an oil bath at approximately 45°C to melt the monomer. Reduced pressure was applied to the flask to degas the reaction mixture for 45 minutes. The flask was back-filled with nitrogen gas, sealed, the temperature of the oil bath was increased to 80°C and stirred for 16 h. The product was a viscous yellow liquid. The flask was removed from the oil bath and allowed to cool to ambient temperature. The reaction mixture was diluted with tetrahydrofuran and added dropwise into hexane. A white precipitate was formed immediately. The white solid was filtered and dried under reduced pressure at 40°C, (4.82 g). The yield was measured gravimetrically to be 47%. SEC: M_n = 1.02 x 10^4 gmol^{-1}, M_w = 1.52 x 10^4 gmol^{-1}, PDI = 1.48.

3.2.8. Attempted RAFT polymerisation of vinyl acetate using RAFT agent 2

3.2.8.1. In bulk

To a 50 ml Schlenk tube containing a magnetic stirrer bar was added VAc (9.34 g, 10.0 ml, 109 mmol), RAFT agent 2 (0.168 g, 0.743 mmol) and AIBN (23.0 mg, 1.40 x 10^{-1} mmol). The polymerisation mixture was thoroughly degassed by four freeze pump thaw cycles. The flask was back-filled with nitrogen, sealed, placed in an oil bath, heated to 80°C and stirred for 40 h. The reaction mixture did not become viscous throughout the polymerisation and no precipitation was observed upon addition to non-solvent. No solid was recovered upon removal of all solvent and excess monomer.

3.2.8.2. In 1, 4 dioxane

To a 50 ml Schlenk tube containing a magnetic stirrer bar was added VAc (9.34 g, 10.0 ml, 109 mmol), RAFT agent 2 (0.244 g, 1.08 mmol), AIBN (22.0 mg, 1.34 x 10^{1} mmol) and 1, 4 dioxane (1 ml). The polymerisation mixture was thoroughly degassed by four freeze pump thaw cycles. The flask was back-filled with nitrogen, sealed, placed in an oil bath, heated to 80°C and stirred for 37 h. The reaction mixture did not become viscous throughout the polymerisation and no precipitation was observed upon addition to non-solvent. No solid was recovered upon removal of all solvent and excess monomer.

3.2.9. RAFT polymerisation of N-vinylpyrrolidone using RAFT agent 3

3.2.9.1. In bulk

To a 50 ml Schlenk tube containing a magnetic stirrer bar, was added NVP (5.23 g, 5.00 ml, 47.0 mmol), RAFT agent 3 (67.0 mg, 3.22 x 10^{-1} mmol) and AIBN (6.50 mg, 5.85 x 10^{-2} mmol). The polymerisation mixture was thoroughly degassed by four freeze pump thaw cycles. The flask was back-filled with nitrogen gas, sealed, placed in an oil bath, heated to 80°C and stirred for 2 h. The flask was removed from the oil bath and allowed to cool to ambient temperature. The product was a very viscous yellow liquid which was dissolved in dichloromethane. The solution was then added dropwise into diethyl ether and a yellow precipitate was formed immediately. The light yellow solid

was filtered and dried under reduced pressure at 40°C, (3.51 g). The yield was measured gravimetrically to be 67%. SEC: M_n = 1.06 x 10^4 $gmol^{-1}$, M_w = 1.55 x 10^4 $gmol^{-1}$, PDI = 1.46.

3.2.9.2. In 2-propanol

To a 50 ml Schlenk tube containing a magnetic stirrer bar, was added NVP (5.23 g, 5.00 ml, 47.0 mmol), RAFT agent 3 (69.0 mg, 3.32 x 10^{-1} mmol), AIBN (6.40 mg, 3.90 x 10^{-2} mmol) and 2-propanol (5 ml). The polymerisation mixture was thoroughly degassed by four freeze pump thaw cycles. The flask by back-filled with nitrogen gas, sealed, placed into an oil bath, the temperature set at 75°C and stirred for 20 h. The flask was then removed from the oil bath and allowed to cool to ambient temperature. The product of the reaction was a slightly yellow viscous liquid. The mixture was diluted with dichloromethane and added dropwise into diethyl ether. A white precipitate was immediately formed. The white solid was filtered and dried under reduced pressure at 40°C, (2.14 g). The yield was measured gravimetrically to be 41%. SEC: M_n = 1.28 x 10^4 $gmol^{-1}$, M_w = 2.25 x 10^4 $gmol^{-1}$, PDI = 1.76.

3.2.9.3. In dimethylformamide

To a 50 ml glass ampoule containing a magnetic stirrer bar, was added NVP (5.23 g, 5.00 ml, 47.0 mmol), RAFT agent 3 (43.0 mg, 2.07 x 10^{-1} mmol), AIBN (7.90 mg, 4.81 x 10^{-2} mmol) and dry dimethylformamide (5 ml). Reaction mixture was thoroughly degassed by four freeze pump thaw cycles and the ampoule sealed under reduced pressure. The ampoule was then placed into an oil bath thermostated at 70°C and stirred for 43 h. A viscous clear yellow/green liquid was produced. The ampoule was removed from the oil bath and allowed to cool to ambient temperature. Dichloromethane was added to dilute the reaction mixture which was subsequently added dropwise into diethyl ether. The white precipitate was formed which was filtered and dried under reduced pressure at 30°C, to give a white solid, (3.94 g). The yield was measured gravimetrically to be 75%. SEC: M_n = 2.42 x 10^4 $gmol^{-1}$, M_w = 3.13 x 10^4 $gmol^{-1}$, PDI = 1.30.

3.2.9.4. In 1, 4 dioxane

To a 50 ml glass ampoule containing a magnetic stirrer bar, was added NVP (5.23 g, 5.00 ml, 47.0 mmol), RAFT agent 3 (38.0 mg, 1.83 x 10^{-1} mmol), AIBN (7.70 mg, 4.69 x 10^{-2} mmol) and 1, 4 dioxane (5 ml). The reaction mixture was thoroughly degassed by four freeze pump cycles and the ampoule was sealed under reduced pressure. The ampoule was then placed in an oil bath thermostated at 80°C and stirred for 39 h. A solid yellow / green gel was formed. The ampoule was taken out of the oil bath and allowed to cool to ambient temperature. The reaction mixture was dissolved in dichloromethane and added dropwise into diethyl ether. A white precipitate was formed immediately, which was filtered and dried under reduced pressure at 35°C to give a white solid, (4.95 g). The yield was measured gravimetrically to be 95%. SEC: M_n = 2.82 x 10^4 gmol^{-1}, M_w = 3.79 x 10^4 gmol^{-1}, PDI = 1.34.

3.2.9.5. In tetrahydrofuran

To a 50 ml Schlenk tube containing a magnetic stirrer bar, was added NVP (5.23 g, 5.00 ml, 47.0 mmol), RAFT agent 3 (71.0 mg, 3.41 x 10^{-1} mmol), AIBN (6.40 mg, 3.90 x 10^{-2} mmol) and dry tetrahydrofuran (5 ml). The reaction mixture was thoroughly degassed by four freeze pump thaw cycles. The flask was back-filled with nitrogen gas, sealed, placed in an oil bath thermostated at 70°C and stirred for 25 h. The product was a yellow clear viscous liquid. The flask was removed from the oil bath and cooled to ambient temperature. The polymerisation mixture was diluted with dichloromethane and added dropwise into diethyl ether. A white precipitate was formed immediately, which was filtered and dried under reduced pressure at 40°C to give a white solid. Conversion was calculated by determining amount of residual monomer in ^{1}H NMR spectrum to be 58%. SEC: M_n = 9.49 x 10^3 gmol^{-1}, M_w = 1.30 x 10^4 gmol^{-1}, PDI = 1.37.

3.2.9.6. In water

To a 50 ml Schlenk tube containing a magnetic stirrer bar, was added NVP (5.23 g, 5.00 ml, 47.0 mmol), RAFT agent 3 (65.0 mg, 3.12 x 10^{-1} mmol), AIBN (6.40 mg, 3.90 x 10^{-2} mmol) and water (5 ml). The reaction mixture was thoroughly degassed by four freeze pump thaw cycles. The flask was back-filled with nitrogen gas, sealed, placed in an oil bath thermostated at 80°C and stirred for 19 h. The product was a light yellow

clear viscous liquid. The flask was removed from the oil bath and cooled to ambient temperature. The polymerisation mixture was diluted with dichloromethane and added dropwise into diethyl ether. A white precipitate was formed immediately, which was filtered and dried under reduced pressure at 40°C to give a white solid, (2.35 g). The yield was measured gravimetrically to be 45%. SEC: M_n = 2.57 x 10^4 $gmol^{-1}$, M_w = 3.55 x 10^4 $gmol^{-1}$, PDI = 1.38.

3.2.9.7. In 2-butoxyethanol

To a 50 ml Schlenk tube containing a magnetic stirrer bar, was added NVP (5.23 g, 5.00 ml, 47.0 mmol), RAFT agent 3 (66.0 mg, 3.17 x 10^{-1} mmol), AIBN (6.60 mg, 4.02 x 10^{-2} mmol) and 2-butoxyethanol (5 ml). The reaction mixture was thoroughly degassed by four freeze pump thaw cycles. The flask was back-filled with nitrogen gas, sealed, placed in an oil bath thermostated at 80°C and stirred for 25 h. The product was a yellow clear viscous liquid. The flask was removed from the oil bath and cooled to ambient temperature. The polymerisation mixture was diluted with dichloromethane and added dropwise into diethyl ether. A white precipitate was formed immediately, which was filtered and dried under reduced pressure at 40°C to give a white solid, (1.50 g). The yield was measured gravimetrically to be 29%. SEC: M_n = 7.13 x 10^3 $gmol^{-1}$, M_w = 1.25 x 10^4 $gmol^{-1}$, PDI = 1.75.

3.2.10. RAFT polymerisation of vinyl acetate using RAFT agent 3

3.2.10.1. In bulk

To a 50 ml Schlenk tube containing a magnetic stirrer bar, was added VAc (4.67 g, 5.00 ml, 54.2 mmol), RAFT agent 3 (78.0 mg, 3.75 x 10^{-1} mmol) and AIBN (7.70 mg, 4.69 x 10^{-2} mmol). The reaction mixture was thoroughly degassed by four freeze pump thaw cycles. The flask was back-filled with nitrogen gas, sealed, placed in oil bath, heated to 80°C and stirred for 17 h. The polymerisation product was solid yellow clear gel. The flask was removed from the oil bath and cooled to ambient temperature. The reaction mixture was dissolved in dichloromethane and resulting solution transferred to another flask. Solvent and excess monomer were removed under reduced pressure to give a white solid, (4.20 g). The yield was measured gravimetrically to be 90%. SEC: M_n = 1.52 x 10^4 $gmol^{-1}$, M_w = 2.23 x 10^4 $gmol^{-1}$, PDI = 1.47. ^{1}H NMR: 1.15 x 10^4 $gmol^{-1}$.

3.2.10.2. In ethyl acetate

To a 50 ml Schlenk tube containing a magnetic stirrer bar, was added VAc (4.67 g, 5.00 ml, 54.2 mmol), RAFT agent 3 (83.0 mg, 3.99 x 10^{-1} mmol), AIBN (7.40 mg, 4.51 x 10^{-2} mmol) and ethyl acetate (5 ml). The reaction mixture was thoroughly degassed by four freeze pump thaw cycles. The flask was back-filled with nitrogen gas, sealed, placed in an oil bath, heated to 80°C and stirred for 16 h. The product of the reaction was a colourless viscous gel. The flask was removed from the oil bath and allowed to cool to ambient temperature. Dichloromethane was added to the reaction mixture and resulting solution was transferred to another flask. Solvent and excess monomer were removed under reduced pressure to give a white solid (4.20 g). The yield was measured gravimetrically to be 90%. SEC: M_n = 1.12 x 10^4 gmol^{-1}, M_w = 1.67 x 10^4 gmol^{-1}, PDI = 1.50. ^{1}H NMR: 1.31 x 10^4 gmol^{-1}.

3.2.10.3. In 2-propanol

To a 50 ml Schlenk tube containing a magnetic stirrer bar, was added VAc (4.67 g, 5.00 ml, 54.2 mmol), RAFT agent 3 (78.0 mg, 3.75 x 10^{-1} mmol), AIBN (7.70 mg, 4.69 x 10^{-2} mmol) and 2-propanol (5 ml). Reaction mixture was thoroughly degassed by four freeze pump thaw cycles and the flask was back-filled with nitrogen gas. The Schlenk tube was sealed under N_2, placed in an oil bath, heated to 75°C and stirred for 17 h. The product of the reaction was a clear colourless liquid. The flask was removed from the oil bath and allowed to cool to ambient temperature. Excess solvent and monomer were removed under reduced pressure to give a white solid, (3.20 g). The yield was measured gravimetrically to be 69%. SEC: M_n = 4.86 x 10^3 gmol^{-1}, M_w = 1.01 x 10^4 gmol^{-1}, PDI = 2.08. ^{1}H NMR: 1.05 x 10^4 gmol^{-1}.

3.2.10.4. In cyclohexane

To a 50 ml Schlenk tube containing a magnetic stirrer bar, was added VAc (4.67 g, 5.00 ml, 54.2 mmol), RAFT agent 3 (76.0 mg, 3.65 x 10^{-1} mmol), AIBN (7.50 mg, 4.57 x 10^{-2} mmol) and cyclohexane (5 ml). Reaction mixture was thoroughly degassed by four freeze pump thaw cycles and the flask was back-filled with nitrogen gas. The Schlenk tube was sealed under N_2, placed in an oil bath, heated to 75°C and stirred for 17 h. The product of the reaction was a clear viscous gel. The flask was removed from the oil

bath and allowed to cool to ambient temperature. Excess solvent and monomer were removed under reduced pressure to give a white solid, (4.34 g). The yield was measured gravimetrically to be 93%. SEC: M_n = 1.17 x 10^4 $gmol^{-1}$, M_w = 2.05 x 10^4 $gmol^{-1}$, PDI = 1.76. ^{1}H NMR: 1.27 x 10^4 $gmol^{-1}$.

3.2.10.5. In water

To a 50 ml Schlenk tube containing a magnetic stirrer bar, was added VAc (4.67 g, 5.00 ml, 54.2 mmol), RAFT agent 3 (79.0 mg, 3.80 x 10^{-1} mmol), AIBN (7.80 mg, 4.75 x 10^{-2} mmol) and water (5 ml). Reaction mixture was thoroughly degassed by four freeze pump thaw cycles and the flask was back-filled with nitrogen gas. The Schlenk tube was sealed under N_2, placed in an oil bath, heated to 80°C and stirred for 16 h. Throughout the reaction there were two layers. The flask was removed from the oil bath and allowed to cool to ambient temperature. Excess solvent and monomer were removed under reduced pressure to give a white solid, (4.17 g). The yield was measured gravimetrically to be 89%. SEC: M_n = 1.42 x 10^4 $gmol^{-1}$, M_w = 2.19 x 10^4 $gmol^{-1}$, PDI = 1.54. ^{1}H NMR: 1.39 x 10^4 $gmol^{-1}$.

3.2.10.6. In acetonitrile

To a 50 ml Schlenk tube containing a magnetic stirrer bar, was added VAc (4.67 g, 5.00 ml, 54.2 mmol), RAFT agent 3 (80.0 mg, 3.85 x 10^{-1} mmol), AIBN (7.50 mg, 4.57 x 10^{-2} mmol) and acetonitrile (5 ml). Reaction mixture was thoroughly degassed by four freeze pump thaw cycles and the flask was back-filled with nitrogen gas. The Schlenk tube was sealed under N_2, placed in an oil bath, heated to 75°C and stirred for 17 h. The product of the reaction was a colourless gel. The flask was removed from the oil bath and allowed to cool to ambient temperature. Excess solvent and monomer were removed under reduced pressure to give a white solid, (4.12 g). The yield was measured gravimetrically to be 88%. SEC: M_n = 1.27 x 10^4 $gmol^{-1}$, M_w = 1.71 x 10^4 $gmol^{-1}$, PDI = 1.35. ^{1}H NMR: 1.23 x 10^4 $gmol^{-1}$.

3.2.10.7. In toluene

To a 50 ml Schlenk tube containing a magnetic stirrer bar, was added VAc (4.67 g, 5.00 ml, 54.2 mmol), RAFT agent 3 (80.0 mg, 3.85 x 10^{-1} mmol), AIBN (7.50 mg, 4.57 x

10^{-2} mmol) and toluene (5 ml). Reaction mixture was thoroughly degassed by four freeze pump thaw cycles and the flask was back-filled with nitrogen gas. The Schlenk tube was sealed under N_2, placed in an oil bath, heated to 75°C and stirred for 17 h. The product of the reaction was a colourless gel. The flask was removed from the oil bath and allowed to cool to ambient temperature. Excess solvent and monomer were removed under reduced pressure to give a white solid, (1.85 g). The yield was measured gravimetrically to be 40%. SEC: M_n = 5.86 x 10^3 $gmol^{-1}$, M_w = 7.56 x 10^3 $gmol^{-1}$, PDI = 1.29. ^{1}H NMR: 6.79 x 10^3 $gmol^{-1}$.

3.2.11. RAFT polymerisation of N-vinylcaprolactam using RAFT agent 3

3.2.11.1. In bulk

To a 50 ml Schlenk tube containing a magnetic stirrer bar, was added NVCL (5.00 g, 35.9 mmol), RAFT agent 3 (51.0 mg, 2.45 x 10^{-1} mmol) and AIBN (4.70 mg, 2.86 x 10^{-2} mmol). The reaction mixture was degassed by heating the polymerisation mixture to 40°C and applying a for 30 minutes. The Schlenk tube was then back-filled with nitrogen gas, the temperature was increased to 80°C and reaction mixture stirred for 16 h. The product from the reaction was a very viscous light yellow gel. The Schlenk tube was removed from the oil bath and allowed to cool to ambient temperature. Dichloromethane was added to dilute the polymerisation mixture which was subsequently added dropwise into diethyl ether. A white precipitate was formed which was filtered and dried under reduced pressure at 50°C to give an off white solid, (2.65 g). The yield was measured gravimetrically to be 53%. SEC: M_n = 1.52 x 10^4 $gmol^{-1}$, M_w = 2.26 x 10^4 $gmol^{-I}$, PDI = 1.48.

3.2.11.2. In 1, 4 dioxane

To a 50 ml glass ampoule containing a magnetic stirrer bar, was added NVCL (5.00 g, 35.9 mmol), RAFT agent 3 (31.0 mg, 1.49 x 10^{-1} mmol), AIBN (5.80 mg, 3.53 x 10^{-2} mmol) and 1, 4 dioxane (5 ml). The polymerisation mixture was thoroughly degassed by four freeze pump thaw cycles and sealed under reduced pressure. The ampoule was then placed in a thermostated oil bath set at 80°C and reaction mixture stirred for 40 h. The product of the reaction was a light yellow viscous liquid. The ampoule was removed from the oil bath and allowed to cool to ambient temperature.

Dichloromethane was added to dilute the reaction mixture and added dropwise into hexane. The white precipitate formed was filtered and dried under reduced pressure at 40°C to give a white solid, (2.46 g). The yield was measured gravimetrically to be 49%. SEC: M_n = 1.65 x 10^4 $gmol^{-1}$, M_w = 2.27 x 10^4 $gmol^{-1}$, PDI = 1.38.

3.2.12. RAFT polymerisation of N-vinylpyrrolidone using RAFT agent 4

3.2.12.1. In bulk

To a 50 ml glass ampoule containing a magnetic stirrer bar, was added NVP (5.23 g, 5.00 ml, 47.0 mmol), RAFT agent 4 (76.0 mg, 3.26 x 10^{-1} mmol) and AIBN (6.70 mg, 4.08 x 10^{-2} mmol). The polymerisation mixture was thoroughly degassed by four freeze pump thaw cycles and sealed under reduced pressure. The ampoule was then placed in an oil bath set at 80°C and reaction mixture stirred for 30 minutes. The product of the reaction was a yellow solid gel. The ampoule was removed from the oil bath and cooled to ambient temperature. The product was dissolved in dichloromethane and added dropwise into diethyl ether to give a white precipitate. The solid was filtered and dried under reduced pressure at 40°C, (4.29 g). The yield was measured gravimetrically to be 82%. SEC: M_n = 1.53 x 10^5 $gmol^{-1}$, M_w = 2.31 x 10^5 $gmol^{-1}$, PDI = 1.51.

3.2.12.2. In 1, 4 dioxane

To a 50 ml glass ampoule containing a magnetic stirrer bar, was added NVP (5.23 g, 5.00 ml, 47.0 mmol), RAFT agent 4 (41.0 mg, 1.76 x 10^{-1} mmol), AIBN (7.70 mg, 4.69 x 10^{-2} mmol) and 1, 4 dioxane (5 ml). The polymerisation mixture was thoroughly degassed by four freeze pump thaw cycles and sealed under reduced pressure. The ampoule was placed in a thermostated oil bath set at 70°C and reaction mixture stirred for 15 h. The polymerisation mixture was a solid clear colourless gel. Dichloromethane was added dissolve the product and was the resulting solution was added dropwise into diethyl ether. A white precipitate was formed which was filtered and dried under reduced pressure at 30°C, (4.80 g). The yield was measured gravimetrically to be 92%. SEC: M_n = 2.16 x 10^5 $gmol^{-1}$, M_w = 3.12 x 10^5 $gmol^{-1}$, PDI = 1.44.

3.2.13. RAFT polymerisation of vinyl acetate using RAFT agent 4.

3.2.13.1. In bulk

To a 50 ml glass ampoule containing a magnetic stirrer bar, was added VAc (4.67 g, 5.00 ml, 54.0 mmol), RAFT agent 4 (52.0 mg, 2.23×10^{-1} mmol), AIBN (9.00 mg, 5.48×10^{-2} mmol) and 1, 4 dioxane (5.0 ml). Polymerisation mixture was thoroughly degassed by four freeze pump thaw cycles. Ampoule was then back-filled with nitrogen gas, placed into an oil bath thermostated at 68°C and stirred for 15 h. The product of the reaction was a clear colourless viscous gel. The ampoule was removed from the oil bath and allowed to cool to ambient temperature. Reaction mixture was dissolved in dichloromethane and resulting solution transferred to another flask. Solvent and excess monomer were removed under reduced pressure to give a white solid, (3.77 g). The yield was measured gravimetrically to be 81%. SEC: $M_n = 8.87 \times 10^3$ gmol^{-1}, $M_w = 2.20 \times 10^4$ gmol^{-1}, PDI = 2.48.

3.2.14. RAFT polymerisation of N-vinylpyrrolidone using RAFT agent 5

3.2.14.1. In bulk

To a 50 ml glass ampoule containing a magnetic stirrer bar, was added NVP (5.00 g, 45.0 mmol), RAFT agent 5 (0.135 g, 4.43×10^{-1} mmol) and AIBN (15.0 mg, 9.14×10^{-2} mmol). The polymerisation mixture was thoroughly degassed by four freeze pump thaw cycles and sealed under reduced pressure. The ampoule was then placed in an oil bath thermostated at 70°C and reaction mixture stirred for 12 h. The product of the reaction was a viscous bright yellow / green gel. Dichloromethane was added to dissolve the mixture and the solution was added dropwise into diethyl ether to give a fine precipitate. The solid was filtered and dried under reduced pressure at 40°C to give a white solid, (3.94 g, 79% gravimetric yield). Conversion was measured by determining the residual monomer by ^{1}H NMR spectrum to be 87%. SEC: $M_n = 1.37 \times 10^4$ gmol^{-1}, $M_w = 1.71 \times 10^4$ gmol^{-1}, PDI = 1.24.

3.2.14.2. In ethanol

To a 50 ml glass ampoule containing a magnetic stirrer bar, was added NVP (5.00 g, 45.0 mmol), RAFT agent 5 (0.134 g, 4.39 x 10^{-1} mmol), AIBN (15.8 mg, 9.62 x 10^{-2} mmol) and ethanol (6 ml). The polymerisation mixture was thoroughly degassed by four freeze pump thaw cycles and sealed under reduced pressure. The ampoule was then placed in an oil bath thermostated at 70°C and reaction mixture stirred for 11 h. The product of the polymerisation was a yellow / gold viscous liquid. The mixture was dissolved in dichloromethane and added dropwise into diethyl ether to give a white solid. The solid was filtered and dried under reduced pressure at 35°C to give a white solid, (2.81 g, 56% gravimetric yield). Conversion was measured by determining the residual monomer by ^{1}H NMR spectrum to be 81%. SEC: M_n = 9.56 x 10^{3} gmol^{-1}, M_w = 1.21 x 10^{4} gmol^{-1}, PDI = 1.27.

3.2.14.3. In tetrahydrofuran

To a 50 ml glass ampoule containing a magnetic stirrer bar, was added NVP (5.00 g, 45.0 mmol), RAFT agent 5 (0.134 g, 4.39 x 10^{-1} mmol), AIBN (15.8 mg, 9.62 x 10^{-2} mmol) and dry tetrahydrofuran (6 ml). The polymerisation mixture was thoroughly degassed by four freeze pump thaw cycles and sealed under reduced pressure. The ampoule was then placed in an oil bath thermostated at 70°C and reaction mixture stirred for 11 h. The product of the polymerisation was a slightly turbid yellow / green liquid. The mixture was dissolved in dichloromethane and added dropwise into diethyl ether to give a white solid. The solid was filtered and dried under reduced pressure at 35°C (2.22 g, 44% gravimetric yield). Conversion was measured by determining the residual monomer by ^{1}H NMR spectrum to be 64%. SEC: M_n = 1.09 x 10^{4} gmol^{-1}, M_w = 1.21 x 10^{4} gmol^{-1}, PDI = 1.13.

3.2.14.4. In water

To a 50 ml glass ampoule containing a magnetic stirrer bar, was added NVP (5.00 g, 45.0 mmol), RAFT agent 5 (0.134 g, 4.39 x 10^{-1} mmol), AIBN (15.4 mg, 9.38 x 10^{-2} mmol) and distilled water (5 ml). The polymerisation mixture was thoroughly degassed by four freeze pump thaw cycles and sealed under reduced pressure. The ampoule was then placed in an oil bath thermostated at 70°C and reaction mixture stirred for 19 h.

The product of the polymerisation was a clear solid gel. The mixture was dissolved in dichloromethane and added dropwise into diethyl ether to give a white solid. The solid was filtered and dried under reduced pressure at 35°C to give a white solid, (3.08 g). The yield was measured gravimetrically to be 62%. SEC: M_n = 3.74 x 10^4 $gmol^{-1}$, M_w = 5.28 x 10^4 $gmol^{-1}$, PDI = 1.41.

3.2.14.5. In acetonitrile

To a 50 ml glass ampoule containing a magnetic stirrer bar, was added NVP (5.90 g, 53.1 mmol), RAFT agent 5 (0.162 g, 5.31 x 10^{-1} mmol), AIBN (15.0 mg, 9.14 x 10^{-2} mmol) and dry acetonitrile (8 ml). The polymerisation mixture was thoroughly degassed by four freeze pump thaw cycles and sealed under reduced pressure. The ampoule was then placed in an oil bath thermostated at 70°C and reaction mixture was stirred for 19 h. The product of the polymerisation was an orange viscous clear liquid. The mixture was dissolved in dichloromethane and added dropwise into diethyl ether to give a white solid. The solid was filtered and dried under reduced pressure at 35°C to give a white solid, (2.14 g, 36% gravimetric yield). Conversion was measured by determining the residual monomer by ^{1}H NMR spectrum to be 51%. SEC: M_n = 7.25 x 10^3 $gmol^{-1}$, M_w = 8.12 x 10^3 $gmol^{-1}$, PDI = 1.12.

3.2.14.6. In 1, 4 dioxane

To a 50 ml glass ampoule containing a magnetic stirrer bar, was added NVP (5.00 g, 45.0 mmol), RAFT agent 5 (0.134 g, 4.39 x 10^{-1} mmol), ACVA (25.0 mg, 8.92 x 10^{-2} mmol) and 1, 4 dioxane (5 ml). The polymerisation mixture was degassed by purging with nitrogen gas for 2 h. The ampoule was then placed in an oil bath thermostated at 70°C and reaction mixture stirred for 17 h. The product of the polymerisation was an yellow / green viscous clear liquid. The mixture was dissolved in dichloromethane and added dropwise into diethyl ether to give a white precipitate. The precipitate was filtered and dried under reduced pressure at 35°C to give a white solid. Conversion was measured by determining the residual monomer by ^{1}H NMR spectrum to be 75%. SEC: M_n = 9.91 x 10^3 $gmol^{-1}$, M_w = 1.23 x 10^4 $gmol^{-1}$, PDI = 1.24.

3.2.14.7. Kinetics of RAFT polymerisation of N-vinylpyrrolidone using RAFT agent 5

To a 50 ml Schlenk tube containing a magnetic stirrer bar fitted with a suba seal and nitrogen inlet, was added NVP (5.00 g, 45.0 mmol), RAFT agent 5 (68.0 mg, 2.23 x 10^{-1} mmol), ACVA (13.0 mg, 4.64 x 10^{-2} mmol) and 1, 4 dioxane (5 ml). The polymerisation mixture was purged with nitrogen gas for 1 h. The polymerisation mixture was then placed in a thermostated oil bath set at 70°C and stirred. Aliquots of the polymerisation mixture were taken after 2, 4, 6 and 8 h. Samples were analysed by SEC and ^{1}H NMR spectroscopy.

3.2.15. RAFT polymerisation of vinyl acetate using RAFT agent 5

3.2.15.1. In bulk

To a 50 ml glass ampoule containing a magnetic stirrer bar, was added VAc (4.67 g, 5.00 ml, 54.0 mmol), RAFT agent 5 (0.165 g, 5.41 x 10^{-1} mmol) and AIBN (17.7 mg, 0.108 mmol). The polymerisation mixture was thoroughly degassed by four freeze pump thaw cycles and sealed under reduced pressure. The ampoule was then placed in an oil bath thermostated at 60°C and reaction mixture stirred for 16 h. The ampoule was then removed from the oil bath and allowed to cool to ambient temperature. The product of the polymerisation was a solid clear gel. Dichloromethane was added to dissolve the material and the resulting solution was transferred to another flask. Excess monomer and solvent were removed under reduced pressure to a give a white solid, (3.73 g). The yield was measured gravimetrically to be 80%. SEC: M_n = 1.07 x 10^4 gmol^{-1}, M_w = 1.36 x 10^4 gmol^{-1}, PDI = 1.27. ^{1}H NMR: 1.28 x 10^4 gmol^{-1}.

3.2.15.2. In ethanol

To a 50 ml glass ampoule containing a magnetic stirrer bar, was added VAc (4.67 g, 5.00 ml, 54.0 mmol), RAFT agent 5 (0.165 g, 5.41 x 10^{-1} mmol), AIBN (18.0 mg, 1.10 x 10^{-1} mmol) and ethanol (5 ml). The polymerisation mixture was thoroughly degassed by four freeze pump thaw cycles and sealed under reduced pressure. The ampoule was then placed in an oil bath thermostated at 68°C and stirred for 19 h. The product of the polymerisation was a clear viscous liquid. Dichloromethane was added to material and

the resulting solution was transferred to another flask. Excess monomer and solvent were removed under reduced pressure to give a white solid, (4.10 g). The yield was measured gravimetrically to be 88%. SEC: M_n = 5.59 x 10^3 $gmol^{-1}$, M_w = 1.06 x 10^4 $gmol^{-1}$, PDI = 1.90. ^{1}H NMR: 9.63 x 10^3 $gmol^{-1}$.

3.2.15.3. In ethyl acetate

To a 50 ml glass ampoule containing a magnetic stirrer bar, was added VAc (4.67 g, 5.00 ml, 54.0 mmol), RAFT agent 5 (0.165 g, 5.41 x 10^{-1} mmol), AIBN (18.0 mg, 1.10 x 10^{-1} mmol) and ethyl acetate (5 ml). The polymerisation mixture was thoroughly degassed by four freeze pump thaw cycles and sealed under reduced pressure. The ampoule was then placed in an oil bath thermostated at 68°C and stirred for 19 h. The product of the polymerisation was a clear viscous liquid. Solvent was added to the material and the resulting solution was transferred to another flask. Excess monomer and solvent were removed under reduced pressure to give a white solid, (4.30 g). The yield was measured gravimetrically to be 92%. SEC: M_n = 9.44 x 10^3 $gmol^{-1}$, M_w = 1.40 x 10^4 $gmol^{-1}$, PDI = 1.49. ^{1}H NMR = 9.16 x 10^3 $gmol^{-1}$.

3.2.16. RAFT polymerisation of N-vinylcaprolactam using RAFT agent 5

3.2.16.1. In 1, 4 dioxane

To a 50 ml glass ampoule containing a magnetic stirrer bar, was added NVCL (5.00 ml, 5.15 g, 37.0 mmol), RAFT agent 5 (55.0 mg, 1.80 x 10^{-1} mmol), ACVA (10.0 mg, 3.57 x 10^{-2} mmol) and 1, 4 dioxane (3 ml). The polymerisation mixture was thoroughly degassed by four freeze pump thaw cycles and sealed under reduced pressure. The ampoule was then placed into a thermostated oil bath set at 70°C and stirred for 17 h. The polymerisation mixture was a slightly yellow viscous gel. Dichloromethane was added to dilute the polymerisation mixture which was subsequently added dropwise to hexane. White precipitate was formed immediately. This was filtered and dried under reduced pressure to give an off-white powder (2.95 g). The yield was measured gravimetrically to be 57%. SEC: M_n = 2.08 x 10^4 $gmol^{-1}$, M_w = 2.82 x 10^4 $gmol^{-1}$, PDI = 1.36.

3.2.17. RAFT polymerisation of N-vinylpyrrolidone using RAFT agent 6

3.2.17.1. In bulk

To a 50 ml glass ampoule containing a magnetic stirrer bar, was added NVP (5.00 g, 45.0 mmol), RAFT agent 6 (0.143 g, 4.48 x 10^{-1} mmol) and AIBN (15.0 mg, 9.14 x 10^{-2} mmol). The polymerisation mixture was thoroughly degassed by four freeze pump thaw cycles and sealed under reduced pressure. The ampoule was then placed in an oil bath thermostated at 70°C and reaction mixture stirred for 16 h. The ampoule was then removed from the oil bath and allowed to cool to ambient temperature. The product of the reaction was a solid yellow / green gel. Dichloromethane was added to dissolve the material and the resulting solution was added dropwise into diethyl ether giving a yellow precipitate. The solid was filtered and dried under reduced pressure at 40°C to give an off white / yellow solid (3.52 g). The yield was measured gravimetrically to be 70%. SEC: M_n = 1.20 x 10^4 gmol^{-1}, M_w = 1.69 x 10^4 gmol^{-1}, PDI = 1.41.

3.2.17.2. In ethanol

To a 50 ml glass ampoule containing a magnetic stirrer bar, was added NVP (5.00 g, 45.0 mmol), RAFT agent 6 (0.143 g, 4.48 x 10^{-1} mmol), AIBN (15.0 mg, 9.14 x 10^{-2} mmol) and ethanol (5 ml). The polymerisation mixture was thoroughly degassed by four freeze pump thaw cycles and sealed under reduced pressure. The ampoule was then placed in an oil bath thermostated at 70°C and reaction mixture stirred for 16 h. The ampoule was then removed from the oil bath and allowed to cool to ambient temperature. The product of the reaction was a clear liquid. Dichloromethane was added to dissolve the material and the resulting solution was added dropwise into diethyl ether giving a white precipitate. The solid was filtered and dried under reduced pressure at 40°C to give a white solid (1.57 g). The yield was measured gravimetrically to be 31%. SEC: M_n = 5.42 x 10^3 gmol^{-1}, M_w = 7.54 x 10^3 gmol^{-1}, PDI = 1.39.

3.2.17.3. Kinetics of RAFT polymerisation of N-vinylpyrrolidone using RAFT agent 6

To a 50 ml Schlenk tube containing a magnetic stirrer bar fitted with a suba seal and nitrogen inlet, was added NVP (5.00 g, 45.0 mmol), RAFT agent 6 (72.0 mg, 2.26 x 10^{-1} mmol), ACVA (13.0 mg, 4.64 x 10^{-2} mmol) and 1, 4 dioxane (5 ml). The polymerisation mixture was purged with nitrogen gas for 1 h. The polymerisation mixture was then placed in a thermostated oil bath set at 70°C and stirred. Aliquots of the polymerisation mixture were taken after 2, 4, 6 and 8 h. Samples were analysed by SEC and ^{1}H NMR spectroscopy.

3.2.18. RAFT polymerisation of N-vinylcaprolactam using RAFT agent 6

3.2.18.1. In 1, 4 dioxane

To a 50 ml glass ampoule containing a magnetic stirrer bar, was added NVCL (5.00 ml, 5.15 g, 37.0 mmol), RAFT agent 6 (57.0 mg, 1.79 x 10^{-1} mmol), ACVA (10.0 mg, 3.57 x 10^{-2} mmol) and 1, 4 dioxane (3 ml). The polymerisation mixture was thoroughly degassed by four freeze pump thaw cycles and sealed under reduced pressure. The ampoule was then placed into a thermostated oil bath set at 70°C and reaction mixture stirred for 17 h. The polymerisation mixture was a slightly yellow viscous gel. Dichloromethane was added to dilute the polymerisation mixture which was subsequently added dropwise to hexane. White precipitate was formed immediately which was filtered and dried under reduced pressure to give an off-white powder, (1.19 g). The yield was measured gravimetrically to be 23%. SEC: M_n = 1.12 x 10^4 gmol^{-1}, M_w = 1.78 x 10^4 gmol^{-1}, PDI = 1.56.

3.2.19. RAFT polymerisation of N-vinylpyrrolidone using RAFT agent 7

3.2.19.1. In bulk

To a 50 ml glass ampoule containing a magnetic stirrer bar, was added NVP (5.00 g, 45.0 mmol), RAFT agent 7 (0.130 g, 4.47 x 10^{-1} mmol) and AIBN (15.0 mg, 9.14 x 10^{-2} mmol). The polymerisation mixture was thoroughly degassed by four freeze pump thaw cycles and sealed under reduced pressure. The ampoule was then placed in an oil

bath thermostated at 70°C and the polymerisation mixture was stirred for 12 h. The product of the polymerisation was a yellow / green solid gel. Dichloromethane was added to dissolve the material and the resulting solution was added dropwise into diethyl ether to give a white precipitate. The solid was filtered and dried under reduced pressure at 40°C to give a white solid (3.85 g, 77% gravimetric yield). Conversion was measured by determining the residual monomer by ^{1}H NMR spectrum to be 85%. SEC: M_n = 1.22 x 10^4 gmol^{-1}, M_w = 1.57 x 10^4 gmol^{-1}, PDI = 1.29.

3.2.19.2. Kinetics of RAFT polymerisation of N-vinylpyrrolidone using RAFT agent 7

Stock solution of NVP (12.0 g, 108 mmol), ACVA (30.0 mg, 1.07 x 10^{-1} mmol), RAFT agent 7 (0.157 g, 5.39 x 10^{-1} mmol) and 1,4 dioxane (12 ml) was prepared and aliquots were transferred to five different ampoules containing a magnetic stirrer bar. Polymerisation mixtures were degassed by four freeze pump thaw cycles and sealed under reduced pressure. Ampoules were then heated and stirred at 70°C and after 1, 2, 4, 8 and 16 h the ampoules were quenched in liquid nitrogen respectively. Samples were taken for SEC and ^{1}H NMR analysis.

3.2.20. RAFT polymerisation of N-vinylcaprolactam using RAFT agent 7

3.2.20.1. In 1, 4 dioxane

To a 50 ml glass ampoule containing a magnetic stirrer bar, was added NVCL (5.00 ml, 5.15 g, 37.0 mmol), RAFT agent 7 (52.0 mg, 1.79 x 10^{-1} mmol), ACVA (10.0 mg, 3.57 x 10^{-2} mmol) and 1, 4 dioxane (3 ml). The polymerisation mixture was thoroughly degassed by four freeze pump thaw cycles and sealed under reduced pressure. The ampoule was then placed into a thermostated oil bath set at 70°C and the reaction mixture was stirred for 17 h. The polymerisation mixture was a slightly yellow viscous gel. Dichloromethane was added to dilute the polymerisation mixture which was subsequently added dropwise to hexane. White precipitate was formed immediately. This was filtered and dried under reduced pressure to give an off-white powder, (3.10 g). The yield was measured gravimetrically to be 60%. SEC: M_n = 2.62 x 10^4 gmol^{-1}, M_w = 3.57 x 10^4 gmol^{-1}, PDI = 1.36.

3.2.21. RAFT polymerisation of N-vinylpyrrolidone using RAFT agent 8 (Cyanomethyl methyl(phenyl)carbamodithioate)

3.2.21.1. In bulk

To a 50 ml glass ampoule containing a magnetic stirrer bar, was added NVP (5.23 g, 5.00 ml, 47.0 mmol), RAFT agent 8 (70.0 mg, 3.15 x 10^{-1} mmol) and AIBN (5.10 mg, 3.11 x 10^{-2} mmol). Polymerisation mixture was thoroughly degassed by four freeze pump thaw cycles. The ampoule was then sealed under reduced pressure, placed in a thermostated oil bath set at 70°C and the reaction mixture was stirred for 18 h. The product of the polymerisation was a clear bright yellow solid gel. The ampoule was removed from the oil bath and allowed to cool to ambient temperature. Dichloromethane was added to the ampoule to dissolve the product and the subsequent solution was added dropwise into diethyl ether to give a white precipitate. The solid was filtered off and dried under reduced pressure at 40°C to give a white solid (4.33 g, 83% gravimetric yield). Conversion was measured by determining the residual monomer by ^{1}H NMR spectrum to be 87%. SEC: M_n= 1.77 x 10^4 gmol^{-1}, M_w = 2.83 x 10^4 gmol^{-1}, PDI = 1.60.

3.2.21.2.In acetonitrile

To a 50 ml glass ampoule containing a magnetic stirrer bar, was added NVP (5.23 g, 5.00 ml, 47.0 mmol), RAFT agent 8 (67.0 mg, 3.01 x 10^{-1} mmol), AIBN (5.30 mg, 3.23 x 10^{-2} mmol) and dry acetonitrile (5 ml). Polymerisation mixture was thoroughly degassed by four freeze pump thaw cycles. The ampoule was then sealed under reduced pressure, placed in a thermostated oil bath set at 70°C and the reaction mixture was stirred for 8.75 h. The product of the polymerisation was a clear bright yellow viscous liquid. The ampoule was removed from the oil bath and allowed to cool to ambient temperature. Dichloromethane was added to the ampoule to dissolve the product and the subsequent solution was added dropwise into diethyl ether to give a white precipitate. The solid was filtered and dried under reduced pressure at 40°C to give a white solid (2.16 g, 41% gravimetric yield). Conversion was measured by determining the residual monomer by ^{1}H NMR spectrum to be 86%. SEC: M_n = 1.59 x 10^4 gmol^{-1}, M_w = 1.99 x 10^4 gmol^{-1}, PDI = 1.25.

3.2.22. RAFT polymerisation of vinyl acetate using RAFT agent 8 (Cyanomethyl methyl(phenyl)carbamodithioate)

3.2.22.1. In bulk

To a 50 ml glass ampoule containing a magnetic stirrer bar, was added VAc (4.67 g, 5.00 ml, 54.0 mmol), RAFT agent 8 (82.0 mg, 3.69×10^{-1} mmol) and AIBN (5.80 mg, 3.53×10^{-2} mmol). The polymerisation mixture was thoroughly degassed by four freeze pump thaw cycles and sealed under reduced pressure. The ampoule was then placed in a thermostated oil bath set at 60°C and the polymerisation mixture was heated for 18 h. The product of the polymerisation was a clear viscous liquid. Excess monomer and was removed under reduced pressure to leave a white solid. Dichloromethane was added to dissolve solid and solution was transferred to sample jar and solvent removed under reduced pressure at 35°C to give a white solid (2.39 g). The yield was measured gravimetrically to be 51%. SEC: $M_n = 9.26 \times 10^3$ gmol^{-1}, $M_w = 1.16 \times 10^4$ gmol^{-1}, PDI = 1.25. ^{1}H NMR = 9.95×10^3 gmol^{-1}.

3.2.22.2. In acetonitrile

To a 50 ml glass ampoule containing a magnetic stirrer bar, was added VAc (4.67 g, 5.00 ml, 54.0 mmol), RAFT agent 8 (80.0 mg, 3.60×10^{-1} mmol), AIBN (6.00 mg, 3.65×10^{-2} mmol) and dry acetonitrile (5 ml). The polymerisation mixture was thoroughly degassed by four freeze pump thaw cycles and sealed under reduced pressure. The ampoule was then placed in a thermostated oil bath set at 65°C and the polymerisation mixture was stirred for 9 h. The product of the polymerisation was a clear pale yellow viscous liquid. Ampoule was removed from oil bath and allowed to cool to ambient temperature. Dichloromethane was added to dilute the mixture and transferred to a round bottomed flask. Solvent and excess monomer was removed under reduced pressure to give a white powder, (4.01 g). The yield was measured gravimetrically to be 86%. SEC: $M_n = 1.02 \times 10^4$ gmol^{-1}, $M_w = 1.41 \times 10^4$ gmol^{-1}, PDI = 1.39. ^{1}H NMR: 1.16×10^4 gmol^{-1}.

3.3. Results and Discussion

3.3.1. Controlled polymerisation of N-vinylpyrrolidone

N-vinylpyrrolidone was polymerised in the presence of synthesised RAFT agent (1-7 and a commercial RAFT agent 8). The data for the homopolymerisations of NVP conducted within this study are collated and represented in Table 3.1.

The extent of the polymerisation was measured in either one of two methods. Initially, the yield was measured gravimetrically (i.e. weighing dried polymer retrieved). Polymers were isolated from the polymerisation mixture by precipitation. Polymeric samples were then filtered and dried under reduced pressure at a temperature of around 30-40°C. If the conversion of the polymerisation was low and monomer was still the samples were re-precipitated until no further monomer was observed by ^{1}H NMR spectroscopy. Hence, this method of calculating the conversion of the polymerisation was not accurate as some polymeric material maybe lost during the re-precipitation process. It was found that measuring conversion by ^{1}H NMR spectroscopy was a more accurate method for determining the extent of the polymerisation. This was achieved by integrating residual monomer CH_2 protons against the polymer backbone CH_2 protons (Section 3.2.3). The theoretical number average molecular weight ($M_{n(theo.)}$) was calculated using Equation 3.1.[27]

$$M_{n\,(theo.)} = \left(\frac{[Mon]\times M_{mon}\times c}{[RAFT]}\right) + M_{RAFT} \qquad \text{Equation 3.1.}$$

Where [Mon] is initial concentration of monomer, [RAFT] is the initial concentration of RAFT agent, M_{mon} is the molecular weight of the monomer, c is the fractional conversion and M_{RAFT} is the RAFT agent's molecular weight. Size exclusion chromatography (SEC) was used to calculate the molecular weight and PDI of the polymers produced. Where possible the molecular weight was also calculated by ^{1}H NMR spectroscopy, by integrating an appropriate proton environment from the chain end to the polymer backbone.

Table 3.1. Polymerisations of NVP using RAFT agents 1-8

Entry	RAFT agent	Solvent	Time (h)	Temp. (°C)	[NVP] / [RAFT agent]	Conversion / Yield (%)	M_n (theo.) (x 10^4 $gmol^{-1}$)	M_n (SEC) (x 10^4 $gmol^{-1}$)	M_w (SEC) (x 10^4 $gmol^{-1}$)	PDI
1	1	1, 4 dioxane	39	80	111	62 (Y)	0.81	0.53	0.66	1.25
2		Bulk	43	80	157	71 (Y)	1.28	1.37	1.61	1.17
3		Toluene	44	80	97	19 (Y)	0.25	0.38	0.50	1.16
4	2	Bulk	40	80	142	65 (Y)	1.07	1.25	1.43	1.15
5		1, 4 dioxane	51	80	94	50 (Y)	0.57	0.51	0.64	1.24
6	3	Bulk	2	80	147	67 (Y)	1.12	1.06	1.55	1.46
7		DMF	43	70	227	75 (Y)	1.91	2.18	3.33	1.53
8		THF	25	70	138	58 (C)	0.92	0.95	1.30	1.37
9		1,4 dioxane	39	80	257	95 (Y)	2.73	2.82	3.79	1.34
10		Water	19	80	150	45 (Y)	0.77	2.57	3.55	1.38 (a)
11		2-propanol	20	75	142	41 (Y)	0.66	1.28	2.25	1.76
12		2-butoxyethanol	25	80	148	29 (Y)	0.49	0.71	1.25	1.75
13	4	Bulk	0.5	80	145	82 (Y)	1.35	15.33	23.12	1.51
14		1,4 dioxane	15	70	267	92 (Y)	2.75	21.63	31.16	1.44
15	5	Bulk	12	70	102	87 (C)	1.02	1.37	1.71	1.24
16		Ethanol	11	70	102	81 (C)	0.94	0.96	1.21	1.27
17		THF	11	70	102	64 (C)	0.76	1.09	1.24	1.13
18		Acetonitrile	19	70	100	51 (C)	0.60	0.73	0.81	1.12
19		1,4 dioxane	17	70	102	75 (C)	0.88	0.99	1.23	1.24
20		Water	19	70	102	62 (Y)	0.73	3.74	5.28	1.41 (a)
21	6	Bulk	16	70	100	70 (Y)	0.81	1.20	1.69	1.41
22		Ethanol	16	70	100	31 (Y)	0.38	0.54	0.75	1.39
23	7	Bulk	12	70	100	85 (C)	0.97	1.2	1.57	1.29
24	8	Bulk	18	70	149	87 (C)	1.44	1.77	2.83	1.60
25		Acetonitrile	9	70	156	86 (C)	1.51	1.59	1.99	1.25

(a) Low molecular weight shoulders observed by SEC

(Y) Extent of reaction measured by yield of polymer

(C) Extent of reaction measured by conversion of monomer to polymer by ^{1}H NMR spectroscopy

RAFT agent 1 was successfully used for the polymerisation of NVP in 1, 4 dioxane. Similar ratios of NVP:DPCM:AIBN of 111:1:0.12 were used to compare the reproducibility of the polymerisation to that in the literature (Table 1; Entry 1).[4] After 39 h the retrieved yield of the polymer was 62%. The PDI of the polymer produced was 1.25 and the observed M_n was 5.30 x 10^3 $gmol^{-1}$ compared to the expected 8.00 x 10^3 $gmol^{-1}$. The results obtained for RAFT agent 1 showed that the M_n, PDI and yield of the polymer were comparable to those found in the literature.[4] NVP was also polymerised in bulk (Table 1; Entry 2). A greater NVP : RAFT agent 1 ratio of 157:1

was used and the found M_n of the polymer (1.37 x 10^4 $gmol^{-1}$) was closer to the theoretical M_n (1.28 x 10^4 $gmol^{-1}$). The PDI remained low at 1.17 at a yield of 71%. When the polymerisation was carried out in toluene (Table 3.1; Entry 3), the PDI was low at 1.16 but the yield of the polymerisation was very low (19%). The reasoning for why the yield is low is discussed in Section 3.3.4.

The polymerisation of NVP in the presence of RAFT agent 2 was carried out in bulk (Table 3.1; Entry 4) and 1,4 dioxane (Table 3.1; Entry 5). The observed molecular weight by SEC was very close to the theoretical molecular weight in both polymerisations. The PDI was 1.15 (bulk) and 1.24 (1, 4 dioxane), indicating a controlled polymerisation. ^{1}H NMR spectroscopy was also used to determine molecular weights. The M_n of 1.20 x 10^4 $gmol^{-1}$ and 4.68 x 10^3 $gmol^{-1}$ was found for bulk and 1, 4 dioxane, respectively. This correlates well with the SEC and theoretical data of the both polymers.

RAFT agent 3 (Rhodixan® A1) has also been used in the literature to control the polymerisation of NVP.[5] In this study, RAFT agent 3 was used to control the polymerisation of NVP in bulk and in a number of solvents. Generally, the PDI's observed of 1.34 - 1.76 were higher than those seen from RAFT agents 1 (1.16 – 1.25) and 2 (1.15 – 1.24). This is likely to be due to the occurrence of hybrid behaviour. The reactivites of the 2-propionic acid ethyl ester radicals (R group radicals) is similar to that of the NVP propagating radicals. Therefore, at the pre-equilibrium stage the radical intermediate can fragment either side of the thiocarbonylthio centre. This is likely to increase the number of propagation steps before the R group is able fragment cleanly and re-initiate the polymerisation. Despite this hybrid behaviour, observed molecular weights measured by SEC are closely related to the theoretical molecular weights (where non-protic solvents are used) (Table 3.1; Entry 6-9). When either water or protic solvents are used (Table 3.1; 10-12) the PDI increases significantly and the molecular weight observed is higher than that which is expected. This is more so for when the polymerisation takes place in an aqueous environment. The effect of solvent is discussed in Section 3.3.4.

NVP was polymerised in the presence of RAFT agent 4 in bulk with a NVP:RAFT agent 4:AIBN ratio of 145 : 1 : 0.13 (Table 3.1; Entry 13). RAFT agent 4 was synthesised with ethyl pyrrolidone as the R group similar to that of the propagating radical to provide more control over the polymerisation, as the propagating chain and R group would have similar reactivites. Hybrid behaviour was expected to possibly occur. The yield of the polymer was 82%. Compared to a conventional FRP of NVP also

conducted in bulk, under the same conditions, without the presence of RAFT agent 4 at 80°C. The yield of the polymer was 79%. SEC analysis of the two polymerisations was compared and shown in Table 3.2. PNVP synthesised conventionally had a M_n of approximately 1.82 x 10^5 $gmol^{-1}$ with a PDI of 1.44, whereas PNVP synthesised in the presence of RAFT agent 4 gave a M_n of approximately 1.53 x 10^5 $gmol^{-1}$ with a PDI of 1.51. It is evident from the data that the polymerisation of NVP using RAFT agent 4 was unsuccessful.

Table 3.2. Comparison between PNVP synthesised with and without RAFT agent 4

Polymerisation	NVP : RAFT agent	NVP : AIBN	RAFT agent : AIBN	$M_{n(theo.)}$ (x 10^4 $gmol^{-1}$)	M_n (SEC) (x 10^5 $gmol^{-1}$)	M_w (SEC) (x 10^5 $gmol^{-1}$)	PDI
Conventional (Bulk)	**N/A**	**1150 : 1**	**N/A**	**N/A**	**1.82**	**2.63**	**1.44**
RAFT (Bulk)	**145 : 1**	**1145 : 1**	**7.9 : 1**	**1.35**	**1.53**	**2.31**	**1.51**

It is thought that RAFT agent 4 is unable to control the polymerisation of NVP due to the nature of the leaving homolytic R group. Having a leaving group similar to the structure of the propagating radical would have been advantageous as they would have had similar reactivites, however RAFT agent 4 fragments to give an unstable primary radical (Scheme 3.2). Therefore, the propagation of the polymer chain is preferred rather than addition to and fragmentation from the RAFT agent.

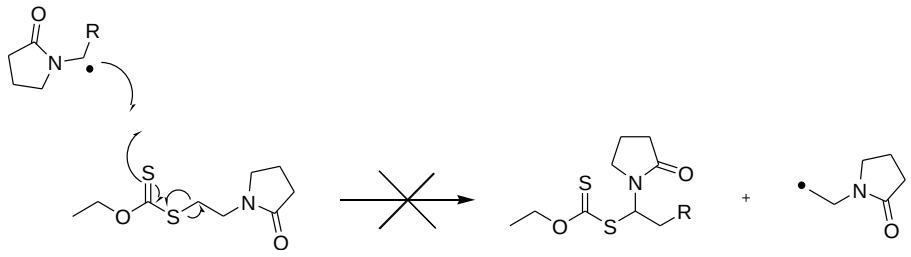

Scheme 3.2. Primary radical instability in RAFT agent 1

To confirm that RAFT agent 4 was unable to control the polymerisation of NVP the experiment was repeated in 1, 4 dioxane (Table 1; Entry 14) and similar results were observed.

RAFT agent 5 is a novel compound which incorporates an ethyl pyrrolidone fragment in the structure of the RAFT agent, as part of the R group. The RAFT agent fragments upon addition of NVP based radicals, to give a secondary R group radical. It was used to control the polymerisation of NVP in bulk (Table 3.1; Entry 15) and in a number of solvents (Table 3.1; Entry 16-20). The found molecular weight data acquired from SEC analysis agrees relatively well with the theoretical molecular weights. PDI's are also low with the only exception being when the controlled polymerisation is carried out in water (Table 3.1; Entry 20). The expected molecular weight is far lower than the observed molecular weight as analysed by SEC. In addition, there is a very broad molecular weight distribution in the SEC trace (discussed in Section 3.3.4). RAFT polymerisation of NVP using RAFT agent 5 was also conducted in 1, 4 dioxane (Scheme 3.3) using a molar ratio [NVP]:[RAFT agent 5]:[ACVA] of 200:1:0.2 at 70°C for 8 h.

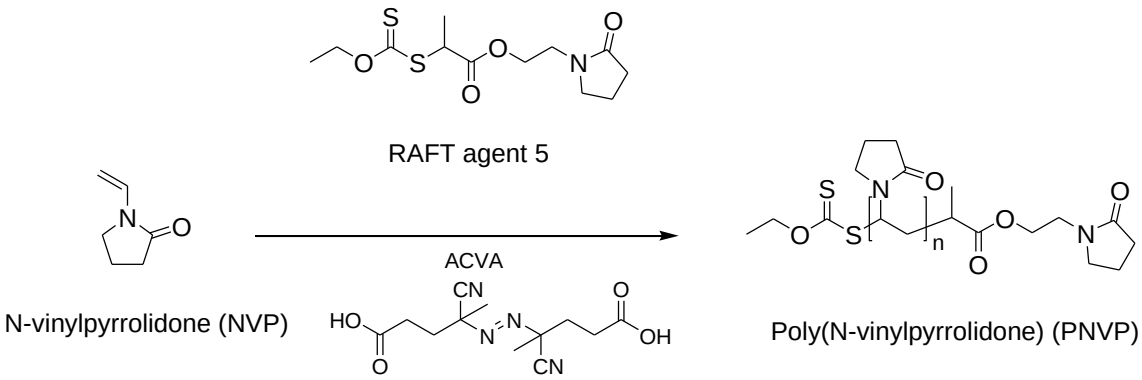

Scheme 3.3. Homopolymerisation of NVP in the presence of RAFT agent 5

A kinetic study was performed by taking an aliquot of the polymerisation mixture out of the reaction vessel and quenched in liquid nitrogen at the required time point. ^{1}H NMR spectroscopy and SEC analysis was conducted on the samples retrieved. Figure 3.2 shows a plot of $\log[([M]_o/[M])]$ against time. The reaction was followed upto 62% conversion of monomer to polymer. It can be clearly seen that $\log[([M]_o/[M])]$ increases linearly, upto 62% conversion, *vs.* time with no indication of any inhibition period. The R^2 value is equal to 0.9917.

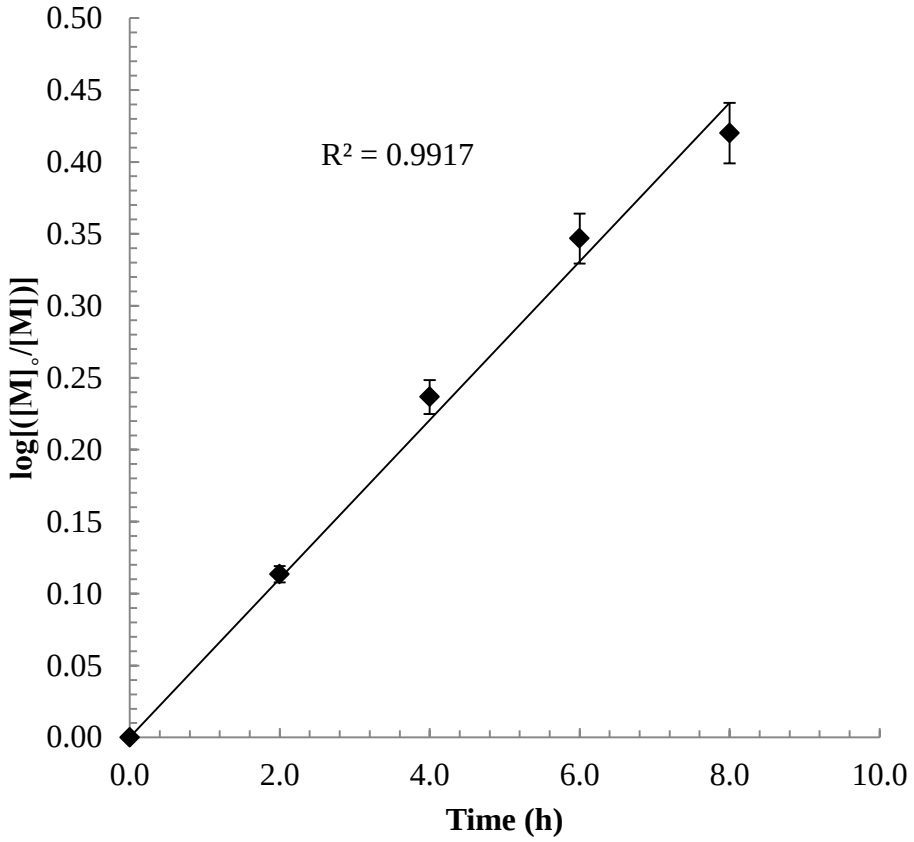

Figure 3.2. Plot of log of monomer concentration against time for polymerisation of NVP (in 1,4 dioxane) in the presence of RAFT agent 5 and ACVA at 70°C. Solid line is line of best fit

Figure 3.3 shows a plot of M_n and PDI against % conversion of monomer to polymer. PDI remained low (1.16 - 1.44) throughout the polymerisation and molecular weight increased in a linear fashion with increasing conversion. The R^2 value was calculated to be 0.9442. After 8 h the M_n was found to be 1.39 x 10^4 $gmol^{-1}$ by SEC, which compared well to the theoretical M_n of 1.41 x 10^4 $gmol^{-1}$. However, at low conversions, higher molecular weight PNVP was produced. After a polymerisation time of 2 h the M_n was found to be 8.46 x 10^3 $gmol^{-1}$ while the theoretical M_n was lower at 5.42 x 10^3 $gmol^{-1}$. This is indicative of hybrid behaviour.[8, 10, 28]

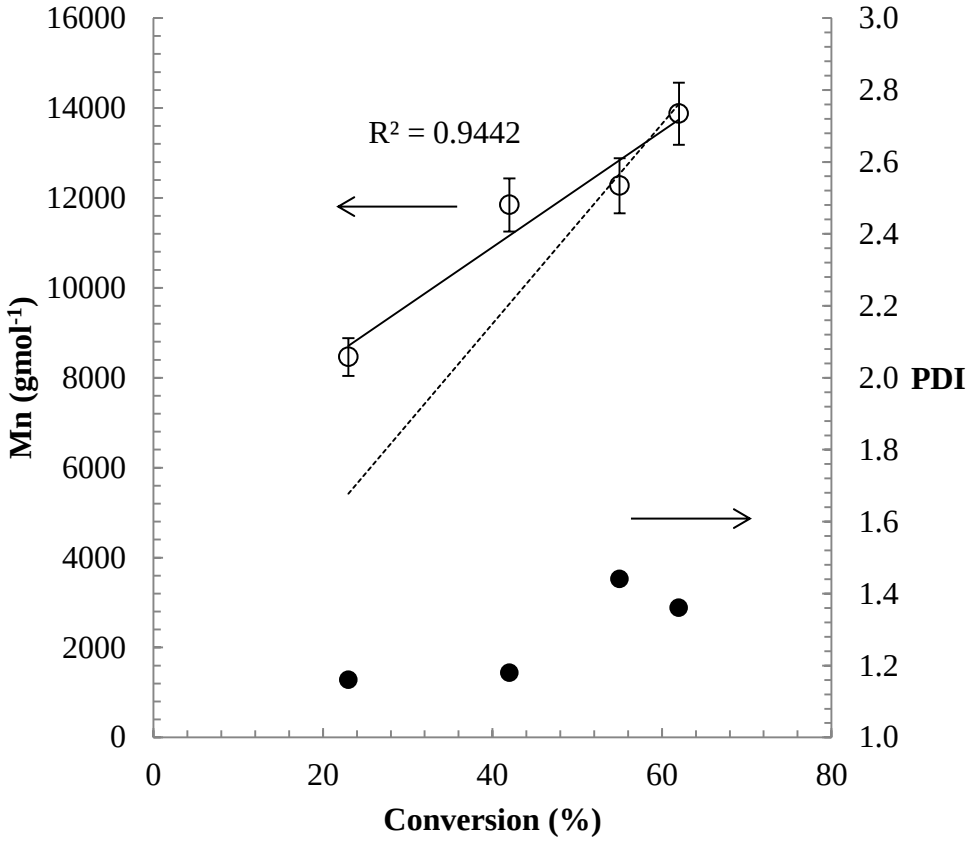

Figure 3.3. Number average molecular weight against % conversion for polymerisation of NVP (in 1,4 dioxane) in the presence of RAFT agent 5 and AVCA at 70°C. Solid line is line of best fit. Dashed line (---) represents theoretical M_n

Figure 3.4 shows the progression of the SEC traces over time. It is shown that there is a gradual increase in the molecular weight with increasing polymerisation time 2 – 8 h. The SEC chromatograms also show the presence of lower molecular weight tails with increasing molecular weight. This is also reflected on the increasing PDI over time. Figure 3.5, a plot of Log M against Wf / dLog M shows the progression of molecular weight distribution. As seen in the SEC chromatograms, similar tailing is observed for samples at higher molecular weight (greater polymerisation times). This suggests the increasing presence of termination products (i.e. dead chains) as conversion increases.

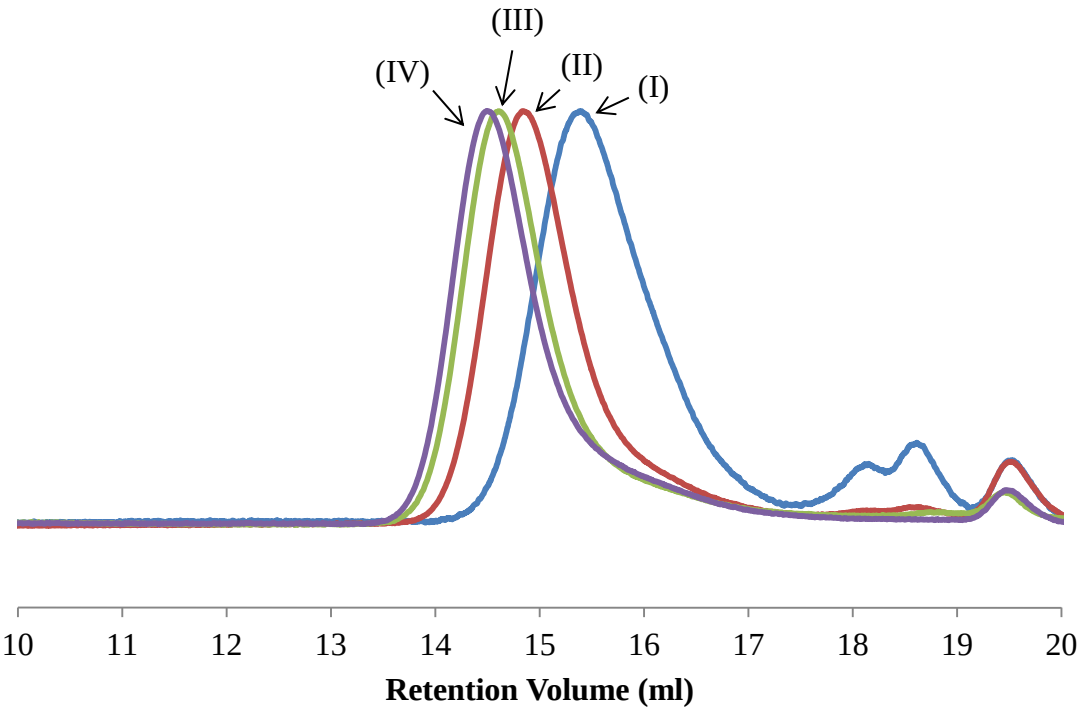

Figure 3.4. SEC traces (refractive index)for the polymerisation of NVP in presence of RAFT agent 5. (I) 2 h, (II) 4 h, (III) 6 h, (IV) 8 h

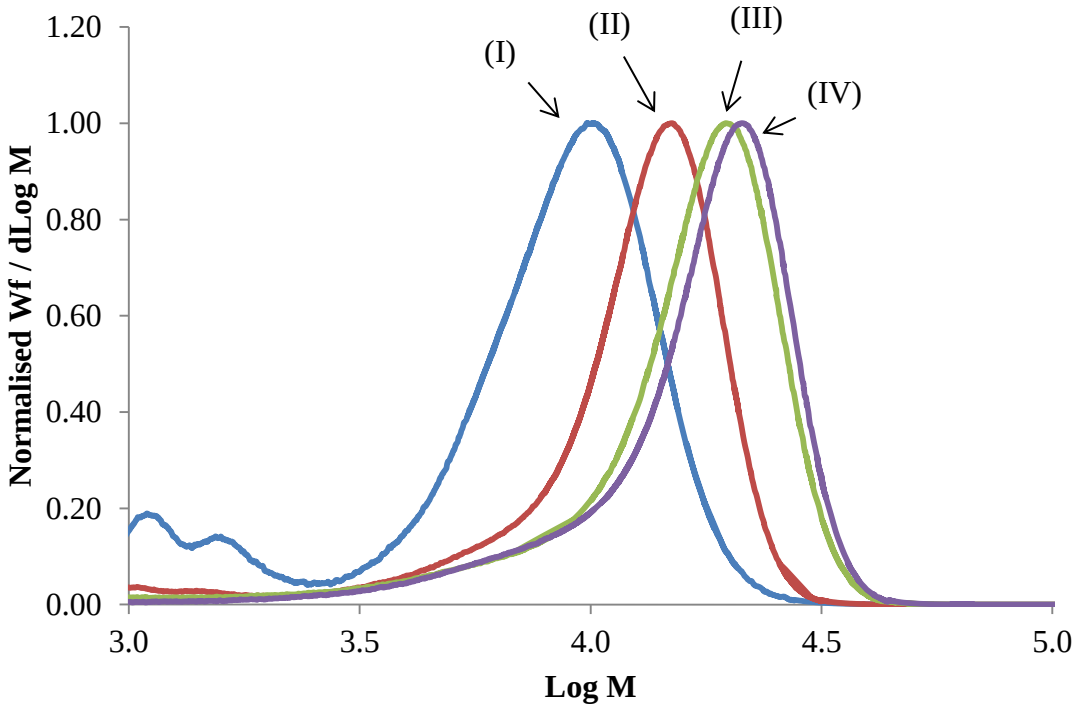

Figure 3.5. Plot of Log M against normalised Wf / dLog M showing the molecular weight distribution for the polymerisation of NVP in the presence of RAFT agent 5. (I) 2 h, (II) 4 h, (III) 6 h, (IV) 8 h

RAFT agent 6 is also a novel compound with the aim of controlling the polymerisation of NVP. It incorporates an ethyl pyrrolidone fragment within its R group. The RAFT agent fragments upon addition of NVP based radicals to give a tertiary R group radical (Scheme 3.4). It was used to control the polymerisation of NVP in bulk and ethanol (Table 3.1; Entry 21 and 22). The PDI's are generally seen to be higher in the polymerisations with RAFT agent 6 (PDI = 1.39 - 1.41) compared to that of RAFT agent 5 (PDI = 1.12 – 1.41). The RAFT polymerisation of NVP using RAFT agent 6 was also conducted in 1, 4 dioxane using a molar ratio [NVP]:[RAFT agent 6]:[ACVA] of 200:1:0.2 at 70°C for 8 h. These are the same conditions used for RAFT agent 5.

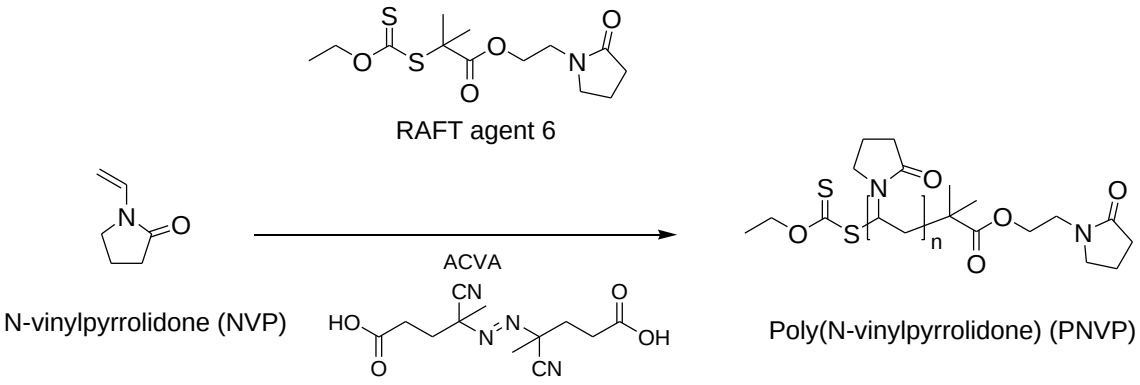

Scheme 3.4 Homopolymerisation of NVP in the presence of RAFT agent 6

A kinetic study was performed by taking an aliquot of the polymerisation mixture out of the reaction vessel and quenched in liquid nitrogen at the required time point (same time point as for RAFT agent 5). ^{1}H NMR spectroscopy and SEC analysis was conducted on the samples retrieved. Figure 3.6 shows a plot of $\log[([M]_o/[M])]$ against time. The reaction was followed upto 57% of conversion of monomer to polymer. It can be clearly seen that $\log[([M]_o/[M])]$ increases linearly, upto 57% conversion, *vs.* time with again no indication of any inhibition period. The R^2 value is equal to 0.9944.

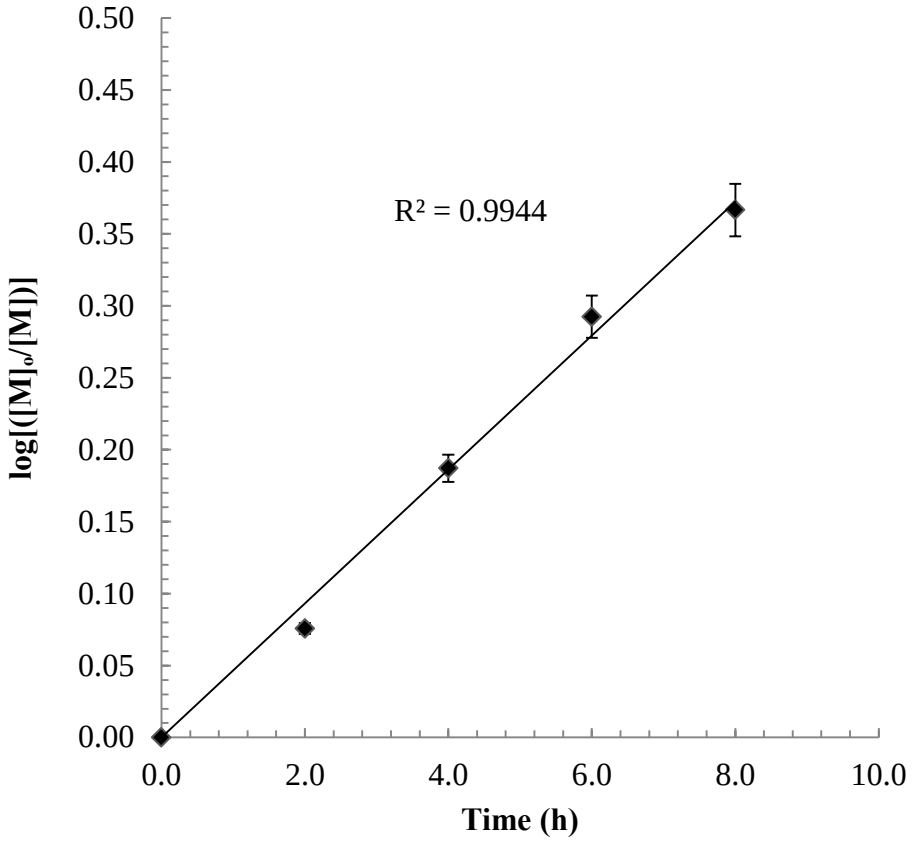

Figure 3.6. Plot of log of monomer concentration against time for polymerisation of NVP (in 1,4 dioxane) in the presence of RAFT agent 6 and ACVA at 70°C. Solid line is line of best fit

Figure 3.7 shows a plot of M_n and PDI against % conversion of monomer to polymer. PDI remained narrow (1.11-1.54) throughout the polymerisation, however, a non-linear relationship was observed, indicating the lack of control over the polymerisation. After 8 h the M_n was found to be 1.31 x 10^4 $gmol^{-1}$ by SEC, which compared well to the theoretical M_n of 1.30 x 10^4 $gmol^{-1}$. Similarly to when RAFT agent 5 was used, hybrid behaviour was exhibited, where higher molecular weight polymer was formed at lower conversions. After a polymerisation time of 2 h the M_n was found to be 7.48 x 10^3 $gmol^{-1}$ while the theoretical M_n was lower at 3.88 x 10^3 $gmol^{-1}$.

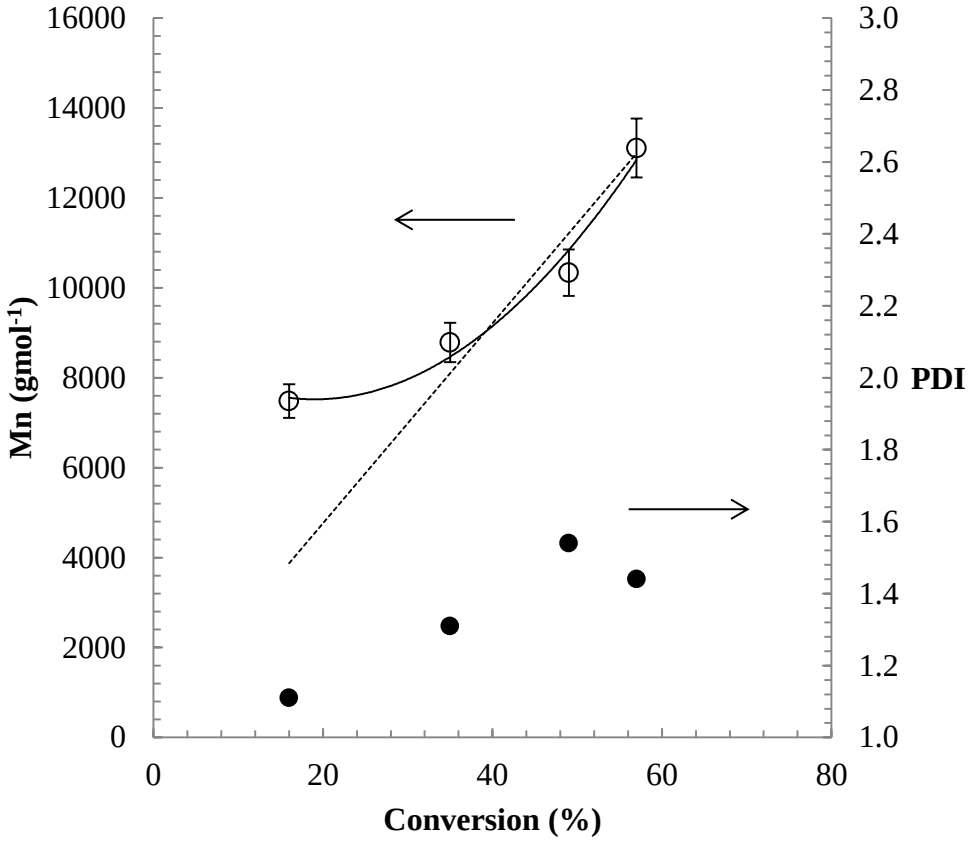

Figure 3.7. Number average molecular weight against % conversion for polymerisation of NVP (in 1,4 dioxane) in the presence of RAFT agent 6 and AVCA at 70°C. Solid line is line of best fit. Dashed line (---) represents theoretical M_n

Figure 3.8 shows the progression of the SEC traces over time. It can be observed that with increasing polymerisation time from 2 – 8 h, there is a gradual shift of the peaks to a higher molecular weight. The SEC chromatograms also show the presence of lower molecular weight tail with increasing molecular weight. This is also reflected in the increased PDI over time. Figure 3.9, a plot of Log M against Wf / dLog M shows the progression of molecular weight distribution. As seen in the SEC chromatograms, significant tailing is observed for samples, especially those at higher molecular weight (greater polymerisation times). This suggests the increasing presence of termination products (i.e. dead chains) as conversion increases.

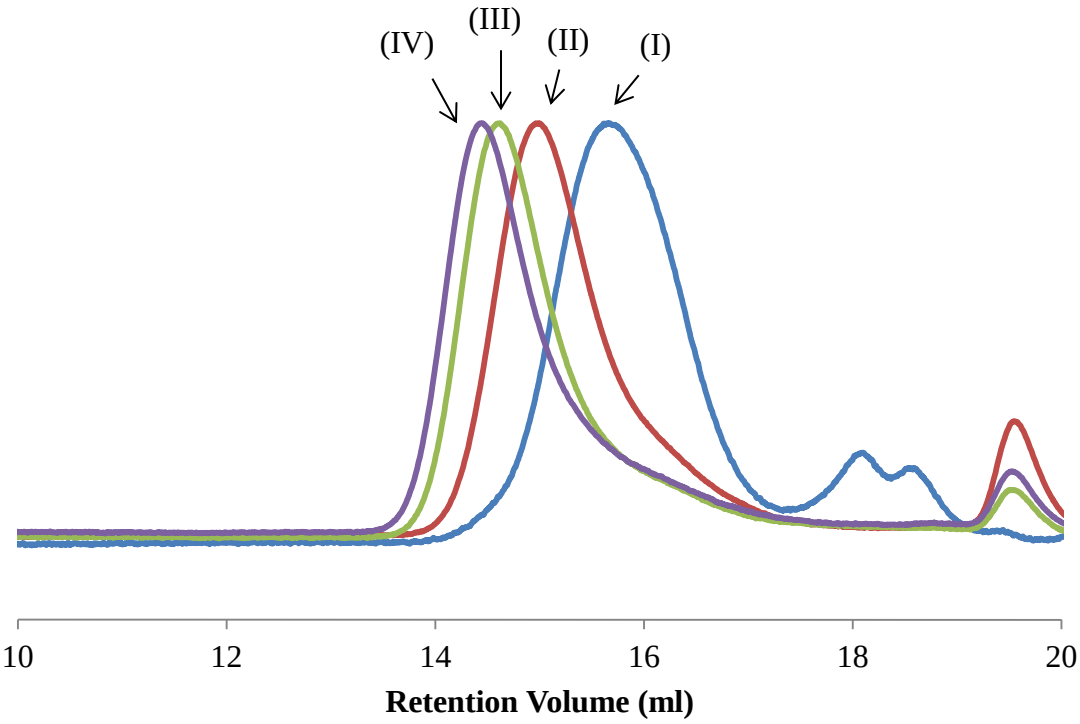

Figure 3.8. SEC traces (refractive index) for the polymerisation of NVP in presence of RAFT agent 6. (I) 2 h, (II) 4 h, (III) 6 h, (IV) 8 h

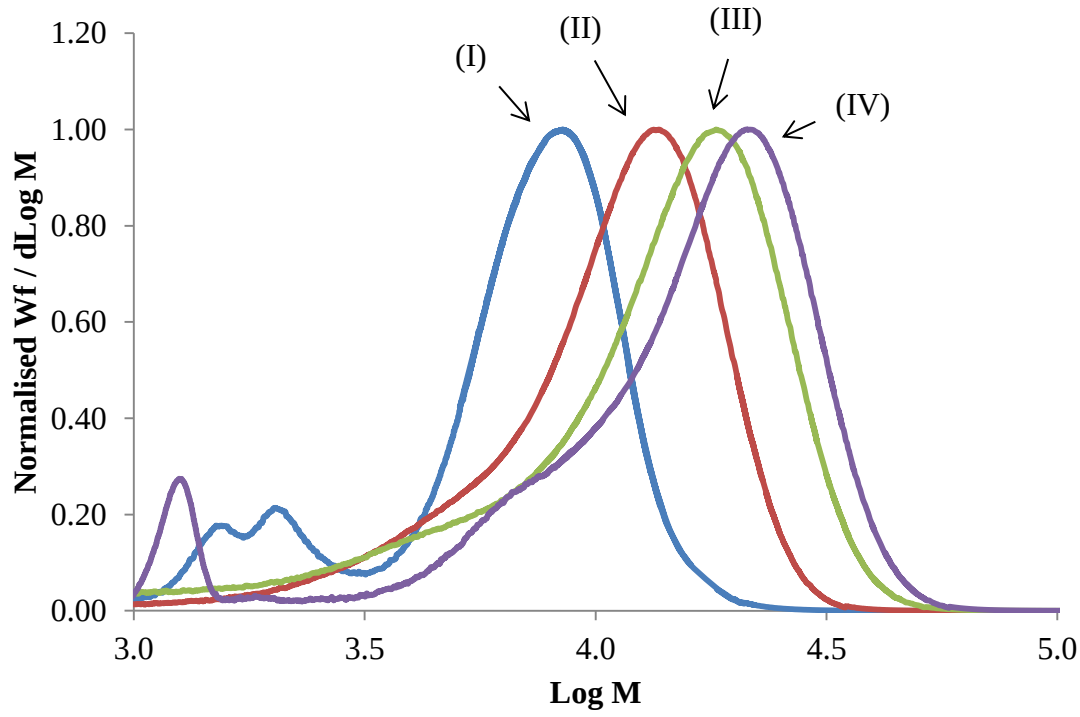

Figure 3.9. Plot of Log M against normalised Wf / dLog M showing the molecular weight distribution for the polymerisation of NVP in the presence of RAFT agent 6. (I) 2 h, (II) 4 h, (III) 6 h, (IV) 8 h

Comparing the kinetic data when conducting a RAFT polymerisation using RAFT agent 5 or 6 suggests that greater control over the polymerisation can be attained when using RAFT agent 5. RAFT agent 6 appears to exhibit a lack of control over the polymerisation, as observed by the non-linear relationship between % conversion and M_n. However, when either using a RAFT agent which fragments to give a secondary or tertiary R group radical (Scheme 3.5), PDI increases with increasing higher molecular weight (due to tailing). This suggests that in both cases termination reactions are occurring, leading to dead chains and therefore higher molecular weight distributions with higher conversions. Furthermore, when RAFT agent 5 is used there are consistently higher conversions observed at each time point.

It is believed that the non-linear relationship (% conversion against M_n) and the lowered conversion at each time point for RAFT agent 6, can be attributed to the increased stability of RAFT agent 6 and lowered reactivity compared to RAFT agent 5 towards initiation of monomeric species.

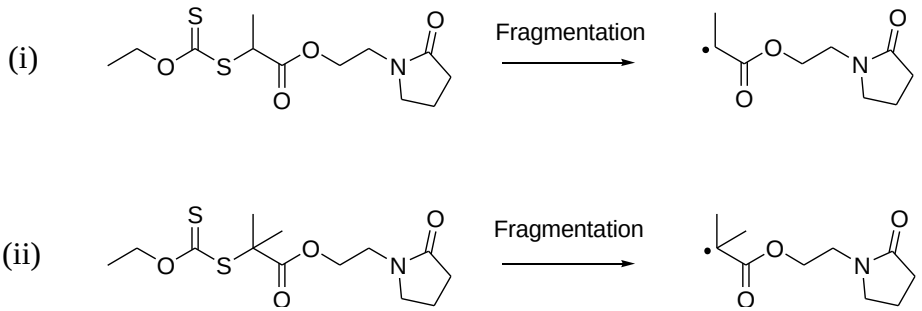

Scheme 3.5. Fragmentation to give (i) secondary radical R group (RAFT agent 5) and (ii) tertiary radical R group (RAFT agent 6)

RAFT agent 7 is also a novel compound, where the Z group includes an ethyl pyrrolidone fragment. The RAFT agent fragments to give a secondary R group radical. It has been used in bulk (Table 3.1; Entry 23). The observed molecular weight of 9.7 x 10^3 $gmol^{-1}$ is relatively close to the expected molecular weight of 1.20 x 10^4 $gmol^{-1}$ and the PDI is low (1.29). This result is comparative to that seen when using RAFT agent 5 in bulk (Table 3.1; Entry 15). Both RAFT agents fragment to give a secondary radical R group. The RAFT polymerisation of NVP using RAFT agent 7 was also conducted in 1, 4 dioxane (Scheme 3.6) using a molar ratio [NVP]:[RAFT agent 7]:[ACVA] of 200:1:0.2 at 70°C for 8 h.

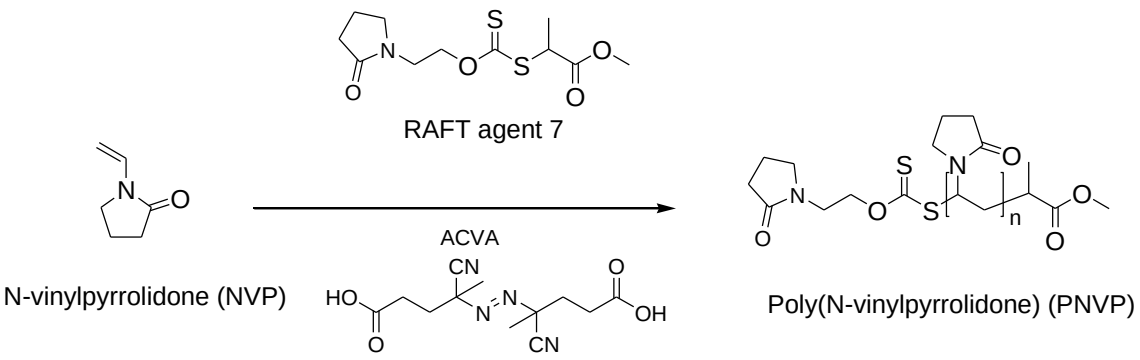

Scheme 3.6. Homopolymerisation of NVP in the presence of RAFT agent 7

A kinetic study was performed by making a stock solution of NVP, RAFT agent 7, 1, 4 dioxane and ACVA. This was then equally separated into a number of glass ampoules and heated to 70°C. At the required time point the ampoules were removed from the oil bath and quenched in liquid nitrogen to stop the polymerisation. The reaction was followed upto 95% of conversion of monomer to polymer. Figure 3.10 shows a plot of $\log[([M]_o/[M])]$ against time and shows good linear correlation. There is no apparent inhibition period in the polymerisation. The R^2 value is equal to 0.9646.

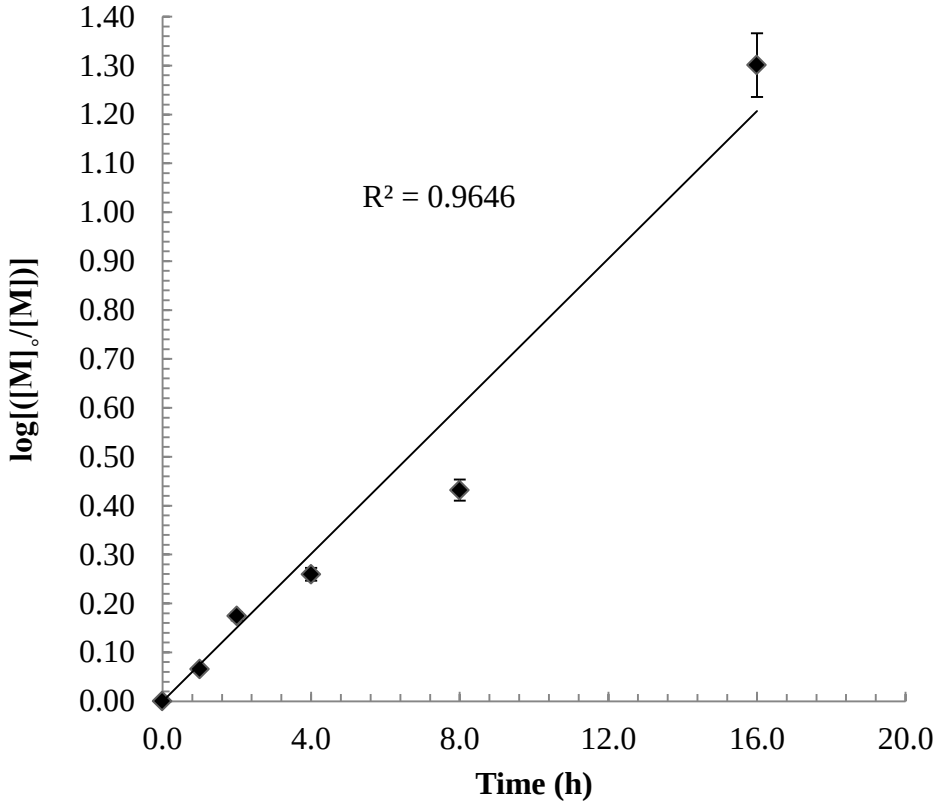

Figure 3.10. Plot of log of monomer concentration against time for polymerisation of NVP (in 1,4 dioxane) in the presence of RAFT agent 4 and ACVA at 70°C. Solid line is line of best fit

Figure 3.11 shows a plot of M_n and PDI against % conversion of monomer to polymer. PDI remained very low (1.14 – 1.21) throughout the polymerisation and molecular weight increased in a linear fashion with increasing conversion. The R^2 value is equal to 0.9987. After 16 h the M_n was 2.38 x 10^4 $gmol^{-1}$ by SEC, which compared well to the theoretical M_n of 2.11 x 10^4 $gmol^{-1}$. There is no evidence of any hybrid behaviour in the polymerisation using RAFT agent 7, unlike with RAFT agents 5 or 6.

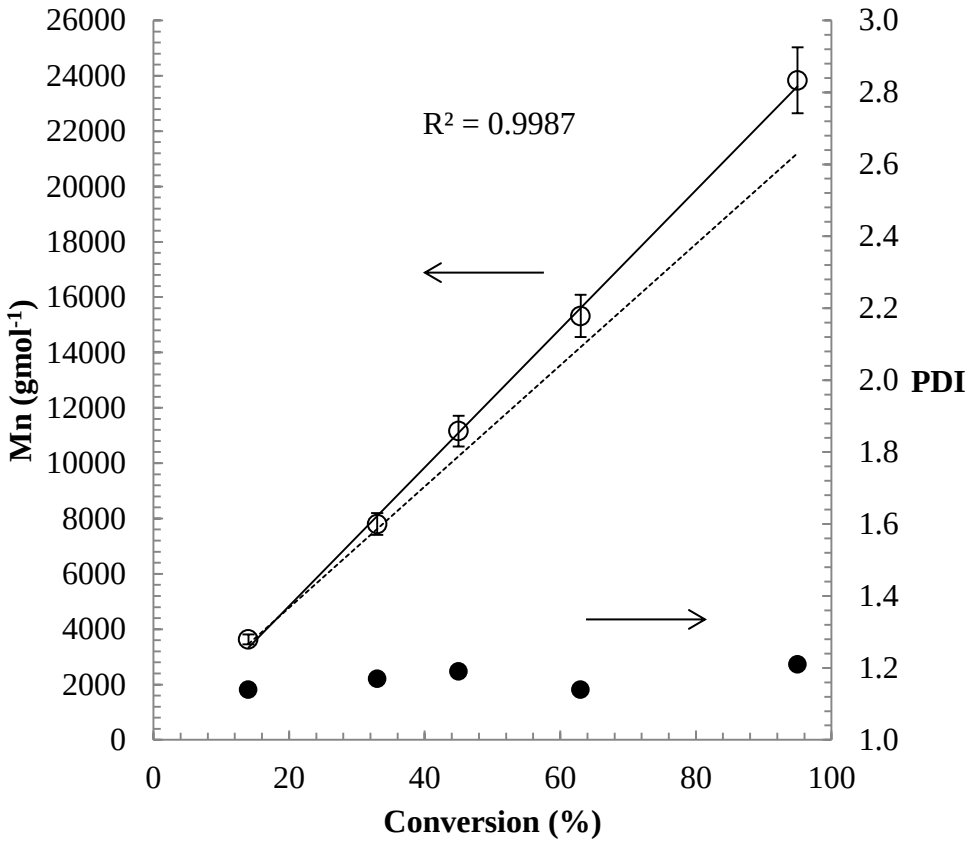

Figure 3.11. Number average molecular weight against % conversion for polymerisation of NVP (in 1,4 dioxane) in the presence of RAFT agent 7 and AVCA at 70°C. Solid line is line of best fit. Dashed line (---) represents theoretical M_n

Figure 3.12 shows the progression of the SEC traces over time. It can be observed that with increasing polymerisation time from 1 – 16 h, there is a gradual shift of the peaks to a higher molecular weight. It is also seen that though the PDI is low even at high conversion, it is apparent that there are still termination products due to the presence of tailing on the lower molecular weight side. This is also be demonstrated in by looking at the progression of the molecular weight distribution, Figure 3.13. A plot

of Log M against Wf / dLog M, shows the evidence of significant tailing with increasing M_n.

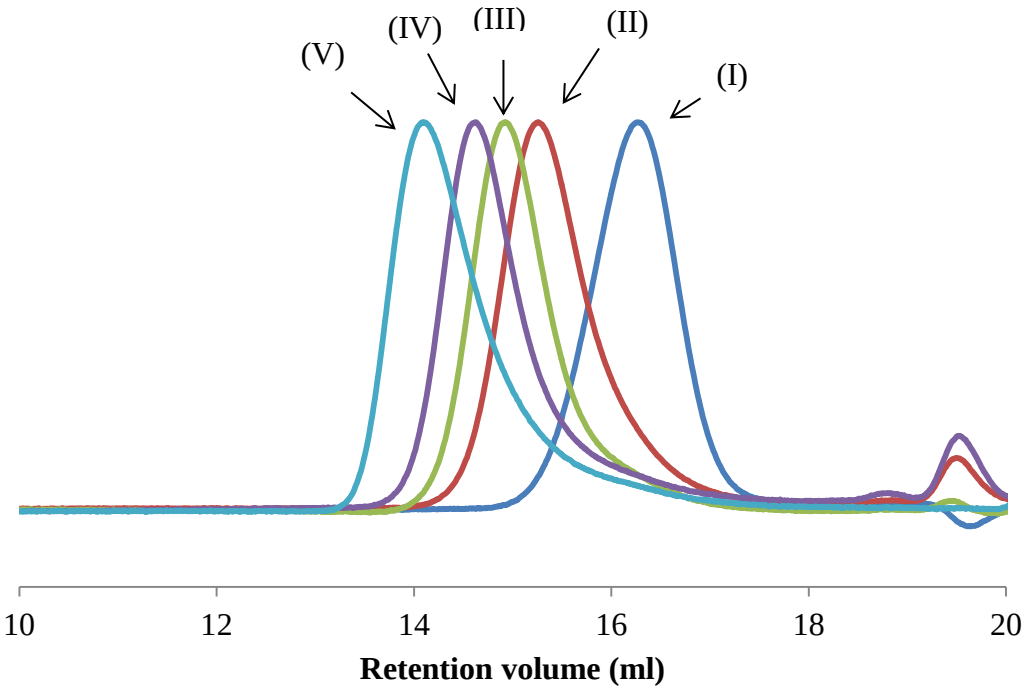

Figure 3.12. SEC traces (refractive index) for the polymerisation of NVP in presence of RAFT agent 7. (I) 1 h, (II) 2 h, (III) 4 h, (IV) 8 h, (V) 16 h

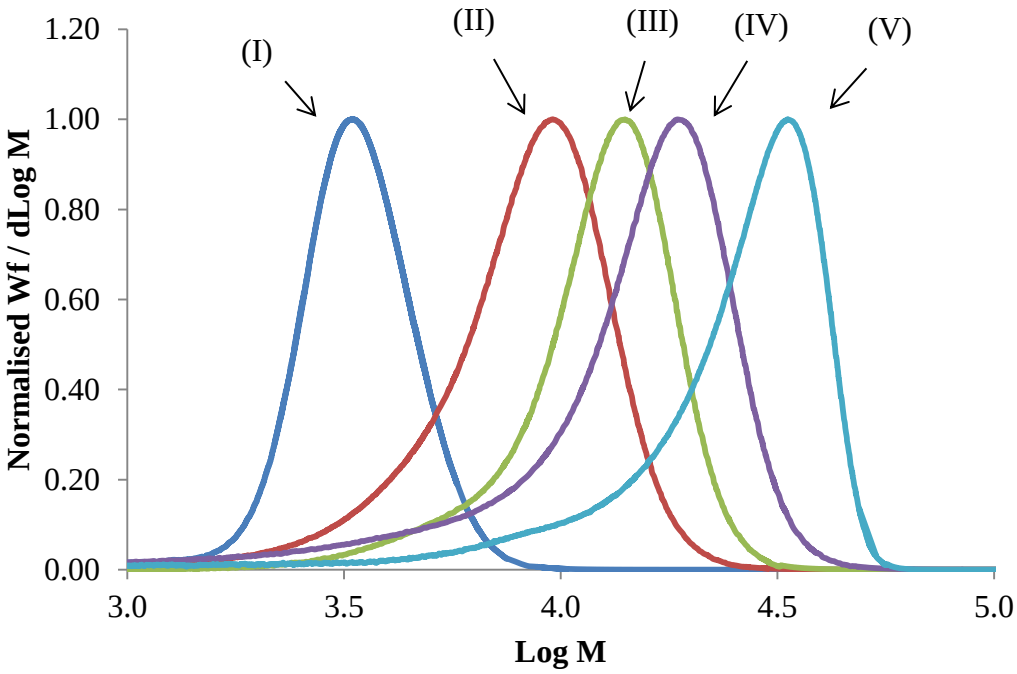

Figure 3.13. Plot of Log M against normalised Wf / dLog M showing the molecular weight distribution for the polymerisation of NVP in the presence of RAFT agent 7. (I) 2 h, (II) 4 h, (III) 6 h, (IV) 8 h

Compared to RAFT agent 5 and 6 the main difference in the kinetic study using RAFT agent 7 is that the polymerisation was conducted under reduced pressure rather nitrogen gas. In addition, a stock solution was made and separate ampoules were removed from the oil bath at regular intervals rather than taking aliquots from one ampoule. The result is that the monomer concentration *vs*. time is more accurate for RAFT agents 5 and 6. Using separate ampoules means there may be slight differences in the reaction conditions from ampoule to ampoule. However, the molecular weight vs. conversion gives a closer correlation to the theoretical using RAFT agent 7. Also PDI values can be observed to be consistently lower throughout the polymerisation. In all of the SEC traces for the three RAFT agents there is no evidence of higher molecular weight shoulders indicating any recombination products.

Cyanomethyl methyl(phenyl)carbamodithioate, RAFT agent 8 (Figure 3.14) is sold by Sigma Aldrich and it is claimed to be able to control the polymerisation of LAMs effectively.

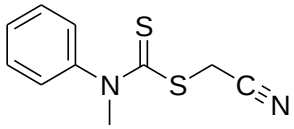

Figure 3.14. Structure of RAFT agent 8 (Cyanomethyl methyl(phenyl)carbamodithioate)

RAFT agent 8 is a dithiocarbamate which fragments to give a primary R group radical, which is stabilised by a cyano group and in the literature it has been used to polymerise VAc. We therefore used it to control the polymerisation of NVP in bulk and acetonitrile (Table 3.1; Entry 24 and 25). In both cases the observed molecular weight is close to that expected. In acetonitrile, the PDI is low (1.25). It is unknown why the PDI is relatively high (1.60) in the polymerisation carried out in bulk.

3.3.2. Controlled polymerisation of vinyl acetate

In this study, the controlled polymerisation of vinyl acetate was attempted using a number of RAFT agents (RAFT agents 1-5 and 8) and the results are shown in Table 3.3.

The extent of the polymerisation was measured gravimetrically by weighing dry PVAc samples. The polymerisation mixture was diluted or dissolved with solvent and then transferred to a flask or jar where all the solvent and excess monomer was removed under reduced pressure to leave the final polymer product. Size exclusion chromatography (SEC) was used to measure the molecular weight and polydispersity of the polymers produced. In addition, ^{1}H NMR spectroscopy was used to measure the molecular weight of the polymers by integrating an appropriate proton environment from the chain end to the polymer backbone.

Table 3.3. Polymerisations of VAc using RAFT agent 1-5 and 8.

Entry	RAFT agent	Solvent	Time (h)	Temp. (°C)	[VAc] / [RAFT agent]	Yield (%)	M_n (theo.) (x 10^4 $gmol^{-1}$)	M_n (NMR) (x 10^4 $gmol^{-1}$)	M_n (SEC) (x 10^4 $gmol^{-1}$)	M_w (SEC) (x 10^4 $gmol^{-1}$)	PDI
1	1	Bulk	39	80	151	92	1.24	1.44	1.58	2.30	1.46
2		1, 4 dioxane	45	80	100	90	0.90	0.96	0.66	1.01	1.53
3		Toluene	44	80	100	47	0.45	0.52	0.60	0.78	1.29
4	2	Bulk	40	80	147	N/A	N/A	N/A	N/A	N/A	N/A
5		1, 4 dioxane	45	80	94	N/A	N/A	N/A	N/A	N/A	N/A
6	3	Bulk	17	80	145	90	1.15	1.17	1.52	2.23	1.47
7		Ethyl acetate	16	80	136	90	1.08	1.31	1.12	1.67	1.50
8		Acetonitrile	17	75	141	88	1.10	1.23	1.27	1.71	1.35
9		Toluene	17	75	141	40	0.51	0.68	0.59	0.76	1.29
10		Cyclohexane	17	75	148	93	1.21	1.27	1.17	2.05	1.76
11		2-propanol	17	75	145	69	0.89	1.05	0.49	1.01	2.08
12	4	1,4 dioxane	15	68	242	81	1.68	N/A	0.89	2.20	2.48
13	5	Bulk	16	60	100	80	0.72	1.28	1.07	1.36	1.27
14		Ethyl acetate	19	68	100	92	0.82	0.92	0.94	1.40	1.49
15		Ethanol	19	68	100	88	0.79	0.96	0.56	1.06	1.90
16	8	Bulk	18	60	147	51	0.67	0.99	0.93	1.16	1.25
17		Acetonitrile	9	65	151	86	1.14	1.16	1.02	1.41	1.39

RAFT agent 1 was used to control the polymerisation of VAc in bulk at 80°C (Table 3.3; Entry 1) and the polymerisation was left for 39 h. A high yield was achieved (92%), the found M_n of 1.44 x 10^4 $gmol^{-1}$, was close to the theoretical M_n of

1.24×10^4 $gmol^{-1}$ and the PDI was relatively low (1.46). This compares well against the data found in the literature.[16] RAFT agent 1 was also used to control the polymerisation of VAc in 1, 4 dioxane (Table 3.3; Entry 2) and toluene (Table 3.3; Entry 3). In both cases, the theoretical molecular weight is in good agreement with the M_n analysed by ^1H NMR spectroscopy. However, the molecular weight data obtained by SEC is lower than expected when 1, 4 dioxane is used as the solvent. The reasoning for why the yield is low when toluene is used as solvent is discussed in Section 3.3.4.

RAFT agent 2 was used to control the polymerisation of VAc. However, whether the polymerisation was carried out in bulk (Table 3.3; Entry 4) or 1, 4 dioxane (Table 3.3; Entry 5) there was no evidence of any polymerisation even after 45 h. Tong *et al*[29] found that RAFT agent 2 had an inhibition period of 48 h. After 72 h, a conversion of only 50% was achieved. This was attributed to the poor reactivity of the 1-phenyl ethyl radical formed from fragmentation of RAFT agent 2, towards VAc. This observation was also found by Pound *et al*.[30]

RAFT agent 3 was used to control the polymerisation of VAc in a number of solvents (Table 3.3; Entry 6 – 11). The molecular weights for Entry 6 – 11 are closely related to the theoretical molecular weight of each polymer. The PDI's are also relatively low and are comparable to that seen in the literature.[31-37] When either cyclohexane (Table 3.3; Entry 10) or 2-propanol (Table 3.3; Entry 11) were used as the solvent, the PDI was observed to be high. This suggests that both solvents are also taking part in the chain transfer process. Any chain transfer of propagating radicals to solvent is expected to result in dead chains and hence a greater PDI. The chain transfer constant to solvent for cyclohexane is; $C_s = 6.59 \times 10^4$ at 60°C [38] and for 2-propanol is; $C_s = 44.6 \times 10^4$ at 70°C [39, 40] which is high. The reasoning for why the yield is low when toluene is used as solvent is discussed in Section 3.3.4.

The controlled polymerisation of VAc was attempted using RAFT agent 4 (Table 3.3; Entry 12). It is clear from the observed high PDI (2.48) than the controlled polymerisation was not successful.

RAFT agent 5 was used in an attempt to control the polymerisation of VAc in bulk, ethyl acetate and ethanol (Table 3.3; Entry 13 - 15). When the polymerisation was carried out in ethanol the PDI of the resulting polymer was high (1.90). This indicates that the solvent is taking part in the chain transfer process. The polymerisation of VAc in ethyl acetate gave a similar result to that seen for RAFT agent 3 (Table 3.3; Entry 7 and 14). The PDI's of the resulting polymers are very similar 1.49 and 1.50. Both molecular weights are close to the expected M_n.

In order to compare to that in the literature, RAFT agent 8 was used for the controlled polymerisation of VAc in bulk and acetonitrile. The results in Table 3.3; Entry 16 – 17 compare well to the results in the literature.[15] The observed molecular weight by ^{1}H NMR spectroscopy and SEC is slightly higher than the expected which also can be seen in the literature. The found molecular weight (1.16 x 10^4 gmol^{-1}) for Entry 17 is close the theoretical value of 1.14 x 10^4 gmol^{-1}. The PDI is observed to be slightly higher when acetonitrile was used as the solvent. In both cases the ^{1}H NMR spectroscopy and SEC data are closely matched.

3.3.3. Controlled polymerisation of N-vinylcaprolactam

In comparison to NVP or VAc little attention has been given to the controlled polymerisation of NVCL by RAFT. In this study RAFT agents 2, 3, 5, 6 and 7 were used to control the polymerisation of NVCL. The data from these polymerisations is represented in Table 3.4. The yield of the polymerisation was measured gravimetrically.

Table 3.4. Polymerisations of NVCL using RAFT agent 2, 3, 5, 6 and 7

Entry	RAFT agent	Solvent	Time (h)	Temp. (°C)	[NVCL] / [RAFT agent]	Yield (%)	M_n (theo.) (x 10^4 gmol^{-1})	M_n (SEC) (x 10^4 gmol^{-1})	M_w (SEC) (x 10^4 gmol^{-1})	PDI
1	2	Bulk	16	80	154	47	1.00	1.02	1.52	1.48
2	3	Bulk	16	80	148	53	1.11	1.52	2.26	1.48 (a)
3		1,4 dioxane	40	80	241	49	1.67	1.65	2.27	1.38 (a)
4	5	1,4 dioxane	17	70	205	57	1.67	2.08	2.82	1.36
5	6	1, 4 dioxane	17	70	206	23	0.69	1.12	1.78	1.56 (b)
6	7	1, 4 dioxane	17	70	206	60	1.76	2.62	3.57	1.36

(a) Low molecular weight shoulder

(b) Bimodal

RAFT agent 2 was used to control the polymerisation of NVCL in bulk at 80°C, using a NVCL:RAFT agent 2 ratio of 154:1 (Table 3.4; Entry 1). A good correlation of found M_n (1.02 x 10^4 gmol^{-1}) and theoretical M_n (1.00 x 10^4 gmol^{-1}) was observed. The RAFT polymerisation of NVCL has also been reported in the literature.[22] However, the found M_n in the literature was observed to be half of the expected M_n.

The controlled polymerisation of NVCL was carried out in bulk and 1,4 dioxane (Table 3.4; Entry 2 – 3) in the presence of RAFT agent 3. The found M_n is relatively close to that of the expected M_n for the polymerisation reactions carried out in bulk and 1, 4 dioxane. For both polymerisations the SEC traces showed small low molecular weight shoulders (Figure 3.15). The reason is unclear but it may well be due to either or a combination of hybrid behaviour and termination reactions. The same observation is seen in the plot of Log M against Wf / dLog M, Figure 3.16, where significant tailing is demonstrated in the lower molecular weight region.

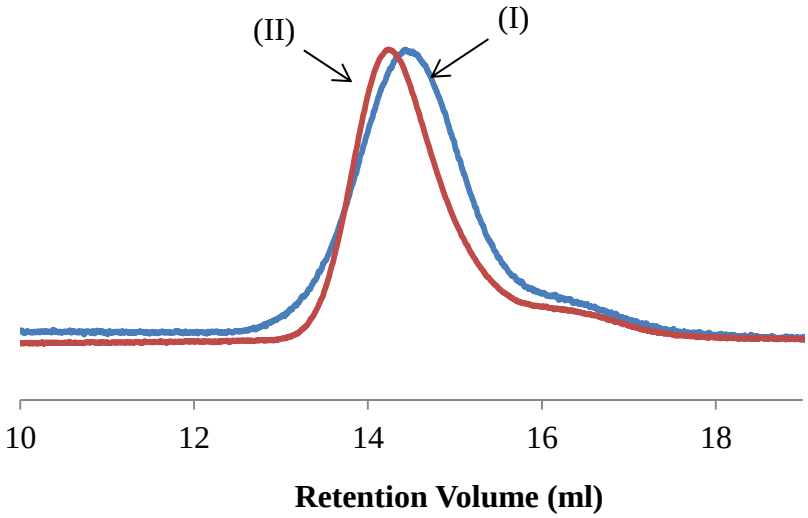

Figure 3.15. SEC traces (refractive index) for RAFT agent 3 in (I) bulk, (II) 1, 4 dioxane

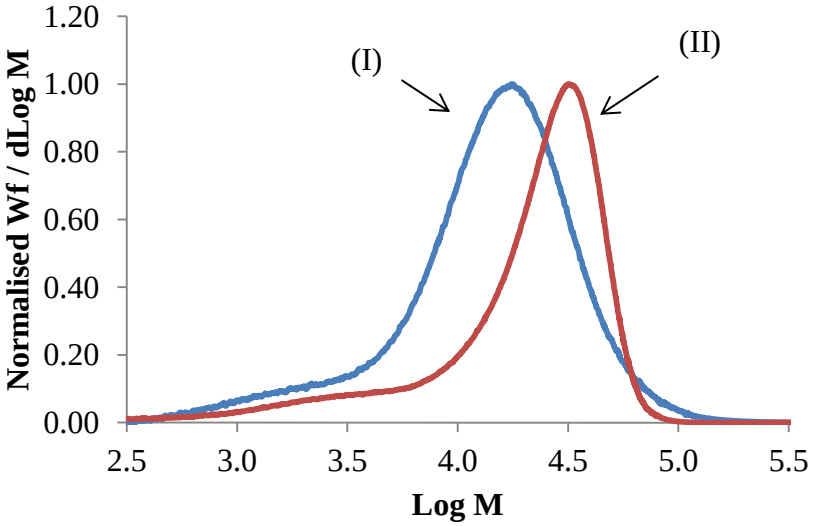

Figure 3.16. Plot of Log M against normalised Wf / dLog M showing the molecular weight distribution for the polymerisation of NVCL in the presence of RAFT agent 3 in (I) bulk, (II) 1, 4 dioxane

The novel RAFT agents 5 - 7 were also used to control the polymerisation of NVCL. The ratio of NVCL:RAFT agent for each polymerisation was 200 : 1 and the polymerisations were carried out in 1, 4 dioxane. The molecular weights for Entries 4 and 6 (Table 3.4) were fairly close to the theoretical M_n and the polydispersity indices were low (PDI = 1.36). It is interesting to see that there is no significant appearance of any low molecular weight shoulders for the polymer samples analysed by SEC when using either RAFT agents 5 or 7 (Figures 3.17, I and III). Unlike RAFT agent 3, the PNVCL prepared by RAFT agents 5 and 7 shower no low molecular weight shoulders in their SEC traces. RAFT agent 5 incorporates an ethyl pyrrolidone moiety as part of the R group, whereas RAFT agent 7 incorporates *O*-ethyl pyrrolidone as the Z group. The results indicate possible effects of incorporation of ethyl pyrrolidone as the R or Z group of the control of the polymerisation of NVCL. The result suggests that ethyl pyrrolidone as R group efficiently re-initiates the polymerisation upon fragmentation from the RAFT agent. Moreover, incorporating ethyl pyrrolidone as the Z group, promotes the activation of C=S bond towards radical addition and the stabilisation of the intermediate radical. When RAFT agent 6 was used for the controlled polymerisation of NVCL, the resulting polymer showed a bimodal distribution (Figure 3.17-II). In terms of structure, RAFT agent 6 is similar to RAFT agent 5 and they only differ on the formation of secondary and tertiary radicals upon fragmentation of the RAFT agent. One explanation for this behaviour, is that the more stable tertiary radicals react more slowly with the monomer and therefore would need longer reactions times for its completion. Also, as the rate of polymerisation is slower, the termination may be more prominent giving an explanation for the bimodal molecular weight distribution observed.

Figure 3.18, a plot of Log M against Wf / dLog M, confirms the results reported from the SEC chromatograms using RAFT agents 5-7. The polymer prepared by RAFT using RAFT agent 6 shows a bimodal molecular weight distribution (Figure 3.18-II) and in the presence of RAFT 5 or 7, monomodal molecular weight distributions are observed, without any significant tailing.

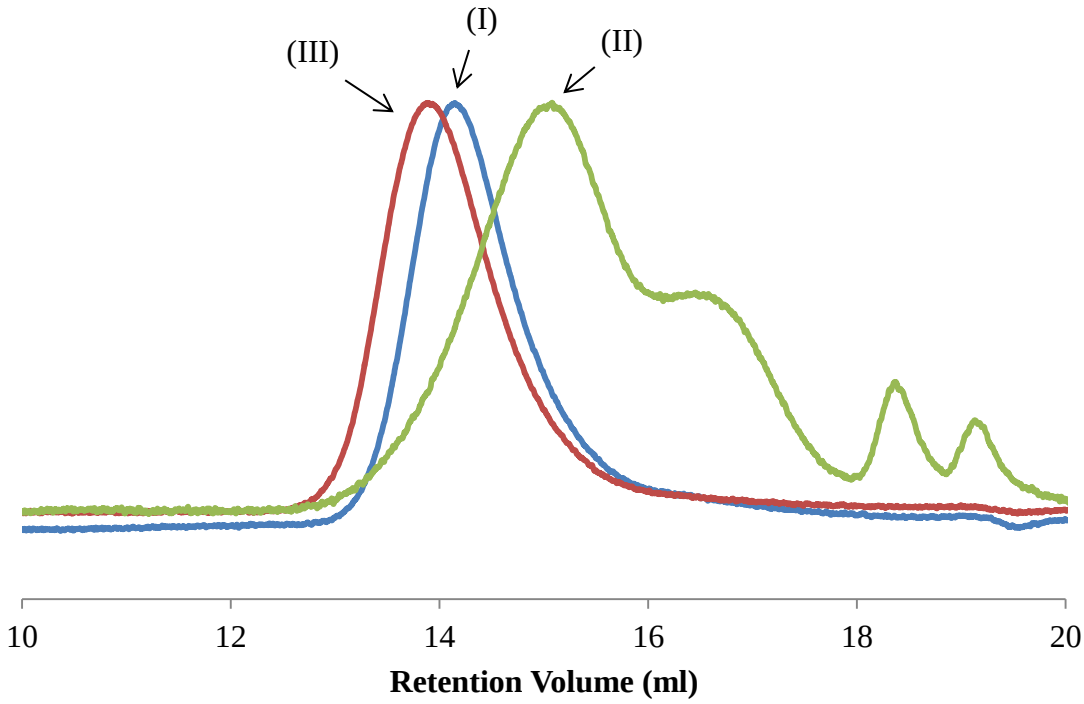

Figure 3.17. SEC traces (refractive index) of PNVCL prepared by (I) RAFT agent 5, (II) RAFT agent 6, (III) RAFT agent 7

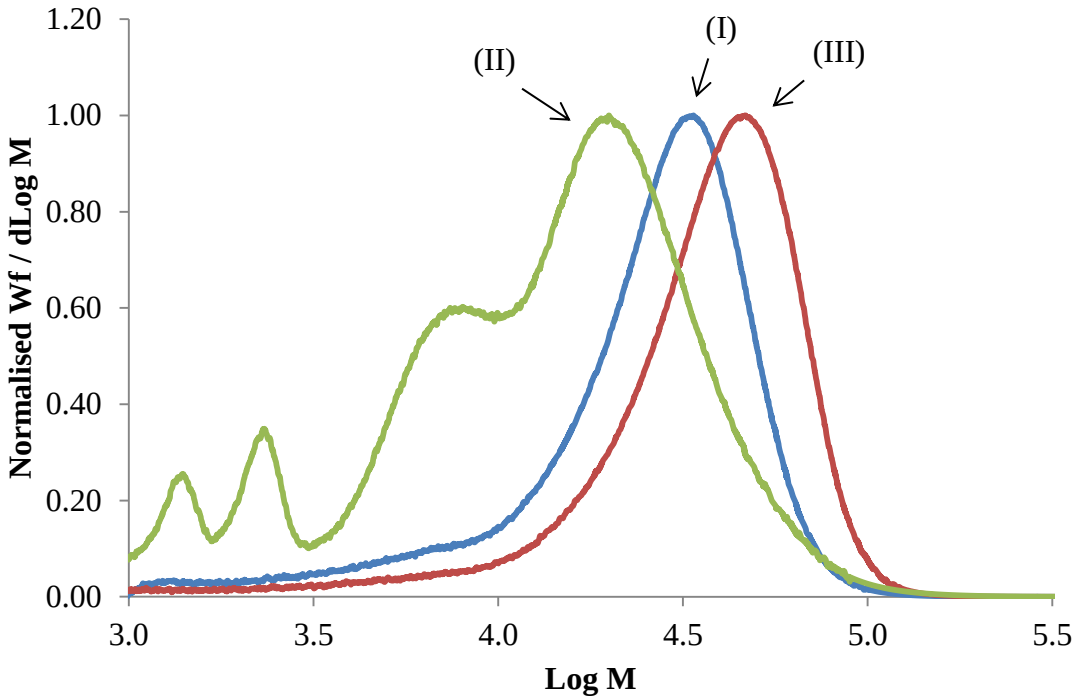

Figure 3.18. Plot of Log M against normalsied Wf / dLog M showing the molecular weight distribution for the polymerisation of NVCL in the presence of (I) RAFT agent 5, (II) RAFT agent 6, (III) RAFT agent 7

3.3.4. Solvent effects in the RAFT polymerisation of N-vinylpyrrolidone and vinyl acetate

The controlled polymerisations of NVP and VAc carried out in bulk, poses a problem in industry, as above approximately 50 - 60% conversion of monomer to polymer, the polymerisation mixture becomes very viscous and difficult to handle. Additionally, this leads to the gel effect and autoacceleration (Trommsdorff – Norrish effect) which can potentially be very dangerous. Therefore, controlled polymerisation in solvents is a more attractive option in industry.

Non-hazardous protic solvents such as 2-propanol are often used in industry for the classical free radical polymerisation of NVP and the final polymer product can be sold in solution. 2-propanol can act as chain transfer agents to reduce the molecular weight of the resulting polymers. Moreover, Zard and co-workers have shown that 2-propanol can effectively be used to remove a xanthate functionality from the polymer chain (Scheme 3.7).[41] The radical generated from the thermal decomposition of dilauroyl peroxide reacts reversible with the xanthate resulting in the expulsion of R•, which subsequently abstracts a secondary hydrogen atom from 2-propanol to generate a hydroxyisopropyl radical. The hydroxyisopropyl radical can then undergo typical termination reactions such as disproportionation to give acetone and 2-propanol. This process will lead to the removal of the xanthate groups if the initiator reacts with the xanthate faster than with 2-propanol. When R• is a propagating chain; as in the RAFT mechanism, then this leads to the formation of dead polymer chains and an increased PDI.

During this study, when either 2-propanol (Table 3.1; Entry 11) or 2-butoxyethanol (Table 3.1; Entry 12) were used as the solvents for the controlled polymerisation of NVP there was a significantly lower yield and greater PDI. Larger PDI's were also observed in the controlled polymerisation of VAc in 2-propanol (Table 3.3; Entry 11) and ethanol (Table 3.3. Entry 15). These observations could well be explained by the cleavage of the xanthate groups by protic solvents.

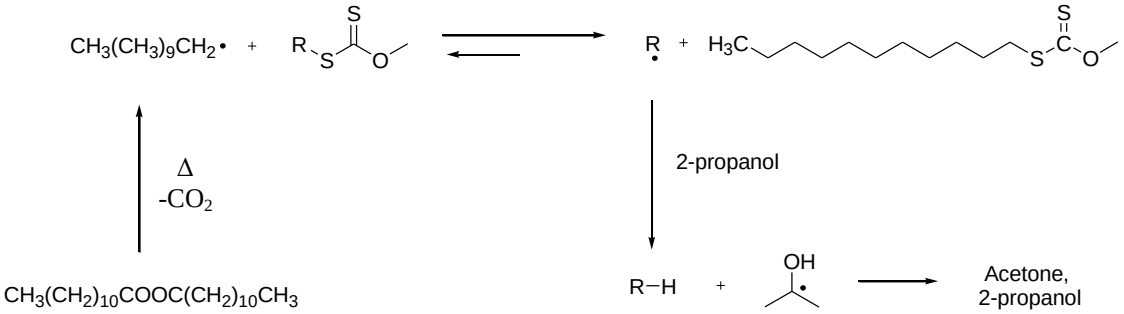

Scheme 3.7. Removal of xanthate group by radical transfer to 2-propanol

In the controlled polymerisations of both NVP and VAc in toluene the yields were low. For NVP the yield of the polymer was 19% after 44 h (Table 3.1; Entry 3). For VAc the yield of the polymers produces was 47% after 44 h (Table 3.3; Entry 3) and 40% 17 h (Table 3.3: Entry 9). It has been reported that the conventional free radical polymerisation of VAc in toluene suffers from retardation.[42-44] It has been postulated that unstable propagating radicals, as those formed in the cases of VAc and NVP, may undergo complexation with the π-electrons of the aromatic ring in toluene and generate a more stabilise radical entity.[45] This would therefore result in the reduction of the rate of polymerisation. However, an alternative explanation is that there is a degradative chain transfer process is occurring between vinyl acetate propagating radicals and toluene (Scheme 3.8).[46] PVAc propagating chains abstract a hydrogen atom from toluene, which then can either react with monomer or undergo primary radical termination with a propagating chain. The rate of addition of benzyl radicals to vinyl acetate is slow and the benzyl radicals then undergo primary termination reactions involving active PVAc chains, having the overall effect of reducing the number of propagating radicals and reducing the rate of polymerisation. NVP may well also be effected by the same rate retardation in toluene as both VAc and NVP generate similar unconjugated unstable propagating radicals. In addition, toluene is a non-solvent for PNVP which may well be a reason for the lowered yield.

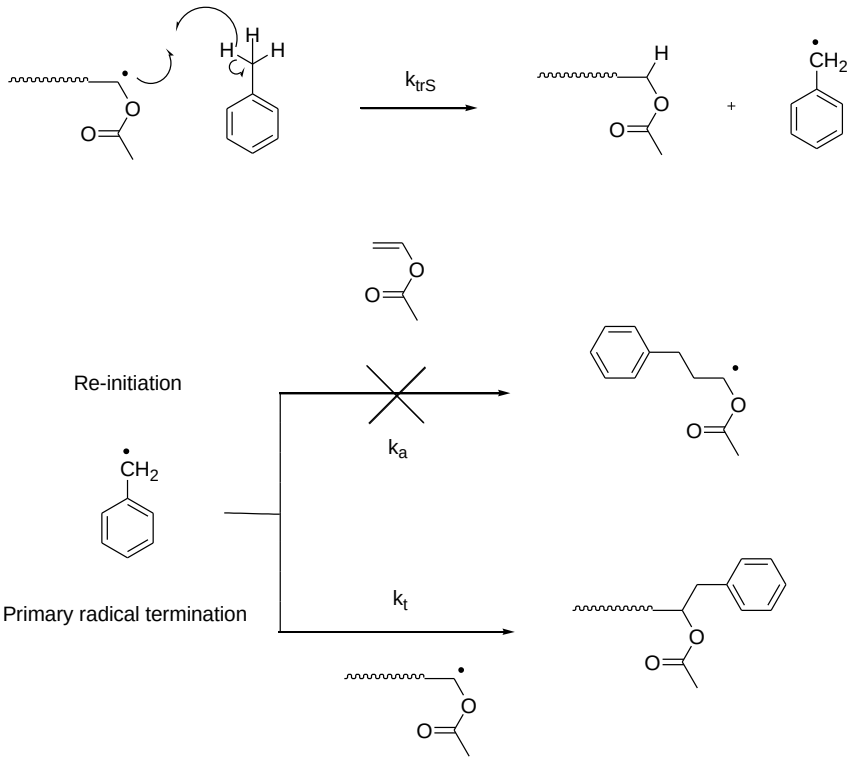

Scheme 3.8. Degradative chain transfer mechanism for free radical polymerisation of VAc in toluene

Pound *et al*.[47] heated a solution of PNVP in water (100 mg/ml) at 40°C for 16 h (Scheme 3.9). ^{1}H NMR spectroscopy revealed the absence of thiocarbonylthio groups and the appearance of hydroxy groups at the chain ends.

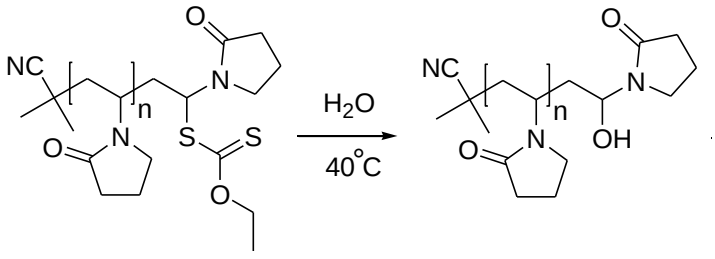

Scheme 3.9. Modification of PNVP xanthate end capped polymers

When the controlled polymerisation of NVP in this work was carried out in water the found M_n was significantly higher than that expected. When RAFT agent 3 was employed, SEC analysis showed the found M_n of 2.57 x 10^4 gmol^{-1} with a PDI of 1.38, which was significantly higher than the theoretical M_n of 7.7 x 10^3 gmol^{-1} (Table 3.1; Entry 10). Similarly, when RAFT agent 5 was used, SEC analysis showed the found M_n of 3.74 x 10^4 gmol^{-1} with a PDI of 1.41, which was also significantly higher

than the theoretical M_n of 7.3 x 10^3 $gmol^{-1}$ (Table 3.1; Entry 20). Moreover, SEC analysis also revealed the presence of low molecular weight shoulders for both PNVP samples (Figure 3.19 and 3.20). The results are most likely indicative of a combination of both conventional free radical and RAFT polymerisation of NVP.

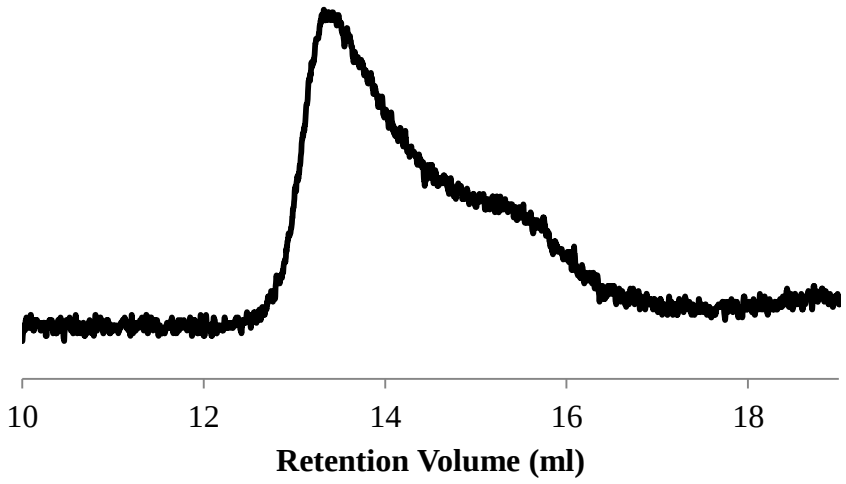

Figure 3.19. SEC trace (refractive index) showing large lower molecular weight shoulder from polymerisation of NVP using RAFT 3 in water (Table 3.1: Entry 10)

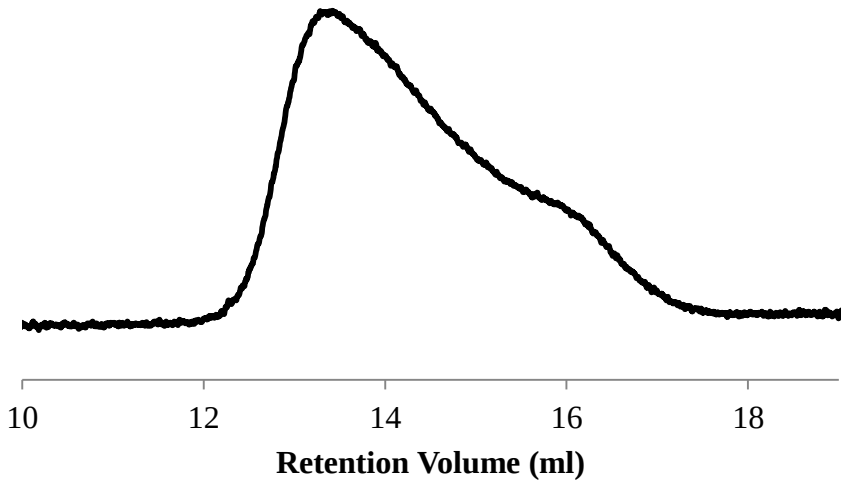

Figure 3.20. SEC trace (refractive index) showing large lower molecular weight shoulder from polymerisation of NVP using RAFT agent 5 in water (Table 3.1; Entry 20)

Figure 3.21, shows the comparison of the molecular weight distributions for the polymer prepared *via* RAFT polymerisation in water using RAFT agent 3 (I) and 5 (II). In both cases, broad bimodal distributions are observed, supporting the results shown in the SEC chromatograms (Figures 3.19 and 3.20).

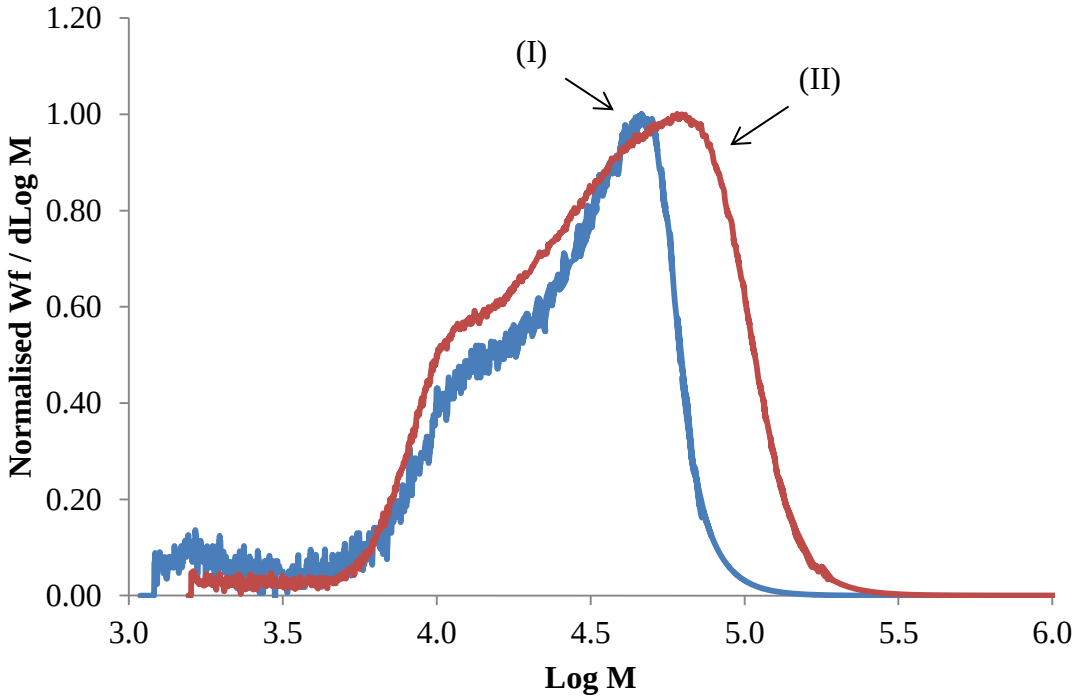

Figure 3.21. Plot of Log M against normalised Wf / dLog M showing the molecular weight distribution for the polymerisation of NVP in water in the presence of (I) RAFT agent 3 (Table 3.1; Entry 10) and (II) RAFT agent 5 (Table 3.1; Entry 20)

3.4. Summary

Controlled radical polymerisations of NVP, VAc and NVCL have been carried out using a number of RAFT agents in various solvents. Both dithiocarbamates and xanthates have been shown to be good RAFT agents in controlling the polymerisation of LAMs. Results from polymerisations of the monomers involving known RAFT agents correspond well with those in the literature.

The controlled polymerisation of NVP using four novel RAFT agents has been investigated. RAFT agent 4 has shown the leaving group ability of the R group is essential in the RAFT process. It is thought the R group is unable to fragment from the RAFT agent due to the lack of any stabilisation of the primary radical formed. Therefore, the polymerisation of NVP in the presence of RAFT agent 4 was of a conventional nature. RAFT agents 5 and 7 have been shown to be effective chain transfer agents to control the molecular weight and lower the PDI of the respective polymers produced. In contrast RAFT agent 6, produced a non-linear relationship between % conversion and M_n, indicating the lack of control over the polymerisation of NVP. It is unclear , but this is believed to be due to the increased stability of the tertiary R group radical formed during the fragmentation process.

NVCL has also been polymerised in the presence of RAFT agents 5-7. RAFT agents 5 and 7 are able to control the polymerisation of NVCL effectively giving mono modal traces in SEC. RAFT agent 6 is unable to control the polymerisation of NVCL.

When water was used as the polymerisation solvent a significantly higher molecular weight polymer than expected is produced. This is due to the chain cleavage of the xanthate chain ends. A similar result is seen when protic solvents are used as the polymerisation solvent. PDI's are observed to be larger than those when polymerisation takes place in bulk or other solvents.

3.5. References

1. Moad, G.; Rizzardo, E.; Thang, S. *Australian Journal of Chemistry* **2005,** 58, (6), 379-410.
2. Moad, G.; Rizzardo, E.; Thang, S. H. *Australian Journal of Chemistry* **2006,** 59, (10), 669-692.
3. Moad, G.; Rizzardo, E.; Thang, S. H. *Australian Journal of Chemistry* **2009,** 62, (11), 1402-1472.
4. Devasia, R.; Bindu, R.; Borsali, R.; Mougin, N.; Gnanou, Y. *Macromolecular Symposia* **2005,** 229, 8-17.
5. Gnanou, Y.; Devasia, R.; Bindu, R.; Mougin, N. *Abstracts of Papers of the American Chemical Society* **2005,** 230, U4144-U4145.
6. Wan, D.; Satoh, K.; Kamigaito, M.; Okamoto, Y. *Macromolecules* **2005,** 38, (25), 10397-10405.
7. Bilalis, P.; Pitsikalis, M.; Hadjichristidis, N. *Journal of Polymer Science Part a-Polymer Chemistry* **2006,** 44, (1), 659-665.
8. Nguyen, T.; Eagles, K.; Davis, T.; Barner-Kowollik, C.; Stenzel, M. *Journal of Polymer Science Part a-Polymer Chemistry* **2006,** 44, (15), 4372-4383.
9. Postma, A.; Davis, T.; Li, G.; Moad, G.; O'Shea, M. *Macromolecules* **2006,** 39, (16), 5307-5318.
10. Pound, G.; McLeary, J.; McKenzie, J.; Lange, R.; Klumperman, B. *Macromolecules* **2006,** 39, (23), 7796-7797.
11. Pound, G.; Eksteen, Z.; Pfukwa, R.; McKenzie, J. M.; Lange, R. F. M.; Klumperman, B. *Journal of Polymer Science Part a-Polymer Chemistry* **2008,** 46, (19), 6575-6593.
12. Benaglia, M.; Chiefari, J.; Chong, Y.; Moad, G.; Rizzardo, E.; Thang, S. *Journal of the American Chemical Society* **2009,** 131, (20), 6914-6915.
13. Yan, Y.; Zhang, W.; Qiu, Y.; Zhang, Z.; Zhu, J.; Cheng, Z.; Zhang, W.; Zhu, X. *Journal of Polymer Science Part a-Polymer Chemistry* **2010,** 48, (22), 5206-5214.
14. Guinaudeau, A.; Mazieres, S.; Wilson, D. J.; Destarac, M. *Polymer Chemistry* **2012,** 3, (1), 81-84.
15. Rizzardo, E.; Chiefari, J.; Mayadunne, R. T. A.; Moad, G.; Thang, S. H., Synthesis of Defined Polymers by Reversible Addition-Fragmentation Chain Transfer: The RAFT Process. In *Controlled/Living Radical Polymerisation*

Progress in ATRP, NMP, and RAFT, Matyjaszewski, K., Ed. ACS Publications: 2000; Vol. 768, pp 278-296.

16. Destarac, M.; Charmot, D.; Franck, X.; Zard, S. Z. *Macromolecular Rapid Communications* **2000,** 21, (15), 1035-1039.
17. Stenzel, M. H.; Cummins, L.; Roberts, G. E.; Davis, T. P.; Vana, P.; Barner-Kowollik, C. *Macromolecular Chemistry and Physics* **2003,** 204, (9), 1160-1168.
18. Wood, M. R.; Duncalf, D. J.; Rannard, S. P.; Perrier, S. *Organic Letters* **2006,** 8, (4), 553-556.
19. Skey, J.; O'Reilly, R. K. *Chemical Communications* **2008**, (35), 4183-4185.
20. Patel, V. K.; Vishwakarma, N. K.; Mishra, A. K.; Biswas, C. S.; Ray, B. *Journal of Applied Polymer Science* **2012,** 125, (4), 2946-2955.
21. Devasia, R.; Borsali, R.; Lecommandoux, S.; Bindu, R.; Mougin, N.; Gnanou, Y. *Abstracts of Papers of the American Chemical Society* **2005,** 230, U4231-U4232.
22. Wan, D. C.; Zhou, Q.; Pu, H. T.; Yang, G. J. *Journal of Polymer Science Part a-Polymer Chemistry* **2008,** 46, (11), 3756-3765.
23. Beija, M.; Marty, J.-D.; Destarac, M. *Chemical Communications* **2011,** 47, (10), 2826-2828.
24. Shao, L. D.; Hu, M. Q.; Chen, L.; Xu, L.; Bi, Y. M. *Reactive & Functional Polymers* **2012,** 72, (6), 407-413.
25. Patel, V. K.; Mishra, A. K.; Vishwakarma, N. K.; Biswas, C. S.; Ray, B. *Polymer Bulletin* **2010,** 65, (2), 97-110.
26. Mishra, A.; Patel, V.; Vishwakarma, N.; Biswas, C.; Raula, M.; Misra, A.; Mandal, T.; Ray, B. *Macromolecules* **2011,** 44, (8), 2465-2473.
27. York, A. W.; Kirkland, S. E.; McCormick, C. L. *Advanced Drug Delivery Reviews* **2008,** 60, (9), 1018-1036.
28. Barner-Kowollik, C.; Quinn, J.; Nguyen, T.; Heuts, J.; Davis, T. *Macromolecules* **2001,** 34, (22), 7849-7857.
29. Tong, Y. Y.; Dong, Y. Q.; Du, F. S.; Li, Z. C. *Macromolecules* **2008,** 41, (20), 7339-7346.
30. Pound, G.; Aguesse, F.; McLeary, J.; Lange, R.; Klumperman, B. *Macromolecules* **2007,** 40, (25), 8861-8871.
31. Charmot, D.; Corpart, P.; Adam, H.; Zard, S. Z.; Biadatti, T.; Bouhadir, G. *Macromolecular Symposia* **2000,** 150, 23-32.

32. Stenzel, M. H.; Davis, T. P.; Barner-Kowollik, C. *Chemical Communications* **2004**, (13), 1546-1547.
33. Shipp, D. A.; Vercoe, K.; Zhang, T. X.; Thopasridharan, M. *Abstracts of Papers of the American Chemical Society* **2005,** 230, U4125-U4126.
34. Theis, A.; Davis, T. P.; Stenzel, M. H.; Barner-Kowollik, C. *Polymer* **2006,** 47, (4), 999-1010.
35. Poly, J.; Wilson, D. J.; Destarac, M.; Taton, D. *Macromolecular Rapid Communications* **2008,** 29, (24), 1965-1972.
36. Girard, E.; Tassaing, T.; Marty, J. D.; Destarac, M. *Polymer Chemistry* **2011,** 2, (10), 2222-2230.
37. Ham, M. K.; HoYouk, J.; Kwon, Y. K.; Kwark, Y. J. *Journal of Polymer Science Part a-Polymer Chemistry* **2012,** 50, (12), 2389-2397.
38. Palit, S. R.; Das, S. K. *Proceedings of the Royal Society of London Series a-Mathematical and Physical Sciences* **1954,** 226, (1164), 82-95.
39. *Polymer Handbook*. Fourth ed.; John Wiley & Sons, INC.: 1999.
40. Vandermeer, R.; Aarts, M.; German, A. L. *Journal of Polymer Science Part a-Polymer Chemistry* **1980,** 18, (4), 1347-1357.
41. Liard, A.; QuicletSire, B.; Zard, S. Z. *Tetrahedron Letters* **1996,** 37, (33), 5877-5880.
42. McKenna, T. F.; Villanueva, A. *Journal of Polymer Science Part a-Polymer Chemistry* **1999,** 37, (5), 589-601.
43. Jovanovic, R.; Dube, M. A. *Journal of Applied Polymer Science* **2001,** 82, (12), 2958-2977.
44. Hatada, K.; Terawaki, Y.; Kitayama, T.; Kamachi, M.; Tamaki, M. *Polymer Bulletin* **1981,** 4, (8), 451-458.
45. Coote, M. L.; Davis, T. P.; Klumperman, B.; Monteiro, M. J. *Journal of Macromolecular Science-Reviews in Macromolecular Chemistry and Physics* **1998,** C38, (4), 567-593.
46. Lonsdale, D. E.; Johnston-Hall, G.; Fawcett, A.; Bell, C. A.; Urbani, C. N.; Whittaker, M. R.; Monteiro, M. J. *Journal of Polymer Science Part a-Polymer Chemistry* **2007,** 45, (16), 3620-3625.
47. Pound, G.; McKenzie, J. M.; Lange, R. F. M.; Klumperman, B. *Chemical Communications* **2008**, (27), 3193-3195.

Chapter 4
Synthesis and characterisation of linear block and random copolymers

4.1. Introduction

This chapter focuses on the synthesis of diblock and random copolymers incorporating varying combinations of poly(N-vinylpyrrolidone) (PNVP), poly(vinyl acetate) (PVAc) and poly(N-vinylcaprolactam) (PNVCL). In Chapter 3, RAFT agents 1-8 and were used to control the homopolymerisation of these "less activated" monomers (LAMs). The homopolymers still have an active RAFT chain end capable of reacting with further monomer. Therefore, these polymers can be regarded as macro chains transfer agents (macroCTA's). Block copolymers can be prepared from the sequential addition of monomers; i.e. synthesising a macroCTA through the homopolymerisation of monomer A, then chain extension of the purified macroCTA with a second monomer, B. Using this method it is possible to get either A-B or B-A diblock copolymers. It is important to polymerise the monomers in order to get the targeted sequence in the block copolymer. Once the first monomer has been polymerised, this polymeric chain becomes the R group (fragmenting radical group). It is therefore important that the first monomer is able to fragment from the active chain end and reinitiate the polymerisation of the second monomer.

Alternative methodologies to synthesise block copolymers incorporating LAMs involving RAFT have also been used in the literature such as; (i) a combination of RAFT and another controlled radical polymerisation technique,[1-5] (ii) modified polymers having a dithiocarbonate end group,[6, 7] (iii) the use of RAFT polymerisation and "click chemistry" [8-11] and (iv) RAFT polymerisation with end groups enabling initiation of ring opening polymerisation (ROP).[10, 12]

4.1.1. Block copolymers incorporating poly(N-vinylpyrrolidone) *via* RAFT

The first examples of block copolymers incorporating PNVP by RAFT were reported by Devasia *et al.*[13] using a PNVP macroCTA (containing an *O* - ethyl xanthate chain end) with a M_n of 1.15 x 10^4 $gmol^{-1}$ and PDI of 1.5, to mediate the polymerisation of either styrene (St) or n-butyl acrylate (*n*-BA), in 1, 4 dioxane at 60°C. However, the blocking efficiencies were found to be poor and the diblock copolymers were isolated from the PNVP homopolymer by repeated precipitation into water or methanol. The isolated block copolymers had molecular weights ranging from 1.22 x 10^4 $gmol^{-1}$ – 1.32 x 10^4 $gmol^{-1}$ and PDI ranging from 1.23 to 1.44. The same group also used PNVP with a xanthate chain end as a macroCTA with a M_n of 8.00 x 10^3 $gmol^{-1}$ and PDI of 1.3, to

synthesise block copolymers of PNVP-*block*-PNVCL and PNVP-*block*-PBA in 1, 4 dioxane at 60°C.[14] Diblock copolymers had to be isolated from the PNVP homopolymer by repeated precipitation into pentane. The copolymerisation reactions lasted from 24 – 52 h and M_n of the block copolymers ranged from 8.9 x 10^3 – 1.2 x 10^4 gmol^{-1}. No information was given on the PDI's of the block copolymers.

A PNVP macroCTA with a trithiocarbonate end group with a M_n of 9.00 x 10^4 gmol^{-1} and PDI of 1.5, was used to control the polymerisation of 2-vinylpyridine (2-VP) in DMF at 75°C.[15] It was reported that the macroCTA was completely consumed during the copolymerisation reaction and after 16 h the diblock copolymer had a M_n of 1.55 x 10^5 gmol^{-1} and PDI of 1.5.

Nguyen *et al*.[16] used a PNVP macroCTA with a M_n of 1.10 x 10^4 gmol^{-1} and PDI of 1.38, with a xanthate chain end, to mediate the polymerisation of VAc in methanol at 60°C. The conversion of VAc to polymer was only 20% after a reaction time of 24 h. The found M_n of the diblock copolymer was measured to be 2.50 x 10^4 gmol^{-1} and PDI of 1.55. A different PNVP macroCTA with a molecular weight of 1.60 x 10^4 gmol^{-1} and PDI of 1.19, was used to mediate the polymerisation of VAc under the same conditions. The conversion of VAc to polymer was only 25% after a reaction time of 24 h. The found M_n of the block copolymer was 3.50 x 10^4 gmol^{-1} and PDI of 1.45. Low molecular weight products were detected by SEC, which were attributed to dead homopolymer produced from termination products.

CSIRO used a "universal switchable" RAFT agent to block copolymerise MAMs and LAMs through the sequential addition of monomers.[17] *N*-(4-pyridinyl)-*N*-methyldithiocarbamates were reported to be effective for the controlled polymerisation of LAMs, whereas in the presence of a strong acid (4-toluenesulphonic acid or trifluoromethanesulphonic acid), the protonated form of the RAFT agent can control the polymerisation of MAMs. A macroCTA of poly(*N*,*N*-dimethylacrylamide) (PDMAm) with a M_n of 3.20 x 10^3 gmol^{-1} and PDI of 1.27, was used to mediate the polymerisation of NVP in acetonitrile at 60°C to give a PDMAm-*block*-PNVP. It was reported that it was not possible to produce any block copolymer in aqueous solution, which was attributed to the hydrolysis of the dithiocarbamate chain end. The M_n of the block copolymer was found to be 1.89 x 10^4 gmol^{-1} with a PDI of 1.33. The conversion of NVP to polymer was reported to be 48% after a reaction time of 16 h. It was reported to be vital that any acid be removed from the polymerisation mixture before the block copolymerisation with NVP, as the pyrrolidone functionality was degraded.

Patel *et al*.[18] used a PNVP macroCTA with a M_n of 3.80 x 10^3 gmol^{-1} and PDI of 1.24, to mediate the polymerisation of NVP and also styrene in DMF at 80°C. The chain extension with NVP gave a polymer with a molecular weight of 5.60 x 10^3 gmol^{-1} and PDI of 1.51 and the conversion of NVP to polymer was 44% after a polymerisation time of 3 h. When the PNVP macroCTA was used to mediate the polymerisation of styrene, the diblock copolymer needed to be purified by repeated precipitation into diethyl ether, to remove PNVP homopolymer. The molecular weight of the diblock copolymer of PNVP-*block*-PS was 5.20 x 10^3 gmol^{-1} with a PDI of 1.24. The conversion of monomer to polymer was 45% after a reaction time of 12 h.

Fandrich *et al*.[19, 20] attempted to chain extend PNVP macroCTA's with VAc in 1,4 dioxane at 70°C. Block copolymers of PNVP-*block*-PVAc with polydispersity indices ranging from 1.50 to 2.23 were synthesised, with PDI increasing with an increase in PVAc content. It was reported that side reactions occurring during the RAFT polymerisation had a great effect on the chain ends, molecular weight and PDI. It was also shown that the use of 1,4 dioxane as solvent led to competitive chain transfer reactions, meaning a loss in the control in the polymerisation of NVP and to an even greater extent during the copolymerisation reactions. In some cases it was suggested that polymer blends were produced rather than block copolymers of PNVP and PVAc.

Amphiphilic diblock copolymers of poly(N-vinylcarbazole)-*block*-poly(N-vinylpyrrolidone) (PNVC-*block*-PNVP) and PNVP-*block*-PNVC were synthesised by the sequential addition of monomers by RAFT.[21] Either a purified PNVC or PNVP macroCTA was used to mediate the polymerisation of the second monomer. In both cases low PDI diblock copolymers were formed and first order kinetics plots were observed with SEC traces being monomodal.

Yan *et al*.[22] used the commercially available isopropylxanthic disulfide (DIP) to mediate the polymerisation of NVP, VAc and NVC (N-vinylcarbazole). Furthermore, PVAc with a M_n of 4.40 x 10^3 gmol^{-1} and PDI of 1.49, was used as a macroCTA to mediate the polymerisation of NVP in THF at 80°C. When the ratio of NVP:PVAc macroCTA was 100:1, the found M_n of diblock copolymer was 1.93 x 10^4 gmol^{-1} with a PDI of 1.88. The conversion of NVP to polymer was reported to be 85% after a reaction time of 1.5 h. A PNVP macroCTA with a M_n of 1.06 x 10^4 gmol^{-1} and PDI of 1.25, was used to mediate the polymerisation of NVP in 2-propanol at 70°C. When the ratio of NVP:PNVP macroCTA was 100:1, the found M_n of the chain extended polymer was 2.62 x 10^4 gmol^{-1} with a PDI of 1.71. The conversion of NVP to polymer was 57%

after a reaction time of 4.5 h. PNVP macroCTA was used to mediate the polymerisation of VAc in 1, 4 dioxane at 80°C. When the ratio of VAc:PNVP macroCTA was 200:1, the found M_n of the block copolymer was 1.52 x 10^4 $gmol^{-1}$ and PDI of 1.51. The conversion of VAc to polymer was 47% after a reaction time of 1.5 h. Furthermore, PNVP macroCTA was used to mediate the polymerisation of NVC in 2-propanol at 80°C. When the ratio of NVC:PNVP macroCTA was 100:1, the found M_n of the block copolymer was 2.27 x 10^4 $gmol^{-1}$ and PDI was much larger at 2.06. It should be pointed out that all chain extended polymers and block copolymers displayed broad PDI which was attributed to the existence of dead polymer chains originating from the initial macroCTA.

More recently Guinaudeau *et al.*[23] have used a poly(acrylamide) (PAm) macroCTA with a xanthate chain end to mediate the polymerisation of NVP in aqueous solution at 25°C. The polymerisation was redox initiated using *tert*-butyl hydroperoxide / ascorbic acid and the PAm macroCTA had a M_n of 3.60 x 10^3 $gmol^{-1}$ and PDI of 1.07. They reported the synthesis of a PAm-*block*-PNVP diblock copolymer with molecular weight 1.22 x 10^4 $gmol^{-1}$ and a PDI of 1.25.

4.1.2. Block copolymers incorporating poly(vinyl acetate) *via* RAFT

The first reports of block copolymers incorporating PVAc were published in 2005 by Batt-Coutrot *et al.*[24] It was reported that a statistical copolymer of EAA and BuA with an *O*-ethyl xanthate chain end was used to mediate the polymerisation of VAc. The random copolymer was found to have a M_n of 3.30 x 10^3 $gmol^{-1}$ and a PDI of 1.90. The M_n of the block copolymer was found to be 7.10 x 10^3 and PDI of 1.30. The conversion of VAc to polymer was reported to be 50% after a reaction time of 6 h.

Lipscomb *et al.*[25] used a PVAc macroCTA (with a xanthate chain end) to control the RAFT polymerisations of vinyl privalate (VPv) and vinyl benzoate (VBz). In both cases diblock copolymers were synthesised with low polydispersity indices (PDI = 1.22 – 1.33) and monomodal traces by SEC. PVPv and PVBz macroCTA's were also used to mediate the RAFT polymerisation VAc, giving diblock copolymers with low PDI (PDI = 1.33 - 1.34). The same group also synthesised, poly(vinyl alcohol)-*block*-poly(vinyl acetate) (PVA-*block*-PVAc) diblock copolymers by hydrolysing poly(vinyl chloroacetate)–block–poly(vinyl acetate) (PVClAc-*block*-PVAc) with polydispersity indices ranging from 1.31 – 1.66.[26]

Moad and co-workers used a "universal switchable" RAFT agent to control the block copolymerisation of methyl methacrylate (MMA) and VAc.[27] VAc generates a poor radical leaving group relative to MAMs, therefore it was reported that MMA should be polymerised first followed by VAc. A PMMA macroCTA of molecular weight 3.30 x 10^4 $gmol^{-1}$ and with a PDI of 1.25 was used to mediate the polymerisation of VAc. The block copolymer has a molecular weight of 5.59 x 10^4 $gmol^{-1}$ and a PDI of 1.39. SEC showed a unimodal peak, although there seemed to be a shoulder on the lower molecular weight side of the block copolymer.

Yan *et al.*[22] used the commercially available DIP (isopropylxanthic disulphide) to mediate the RAFT polymerisations of VAc, NVP and NVC. VAc was polymerised in THF with various conditions and molecular weights ranged from 2.50 x 10^3 – 7.60 x 10^3 $gmol^{-1}$ and PDI's of 1.22 - 1.82. PVAc with a M_n of 3.00 x 10^3 $gmol^{-1}$ and PDI of 1.35, was used as a macroCTA for chain extension with VAc. The molecular weight increased to 5.4 x 10^3 $gmol^{-1}$ with PDI increasing to 1.77. A PVAc macroCTA was also extended with NVC and NVP at 80°C and the diblock copolymers also had PDI's of 2.77 and 1.88, respectively. It should be pointed out that all chain extended polymers and block copolymers displayed broad PDI which was attributed to the existence of dead polymer chains originating from the initial macroCTA.

Ieong *et al.*[28] prepared amphiphilic diblock copolymers of poly(N-vinylpiperidone)-*block*-poly(vinyl acetate) (PVPip-*block*-PVAc). They initially polymerised VPip in 1, 4 dioxane at 70°C using a xanthate CTA. This was then used as a macroCTA in the RAFT polymerisation of VAc in 1, 4 dioxane at 60°C for 68 h. They found that bimodal molecular weight distributions were observed by SEC when the concentration of VAc was 4 M in 1, 4 dioxane. By reducing the concentration to 1 M VAc in 1, 4 dioxane and lowering the temperature to 60°C and limiting conversion to 50% gave fairly well-defined (PDI = 1.46 – 1.55) amphiphilic PVPip-*block*-PVAc diblock copolymers. The diblock copolymers were recovered by multiple precipitations into diethyl ether.

Patel *et al.*[29] used a PVAc macroCTA with a M_n of 5.00 x 10^3 $gmol^{-1}$ and PDI of 1.12, with a xanthate chain end to control the polymerisation of VAc and NVP in DMF at 60°C. After 24 h the conversion of VAc to polymer was only 14%. The resulting chain extended polymer had a molecular weight of 5.20 x 10^3 $gmol^{-1}$ and a PDI of 1.30. After the same time period, the conversion of NVP to polymer was 27%. The molecular weight of the diblock copolymer was 5.40 x 10^3 $gmol^{-1}$ with a PDI of 1.16.

4.1.3. Block copolymers incorporating poly(N-vinylcaprolactam) *via* RAFT

The first report of block copolymers incorporating PNVCL *via* RAFT was published in 2005. Devasia *et al.*[30] used a PNVCL macroCTA with a xanthate chain end to mediate the copolymerisation with NVP. The macroCTA had a molecular weight of 9.64 x 10^3 $gmol^{-1}$ and PDI of 1.31. After a polymerisation time of 36 h, the M_n was 2.33 x 10^4 $gmol^{-1}$ with a PDI of 1.68.

Wan *et al.*[31] synthesised PVAc-*block*-PNVCL and PNVCL-*block*-PVAc diblock copolymers through the sequential addition of monomers *via* RAFT polymerisation. A PVAc macroCTA with a M_n of 8.10 x 10^3 $gmol^{-1}$ and PDI of 1.42, with a dithiocarbamate group at the chain end was extended with NVCL to give a diblock copolymer of molecular weight of 1.12 x 10^4 $gmol^{-1}$ and PDI of 1.37. SEC traces were reported to be monomodal. However, when a PNVCL macroCTA with a M_n of 3.7 x 10^3 $gmol^{-1}$ and a PDI of 1.43 was used to control the polymerisation of VAc, the block copolymerisation was less well controlled and polydispersity indices were observed to be broader (PDI = 1.58 - 1.69). There was tailing on the lower molecular weight side which was explained by the radical coupling of PNVCL chains or having no dithiocarbamate groups at the chain end. No data for the conversion of the second block was detailed.

4.1.4. Random copolymers *via* RAFT incorporating N-vinylpyrrolidone, vinyl acetate or N-vinylcaprolactam

VAc and NVP were copolymerised with other monomers in the presence of a RAFT agent. Moad *et al.*[32] copolymerised *tert*-butyl acrylate (*t*-BA) and VAc using a xanthate CTA. Due to the reactivity ratios of *t*-BA ($r_{t\text{-BA}} \approx 5.93$) and VAc ($r_{VAc} \approx 0.026$), blocky random copolymers have been obtained, exhibiting M_n of 1.65 x 10^4 $gmol^{-1}$ with a PDI of 1.31. The same group also copolymerised VAc ($r_{VAc} \approx 0.1$) and methyl acrylate (MA) ($r_{MA} \approx 9$) in the presence of a xanthate CTA.[33] A similar blocky random copolymer was produced with a M_n of 1.40 x 10^4 $gmol^{-1}$ and a PDI of 1.34.

Moad *et al*. have also copolymerised NVP with octadecyl acrylate (ODA).[34] Gradient copolymers were synthesised for the use as dispersants for polymer-clay nanocomposites. Molecular weights ranged from 1.44 x 10^4 $gmol^{-1}$ – 1.62 x 10^4 $gmol^{-1}$ and PDI's ranged from 1.16 – 1.25.

Zhu *et al.*[35] copolymerised NVC and VAc in the presence of a xanthate (*S*-benzyl-*O*-ethyl dithiocarbonate), in 1, 4 dioxane at 70°C for a polymerisation time of 48 h. Low PDI copolymers of PNVC-*ran*-PVAc were synthesised (PDI = 1.30 - 1.35), with M_n ranging from 9.1 x 10^3 – 1.58 x 10^4 gmol^{-1}.

Moreover, random copolymers synthesised *via* RAFT of VAc with vinyl butyrate (VBu), vinyl octanoate (VOc) and vinyl privalate (PVPi), were used as stabilizers in the dispersion polymerisation of NVP in super critical CO_2. *O*-ethyl xanthate CTA's were used to control the molecular weight and PDI of the random copolymers.[36-38] *Lee et al.* synthesised PVAc-*ran*-PVBu with M_n ranging from 2.4 x 10^3 - 4.0 x 10^3 gmol^{-1} with polydispersity indices of 1.29 – 1.45.[36] Park *et al.* synthesised PVAc-*ran*-PVBu with M_n ranging from 6.7 x 10^3 to 1.02 x 10^4 gmol^{-1} and polydispersity indices of 1.27 – 1.87. In addition, they also reported the synthesis of PVAc-*ran*-PVOc with M_n ranging from 9.1 x 10^3 to 1.10 x 10^4 gmol^{-1} with polydispersity indices of 1.44 – 1.46.[37] The same group, in a separate communication, also synthesised PVAc-*ran*-PVPi with M_n ranging from 8.9 x 10^3 to 1.56 x 10^4 gmol^{-1} and polydispersity indices of 1.4 – 1.6.[38]

To the best of our knowledge, there have been no reported syntheses of random copolymers *via* RAFT of PNVP-*ran*-PVAc, PNVCL-*ran*-PVAc or PNVP-*ran*-PNVCL in the literature.

4.2. Experimental

4.2.1. Materials

N-vinylpyrrolidone (ISP) and vinyl acetate (Sigma Aldrich, ≥99%) were distilled under reduced pressure and stored under reduced pressure at -4°C. N-vinylcaprolactam (ISP) was recrystallised from either pentane or hexane then distilled under reduced pressure and stored under nitrogen at -4°C. 4,4'-Azobis(4-cyanovaleric acid) (ACVA) (Sigma Aldrich, ≥98%) used as supplied. 2, 2'-Azobis(isobutyonitrile) (AIBN) (Sigma Aldrich) was recrystallized from methanol. 1,4 dioxane was dried over calcium hydride and distilled under reduced pressure. All dry solvents were obtained from Durham Chemistry Department Solvent Purification System (SPS). Purification grade (HPLC) solvent was pushed from its storage container under low argon pressure through two stainless steel columns containing activated alumina or copper catalyst depending on solvent used. Trace amounts of water were removed by the alumina, producing a dry solvent. In addition, deoxygenated solvent was achieved when it was suitable for a copper catalyst column to be used. Water content values - DCM < 25.1ppm, DMF < 735.1ppm, Toluene < 21.3ppm, THF < 35.7 ppm, Chloroform < 20.9ppm, Diethyl ether < 19.1ppm, Hexane < 7.6 ppm and Acetonitrile < 8.7ppm. All other solvents were analytical grade and used without any purification.

4.2.2. Characterisation techniques

Nuclear Magnetic Resonance (NMR) Spectroscopy – ^{1}H NMR spectroscopy was performed on a Bruker Avance-400MHz, Varian iNova-500 or VNMRS 700. ^{1}H NMR spectra were recorded at either 400, 500 or 700MHz. Samples of RAFT / MADIX agents and polymers were analysed in deuterated chloroform ($CDCl_3$ - Sigma-Aldrich) or DCM (CD_2Cl_2 – Goss Scientific). The following abbreviations are used in listing NMR spectra: s = singlet, d = doublet, t = triplet, q = quartet, quin = quintet, m = multiplet, b = broad.

Size exclusion chromatography (SEC) analysis on poly(N-vinylpyrrolidone) and poly(N-vinylcaprolactam) was carried out using a Viscotek TDA 302 with triple detection (refractive index, viscosity and light scattering), using 2 x 300ml PLgel 5µm C columns and DMF (containing 0.1% w/v LiBr) as the eluent at a flow rate of 1ml/min (70°C). The system was calibrated using narrowly polydisperse polystyrene standards.

A value of 0.099 mL/g was used for the dn/dc of poly(N-vinylpyrrolidone). SEC analysis on poly(vinyl acetate) was carried out on a Viscotek TDA 302 with triple detection (refractive index, viscosity and light scattering), using 2 x 300ml PLgel 5µm C columns using THF as the eluent at a flow rate of 1ml/min (30°C). The system was calibrated with narrowly polydisperse polystyrene standards. A value of 0.058 mL/g was used for the dn/dc of poly(vinyl acetate).

4.2.3. Synthesis of poly(N-vinylpyrrolidone)-*block*-poly(vinyl acetate)

4.2.3.1. In dimethylformamide

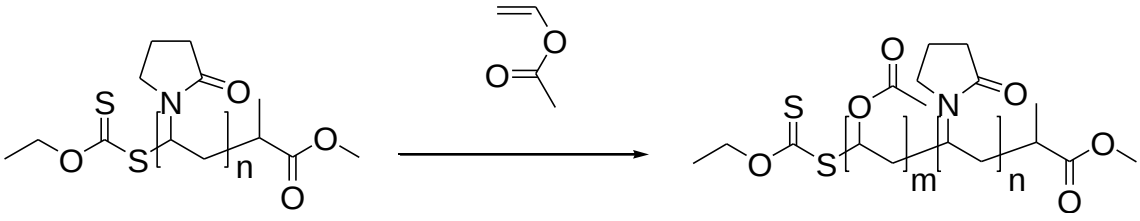

MacroCTA 12

Scheme 4.1

To a 50 ml glass ampoule was added a PNVP macroCTA (1.00 g, 4.59 x 10^{-2} mmol, M_n = 2.18 x 10^4 $gmol^{-1}$, PDI = 1.53), VAc (770 mg, 8.94 mmol), AIBN (1.50 mg, 9.14 x 10^{-3} mmol) and dimethylformamide (3.0 ml). The polymerisation mixture was thoroughly degassed by four freeze pump thaw cycles. The vacuum was replaced with nitrogen gas, the ampoule was sealed, placed into an oil bath thermostated at 70°C and the mixture was heated for 25 h. The ampoule was then removed from the oil bath and allowed to cool to ambient temperature. The polymerisation mixture a yellow / green slightly viscous liquid, was added dropwise to diethyl ether and white precipitate was immediately formed. The solid was filtered and dried under reduced pressure at 40°C to give an off-white powder (1.01 g, 1 % yield).

4.2.3.2. In acetonitrile

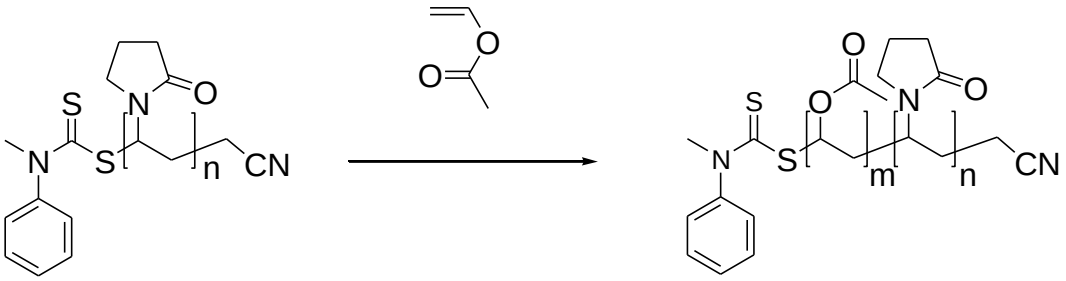

MacroCTA 13

Scheme 4.2.

To a 50 ml glass ampoule was added a PNVP macroCTA (1.00 g, 6.29 x 10^{-2} mmol, M_n = 1.59 x 10^4 gmol^{-1}, PDI = 1.25), VAc (2.58 g, 30.0 mmol), AIBN (2.00 mg, 1.22 x 10^{-2} mmol) and dry acetonitrile (5.0 ml). The polymerisation mixture was thoroughly degassed by four freeze pump thaw cycles and sealed under vacuum. The ampoule was placed into an oil bath thermostated at 70°C and stirred for 41 h and then removed from the oil bath and allowed to cool to ambient temperature. The polymerisation mixture was seen to be a light yellow / green viscous liquid. Solvent and excess monomer were removed under reduced pressure and the residue was dissolved in dichloromethane and added dropwise to diethyl ether and white precipitate was formed. The solid was filtered and dried under reduced pressure at 40°C to give a white solid (2.10 g, 43% yield).

4.2.3.3. In tetrahydrofuran

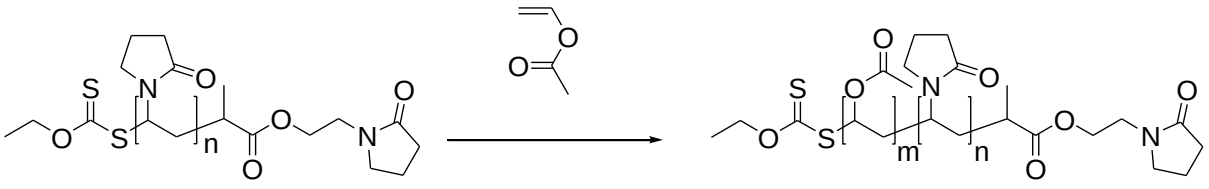

MacroCTA 14

Scheme 4.3.

To a 50 ml glass ampoule was added a PNVP macroCTA (1.00 g, 9.17 x 10^{-2} mmol, M_n = 1.09 x 10^4 gmol^{-1}, PDI = 1.13), VAc (2.96 g, 34.4 mmol), AIBN (2.80 mg, 1.71 x 10^{-2} mmol) and tetrahydrofuran (5.0 ml). The polymerisation mixture was thoroughly degassed by four freeze pump thaw cycles and sealed under vacuum. The ampoule was

placed into an oil bath thermostated at 70°C and stirred for 16 h and then removed from the oil bath and allowed to cool to ambient temperature. The polymerisation mixture was seen to be a light yellow / green viscous gel. Solvent and excess monomer were removed under reduced pressure and the residue was dissolved in dichloromethane and added dropwise to diethyl ether and white precipitate was formed. The solid was filtered and dried under reduced pressure at 40°C to give a white solid (3.26 g, 76% yield).

4.2.3.4. In 1, 4 dioxane

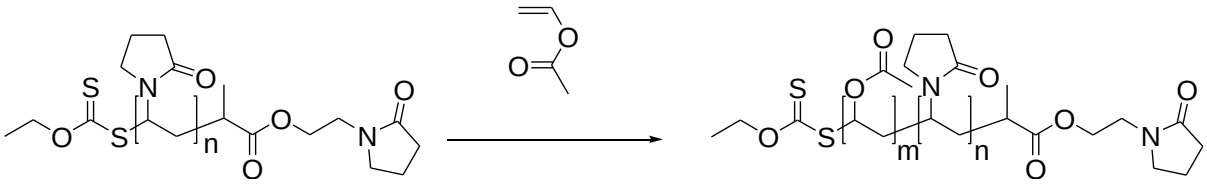

MacroCTA 14

Scheme 4.4.

To a 50 ml glass ampoule was added a PNVP macroCTA (0.500 g, 5.05 x 10^{-2} mmol, M_n = 9.91 x 10^3 $gmol^{-1}$, PDI = 1.24), VAc (2.44 g, 28.3 mmol), ACVA (4.00 mg, 1.43 x 10^{-2} mmol) and 1, 4 dioxane (5.0 ml). Components were added together in a nitrogen filled glove box. The ampoule was sealed under nitrogen and placed into an oil bath thermostated at 70°C and stirred for 24 h and then removed from the oil bath and allowed to cool to ambient temperature. The polymerisation mixture was heated for 24 h. A white opaque gel was formed. The mixture was dissolved in dichloromethane and added dropwise to diethyl ether to give a white precipitate. The product was purified by a further two re-precipitations from dichloromethane / diethyl ether. The solid was recovered by filtration and dried under reduced pressure at 30°C (2.60 g, 86% yield).

4.2.4. Synthesis of poly(N-vinylpyrrolidone)-*block*-poly(N-vinylcaprolactam)

4.2.4.1. In 1, 4 dioxane

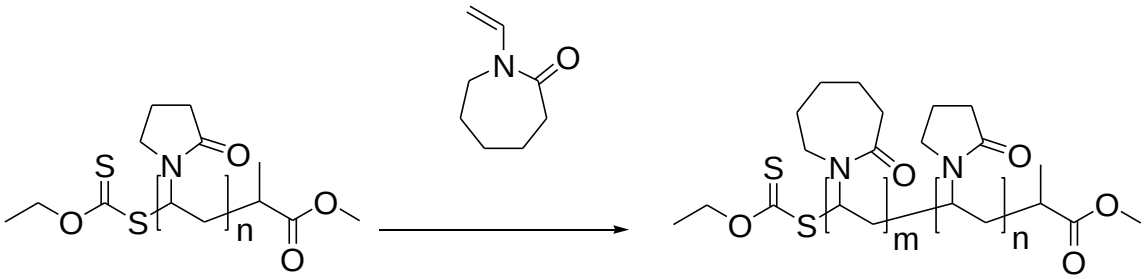

MacroCTA 12

Scheme 4.5.

To a 50 ml glass ampoule was added a PNVP macroCTA (1.00 g, 3.55 x 10^{-2} mmol, M_n = 2.82 x 10^4 $gmol^{-1}$, PDI = 1.34), NVCL (1.25 g, 8.98 mmol), AIBN (1.60 mg, 9.74 x 10^{-3} mmol) and 1,4 dioxane (3.5 ml). The polymerisation mixture was thoroughly degassed by four freeze pump thaw cycles and sealed under vacuum. The ampoule was placed into an oil bath thermostated at 80°C and stirred for 40 h and then removed from the oil bath and allowed to cool to ambient temperature. The polymerisation mixture, a yellow solid gel which was subsequently dissolved in dichloromethane and added dropwise to hexane and white precipitate was formed. The solid was filtered and dried under reduced pressure at 35°C to give a white solid (2.24 g, 99% yield).

4.2.4.2. In 1, 4 dioxane

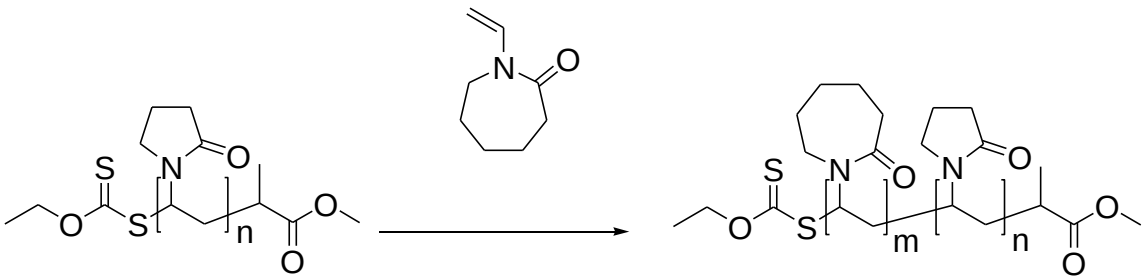

MacroCTA 12

Scheme 4.6.

To a 50 ml glass ampoule was added a PNVP macroCTA (1.00 g, 3.55 x 10^{-2} mmol, M_n = 2.82 x 10^4 $gmol^{-1}$, PDI = 1.34), NVCL (11.7 g, 84.0 mmol), AIBN (1.40 mg, 8.53 x

10^{-3} mmol) and 1, 4 dioxane (15.0 ml). The polymerisation mixture was thoroughly degassed by four freeze pump thaw cycles. The vacuum was replaced with nitrogen gas, the ampoule was sealed, placed into an oil bath thermostated at 80°C and the mixture was heated for 17 h. The ampoule was then removed from the oil bath and allowed to cool to ambient temperature. The polymerisation mixture, a yellow / green slightly viscous liquid, was added dropwise to diethyl ether and white precipitate was immediately formed. The solid was filtered and dried under reduced pressure at 40°C. (10.2 g, 79% yield)

4.2.4.3. In 1, 4 dioxane

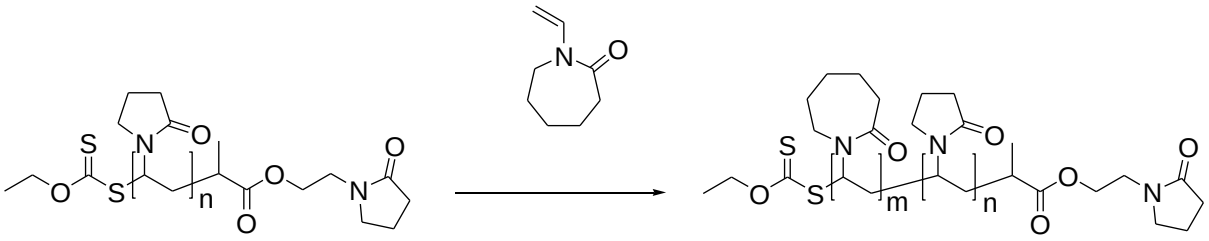

MacroCTA 14

Scheme 4.7.

To a 50 ml glass ampoule was added a PNVP macroCTA (500 mg, 5.05 x 10^{-2} mmol, M_n = 9.91 x 10^3 $gmol^{-1}$, PDI = 1.24), NVCL (3.90 g, 28.0 mmol), ACVA (4.00 mg, 1.43 x 10^{-2} mmol) and 1, 4 dioxane (5.0 ml). Components were added together in a nitrogen filled glove box. The ampoule was sealed under nitrogen and placed into an oil bath thermostated at 70°C and stirred for 24 h and then removed from the oil bath and allowed to cool to ambient temperature. A white opaque gel was formed, which was subsequently dissolved in dichloromethane and added dropwise to diethyl ether to give a white precipitate. The product was purified by a further two re-precipitations from dichloromethane / diethyl ether. The solid was recovered by filtration and dried under reduced pressure at 30°C (2.10 g, 41% yield).

4.2.5. Synthesis of poly(vinyl acetate)-*block*-poly(N-vinylpyrrolidone)

4.2.5.1. In 1, 4 dioxane

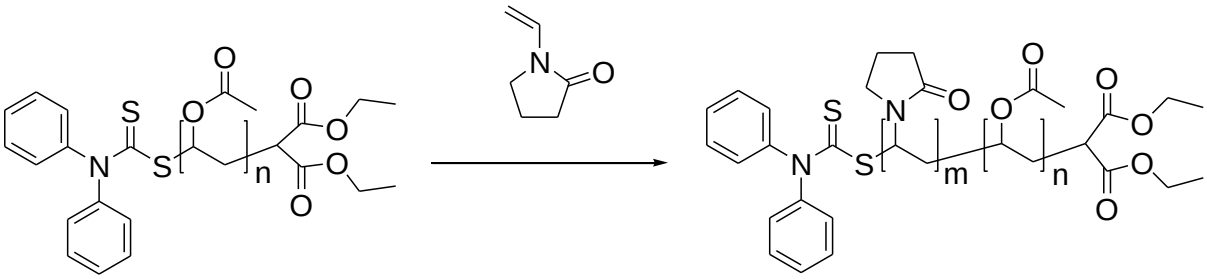

MacroCTA 15

Scheme 4.8.

To a 50 ml Schlenk tube was added a PVAc macroCTA (1.00 g, 0.152 mmol, M_n = 6.60 x 10^3 $gmol^{-1}$, PDI = 1.53), NVP (1.48 ml, 1.55 g, 13.9 mmol), AIBN (5.00 mg, 3.05 x 10^{-2} mmol) and 1, 4 dioxane (1.0 ml). The polymerisation mixture was thoroughly degassed by four freeze pump thaw cycles. The flask was back filled with nitrogen gas, placed in an oil bath and the temperature was increased to 80°C. The polymerisation mixture was heated for 16 h and then was the flask was removed from the oil bath and allowed to cool to ambient temperature. The product of the reaction, a white solid gel was dissolved in tetrahydrofuran and added dropwise to hexane to give a white precipitate. The solid was filtered off and dried under reduced pressure at 30°C (2.0 g, 65% yield).

4.2.5.2. In 1, 4 dioxane

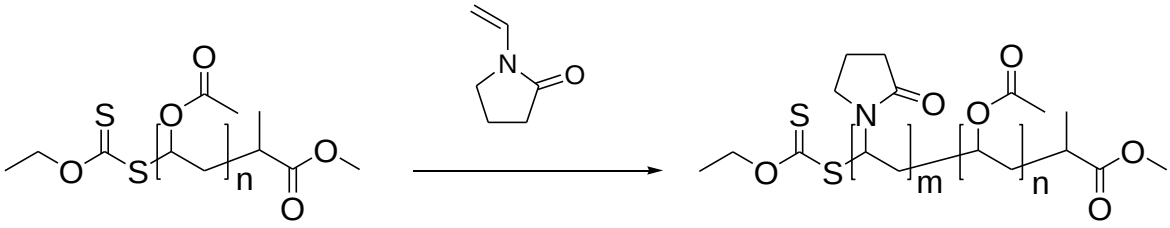

MacroCTA 16

Scheme 4.9.

To a 50 ml glass ampoule was added a PVAc macroCTA (1.00 g, 7.87 x 10^{-2} mmol, M_n = 1.27 x 10^4 $gmol^{-1}$, PDI = 1.35), NVP (1.23 ml, 1.29 g, 11.6 mmol), AIBN (2.00 mg,

1.22 x 10^{-2} mmol) and 1, 4 dioxane (3.5 ml). The polymerisation mixture was thoroughly degassed by four freeze pump thaw cycles and the ampoule was then sealed under vacuum. The ampoule was then placed in a thermostated oil bath set at 80°C and stirred for 35 h, then removed from the oil bath. The product of the reaction, a white solid gel was dissolved in dichloromethane and subsequently added dropwise to diethyl ether to give a white precipitate. This solid was filtered and dried under reduced pressure at 35°C (2.27 g, 98% yield).

4.2.5.3. In acetonitrile

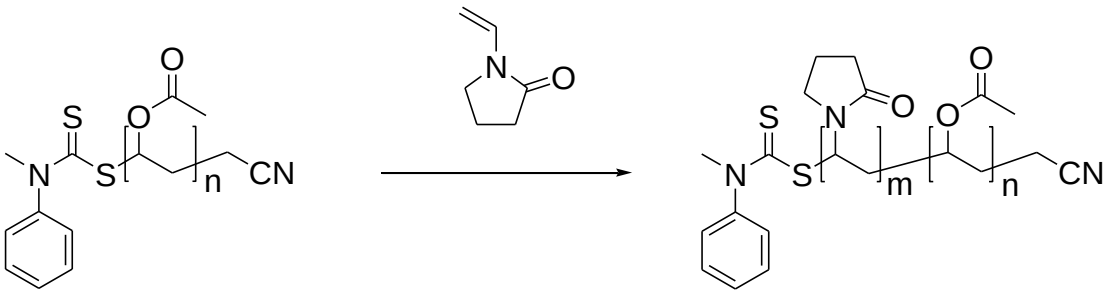

MacroCTA 17

Scheme 4.10.

To a 50 ml glass ampoule was added a PVAc macroCTA (1.00 g, 9.80 x 10^{-2} mmol, 1.02 x 10^{4} $gmol^{-1}$, PDI = 1.39), NVP (1.50 g, 13.5 mmol), AIBN (2.00 mg, 1.22 x 10^{-2} mmol) and dry acetonitrile (3.0 ml). The polymerisation mixture was thoroughly degassed by four freeze pump thaw cycles and the ampoule was sealed under vacuum. The ampoule was then placed in an oil bath thermostated at 70°C and heated for 25 h. The product of the reaction was a very viscous white liquid. The polymerisation mixture was allowed to cool to ambient temperature, diluted with dichloromethane and subsequently added dropwise to diethyl ether to give a white precipitate. This was filtered and dried under reduced pressure at 40°C (1.90 g, 60% yield).

4.2.6. Synthesis of poly(vinyl acetate)-*block*-poly(N-vinylcaprolactam)

4.2.6.1. In ethyl acetate

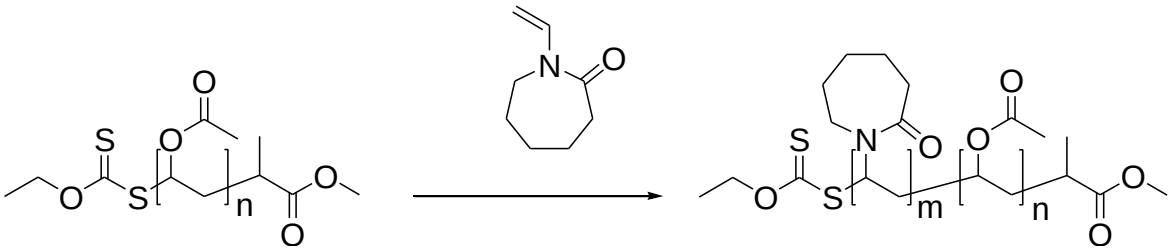

MacroCTA 16

Scheme 4.11.

To a 50 ml Schlenk tube was added a PVAc macroCTA (1.00 g, 5.68 x 10^{-2} mmol, 1.76 x 10^{4} $gmol^{-1}$, PDI = 1.39), NVCL (1.60 g, 11.5 mmol), AIBN (5.00 mg, 3.05 x 10^{-2} mmol) and ethyl acetate (4.0 ml). The polymerisation mixture was thoroughly degassed by four freeze pump thaw cycles. The flask was back filled with nitrogen gas, placed in an oil bath, temperature was raised to 80°C and the mixture was heated for 19 h. Solvent was removed under reduced pressure and residue was dissolved in dichloromethane and added dropwise to diethyl ether to give a white precipitate. The solid was filtered off and dried under reduced pressure to give a white solid (1.72 g, 45% yield).

4.2.6.2. In 1, 4 dioxane

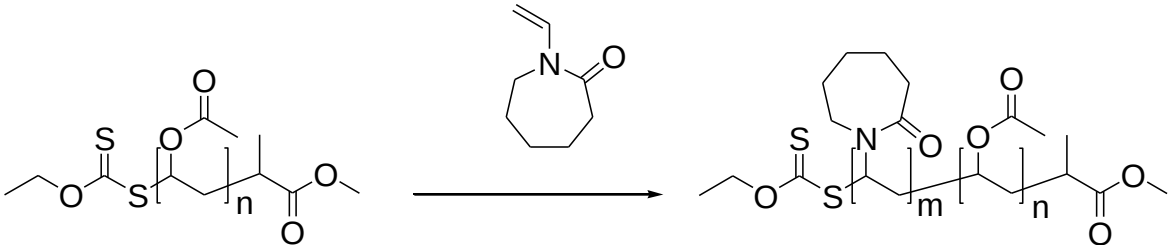

MacroCTA 16

Scheme 4.12.

To a 50 ml glass ampoule was added a PVAc macroCTA (1.00 g, 7.87 x 10^{-2} mmol, 1.27 x 10^{4} $gmol^{-1}$, PDI = 1.35), NVCL (1.63 g, 11.7 mmol), AIBN (2.00 mg, 1.22 x 10^{-2} mmol) and 1,4 dioxane (3.5 ml). The polymerisation mixture was thoroughly degassed

by four freeze pump thaw cycles and sealed under vacuum. The ampoule was then placed in an oil bath thermostated at 80°C and heated for 40 h. The product of the reaction was a solid white gel, which was dissolved in dichloromethane and the resulting solution was added dropwise to hexane. A white precipitate was immediately formed, which was subsequently filtered and dried under reduced pressure at 35°C to give a white solid (2.56 g, 96% yield).

4.2.7. Synthesis of poly(N-vinylpyrrolidone)-*ran*-poly(vinyl acetate) *via* RAFT

To a 50 ml glass ampoule was added NVP (2.58 g, 23.2 mmol), VAc (2.00 g, 23.2 mmol), RAFT agent 5 (66.0 mg, 0.216 mmol), ACVA (14.0 mg, 5.00×10^{-2} mmol) and 1,4 dioxane (5.0 ml) inside a nitrogen filled glove box. The ampoule was removed from glove box and heated at 70°C for 12 h. Polymerisation mixture, a gel, was dissolved in dichloromethane and precipitated into diethyl ether to give a white precipitate. Solid polymer was filtered and dried under reduced pressure at ambient temperature to give a white powder (3.65 g, 80% yield).

4.2.8. Synthesis of poly(N-vinylcaprolactam)-*ran*-poly(vinyl acetate) *via* RAFT

To a 50 ml glass ampoule was added NVCL (3.23 g, 23.2 mmol), VAc (2.00 g, 23.2 mmol), RAFT agent 5 (67.0 mg, 0.220 mmol), ACVA (12.4 mg, 4.42×10^{-2} mmol) and 1,4 dioxane (5.0 ml) inside a nitrogen filled glove box. The ampoule was removed from glove box and heated at 70°C for 12 h. Polymerisation mixture, a gel, was dissolved in dichloromethane and precipitated into hexane to give a white precipitate. Solid polymer was filtered and dried under reduced pressure at ambient temperature to give a white powder (3.94 g, 75% yield).

4.2.9. Synthesis of poly(N-vinylpyrrolidone)-*ran*-poly(N-vinylcaprolactam) *via* RAFT

To a 50 ml glass ampoule was added NVP (2.58 g, 23.2 mmol), NVCL (3.23 g, 23.2 mmol), RAFT agent 5 (68.0 mg, 0.223 mmol), ACVA (12.4 mg, 4.42×10^{-2} mmol) and 1,4 dioxane (5.0 ml) inside a nitrogen filled glove box. The ampoule was removed from glove box and heated at 70°C for 12 h. Polymerisation mixture, a gel, was dissolved in dichloromethane and precipitated into diethyl ether to give a white precipitate. Solid

polymer was filtered and dried under reduced pressure at ambient temperature to give a white powder (2.23 g, 38% yield).

4.2.10. Synthesis of poly(N-vinylpyrrolidone)-*ran*-poly(vinyl acetate) *via* conventional free radical polymerisation

To a 50 ml glass ampoule was added NVP (2.58 g, 23.2 mmol), VAc (2.00 g, 23.2 mmol), ACVA (14.0 mg, 5.00 x 10^{-2} mmol) and 1, 4 dioxane (4.5 ml) inside a nitrogen filled glove box. The ampoule was removed from glove box and heated at 70°C for 1.5 h. Polymerisation mixture, a gel, was dissolved in dichloromethane and precipitated into diethyl ether to give a white precipitate. Solid polymer was filtered and dried under reduced pressure at 30°C to give a white powder (3.66 g, 80% yield).

4.2.11. Synthesis of poly(N-vinylcaprolactam)-*ran*-poly(vinyl acetate) *via* conventional free radical polymerisation

To a 50 ml glass ampoule was added NVCL (3.23 g, 23.2 mmol), VAc (2.00 g, 23.2 mmol), ACVA (14.0 mg, 5.00 x 10^{-2} mmol) and 1,4 dioxane (4.5 ml) inside a nitrogen filled glove box. The ampoule was removed from glove box and heated at 70°C for 1.5 h. Polymerisation mixture, a gel, was dissolved in dichloromethane and precipitated into hexane to give a white precipitate. Solid polymer was filtered and dried under reduced pressure at ambient temperature to give a white powder (3.98 g, 76% yield).

4.2.12. Synthesis of poly(N-vinylpyrrolidone)-*ran*-poly(N-vinylcaprolactam) *via* conventional free radical polymerisation

To a 50 ml glass ampoule was added NVP (2.58 g, 23.2 mmol), NVCL (3.23 g, 23.2 mmol), ACVA (14.0 mg, 5.00 x 10^{-2} mmol) and 1,4 dioxane (4.5 ml) inside a nitrogen filled glove box. The ampoule was removed from glove box and heated at 70°C for 1.5 h. Polymerisation mixture, a gel, was dissolved in dichloromethane and precipitated into diethyl ether to give a white precipitate. Solid polymer was filtered and dried under reduced pressure at ambient temperature to give a white powder (5.67 g, 98% yield).

4.3. Results and Discussion

4.3.1. Synthesis of block copolymers

Homopolymers of NVP and VAc, prepared in Chapter 3 *via* RAFT polymerisation using RAFT agents 1-8, were utilised as macroCTA's to produce block copolymers. PNVP and PVAc macroCTA's 12-17, Figure 4.1, were used to synthesise PNVP-*block*-PVAc, PNVP-*block*-PNVCL, PVAc-*block*-PNVP and PVAc-*block*-PNVCL.

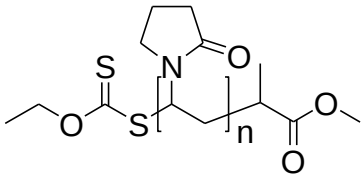

MacroCTA 12

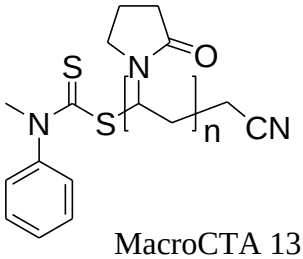

MacroCTA 13

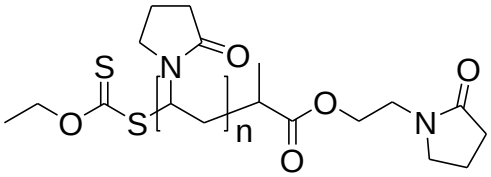

MacroCTA 14

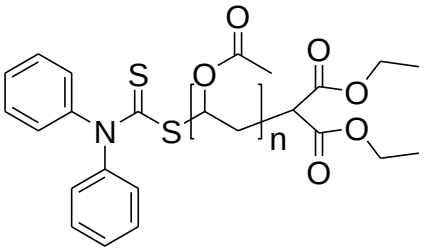

MacroCTA 15

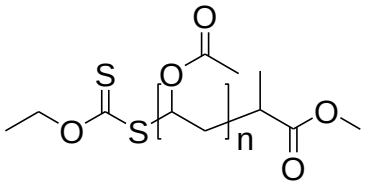

MacroCTA 16

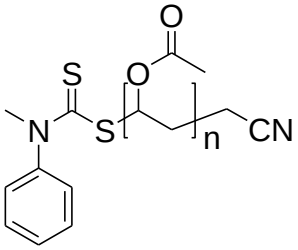

MacroCTA 17

Figure 4.1. Structures of macroCTA 12 – 17

4.3.1.1. Poly(N-vinylpyrrolidone)-*block*-poly(vinyl acetate)

PNVP macroCTA's 12-14 were used for the controlled polymerisation of VAc, to prepare PNVP-*block*-PVAc, Table 4.1.

Table 4.1. Synthesis of PNVP-*block*-PVAc, at 70°C

Entry	MacroCTA Details			Solvent	Molar ratio [VAc] : [PNVP]	Time (h)	Copolymer Product		
	Number	M_n (SEC) ($gmol^{-1}$) (x 10^4)	PDI				Yield (%)	M_P (SEC) ($gmol^{-1}$) (x 10^4)	PDI
1	12	2.18	1.53	DMF	194:1	25	1	2.28 (M_n)	1.39
2	13	1.59	1.25	Acetonitrile	476:1	41	43	4.75	1.70
3	14	1.09	1.13	THF	374:1	16	76	2.00	1.14
4	14	0.99	1.24	1, 4 dioxane	566:1	24	86	6.02	1.88

MacroCTA 12 (M_n = 2.18 x 10^4 $gmol^{-1}$, PDI = 1.53) was used to mediate the polymerisation of VAc in DMF (Table 4.1, Entry 1). The resulting copolymer product was analysed by ^{1}H NMR spectroscopy (Appendix 1, Figure 1) and SEC (Figure 4.2).

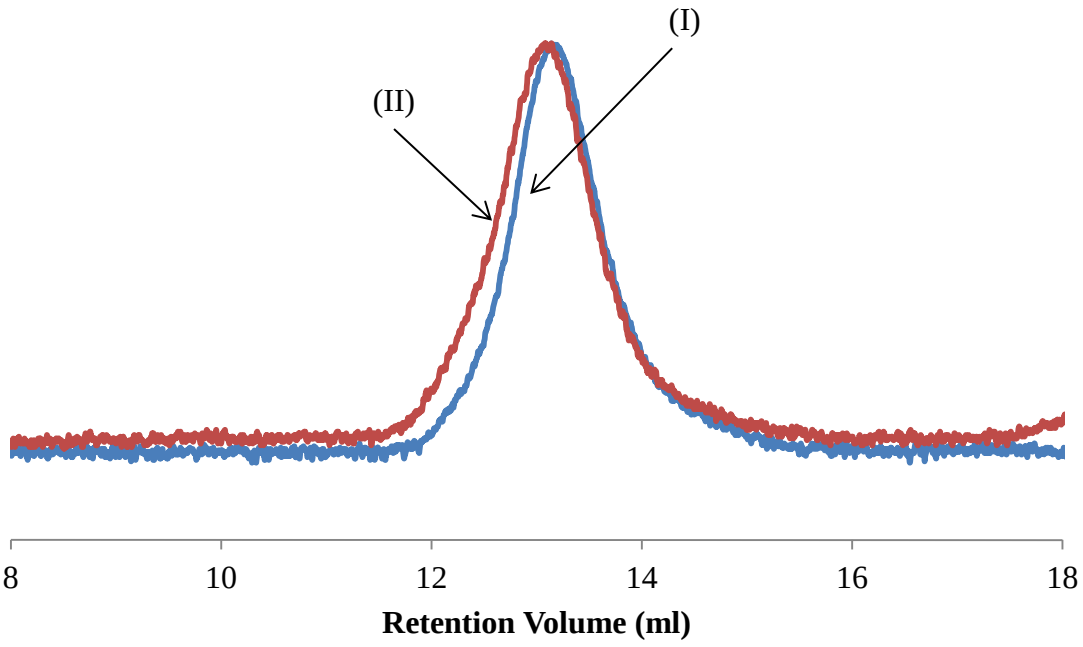

Figure 4.2. SEC traces (refractive index) of (I) PNVP macroCTA 12 and (II) copolymer product

The comparison of ^{1}H NMR spectra of the macroCTA 12 and copolymer product, shows that only a small amount of PVAc has been incorporated (Appendix 1, Figure 1, I-III). Integration of the CH protons on the backbone chain of PVAc (4.70-4.95 ppm) and PNVP (3.45-4.10 ppm), gives a ratio of 1 : 14.58 and this equates to approximately 6% incorporation of PVAc in the copolymer product. Furthermore, comparison of the SEC traces of macroCTA 12 (Figure 4.2-I) and copolymer product (Figure 4.2-II) shows only a slight shift; the M_p of macroCTA 12 and copolymer product were found to be 3.01 x 10^4 gmol^{-1} and 2.94 x 10^4 gmol^{-1}, respectively. It is believed that the reason why VAc incorporation is low in PNVP-*block*-PVAc is due to DMF promoting xanthate cleavage. The same observation has been reported previously.[29]

MacroCTA 13 (M_n = 1.59 x 10^4 gmol^{-1}, PDI = 1.25) was also used for the polymerisation of VAc (Table 4.1; Entry 2) and the copolymer product was analysed by ^{1}H NMR spectroscopy (Appendix 1, Figure 2) and SEC (Figure 4.3).

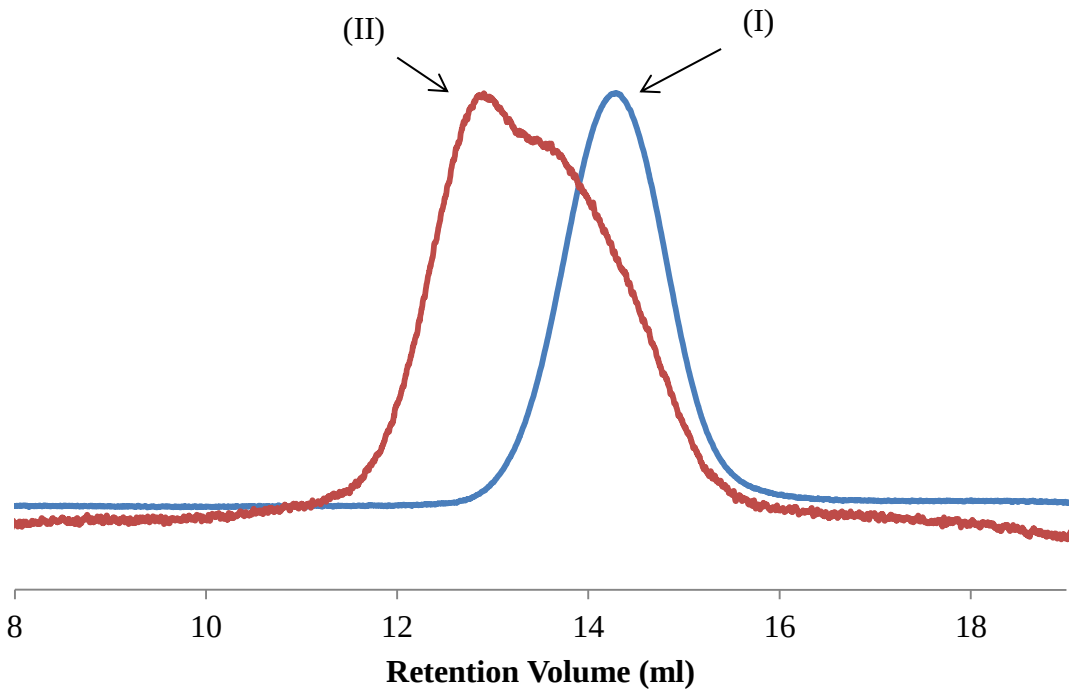

Figure 4.3 SEC traces (refractive index) of (I) PNVP macroCTA 13 and (II) copolymer product

From comparing the ^{1}H NMR spectra of macroCTA 13 and the copolymer product, resonances corresponding to both PNVP and PVAc can be observed (Appendix 1, Figure 2, I-III). Integration of the CH protons on the backbone of each polymer,

gives a ratio 2:1 (PVAc : PNVP) indicating that approximately 67% of the copolymer product is PVAc. Furthermore, the SEC trace for the product shows a bimodal molecular weight distribution with PDI of 1.70, Figure 4.3-II. The lower molecular weight shoulder is believed to be due to the presence of macroCTA 13, Figure 4.3-I. The M_p of the copolymer product (higher molecular weight distribution) is found to be 4.75 x 10^4 $gmol^{-1}$. This result indicates that the copolymerisation reaction is performed better in acetonitrile as the solvent.

MacroCTA 14 (M_n = 1.09 x 10^4 $gmol^{-1}$, PDI = 1.13) was used to mediate the polymerisation of VAc in THF (Table 4.1, Entry 3). The resulting copolymer product was analysed by ^{1}H NMR spectroscopy (Appendix 1, Figure 3) and SEC (Figure 4.4).

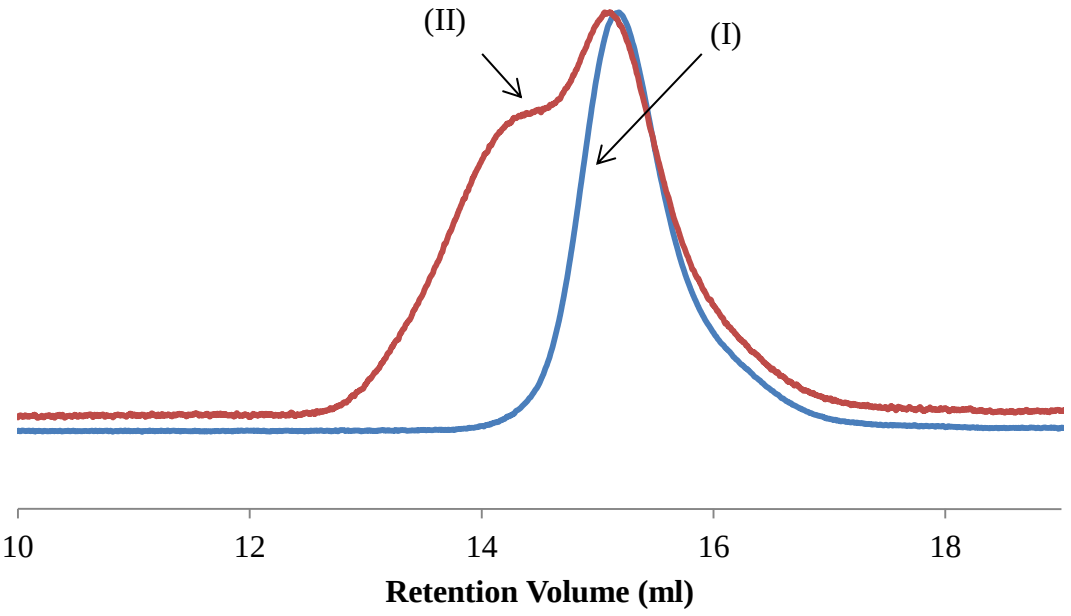

Figure 4.4. SEC traces (refractive index) of (I) PNVP macroCTA 14 and (II) copolymer product

The comparison of the ^{1}H NMR spectrum of macroCTA 14 and the copolymer product shows resonances for both PNVP and PVAc (Appendix 1, Figure 3, I-III). By integrating the CH protons of the backbone of both polymers, the ratio of PVAc:PNVP is observed to be 1 : 1.57, indicating that PVAc accounts for approximately 39% of the copolymer product. Furthermore, the SEC trace of the copolymer product shows a bimodal molecular weight distribution (Figure 4.4-II); the lower molecular weight peak is believed to be due to the presence of macroCTA 14, Figure 4.4-I. The M_p of the

copolymer product (higher molecular weight distribution) increased to 2.00 x 10^4 $gmol^{-1}$.

In order to investigate the effect of solvent, the copolymerisation reaction was also conducted in 1, 4 dioxane (Table 4.1; Entry 4) using macroCTA 14 (M_n = 9.90 x 10^3 $gmol^{-1}$, PDI = 1.24). The resulting copolymer product was analysed by ^{1}H NMR spectroscopy (Appendix 1, Figure 4) and SEC (Figure 4.5).

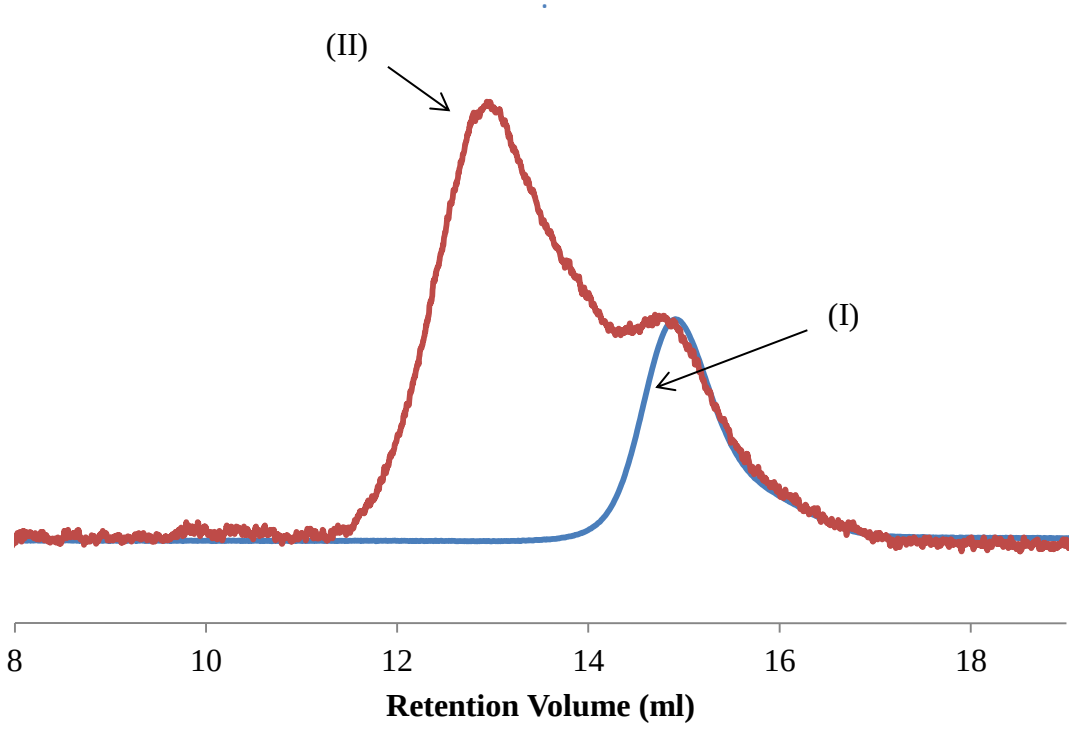

Figure 4.5. SEC traces (refractive index) of (I) PNVP macroCTA 14 and (II) copolymer product

The comparison of the ^{1}H NMR spectra of macroCTA 14 and the copolymer product shows resonances for both PNVP and PVAc (Appendix 1, Figure 4, I-III). Integration of the CH protons in the backbone for both polymers, gives a ratio of 4:1 (PVAc:PNVP), indicating PVAc content of approximately 80% of the copolymer product. SEC trace for the copolymer product shows a bimodal molecular weight distribution with PDI of 1.88, Figure 4.5-II. The lower molecular weight shoulder is due to the presence of macroCTA 14 (Figure 4.5-I). The M_p of the copolymer product (higher molecular weight distribution) is found to be 6.02 x 10^4 $gmol^{-1}$. The comparison of the PVAc content of 39% in THF to 80% in 1, 4 dioxane, indicates that the copolymerisation reaction is conducted better in 1, 4 dioxane.

4.3.1.2. Poly(N-vinylpyrrolidone)-*block*-poly(N-vinylcaprolactam)

PNVP macroCTA's 12-14 were also used for the controlled polymerisation of NVCL in 1, 4 dioxane and acetonitrile, to prepare PNVP-*block*-PNVCL, Table 4.2.

Table 4.2. Synthesis of PNVP-*block*-PNVCL, in 1, 4 dioxane

Entry	MacroCTA Details			Molar ratio [NVCL] : [PNVP]	Time (h)	Temp (°C)	Copolymer Product		
	Number	M_n (SEC) ($gmol^{-1}$) (x 10^4)	PDI				Yield (%)	M_p (SEC) ($gmol^{-1}$) (x 10^4)	PDI
1	12	2.82	1.34	257:1	40	80	99	10.26	2.29
2	12	2.82	1.34	2399:1	17	80	79	33.07	2.23
3	14	0.99	1.24	566:1	24	70	41	16.99	2.47

MacroCTA 12 (M_n = 2.82 x 10^4 $gmol^{-1}$, PDI = 1.34) was used to mediate the polymerisation of NVCL, in 1, 4 dioxane (Table 4.2; Entry 1). The molar ratio of monomer to macroCTA 12 was 257 : 1 and the copolymer product was analysed by ^1H NMR spectroscopy (Appendix 1, Figure 5) and SEC (Figure 4.6).

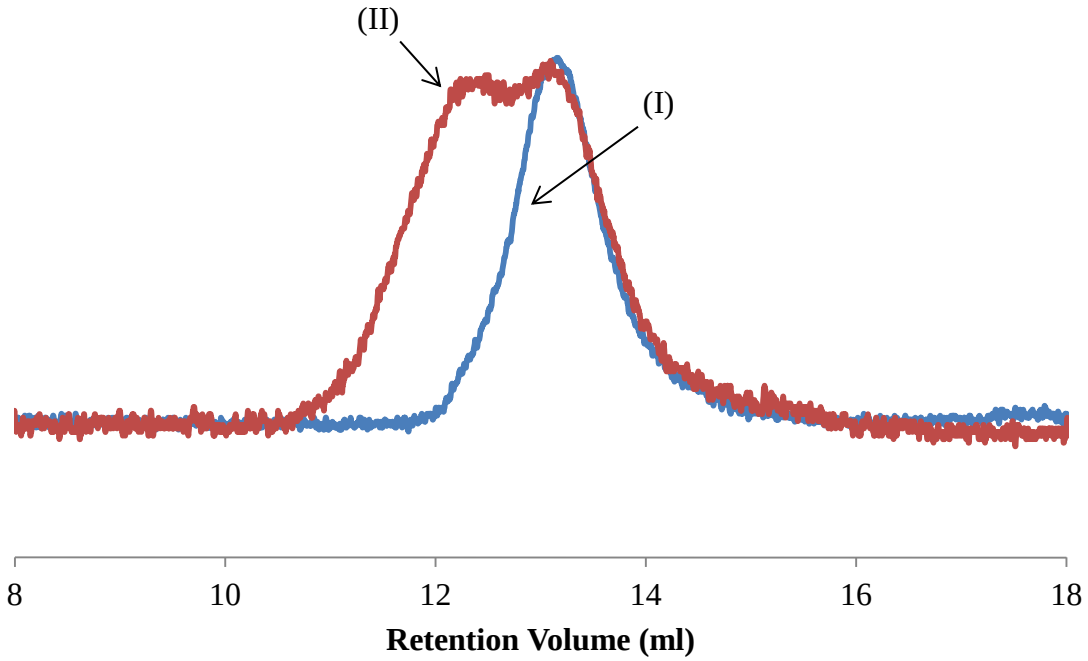

Figure 4.6. SEC traces (refractive index) of (I) PNVP macroCTA 12 and (II) copolymer product

The comparison of the ^{1}H NMR spectra of macroCTA 12 and copolymer product shows the resonances for both PNVP and PNVCL (Appendix 1, Figure 5, I-III). Integration of the CH protons in the backbone chain for both polymers gives the ratio of PNVCL : PNVP was 1 : 1.16, indicating the PNVCL content in the copolymer product was approximately 46%. SEC trace for the product shows a bimodal molecular weight distribution with a PDI of 2.29, Figure 4.6-II. The lower molecular weight shoulder is due to the presence of macroCTA 12 (Figure 4.6-I). The M_p of the copolymer product (higher molecular weight distribution) is found to be 10.26 x 10^4 gmol^{-1}. The existence of low molecular weight shoulders in the SEC traces of the block copolymers, could be attributed to: (a) presence of a small amount of homopolymer of the second monomer, see Section 4.3.1.5; (b) macroCTA with cleaved xanthate or dithiocarbamate end groups, unable to be chain extended; (c) the rate of propagation being faster than the rate of initiation and insufficient amount of second monomer to achieve full consumption of the macroCTA. However, the combination of all these factors may well be possible.

In order to investigate the effect of the addition of more NVCL monomer, the reaction was repeated with a higher ratio of NVCL:PNVP. MacroCTA 12 (M_n = 2.82 x 10^4 gmol^{-1}, PDI = 1.34) was used to control the polymerisation of NVCL, in an increased NVCL : macroCTA ratio of 2399 : 1 (Table 4.2; Entry 2). The resulting copolymer product was analysed by ^{1}H NMR spectroscopy (Appendix 1, Figure 6) and SEC (Figure 4.7).

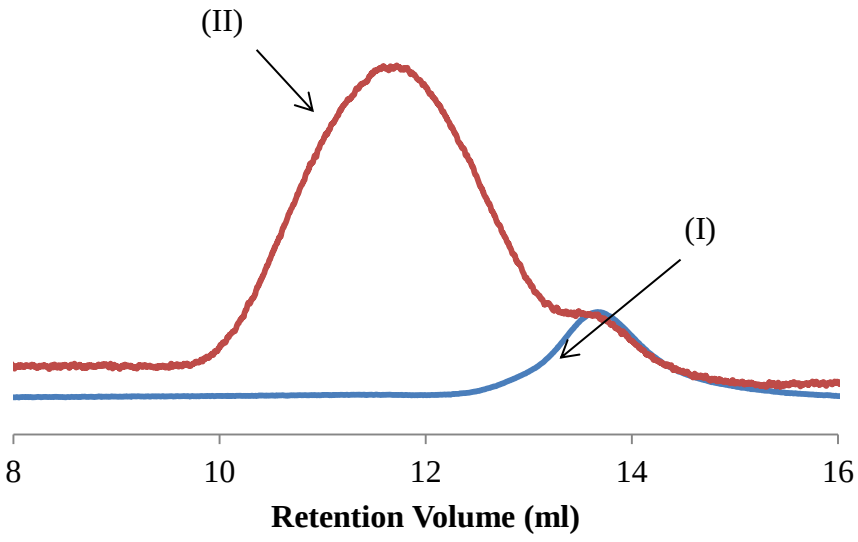

Figure 4.7. SEC traces (refractive index) of (I) PNVP macroCTA 12 and (II) copolymer product

Expectedly as the ratio of NVCL : macroCTA 12 was increased, the ^{1}H NMR spectrum of the copolymer product, shows resonances predominately for PNVCL (Appendix 1, Figure 6, I-III). The SEC trace for the copolymer product shows a bimodal molecular weight distribution with a PDI of 2.23, Figure 4.7-II. The lower molecular weight peak is believed to be due to the presence of macroCTA 12 (Figure 4.7-I). The M_p of the copolymer product (higher molecular weight distribution) was analysed to be 33.07 x 10^4 gmol^{-1}. This result is believed to be indicating the presence of PNVP chains with cleaved xanthate end groups. However, the existence of the homopolymer of the second block (PNVCL) cannot be ruled out.

MacroCTA 14 (M_n = 9.91 x 10^3 gmol^{-1}, PDI = 1.24) was used to mediate the polymerisation of NVCL in 1, 4 dioxane (Table 4.2; Entry 3). The resulting copolymer product was analysed by ^{1}H NMR spectroscopy (Appendix 1, Figure 7) and SEC (Figure 4.8).

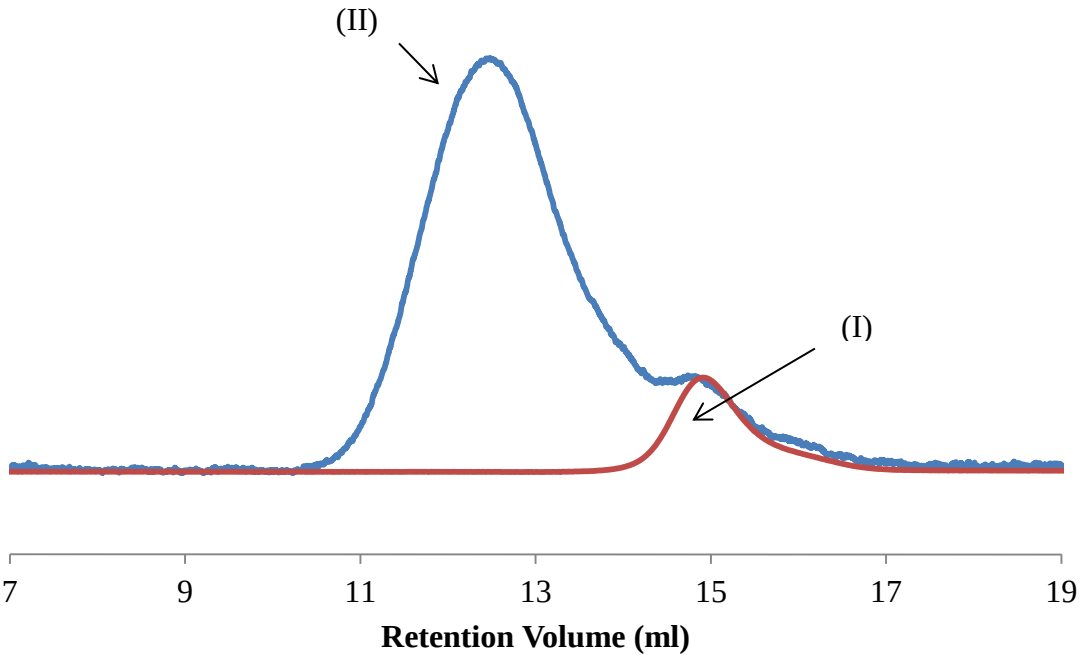

Figure 4.8. SEC traces (refractive index) of (I) PNVP macroCTA 14 and (II) copolymer product

From comparing the ^{1}H NMR of macroCTA 14 and the copolymer product, resonances for both PNVCL and PNVP can be observed (Appendix 1, Figure 7, I-III). Integration of the CH protons on the backbone of each polymer gives a ratio of approximately 3.7 : 1 (PNVCL : PNVP), indicating that PNVCL accounts for around 80% of the copolymer product. The SEC trace of the copolymer product (Figure 4.8-II)

shows a bimodal molecular weight distribution with a PDI of 2.47. The lower molecular weight peak is due to the presence of macroCTA 14 (Figure 4.8-I). The M_p of the copolymer product (higher molecular weight distribution) was analysed by SEC to be 16.97 x 10^4 $gmol^{-1}$. As discussed for the copolymerisation reactions using macroCTA 12, this result is also believed to be indicating the presence of PNVP chains with cleaved xanthate end groups.

4.3.1.3. Poly(vinyl acetate)-*block*-poly(N-vinylpyrrolidone)

PVAc macroCTA's 15-17 were used for the controlled polymerisation of NVP, to synthesise PVAc-*block*-PNVP, (Table 4.3).

Table 4.3. Synthesis of PVAc-*block*-PNVP

Entry	MacroCTA Details			Solvent	Molar ratio [NVP] : [PVAc]	Time (h)	Temp (°C)	Copolymer Product		
	Number	M_n (SEC) ($gmol^{-1}$) (x 10^4)	PDI					Yield (%)	M_p (SEC) ($gmol^{-1}$) (x 10^4)	PDI
1	15	0.66	1.53	1, 4 dioxane	93:1	16	80	65	10.06	2.09
2	16	1.27	1.35	1, 4 dioxane	147:1	35	80	98	17.50	1.91
3	17	1.02	1.39	Acetonitrile	138:1	25	70	60	12.34	3.18

MacroCTA 15 (M_n = 6.60 x 10^3 $gmol^{-1}$, PDI = 1.53) was used to mediate the polymerisation of NVP in 1, 4 dioxane (Table 4.3; Entry 1). The molar ratio of NVP to macroCTA 15 was 93 : 1. The resulting copolymer product was analysed by ^{1}H NMR spectroscopy (Appendix 1, Figure 8) and SEC (Figure 4.9).

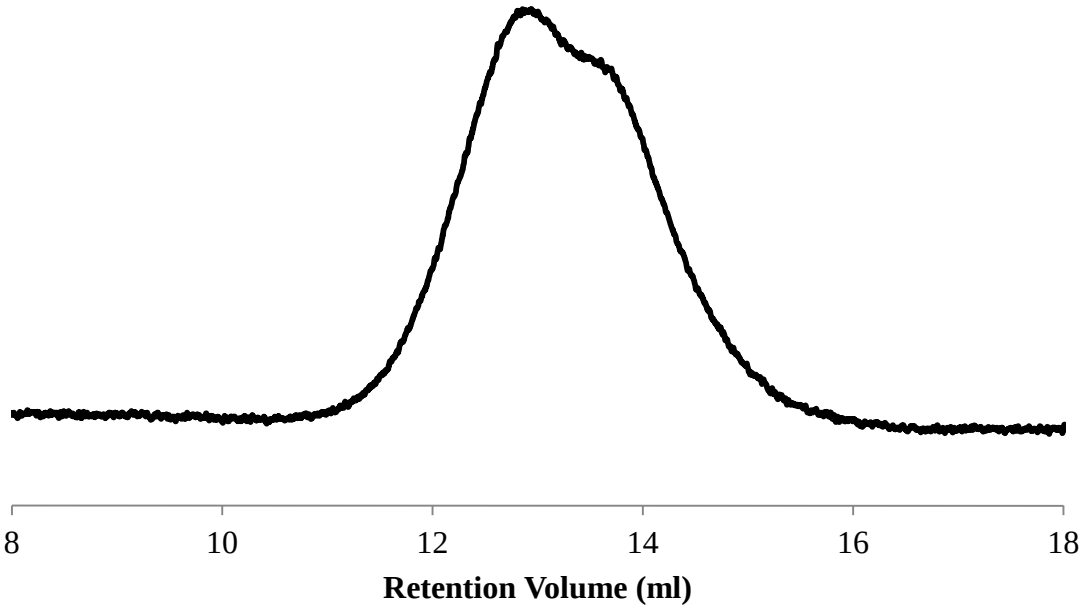

Figure 4.9. SEC trace (refractive index) of copolymer product

From comparing the ^{1}H NMR spectrum of the macroCTA 15 and copolymer product, resonances due to both PVAc and PNVP can be observed (Appendix 1, Figure 8, I-III). Integration of the CH protons on the backbone chain of each polymer gives a ratio of 1 : 1.19 (PVAc : PNVP), indicating that PNVP accounts for approximately 54% of the copolymer product. The SEC trace for the copolymer product shows a bimodal molecular weight distribution with a PDI of 2.09, Figure 4.9. The M_p of the higher molecular weight peak is 10.06 x 10^4 gmol^{-1} and the low molecular weight distribution is believed to be due to the presence of macroCTA 15.

MacroCTA 16 (M_n = 1.27 x 10^4 gmol^{-1}, PDI = 1.35) was used to mediate the polymerisation of NVP, in 1, 4 dioxane with a NVP : macroCTA 16 ratio of 147:1 (Table 4.3; Entry 2). The resulting copolymer product was analysed by ^{1}H NMR spectroscopy (Appendix 1, Figure 9) and SEC (Figure 4.10).

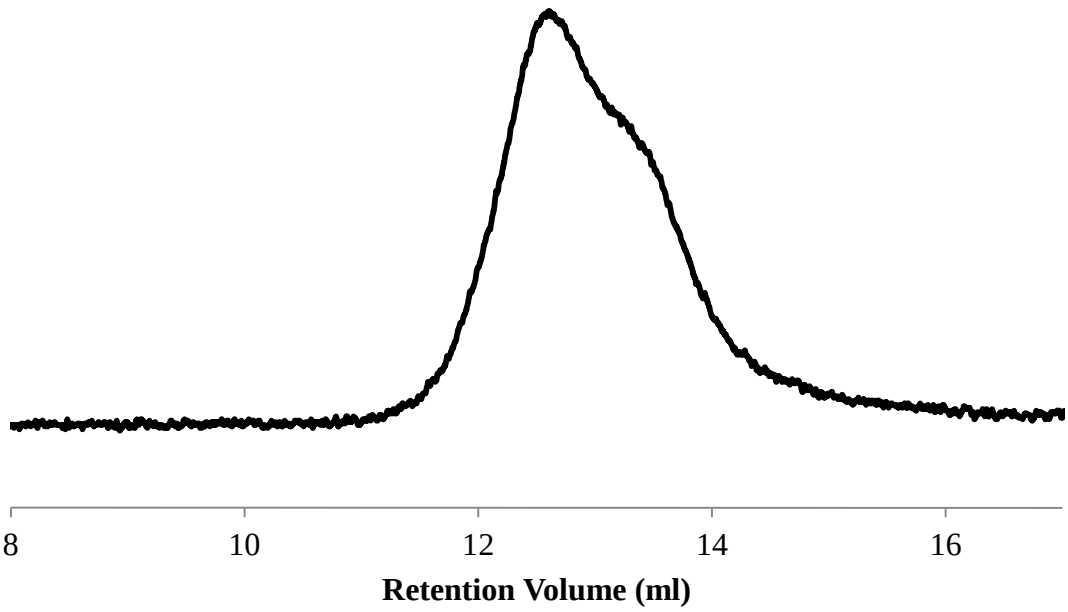

Figure 4.10. SEC trace (refractive index) of copolymer product

From comparing the ^{1}H NMR spectra of macroCTA 16 and the copolymer product, resonances for both the PVAc and PNVP can be observed (Appendix 1, Figure 9, I-III). Integration of the CH protons on the backbone chain of the polymers gives a ratio of 1 : 1.65 (PVAc : PNVP), indicating that PNVP accounts for approximately 62% of the copolymer product. The SEC trace for the copolymer product shows a bimodal molecular weight distribution with a PDI of 1.91, Figure 4.10. The M_p of the higher molecular weight peak is 17.50 x 10^4 gmol^{-1} and the low molecular weight distribution is believed to be due to the presence of macroCTA 16.

MacroCTA 17 (1.02 x 10^4 gmol^{-1}, PDI = 1.39) was used to mediate the polymerisation of NVP, in acetonitrile (Table 4.3; Entry 3). The resulting copolymer product was analysed by ^{1}H NMR spectroscopy (Appendix 1, Figure 10) and SEC (Figure 4.11).

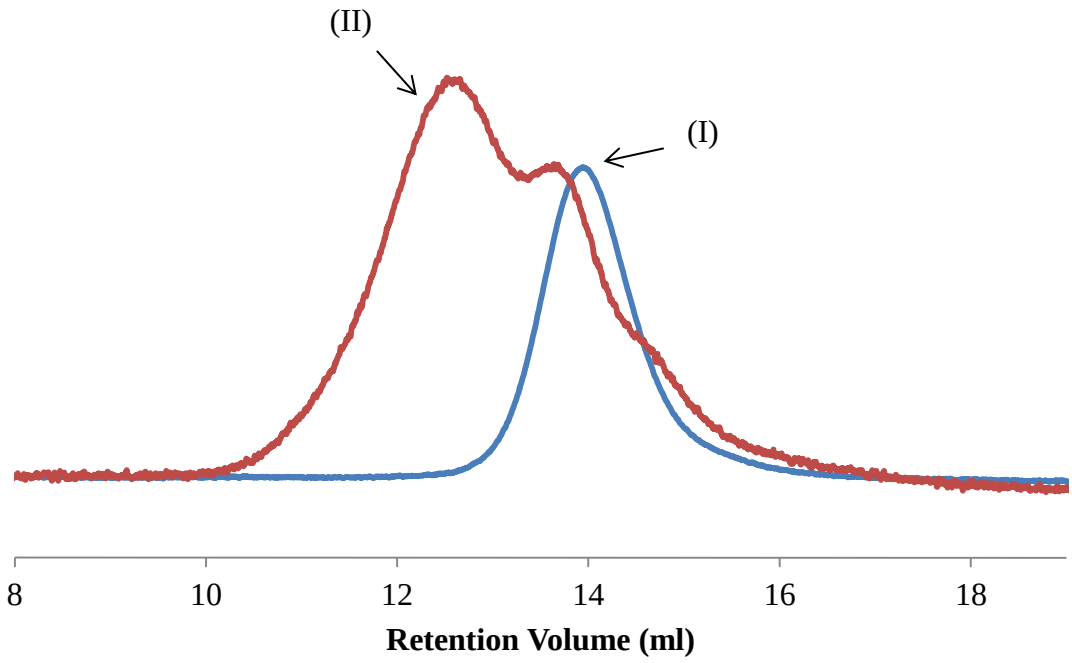

Figure 4.11. SEC traces (refractive index) of (I) PVAc macroCTA 17 and (II) copolymer product

The comparison of the ^{1}H NMR spectra of macroCTA 17 and the copolymer product, shows resonances for both the PVAc and PNVP (Appendix 1, Figure 10, I-III). Integration of the CH protons of the backbone chain of each polymers gives the ratio is 1 : 1.84 (PVAc : PNVP), indicating that PNVP accounts for approximately 65% of the copolymer product. The SEC trace of the copolymer product shows a bimodal molecular weight distribution with a PDI of 3.18, Figure 4.11-II. The lower molecular weight peak is believed to be due to the presence of macroCTA 17 (Figure 4.11-I). The M_p of the copolymer product (higher molecular weight distribution) is 12.34 x 10^4 $gmol^{-1}$.

It is interesting to note that the second monomer content (PNVP) in the block copolymer using macroCTA 15-17, is approximately the same (average of 60%). The reason for the SEC traces being bimodal may well be due to the presence of PVAc chains with cleaved xanthate or dithiocarbamate groups. Although here again the presence of homo PNVP cannot be ruled out.

4.3.1.4. Poly(vinyl acetate)-*block*-poly(N-vinylcaprolactam)

PVAc macroCTA 16 was used for the controlled polymerisation of NVCL to synthesise PVAc-*block*-PNVP, shown in Table 4.4.

Table 4.4. Synthesis of PVAc-*block*-PNVCL, at 80°C

Entry	MacroCTA Details			Solvent	Molar ratio [NVCL] : [PVAc]	Time (h)	Copolymer Product		
	Number	M_n (SEC) ($gmol^{-1}$) ($x\ 10^4$)	PDI				Yield (%)	M_p (SEC) ($gmol^{-1}$) ($x\ 10^4$)	PDI
1	16	1.76	1.39	Ethyl acetate	202:1	19	45	8.33	2.23
2	16	1.27	1.35	1, 4 dioxane	148:1	40	96	10.76	1.62

MacroCTA 16 (1.76×10^4 $gmol^{-1}$, PDI = 1.39) was used to mediate the polymerisation of NVCL, in ethyl acetate (Table 4.4; Entry 1) and the NVCL : macroCTA 16 ratio, was 202 : 1. The resulting copolymer product was analysed by ^1H NMR spectroscopy (Appendix 1, Figure 11) and SEC (Figure 4.12).

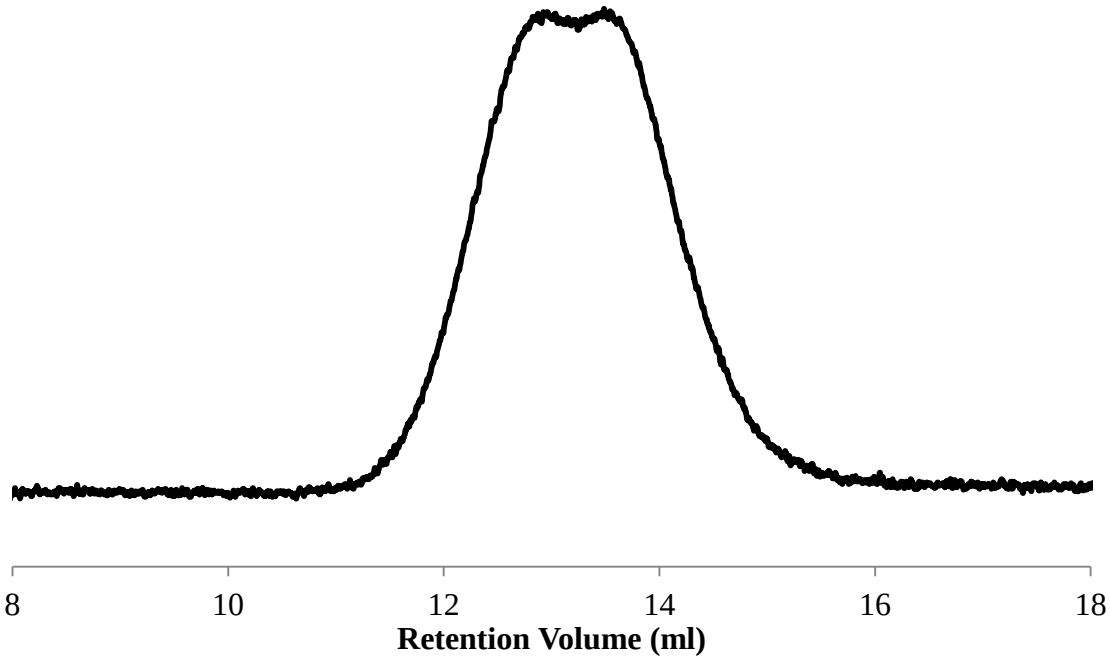

Figure 4.12. SEC trace (refractive index) of copolymer product

The comparison of the ^{1}H NMR spectra of macroCTA 16 and the copolymer product, shows resonances for both PVAc and PNVCL (Appendix 1, Figure 11, I-III). Integration of the CH protons of the two polymers backbone chain gives a ratio of 1 : 1, indicating that both PNVCL and PVAc account for 50% of the copolymer product. The SEC trace for the copolymer product shows a bimodal molecular weight distribution with a PDI of 2.23, Figure 4.12. The M_p of the higher molecular weight peak is 8.33 x 10^4 gmol^{-1} and the lower molecular weight peak is believed to be due to the presence of macroCTA 16.

MacroCTA 16 (M_n = 1.27 x 10^4 gmol^{-1}, PDI = 1.35) was also to mediate the polymerisation of NVCL, in 1, 4 dioxane (Table 4.4; Entry 2) and the NVCL : macroCTA 16, was 148:1. The resulting copolymer product was analysed by ^{1}H NMR spectroscopy (Appendix 1, Figure 12) and SEC (Figure 4.13).

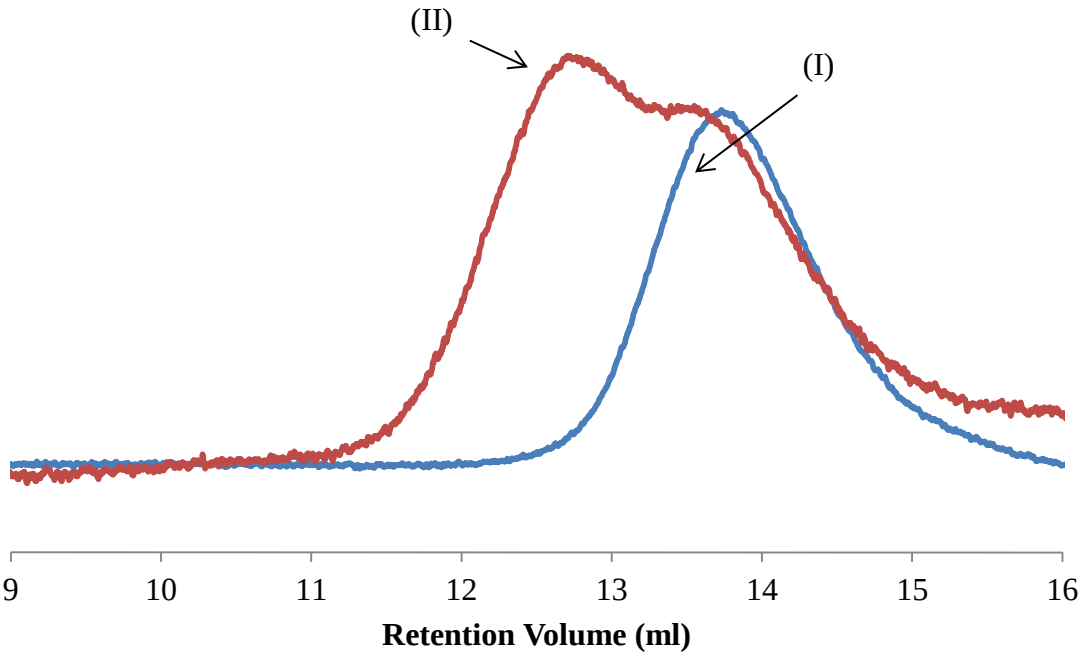

Figure 4.13. SEC traces (refractive index) of (I) PVAc macroCTA 16 and (II) copolymer product

From comparing of the ^{1}H NMR spectra of macroCTA 16 and the copolymer product, resonances for both the PVAc and PNVCL can be observed (Appendix 1, Figure 12, I-III). Integration of the CH protons from the polymer backbone of the two polymers gives a ratio of 1 : 0.83 (PVAc : PNVCL) indicating that PNVCL accounts for

approximately 45% of the copolymer product. The SEC trace from the copolymer product shows bimodal molecular weight distribution with a PDI of 1.62, Figure 4.13-II. The lower molecular weight shoulder is believed to be due to the presence of macroCTA 16 (Figure 4.13-I). The M_p of the copolymer product (higher molecular weight distribution) is 10.76 x 10^4 $gmol^{-1}$.

Similar behaviour to the synthesis of PNVP-block-PVAc, PNVP-block-PNVCL and PVAc-block-PNVP SEC traces are observed to be bimodal. The reason for this behaviour has been discussed in the previous sections.

4.3.1.5. Explanation of bimodal molecular weight distributions in SEC analysis

All the block copolymers synthesised in this chapter exhibited bimodal molecular weight distributions by SEC analysis. The existence of low molecular weight shoulders in the SEC traces of the block copolymers, could be attributed to: (a) presence of a small amount of homopolymer of the second monomer; (b) macroCTA with cleaved xanthate or dithiocarbamate end groups, unable to be chain extended; (c) the rate of propagation being faster than the rate of initiation and insufficient amount of second monomer to achieve full consumption of the macroCTA. However, the combination of all these factors may well be possible.

(a) Formation of homopolymers of the second monomer

The mechanism shown in Scheme 4.13 for block copolymerisations *via* RAFT, clearly indicates the possibility for the formation of homopolymer of the second block.

Propagating homopolymer ($\mathbf{P_2}$•) initiated from the radical intiator (e.g. thermal decomposition of AIBN) can react with the macroCTA (**A**) to give an intermediate radical (**B**) which can either fragment to give the initial macroCTA (**A**) or a macroCTA incorporating the second block homopolymer (**C**). If (**C**) is generated, then the propagating radicals P_1• can reinitiate the polymerisation of the second monomer to produce diblock copolymer, P_1P_2•. P_1P_2• can now either add to the initial macroCTA (**A**) or second monomer derived macroCTA (**C**). Addition to (**A**) generates a P_1• capable producing diblock copolymer, P_1P_2•. Addition to (**C**) generates P_2•, which can further react with monomer to extend the homopolymer chain, P_2. The amount of P_2 homopolymer, depends on the concentration of the initiating radicals. As this is generally kept low in RAFT polymerisations, to reduce termination reactions, P_2 can be

minimised. Termination reactions still occur by coupling or disproportionation to give dead polymer chains of homopolymer, diblock copolymer or theoretically triblock copolymers through the coupling of the diblocks.[39] Although no higher molecular weight coupling products were observed in any of the SEC chromatograms in this study.

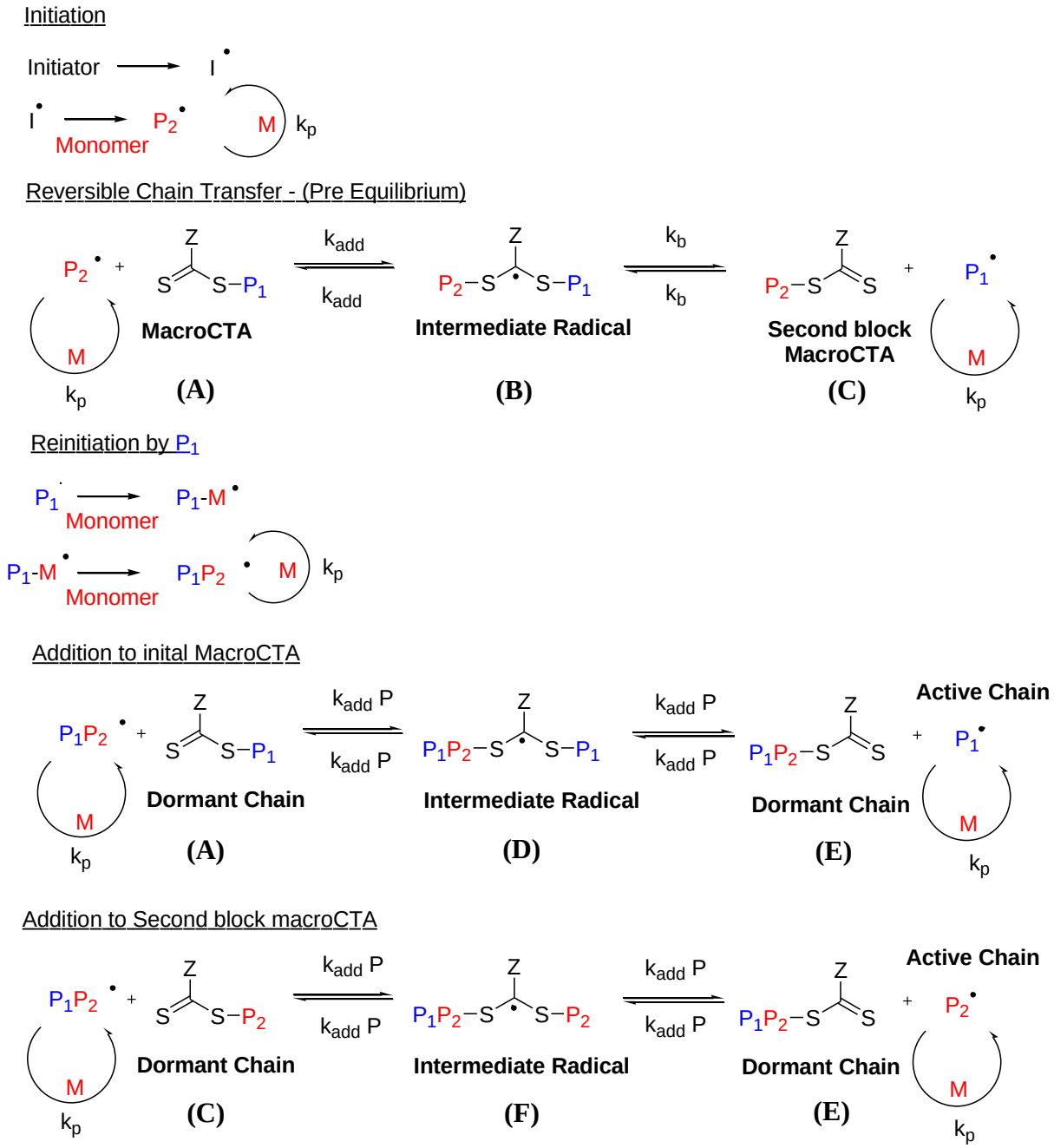

Scheme 4.13. Block copolymerisation mechanism in RAFT

(Where, **P_1** = Polymer 1, **P_2** = Polymer 2, **P_1P_2** = diblock copolymer)

(b) Cleavage of xanthate and dithiocarbamate groups

There are several possibilities for the cleavage of xanthate or dithiocarbamates groups at the chain end. These include the temperature of the (co)polymerisation / nature of Z group, solvent effects and reaction time.

Perrier and co-workers reported that RAFT agent 3 had a decomposition temperature of 75°C and loses 50% of its weight at 131°C.[40] The Z group was found to affect the thermal stability of the thio carbonyl groups in the order of dithiobenzoates > trithiocarbonates > xanthates. The C-S single bond is the most labile bond within the RAFT agent structure and is strengthened by electron donating Z groups, such as dithiobenzoates. However, electron withdrawing groups such as xanthates or dithiocarbamates weaken the C-S bond and thus the decomposition temperature is lowered. In addition, it was found that when the Z group contains an aromatic group the thermal stability of the compounds was increased. They concluded that polymerisations carried out at temperatures above 75°C will possibly experience some decomposition of the *O*-ethyl xanthate chain end; dithiocarbamate was seen to have a decomposition temperature of 242°C and loses 50% of its weight at 284°C.

Postma *et al.*[41] found that PVAc (M_n = 2.30 x 10^3 $gmol^{-1}$, PDI = 1.24) with an *O*-ethyl xanthate chain end formed higher molecular weight polymer (M_n = 4.25 x 10^3 $gmol^{-1}$, PDI = 1.70) and the loss of xanthate groups, when heated at 220°C for 3 h. It was suggested that the chain end is lost by the homolysis of the C-S bond to give PVAc propagating radicals, which can couple together to give higher molecular weight polymer (Scheme 4.14).

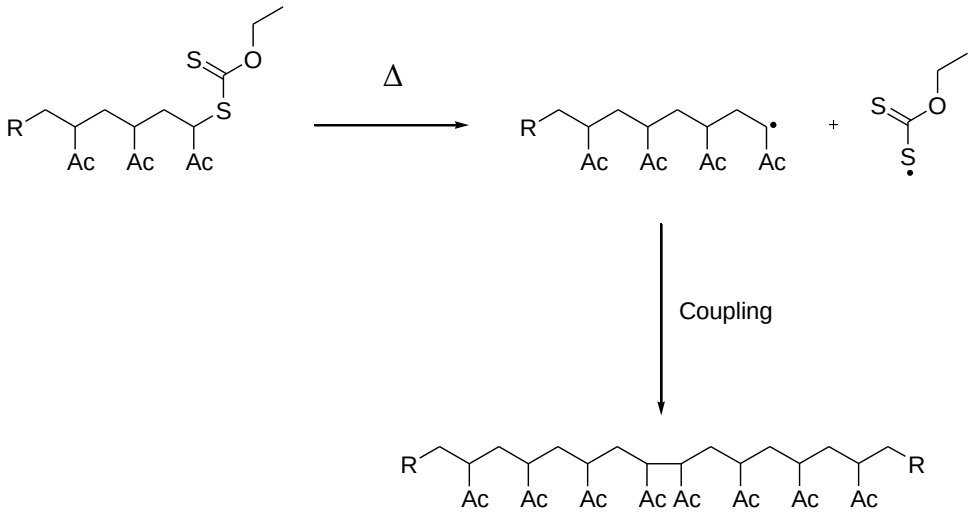

Scheme 4.14. Thermolysis of xanthate terminated PVAc

Pound *et al.*[42] have described the lability of the *O*-ethyl xanthate moiety next to an NVP adduct as exceptional. They conducted *in situ* ^{1}H NMR initialisation experiments and identified an unsaturated xanthate elimination product (X-EP) (Scheme 4.15 – I).

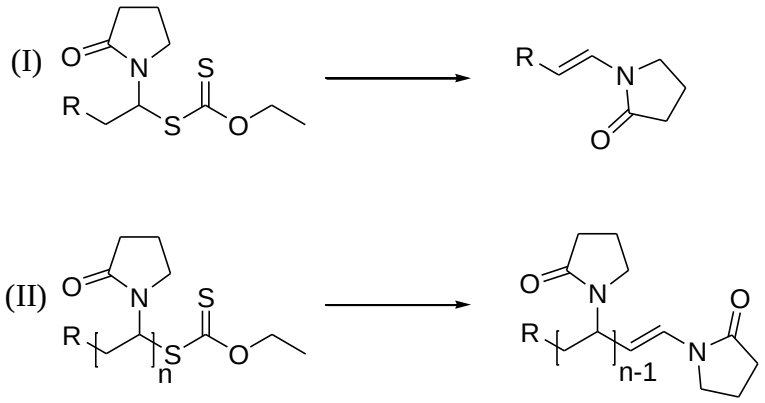

Scheme 4.15. Xanthate elimination[42]

Beyond initialisation (Scheme 4.15 - II), when polymer is formed, xanthate elimination leads to unsaturated chain ends. They concluded that the formation of unsaturated products during the polymerisation of NVP can depend on the nature of the solvent and reaction temperature.

In this study, the temperature at which polymerisations and block copolymerisations were carried out was between 60 - 80°C and in solvent. The SEC traces of the copolymer products showed bimodal molecular weight distribution where an *O*-ethyl xanthate Z group is present in the macroCTA. The lower molecular weight distribution could well be due to the presence of un-extended macroCTA as the result of the loss of xanthate end group during the copolymerisation reaction. Moreover, this could also be explained as the result of the presence of some homopolymer chains without xanthate active ends within the initial macroCTA. The chain extension ability of the macroCTA is not dependent on the nature of the homopolymer. Both PNVP and PVAc macroCTA's were unable to be fully chain extended in the block copolymerisation reactions.

It is interesting to note that copolymer products synthesised in the presence of macroCTA's 13, 15 and 17, exhibited bimodal molecular weight distributions. The presence of the lower molecular weight distributions could be discussed as that for xanthates. This observation is due to the dithiocarbamate chain end, withdrawing

electron density and weakening the C-S bond, similar to that seen in xanthates, thus lowering the decomposition temperature.

A number of solvents were used in the synthesis of block copolymers in this study. In general, carrying out RAFT polymerisations in solution is problematic, due to the chain transfer ability of the solvent used, Table 4.5. As described in Chapter 3, Section 3.3.4, protic solvents, such as 2-propanol can be effective in the elimination of xanthate moieties from the chain end of a polymer.

Table 4.5. Solvent chain transfer constants for VAc[43]

Solvent	**VAc (C_s (x 10^4))**
Acetonitrile	10 (60°C)[44]
Dimethylformamide	50 (70°C)[45]
Ethyl Acetate	3.4 (60°C)[46]
1, 4 dioxane	20 (60°C)[44]
2-propanol	44.6 (70°C)[45]

Furthermore, 1, 4 dioxane and THF are known to generate peroxides,[47] which could decompose and also initiate the polymerisation. A RAFT end capped polymer left in THF solution can have the sulphur atom of the dithiocarbonate moiety exchanged with an oxygen atom, resulting in dead polymer chains.[48] It has been reported also that block copolymerisations conducted in 1, 4 dioxane were observed to have incomplete chain extension and residual macroCTA observed by SEC [39, 49, 50] This is evident from our results as the block polymerisations conducted in either THF or 1, 4 dioxane resulted in a significant amount of dead macroCTA chains.

When DMF was used as the copolymerisation solvent in the synthesis of PNVP-*block*-PVAc, it was found that the incorporation of VAc in the copolymer product was 6% based on NMR. It is thought that DMF promotes the cleavage of the xanthate moiety from the polymer. Patel et al.[29] reported a similar observation in the synthesis of PVAc-*block*-PNVP, using xanthate containing macroCTA's in DMF.

In this study, the synthesis of macroCTA's has been achieved on a timescale in the region of 16 – 40 h, in order to achieve high conversion of monomer to polymer and to minimise residual monomer in the product. However, leaving polymerisation reactions this long increases the potential of termination reactions, such as disproportionation and the coupling of polymer chains. In RAFT block

copolymerisation reactions involving "less activated" monomers (LAMs), generally the conversion of monomer to polymer is kept low (< 50%), in order to minimise these side reactions.[18, 21, 28, 2]

(c) Rate of propagation *vs.* Rate of Initiation

The third possibility was that the rate of propagation was faster than the rate of initiation of the second monomer from the macroCTA. A consequence of this is that there is incomplete conversion of macroCTA to block copolymer, due to there being an insufficient amount of the second monomer present. Therefore, the lower molecular weight distribution in the bimodal block copolymer SEC traces may be due to the presence of unreacted macroCTA. However, we found that adding a large excess of monomer (Table 4.2; Entry 2), still resulted in the presence of un-extended macroCTA. This result may well rule out this possibility. However, we have not completed any detailed kinetics on the block copolymerisation reactions and therefore have no data to make a definite conclusion.

4.3.2. Synthesis of random RAFT copolymers

PNVP-*ran*-PVAc, PNVCL-*ran*-PVAc and PNVP-*ran*-PNVCL were prepared in the presence of RAFT agent 5. To the best of our knowledge, there are no reports that these random copolymers have previously been prepared in the literature by a controlled polymerisation method.

4.3.2.1. Poly(N-vinylpyrrolidone)-*ran*-poly(vinyl acetate)

The random copolymerisation of NVP and VAc, was conducted in 1, 4 dioxane using a monomer molar feed ratio of 50:50 in the presence of RAFT agent 5. The conventional random copolymerisation of NVP and VAc was also carried out in the absence of RAFT agent 5 for comparison. Figure 4.14 shows the ^{1}H NMR spectra of the copolymer products of the conventional (I) and RAFT copolymerisations (II) of NVP and VAc.

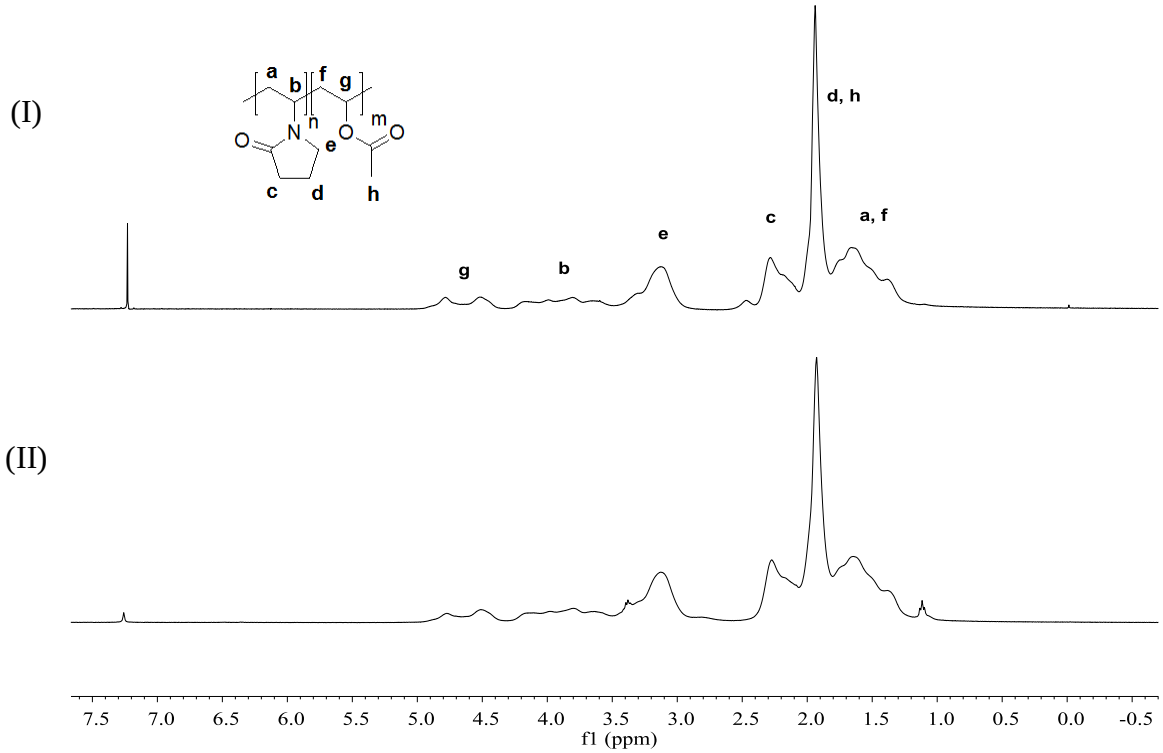

Figure 4.14. 400 MHz-^{1}H NMR of (I) PNVP-*ran*-PVAc without RAFT agent, (II) PNVP-*ran*-PVAc with RAFT agent in $CDCl_3$

It can be observed that peaks are present corresponding to the protons environments for both PNVP and PVAc. The composition of the copolymer can be determined by comparing the ratio of the integrals of the CH from PVAc backbone (Figure 4.14; **g**) and CH_2 adjacent to the nitrogen atom from PNVP (Figure 4.14; **e**). The ratio of PNVP to PVAc was 61:39 and 66:34 for the conventional and RAFT mediated copolymerisations, respectively. Within experimental error (≈20%) it is shown that the composition of NVP and VAc is the same for both copolymerisation processes. Furthermore, the yields of the conventional and RAFT mediated copolymerisation were 80%.

From the SEC traces (Figure 4.15), it can be seen that there is a significant difference in molecular weight and PDI of the two copolymerisation methods. The molecular weight distribution of the RAFT random copolymer (Figure 4.15-II) is monomodal with narrow PDI of 1.21 and M_n of 2.60 x 10^4 gmol^{-1}. In contrast, the conventional radical copolymerisation of NVP and VAc gave higher molecular weight copolymer (M_n = 6.80 x 10^4 gmol^{-1}) with a broad PDI (PDI = 2.72) and a low molecular weight shoulder. Figure 4.16, a plot of Log M against Wf / dLog M further confirms the outcome of the SEC trace. The distribution for the random copolymer synthesised

via conventional FRP shows a bimodal distribution. This may be due to termination reactions. PNVP-*ran*-PVAc synthesised *via* RAFT polymerisation shows a monomodal distribution.

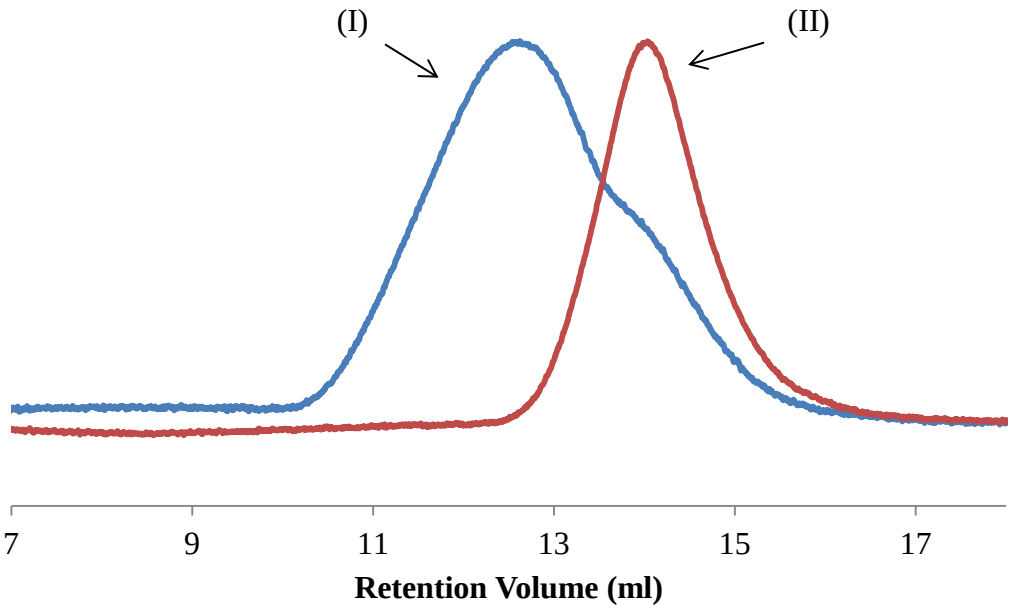

Figure 4.15. Comparison between SEC traces (refractive index) for (I) PNVP-*ran*-PVAc synthesised *via* conventional radical polymerisation and (II) PNVP-*ran*-PVAc synthesised *via* RAFT

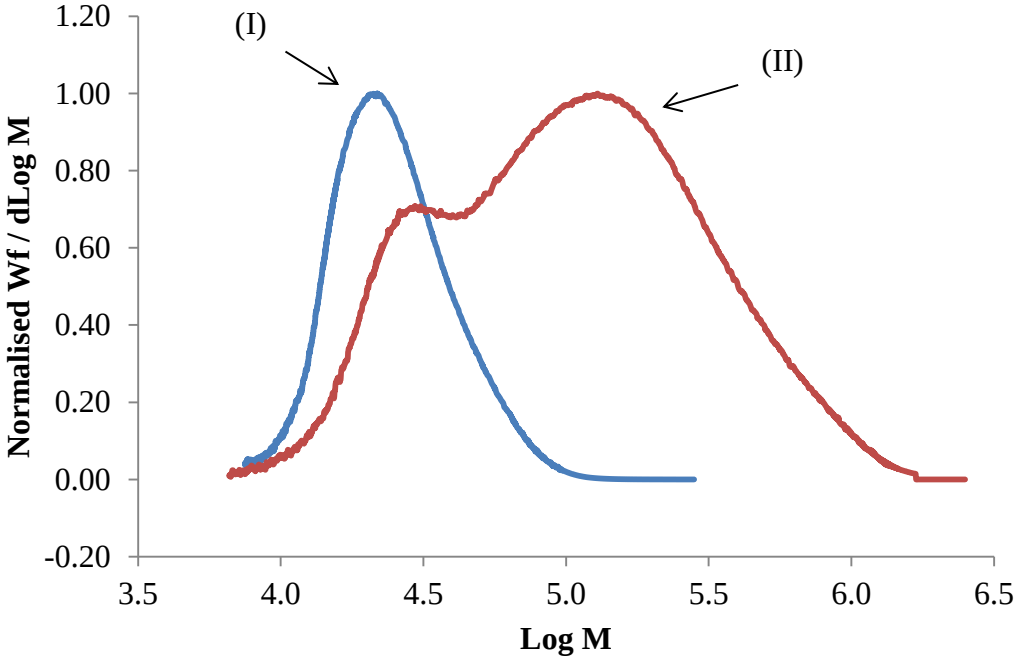

Figure 4.16. Pot of Log M against normalised Wf / dLog M showing molecular weight distribution of PNVP-*ran*-PVAc *via* (I) RAFT and (II) conventional FRP

The Mark Houwink α parameter values for PNVP-*ran*-PVAc *via* RAFT and conventional FRP were 0.59 and 0.54, respectively. This suggests that there is the possibility of branching present in the random copolymer synthesised *via* conventional FRP.

4.3.2.2. Poly(N-vinylpyrrolidone)-*ran*-poly(N-vinylcaprolactam)

The random copolymerisation of NVP and NVCL was conducted in 1, 4 dioxane using a monomer feed molar ratio of 50:50 in the presence of RAFT agent 5. The conventional random copolymerisation of NVP and VAc was also carried out in the absence of RAFT agent 5 for comparison. Figure 4.17 shows the ^{1}H NMR spectra of the copolymer products of the conventional (I) and RAFT copolymerisations (II) of NVP and NVCL.

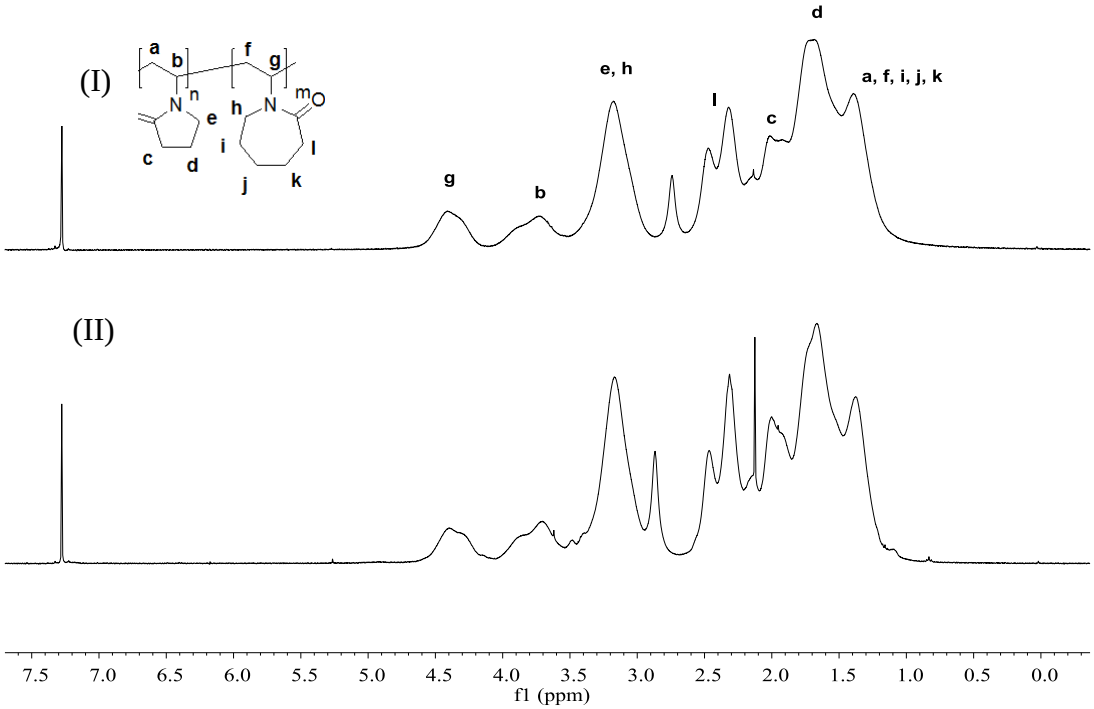

Figure 4.17. 400 MHz-^{1}H NMR of (I) PNVP-*ran*-PNVCL without RAFT agent, (II) PNVP-*ran*-PNVCL with RAFT agent in $CDCl_3$

Peaks representing the differing proton environments for both PNVP and PNVCL can be observed. The composition of the copolymer can be determined by comparing the ratios of the integrals of the CH (Figure 4.17; **b** and **g**) from each of the repeat units. The ratio of PNVP to PNVCL was 52:48 and 56:44 for the conventional

and RAFT mediated copolymerisation, respectively. The results indicate, that within the experimental error (≈20%), that the composition of NVP and VAc is the same for both copolymerisation processes. Furthermore, the yields of the conventional and RAFT mediated copolymerisations were 98% and 38%, respectively.

From the SEC traces (Figure 4.18), it can be seen that there is a significant difference in molecular weight and PDI of the two copolymerisation methods. The molecular weight distribution of the RAFT random copolymer (Figure 4.18-II) is monomodal with narrow PDI of 1.25 and M_n of 1.40 x 10^4 $gmol^{-1}$. In contrast, the conventional radical copolymerisation of NVP and NVCL gave a far higher molecular weight copolymer (M_n = 2.19 x 10^5 $gmol^{-1}$) with a broad PDI (PDI = 2.77) and tailing present on both the high and low molecular weight side. Figure 4.19, a plot of Log M against Wf / dLog M further confirms the outcome of the SEC trace. The distribution for the random copolymer synthesised *via* conventional FRP shows a bimodal distribution. This may be due to termination reactions. PNVP-*ran*-PNVCL synthesised *via* RAFT polymerisation shows a monomodal distribution.

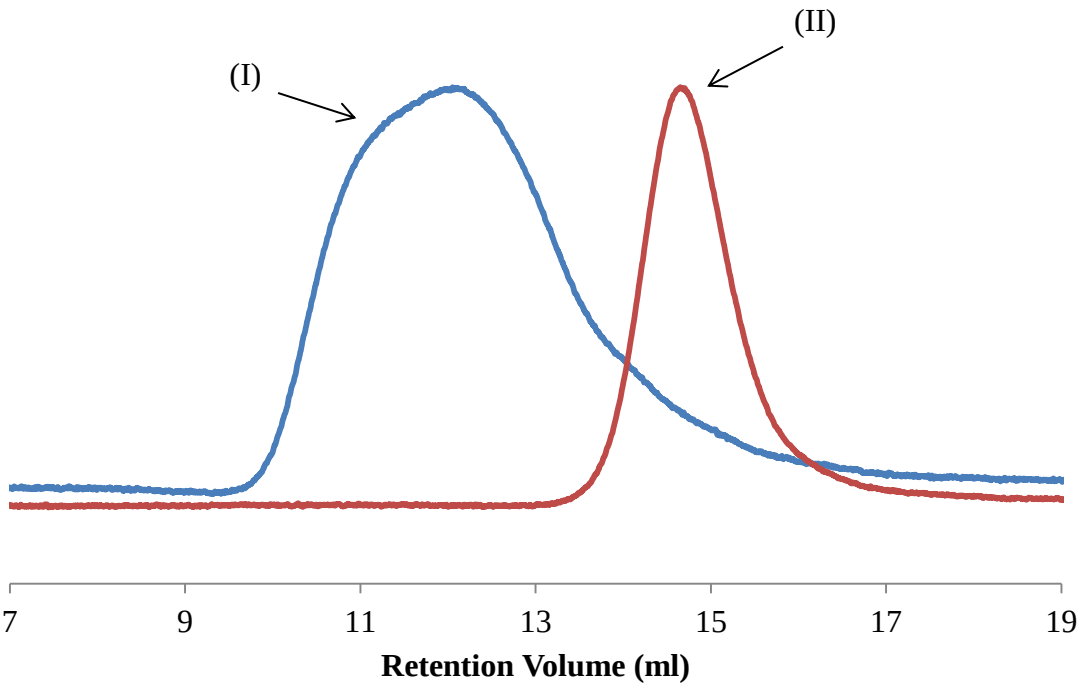

Figure 4.18. Comparison between SEC traces (refractive index) for (I) PNVP-*ran*-PNVCL synthesised *via* conventional radical polymerisation and (II) PNVP-*ran*-PNVCL synthesised *via* RAFT

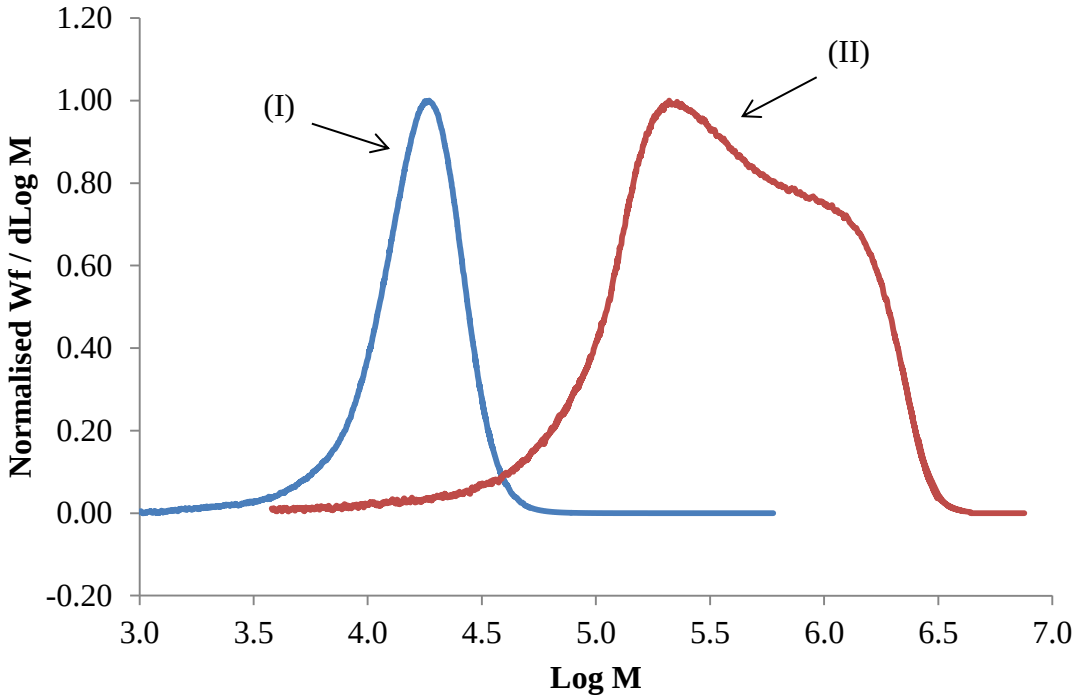

Figure 4.19. Pot of Log M against normalised Wf / dLog M showing molecular weight distribution of PNVP-*ran*-PNVCL *via* (I) RAFT and (II) conventional FRP

The Mark Houwink α parameter values for PNVP-*ran*-PNVCL *via* RAFT and conventional FRP were 0.61 and 0.55, respectively. This suggests that there is the possibility of branching present in the random copolymer synthesised *via* conventional FRP.

4.3.2.3. Poly(N-vinylcaprolactam)-*ran*-poly(vinyl acetate)

The random copolymerisation of NVCL and VAc was conducted in 1, 4 dioxane using a monomer feed molar ratio of 50:50 in the presence of RAFT agent 5. The conventional random copolymerisation of NVP and VAc was also carried out in the absence of RAFT agent 5 for comparison. Figure 4.20 shows the ^{1}H NMR spectra of the copolymer products of the conventional (I) and RAFT copolymerisations (II) of NVCL and VAc.

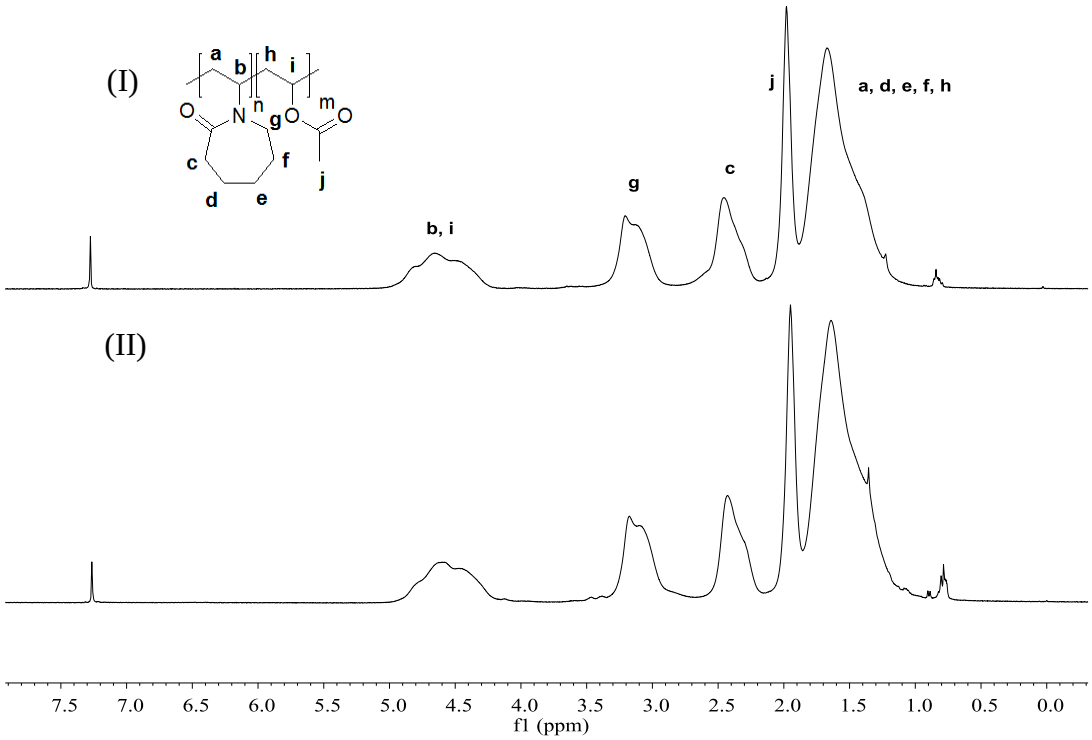

Figure 4.20. 400 MHz-^{1}H NMR of (I) PNVCL-*ran*-PVAc without RAFT agent, (II) PNVCL-*ran*-PVAc with RAFT agent in $CDCl_3$

Peaks present for the resonances due to both PNVCL and PVAc blocks can be observed. The composition of the copolymer can be determined by comparing the ratio of the integrals of the CH's from each of the repeated units (Figure 4.20; **b** and **i**) and the CH_2 on the lactam ring (Figure 4.20; **g**). The ratio of PNVCL to PVAc was 58:42 and 64:36 for the conventional and RAFT mediated copolymerisation, respectively. Within experimental error (≈20%) it is shown that the composition of NVCL and VAc is the same for both copolymerisation processes. Furthermore, the yields of the conventional and RAFT mediated copolymerisations were 76% and 75%, respectively.

From the SEC traces (Figure 4.21), it can be seen that there is a significant difference in molecular weight and PDI of the two copolymerisation methods. The molecular weight distribution of the RAFT random copolymer (Figure 4.21-II) is monomodal with narrow PDI of 1.18 and M_n of 2.80 x 10^4 gmol^{-1}. In contrast, the conventional copolymerisation of NVCL and VAc gave higher molecular weight copolymer (M_n = 6.60 x 10^4 gmol^{-1}) with a broad PDI (PDI = 2.88) and a low molecular weight shoulder. Figure 4.22, a plot of Log M against Wf / dLog M further confirms the outcome of the SEC trace. The distribution for the random copolymer synthesised *via* conventional FRP shows a bimodal distribution. This may be due to termination

reactions. PNVCL-*ran*-PVAc synthesised *via* RAFT polymerisation shows a monomodal distribution.

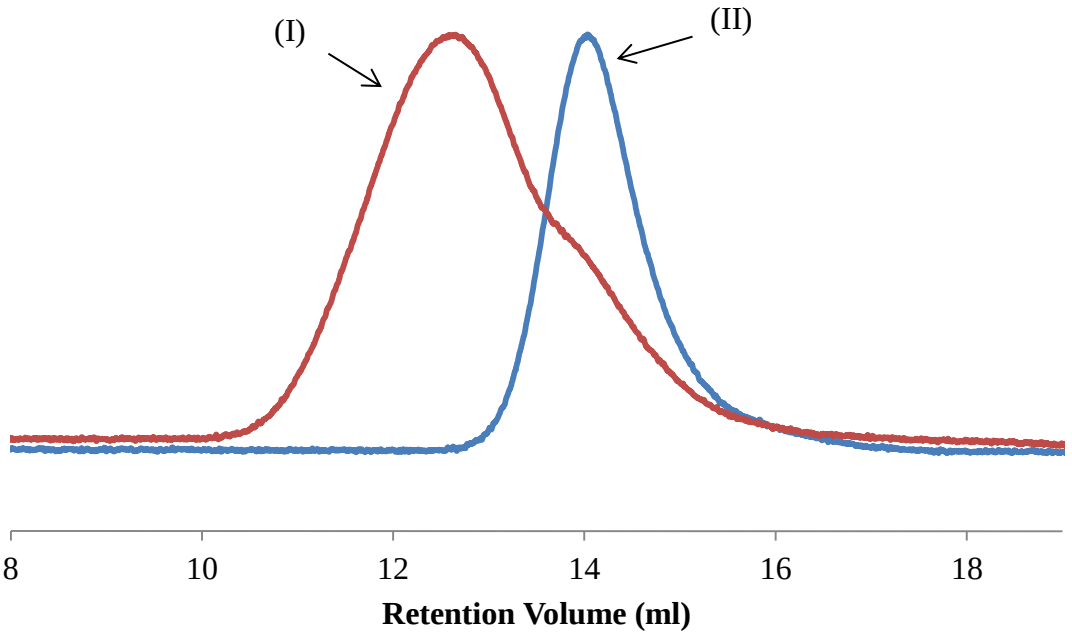

Figure 4.21. Comparison between SEC traces (refractive index) for (I) PNVCL-*ran*-PVAc synthesised *via* conventional radical polymerisation and (II) PNVCL-*ran*-PVAc synthesised *via* RAFT

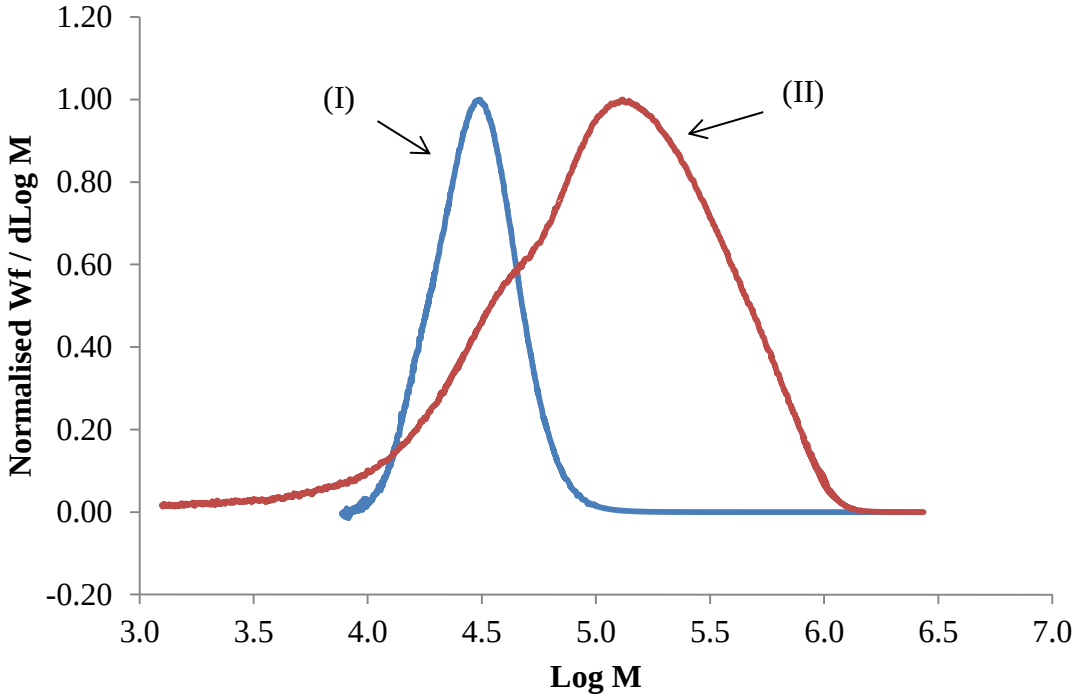

Figure 4.22. Pot of Log M against normalised Wf / dLog M showing molecular weight distribution of PNVCL-*ran*-PVAc *via* (I) RAFT and (II) conventional FRP

The Mark Houwink α parameter values for PNVCL-*ran*-PVAc *via* RAFT and conventional FRP were 0.62 and 0.56, respectively. This suggests that there is the possibility of branching present in the random copolymer synthesised *via* conventional FRP.

4.4. Summary

4.4.1. Block copolymerisations

PNVP-*block*-PVAc, PNVP-*block*-PNVCL, PVAc-*block*-PNVP and PVAc-*block*-PNVCL were synthesised using macroCTA's 12-17. However, the resulting products exhibited bimodal molecular weight distributions. This result was attributed to a number of possibilities. The first, the presence of a small amount of homopolymer of the second monomer, which is inherent in RAFT block polymerisations. The second, the cleavage of xanthate or dithiocarbamate groups from the macroCTA due to longer reaction times or temperature and solvent effects, produced un-extended macroCTA. The third, the rate of propagation being faster than the rate of initiation and insufficient amount of second monomer to achieve full consumption of macroCTA. This reason may well be ruled out as when a large excess of second monomer was added, the resulting product still exhibited bimodal molecular weight distribution.

4.4.2. Random copolymerisations

PNVP-*ran*-PVAc, PNVCL-*ran*-PVAc and PNVCL-*ran*-PVAc, were successfully synthesised in the presence of RAFT agent 5 with monomodal distributions and narrow PDI. In contrast, the SEC chromatograms of the random copolymers synthesised *via* conventional FRP exhibited much broader PDI's and far greater M_n. PNVP-*ran*-PVAc synthesised *via* RAFT was found to have an M_n of 2.60 x 10^4 $gmol^{-1}$ with a PDI of 1.21, compared to that synthesised *via* conventional FRP with an M_n of 6.80 x 10^4 $gmol^{-1}$ and a PDI of 2.72. Moreover, PNVP-*ran*-PNVCL synthesised *via* RAFT was found to have an M_n of 1.40 x 10^4 $gmol^{-1}$ with a PDI of 1.25, compared to that synthesised *via* conventional FRP with an M_n of 2.19 x 10^5 $gmol^{-1}$ and a PDI of 2.77. Furthermore, PNVCL-*ran*-PVAc synthesised *via* RAFT was found to have an M_n of 2.80 x 10^4 $gmol^{-1}$ with a PDI of 1.18, compared to that synthesised *via* conventional FRP with an M_n of 6.60 x 10^4 $gmol^{-1}$ and a PDI of 2.88. The compositions of the conventional and RAFT mediated random copolymerisations were found to be the same, within the experimental error.

4.5. References

1. Hussain, H.; Tan, B.; Gudipati, C.; Liu, Y.; He, C.; Davis, T. *Journal of Polymer Science Part a-Polymer Chemistry* **2008,** 46, (16), 5604-5615.
2. Huang, C.; Nicolay, R.; Kwak, Y.; Chang, F.; Matyjaszewski, K. *Macromolecules* **2009,** 42, (21), 8198-8210.
3. Nicolay, R.; Kwak, Y.; Matyjaszewski, K. *Chemical Communications* **2008**, (42), 5336-5338.
4. Petruczok, C. D.; Barlow, R. F.; Shipp, D. A. *Journal of Polymer Science Part a-Polymer Chemistry* **2008,** 46, (21), 7200-7206.
5. Tong, Y. Y.; Dong, Y. Q.; Du, F. S.; Li, Z. C. *Macromolecules* **2008,** 41, (20), 7339-7346.
6. Pound, G.; Aguesse, F.; McLeary, J.; Lange, R.; Klumperman, B. *Macromolecules* **2007,** 40, (25), 8861-8871.
7. Tong, Y. Y.; Dong, Y. Q.; Du, F. S.; Li, Z. C. *Journal of Polymer Science Part a-Polymer Chemistry* **2009,** 47, (7), 1901-1910.
8. Quemener, D.; Davis, T. P.; Barner-Kowollik, C.; Stenzel, M. H. *Chemical Communications* **2006**, (48), 5051-5053.
9. Quemener, D.; Le Hellaye, M.; Bissett, C.; Davis, T. P.; Barner-Kowollik, C.; Stenzel, M. H. *Journal of Polymer Science Part a-Polymer Chemistry* **2008,** 46, (1), 155-173.
10. Glaied, O.; Delaite, C.; Riess, G. *Polymer Bulletin* **2012,** 68, (3), 607-621.
11. Ting, S. R. S.; Granville, A. M.; Quemener, D.; Davis, T. P.; Stenzel, M. H.; Barner-Kowollik, C. *Australian Journal of Chemistry* **2007,** 60, (6), 405-409.
12. Mishra, A.; Patel, V.; Vishwakarma, N.; Biswas, C.; Raula, M.; Misra, A.; Mandal, T.; Ray, B. *Macromolecules* **2011,** 44, (8), 2465-2473.
13. Devasia, R.; Bindu, R.; Borsali, R.; Mougin, N.; Gnanou, Y. *Macromolecular Symposia* **2005,** 229, 8-17.
14. Gnanou, Y.; Devasia, R.; Bindu, R.; Mougin, N. *Abstracts of Papers of the American Chemical Society* **2005,** 230, U4144-U4145.
15. Bilalis, P.; Pitsikalis, M.; Hadjichristidis, N. *Journal of Polymer Science Part a-Polymer Chemistry* **2006,** 44, (1), 659-665.
16. Nguyen, T.; Eagles, K.; Davis, T.; Barner-Kowollik, C.; Stenzel, M. *Journal of Polymer Science Part a-Polymer Chemistry* **2006,** 44, (15), 4372-4383.

17. Keddie, D. J.; Guerrero-Sanchez, C.; Moad, G.; Rizzardo, E.; Thang, S. H. *Macromolecules* **2011,** 44, (17), 6738-6745.

18. Patel, V. K.; Mishra, A. K.; Vishwakarma, N. K.; Biswas, C. S.; Ray, B. *Polymer Bulletin* **2010,** 65, (2), 97-110.

19. Fandrich, N.; Falkenhagen, J.; Weidner, S. M.; Pfeifer, D.; Staal, B.; Thuenemann, A. F.; Laschewsky, A. *Macromolecular Chemistry and Physics* **2010,** 211, (8), 869-878.

20. Fandrich, N.; Falkenhagen, J.; Weidner, S. M.; Staal, B.; Thuenemann, A. F.; Laschewsky, A. *Macromolecular Chemistry and Physics* **2010,** 211, (15), 1678-1688.

21. Huang, C.; Yoon, J.; Matyjaszewski, K. *Canadian Journal of Chemistry-Revue Canadienne De Chimie* **2010,** 88, (3), 228-235.

22. Yan, Y.; Zhang, W.; Qiu, Y.; Zhang, Z.; Zhu, J.; Cheng, Z.; Zhang, W.; Zhu, X. *Journal of Polymer Science Part a-Polymer Chemistry* **2010,** 48, (22), 5206-5214.

23. Guinaudeau, A.; Mazieres, S.; Wilson, D. J.; Destarac, M. *Polymer Chemistry* **2012,** 3, (1), 81-84.

24. Batt-Coutrot, D.; Robin, J. J.; Bzducha, W.; Destarac, M. *Macromolecular Chemistry and Physics* **2005,** 206, (17), 1709-1717.

25. Lipscomb, C. E.; Mahanthappa, M. K. *Macromolecules* **2009,** 42, (13), 4571-4579.

26. Repollet-Pedrosa, M. H.; Weber, R. L.; Schmitt, A. L.; Mahanthappa, M. K. *Macromolecules* **2010,** 43, (19), 7900-7902.

27. Benaglia, M.; Chiefari, J.; Chong, Y.; Moad, G.; Rizzardo, E.; Thang, S. *Journal of the American Chemical Society* **2009,** 131, (20), 6914-6915.

28. Ieong, N. S.; Redhead, M.; Bosquillon, C.; Alexander, C.; Kelland, M.; O'Reilly, R. K. *Macromolecules* **2011,** 44, (4), 886-893.

29. Patel, V. K.; Vishwakarma, N. K.; Mishra, A. K.; Biswas, C. S.; Ray, B. *Journal of Applied Polymer Science* **2012,** 125, (4), 2946-2955.

30. Devasia, R.; Borsali, R.; Lecommandoux, S.; Bindu, R.; Mougin, N.; Gnanou, Y. *Abstracts of Papers of the American Chemical Society* **2005,** 230, U4231-U4232.

31. Wan, D. C.; Zhou, Q.; Pu, H. T.; Yang, G. J. *Journal of Polymer Science Part a-Polymer Chemistry* **2008,** 46, (11), 3756-3765.

32. Moad, G.; Mayadunne, R. T. A.; Rizzardo, E.; Skidmore, M.; Thang, S. H. *Macromolecular Symposia* **2003,** 192, 1-12.

33. Moad, G.; Rizzardo, E.; Thang, S. *Australian Journal of Chemistry* **2005,** 58, (6), 379-410.

34. Moad, G.; Dean, K.; Edmond, L.; Kukaleva, N.; Li, G. X.; Mayadunne, R. T. A.; Pfaendner, R.; Schneider, A.; Simon, G.; Wermter, H. *Macromolecular Symposia* **2006,** 233, 170-179.

35. Zhu, J.; Zhu, X.; Cheng, Z.; Zhang, Z. *Macromolecular Symposia* **2008,** 261, 46-53.

36. Lee, H.; Terry, E.; Zong, M.; Arrowsmith, N.; Perrier, S.; Thurecht, K.; Howdle, S. *Journal of the American Chemical Society* **2008,** 130, (37), 12242-12243.

37. Park, E.; Richez, A.; Birkin, N.; Lee, H.; Arrowsmith, N.; Thurecht, K.; Howdle, S. *Polymer* **2011,** 52, (24), 5403-5409.

38. Birkin, N. A.; Arrowsmith, N. J.; Park, E. J.; Richez, A. P.; Howdle, S. M. *Polymer Chemistry* **2011,** 2, (6), 1293-1299.

39. *Handbook of RAFT Polymerization*. Wiley-VCH: 2008.

40. Legge, T. M.; Slark, A. T.; Perrier, S. *Journal of Polymer Science Part a-Polymer Chemistry* **2006,** 44, (24), 6980-6987.

41. Postma, A.; Davis, T.; Li, G.; Moad, G.; O'Shea, M. *Macromolecules* **2006,** 39, (16), 5307-5318.

42. Pound, G.; Eksteen, Z.; Pfukwa, R.; McKenzie, J. M.; Lange, R. F. M.; Klumperman, B. *Journal of Polymer Science Part a-Polymer Chemistry* **2008,** 46, (19), 6575-6593.

43. *Polymer Handbook*. Fourth ed.; John Wiley & Sons, INC.: 1999.

44. Clarke, J. T.; Howard, R. O.; Stockmayer, W. H. *Makromolekulare Chemie* **1961,** 44-6, 427-447.

45. Vandermeer, R.; Aarts, M.; German, A. L. *Journal of Polymer Science Part a-Polymer Chemistry* **1980,** 18, (4), 1347-1357.

46. Bevington, J. C.; Sheen, J. P.; Johnson, M. *European Polymer Journal* **1972,** 8, (2), 209-213.

47. Clark, D. E. *Chemical Health & Safety* **2001,** 8, (5), 12-22.

48. Vana, P.; Albertin, L.; Barner, L.; Davis, T. P.; Barner-Kowollik, C. *Journal of Polymer Science Part a-Polymer Chemistry* **2002,** 40, (22), 4032-4037.

49. Relogio, P.; Charreyre, M. T.; Farinha, J. P. S.; Martinho, J. M. G.; Pichot, C. *Polymer* **2004,** 45, (26), 8639-8649.

50. Hao, X. J.; Stenzel, M. H.; Barner-Kowollik, C.; Davis, T. P.; Evans, E. *Polymer* **2004,** 45, (22), 7401-7415.

Chapter 5
Synthesis and characterisation of star-like polymeric materials

5.1. Introduction

This chapter focuses on the synthesis of homopolymers, as well as block and random copolymers incorporating "less activated" monomers (LAMs) with multi-arm architectures. Star polymers can be defined as having linear chains (arms) connected to a central point (core).[1] Anionic polymerisation has historically been the main route to produce polymeric star structures.[2, 3] However, with the emergence of controlled radical polymerisation methods it is now possible to synthesise star polymers with a wider range of monomers.[4-6] Star polymers are of interest due to their compact structure compared to linear polymers, which gives the unique solution property of having lower viscosity.

Star polymers can be classified into two categories; (1) regular arm star and (2) mikto-arm star polymers.[7] Regular arm star polymers consist of a symmetrical structure and composition. In contrast, mikto-arm star polymers have chemically different arms. Star polymers can be prepared by either starting with (i) an arm-first technique or (ii) core-first technique. An arm-first technique involves the synthesis of separate linear polymer chains and then attaching them together *via* a crosslinking agent or multifunctional molecule. A core-first technique involves a central core either being an initiator or CTA in which polymer chains can be polymerised from. The number of arms is governed by the active sites on the central core.

There are two routes in which star polymers can be synthesised using core-first methodology; R group and Z group approach. An R group approach requires that the core of the RAFT agent is attached to the arms through the R group. Therefore, when fragmentation takes place, the radical is located on the central core and polymer is formed from the core outwards (Scheme 5.1).

Initation

Initiator → I•

I• + monomer → Pn•

RAFT process

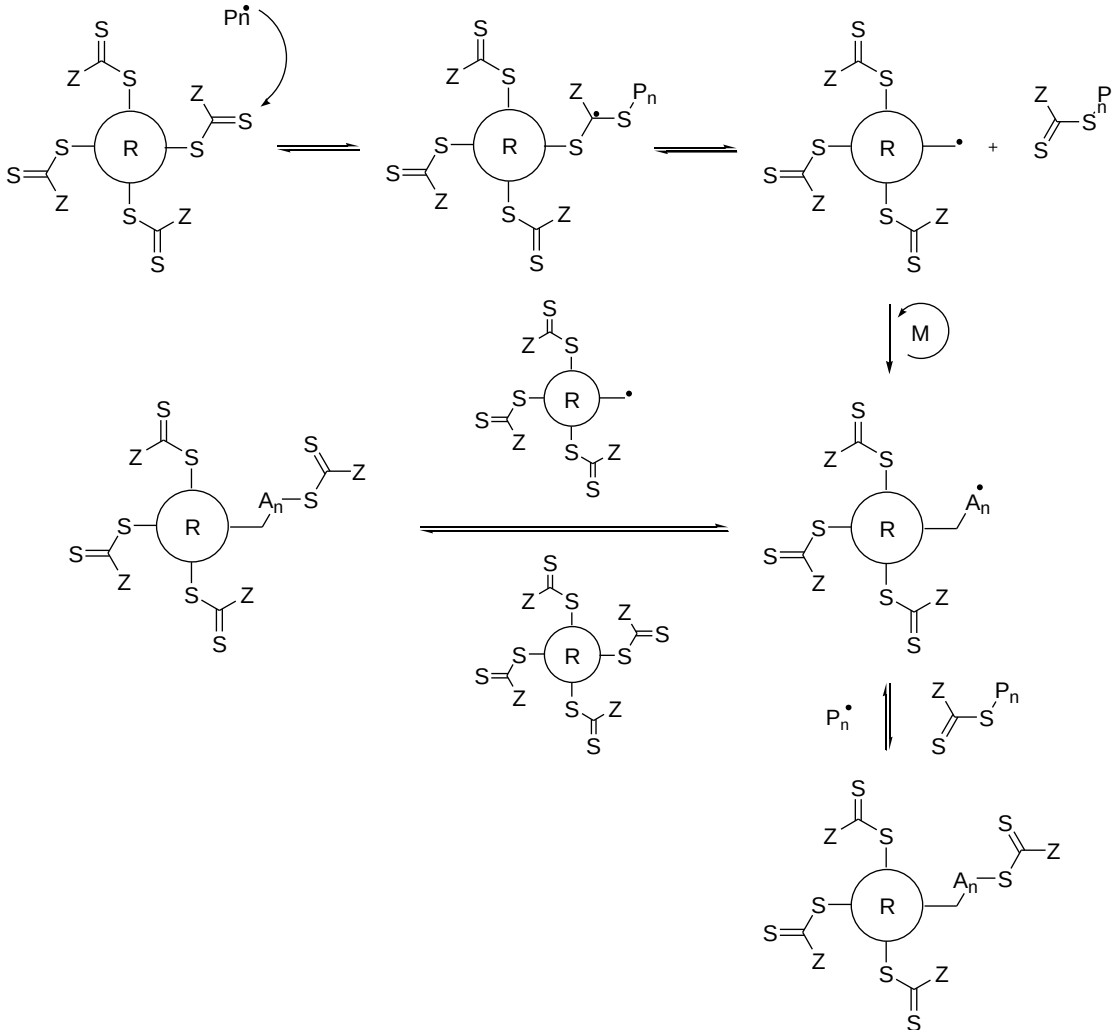

Scheme 5.1. Synthesis of star polymers *via* a R group approach[8]

Termination can occur through the coupling of stars and linear species and also disproportionation (Scheme 5.2). The termination step can result in the coupling of two stars (Scheme 5.2-I), coupling of a star with a linear chain (Scheme 5.2-II) or the coupling of two linear chains (Scheme 5.2-III).

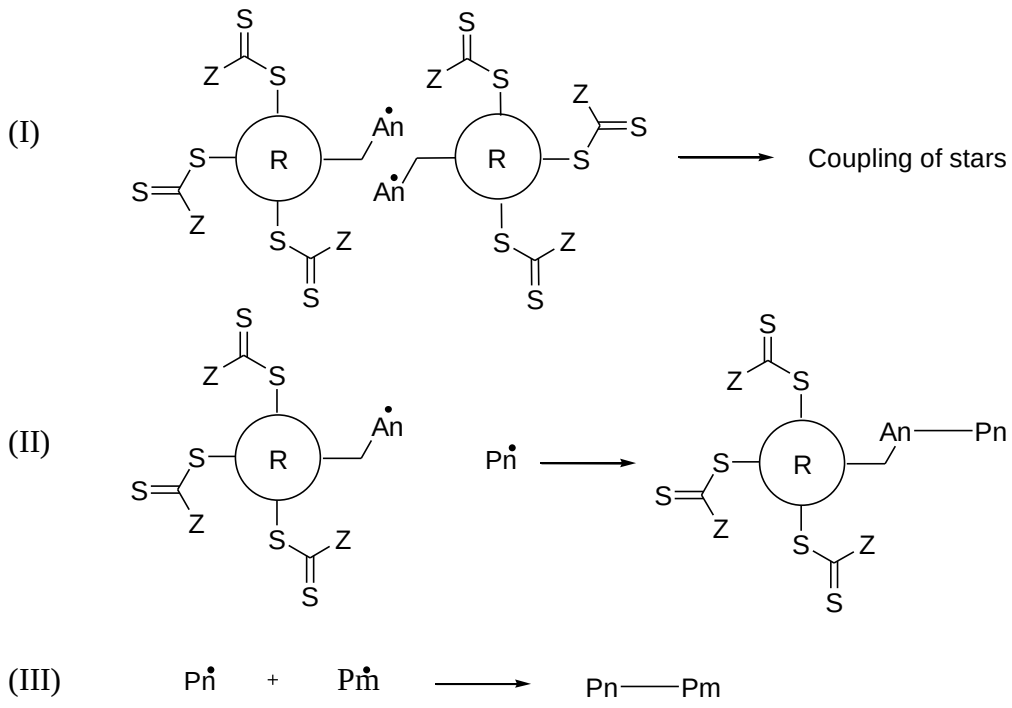

Scheme 5.2. Termination reactions

A Z group approach is the direct opposite of the R group approach, where the central core is attached to the RAFT agent through the Z group. Therefore, when fragmentation occurs, the generated radical which is not on the core, propagates linear chains (P•). The linear chains then react with the core and become dormant (Scheme 5.3). This method prevents the possibility of coupled star structures *via* termination.

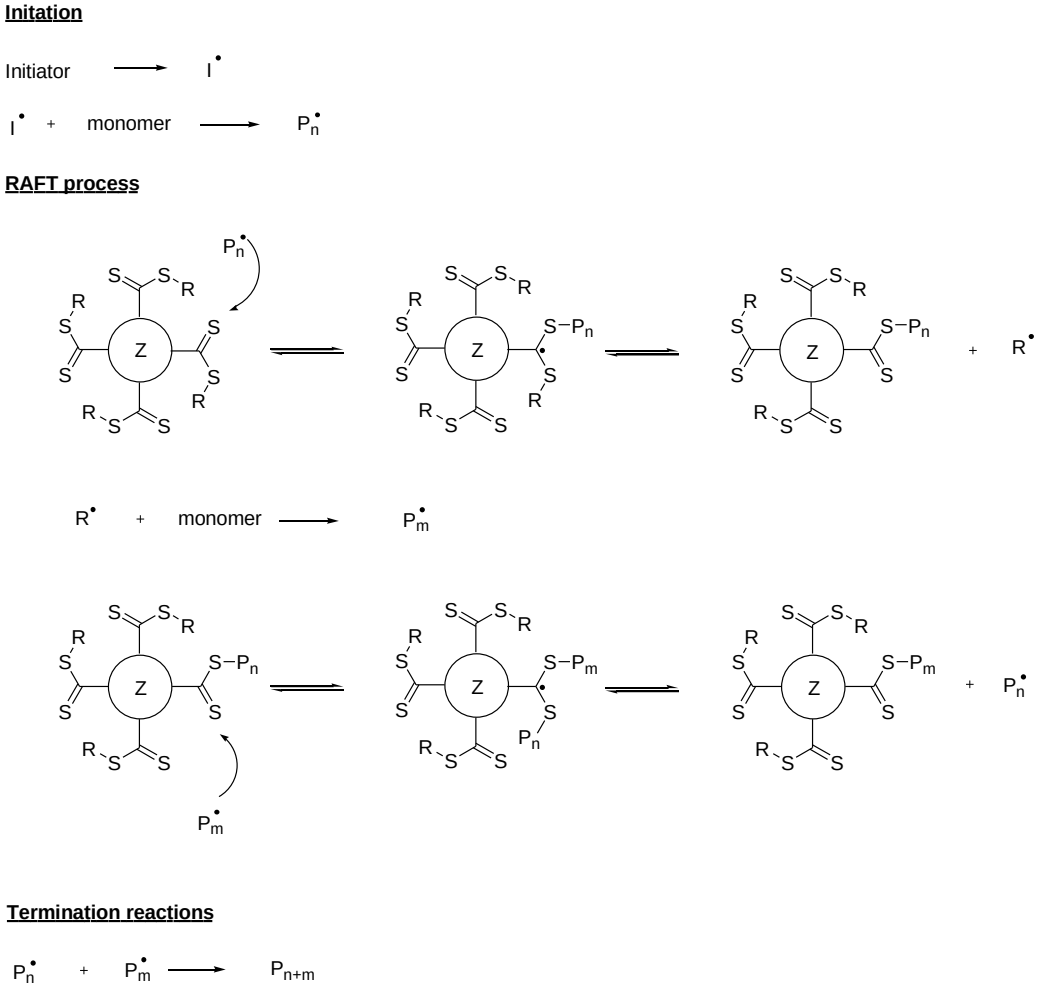

Scheme 5.3. Synthesis of star polymers *via* a Z group approach[8]

Star homopolymers of poly(N-vinylpyrrolidone) (PNVP) have been prepared previously in the literature. Nguyen *et al.*[9] have synthesised PNVP four-arm star polymers using a core first, R group approach. The R group at the core was a benzyl radical. They reported conversion of monomer to polymer increasing linearly with molecular weight upto 70% with PDI's remaining low (PDI = 1.15 – 1.25) throughout. There was no evidence of any multi modal distributions by SEC, which was attributed to low radical concentrations and fast propagation of the monomer. However, at higher conversions, broader PDI's were observed (PDI = 1.35) which were due to side reactions, i.e. star couplings.

The synthesis of poly(vinyl acetate) (PVAc) three and four armed star polymers using an R group approach have been reported in the literature.[10] A xanthate end group was attached to either pentaerythritol or 1, 1, 1-tris(hydroxymethyl)propane, to form a four or three armed star RAFT agent, respectively. Using SEC analysis, molecular weight was observed to deviate from the calculated M_n even at low conversion, which

was attributed to the different hydrodynamic volume of the star polymers compared to that of linear PVAc. PDI remained relatively low throughout the polymerisation (PDI = 1.2 – 1.5), however became broader at higher conversions due to termination reactions. Hydrolysis of the stars led to poly(vinyl alcohol) (PVA) stars, with no evidence of the destruction of the star structure. The same group also increased the scope of their research and compared the polymerisation of VAc in the presence of star RAFT agents, based on R and Z group approaches.[11] When an R group approach was utilised, the polymerisation of VAc proceeded with pseudo first order kinetics and PDI remained low even at high conversion (PDI = 1.1 – 1.4). The SEC traces were monomodal which indicated that star-star coupling or linear chains were not present. Moreover, when a Z group approach was adopted, monomodal molecular weight distributions were observed. However, the PDI broadened significantly (PDI = 1.2 – 2.0) with increasing conversion, which was attributed to steric shielding due to the increasing length of separated polymer chains. Unlike the R group approach, the Z group approach led to the destruction of the star structure, when PVAc was hydrolysed to give PVA.

Boschmann *et al*.[12] have synthesised four arm PVAc star polymers *via* a Z group approach based on a xanthate star RAFT agent at low conversions and found a linear relationship between conversion (of monomer to polymer) and M_n. However, as conversion of monomer to polymer increased, the relationship was less linear. This effect was greatest at low concentrations of RAFT agent. This was explained by the longer polymer chains (arms) shielding any incoming propagating radicals from reacting with the core. This behaviour has also been reported by Fleet *et al*.[13]

In this study, we synthesised polymeric three and four armed star structures comprising “less activated” monomers (LAMs) by using multifunctional RAFT agents. The RAFT agents used were synthesised with a core first R group approach in mind. Therefore, the polymer will grow from the core outwards. This is in contrast to Boschmann *et al*.[12] and Fleet *et al*.[13] as they used a Z group approach, resulting in poorly controlled RAFT polymerisations. As described earlier there has only been one example of PNVP with a star structure using a core first R group approach.[9] The R group was a benzyl radical and four arms were grown from the core. We have chosen to use a methyl propionate R group in all of our RAFT agents, so that the fragmentation and re-initiation steps are efficient for NVP, NVCL and VAc. It was believed that this route would give benefit for the random and block copolymerisation reactions.

NVP was polymerised in the presence of RAFT agents 9-11 (Chapter 2), in order to synthesise star polymers with low PDI’s. To the best of our knowledge there

have been no report of PNVP with 3-arms. A 4 arm star of PNVP (Star 3) was used as a macroCTA to mediate the polymerisation of VAc and NVCL to prepare star PNVP-*block*-PVAc and PNVP-*block*–PNVCL 4 arm star copolymers, respectively. Moreover, VAc was polymerised in the presence of RAFT agent 11 to synthesise a four armed PVAc star homopolymer. This was then used as a macroCTA to mediate the polymerisation of NVP and NVCL to synthesise PVAc–*block*–PNVP and PVAc–*block*–PNVCL star copolymers, respectively. To the best of our knowledge there are no reports of the synthesis of star-block copolymers incorporating NVP, NVCL or VAc. RAFT agents 9 and 11 were also used to mediate the polymerisation of NVCL to give three and four armed homopolymers of PNVCL. There are no reports of PNVCL star polymers prepared by RAFT in the literature.

Furthermore, RAFT agents 9 and 11 were used to mediate the random copolymerisation of NVP, VAc and NVCL in various combinations to prepare three and four armed statistical copolymers of PNVP–*ran*–PVAc, PNVCL–*ran*-PVAc and PNVP–*ran*–PNVCL. To the best of our knowledge this has not be described before.

5.2. Experimental

5.2.1. Materials

N-vinylpyrrolidone (ISP) and vinyl acetate (Sigma Aldrich, ≥99%) were distilled under reduced pressure and stored under reduced pressure at -4°C. N-vinylcaprolactam (ISP) was recrystallised from either pentane or hexane then distilled under reduced pressure and stored under nitrogen at -4°C. 4,4'-Azobis(4-cyanovaleric acid) (ACVA) (Sigma Aldrich, ≥98%) used as supplied. 2, 2'-Azobis(isobutyonitrile) (AIBN) (Sigma Aldrich) was recrystallized from methanol. 1,4 dioxane was dried over calcium hydride and distilled under reduced pressure. All dry solvents were obtained from Durham Chemistry Department Solvent Purification System (SPS) - Purification grade (HPLC) solvent was pushed from its storage container under low argon pressure through two stainless steel columns containing activated alumina or copper catalyst depending on solvent used. Trace amounts of water were removed by the alumina, producing a dry solvent. In addition, deoxygenated solvent was achieved when it was suitable for a copper catalyst column to be used. Water content values - DCM < 25.1ppm, DMF < 735.1ppm, Toluene < 21.3ppm, THF < 35.7 ppm, Chloroform < 20.9ppm, Diethyl ether < 19.1ppm, Hexane < 7.6 ppm and Acetonitrile < 8.7ppm. All other solvents were analytical grade and used without any purification.

5.2.2. Characterisation techniques

Nuclear Magnetic Resonance (NMR) Spectroscopy – ^{1}H NMR and ^{13}C NMR was performed on a Bruker Avance-400MHz, Varian iNova-500 or VNMRS 700. ^{1}H NMR spectra were recorded at either 400, 500 or 700 MHz. Samples of RAFT / MADIX agents and polymers were analysed in deuterated chloroform ($CDCl_3$ - Sigma-Aldrich).

Size exclusion chromatography (SEC) analysis on poly(N-vinylpyrrolidone) and poly(N-vinylcaprolactam) was carried out using a Viscotek TDA 302 with triple detection (refractive index, viscosity and light scattering), using 2 x 300ml PLgel 5µm C columns and DMF (containing 0.1% w/v LiBr) as the eluent at a flow rate of 1ml/min (70°C). The system was calibrated using narrowly polydisperse polystyrene standards. A value of 0.099 mL/g was used for the dn/dc of poly(N-vinylpyrrolidone). SEC analysis on poly(vinyl acetate) was carried out on a Viscotek TDA 302 with triple detection (refractive index, viscosity and light scattering), using 2 x 300ml PLgel 5µm

C columns using THF as the eluent at a flow rate of 1ml/min (30°C). The system was calibrated with narrowly polydisperse polystyrene standards. A value of 0.058 mL/g was used for the dn/dc of poly(vinyl acetate).

5.2.3. Synthesis of Star 1

A stock solution from a mixture of NVP (10.0 g, 90.0 mmol), RAFT agent 9 (0.199 g, 0.301 mmol) and ACVA (17.0 mg, 6.07 x 10^{-2} mmol) was prepared. Aliquots were transferred to five ampoules containing a magnetic stirrer bar in a nitrogen filled glove-box. The ampoules were sealed and removed from the glove-box and placed into an oil bath at 70°C. Ampoules were removed from the oil bath after 2, 4, 5, 7 and 24 h. Samples were taken for SEC and ^{1}H NMR spectroscopy analysis.

5.2.4. Synthesis of Star 2

A stock solution from a mixture of NVP (10.0 g, 90.0 mmol), RAFT agent 10 (0.189 g, 0.225 mmol) and ACVA (13.0 mg, 4.64 x 10^{-2} mmol) was prepared. Aliquots were transferred to five ampoules containing a magnetic stirrer bar in a nitrogen filled glove-box. The ampoules were sealed and removed from the glove-box and placed into an oil bath at 70°C. Ampoules were removed from the oil bath after 2, 4, 5, 7 and 24 h. Samples were taken for SEC and ^{1}H NMR spectroscopy analysis.

5.2.5. Synthesis of Star 3

To a 50 ml glass ampoule containing a magnetic stirrer bar, was added NVP (5.00 g, 45.0 mmol), RAFT agent 11 (0.102 g, 0.107 mmol) and ACVA (6.30 mg, 2.25 x 10^{-2} mmol). The polymerisation mixture was degassed thoroughly by four freeze pump thaw cycles and the ampoule was sealed under reduced pressure. The ampoule was placed in an oil bath at 70°C and heated for 19 h. The product of the reaction was a lime coloured viscous gel. Conversion of monomer to polymer was measured by determining the residual monomer by ^{1}H NMR spectroscopy and found to be 51%. Dichloromethane was added to dissolve the polymerisation product and the resulting solution was added dropwise to diethyl ether. White precipitate was formed, which was filtered off and dried under reduced pressure at 35°C. SEC: M_n = 2.52 x 10^4 gmol^{-1}, M_w = 2.96 x 10^4 gmol^{-1}, PDI = 1.17.

5.2.6. Synthesis of Star-block 1

To a 50 ml glass ampoule containing a magnetic stirrer bar, was added VAc (2.15 g, 25.0 mmol), PNVP macroCTA (0.500 g, 0.198 mmol, M_n = 2.52 x 10^4 $gmol^{-1}$, PDI = 1.17), ACVA (1.20 mg, 4.28 x 10^{-3} mmol) and 1,4 dioxane (3 ml). The polymerisation mixture was degassed thoroughly by four freeze pump thaw cycles. The ampoule was placed in an oil bath at 65°C and heated for 24 h. The ampoule was taken from the oil bath and allowed to cool to ambient temperature. Residual monomer was removed from the polymerisation mixture under reduced pressure to give a white crystalline solid (1.40 g, 42% yield). No further purification by re-precipitation was necessary.

5.2.7. Synthesis of Star-block 2

To a 50 ml glass ampoule containing a magnetic stirrer bar, was added NVCL (3.47 g, 24.9 mmol), PNVP macroCTA (0.500 g, 0.198 mmol, M_n = 2.52 x 10^4 $gmol^{-1}$, PDI = 1.17), ACVA (1.20 mg, 4.28 x 10^{-3} mmol) and 1,4 dioxane (7 ml). The polymerisation was degassed thoroughly by four freeze pump thaw cycles. The ampoule was placed in an oil bath at 70°C and heated for 24 h. The ampoule was then taken from the oil bath and allowed to cool to ambient temperature. Dichloromethane was added to dissolve the polymerisation product and the resulting solution was added dropwise to diethyl ether to give a white precipitate. This was filtered off and dried under reduced pressure at 30°C to give a white powder (1.46 g, 28% yield).

5.2.8. Synthesis of Star 4

To a 50 ml glass ampoule containing a magnetic stirrer bar, was added VAc (5.00 g, 58.1 mmol), RAFT agent 11 (0.139 g, 0.146 mmol) and ACVA (8.00 mg, 2.90 x 10^{-2} mmol). The polymerisation mixture was thoroughly degassed by four freeze pump thaw cycles and the ampoule was subsequently back filled with nitrogen gas. The ampoule was placed in an oil bath at 65°C and heated for 16 h. The product of the reaction was a viscous pale green gel. The ampoule was then taken from the oil bath and allowed to cool to ambient temperature. Residual monomer was removed by evaporation under reduced pressure to give an off white crystalline solid (3.07 g, 61% yield). SEC: M_n = 2.14 x 10^4 $gmol^{-1}$, M_w = 3.08 x 10^4 $gmol^{-1}$, PDI = 1.44.

5.2.9. Synthesis of Star-block 3

To a 50 ml glass ampoule containing a magnetic stirrer bar, was added NVP (5.56 g, 50.0 mmol), PVAc macroCTA (1.00 g, 4.67 x 10^{-2} mmol, M_n = 2.14 x 10^4 $gmol^{-1}$, PDI = 1.44), ACVA (7.00 mg, 2.50 x 10^{-2} mmol) and 1, 4 dioxane (5 ml). The polymerisation mixture was thoroughly degassed by four freeze pump thaw cycles. The ampoule was sealed under reduced pressure and placed in an oil bath set at 70°C and heated for 20 h. The ampoule was then removed from the oil bath and allowed to cool to ambient temperature. The product of the reaction was a viscous light yellow gel. Conversion of monomer to polymer was measured by determining the residual monomer by ^{1}H NMR spectroscopy and found to be 72%. Dichloromethane was added to dissolve the product and the resulting solution was added dropwise to diethyl ether to give a white precipitate. This was subsequently filtered off and dried under reduced pressure at 30°C to give a white powder (5.46 g, 80% gravimetric yield).

5.2.10. Synthesis of Star-block 4

To a 50 ml glass ampoule containing a magnetic stirrer bar, was added NVCL (6.96 g, 50.0 mmol), PVAc macroCTA (1.00 g, 4.67 x 10^{-2} mmol, M_n = 2.14 x 10^4 $gmol^{-1}$, PDI = 1.44), ACVA (7.00 mg, 2.50 x 10^{-2} mmol) and 1, 4 dioxane (8 ml). The polymerisation mixture was thoroughly degassed by four freeze pump thaw cycles. The ampoule was sealed under reduced pressure and placed in an oil bath set at 70°C and heated for 20 h. The ampoule was then removed from the oil bath and allowed to cool to ambient temperature. The product of the reaction was a viscous light yellow gel. Dichloromethane was added to dissolve the product and the resulting solution was added dropwise to hexane to give a white precipitate. This was subsequently filtered off and dried under reduced pressure at 40°C to give a white powder (3.85 g, 41% yield).

5.2.11. Synthesis of Star 5

To a 50 ml glass ampoule containing a magnetic stirrer bar, was added NVCL (5.00 g, 35.9 mmol), RAFT agent 9 (79.0 mg, 1.19 x 10^{-1} mmol), ACVA (7.00 mg, 2.50 x 10^{-2} mmol) and 1,4 dioxane (5 ml). The polymerisation mixture was thoroughly degassed by four freeze pump thaw cycles and sealed under vacuum. The ampoule was placed in an oil bath thermostated at 70°C and heated for 18 h. The ampoule was then removed

from the oil bath and allowed to cool to ambient temperature. The product of the reaction was a slightly viscous clear liquid. The polymerisation mixture was added dropwise to hexane to give a white precipitate. The polymer was purified by repeated precipitations by dissolving the polymer material in dichloromethane and the resulting solution added dropwise to hexane. The solid retrieved by filtration was dried under reduced pressure at 40°C to give a white powder (1.20 g, 24% yield).

5.2.12. Synthesis of Star 6

To a 50 ml glass ampoule containing a magnetic stirrer bar, was added NVCL (5.00 g, 35.9 mmol), RAFT agent 11 (86.0 mg, 9.01 x 10^{-2} mmol), ACVA (5.00 mg, 1.78 x 10^{-2} mmol) and 1,4 dioxane (5 ml). The polymerisation mixture was thoroughly degassed by four freeze pump thaw cycles and sealed under vacuum. The ampoule was placed in an oil bath thermostated at 70°C and heated for 18 h. The ampoule was then removed from the oil bath and allowed to cool to ambient temperature. The product of the reaction was a slightly viscous clear liquid. The polymerisation mixture was added dropwise to hexane to give a white precipitate. The polymer was purified by repeated precipitations by dissolving the polymer material in dichloromethane and the resulting solution added dropwise to hexane. The solid retrieved by filtration was dried under reduced pressure at 40°C to give a white powder (0.840 g, 17% yield).

5.2.13. Synthesis of Star-random 1

To a 50 ml glass ampoule containing a magnetic stirrer bar, was added NVP (2.58 g, 23.2 mmol), VAc (2.00 g, 23.2 mmol), RAFT agent 9 (50.0 mg, 7.55 x 10^{-2} mmol) and ACVA (4.00 mg, 1.43 x 10^{-2} mmol). The polymerisation mixture was thoroughly degassed by four freeze pump thaw cycles. The ampoule was placed in an oil bath at 70°C and heated for 16 h. The ampoule was removed from the oil bath and allowed to cool to ambient temperature. The product of the reaction was a light yellow / green viscous gel. Dichloromethane was added to dissolve the product and the resulting solution was added dropwise to diethyl ether to give a white precipitate. This solid was filtered off and dried under reduced pressure to give a white powder (1.78 g, 39% yield).

5.2.14. Synthesis of Star-random 2

To a 50 ml glass ampoule containing a magnetic stirrer bar, was added NVCL (3.23 g, 23.2 mmol), VAc (2.00 g, 23.2 mmol), RAFT agent 9 (51.0 mg, 7.70 x 10^{-2} mmol) and ACVA (4.00 mg, 1.43 x 10^{-2} mmol). The polymerisation mixture was thoroughly degassed by four freeze pump thaw cycles. The ampoule was placed in an oil bath at 70°C and heated for 16 h. The ampoule was removed from the oil bath and allowed to cool to ambient temperature. The product of the reaction was a light yellow / green viscous gel. Dichloromethane was added to dissolve the product and the resulting solution was added dropwise to hexane to give a white precipitate. This solid was filtered off and dried under reduced pressure to give a white powder (1.25 g, 24% yield).

5.2.15. Synthesis of Star-random 3

To a 50 ml glass ampoule containing a magnetic stirrer bar, was added NVP (2.58 g, 23.2 mmol), NVCL (3.23 g, 23.2 mmol), RAFT agent 9 (51.0 mg, 7.70 x 10^{-2} mmol) and ACVA (4.00 mg, 1.43 x 10^{-2} mmol). The polymerisation mixture was thoroughly degassed by four freeze pump thaw cycles. The ampoule was placed in an oil bath at 70°C and heated for 16 h. The ampoule was removed from the oil bath and allowed to cool to ambient temperature. The product of the reaction was a light yellow / green viscous gel. Dichloromethane was added to dissolve the product and the resulting solution was added dropwise to diethyl ether to give a white precipitate. This solid was filtered off and dried under reduced pressure to give a white powder. The polymer was purified by re-precipitation by dissolving the polymer material in dichloromethane and the resulting solution added dropwise to diethyl ether. The resulting precipitate was filtered off and dried under reduced pressure to give a white solid (1.30 g, 22% yield).

5.2.16. Synthesis of Star-random 4

To a 50 ml glass ampoule containing a magnetic stirrer bar, was added NVP (2.58 g, 23.2 mmol), VAc (2.00 g, 23.2 mmol), RAFT agent 11 (60.0 mg, 6.29 x 10^{-2} mmol) and ACVA (3.00 mg, 1.07 x 10^{-2} mmol). The polymerisation mixture was thoroughly degassed by four freeze pump thaw cycles. The ampoule was placed in an oil bath at 70°C and heated for 16 h. The ampoule was removed from the oil bath and allowed to

cool to ambient temperature. The product of the reaction was a light yellow / green viscous gel. Dichloromethane was added to dissolve the product and the resulting solution was added dropwise to diethyl ether to give a white precipitate. This solid was filtered off and dried under reduced pressure to give a white powder (2.17 g, 47% yield).

5.2.17. Synthesis of Star-random 5

To a 50 ml glass ampoule containing a magnetic stirrer bar, was added NVCL (3.23 g, 23.2 mmol), VAc (2.00 g, 23.2 mmol), RAFT agent 11 (70.0 mg, 7.34×10^{-2} mmol) and ACVA (3.00 mg, 1.07×10^{-2} mmol). The polymerisation mixture was thoroughly degassed by four freeze pump thaw cycles. The ampoule was placed in an oil bath at 70°C and heated for 16 h. The ampoule was removed from the oil bath and allowed to cool to ambient temperature. The product of the reaction was a light yellow / green viscous gel. Dichloromethane was added to dissolve the product and the resulting solution was added dropwise to hexane to give a white precipitate. This solid was filtered off and dried under reduced pressure to give a white powder (1.57 g, 30% yield).

5.2.18. Synthesis of Star-random 6

To a 50 ml glass ampoule containing a magnetic stirrer bar, was added NVP (2.58 g, 23.2 mmol), NVCL (3.23 g, 23.2 mmol), RAFT agent 11 (57.0 mg, 5.97×10^{-2} mmol) and ACVA (3.00 mg, 1.07×10^{-2} mmol). The polymerisation mixture was thoroughly degassed by four freeze pump thaw cycles. The ampoule was placed in an oil bath at 70°C and heated for 16 h. The ampoule was removed from the oil bath and allowed to cool to ambient temperature. The product of the reaction was a light yellow / green viscous gel. Dichloromethane was added to dissolve the product and the resulting solution was added dropwise to diethyl ether to give a white precipitate. This solid was filtered off and dried under reduced pressure to give a white powder. The polymer was purified by re-precipitation by dissolving the polymer material in dichloromethane and the resulting solution added dropwise to diethyl ether. The resulting precipitate was filtered off and dried under reduced pressure to give a white solid (1.45 g, 25% yield).

5.3. Results and discussion

5.3.1. Synthesis of Star 1-6

RAFT agents 9-11 (Chapter 2, Figure 2.3) were used to synthesise Star 1-6, containing either PNVP, PVAc or PNVCL, Figure 5.1. RAFT agent 9 and 10-11 allow the synthesis of three (Star 1 and 5) and four (Star 2-4, 6) armed polymeric star structures, respectively.

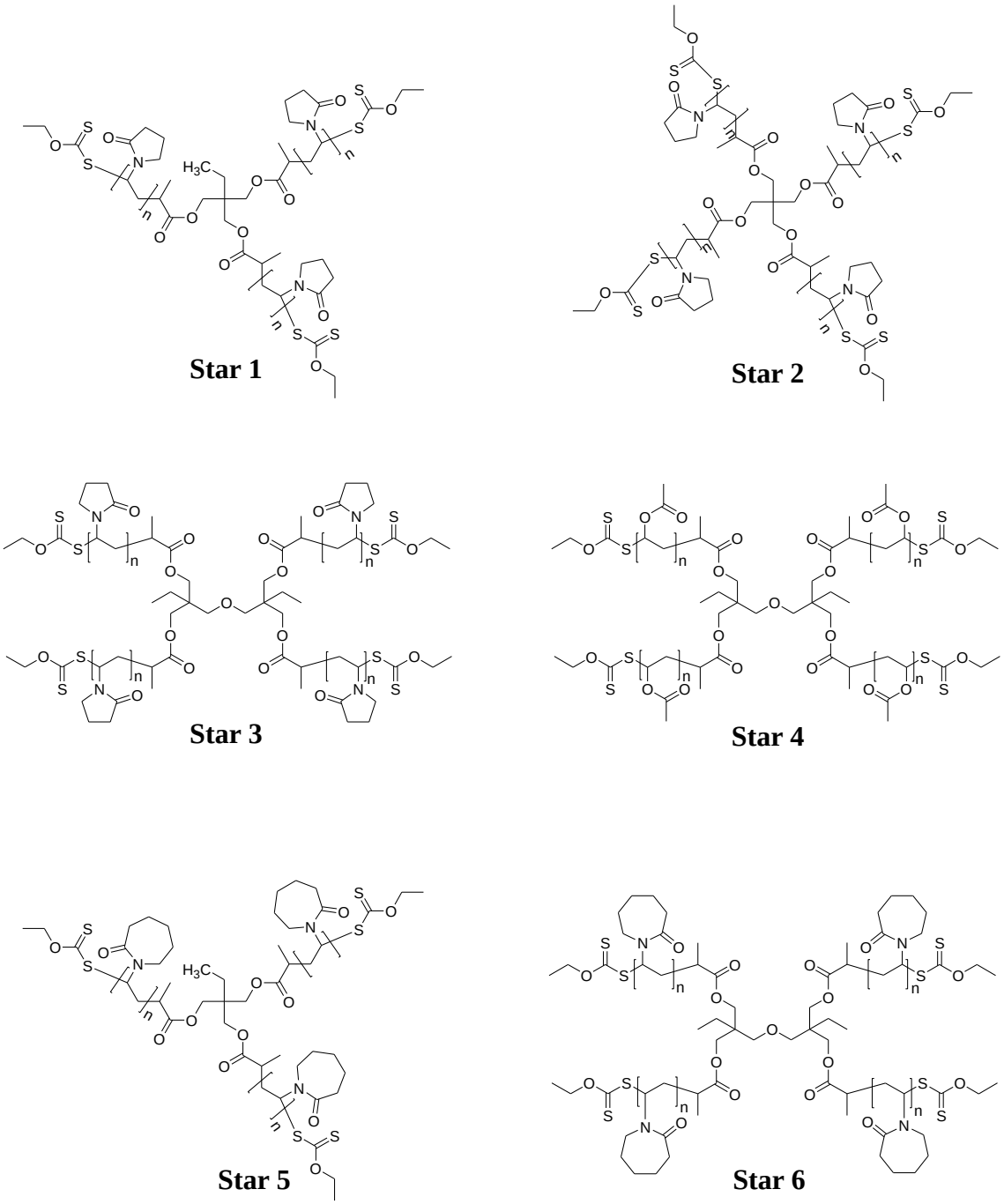

Figure 5.1. Structures of Star 1-6

5.3.1.1. Synthesis of Star 1

NVP was polymerised in bulk using ACVA as initiator, in the presence of RAFT agent 9, to synthesise Star 1 (Scheme 5.4). Star 1 comprised of 1,1,1-trimethoxypropane as a core and three PNVP arms. The chain ends are *O*-ethyl xanthate moieties.

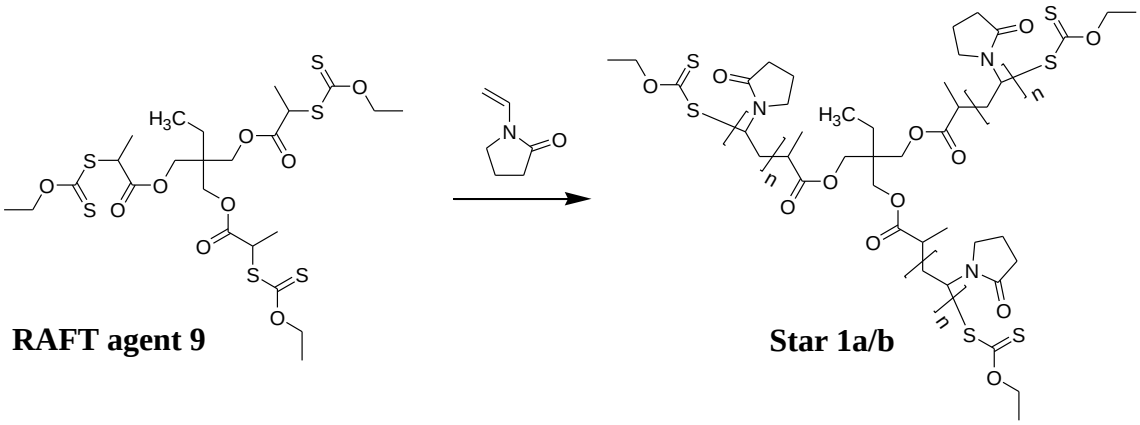

Scheme 5.4. Synthesis of Star 1

Samples of the polymerisation mixtures at 2, 4, 5, 7 and 24 h, were analysed by ^{1}H NMR spectroscopy and SEC. Figure 5.2 shows the plot of time against $\log[([M]_o/[M])]$. For upto 5 h the plot shows a linear relationship between time and conversion of monomer to polymer. After this point, due to the increased viscosity of the polymerisation medium, the correlation becomes less linear and conversion of monomer to polymer was curtailed at approximately 50%. There was no appearance of any apparent inhibition period.

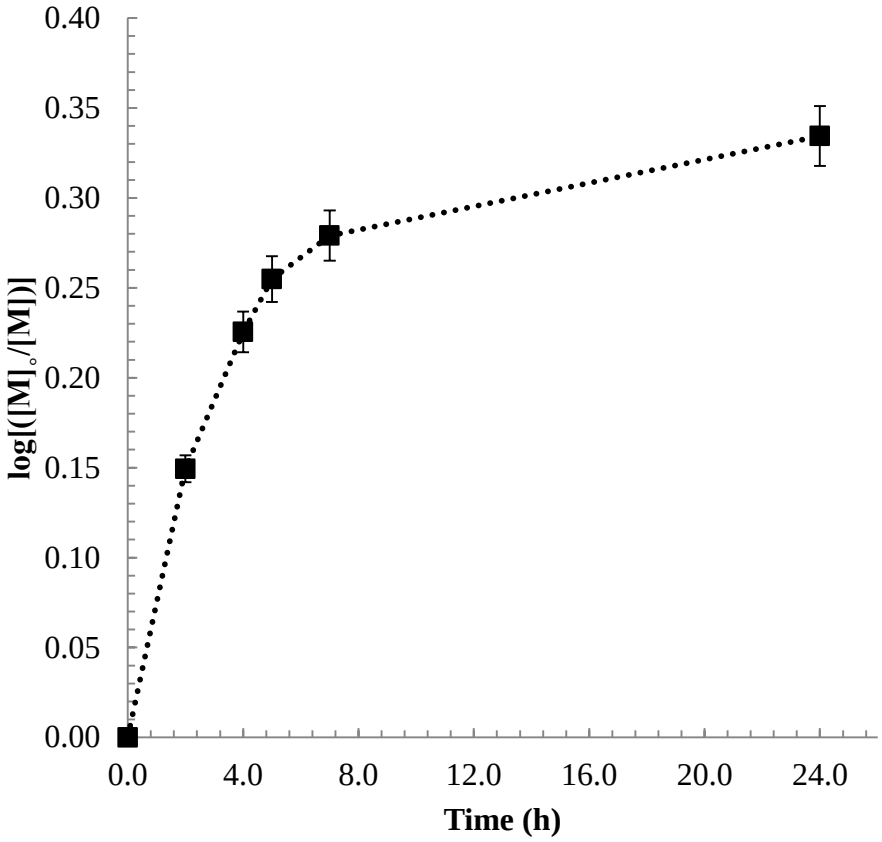

Figure 5.2. Plot of log of monomer concentration against time for polymerisation of NVP in bulk. Dashed line (---) is only a guide to the eye

Figure 5.3 shows a plot of M_n and PDI against % conversion of monomer to polymer. PDI remained low (1.06 – 1.22) throughout the polymerisation and molecular weight increased in a linear fashion with increasing conversion. The R^2 value is 0.9389. After 24 h the overall M_n was found to be 2.20 x 10^4 $gmol^{-1}$ by SEC, indicating a $\overline{DP}$ of 66 in each arm. This was in relatively good agreement with the theoretical M_n of 1.86 x 10^4 $gmol^{-1}$.

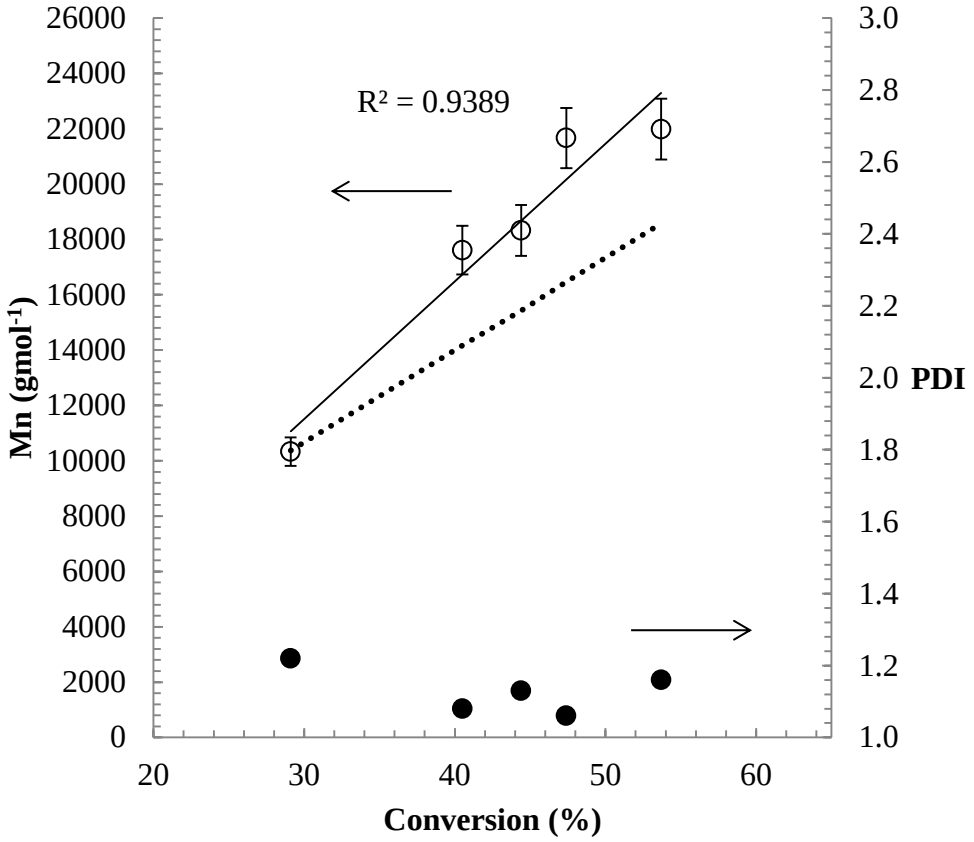

Figure 5.3. M_n against % conversion for polymerisation of NVP in bulk. Solid line is line of best fit. Dashed line (---) represents theoretical M_n

Figure 5.4 shows the ^{1}H NMR spectrum of Star 1 (after 24 h). Integration of the CH_3 protons (**1**) from the core, against CH protons from PNVP backbone (**2**), gives a ratio of approximately 1:60. This represents the degree of polymerisation ($\overline{DP}$) for each of the arms, indicating M_n of approximately 6.67 x 10^3 gmol^{-1}. The overall M_n of Star 1 (after 24 h) is found to be 2.00 x 10^4 gmol^{-1}, which is in good agreement with the M_n obtained by SEC and with the theoretical M_n. The integration of the CH_3 protons (**3**) of the *O*-ethyl xanthate moiety against the CH_3 protons (**1**) of the core reveals a ratio of 3.5:1, indicating the existence of three arms in Star 1 (after 24 h).

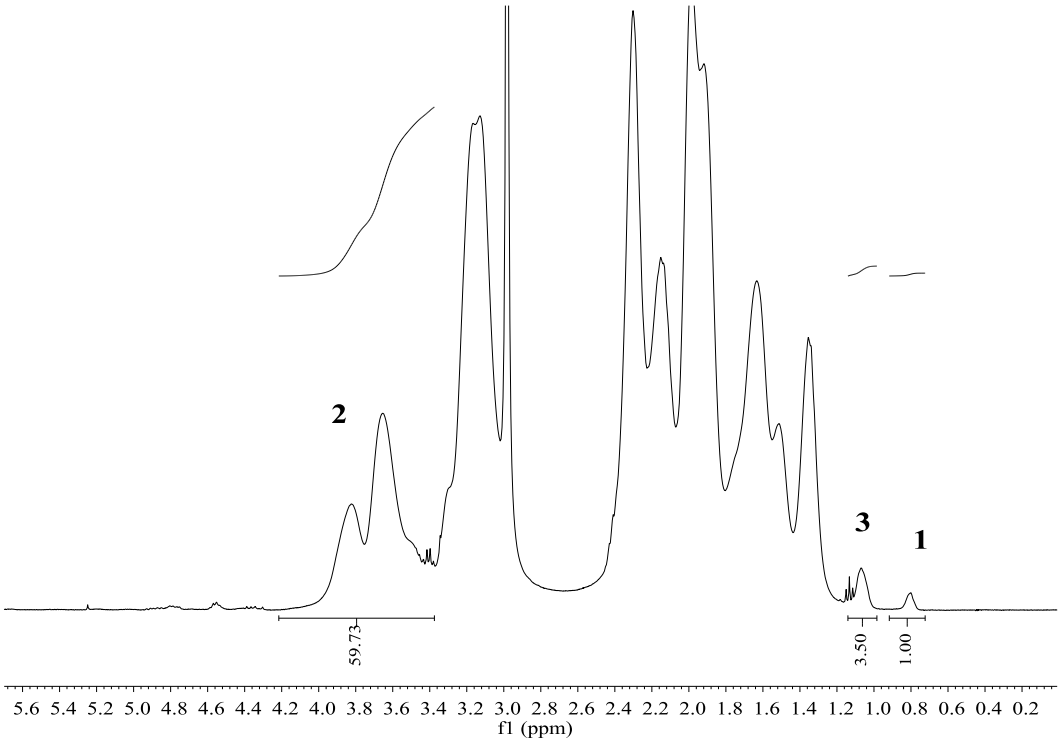

Figure 5.4. 400 MHz-^{1}H NMR spectrum of Star 1 (after 24 h)

Figure 5.5 shows the progression of SEC traces over the polymerisation reaction time. It is shown that there is a gradual increase in the molecular weight with increasing polymerisation time from 2 – 24 h (traces I – V). All SEC traces are observed as monomodal, however on the lower molecular weight side there is evidence of significant tailing. After 24 h the Mark Houwink α parameter was calculated to be 0.45. In comparison, a typical value for linear PNVP within this study was between 0.66 and 0.73. This therefore suggests that there is a degree of branching within the structure of Star 1.

Figure 5.6, a plot of Log M against Wf / dLog M shows the progression of molecular weight distribution for samples collected after 5h, 7h and 24 h. In all cases the distributions are observed to be monomodal, however there is evidence of tailing on the lower molecular weight side. This indicates the presence of termination reactions, leading to the possibility of star structures with differing arm lengths.

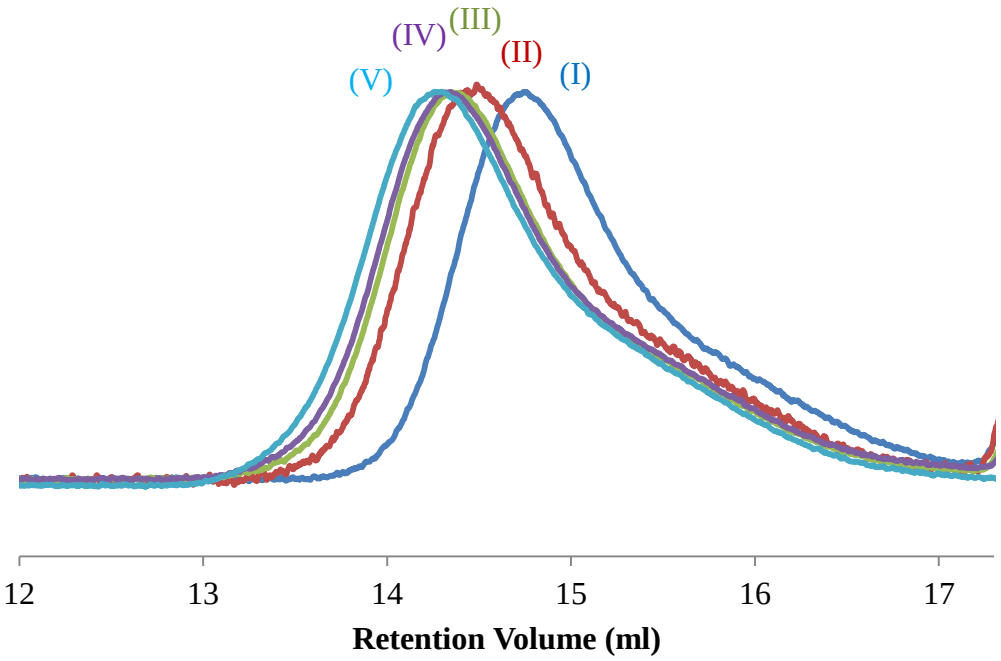

Figure 5.5. Progression of SEC traces (refractive index) after (I) 2 h, (II) 4 h, (III) 5 h, (IV) 7 h and (V) 24 h

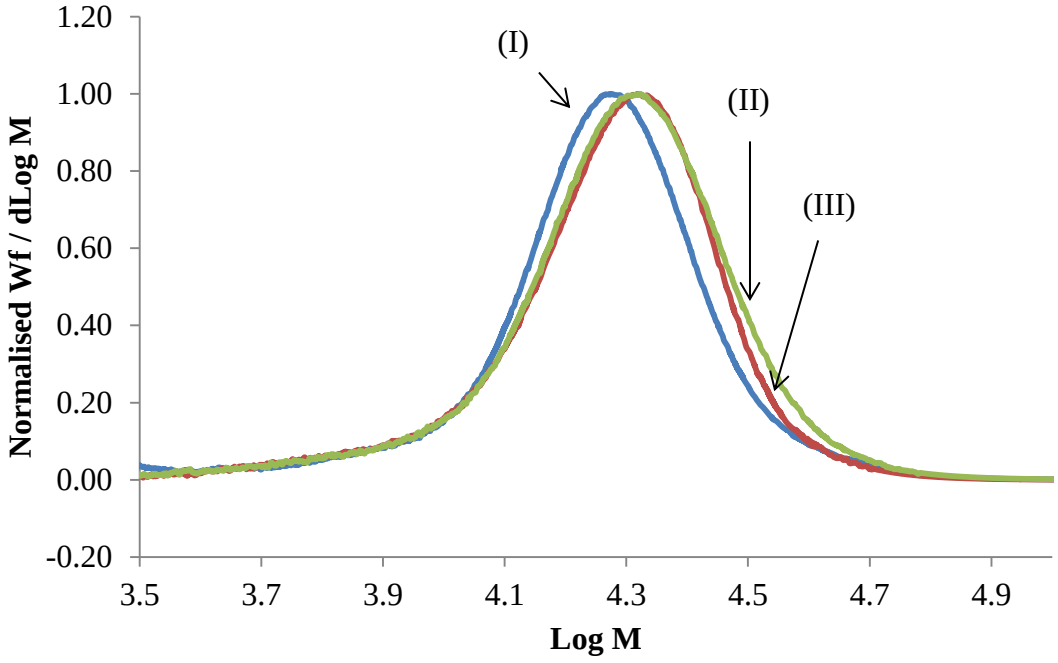

Figure 5.6. Plot of Log M against normalised Wf / dLog M showing the molecular weight distribution for the polymerisation of NVP in the presence of RAFT agent 9. (I) 5 h, (II) 7 h, (III) 24 h

5.3.1.2. Synthesis of Star 2

NVP was also polymerised in bulk using ACVA as initiator, in the presence of RAFT agent 10, to synthesise Star 2, Scheme 5.5. Star 2 comprised of a pentaerythritol core and four PNVP arms. The chain ends are *O*-ethyl xanthate moieties.

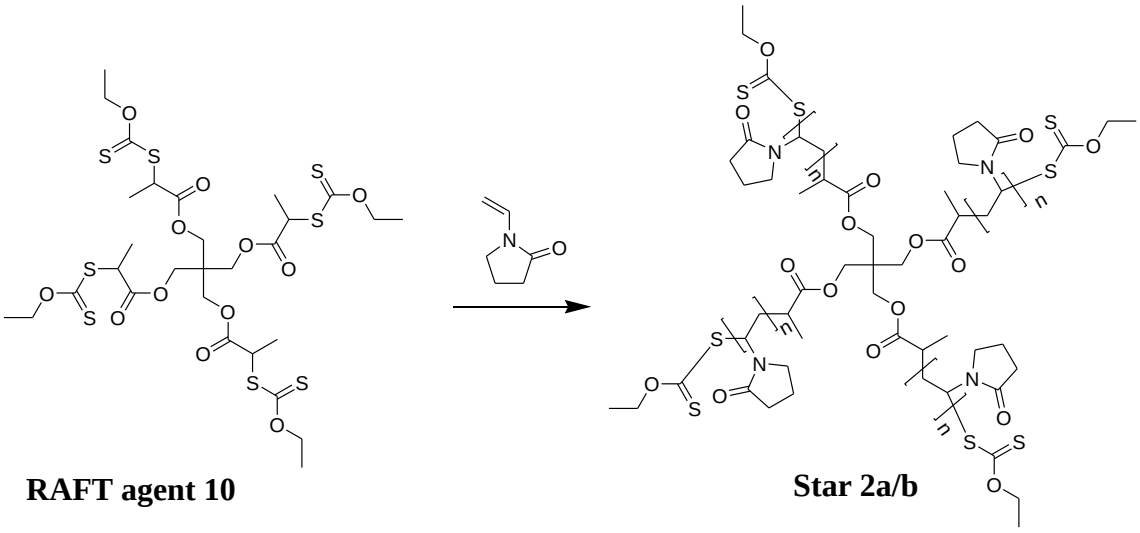

RAFT agent 10 **Star 2a/b**

Scheme 5.5. Synthesis of Star 2

Samples of the polymerisation mixtures after 2, 4, 5, 7 and 24 h were analysed by ^{1}H NMR spectroscopy and SEC. Figure 5.7 shows the plot of time against $\log[([M]_o/[M])]$. The plot shows a linear relationship between time and conversion of monomer to polymer, upto 5 h, as observed for Star 1. After this point however, due to the increased viscosity of the polymerisation medium the correlation became less linear and conversion was curtailed at approximately 40%. There was no appearance of any apparent inhibition period.

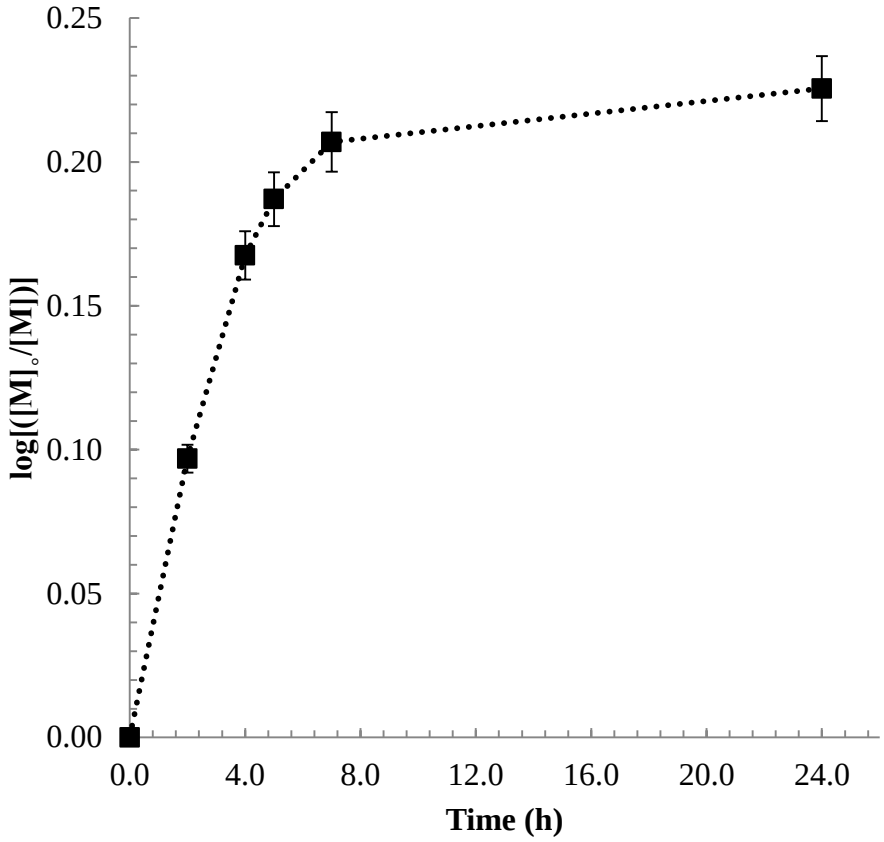

Figure 5.7. Plot of log of monomer concentration against time for polymerisation of NVP in bulk. Dashed line (---) is only a guide to the eye

Figure 5.8 shows the plot of M_n and PDI against % conversion of monomer to polymer. PDI remained low (1.04 – 1.19) throughout the polymerisation and molecular weight increased in a linear fashion with increasing conversion. The R^2 value is 0.9256. After 24 h the overall M_n was found to be 2.21 x 10^4 $gmol^{-1}$ by SEC, indicating a $\overline{DP}$ of 50 in each arm. This was in relatively good agreement with the theoretical M_n of 1.90 x 10^4 $gmol^{-1}$.

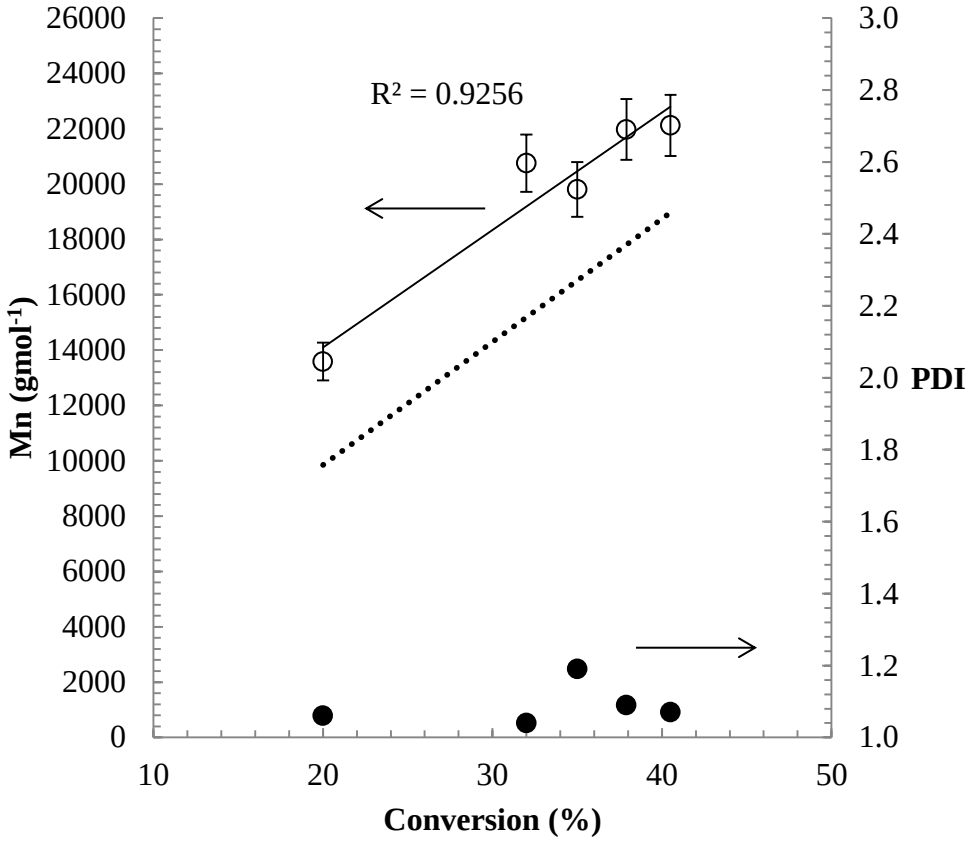

Figure 5.8. Mn against % conversion for polymerisation of NVP in bulk. Solid line is line of best fit. Dashed line (---) represents theoretical Mn

Figure 5.9 shows the ^{1}H NMR spectrum of Star 2 (after 24 h). Integration of the CH_3 protons of the *O*-ethyl xanthate moiety (**1**), against the CH protons of the backbone chain of PNVP (**2**), gives a ratio of approximately 1:12. This equates to the $\overline{DP}$ for each of the arms being 36, indicating M_n of approximately 4.0 x 10^3 gmol^{-1}. The $\overline{DP}$ value is lower than reported for SEC. The overall M_n of Star 2 (after 24 h) is found to be 1.60 x 10^4 gmol^{-1}, which is also in relatively good agreement with the theoretical M_n. This indicates the existence of four arms in the structure of Star 2 (after 24 h).

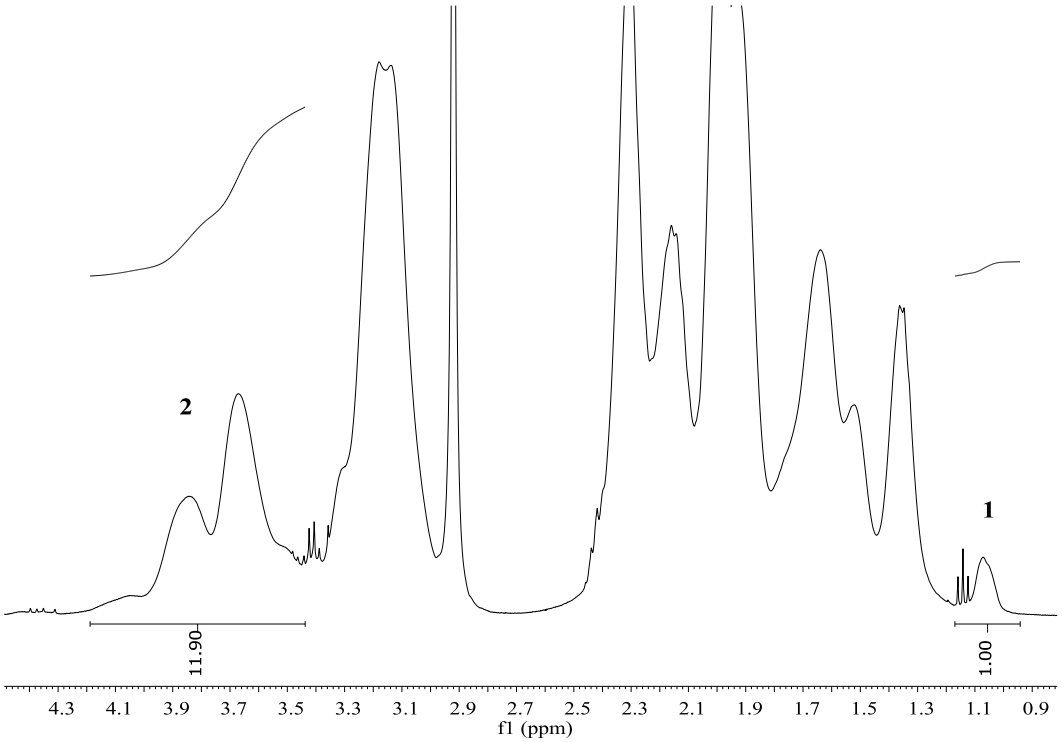

Figure 5.9. 400 MHz-^{1}H NMR spectrum of Star 2b

Figure 5.10 shows the progression of SEC traces over the polymerisation reaction time. It is shown that there is a gradual increase in the molecular weight with increasing polymerisation time form 2 – 24 h (traces I-V). All SEC traces are observed as monomodal, however on the lower molecular weight side there is evidence of significant tailing. After 24 h the Mark Houwink α parameter was calculated to be 0.46. In comparison, a typical value for linear PNVP within this study was between 0.66 and 0.73. This therefore suggests that there is a degree of branching within the structure of Star 2.

Figure 5.11, a plot of Log M against Wf / dLog M shows the progression of molecular weight distribution for samples collected after 5h, 7h and 24 h. In all cases the distributions are observed to be monomodal, however there is evidence of tailing on the lower molecular weight side. This indicates the presence of termination reactions, leading to the possibility of star structures with differing arm lengths.

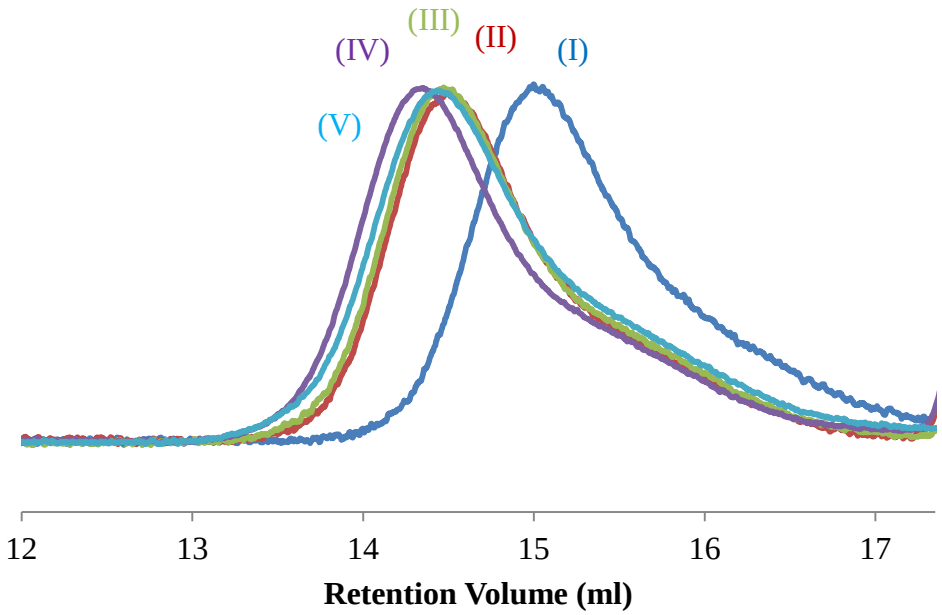

Figure 5.10. Progression of SEC traces (refractive index) after (I) 2 h, (II) 4 h, (III) 5 h, (IV) 7 h and (V) 24 h

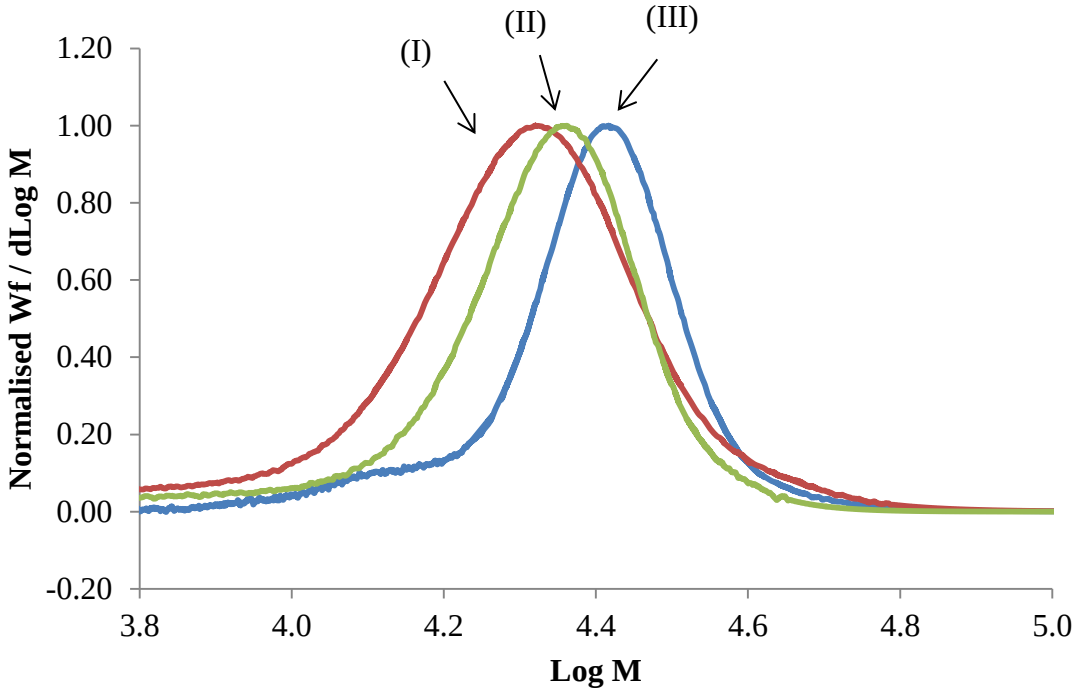

Figure 5.11. Plot of Log M against normalised Wf / dLog M showing the molecular weight distribution for the polymerisation of NVP in the presence of RAFT agent 10. (I) 5 h, (II) 7 h, (III) 24 h

5.3.1.3. Synthesis of Star 3

NVP was polymerised in bulk using ACVA as initiator, in a ratio of approximately 420 : 1 with respect to RAFT agent 11, to synthesise Star 3, Scheme 5.6. Star 3 comprised of di(trimethoxypropane) as a core and four PNVP arms. The chain ends are *O*-ethyl xanthate moieties.

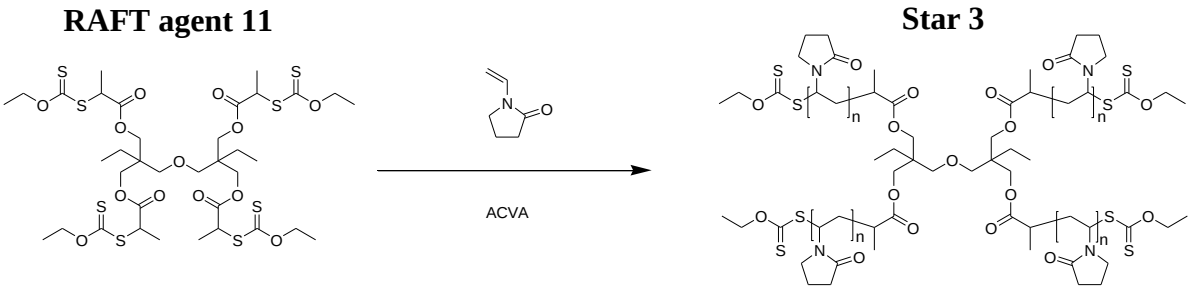

Scheme 5.6. Synthesis of Star 3

The conversion of monomer to polymer was measured by ^{1}H NMR spectroscopy to be 51% (Chapter 3, Section 3.2.3). SEC analysis (Figure 5.12) of Star 3 gave a M_n of 2.46 x 10^4 gmol^{-1} with a PDI of 1.19, indicating a $\overline{DP}$ of 55 in each arm. The theoretical M_n of Star 3, was calculated to be 2.48 x 10^4 gmol^{-1} and therefore is in very good agreement with the found M_n. The Mark Houwink α parameter was calculated to be 0.37. In comparison, a typical value for linear PNVP within this study was between 0.66 and 0.73. This therefore suggests that there is a degree of branching within the structure of Star 3.

Figure 5.13, a plot of Log M against Wf / dLog M shows the progression of molecular weight distribution, which is observed to be monomodal. However there is evidence of significant tailing on the lower molecular weight side. This indicates the presence of termination reactions, leading to the possibility of star structures with differing arm lengths.

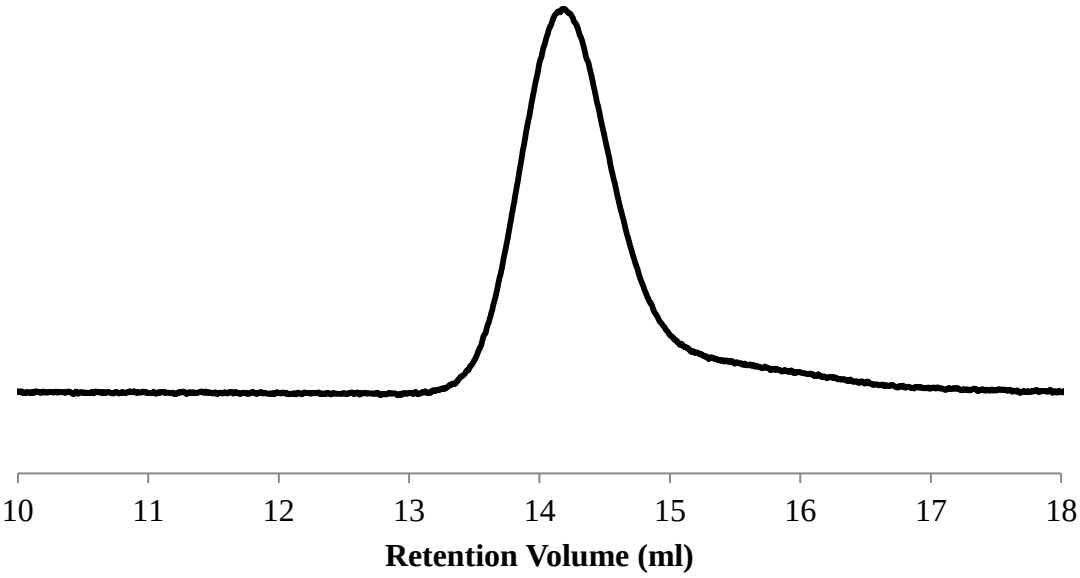

Figure 5.12. SEC chromatogram (refractive index) of Star 3

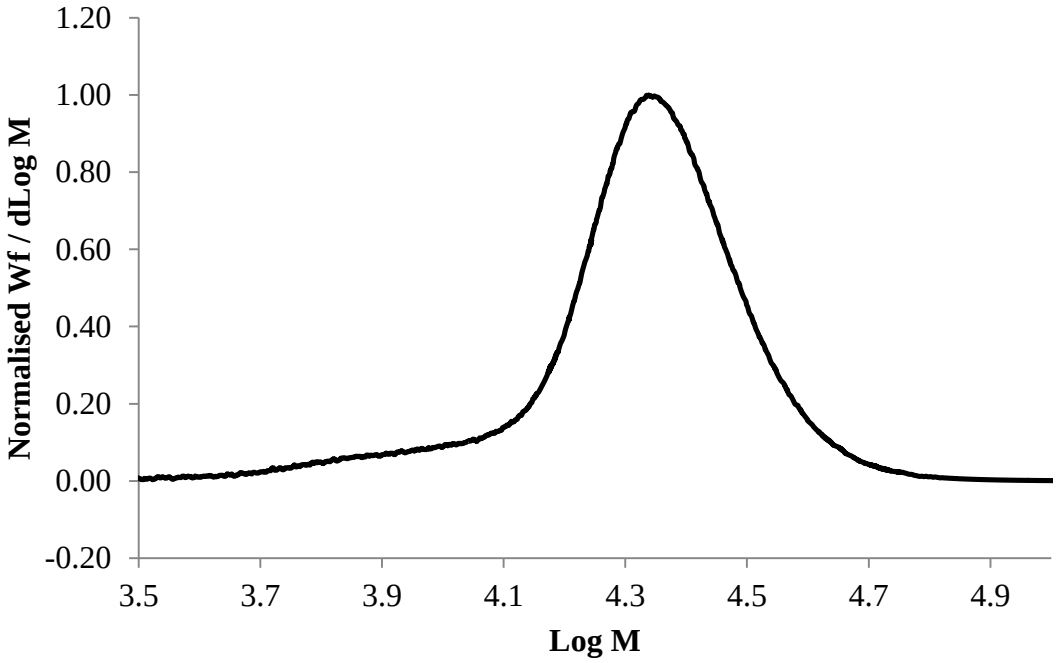

Figure 5.13. Plot of Log M against normalised Wf / dLog M showing the molecular weight distribution for the polymerisation of NVP in the presence of RAFT agent 11

Figure 5.14 shows the ^{1}H NMR spectrum of Star 3. Integration of the CH_3 protons (**1**) from the core, against the CH protons from PNVP backbone, gives a ratio of approximately 6:217. This equates to the $\overline{DP}$ for each of the arms as being 54, indicating M_n of approximately 6.0 x 10^3 $gmol^{-1}$. The overall M_n of Star 3 is found to be 2.41 x 10^4 $gmol^{-1}$, which is in good agreement with the theoretical M_n and that obtained by SEC. Furthermore, integration of the CH_3 protons (**3**) of the *O*-ethyl xanthate moiety against the CH_3 protons (**1**) from the core, shows that the ratio is approximately 2:1, indicating the existence of four arms in Star 3.

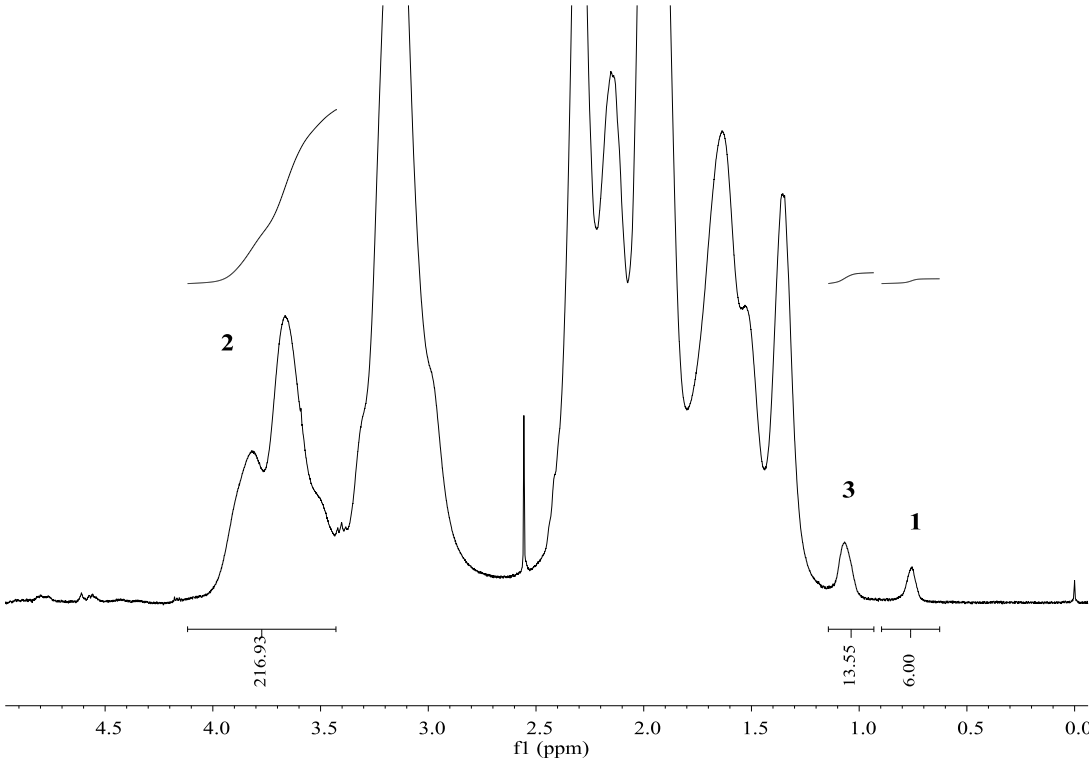

Figure 5.14. 400 MHz-^{1}H NMR spectrum of Star 3

5.3.1.4. Synthesis of Star 4

VAc was polymerised in bulk using ACVA as initiator, in a ratio of approximately 400 : 1 with respect to RAFT agent 11, to synthesise Star 4, Scheme 5.7. Star 4 comprised of di(trimethylolpropane) as a core and four PVAc arms. The chain ends are *O*-ethyl xanthate moieties.

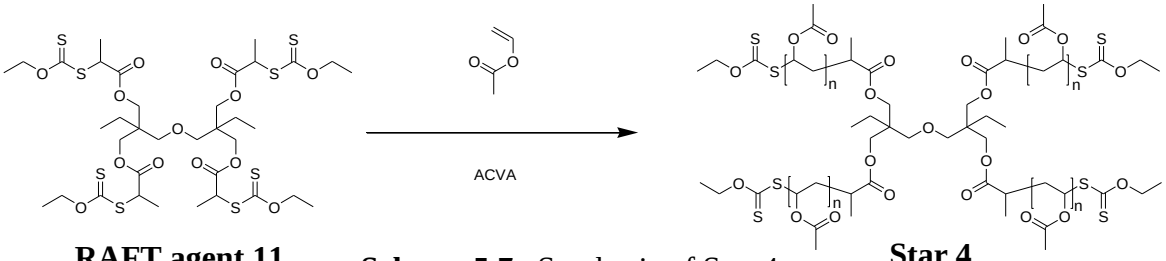

RAFT agent 11 **Star 4**

Scheme 5.7. Synthesis of Star 4

The yield of the polymerisation was measured gravimetrically as 61%. SEC analysis (Figure 5.15) of Star 4 gave a M_n of 2.14 x 10^4 $gmol^{-1}$ with a PDI of 1.44, indicating a $\overline{DP}$ of 62 in each arm. The theoretical M_n of Star 4, was calculated to be 2.20 x 10^4 $gmol^{-1}$ and therefore in good agreement with the found M_n. The Mark Houwink α parameter was calculated to be 0.41. In comparison, a typical value for linear PVAc within this study was between 0.62 and 0.75. This therefore suggests that there is a degree of branching within the structure of Star 4.

Figure 5.16, a plot of Log M against Wf / dLog M shows the progression of molecular weight distribution, which is observed to be monomodal. However there is evidence of tailing on the lower molecular weight side. This indicates the presence of termination reactions, leading to the possibility of star structures with differing arm lengths.

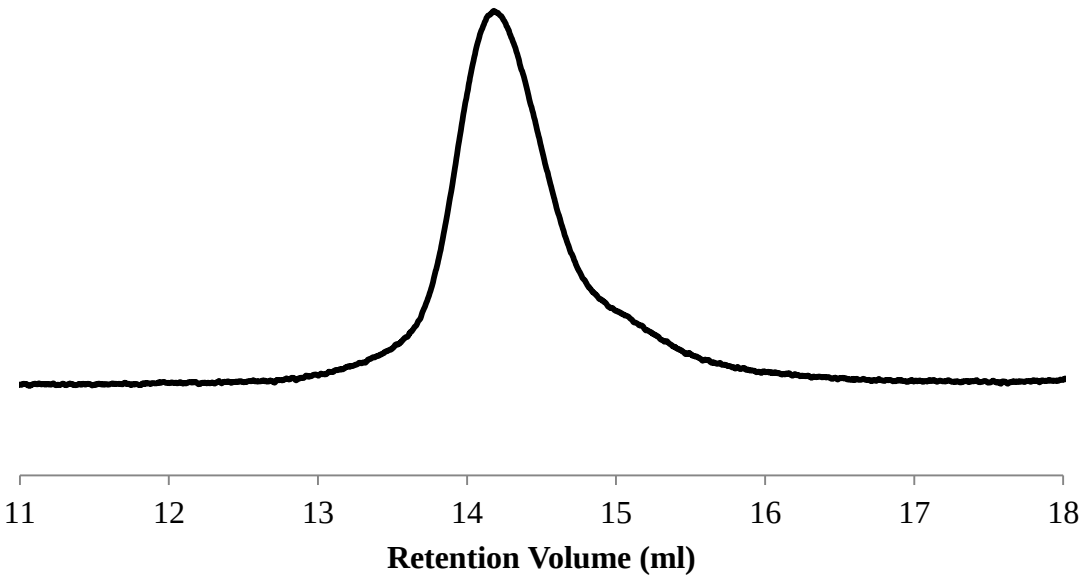

Figure 5.15. SEC chromatogram (refractive index) of Star 4

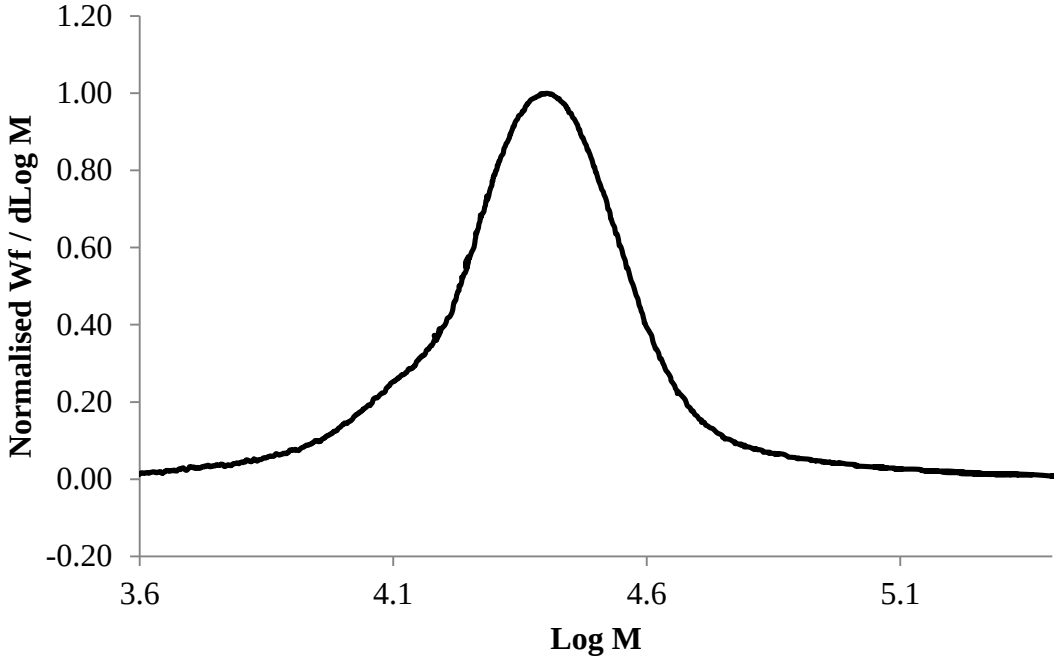

Figure 5.16. Plot of Log M against normalised Wf / dLog M showing the molecular weight distribution for the polymerisation of VAc in the presence of RAFT agent 11

Figure 5.17 shows the ^{1}H NMR spectrum of Star 4. Integration of the CH_3 protons (**1**) from the core, against CH protons from PVAc backbone, gives a ratio of approximately 6:296. This equates to the $\overline{DP}$ for each of the arms as being 74, indicating M_n of 6.4 x 10^3 gmol^{-1}. The $\overline{DP}$ value is larger than reported by SEC. The overall M_n of Star 4 is found to be 2.55 x 10^4 gmol^{-1}, which is also in good agreement with the theoretical M_n. Furthermore, integration of the CH_3 protons (**3**) of the *O*-ethyl xanthate moiety against the CH_3 protons (**1**) from the core, shows that the ratio is 2:1, indicating the existence of four arms in Star 4.

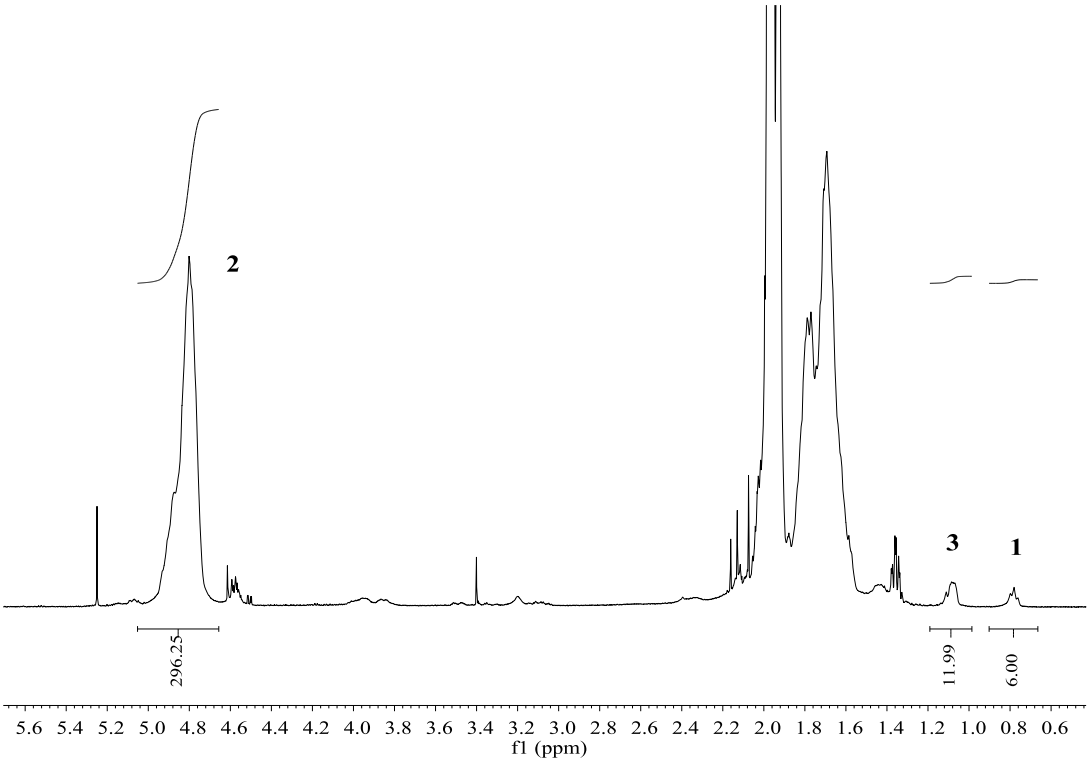

Figure 5.17. 400 MHz-^{1}H NMR spectrum of Star 4

5.3.1.5. Synthesis of Star 5

RAFT agent 9 was used to mediate the polymerisation of NVCL in 1,4 dioxane, using ACVA as intiator at 70°C for 18 h, Scheme 5.8. The ratio of monomer to RAFT agent 9 was approximately 300:1. The yield of the reaction was low at 24%. Star 5 comprised 1,1,1-trimethoxypropane as the core and three PNVCL arms. The chain ends are *O*-ethyl xanthate moieties.

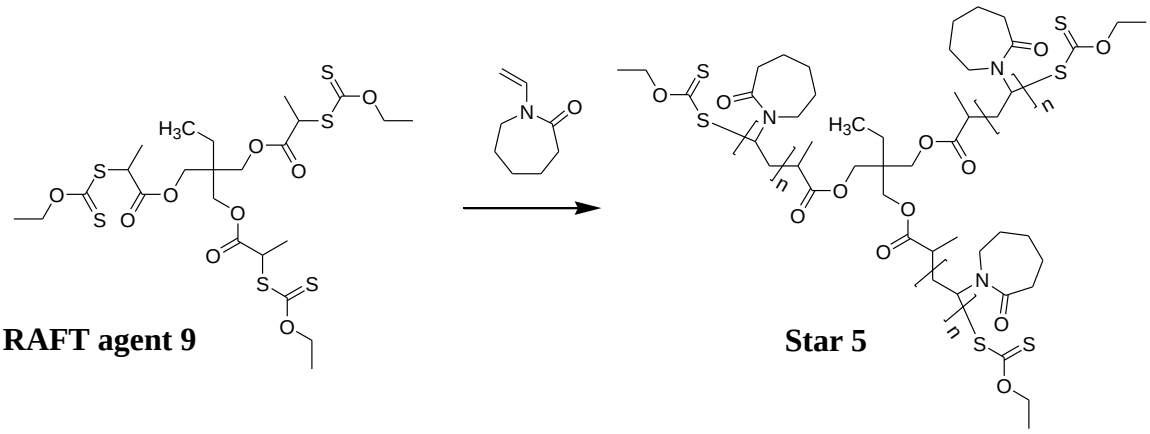

Scheme 5.8. Polymerisation of NVCL in the presence of RAFT agent 9

^{1}H NMR spectrum of Star 5 is shown in Appendix 2, Figure 1 and shows the typical proton resonances for PNVCL. Integration of the CH_3 protons (**1**) form the core, against CH protons (**2**) from PNVCL backbone, gives a ratio of approximately 3:24, indicating that the overall M_n is 3.34 x 10^3 gmol^{-1}. Figure 5.18 shows the SEC trace for Star 5 and it is apparent that it is bimodal with a PDI of 2.80. The M_p of the higher molecular weight distribution is 1.13 x 10^4 gmol^{-1} indicating a $\overline{DP}$ of 27 for each arm. The M_p of the lower molecular weight distribution was approximately 3.00 x 10^3 gmol^{-1}, indicating a $\overline{DP}$ of 22. This suggests that this distribution is single armed. The RAFT polymerisation of NVCL is problematic and bimodal molecular weight distributions are even observed during linear homopolymerisation reactions. The presence of bimodal molecular weight distribution is attributed to hybrid behaviour and terminations reactions (Chapter 3, Section 3.3.3).

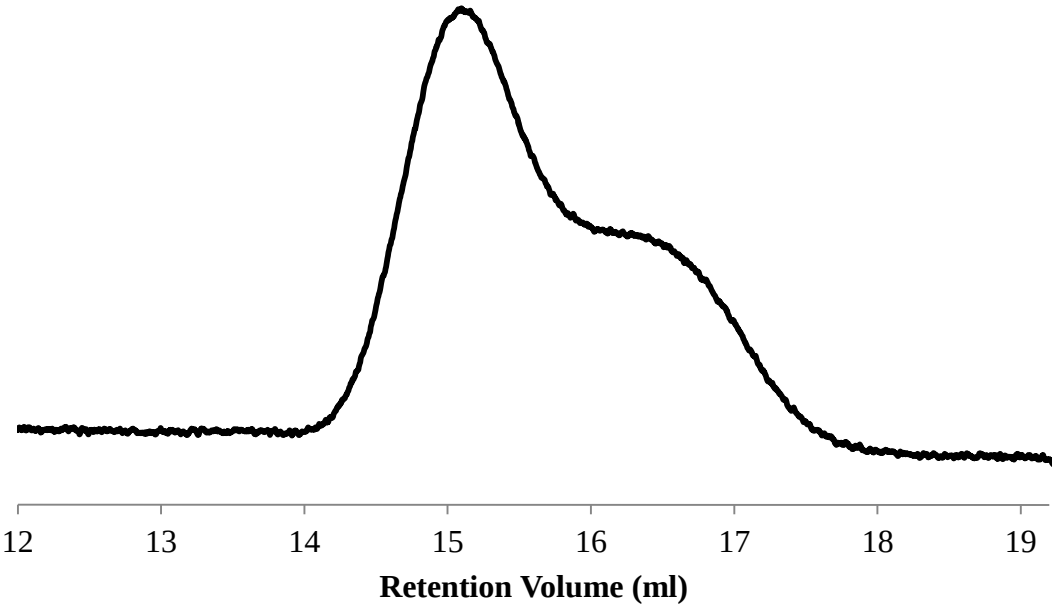

Figure 5.18. SEC trace (refractive index) of Star 5

5.3.1.6. Synthesis of Star 6

RAFT agent 11 was also used to mediate the polymerisation of NVCL in 1,4 dioxane, using ACVA as initiator at 70°C for 18 h, Scheme 5.9. The ratio of monomer to RAFT agent 11 was approximately 400:1. The yield of the reaction was 17%. Star 6 comprised di(trimethylolpropane) as the core and four PNVCL arms. The chain ends are *O*-ethyl xanthate moieties.

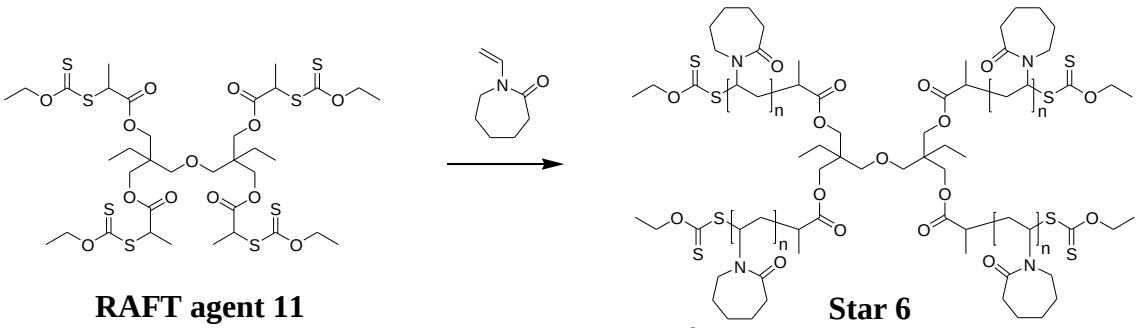

RAFT agent 11 **Star 6**

Scheme 5.9. Synthesis of Star 6

^{1}H NMR spectrum of Star 6 is shown in Appendix 2, Figure 2 and shows the typical proton resonances for PNVCL. Integration of the CH_3 protons (**1**) from the core, against CH protons (**2**) from PNCL backbone, gives a ratio of approximately 6:56, indicating that the overall M_n is 7.8 x 10^3 gmol^{-1}. Figure 5.19 shows the SEC trace for Star 6 and it is apparent that it is bimodal with a PDI of 3.70. The M_p of the higher molecular weight distribution is 1.34 x 10^4 gmol^{-1}, indicating a $\overline{DP}$ of 24 for each arm. The M_p of the lower molecular weight distribution was approximately 4.50 x 10^3 gmol^{-1}, indicating a $\overline{DP}$ of 32. This suggests that this distribution is mainly single armed. Similar observations were found as discussed for Star 5.

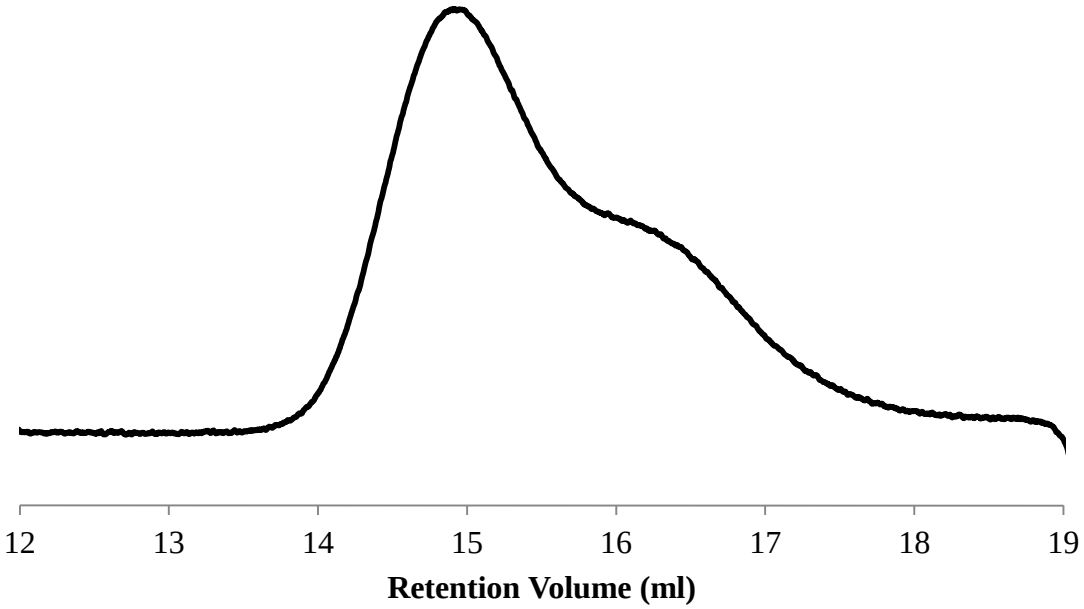

Figure 5.19. SEC trace (refractive index) of Star 6

Figure 5.20 compares a plot of Log M against Wf / dLog M for Star 5 and Star 6. This confirms the results reported from the SEC chromatograms using RAFT agents 9 and 11. Both molecular weight distributions show either extensive tailing on the lower molecular weight side (Star 6) or a definite bimodal molecular weight distribution (Star 5).

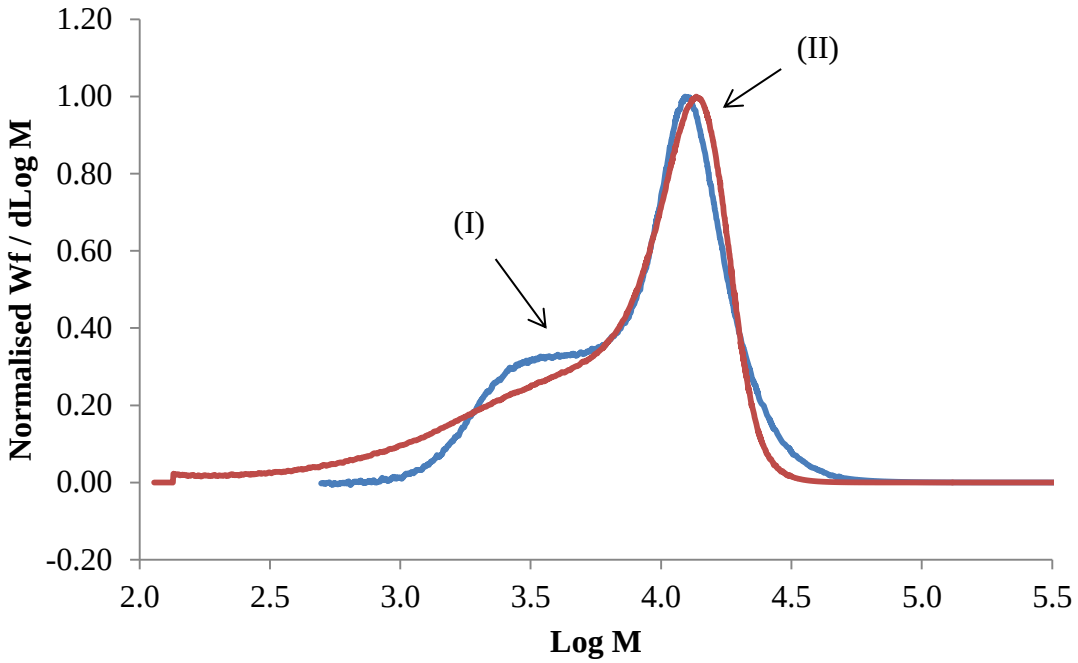

Figure 5.20. Plot of Log M against normalised Wf / dLog M showing the molecular weight distribution for the polymerisation of NVCL in the presence of (I) RAFT agent 9 (Star 5) and (II) RAFT agent 11 (Star 6)

5.3.2. Synthesis of Star-block 1-4

Star 1-4 (Section 5.3.1) were used as macroCTA's to synthesise Star-block 1-4, containing PNVP, PVAc or PNVCL, Figure 5.21.

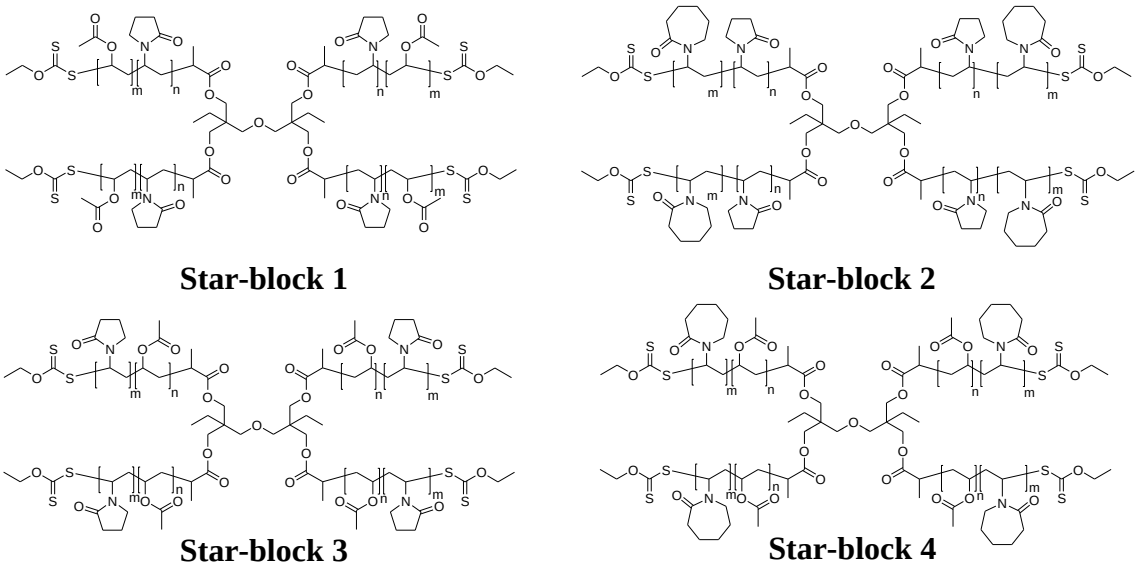

Figure 5.21. Structures of Star-block 1-4

5.3.2.1. Synthesis of Star-block 1

Star 3 was used as a macroCTA to control the polymerisation of VAc at 70°C using ACVA as initiator, to synthesise Star-block 1, (Scheme 5.10).

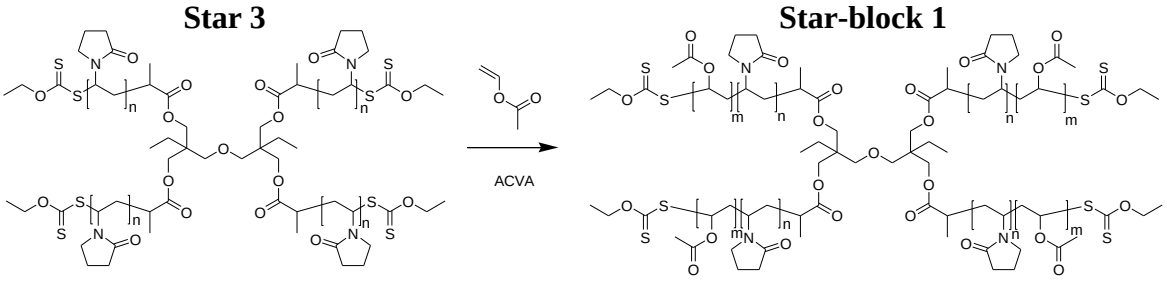

Scheme 5.10. Synthesis of Star-block 1

^{1}H NMR spectra of Star-block 1, along with Star 3 and PVAc are shown in Appendix 2, Figure 3. The figure clearly shows the presence of proton environments for both PNVP and PVAc. The integration of the resonances due to the CH protons of backbone of PVAc block (4.7 – 5.0 ppm) against the CH_2 protons adjacent to nitrogen atom on the pyrrolidone ring of PNVP block (3.0 – 3.5 ppm) gives a ratio of 1:0.23, indicating PVAc content of 81%.

Star-blocks generally have very complex structures and hence hydrodynamic volumes in comparison with their linear homopolymers. Therefore, M_n values obtained

by SEC are not that reliable however, M_p and PDI provide useful information on their formation.

Figure 5.22 shows the comparison of the SEC traces for Star 3 (I) and Star-block 1 (II). Star-block 1 has a bimodal molecular weight distribution and the lower molecular weight peak is superimposable with that of Star 3. Star-block 1 shows a significantly broader molecular weight distribution than that of Star 3; PDI increased from 1.17 (Star 3) to 2.16 (Star-block 1). Moreover, the M_p increased from 3.1 x 10^4 $gmol^{-1}$ (Star 3) to 6.0 x 10^4 $gmol^{-1}$ (Star-block 1, higher molecular weight distribution), suggesting that approximately 2.9 x 10^4 $gmol^{-1}$ of the molecular weight is due to PVAc. This indicates that the molecular weight and $\overline{DP}$ of PVAc for each arm is 7.5 x 10^3 $gmol^{-1}$ and 84, respectively. This calculation shows that the overall $\overline{DP}$ of each arm is now 139. Broad PDI may indicate that for the formation of Star-block 1, there is variable PVAc content.

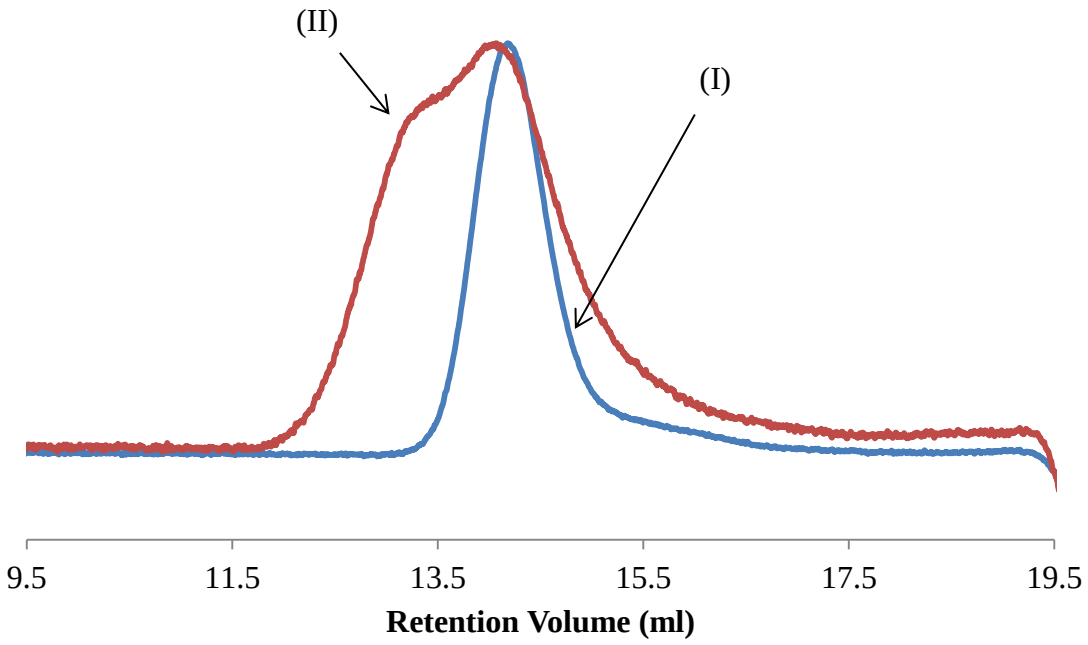

Figure 5.22. SEC traces (refractive index) of (I) Star 3 and (II) Star-block 1

5.3.2.2. Synthesis of Star-block 2

Star 3 was also used to mediate the polymerisation of NVCL, to synthesise Star-block 2, (Scheme 5.11).

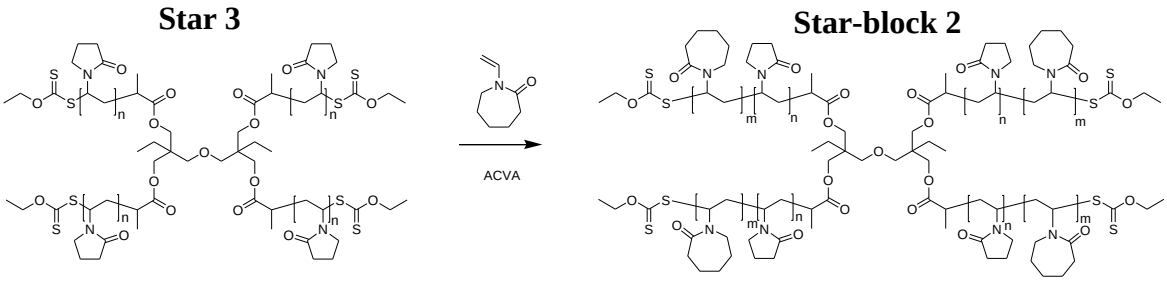

Scheme 5.11. Synthesis of Star-block 2

^{1}H NMR spectra of Star-block 2, along with Star 3 and PNVCL are shown in Appendix 2, Figure 4. The figure clearly shows the presence of proton environments for both PNVP and PNVCL. The integration of the resonances due to the CH protons of the backbone of PNVCL block (4.2 – 4.7 ppm) against CH protons of the backbone of PNVP block (3.5 – 4.0 ppm) gives a ratio of 1:0.19, indicating PNVCL content of 84%.

Figure 5.23 shows the comparison of the SEC trace for Star 3 (I) and Star-block 2 (II). Star-block 2 has a bimodal molecular weight distribution and the lower molecular weight peak is superimposable with that of Star 3. Star-block 2 shows a significantly broader molecular weight distribution that that of Star 3: PDI increased from 1.17 (Star 3) to 2.08 (Star-block 2). Moreover, the M_p increased from 3.1 x 10^4 $gmol^{-1}$ (Star 3) to 1.21 x 10^5 $gmol^{-1}$ (Star-block 2), suggesting that approximately 9.0 x 10^4 $gmol^{-1}$ of the molecular weight is due to PNVCL. This indicates that the molecular weight and $\overline{DP}$ of PVAc for each arm is 2.25 x 10^4 $gmol^{-1}$ and 161, respectively. This calculation shows that the overall $\overline{DP}$ of each arm is now 216. Broad PDI may indicate the formation of Star-block 2, there is variable PNVCL content.

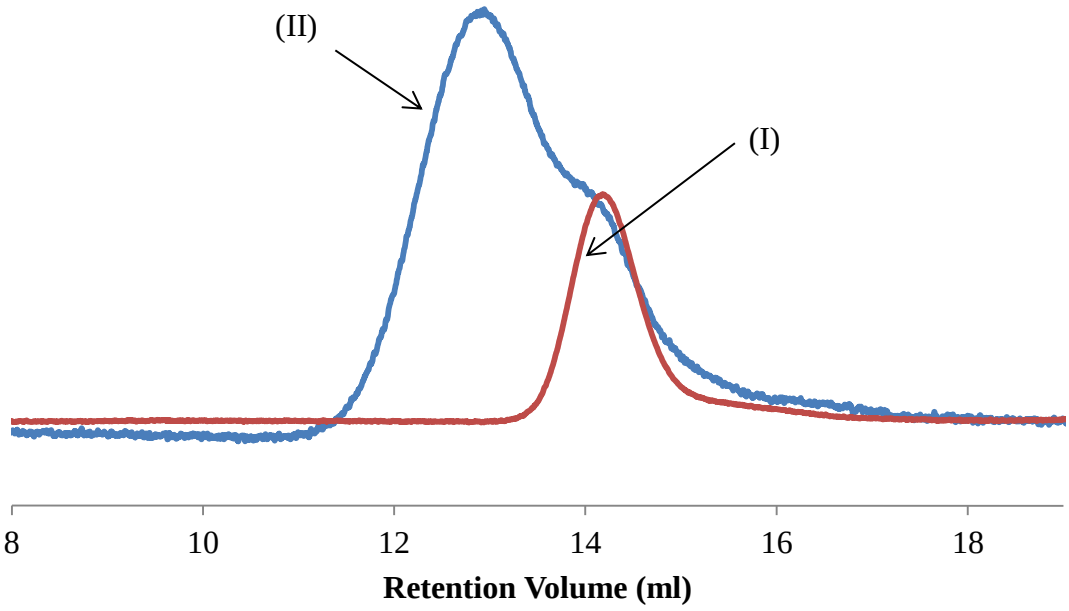

Figure 5.23. SEC traces (refractive index) of (I) Star 3 and (II) Star-block 2

5.3.2.3. Synthesis of Star-block 3

Star 4 was used as a macroCTA to mediate the polymerisation of NVP, to synthesise Star-block 3 (four arm PVAc-*block*-PNVP star), Scheme 5.12.

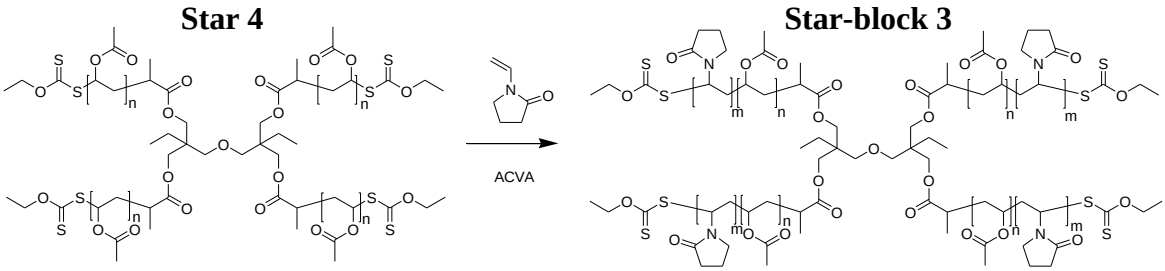

Scheme 5.12. Synthesis of Star-block 3

^{1}H NMR spectra of Star-block 3, along with Star 4 and PNVP are shown in Appendix 2, Figure 5. The figure clearly shows the presence of proton environments for both PNVP and PVAc. The conversion of NVP to PNVP was 72%, as measured by ^{1}H NMR spectroscopy (Chapter 3, Section 3.2.3). The integration of the resonances due to the CH protons of the backbone of PVAc block (4.7 – 5.0 ppm) against the CH_2 protons adjacent to nitrogen on the pyrrolidone ring of PNVP block (3.0 – 3.5 ppm) gives a ratio of 1:4.1, indicating PNVP content of 80%.

Figure 5.24 shows the comparison of the SEC traces for Star 4 (I) and Star-block 3 (II). Star-block 3 shows a significantly broader molecular weight distribution than that for Star 4; PDI increased from 1.44 (Star 4) to 1.76 (Star-block 3). Moreover, the M_p increased from 2.67 x 10^4 gmol^{-1} (Star 4) to 2.27 x 10^5 gmol^{-1} (Star-block 3), suggesting that approximately 2.0 x 10^5 gmol^{-1} is due to PNVP. This indicates that the molecular weight and $\overline{DP}$ of PNVP for each arm is 5.0 x 10^4 gmol^{-1} and 450, respectively. This calculation shows that the overall $\overline{DP}$ of each arm is now 512. Broader PDI may indicate that for the formation of Star-block 3, there is variable PNVP content.

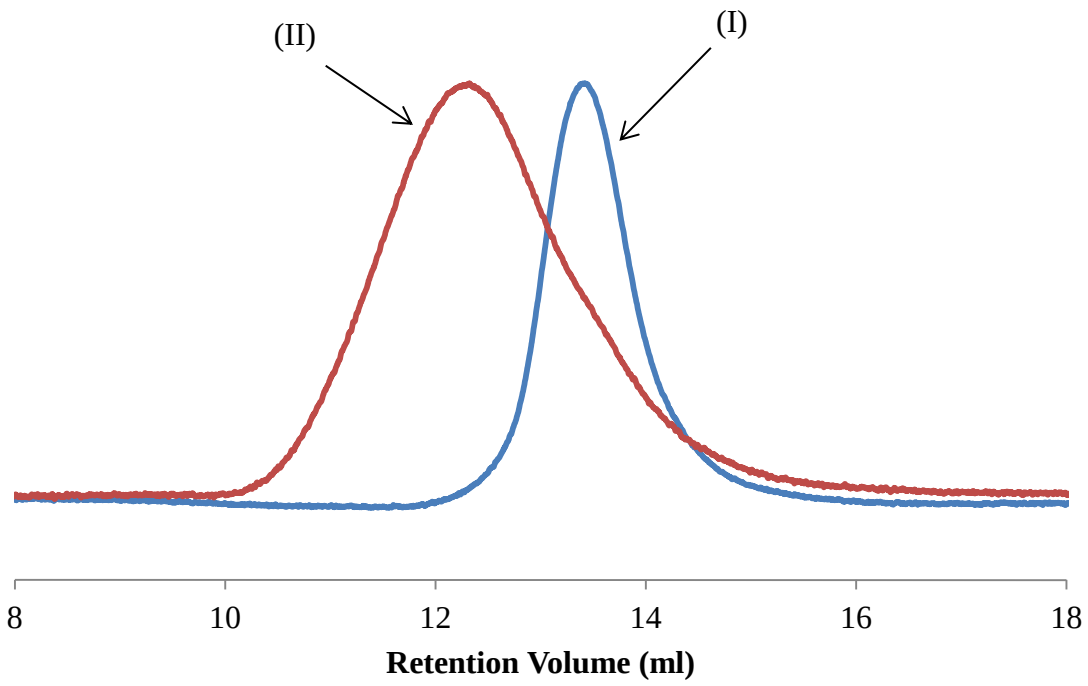

Figure 5.24. SEC traces (refractive index) of (I) Star 4 and (II) Star-block 3

5.3.2.4. Synthesis of Star-block 4

Star 4 was also used to mediate the polymerisation of NVCL to synthesise Star-block 4 (4 arm PVAc-*block*–PNVCL star), Scheme 5.13.

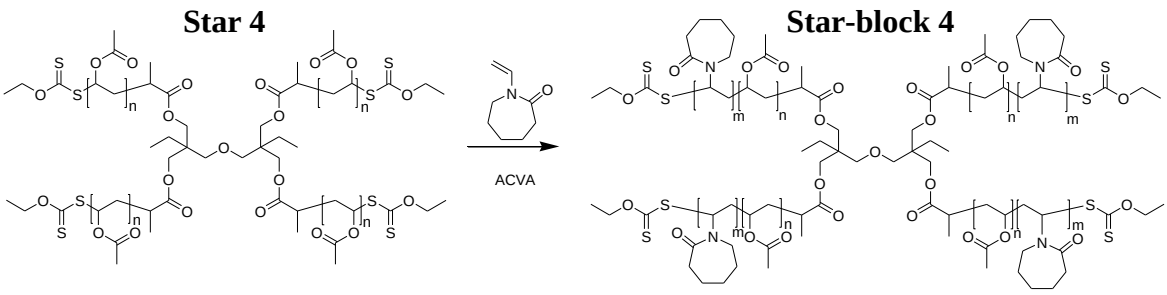

Scheme 5.13. Synthesis of Star-block 4

^{1}H NMR spectra of Star-block 4, along with Star 4 and PNVCL are shown in Appendix 2, Figure 6. The figure clearly shows the presence of protons environments for both PNVCL and PVAc. The yield of the polymerisation of NVCL in the presence of the PVAc macroCTA measured gravimetrically was 41%. The integration of the resonances due to the CH protons of the backbone of PVAc block (4.7 – 5.0 ppm) against the CH protons of the backbone of PNVCL block (4.2 – 4.7 ppm) gives a ratio of 1:1.7, indicating PNVCL content of 63%.

Figure 5.25 shows the comparison of the SEC traces for Star 4 (I) and Star-block 4 (II). Star-block 4 has a bimodal molecular weight distribution and the lower molecular weight peak corresponds to that of Star 4; PDI increased from 1.44 (Star 4) to 1.68 (Star-block 4). Moreover, the M_p increased from 2.67 x 10^4 gmol^{-1} (Star 4) to 8.69 x 10^4 gmol^{-1} (Star-block 4), suggesting that approximately 6.0 x 10^4 gmol^{-1} is due to PNVCL. This indicates that the molecular weight and $\overline{DP}$ of PNVCL for each arm is 1.5 x 10^4 gmol^{-1} and 108, respectively. This calculation shows that the overall $\overline{DP}$ of each arm is now 170. Broader PDI may indicate for the formation of Star-block 4, there is variable PNVCL content.

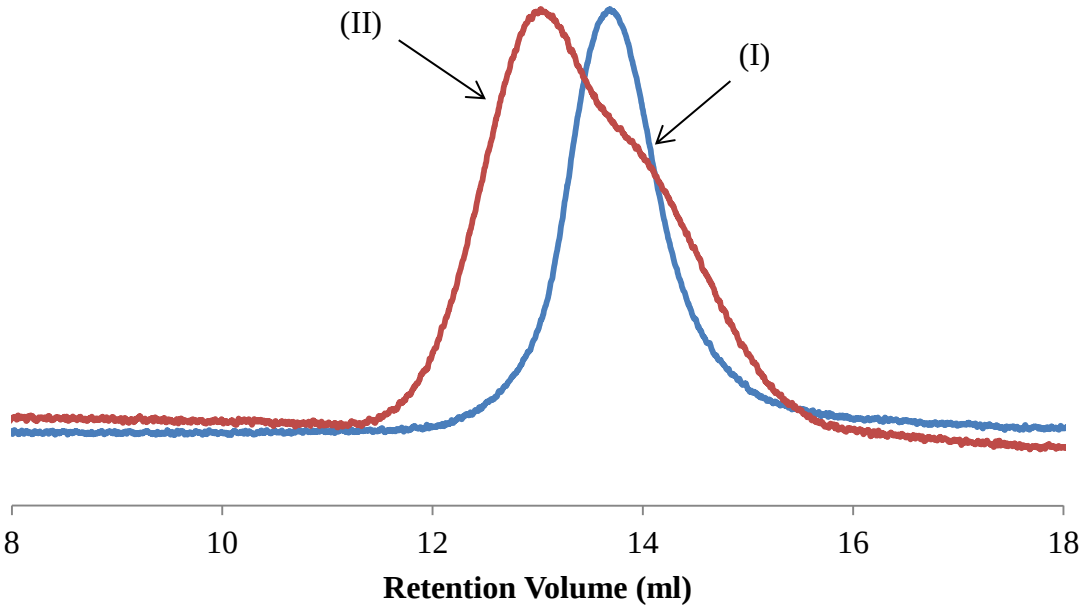

Figure 5.25. SEC traces (refractive index) of (I) Star 4 and (II) Star-block 4

5.3.3. Synthesis of Star-random 1-6

With the addition of multi-armed RAFT agents to a polymerisation mixture it is possible to make more complex random copolymer architectures, such as stars. RAFT agents 9 and 11 were used to synthesise PNVP-*ran*-PVAc, PNVCL-*ran*-PVAc and PNVP-*ran*-PNVCL with three (Star-random 1-3) and four (Star-random 4-6) arms, respectively, Figure 5.26. To the best of our knowledge, there are no reports in the literature concerning the synthesis of random star polymer structures formed *via* RAFT polymerisation.

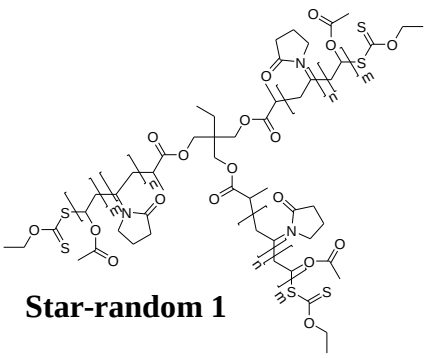

Star-random 1

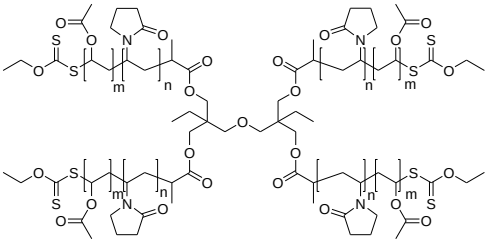

Star-random 4

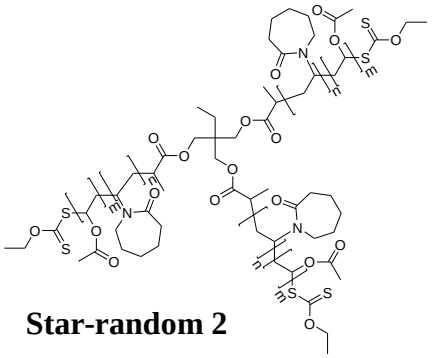

Star-random 2

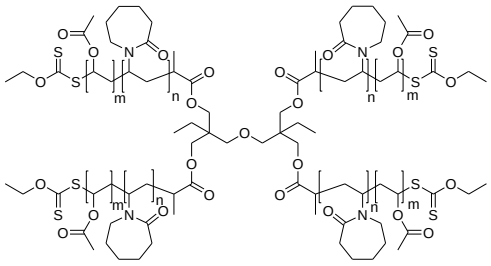

Star-random 5

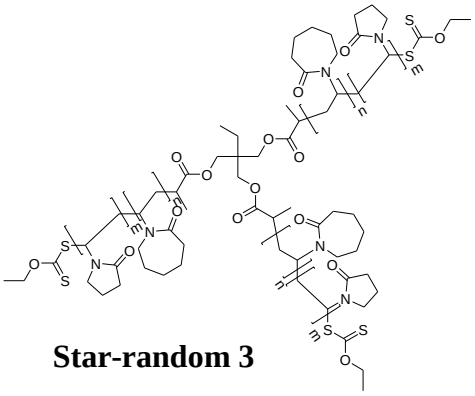

Star-random 3

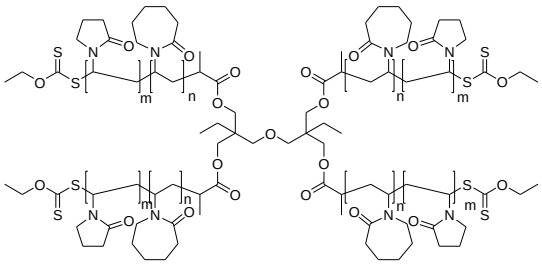

Star-random 6

Figure 5.26. Structures of Star-random 1-6

5.3.3.1. Synthesis of Star-random 1 and 4

Star random 1 (three arm) and 4 (four arm) were synthesised using RAFT agents 9 and 11 for the copolymerisation of NVP and VAc in a monomer molar feed ratio of 50:50 (NVP:VAc), Scheme 5.14 (I and II).

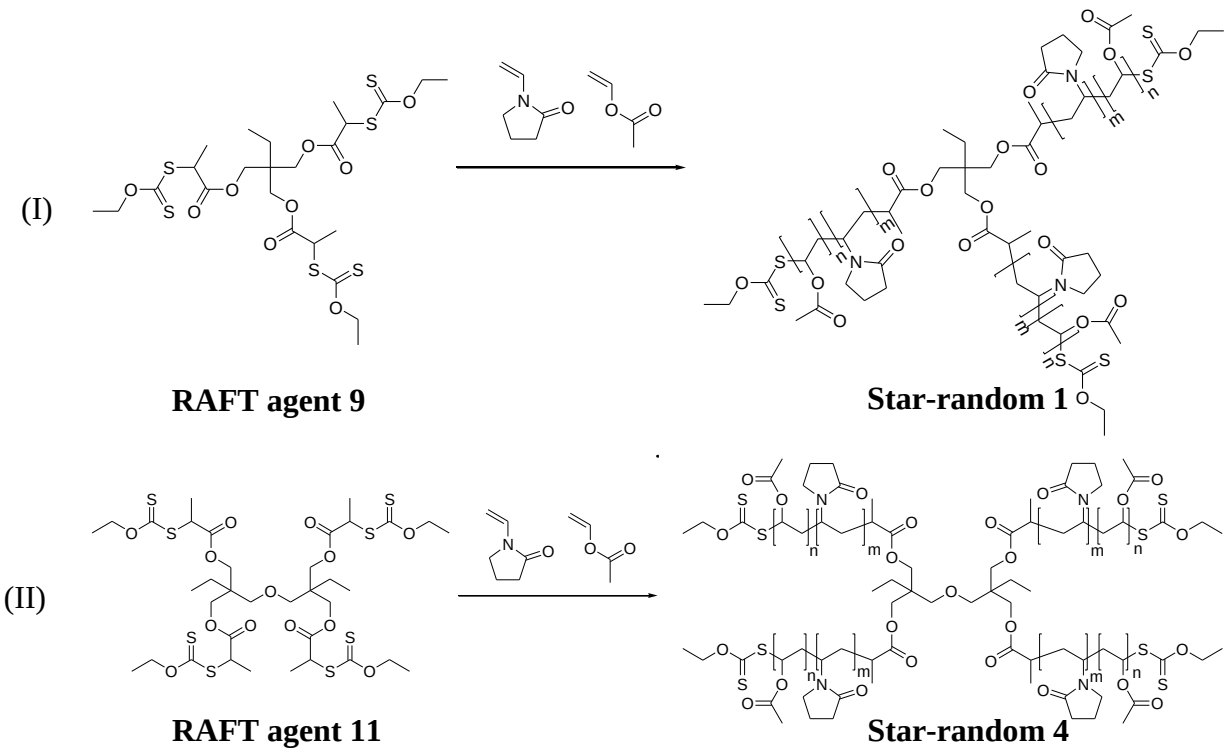

Scheme 5.14. Synthesis of (I) Star-random 1 and (II) Star-random 4

^{1}H NMR spectra of Star-random 1 and 4 are compared in Appendix 2, Figure 7. Both spectra show the typical proton resonances for PNVP and PVAc in PNVP-*ran*-PVAc products. The composition of the copolymer can be determined by comparing the ratio of the integrals of the CH from PVAc backbone (4.4 – 5.1 ppm) and CH_2 adjacent to the nitrogen atom from PNVP (2.9 – 3.5 ppm). The compositions were analysed as 72 : 28 (PNVP : PVAc) in both random copolymers. The yields of Star-random 1 and Star-random 4 were 39% and 47%, respectively. The SEC traces of Star-random 1 and 4 are shown in Figure 5.27. The M_n of Star-random 1 (Figure 5.27-I) was measured by SEC as 2.74 x 10^4 gmol^{-1} with a PDI of 1.18. Therefore, the M_n of each arm is approximately 9.1 x 10^3 gmol^{-1}, indicating that there are 59 repeat units of NVP and 30 repeat units for VAc in each arm, based on composition of PNVP:PVAc (72:28). In comparison, the M_n of Star-random 4 (Figure 5.27-II) was measured by SEC as 5.15 x 10^4 gmol^{-1} with a PDI of 1.22. Therefore, the M_n of each arm is approximately 1.3 x 10^4 gmol^{-1}, indicating that there are 83 repeat units of NVP and 42 repeat units for VAc in each arm, based on composition of PNVP:PVAc (72:28). It should be noted, these Star-random copolymers have, due to their structures complex hydrodynamic volumes and the molecular weight measured by SEC is not accurate.

However, the traces are single mode and PDI is narrow, indicating the formation of Star-random copolymers.

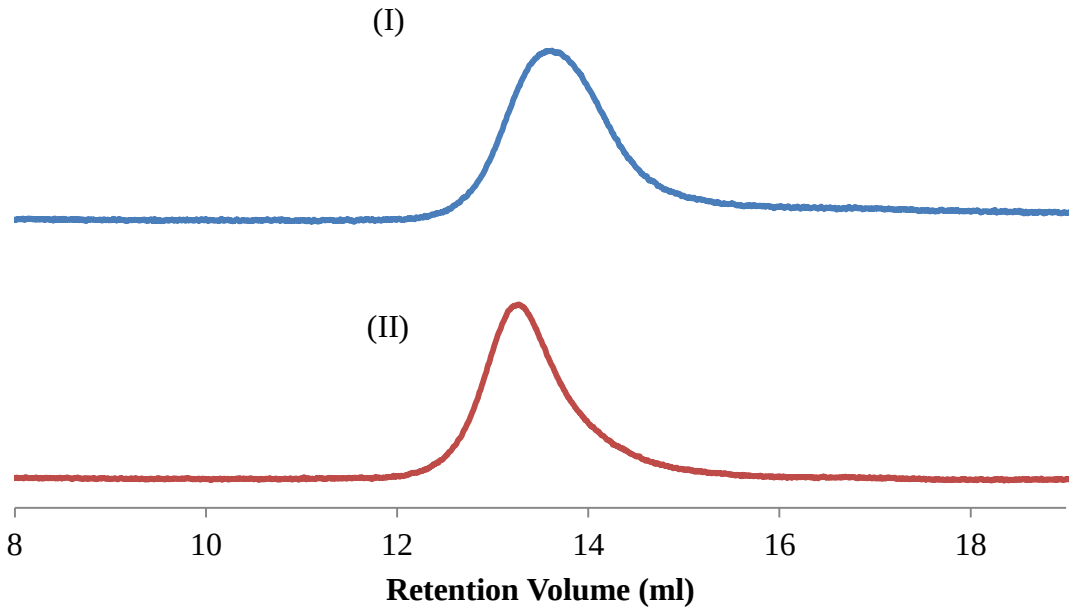

Figure 5.27. Comparison of SEC traces (refractive index) of (I) Star-random 1 and (II) Star-random 4

Figure 5.28, a plot of Log M against Wf / dLog M, shows the comparison of molecular weight distributions between Star-random 1 and 4. Both distributions are monomodal which supports the result observed in Figure 5.27.

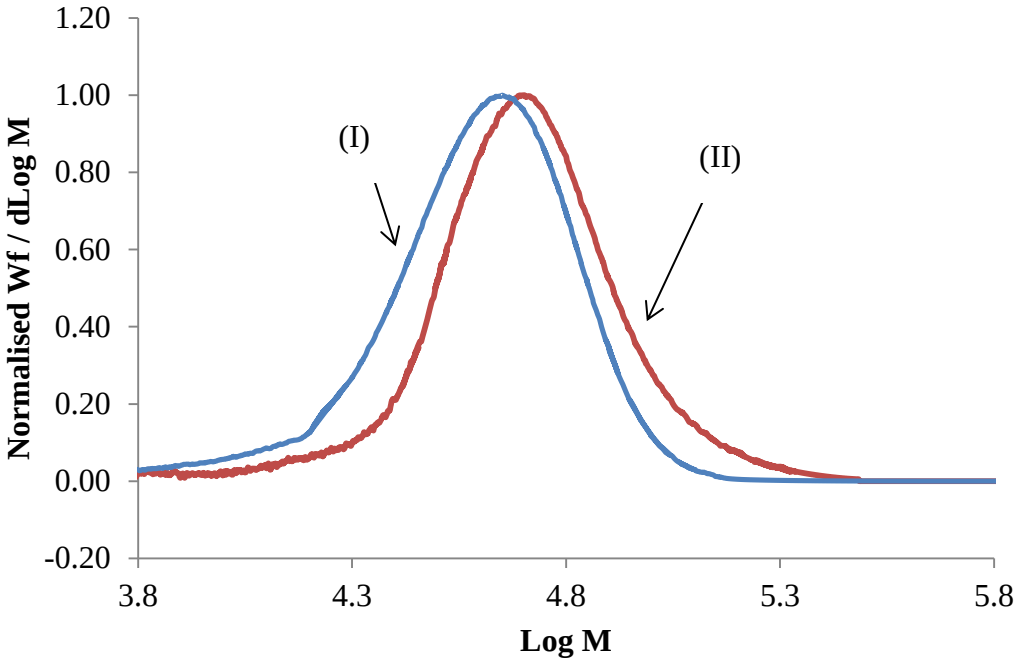

Figure 5.28. Plot of Log M against normalised Wf / dLog M showing the molecular weight distribution for (I) Star-random 1 and (II) Star-random 4

5.3.3.2. Synthesis of Star-random 2 and 5

Star random 2 (three arm) and 5 (four arm) were synthesised using RAFT agents 9 and 11 for the copolymerisation of NVCL and VAc in a monomer molar feed ratio of 50:50 (NVCL:VAc), Scheme 5.15 (I and II).

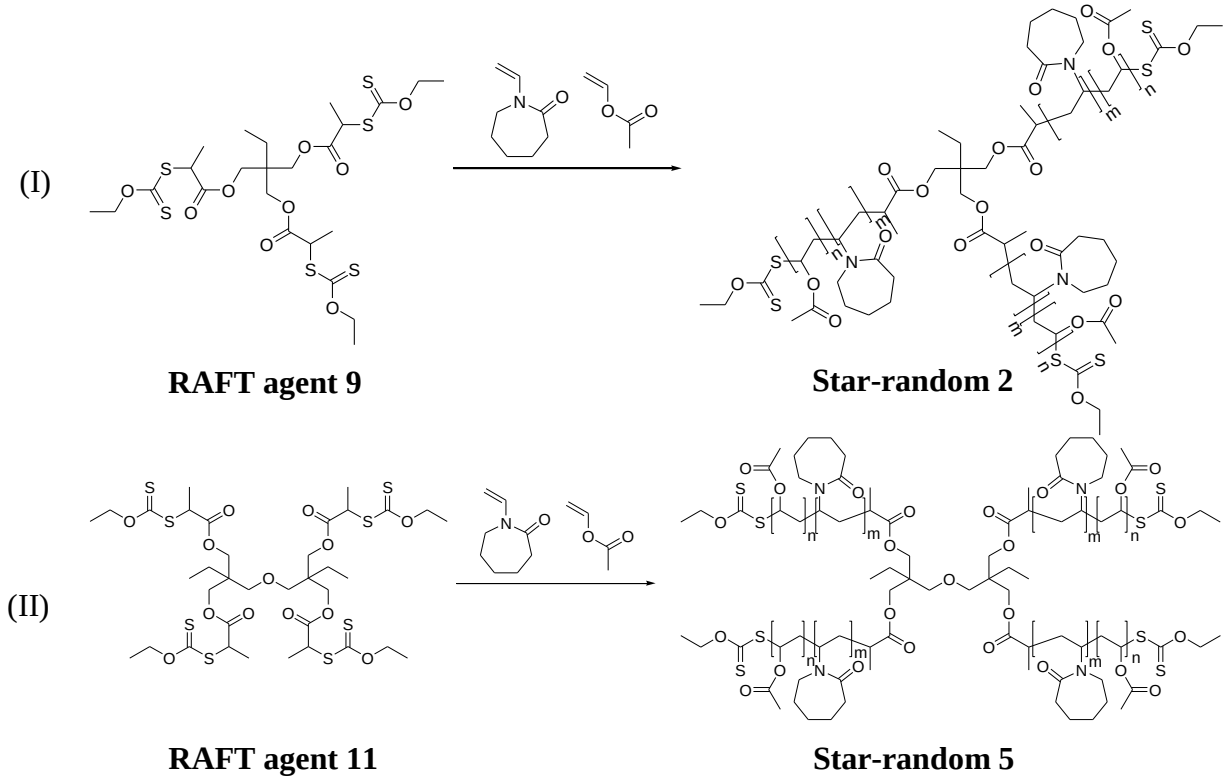

Scheme 5.15. Synthesis of (I) Star-random 2 and (II) Star-random 5

^{1}H NMR spectra of Star-random 2 and 5 are compared in Appendix 2, Figure 8. Both spectra show the typical proton resonances for PNVCL and PVAc in PNVCL-*ran*-PVAc products. By integrating the CH protons from each of the repeat units (4.1 – 5.0 ppm) and the CH_2 of PNVCL at 2.8 – 3.3 ppm, the composition of Star-random 2 was analysed to be 72:28 (PNVCL:PVAc). In addition, Star-random 5 has a composition of 76:24 (PNVCL:PVAc). The yields of Star-random 2 and Star-random 5 were 24% and 30%, respectively. The SEC traces of Star-random 2 and 5 are shown in Figure 5.29. The M_n of Star-random 2 (Figure 5.29-I) was measured by SEC as 2.64 x 10^4 gmol^{-1} with a PDI of 1.31. Therefore, the M_n of each arm is approximately 8.8 x 10^3 gmol^{-1}, indicating that there are 46 repeat units of NVCL and 29 repeat units for VAc in each arm, based on composition of PNVCL:PVAc (72:28). In comparison, the M_n of Star-random 5 (Figure 5.29-II) was measured by SEC as 2.35 x 10^4 gmol^{-1} with a PDI of 1.23. Therefore, the M_n of each arm is approximately 5.9 x 10^4 gmol^{-1}, indicating that there are 36 repeat units of NVCL and 16 repeat units for VAc in each arm, based on composition of PNVCL:PVAC (76:24). It should be noted, these Star-random copolymers have, due to their structures complex hydrodynamic volumes and the molecular weight measured by SEC is not accurate.

However, the traces are single mode and PDI is narrow, indicating the formation of Star-random copolymers.

Figure 5.30, a plot of Log M against Wf / dLog M, shows the comparison of molecular weight distributions between Star-random 2 and 5. Both distributions are monomodal which supports the result observed in Figure 5.29.

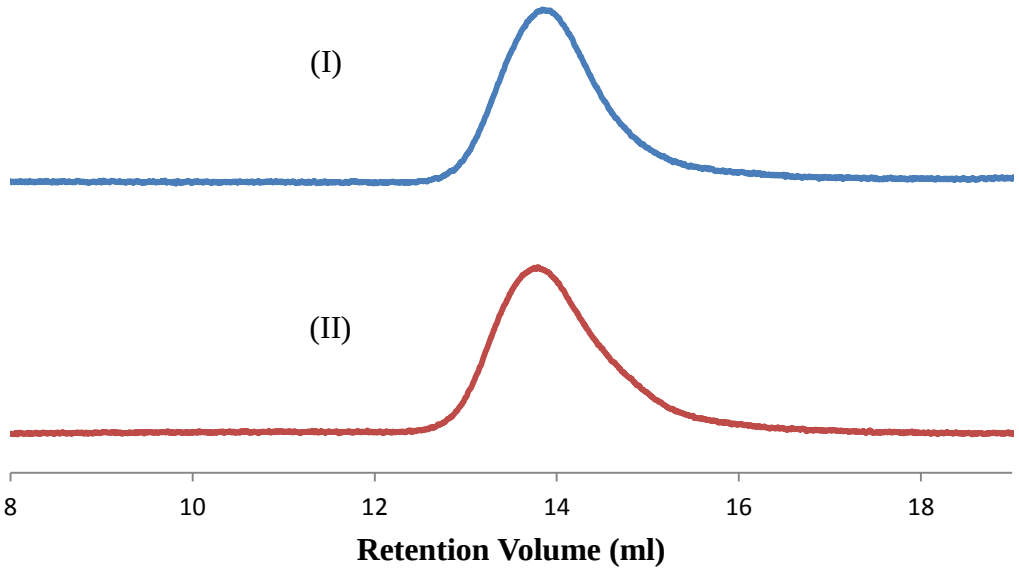

Figure 5.29. Comparison of SEC traces (refractive index) of (I) Star-random 2 and (II) Star-random 5

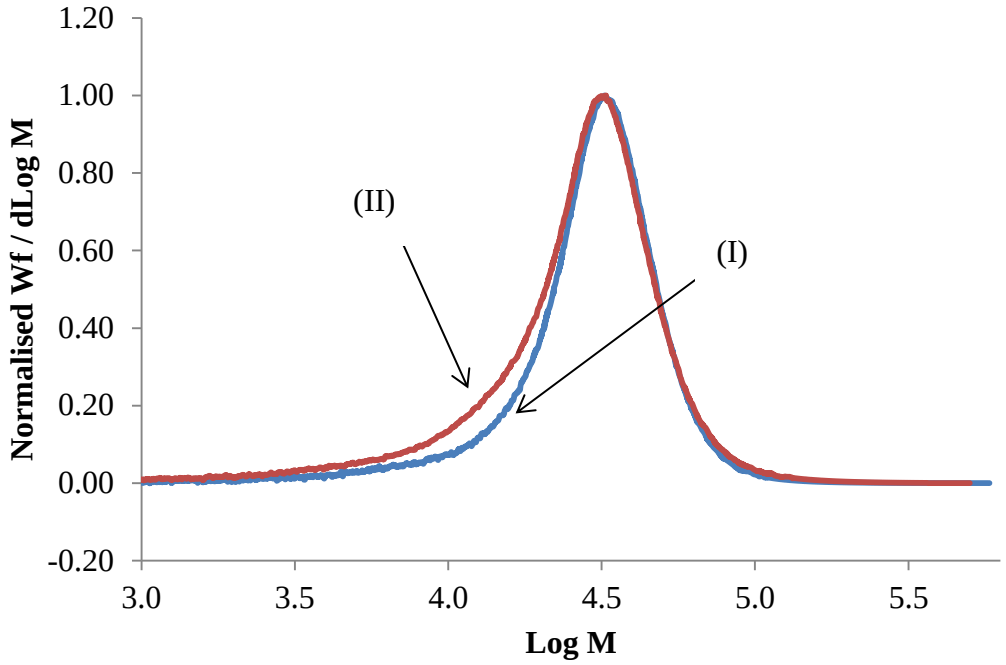

Figure 5.30. Plot of Log M against normalised Wf / dLog M showing the molecular weight distribution of (I) Star-random 2 and (II) Star-random 5

5.3.3.3. Synthesis of Star-random 3 and 6

Star random 3 (three arm) and 6 (four arm) were synthesised using RAFT agents 9 and 11 for the copolymerisation of NVP and NVCL in a monomer molar feed ratio of 50:50 (NVP:NVCL), Scheme 5.16 (I and II).

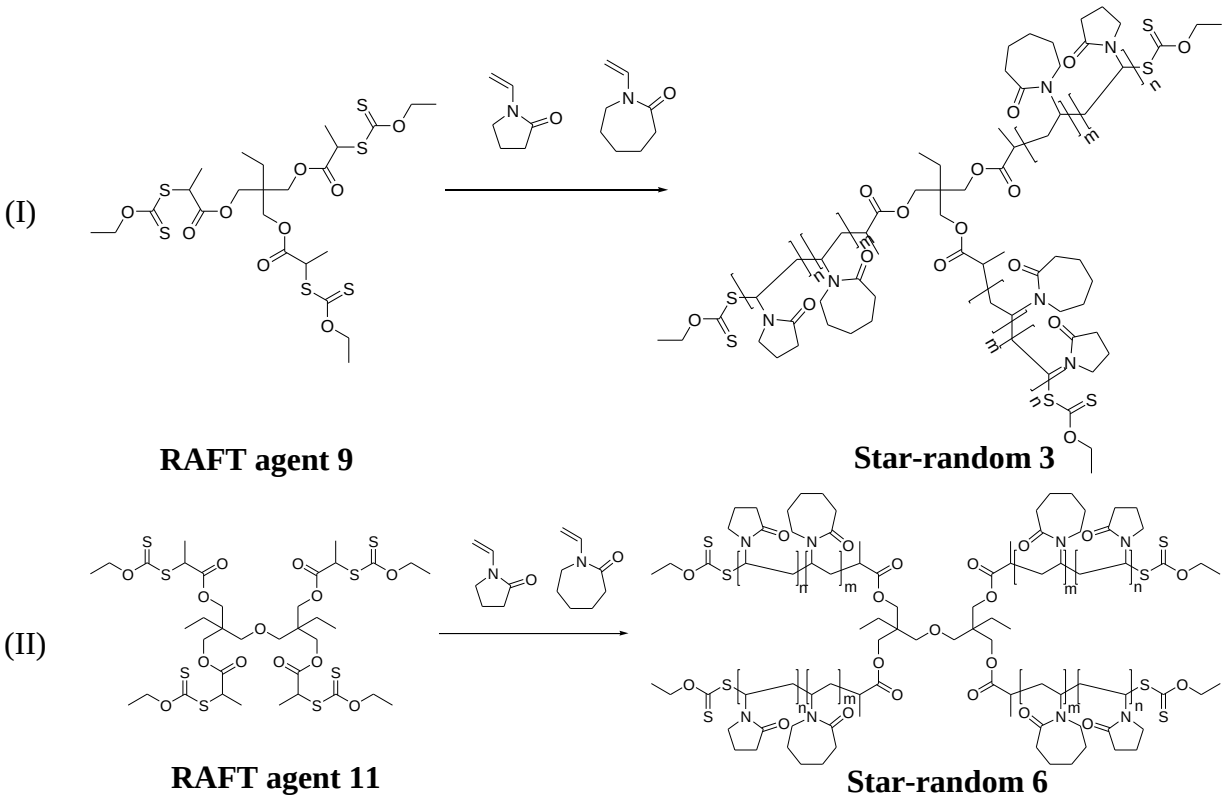

Scheme 5.16. Synthesis of (I) Star-random 3 and (II) Star-random 6

^{1}H NMR spectra of Star-random 3 and 6 are compared in Appendix 2, Figure 9. Both spectra show the typical proton resonances for PNVP and PNVCL in PNVP-*ran*-PNVCL products. The composition of the copolymer can be determined by comparing the ratio of the integrals of the CH from PNVP backbone (3.5 – 4.1 ppm) and CH from PNVCL backbone (4.1 – 4.6 ppm). The composition was analysed as 57:43 (PNVP:PNVCL) for Star-random 3 and 56:44 (PNVP:PNVCL) for Star-random 6. The yields of Star-random 3 and Star-random 6 were 22% and 25%, respectively. The SEC traces of Star-random 3 and 6 are shown in Figure 5.31. The M_n of Star-random 3 (Figure 5.31-I) was measured by SEC as 2.11 x 10^4 gmol^{-1} with a PDI of 1.42. Therefore, the M_n of each arm is approximately 7.0 x 10^3 gmol^{-1}, indicating that there are 36 repeat units of NVP and 22 repeat units for NVCL in each arm, based on composition of PNVP:PNVCL (57:43). In comparison, the M_n of Star-random 6 (Figure 5.31-II) was measured by SEC as 2.73 x 10^4 gmol^{-1} with a PDI of 1.36. Therefore, the M_n of each arm is approximately 6.8 x 10^4 gmol^{-1}, indicating that there are 34 repeat units of NVP and 22 repeat units for VAc in each arm, based on composition of PNVP:PNVCL (56:44). Figure 5.32, a plot of Log M against Wf / dLog

M, shows the comparison of molecular weight distributions between Star-random 3 and 6. Both distributions are monomodal which supports the result observed in Figure 5.31.

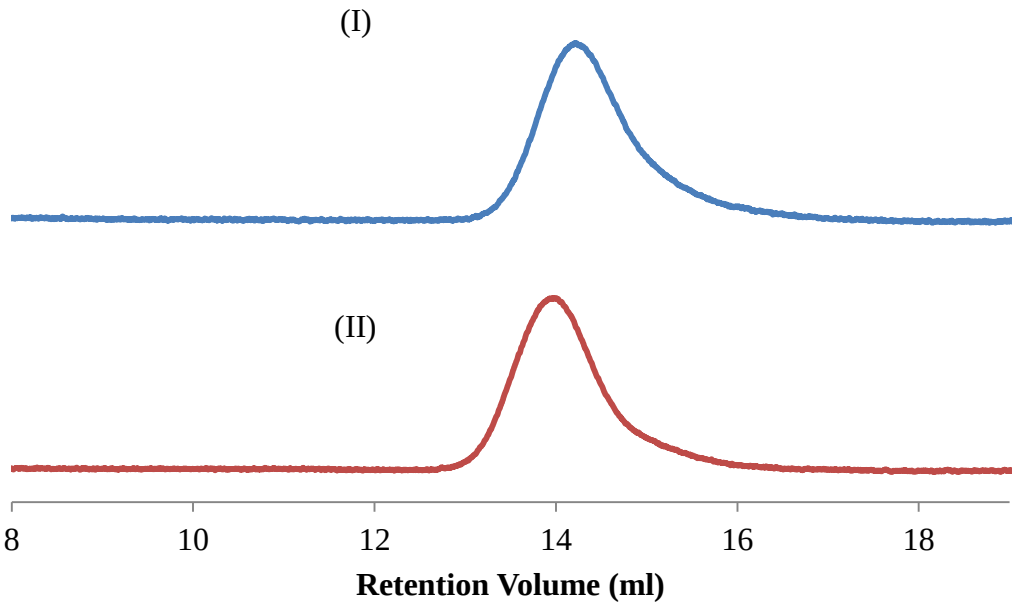

Figure 5.31. Comparison of SEC traces (refractive index) of (I) Star-random 3 and (II) Star-random 6

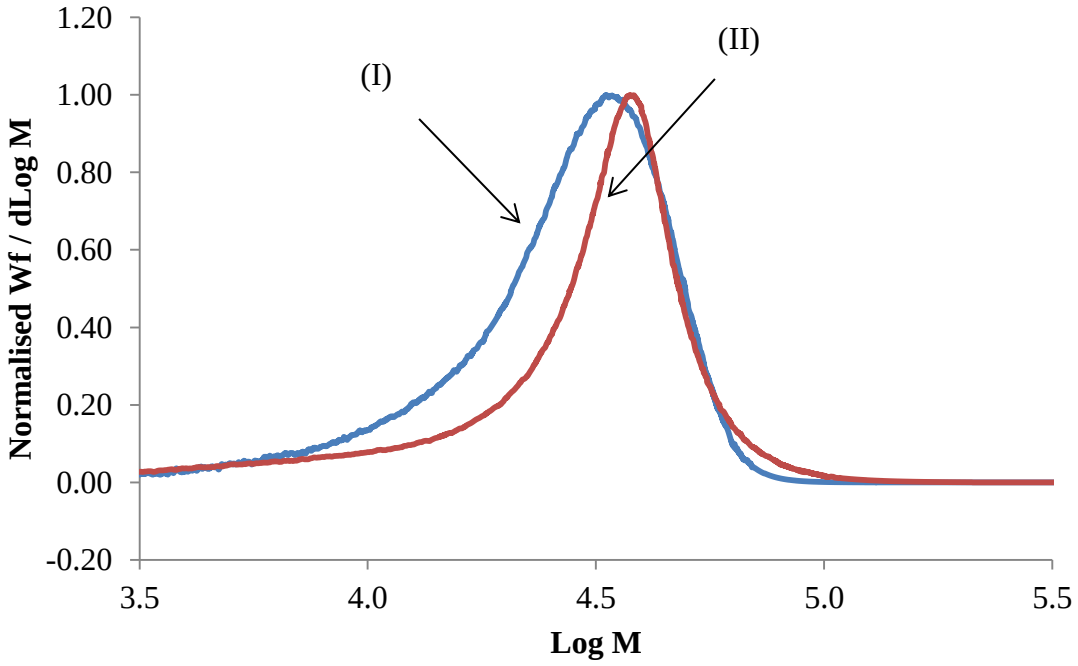

Figure 5.32. Plot of Log M against normalised Wf / dLog M showing the molecular weight distribution of (I) Star-random 3 and (II) Star-random 6

5.4. Summary

5.4.1. Star 1-6

RAFT agents 9-11, were used to synthesise Star 1-6, containing either PNVP, PVAc or PNVCL. The homopolymerisation of NVP in the presence of RAFT agents 9 and 10 in bulk, were shown to have living characteristics. SEC showed single mode molecular weight distribution with narrow PDI. M_n increased in a linear fashion with increasing conversion in the case of Star 1 and 2. For Star 1 and 2 the $\overline{DP}$ of each arm was calculated to be 66 and 50, respectively. RAFT agent 11 was also used to mediate the polymerisation of NVP and VAc to synthesise Star 3 and 4, respectively. The M_n found experimentally by SEC and NMR spectroscopy for Stars 3 and 4 were observed to be close to the respective theoretical M_n. SEC showed single mode molecular weight distribution with narrow PDI. For Star 3 and 4 the $\overline{DP}$ of each arm was calculated to be 55 and 62, respectively. RAFT agents 9 and 11 were used to mediate the polymerisation of NVCL, in order to synthesise three (Star 5) and four (Star 6) armed PNVCL, respectively. However, bimodal molecular weight distributions and broad PDI were observed in both cases. This could be attributed to hybrid behaviour and termination reactions.

5.4.2. Star-block 1-4

Star 3 and 4, were used to synthesise Star-block 1-4, containing either PNVP, PVAc or PNVCL. Star-blocks generally have very complex structures and hence hydrodynamic volumes in comparison with their linear homopolymers. Therefore, M_n values obtained by SEC are not that reliable however, M_p and PDI provide useful information on their formation. Star 3 (PNVP 4 arm star) and 4 (PVAc 4 arm star), were used as macroCTA's to synthesise Star-block 1-4, containing PNVP, PVAc or PNVCL. Star 3 was used to mediate the polymerisation of VAc and NVCL, to synthesise Star-block 1 and 2, respectively. Comparison of SEC traces for Star 3 against Star-block 1 and 2 showed bimodal molecular weight distributions with PDI and M_p increasing significantly. For Star-block 1 and 2 the overall $\overline{DP}$ of each arm was calculated to be 139 and 216, respectively. Star 4 was used to mediate the polymerisation of NVP and NVCL to synthesise, Star-block 3 and 4, respectively. Comparison of SEC traces for

Star 4 against Star-block 3 and 4 showed SEC with broader PDI and increasing M_p. For Star-block 3 and 4 the overall $\overline{DP}$ of each arm was calculated to be 512 and 170, respectively.

5.4.3. Star-random 1-6

RAFT agents 9 and 11 were used to control the random copolymerisation reactions of various combinations of NVP, VAc and NVCL, to prepare Star-random 1-6. All SEC traces of Star-random 1-6 showed monomodal molecular weight distributions and narrow PDI. All the star random copolymers synthesised in this study are soluble in water at ambient temperature.

Star-random 1 was found to have 59 repeat units of NVP and 30 repeat units of VAc in each arm, whilst Star-random 4 was found to have 83 repeat units of NVP and 42 repeat units of VAc. Both calculations were based on a composition of 72:28 (PNVP:PVAc). Star-random 2 was found to have 46 repeat units of NVCL and 29 repeat units of VAc in each arm, based on a composition of 72:28 (PNVCL:PVAc). Star-random 5 was found to have 36 repeat units of NVCL and 16 repeat units of VAc in each arm, based on a composition of 76:24 (PNVCL:PVAc). Star random 3 was found to have 36 repeat units of NVP and 22 repeat units of NVCL in each arm, based on a composition of 57:43 (PNVP:PNVCL). Star-random 6 was found to have 34 repeat units of NVP and 22 repeat units of NVCL in each arm, based on a composition of 56:44.

5.5. References

1. Roovers, J., In *In Star and Hyperbranched Polymers*, Mishra, M.; Kobayashi, K., Eds. Marcel Dekker: New York, 1998; p 285.
2. Hadjichristidis, N.; Pitsikalis, M.; Pispas, S.; Iatrou, H. *Chemical Reviews* **2001,** 101, (12), 3747-3792.
3. Inoue, K. *Progress in Polymer Science* **2000,** 25, (4), 453-571.
4. Barner-Kowollik, C.; Davis, T. P.; Stenzel, M. H. *Australian Journal of Chemistry* **2006,** 59, (10), 719-727.
5. Hawker, C. J. *Angewandte Chemie-International Edition in English* **1995,** 34, (13-14), 1456-1459.
6. Matyjaszewski, K.; Xia, J. H. *Chemical Reviews* **2001,** 101, (9), 2921-2990.
7. Hadjichristidis, N.; Iatrou, H.; Pitsikalis, M.; Mays, J. *Progress in Polymer Science* **2006,** 31, (12), 1068-1132.
8. *Handbook of RAFT Polymerization*. Wiley-VCH: 2008.
9. Nguyen, T.; Eagles, K.; Davis, T.; Barner-Kowollik, C.; Stenzel, M. *Journal of Polymer Science Part a-Polymer Chemistry* **2006,** 44, (15), 4372-4383.
10. Stenzel, M. H.; Davis, T. P.; Barner-Kowollik, C. *Chemical Communications* **2004**, (13), 1546-1547.
11. Bernard, J.; Favier, A.; Zhang, L.; Nilasaroya, A.; Davis, T. P.; Barner-Kowollik, C.; Stenzel, M. H. *Macromolecules* **2005,** 38, (13), 5475-5484.
12. Boschmann, D.; Vana, P. *Polymer Bulletin* **2005,** 53, (4), 231-242.
13. Fleet, R.; McLeary, J. B.; Grumel, V.; Weber, W. G.; Matahwa, H.; Sanderson, R. D. *Macromolecular Symposia* **2007,** 255, 8-19.

Chapter 6

Temperature responsive polymers

6.1. Introduction

"Smart materials" are those which can respond to an external stimuli such as; pH, ionic strength, electric / magnetic field, light or temperature. Polymeric materials which respond to a change in temperature or pH are the most studied and important in biomedical applications.[1-10] This chapter focuses on stimuli responsive polymers which respond to a change in temperature, i.e. temperature responsive polymers. Temperature responsive polymers can exhibit a change in their solubility / conformation in a given solvent, upon heating or cooling. An upper critical solution temperature (UCST) is observed for polymers which demix on cooling; generally in organic solvents.[11] Polymers which are soluble in aqueous solution can exhibit a lower critical solution temperature (LCST); demixing as temperature rises.[12-14] The polymer is soluble below the LCST and has a coil conformation. However, as temperature is increased above the LCST, the polymer undergoes a phase transition and a globule conformation is subsequently formed, thus the solution becomes cloudy, Figure 6.1.[15]

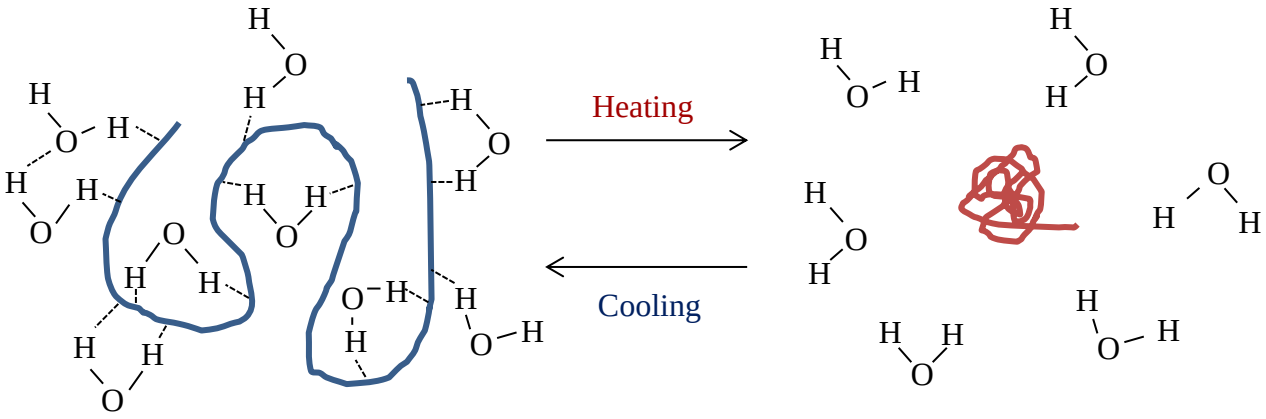

Figure 6.1. Effect on phase transition by heating and cooling an aqueous polymer solution above and below the LCST

The LCST of the polymer depends on the hydrophilic / hydrophobic balance of the monomer units and its capability of creating hydrogen bonds with water. Polymers which are soluble in water and exhibit an LCST, contain hydrophilic groups (which can readily form hydrogen bonds with water) in addition to hydrophobic groups (carbon – carbon backbone chain). The phase transition can be explained by the hydrophobic effect.[16, 17] Polymer dissolution is given by the Gibbs free energy equation (Equation 6.1).

$$\Delta G_{mix} = \Delta H_{mix} - T\Delta S_{mix}$$ Equation 6.1

Typically, mixing between solvent and polymer occurs when the ΔG_{mix} at a certain temperature is negative. This can be achieved through the presence of H-bonding interactions between water molecules and polymer chains, or alternatively by increasing the temperature of the solution. Hence, the formation of hydrogen bonds between water molecules and hydrophilic groups on the polymer means a gain in enthalpy (ΔH) and favourability for dissolution. In terms of the hydrophobic groups present in the polymer, the water molecules need to reorganise around these groups which leads to an unfavourable loss of entropy (ΔS); both $\Delta H_{mix\ and}$ ΔS_{mix} are negative. As temperature rises, previously bonded water molecules are released from the polymer and the contribution of $T\Delta S_{mix}$ is greater than that for $\Delta H_{mix.}$ This results in the Gibbs free energy changing from negative (favourable) to positive (unfavourable) and ultimately phase separation.[13, 18]

The most widely studied polymer which exhibits an LCST in aqueous solution is poly(N-isopropylacrylamide) (PNIPAAm).[19, 20] This occurs in water at approximately 32°C, which is useful, as it is close to the lower end of the physiological range (30-40°C).[14, 20] PNIPAAm exhibits Type II Flory-Huggins behaviour, meaning that the LCST is almost independent of polymer chain length.[21] The LCST can be altered by copolymerising with either hydrophilic or hydrophobic monomers.[22-24] It has been reported that the presence of multiple secondary amide functions in PNIPAAm may lead to the formation of cooperative hydrogen bonding with other amide containing polymers, or more importantly proteins.[25, 26] Furthermore, PNIPAAm has been reported to break under hydrolysis and form small toxic amide compounds.[27, 28] Unlike PNIPAAm, poly(N-vinylcaprolactam) (PNVCL) has the advantage that upon hydrolysis there are no small amide compounds produced. However, neither PNVCL nor PNIPAAm can be considered bio inert due the presence of the hydrocarbon backbone chain which is not biodegradable.

PNVCL is also a polymer which exhibits an LCST in aqueous solution, generally observed between 31°C - 51°C.[27, 29-31] This range is attributed to PNVCL showing "classical" Flory-Huggins (Type I) temperature responsive phase behaviour, as the LCST is dependent on polymer concentration and chain length.[21] The LCST is lowered when either of the polymer concentration or chain length is increased. PNVCL

is well known to be a biocompatible polymer which is of particular interest in the pharmaceutical industry.[27, 32-34]

The phase transition of aqueous PNVCL solutions has been investigated using light scattering,[30, 35] calorimetry,[30, 35, 36] fluorescence,[37] small-angle X-ray scattering,[38] infrared spectroscopy,[39, 40] NMR spectroscopy[38] and absorption millimetre-wave measurements.[41] Figure 6.2 shows the hydration behaviour of PNVCL compared to that of PNIPAAm.[40]

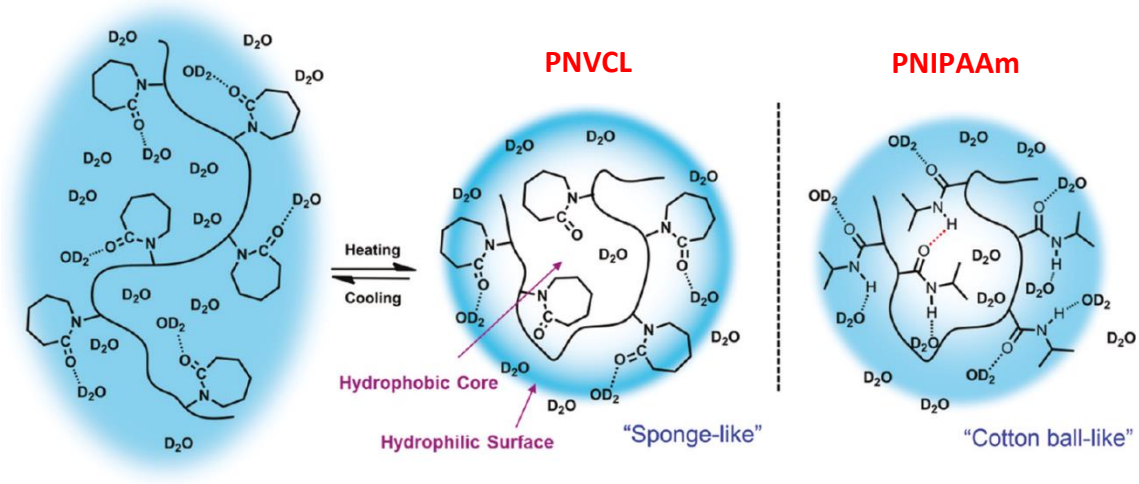

Figure 6.2. Comparison of the hydration behaviour of PNVCL with PNIPAAm

Sun *et al.* found that upon heating an aqueous solution of PNVCL, the phase transition is initially driven in the first stage (below the LCST) *via* a hydrogen bonding transformation of the amide groups, followed by the hydrophobic interactions above the LCST.[40] PNVCL mesoglobules were reported to form "sponge-like" structures above the LCST, whilst PNIPAAm mesoglobules were reported to form "cotton ball-like" structures, which are more compact due to the hydrogen bonding between polymer chains. Moreover, it was concluded that there is a distribution gradient of water molecules in PNVCL mesoglobules, which is not observed in PNIPAAm mesoglobules. Spěváček *et al.* have recently reported that PNVCL exhibits a strong tendency to aggregate and shows that the amount of fully dehydrated carbonyl groups in PNVCL mesoglobules is relatively small.[38] This was attributed to the lack of hydrogen bonding between polymer chains, indicating that water molecules trapped inside the mesoglobules, serve as intermediaries of interactions between PNVCL moieties.

The LCST range of PNVCL aqueous solutions can be widened further *via* copolymerisation with either hydrophilic or hydrophobic monomers.[42] It has been

reported that when NVCL is copolymerised with vinyl acetate (VAc) to synthesise PNVCL-*ran*-PVAc, the LCST is lowered due to the incorporation of PVAc, which is hydrophobic. For example, PNVCL-*ran*-PVAc with 66 mol % PVAc showed an LCST in aqueous solution at 5.0°C.[43-46] NVCL has also been copolymerised with the hydrophilic monomer, N-vinylpyrrolidone (NVP) and a copolymer with 66 mol % PNVP was reported to show an LCST in aqueous solution at approximately 80°C.[46-48]

The use of RAFT enables the synthesis of PNVCL chains with controllable molecular weights and PDI's. Therefore, it is possible for the LCST to be easily altered by changing polymer chain length. Recently, several groups have used RAFT agents to produce well defined PNVCL with controlled molecular weights. *O*-ethyl-*S*-(1-methoxycarbonyl)ethyl dithiocarbonate (Rhodixan® A1) was used to mediate the polymerisation of NVCL in 1,4 dioxane at 60°C.[49] PNVCL polymers ranging from 1.80 x 10^4 - 1.50 x 10^5 gmol^{-1} were synthesised with low PDI's (< 1.2) and cloud points ranging from 33 - 46°C, depending on molecular weight.

Shao *et al.* used *S*-benzyl-*S*-(benzyl propionate) trithiocarbonate and *N*, *N*-diethyl-*S*-(α, α-dimethyl-α-acetic acid) dithiocarbamate as RAFT agents, to mediate the polymerisation of NVCL.[50] It was reported that a PNVCL sample with a M_n of 6.80 x 10^3 gmol^{-1} and PDI of 1.29, containing a hydrophobic end group exhibited a sharper phase transition at a low temperature compared to PNVCL (M_n = 7.20 x 10^3, PDI = 1.15) without a hydrophobic chain end. PNVCL samples with molecular weights ranging from 3.72 x 10^3 – 2.06 x 10^4 gmol^{-1} were observed to have LCST's ranging from 45°C - 34°C.

This chapter describes the analysis of polymer samples containing NVCL, synthesised in Chapters 3-5, to determine their temperature responsive behaviour. PNVCL synthesised *via* RAFT, with M_n ranging from 1.02 x 10^4 – 2.62 x 10^4 gmol^{-1} and PDI ranging from 1.36 - 1.48, were analysed by UV-Visible spectroscopy to compare their temperature responsive behaviour. For comparison, a PNVCL sample was also synthesised *via* conventional free radical polymerisation (FRP), with a M_n of 9.97 x 10^4 gmol^{-1} and a PDI of 2.92. PNVCL-*ran*-PVAc and PNVCL-*ran*-PNVP samples synthesised *via* RAFT were also investigated to determine their temperature responsive behaviour in water. Furthermore, random copolymers synthesised *via* conventional FRP were analysed for comparison with those synthesised *via* RAFT. To the best of our knowledge, there are no reports on the temperature responsive behaviour of star random copolymers containing NVCL.

Star 5-6 and PNVP-*block*-PNVCL samples were investigated for their temperature responsive behaviour, but since they all exhibited bimodal molecular weight distributions in SEC, the resulting LCST's were believed not to be accurate. Therefore, the results are not reported here.

6.2. Experimental

6.2.1. Materials

N-vinylcaprolactam (ISP) was recrystallised from either pentane or hexane then distilled under reduced pressure and stored under nitrogen at -4°C. 4,4'-Azobis(4-cyanovaleric acid) (ACVA) (Sigma Aldrich, ≥98%) used as supplied. 2, 2'-Azobis(isobutyonitrile) (AIBN) (Sigma Aldrich) was recrystallized from methanol. 1,4 dioxane was dried over calcium hydride and distilled under reduced pressure. All dry solvents were obtained from Durham Chemistry Department Solvent Purification System (SPS). Purification grade (HPLC) solvent was pushed from its storage container under low argon pressure through two stainless steel columns containing activated alumina or copper catalyst depending on solvent used. Trace amounts of water were removed by the alumina, producing a dry solvent. In addition, deoxygenated solvent was achieved when it was suitable for a copper catalyst column to be used. Water content values - DCM < 25.1ppm, DMF < 735.1ppm, Toluene < 21.3ppm, THF < 35.7 ppm, Chloroform < 20.9ppm, Diethyl ether < 19.1ppm, Hexane < 7.6 ppm and Acetonitrile < 8.7ppm. All other solvents were analytical grade and used without any purification.

6.2.2. Characterisation techniques

Size exclusion chromatography (SEC) analysis on PNVCL sample was carried out as in Chapter 3, Section 3.2.2.

The LCST of aqueous polymer samples at 500nm was determined by using a Varian Cary – 100 UV-Visible spectrophotometer attached with temperature controller. Polymer samples were prepared in deionised water with a concentration of 2 mg/ml. The rate at which temperature was increased was 1°C / min and then temperature was held for a further 1 minute before each measurement was taken. The temperature was increased above the LCST and the polymer solution was subsequently cooled below the LCST at the same rate and held for 1 minute at each time-point. LCST was taken at the point where transmittance began to decrease.

Images were also taken using an optical microscope to observe the reversible change in conformation and LCST. The optical micrographs of the aqueous polymer solution were taken by Olympus BX50WI microscope with 50 x optical zoom lens, cross

polarizers, 589nm tint plate and TMS 93 controller linked to T600 hotstage connect to a Pixelink A60z firewire camera through a Linkam Linksys32 software.

Photographic images were taken using a standard digital camera.

6.2.3. Synthesis of poly(N-vinylcaprolactam) *via* conventional free radical polymerisation

To a 50 ml Schlenk tube containing a magnetic stirrer bar was added NVCL (2.06 g, 14.8 mmol), AIBN (5.00 mg, 3.05 x 10^{-2} mmol) and 1, 4 dioxane (2 ml). The polymerisation mixture was thoroughly degassed by four freeze pump thaw cycles. The Schlenk tube was then back-filled with nitrogen gas, placed in an oil bath set at 80°C and stirred for 16 h. The Schlenk tube was removed from the oil bath and allowed to cool to ambient temperature. The polymerisation mixture was a pale cream solid gel. Tetrahydrofuran (20 ml) was added to the mixture to dissolve the product and then added drop wise to stirring hexane (200 ml). A white precipitate immediately formed which was filtered off and dried under reduced pressure to give a white solid of PNVCL (1.56 g, 76% yield).

6.2.4. Synthesis of NVCL containing polymers *via* RAFT

PNVCL samples synthesised *via* RAFT are described in Chapter 3 (Sections 3.2.7, 3.2.11, 3.2.16 and 3.2.20). Linear PNVCL-*ran*-PVAc samples were synthesised in Chapter 4 (Sections 4.2.8 and 4.2.11). Linear PNVCL-*ran*-PNVP samples were synthesised in Chapter 4 (Sections 4.2.9 and 4.2.12). Star PNVCL-*ran*-PVAc samples were synthesised in Chapter 5 (Sections 5.2.16 and 5.2.19). Star PNVCL-*ran*-PNVP samples were synthesised in Chapter 5 (Sections 5.2.17 and 5.2.20)

6.3. Results and Discussion

6.3.1. Temperature responsive poly(N-vinylcaprolactam)

PNVCL with controlled molecular weights and architectures, reported in Chapters 3 - 5, were analysed to determine their temperature responsive behaviour in water. The cloud point was analysed using UV - Visible spectroscopy

6.3.1.1. Linear poly(N-vinylcaprolactam)

PNVCL (M_n = 1.02 x 10^4 $gmol^{-1}$, PDI = 1.48) synthesised *via* RAFT using RAFT agent 2, was investigated for its temperature responsive behaviour. Figure 6.3 shows the plot of % transmittance against temperature (°C). The % transmittance of the polymer solution remained steady at 95% until 40°C; the solution was homogeneous and clear. After 40°C, the polymer solution quickly started to become cloudy and there was a significant drop in the % transmittance, reaching 0% at approximately 42°C. Therefore, the LCST was determined to be at 40°C. The polymer solution was then cooled to 25°C. The polymer solution stayed cloudy until 38°C and then a significant rise in the % transmittance occurred. The polymer solution became clear again at 36°C and this remained constant as temperature decreased to 25°C. The system is reversible; however there is a significant hysteresis, as there is a 4°C difference between the heating and cooling traces. This is explained further in Section 6.4. Furthermore, the aqueous polymer sample was re-heated then re-cooled and superimposable traces were obtained, indicating that the system is reproducible.

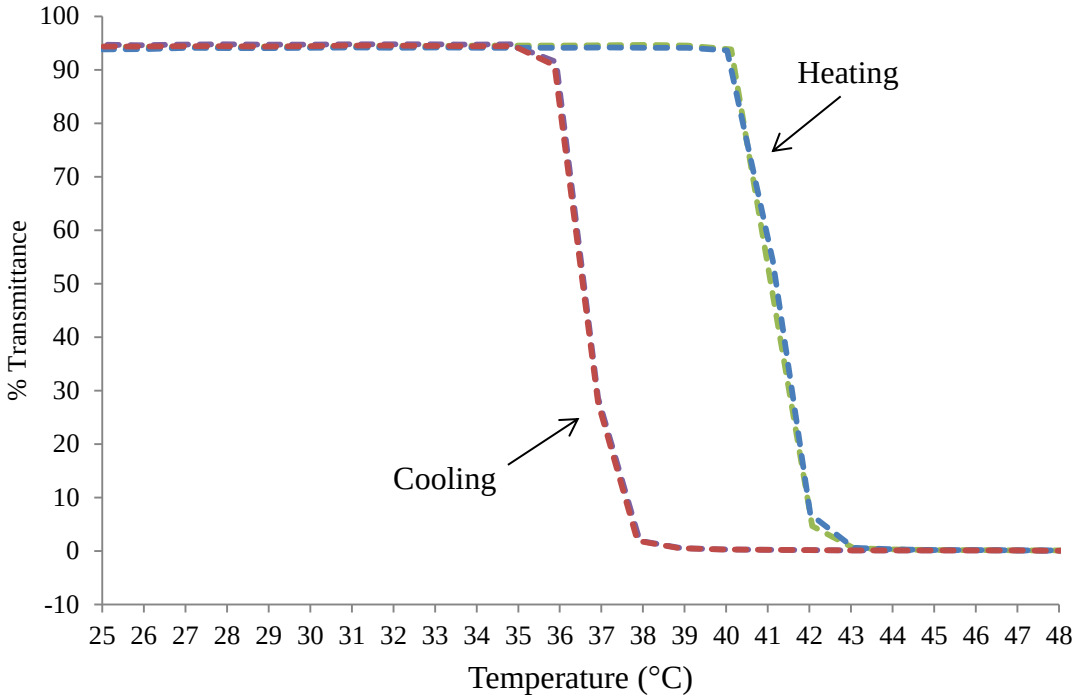

Figure 6.3. Plot showing % transmittance against temperature (°C) for PNVCL synthesised in the presence of RAFT agent 2. (Green / purple lines for 1st heating - cooling cycle, blue / red lines for 2nd heating – cooling cycle)

Figure 6.4 shows the comparison of photographic images of the PNVCL solution, below and above the LCST. Below the LCST (Figure 6.4-I) the sample is clear and homogenous and above the LCST (Figure 6.4-II), the sample is very turbid.

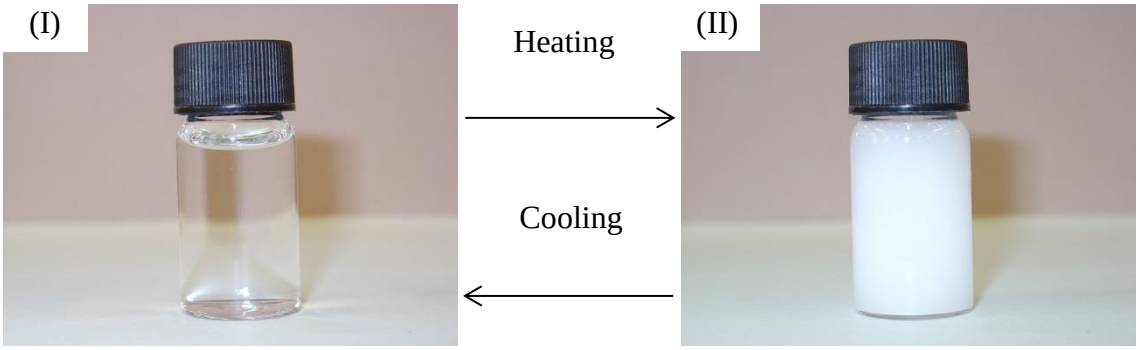

Figure 6.4. Comparison of photographic images of PNVCL synthesised via RAFT in aqueous solution

Figure 6.5 shows the optical microscope images of the PNVCL sample taken below and above the LCST. Below the LCST the polymer chains are soluble and are in

a hydrated coil conformation (Figure 6.5-I). Above the LCST the polymer chains collapse and form globules which are apparent in the image (Figure 6.5-II).

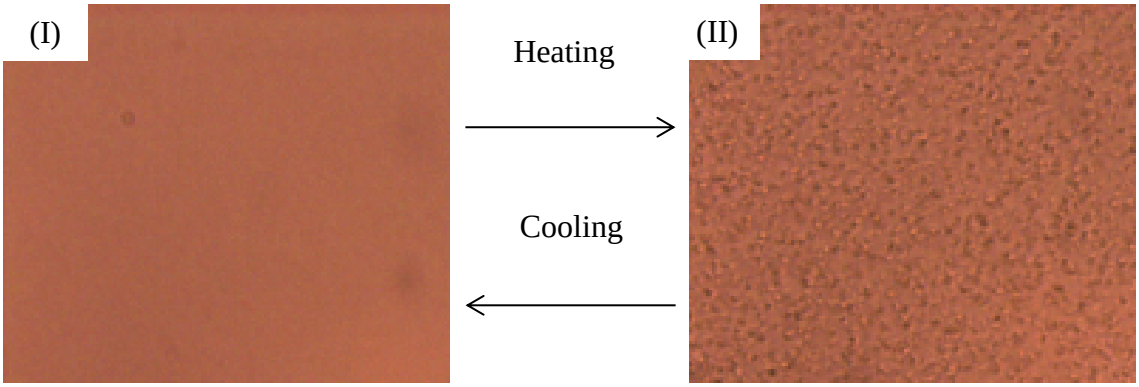

Figure 6.5. Comparison of optical microscope images (I) above and (II) below the LCST for PNVCL synthesised in the presence of RAFT agent 2

PNVCL (M_n = 1.52 x 10^4 $gmol^{-1}$, PDI = 1.48) synthesised *via* RAFT using RAFT agent 3 was investigated for its temperature responsive behaviour. Appendix 3, Figure 1 shows the plot of % transmittance against temperature (°C). The % transmittance of the polymer solution remained steady at 100% until 39°C; the solution was homogeneous and clear. After 39°C, the polymer solution quickly started to become cloudy and there was a significant drop in the % transmittance, reaching 0% at approximately 42°C. Therefore, the LCST was determined to be at 39°C. The polymer solution was then cooled to 25°C. The polymer solution stayed cloudy until 36°C and then a significant rise in the % transmittance occurred. The polymer solution became clear again at 33°C and this remained constant as temperature decreased to 25°C. The system is reversible; however there is a significant hysteresis, as there is a 4°C difference between the heating and cooling traces. This is explained further in Section 6.4.

Appendix 3, Figure 2 shows the optical microscope images taken of the PNVCL sample below and above the LCST. Below the LCST the polymer chains are soluble and are in a hydrated coil conformation (Appendix 3, Figure 2-I). Above the LCST the polymer chains collapse and form globules which are apparent in the image (Appendix 3, Figure 2-II).

A PNVCL sample (M_n = 1.65 x 10^4 $gmol^{-1}$, PDI = 1.38) synthesised *via* RAFT also using RAFT 3 was investigated for its temperature responsive behaviour.

Appendix 3, Figure 3 shows the plot of % transmittance against temperature (°C). The % transmittance of the polymer solution remained steady at 100% until 40°C; the solution was homogeneous and clear. After 40°C, the polymer solution quickly started to become cloudy and there was a significant drop in the % transmittance, reaching 0% at approximately 42°C. Therefore, the LCST was determined to be at 40°C. The polymer solution was then cooled to 25°C. The polymer solution stayed cloudy until 38°C and then a significant rise in the % transmittance occurred. The polymer solution became clear again at 36°C and this remained constant as temperature decreased to 25°C. The system is reversible; however there is a significant hysteresis, as there is a 4°C difference between the heating and cooling traces. This is explained further in Section 6.4.

Appendix 3, Figure 4 shows the optical microscope images of the PNVCL sample taken below and above the LCST. Below the LCST the polymer chains are soluble in aqueous solution and are in a hydrated coil conformation (Appendix 3, Figure 4-I). Above the LCST the polymer chains collapse and form globules which are apparent in the image (Appendix, Figure 4-II).

PNVCL (M_n = 2.08 x 10^4 $gmol^{-1}$, PDI = 1.36) synthesised *via* RAFT using RAFT agent 5 was investigated for its temperature responsive behaviour. Appendix 3, Figure 5 shows the plot of % transmittance against temperature (°C). The % transmittance of the polymer solution remained steady at approximately 100% until 39°C; the polymer solution was homogeneous and clear. After 39°C, the polymer solution quickly started to become cloudy and there was a significant drop in the % transmittance, reaching 0% at approximately 41°C. Therefore, the LCST was determined to be at 39°C. The polymer solution was then cooled to 25°C. The polymer solution remained cloudy until 37°C and then a significant rise in % transmittance occurred. The polymer solution became clear again at 35°C and this remained constant as temperature decreased to 25°C. The system is reversible; however there is a significant hysteresis as there is a 4°C difference between the heating and cooling traces. This is explained further in Section 6.4.

Appendix 3, Figure 6 shows the optical microscope images of the PNVCL sample taken below and above the LCST. Below the LCST the polymer chains are soluble in aqueous solution and are in a hydrated coil conformation (Appendix 3, Figure 6-I). Above the LCST, the polymer chains collapse and form globules which are apparent in the image (Appendix 3, Figure 6-II).

PNVCL (M_n = 2.62 x 10^4 $gmol^{-1}$, PDI = 1.36) synthesised *via* RAFT using RAFT agent 7 was investigated for it temperature responsive behaviour. Appendix 3, Figure 7 shows the plot of % transmittance against temperature (°C). The % transmittance of the polymer solution remained steady at 100% until 38°C; the solution was homogeneous and clear. After 38°C, the polymer solution quickly started to become cloudy and there was a significant drop in the % transmittance, reaching 0% at 40°C. Therefore, the LCST was determined to be at 38°C. The polymer solution was then cooled to 25°C. The polymer solution remained cloudy until 36°C and then a significant rise in the % transmittance occurred. The polymer solution became clear again at 34°C and this remained constant as temperature decreased to 25°C. The system is reversible; however there is a significant hysteresis, as there is a 4°C difference between the heating and cooling traces. This is explained further in Section 6.4.

Appendix 3, Figure 8 shows the optical microscope images of the PNVCL sample taken below and above the LCST. Below the LCST the polymer chains are soluble in aqueous solution and are in a hydrated coil conformation (Appendix 3, Figure 8-I). Above the LCST, the polymer chains collapse and form globules which are apparent in the image (Appendix 3, Figure 8-II).

6.3.1.2. Poly(N-vinylcaprolactam) *via* conventional free radical polymerisation

The temperature responsive behaviour of PNVCL (M_n = 9.97 x 10^4 $gmol^{-1}$, PDI = 2.92) synthesised *via* conventional FRP was investigated to provide comparison with PNVCL samples prepared *via* RAFT. Appendix 3, Figure 9 shows the plot of % transmittance against temperature (°C). The % transmittance of the polymer solution remained steady at approximately 100% until 33.5°C; the polymer solution was homogeneous and clear. After 33.5°C, the polymer solution quickly started to become cloudy and there was a significant drop in the % transmittance, reaching 0% at approximately 35.5°C and then stayed constant. Therefore, the LCST was determined to be at 33.5°C. The polymer solution was then cooled to 25°C. The polymer solution stayed cloudy until 30.5°C and then a significant rise in the % transmittance occurred. The polymer solution became clear again at 28.5°C and this remained constant as temperature decreased to 25°C. The system is reversible; however there is a significant hysteresis, as there is a 5°C difference between the heating and cooling traces. This is explained further in Section 6.4.

Appendix 3, Figure 10 shows the optical microscope images of the PNVCL sample taken below and above the LCST. Below the LCST the polymer chains are soluble in aqueous solution and are in a hydrated coil conformation (Appendix 3, Figure 10-I). Above the LCST the polymer chains collapse and form globules which are apparent in the image (Appendix 3, Figure 10-II).

6.3.1.3. Comparison of LCST for poly(N-vinylcaprolactam)

Table 6.1 shows a comparison of the LCST's exhibited by various PNVCL homopolymers analysed within this chapter.

Table 6.1. Comparison of M_n, PDI and LCST for PNVCL homopolymers

Entry	RAFT agent	M_n (x 10^4 $gmol^{-1}$)	PDI	LCST (°C)
1	-	9.97	2.92	33
2	2	1.02	1.48	40
3	3	1.52	1.48	39
4	3	1.65	1.38	40
5	5	2.08	1.36	39
6	7	2.62	1.36	38

PNVCL synthesised here *via* conventional free radical polymerisation (M_n = 9.97 x 10^4 $gmol^{-1}$, PDI = 2.92) exhibited an LCST of 33°C (Table 6.1; Entry 1), which is comparable to that reported in the literature.[28, 37] PNVCL samples with M_n ranging from 1.02 x 10^4 $gmol^{-1}$ – 2.08 x 10^4 $gmol^{-1}$ and PDI ranging from 1.36-1.48 (Entry 2-5), were observed to exhibit comparable LCST's in the region of 39-40°C; known as fever temperature.[51, 52]

The effect of molecular weight on PNVCL prepared *via* RAFT was investigated. PNVCL with M_n of 1.02 x 10^4 $gmol^{-1}$ (Entry 2) showed an LCST at 40°C, whereas PNVCL with a M_n of 2.62 x 10^4 $gmol^{-1}$ exhibited an LCST at 38°C. This result is believed to be due to PNVCL exhibiting "classical" Flory-Huggins (Type 1) behaviour.[21] This is more evident when PNVCL synthesised *via* RAFT is compared with PNVCL synthesised *via* conventional FRP, where the molecular weight is far greater and the LCST exhibited is far lower.

6.3.2. Temperature responsive random copolymers

Linear and star random copolymers of PNVCL-*ran*-PVAc and PNVCL-*ran*-PNVP were analysed to determine their LCST. The resulting LCST's were compared to that determined for the conventional random copolymerisations *via* FRP.

6.3.2.1. PNVCL-*ran*-PVAc

6.3.2.1.1. Linear PNVCL-*ran*-PVAc *via* RAFT

Linear PNVCL-*ran*-PVAc (M_n = 2.79 x 10^4 $gmol^{-1}$, PDI = 1.18) synthesised *via* RAFT using RAFT agent 5, with a composition of 64:36 (PNVCL:PVAc), was investigated for its temperature responsive behaviour. At ambient temperature the polymer solution was cloudy. Hence, the solution was cooled to 3°C and a clear, homogenous colourless liquid was observed. Figure 6.6 shows the plot of % transmittance against temperature (°C). The % transmittance of the polymer solution remained relatively steady until 18°C. The small fluctuations are due to condensation on the UV cuvette. After 18°C, the polymer solution quickly started to become cloudy and there was a significant drop in the % transmittance, reaching 0% at approximately 22°C. Therefore, the LCST was determined to be at 18°C. The polymer solution was then cooled to 3°C. The polymer solution remained cloudy until 16°C and then a significant rise in % transmittance occurred. The polymer solution became clear again at 13°C and this remained constant as temperature decreased to 3°C. The system is reversible; however there is a significant hysteresis, there is a 5°C difference between the heating and cooling traces. This is explained further in Section 6.4.

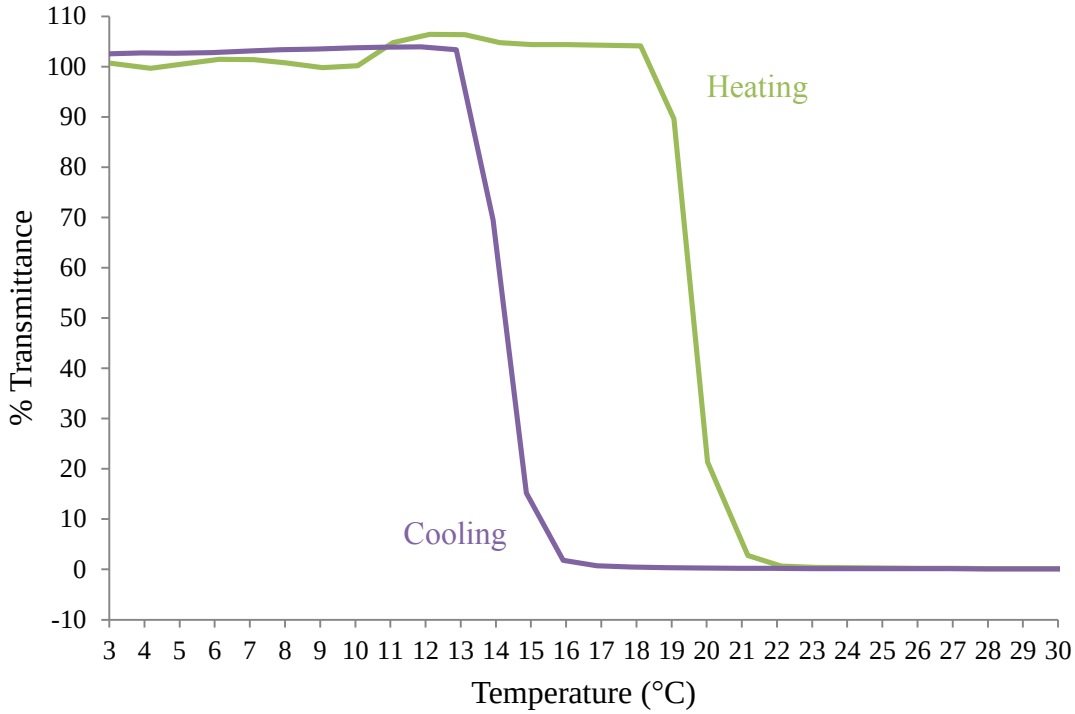

Figure 6.6. Plot showing % transmittance against temperature (°C) for PNVCL-*ran*-PVAC prepared in the presence of RAFT agent 5

Figure 6.7 shows the comparison of photographic images of PNVCL-*ran*-PVAc solution below and above the LCST. The aqueous solution was cooled to 15°C and found to be a clear homogenous solution (Figure 6.7-I). At 23°C the sample was observed to be very turbid (Figure 6.7-II).

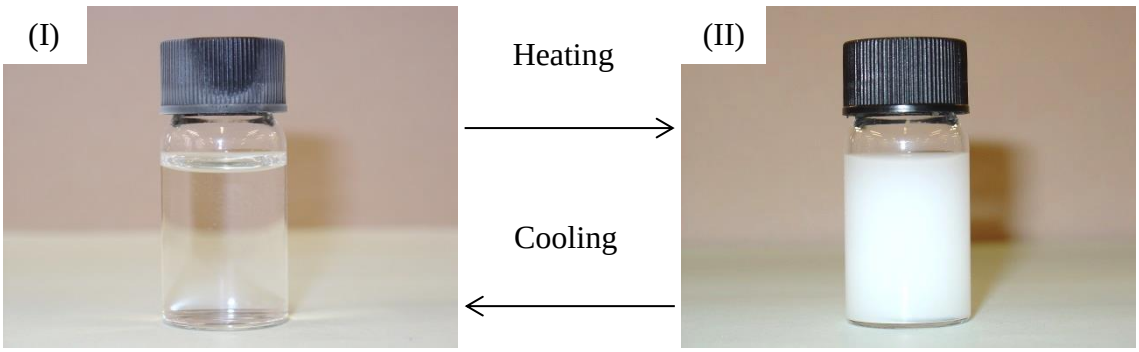

Figure 6.7. Comparison of photographic images of PNVCL-*ran*-PVAc synthesised *via* RAFT in aqueous solution

Figure 6.8 shows the optical microscope images of PNVCL-*ran*-PVAc solution taken below and above the LCST. Below the LCST the polymer chains are soluble solution and are in a hydrated coil conformation (Figure 6.8-I). Above the LCST, the

polymer chains collapse and form globules which are apparent in the image (Figure 6.8-II).

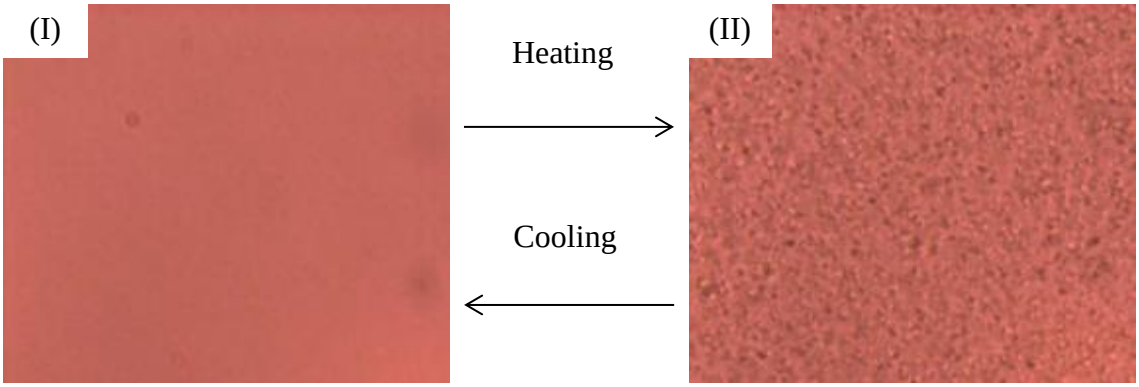

Figure 6.8. Comparison of optical microscope images above and below the LCST for PNVCL-*ran*-PVAc synthesised in presence of RAFT agent 5

6.3.2.1.2. Star-random 2

Three armed star PNVCL-*ran*-PVAc (Star-random 2) (M_n = 2.65 x 10^4 $gmol^{-1}$, PDI = 1.31) synthesised *via* RAFT using RAFT agent 9, with a composition of 72:28 (PNVCL:PVAc), was and investigated for its temperature responsive behaviour. At ambient temperature the polymer solution was cloudy. Hence, the solution was cooled to 3°C and a clear, homogenous colourless liquid was observed. Appendix 3, Figure 11 shows the plot of % transmittance against temperature (°C). The % transmittance of the polymer solution remained relatively steady until 19°C. The fluctuations are due to condensation on the UV cuvette. After 19°C, the polymer solution quickly started to become cloudy and there was a significant drop in the % transmittance, reaching 0% at 21°C. Therefore, the LCST was determined to be at 19°C. The polymer solution was then cooled to 3°C. The polymer solution remained cloudy until 15°C and then a significant rise in the % transmittance took place. The polymer solution became clear again at 13°C and this remained constant as temperature decreased to 3°C. The system is reversible; however there is a significant hysteresis, as there is a 6°C difference between the heating and cooling traces. This is explained further in Section 6.4.

Appendix 3, Figure 12 shows the optical microscope images of the PNVCL-*ran*-PVAc solution taken below and above the LCST. Below the LCST the polymer chains are soluble and are in a hydrated coil conformation (Appendix 3, Figure

12-I). Above the LCST, the polymer chains collapse and form globules which are apparent in the image (Appendix 3, Figure 12-II).

6.3.2.1.3. Star-random 5

Four armed star PNVCL-ran-PVAc (Star-random 5) (M_n = 2.35 x 10^4 $gmol^{-1}$, PDI = 1.23) synthesised *via* RAFT using RAFT agent 11, with a composition of 76:24 (PNVCL:PVAc), was investigated for its temperature responsive behaviour. At ambient temperature the polymer solution was cloudy. Hence, the solution was cooled to 3°C and a clear colourless liquid was observed. Appendix 3, Figure 13 shows the plot of % transmittance against temperature (°C). The % transmittance of the polymer solution remained relatively steady until 16°C. The fluctuations are due to condensation on the UV cuvette. After 16°C, the polymer solution quickly started to become cloudy and there was a significant drop in the % transmittance, reaching 0% at 19.5°C. Therefore, the LCST was determined to be at 16°C. The polymer solution was then cooled to 3°C. The polymer solution remained cloudy until 14°C and then a significant rise in the % transmittance was observed. The polymer solution became clear again at 10.5°C and this remained constant as temperature decreased to 3°C. The system is reversible, however there is a significant hysteresis, as there is a 5.5°C difference between the heating and cooling traces. This is explained further in Section 6.4.

Appendix 3, Figure 14 shows the optical microscope images of the PNVCL-*ran*-PVAc solution taken below and above the LCST. Below the LCST the polymer chains are soluble in aqueous solution and are in a hydrated coil conformation (Appendix 3, Figure 14-I). Above the LCST, the polymer chains collapse and form globules which are apparent in the image (Appendix 3, Figure 14-II).

6.3.2.1.4. PNVCL-*ran*-PVAc *via* conventional free radical polymerisation

PNVCL-*ran*-PVAc synthesised *via* conventional free radical polymerisation (M_n = 6.62 x 10^4 $gmol^{-1}$, PDI = 2.88), with a composition of 58:42 (PNVCL:PVAc), was also investigated for its temperature responsive behaviour to provide data for comparison. At ambient temperature the solution was cloudy. Hence, the polymer solution was cooled to 3°C and the temperature was slowly risen to 30°C. The polymer solution turned into a homogenous clear liquid upon cooling. Figure 6.9 shows the plot of % transmittance against temperature (°C). The % transmittance of the polymer solution

remained steady until 6°C. After 6°C, the polymer solution slowly started to become cloudy and there is a slow decrease in the % transmittance, reaching 0% at 20°C. Therefore, the LCST was determined to be at approximately 6°C. The polymer solution was then cooled to 3°C. The polymer solution remained cloudy until approximately 15°C and then slowly there was a rise in % transmittance. Due to limitations of the UV-Visible spectrometer the temperature was unable to go below 3°C in the required timeframe. However, at 3°C the % transmittance was close to the starting % transmittance. The system is reversible, however there is a significant hysteresis, as there is a 5°C difference between the heating and cooling traces. This is explained further in Section 6.4. Furthermore, the LCST range of approximately 14°C is very broad.

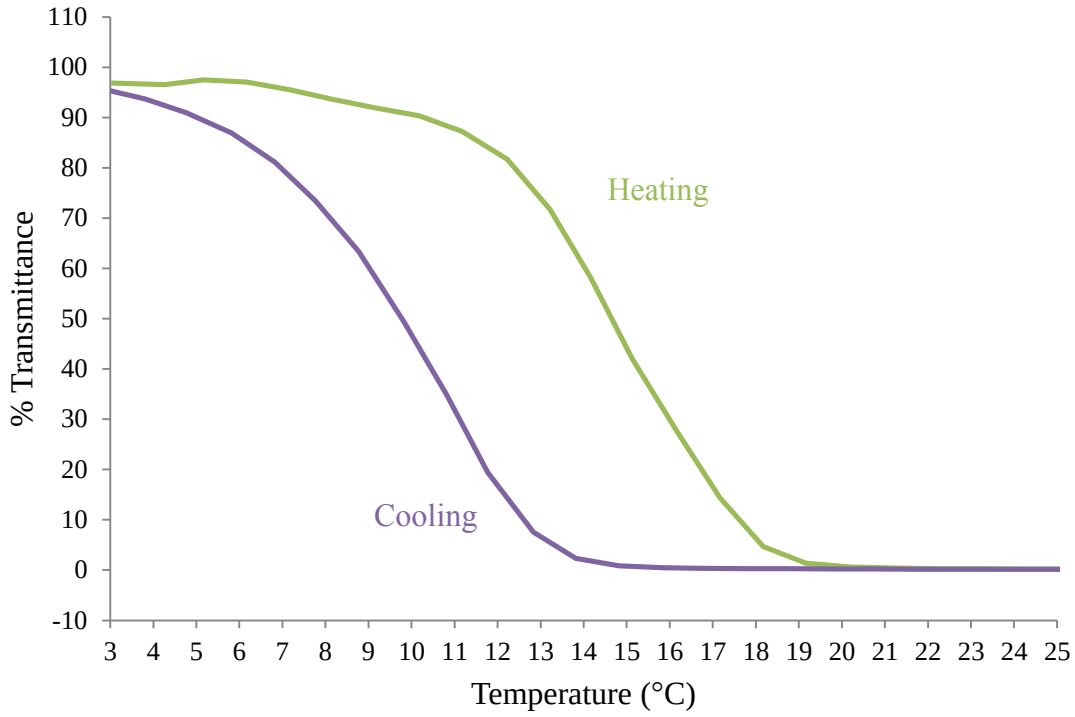

Figure 6.9. Plot showing % transmittance against temperature (°C) for conventional PNVCL-*ran*-PVAc

Appendix 3, Figure 15 shows the optical microscope images of the PNVCL-*ran*-PVAc solution taken below and above the LCST. Below the LCST the polymer chains are soluble in aqueous solution and are in a hydrated coil conformation (Appendix 3, Figure 15-I). Above the LCST, the polymer chains collapse and form globules which are apparent in the image (Appendix 3, Figure 15-II).

6.3.2.1.5. Comparison of PNVCL-*ran*-PVAc

Table 6.2 shows the comparison of the LCST's exhibited by various PNVCL-*ran*-PVAc samples and PNVCL.

Table 6.2. Comparison of M_n, PDI and LCST for PNVCL-*ran*-PVAc and PNVCL

Entry	Sample	Composition (NVCL:VAc)	M_n (x 10^4 $gmol^{-1}$)	PDI	LCST (°C)
1	PNVCL	100:0	2.62	1.36	38
2	Conventional	58:42	6.62	2.88	6
3	RAFT	64:36	2.79	1.18	18
4	Star-random 2	72:28	2.65	1.31	19
5	Star-random 5	76:24	2.35	1.23	16

The LCST of PNVCL of 38°C (Entry 1) is already discussed in Section 6.3.1.3. PVAc does not exhibit an LCST in water, due to its insolubility. The introduction of hydrophobic monomers is known to reduce the LCST of the resulting material. The LCST of PNVCL-*ran*-PVAc with a composition of 34:66 (NVCL:VAc) is reported to be 5°C, although the M_n is unknown.[43-46] PNVCL-*ran*-PVAc synthesised in the presence of RAFT agent 5 exhibited an LCST of 18°C, in comparison to that of 38°C for PNVCL homopolymer of almost the same M_n. This is a clear indication that the introduction of VAc reduces the LCST. PNVCL-*ran*-PVAc synthesised *via* conventional FRP (Entry 2) exhibited an LCST of 6°C, which is lower than that reported for the same copolymer made *via* RAFT (Entry 3) with similar compositions. The low LCST for the conventional random copolymer is believed to be due to the combination of higher molecular weight, broader PDI and greater incorporation of VAc repeat units. Furthermore, the LCST transition ranged from 6-19°C (13°C) for the conventional random copolymer (Figure 6.9), whereas the copolymer synthesised *via* RAFT showed a narrow transition of 3°C (18-21°C).

Star-random 2 (3 armed star) (Entry 4) showed an LCST of 19°C, which is similar to that obtained for linear random PNVCL-*ran*-PVAc prepared via RAFT (Entry 3). However, Star-random 5 (4 armed star) showed an LCST of 16°C. The reason for the lower LCST is not clear, but it may well be due to the presence of 4 arms instead of 3 arms, which could facilitate its aggregation. It should be noted that there is an oxygen

atom in the central unit of Star-random 5 (Chapter 5, Figure 5.21), which could also have an effect on the aggregation of the material.

6.3.2.2. PNVCL-*ran*-PNVP

Due to the higher temperatures needed to observe the LCST of the PNVCL-*ran*-PNVP random copolymer, UV – Visible spectroscopy could not be used. Therefore, the less accurate optical microscopy technique was employed.

6.3.2.2.1. Linear PNVCL-*ran*-PNVP *via* RAFT

Linear PNVCL-*ran*-PNVP (M_n = 1.40 x 10^4 $gmol^{-1}$, PDI = 1.25) synthesised *via* RAFT using RAFT agent 5, with a composition of 44:56 (PNVCL:PNVP), was investigated for its temperature responsive behaviour. Appendix 3, Figure 17 shows the images taken below and above the LCST of the PNVCL-*ran*-PNVP sample using an optical microscope. The LCST was found to be 87.9°C. Below the LCST the polymer chains are soluble in aqueous solution and are in a hydrated coil conformation (Appendix 3, Figure 17-I). Above the LCST, the polymer chains collapse and form globules which are apparent in the image (Appendix 3, Figure 17-II).

6.3.2.2.2. Star-random 3

Three armed star PNVCL-*ran*-PNVP (Star-random 3) (M_n = 2.11 x 10^4 $gmol^{-1}$, PDI = 1.42) synthesised *via* RAFT using RAFT agent 9, with a composition of 43:57 (PNVCL:PNVP), was investigated for its temperature responsive behaviour. Appendix 3, Figure 18 shows the images taken below and above the LCST of Star-random 3, using an optical microscope. The LCST was found to be 74.0°C. Below the LCST the polymer chains are soluble in aqueous solution and are in a hydrated coil conformation (Appendix 3, Figure 18-I). Above the LCST, the polymer chains collapse and form globules which are apparent in the image (Appendix 3, Figure 18-II).

6.3.2.2.3. Star-random 6

Four armed star PNVCL-*ran*-PNVP (Star-random 6) (M_n = 2.73 x 10^4 $gmol^{-1}$, PDI = 1.36) synthesised *via* RAFT using RAFT agent 9, with a composition of 44:56

(PNVCL:PNVP), was investigated for its temperature responsive behaviour. Appendix 3, Figure 19 shows the images taken below and above the LCST of Star-random 6, using an optical microscope. The LCST was found to be 72.0°C. Below the LCST the polymer chains are soluble in aqueous solution and are in a hydrated coil conformation (Appendix 3, Figure 19-I). Above the LCST, the polymer chains collapse and form globules which are apparent in the image (Appendix 3, Figure 19-II).

6.3.2.2.4. PNVCL-*ran*-PNVP *via* conventional free radical polymerisation

PNVCL-*ran*-PNVP synthesised *via* conventional free radical polymerisation (M_n = 2.19 x 10^5 $gmol^{-1}$, PDI = 2.77), with a composition of 48:52 (PNVCL:PNVP), was investigated for its temperature responsive behaviour. Appendix 3, Figure 20 shows the images taken below and above the LCST of Star-random 6, using an optical microscope. The LCST was found to be 59.4°C. Below the LCST the polymer chains are soluble in aqueous solution and are in a hydrated coil conformation (Appendix 3, Figure 20-I). Above the LCST, the polymer chains collapse and form globules which are apparent in the image (Appendix 3, Figure 20-II).

6.3.2.2.5. Comparison of PNVCL-*ran*-PNVP

Table 6.3 shows the comparison of the LCST's exhibited by various PNVCL-*ran*-PNVP samples and PNVCL.

Table 6.3. Comparison of M_n, PDI and LCST for PNVCL-ran-PNVP and PNVCL

Entry	Sample	Composition (NVCL:NVP)	M_n (x 10^4 $gmol^{-1}$)	PDI	LCST (°C)
1	PNVCL	100:0	1.52	1.48	39.0
2	Conventional	48:52	21.90	2.77	59.4
3	RAFT	44:56	1.40	1.25	87.9
4	Star-random 3	43:57	2.11	1.42	74.0
5	Star-random 6	44:56	2.73	1.36	72.0

The LCST of PNVCL of 39°C (Entry 1) is already discussed in Section 6.3.1.3. PNVP is water soluble and only exhibits phase transitions when in solution with the addition of an additive, such as a salt.[39, 53-55] The introduction of hydrophilic monomers

are known to increase the LCST of the resulting material. The LCST of PNVCL-*ran*-PNVP with a composition of 34:66 (NVCL:NVP) is reported to be 80°C, although the M_n is unknown.[46-48] PNVCL-*ran*-PNVP synthesised in the presence of RAFT agent 5 (Entry 3), exhibited an LCST of 87.9°C, in comparison to that of 39.0°C for PNVCL of almost the same M_n. This is a clear indication that the introduction of PNVP increases the LCST. PNCVL-*ran*-PNVP synthesised *via* conventional FRP (Entry 2) exhibited an LCST of 59.4°C, which is lower than that reported for the same copolymer made *via* RAFT (Entry 3) with a similar composition. The lower LCST for the conventional random copolymer is believed to be due to the higher molecular weight and broader PDI. LCST of Star-random 3 (3 armed star) (Entry 4) and Star-random 6 (4 armed star) (Entry 5) was found to be 74.0°C and 72.0°C, respectively. The reason for low LCST for the four armed random copolymer is discussed in Section 6.3.2.1.5.

6.4. Origin of hysteresis

For all PNVCL containing samples investigated here, the demixing of the polymer solution is reversible, however the rate of re-dissolution of the polymer is found to be slower and chain expansion takes place at a lower temperature, i.e. a thermal hysteresis occurs.[56, 57] The hysteresis can be attributed to the limited diffusion of water molecules into the collapsed PNVCL aggregates and therefore upon cooling there is a delay in the hydration and hence re-dissolution of the polymer.

PNIPAAm has been found to undergo intramolecular coil collapse into globules followed by intermolecular aggregation of the collapsed globules, above the LCST. The formation of aggregates (mesoglobules) can be attributed to inter-chain and intra-chain hydrogen bonds between carbonyl and amide moieties of the pendant groups (>C=O ⋯ H-N<) in PNIPAAm. Although the LCST behaviour of PNIPAAm is reversible, it shows a hysteresis.[58, 59] This was reported to be attributed, to the retardation in the dissociation process of the hydrogen bonding interactions between carbonyl and amide moieties. In contrast, PNVCL is unable to form inter-chain or intra-chain hydrogen bonds between polymer chains due to the lack of hydrogen on the amide group. However, two induced phase transitions have been reported to occur, the first was attributed to the microsegregation of hydrophobic domains and the second due to the volume collapse of the gel.[37, 60]

As discussed in the introduction (Section 6.1), PNVCL exhibits a strong tendency to aggregate and the amount of fully dehydrated carbonyl groups is relatively low, indicating that water molecules are trapped inside the mesoglobules. Similar phase transition behaviour has been observed for poly(3-ethyl-N-vinylpyrrolidone) (C_2PNVP) by Lai *et al.* They reported the strong presence of weak cross-linking between carbonyl groups from the polymer and D_2O (>C=O ⋯ D_2O ⋯ O=C<) in C_2PNVP mesoglobules, Figure 6.10.[61] Moreover, upon cooling free carbonyl groups were found to be more eager to form hydrogen bonds with water rather than the carbonyl groups "cross-linked".

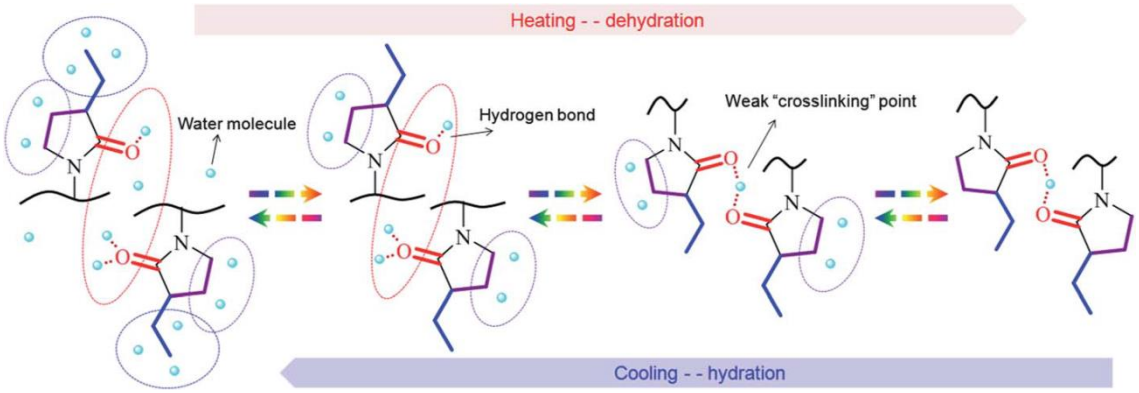

Figure 6.10. Mechanism of phase transition for aqueous C_2PNVP solution upon heating and cooling

Therefore, the thermal hysteresis in our NVCL containing samples could well be due to the presence of weak cross-linking between carbonyl groups from the polymer chains and trapped water molecules in PNVCL mesoglobules.

6.5. Summary

The temperature responsive behaviour of PNVCL, PNVCL-*ran*-PNVP and PNVCL-*ran*-PVAc was investigated using UV-Visible spectroscopy and optical microscopy.

6.5.1. Temperature responsive behaviour of PNVCL

PNVCL synthesised *via* conventional FRP (M_n = 9.97 x 10^4, PDI = 2.92) was found to have an LCST of 33°C. This is typical for PNVCL of higher molecular weight. Linear PNVCL samples with M_n ranging from 1.02 x 10^4 to 2.62 x 10^4 $gmol^{-1}$ and PDI's ranging from 1.36 – 1.48, were investigated for their temperature responsive behaviour and LCST's were found to be in the region of 38 – 40°C, which is greater than that observed for PNVCL synthesised *via* conventional FRP. This suggests that the exhibited LCST is dependent on the polymer chain length; i.e. "classical" (Type 1) Flory-Huggins behaviour. Interestingly, PNVCL synthesised *via* RAFT using RAFT agents 2-5 exhibited LCST's in the region of 39-40°C, which is known as fever temperature.

6.5.2. Temperature responsive behaviour of PNVCL-*ran*-PVAc and PNVCL-*ran*-PNVP

Linear, Star-random 2, Star-random 5 containing PNVCL-*ran*-PVAc as well as linear, Star-random 3, Star-random 6 containing PNVCL-*ran*-PNVP were analysed to determine their temperature responsive behaviour. The results were then compared with random copolymers synthesised *via* conventional FRP.

Comparison of PNVCL and linear PNVCL-*ran*-PVAc syntheised *via* RAFT with similar M_n, showed that the introduction of VAc reduces the LCST from 38°C to 18°C. The LCST of 6°C for PNVCL-*ran*-PVAc synthesised *via* conventional FRP was found to be lower than that exhibited for the same copolymer *via* RAFT. This is believed to be due to a combination of higher molecular weight, broader PDI and greater incorporation of VAc repeat units. The LCST transition range was also observed to be broader for the random copolymer synthesised *via* conventional FRP. Star-random 2 (3 armed star) and Star-random 5 (4 armed star) showed LCST's of 19°C and 16°C, respectively. The reason for the LCST is not clear, but it may well be due to

the presence of 4 arms instead of 3 arms, which could facilitate it's aggregation. The presence of an oxygen atom at the center of the Star-random 5 could also have an effect on the aggregation of the material. Comparison of PNVCL and linear PNVCL-*ran*-PNVP syntheised *via* RAFT with similar M_n, showed that the introduction of NVP increases the LCST from 39.0°C to 87.9°C. The LCST of 59.4°C for PNVCL-*ran*-PNVP synthesised *via* conventional FRP is lower than that exhibited for the same copolymer *via* RAFT. This is believed to be due to a combination of higher molecular weight and broader PDI. Star-random 3 (3 armed star) and Star-random 6 (4 armed star) showed LCST's of 74.0C and 72.0°C, respectively. The reason for the low LCST for the four armed PNVCL-*ran*-PNVP is similar to that for PNVCL-*ran*-PVAc.

Although all samples containing PNVCL showed reversible behaviour, they exhibited a thermal hysteresis. This is believed to be due to weak cross-linking interactions between the carbonyl groups of PNVCL and molecules of water.

6.6. References

1. Shimizu, K.; Fujita, H.; Nagamori, E. *Biotechnology and Bioengineering* **2010,** 106, (2), 303-310.
2. Twaites, B. R.; Alarcon, C. D. H.; Lavigne, M.; Saulnier, A.; Pennadam, S. S.; Cunliffe, D.; Gorecki, D. C.; Alexander, C. *Journal of Controlled Release* **2005,** 108, (2-3), 472-483.
3. Doorty, K. B.; Golubeva, T. A.; Gorelov, A. V.; Rochev, Y. A.; Allen, L. T.; Dawson, K. A.; Gallagher, W. M.; Keenan, A. K. *Cardiovascular Pathology* **2003,** 12, (2), 105-110.
4. Stile, R. A.; Healy, K. E. *Biomacromolecules* **2001,** 2, (1), 185-194.
5. Hacker, M. C.; Klouda, L.; Ma, B. B.; Kretlow, J. D.; Mikos, A. G. *Biomacromolecules* **2008,** 9, (6), 1558-1570.
6. Klouda, L.; Mikos, A. G. *European Journal of Pharmaceutics and Biopharmaceutics* **2008,** 68, (1), 34-45.
7. Vihola, H.; Laukkanen, A.; Tenhu, H.; Hirvonen, J. *Journal of Pharmaceutical Sciences* **2008,** 97, (11), 4783-4793.
8. Vihola, H.; Marttila, A.-K.; Pakkanen, J. S.; Andersson, M.; Laukkanen, A.; Kaukonen, A. M.; Tenhu, H.; Hirvonen, J. *International Journal of Pharmaceutics* **2007,** 343, (1-2), 238-246.
9. Liu, F.; Urban, M. W. *Progress in Polymer Science* **2010,** 35, (1-2), 3-23.
10. Pasparakis, G.; Vamvakaki, M. *Polymer Chemistry* **2011,** 2, (6), 1234-1248.
11. Schulz, D. N.; Peiffer, D. G.; Agarwal, P. K.; Larabee, J.; Kaladas, J. J.; Soni, L.; Handwerker, B.; Garner, R. T. *Polymer* **1986,** 27, (11), 1734-1742.
12. Gil, E. S.; Hudson, S. M. *Progress in Polymer Science* **2004,** 29, (12), 1173-1222.
13. Dimitrov, I.; Trzebicka, B.; Muller, A. H. E.; Dworak, A.; Tsvetanov, C. B. *Progress in Polymer Science* **2007,** 32, (11), 1275-1343.
14. Schild, H. G. *Progress in Polymer Science* **1992,** 17, (2), 163-249.
15. Vihola, H. Studies on Thermosensitive Poly(N-vinylcaprolactam) Based Polymers for Pharmaceutical Applications. University of Helsinki, Helsinki, 2007.
16. Chandler, D. *Nature* **2005,** 437, (7059), 640-647.
17. Southall, N. T.; Dill, K. A.; Haymet, A. D. J. *Journal of Physical Chemistry B* **2002,** 106, (3), 521-533.

18. Chee, C. K.; Hunt, B. J.; Rimmer, S.; Rutkaite, R.; Soutar, I.; Swanson, L. *Soft Matter* **2009,** 5, (19), 3701-3712.
19. Heskins, M.; Guillet, J. E. *Journal of Macromolecular Science, Part A* **1968,** 2, 1441 - 1455.
20. Bokias, G.; Hourdet, D.; Iliopoulos, I. *Macromolecules* **2000,** 33, (8), 2929-2935.
21. Meeussen, F.; Nies, E.; Berghmans, H.; Verbrugghe, S.; Goethals, E.; Du Prez, F. *Polymer* **2000,** 41, (24), 8597-8602.
22. Chee, C. K.; Rimmer, S.; Shaw, D. A.; Soutar, I.; Swanson, L. *Macromolecules* **2001,** 34, (21), 7544-7549.
23. Hopkins, S.; Carter, S.; MacNeil, S.; Rimmer, S. *Journal of Materials Chemistry* **2007,** 17, (38), 4022-4027.
24. Destarac, M.; Papon, A.; Van Gramberen, E.; Karagianni, K. *Australian Journal of Chemistry* **2009,** 62, (11), 1488-1491.
25. Keerl, M.; Smirnovas, V.; Winter, R.; Richtering, W. *Angewandte Chemie-International Edition* **2008,** 47, (2), 338-341.
26. Wu, J. Y.; Liu, S. Q.; Heng, P. W. S.; Yang, Y. Y. *Journal of Controlled Release* **2005,** 102, (2), 361-372.
27. Lau, A. C. W.; Wu, C. *Macromolecules* **1999,** 32, (3), 581-584.
28. Vihola, H.; Laukkanen, A.; Valtola, L.; Tenhu, H.; Hirvonen, J. *Biomaterials* **2005,** 26, (16), 3055-3064.
29. Kirsh, Y. E., *Water Soluble Poly-N-Vinylamides. Synthesis and Physicochemical Properties*. 1998.
30. Laukkanen, A.; Valtola, L.; Winnik, F. M.; Tenhu, H. *Macromolecules* **2004,** 37, (6), 2268-2274.
31. Yanul, N. A.; Zemljanova, O. Y.; Kalninsh, K. K.; Kirsh, Y. E. *Zurnal Fiziceskoj Chimii* **1998,** 72, 1037.
32. Peng, S. F.; Wu, C. *Macromolecular Symposia* **2000,** 159, (1), 179-186.
33. Markvicheva, E. A.; Tkachuk, N. E.; Kuptsova, S. V.; Dugina, T. N.; Strukova, S. M.; Kirsh, Y. E.; Zubov, V. P.; Rumsh, L. D. *Applied Biochemistry and Biotechnology* **1996,** 61, (1-2), 75-84.
34. Vihola, H.; Laukkanen, A.; Hirvonen, J.; Tenhu, H. *European Journal of Pharmaceutical Sciences* **2002,** 16, (1-2), 69-74.
35. Aseyev, V.; Hietala, S.; Laukkanen, A.; Nuopponen, M.; Confortini, O.; Du Prez, F. E.; Tenhu, H. *Polymer* **2005,** 46, (18), 7118-7131.

36. Dubovik, A. S.; Makhaeva, E. E.; Grinberg, V. Y.; Khokhlov, A. R. *Macromolecular Chemistry and Physics* **2005,** 206, (9), 915-928.

37. Chee, C. K.; Rimmer, S.; Soutar, I.; Swanson, L. *Reactive & Functional Polymers* **2006,** 66, (1), 1-11.

38. Spevacek, J.; Dybal, J.; Starovoytova, L.; Zhigunov, A.; Sedlakova, Z. *Soft Matter* **2012,** 8, (22), 6110-6119.

39. Maeda, Y.; Nakamura, T.; Ikeda, I. *Macromolecules* **2002,** 35, (1), 217-222.

40. Sun, S. T.; Wu, P. Y. *Journal of Physical Chemistry B* **2011,** 115, (40), 11609-11618.

41. Vorob'ev, M. M.; Burova, T. V.; Grinberg, N. V.; Dubovik, A. S.; Faleev, N. G.; Lozinsky, V. I. *Colloid and Polymer Science* **2010,** 288, (14-15), 1457-1463.

42. Zhang, L.; Liang, Y.; Meng, L. *Polymers for Advanced Technologies* **2010,** 21, (10), 720-725.

43. Boyko, D. V. B. N-Vinylcaprolactam based Bulk and Microgels: Synthesis, Structural Formation and Characterization by Dynamic Light Scattering. Dresden University of Technology, 2004.

44. Kirsh, Y. E.; Soos, T. A.; Karaputadze, T. M. *Vysokomolekuljarnye Soedinenija A* **1993,** 35, 481.

45. Sabey, M. Z.; Dmitrieva, S. N.; Meos, A. N. *Vysokomolekuljarnye Soedinenija* **1970,** 12, 243.

46. Skornikova, E. E.; Karaputadze, T. M.; Ovsepyan, A. M.; Aksenov, A. I.; Kirsh, Y. E. *Vysokomolekuljarnye Soedinenija B* **1985,** 27, 869.

47. Yanul, N. A.; Kirsh, Y. E.; Anufrieva, E. V. *Journal of Thermal Analysis and Calorimetry* **2000,** 62, (1), 7-14.

48. Kirsh, Y. E.; Soos, T. A.; Karaputadze, T. M. *Vysokomolekuljarnye Soedinenija A* **1979,** 21, 519.

49. Beija, M.; Marty, J.-D.; Destarac, M. *Chemical Communications* **2011,** 47, (10), 2826-2828.

50. Shao, L. D.; Hu, M. Q.; Chen, L.; Xu, L.; Bi, Y. M. *Reactive & Functional Polymers* **2012,** 72, (6), 407-413.

51. Eissa, A. M.; Khosravi, E. *European Polymer Journal* **2011,** 47, (1), 61-69.

52. Lutz, J. F.; Hoth, A. *Macromolecules* **2006,** 39, (2), 893-896.

53. Pakuro, N. I.; Nakhmanovich, B. I.; Pergushov, D. V.; Chibirova, F. K. *Polymer Science Series A* **2011,** 53, (1), 6-11.

54. Nakhmanovich, B. I.; Pakuro, N. I.; Akhmet'eva, E. I.; Litvinenko, G. I.; Arest-Yakubovich, A. A. *Polymer Science Series B* **2007,** 49, (5-6), 136-138.

55. Pakuro, N.; Yakimansky, A.; Chibirova, F.; Arest-Yakubovich, A. *Polymer* **2009,** 50, (1), 148-153.

56. Aseyev, V.; Tenhu, H.; Winnik, F. M., Non-ionic Thermoresponsive Polymers in Water. In *Self Organized Nanostructures of Amphiphilic Block Copolymers Ii*, Muller, A. H. E.; Borisov, O., Eds. Springer-Verlag Berlin: Berlin, 2011; Vol. 242, pp 29-89.

57. Wang, X. H.; Qiu, X. P.; Wu, C. *Macromolecules* **1998,** 31, (9), 2972-2976.

58. Wu, C.; Wang, X. H. *Physical Review Letters* **1998,** 80, (18), 4092-4094.

59. Cheng, H.; Shen, L.; Wu, C. *Macromolecules* **2006,** 39, (6), 2325-2329.

60. Mikheeva, L. M.; Grinberg, N. V.; Mashkevich, A. Y.; Grinberg, V. Y.; Thanh, L. T. M.; Makhaeva, E. E.; Khokhlov, A. R. *Macromolecules* **1997,** 30, (9), 2693-2699.

61. Lai, H. J.; Chen, G. T.; Wu, P. Y.; Li, Z. C. *Soft Matter* **2012,** 8, (9), 2662-2670.

Chapter 7
Summary of work, general conclusions and future work

7.1. Summary of work

The use of reversible addition fragmentation chain transfer (RAFT) polymerisation was successfully demonstrated for the controlled polymerisation of "less activated" monomers (LAMs) such as, N-vinylpyrrolidone (NVP), vinyl acetate (VAc) and N-vinylcaprolactam (NVCL). This resulted in the synthesis of well-defined polymeric materials.

RAFT agents 1-7 and 9-11 were synthesised to a high degree of purity *via* nucleophilic substitution reactions and fully characterised by ^{1}H and ^{13}C NMR spectroscopy. RAFT agents 1-3 were known in the literature to work as efficient chain transfer agents in the polymerisations of LAMs and were initially synthesised to gain an insight and familiarity into the RAFT polymerisations of NVP, VAc and NVCL. Novel linear RAFT agents (RAFT agents 4-7), in which primary (RAFT agent 4), secondary (RAFT agents 5 and 7) and tertiary radicals (RAFT agent 6) are produced upon fragmentation, were successfully synthesised. RAFT agents 4-6 incorporated pyrrolidone functionality as part of the R group and in contrast RAFT agent 7 incorporated pyrrolidone functionality as part of the Z group. Multi-armed RAFT agents 9 (3-arm) and 10 (4-arm) as well as the novel multi-armed RAFT agent 11 (4 arm), were also successfully synthesised and characterised.

RAFT agents 1-8 were then utilised to mediate the homopolymerisation of NVP, VAc and NVCL. Both dithiocarbamate (RAFT agents 1 and 8) and xanthate (RAFT agents 2-7) RAFT agents were shown to mediate the polymerisation of the LAMs, generating homopolymers with controlled molecular weight close to theoretical values and with narrow molecular weight distributions (PDI). RAFT agent 4 was shown to be ineffective for the polymerisation of NVP, as the found molecular weight was comparable to that observed *via* conventional free radical polymerisation methodology. This is believed to be due to the lack of stabilisation of the primary radical formed upon fragmentation. RAFT agents 5-7 were shown to be effective in mediating the polymerisation of NVP. Kinetics investigation showed molecular weight increasing in a linear fashion with conversion and conversion increasing in a linear fashion against time. The choice of solvent was found to effect the RAFT polymerisations of NVP and VAc. When toluene was used as the polymerisation solvent for both NVP and VAc, the yield was low. This was attributed to the possibility of a degradative chain transfer process occurring between monomer propagating radicals and toluene. RAFT

polymerisations in 2-propanol and 2-butoxyethanol produced polymers with broad PDI, believed to be due to the role of the alcoholic solvents as chain transfer agents. Furthermore, when water was used as the polymerisation solvent, significantly high molecular weight polymer than expected was produced. This was attributed to the chain cleavage of the RAFT chains ends, indicating a combination of both conventional FRP and RAFT polymerisation of NVP.

For the RAFT polymerisation of NVCL, novel RAFT agent 5 and 7 were effective in controlling the polymerisation. However, when novel RAFT agent 6 was used, the controlled polymerisation of NVCL was ineffective, as bimodal molecular weight distribution were observed. This is explained in terms of more stable tertiary radicals, generated *via* the fragmentation of RAFT agent 6, reacting more slowly with NVCL and therefore requiring longer reaction times for its completion. Hence, as the rate of polymerisation is slower, the termination reactions may well be more prominent which could result in the bimodal molecular weight distribution.

The research then moved onto synthesising block copolymers incorporating LAMs. This was accomplished using PNVP and PVAc homopolymers synthesised in Chapter 3 as macro RAFT agent (macroCTA 12-17). Linear copolymers of PNVP-*block*-PVAc, PNVP-*block*-PNVCL, PVAc-*block*-PNVP and PVAc-*block*-PNVCL were synthesised. However, the resulting polymeric products exhibited bimolecular molecular weight distributions, which were attributed to number of possibilities. The first was the presence of a small amount of homopolymer of the second monomer, which is inherent in the mechanism of RAFT block copolymerisations, due to the polymerisation of the co-monomer by added initiator. The second possibility was the cleavage of xanthate or dithiocarbamate groups from the macroCTA due to a combination of longer reaction times, temperature and solvent effects, resulting in un-extended macroCTA. The third possibility was the rate of propagation being faster than the rate of initiation and insufficient amount of second monomer to achieve full consumption of macroCTA. This reason may well be ruled out as when a large excess of second monomer was added, the resulting product still exhibited bimodal molecular weight distribution. The inability to synthesise clean block copolymers highlights the limitations of RAFT polymerisation in industry.

RAFT polymerisation was also used to synthesise linear novel random copolymers of PNVP-*ran*-PVAc, PNVCL-*ran*-PVAc and PNVCL-*ran*-PNVP using RAFT agent 5. The RAFT copolymers were compared with random copolymers synthesised *via* conventional FRP. The RAFT random copolymers showed narrow

monomodal molecular weight distributions by SEC, in contrast with random copolymer synthesised *via* conventional FRP with broad molecular weight distributions and far greater M_n. The composition of the conventional and RAFT mediated random copolymerisations were found to be the same, indicating similar monomer reactivity ratios.

More complex architectures were then prepared *via* RAFT polymerisation, using Multi-RAFT agents (RAFT agents 9-11). This lead to the synthesis of Star 1 (PNVP three armed star), Star 2 and 3 (PNVP four armed star), Star 4 (PVAc four armed star), Star 5 (PNVCL 3 armed star) and Star 6 (PNVCL 4 armed star). A "core first" R group approach was implemented, as to retain the structural integrity of the three and four armed stars. Kinetics for the RAFT polymerisation to produce PNVP stars (Star 1 and 2); using RAFT agents 9 and 10 were followed by ^{1}H NMR spectroscopy and SEC. The RAFT polymerisations were shown to have controlled / living characteristics, with narrow monomodal SEC traces, along with M_n increasing in a linear fashion with increasing conversion. Moreover, novel RAFT agent 11 was also used to mediate the polymerisation of NVP stars (Star 3) and VAc stars (Star 4), with the products exhibiting narrow monomodal SEC traces and found M_n close to the theoretical value. The narrow monomodal SEC traces indicate the formation of stars without the presence of linear homopolymer. NVCL was also polymerised in the presence of RAFT agent 9 and the novel RAFT agent 11, to produce Star 5 and Star 6, respectively. However, bimodal molecular weight distributions were observed with broad PDI, attributed to termination reactions.

Four arm stars of PNVP (Star 3) and PVAc (Star 4) were then used as macroCTA's to synthesise Star-block 1-4, containing PNVP, PVAc or PNVCL. In all cases the PDI's of the Star-blocks were broader than those observed for the Stars, indicating that the products had variable chain extension. RAFT polymerisation was also used to synthesise novel star-like random copolymers of PNVP-*ran*-PVAc (Star-random 1 and 4), PNVCL-*ran*-PVAc (Star-random 2 and 5) and PNVCL-*ran*-PNVP (Star-random 3 and 6), with three and four arms, using RAFT agent 9 and novel RAFT agent 11. Star-random 1-6 were shown to have narrow monomodal molecular weight distributions. This demonstrates the ability of RAFT to synthesise star-like random copolymers of vinyl monomers. Comparison of the monomer compositions of the three and four armed random stars shows that they are the same within experimental error.

The temperature responsive behaviour of polymeric materials containing NVCL synthesised *via* RAFT polymerisation was investigated. PNVCL samples synthesised

via RAFT showed an LCST approximately between 38-40°C, for M_n ranging from 1.02 x 10^4 - 2.62 x 10^4 $gmol^{-1}$. This was greater than the LCST of 33°C, exhibited for PNVCL synthesised *via* conventional FRP. This suggests that the exhibited LCST is dependent on the polymer chain length; i.e. "classical" (Type 1) Flory-Huggins behaviour. Therefore, the LCST of PNVCL can be finely tuned using RAFT polymerisation, to give a targeted LCST. PNVCL synthesised *via* RAFT using RAFT agents 2-5 exhibited LCST's in the region of 39-40, which is known as fever temperature.

Comparison of PNVCL and novel linear PNVCL-*ran*-PVAc syntheised *via* RAFT with similar M_n, showed that the introduction of VAc reduces the LCST from 38°C to 18°C. Novel Star-random 2 and 5 were observed to exhibit an LCST of 19°C and 16°C, respectively. The lower LCST for Star-random 5 may well be due to the presence of four arms instead of three, which could facilitate it's aggregation. Furthermore, the presence of an oxygen atom at the center of Star-random 5 could also have an effect on the aggregation of the material. All the PNVCL-*ran*-PVAc samples synthesised *via* RAFT were shown to have narrow phase transitions. In contrast, PNVCL-*ran*-PVAc synthesised *via* conventional FRP, was observed to exhibit an LCST of 6°C, with a broad phase transtition. Comparison of PNVCL and linear PNVCL-*ran*-PNVP syntheised *via* RAFT with similar M_n, showed that the introduction of NVP increases the LCST from 39.0°C to 87.9°C. PNVCL-*ran*-PNVP synthesised *via* conventional FRP was observed to exhibit a lower LCST at 59.4°C, despite both copolymers having similar compositions. It is believed that this is due to a combination of the increased molecular weight and broad PDI for the random copolymer synthesised *via* conventional FRP. Novel Star-random 3 and 6 were observed to exhibit an LCST of 74°C and 72°C, respectively. The reason for the low LCST for Star-random 6 is similar to that explained for Star-random 5.

7.2. General conclusions

This work was successful in producing well-defined linear and multi-armed homo, block and random copolymers, incorporating NVP, NVCL and VAc utilising RAFT polymerisation. A range of literature based and novel RAFT agents, with either xanthate or dithiocarbamate structures were used to mediate the polymerisation of the less activated monomers.

It is evident from looking at the results from Chapters 3-5, that significant improvements are needed in the field of controlled radical polymersations to be able to use this methodoly to great effect within an industrial environment. There are several majors hurdles which will need to be overcome to achieve this.

Firstly, for the homopolymerisation reactions of LAMs, the conversion / yield will be required to be increased to a level where residual monomer concentration is on the scale of ppm. (This is also to be achieved within a much shorter time frame than is currently possible). Presently, in the polymerisation reaction of LAMs, best efforts give conversions / yields in the region of 90-95% after a reaction time in the region of 24 h. A further complication in this respect, is the difficulty of the NVCL radical polymerisation, where conversions tend to be even lower. This is due to the comparative unavailability of the C=C bond in NVCL compared to NVP. The "chair" conformation in NVCL means the C=C bond is rigid (less reactive) and partialy hindered by the C=O bond on the lactam ring. In constrast, NVP (and VAc) has a planar conformation and the C=C is far more available.

Secondly, as demonstrated in Chapters 3-5, the retention of the chain end is essential in synthesising clean block copolymers, free of homopolymer impurities. However, due to the nature of radical chemistry and the ease of xanthates / dithiocarbamates to be cleaved from the polymer chains either by solvent interactions or raised temperature conditions, it is believed that this will be extremely hard to achieve. In addition, due to the inherent problem of producing homopolymer of the second monomer within the RAFT process, generating clean block copolymers to a high degree of purity and conversion is practically impossible. Recycling of unused monomer or further purification steps would need to be implemented to produce block coolymers close to the wanted specification. The literature tends to have a more positive outlook on block copolymer synthesis *via* RAFT polymerisation. Clean block copolymers with monomodal SEC chromatographs are often shown. However, either (i) optimised SEC chromatography conditions are used, (ii) macroCTA's are extensively purified before

further use for block copolymer synthesis or (ii) the polymerisation time to synthesise the macroCTA is stopped short to retain as much chain end functionality as possible.

It is therefore believed that much work is needed to be conducted in the area of controlled / living polymerisations of LAMs (not necessarily by radical means) in order to meet the requirements set by industry. This can also be said for RAFT polymerisation in general, although radical polymerisation of MAMs has been widely studied and the knowledge of these systems is more advanced. MAMs also have the advantage of being able to be polymerised by other methods such as ATRP, SET-LRP and NMP. Therefore, more further research is needed in these areas for the controlled / living polymerisation of LAMs.

7.3. Future work

In this study, RAFT polymerisation was shown to be useful in synthesising linear and star homopolymer structures with narrow single mode molecular weight distributions.

Firstly, it is believed that further characterisation work is needed of the polymeric materials, as this would lead to a better understanding of the chemistry present. Within this study there was a heavy reliance of SEC and NMR spectroscopy for the polymer samples. A combination of the two characterisation methods, where samples were analysed using an on-line SEC–NMR system would allow the precise determination of M_n, M_w and molar mass distributions. It would also give the ability to separate and analyse the different compositions within the copolymer product (i.e. block copolymer and homopolymer impurities) more accurately. The application of high performance liquid chromatography (HPLC) would allow the accurate determination of whether the block copolymer samples were either a blend or actually covalently linked (block copolymer). In addition, this technology would also give an insight into the chain ends present in the polymer samples, the degree of functionality as well as further molecular weight data.

The main aim of this research was to synthesise pure block copolymers containing LAMs with high conversions and single mode molecular weight distributions. This is known in the literature to be difficult to achieve and it is also found to be problematic here, as results show the incomplete conversion of macroCTA to block copolymer. One reason identified as a possible cause for the cleavage of active macroCTA chain ends, was high temperature of the polymerisation reaction. In order to

eliminate this possibility, it is suggested that the RAFT polymerisation of LAMs be conducted at a lower temperature (ambient temperature) with redox initiation being adopted to generate radicals. Moreover, lowering the temperature may also reduce the number of side reactions; i.e. radical recombination and disproportionation.

Furthermore, an alternative to using RAFT polymerisation is single electron transfer – living radical polymerisation (SET-LRP) which may well be beneficial for synthesising pure block copolymers. SET-LRP has been shown to be effective in synthesising high molecular weight polymers with short reaction times with a high degree of chain end functionality. This route may be a possibility in controlling the polymerisation of LAMs to high conversion and subsequently using them as macro-initiators to generate pure block copolymers. This process could also be extended for the synthesis of well-defined Star-block copolymers. Using SET-LRP may also allow the synthesis of block copolymers of LAMs-*block*-MAMs. As SET-LRP often uses Cu(0) in the form of copper wire or pipe, this may remove any copper contamination.

NVP, NVCL and VAc have predominantly been polymerised by radical means. Little attention has been focused on the cationic polymerisation of these monomers. The results from the reactions that have utilised this polymerisation method have been disappointing to say the least. However, from a theoretical point of view, the cationic polymerisation of these non-conjugated monomers should be possible and it may be of benefit to re-look at this.

To further the research into more complex architectures, it will be interesting to attach a RAFT agent to a polyol, such as ring-opened epoxidised natural oil. The conversion of the hydroxyl groups from polyol to xanthate moieties would allow the controlled / living polymerisation of LAMs. If the monomer used is NVP, then this would hopefully produce a biodegradable water soluble material. If the monomer used is NVCL, then this would hopefully produce a biodegradable temperature responsive material.

Appendix 1

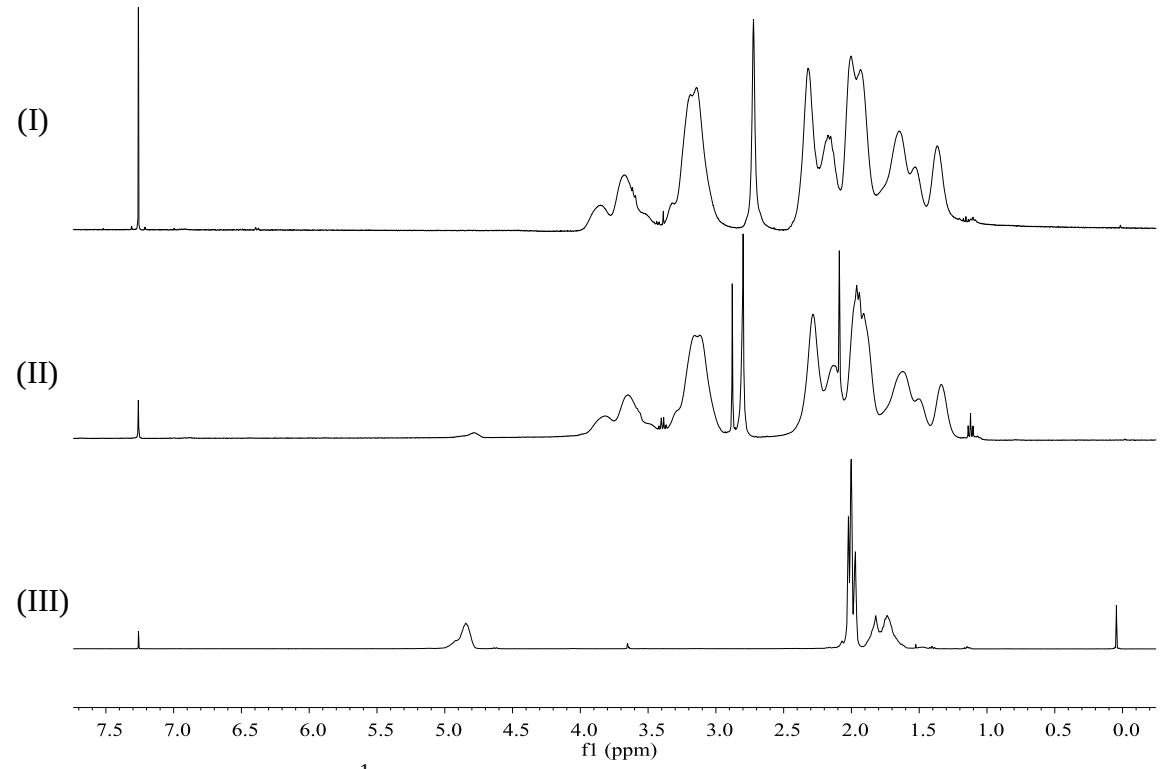

Figure 1. 400 MHz-^{1}H NMR spectra of (I) PNVP macroCTA 12, (II) copolymer product (Table 4.1; Entry 1) and (III) PVAc in $CDCl_3$

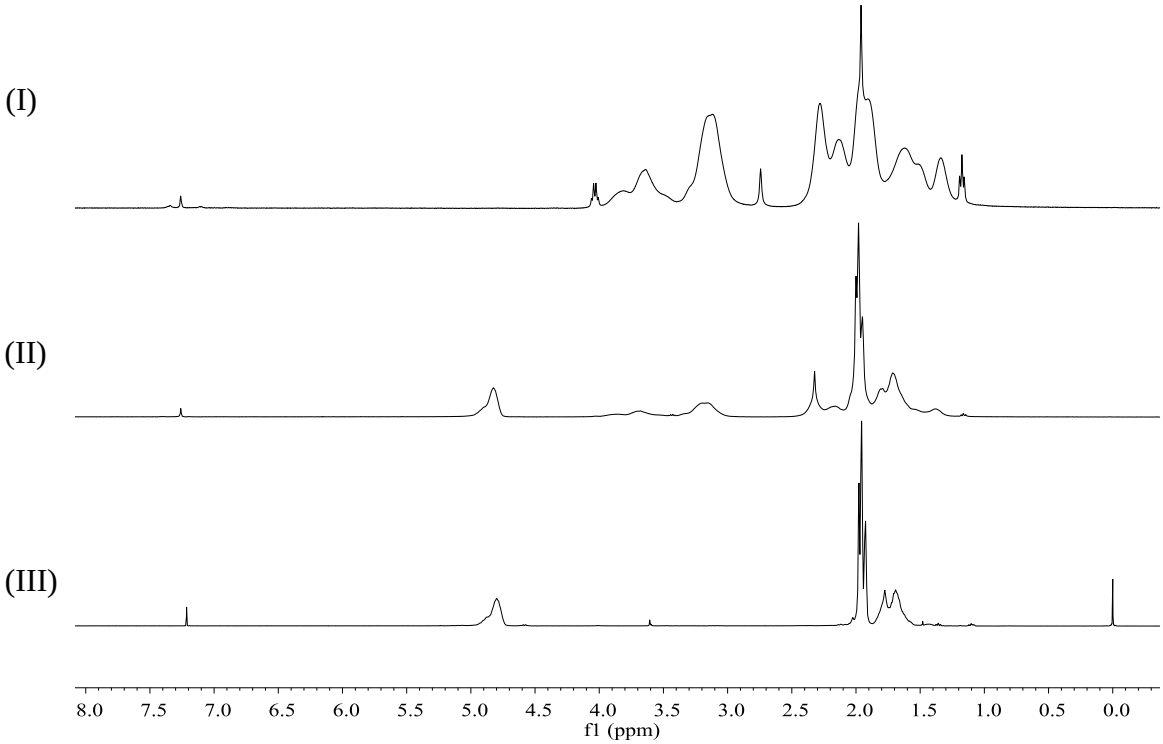

Figure 2. 400 MHz-^{1}H NMR spectra of (I) PNVP macroCTA 13, (II) copolymer product (Table 4.1; Entry 2) and (III) PVAc in $CDCl_3$

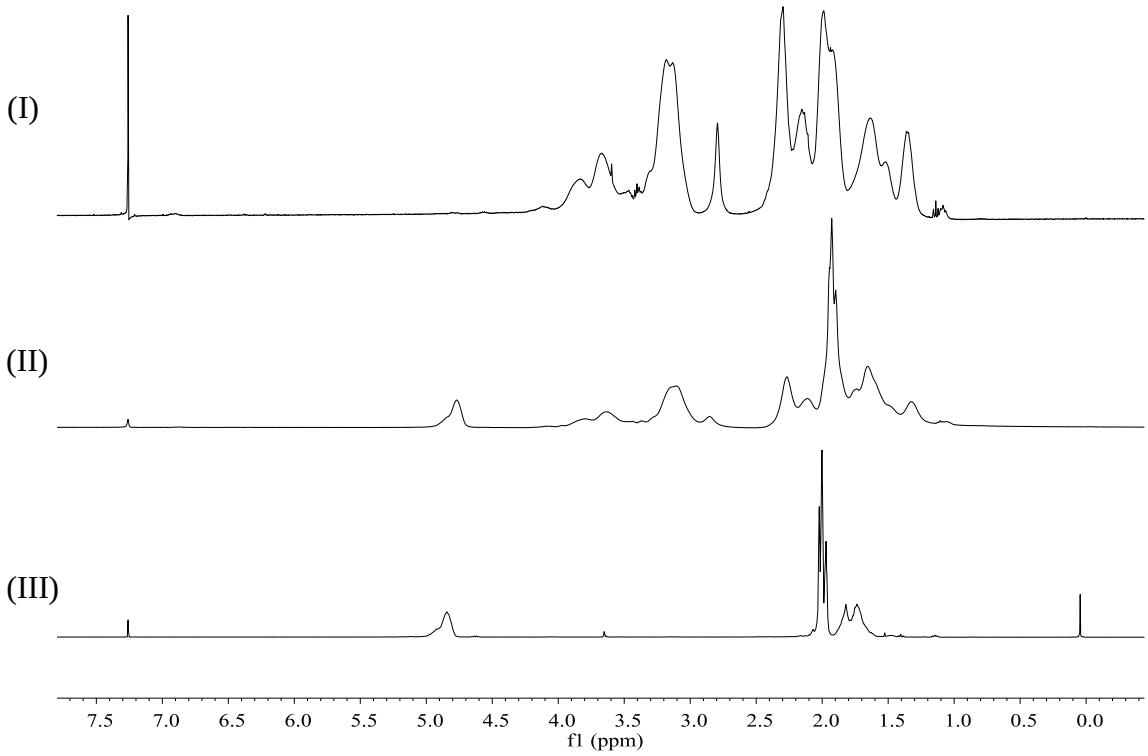

Figure 3. 400 MHz-^{1}H NMR spectra of (I) PNVP macroCTA 14, (II) copolymer product (Table 4.1; Entry 3) and (III) PVAc in $CDCl_3$

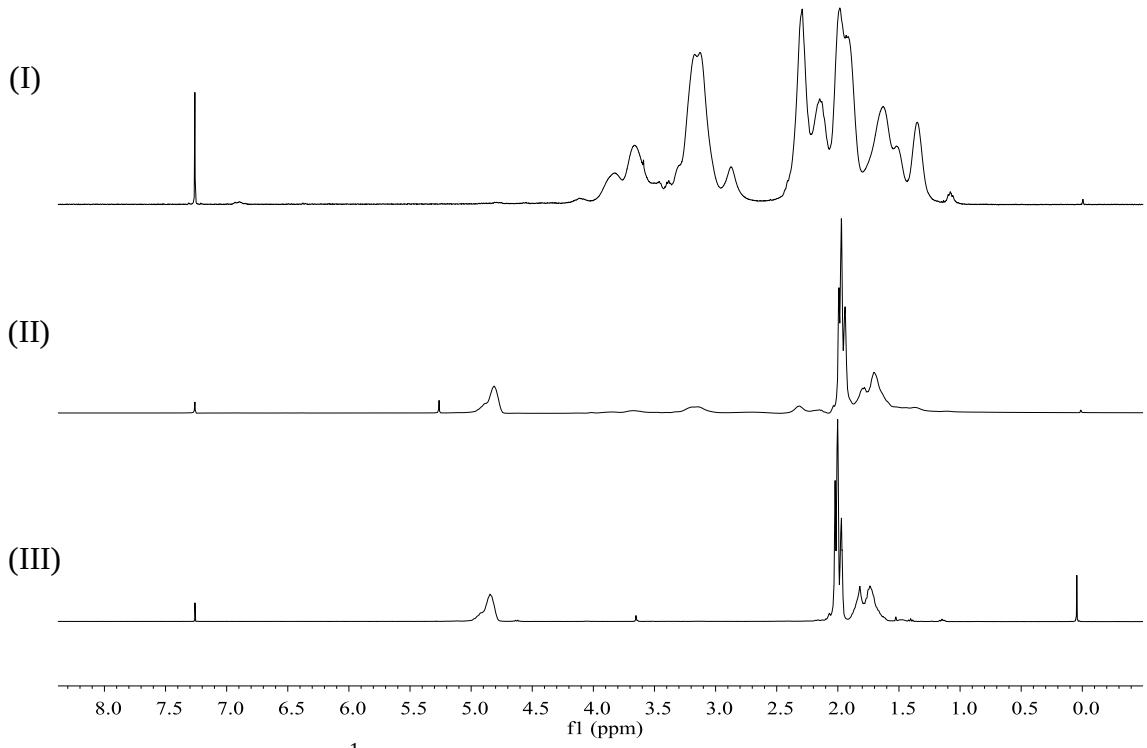

Figure 4. 400 MHz-^{1}H NMR spectra of (I) PNVP macroCTA 14, (II) copolymer product (Table 4.1; Entry 4) and (III) PVAc in $CDCl_3$

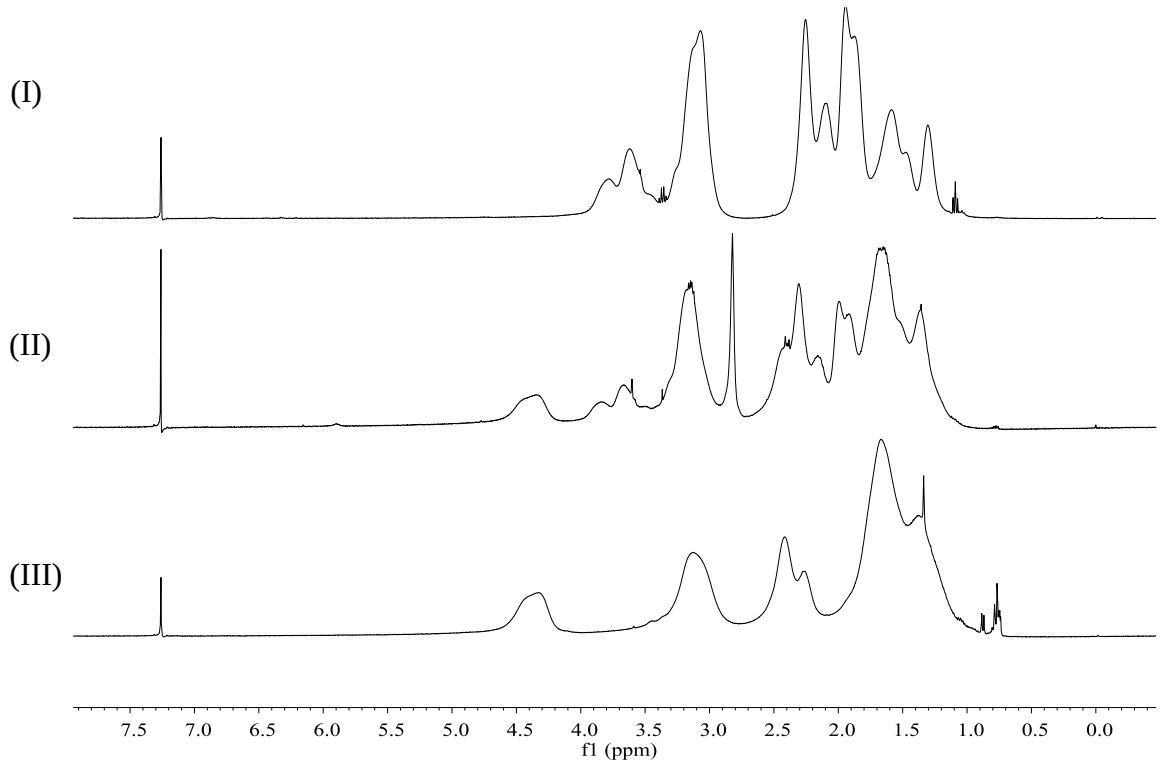

Figure 5. 400 MHz-^{1}H NMR spectra of (I) PNVP macroCTA 12, (II) copolymer product (Table 4.2; Entry 1) and (III) PNVCL in $CDCl_3$

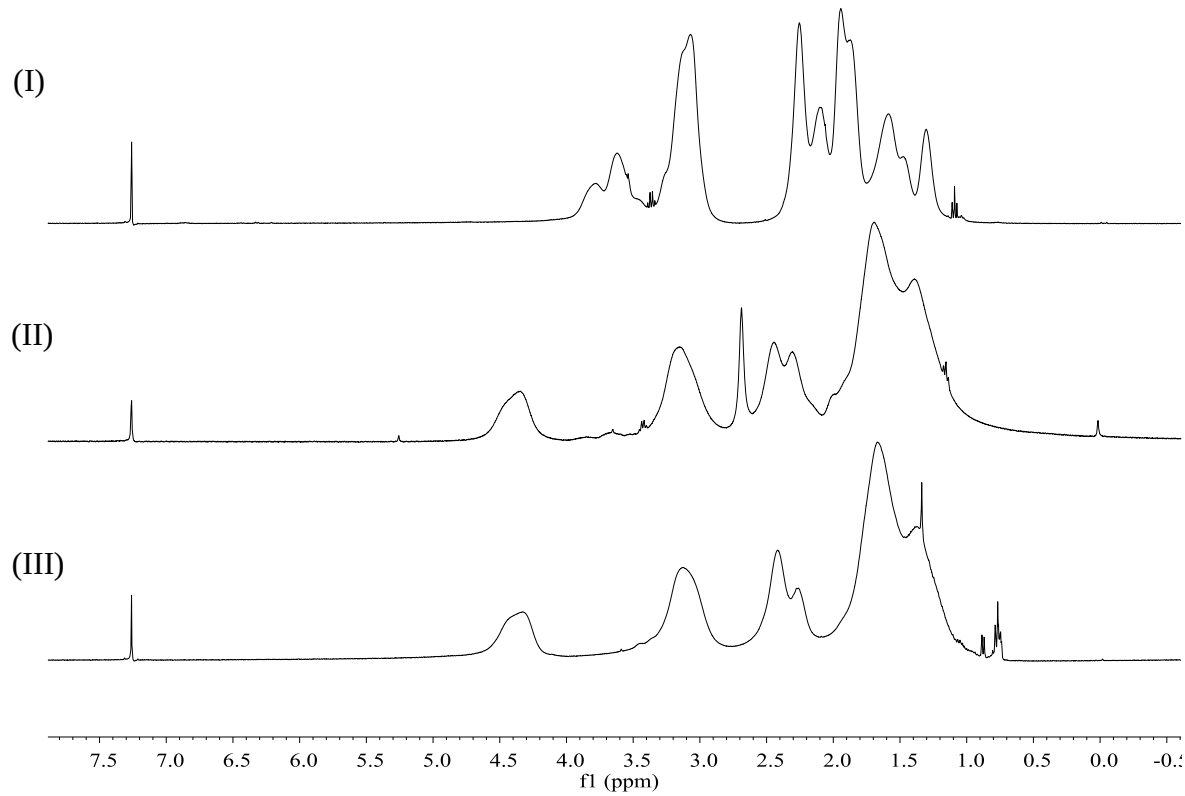

Figure 6. 400 MHz-^{1}H NMR spectra of (I) PNVP macroCTA 12, (II) copolymer product (Table 4.2; Entry 2) and (III) PNVCL in $CDCl_3$

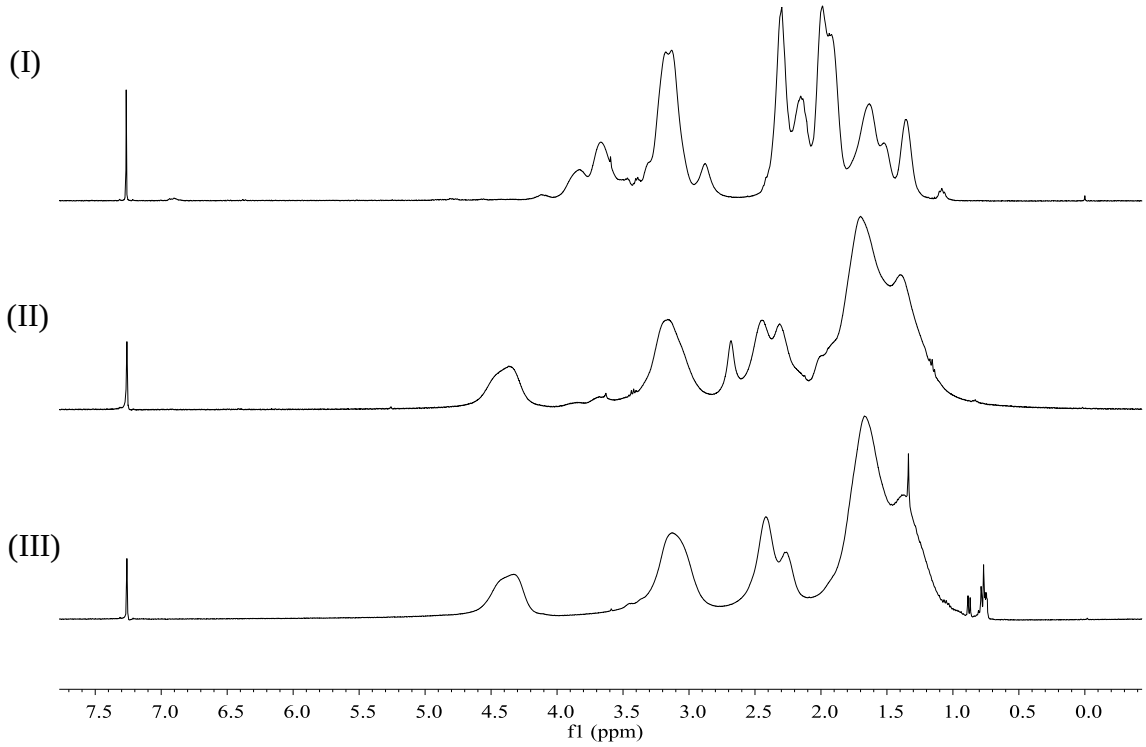

Figure 7. 400 MHz-^{1}H NMR spectra of (I) PNVP macroCTA 14, (II) copolymer product (Table 4.2; Entry 3) and (III) PNVCL in $CDCl_3$

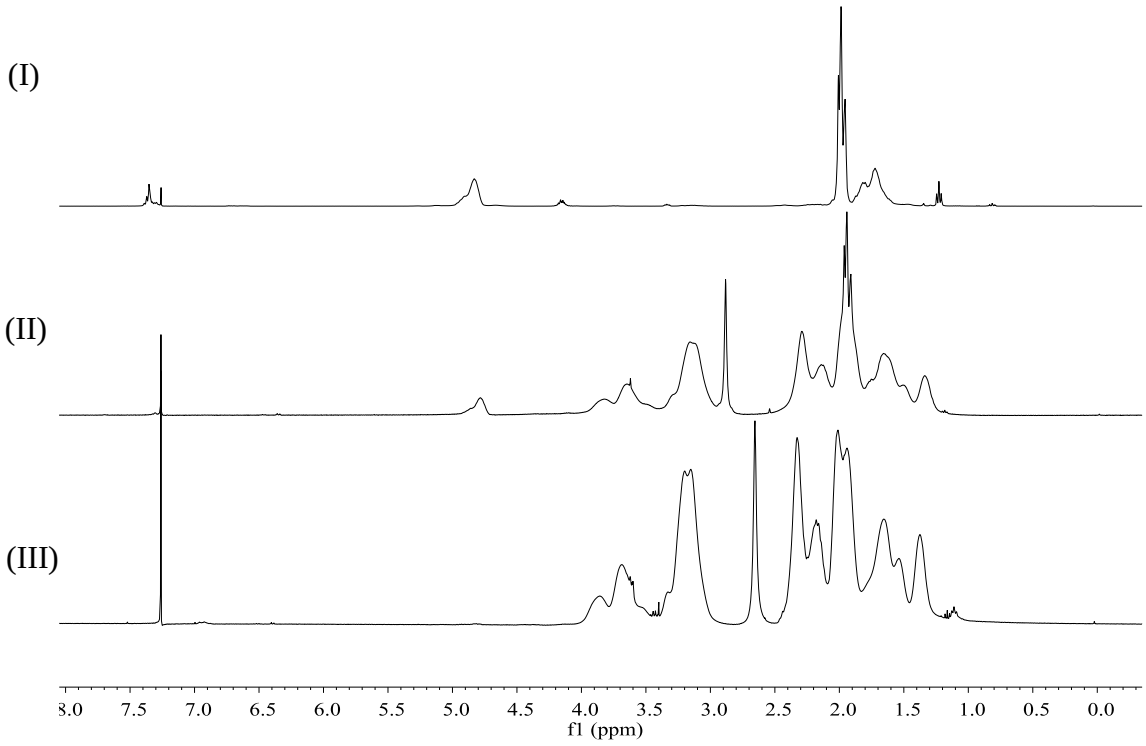

Figure 8. 400 MHz-^{1}H NMR spectra of (I) PVAc macroCTA 15, (II) copolymer product (Table 4.3; Entry 1) and (III) PNVP in $CDCl_3$

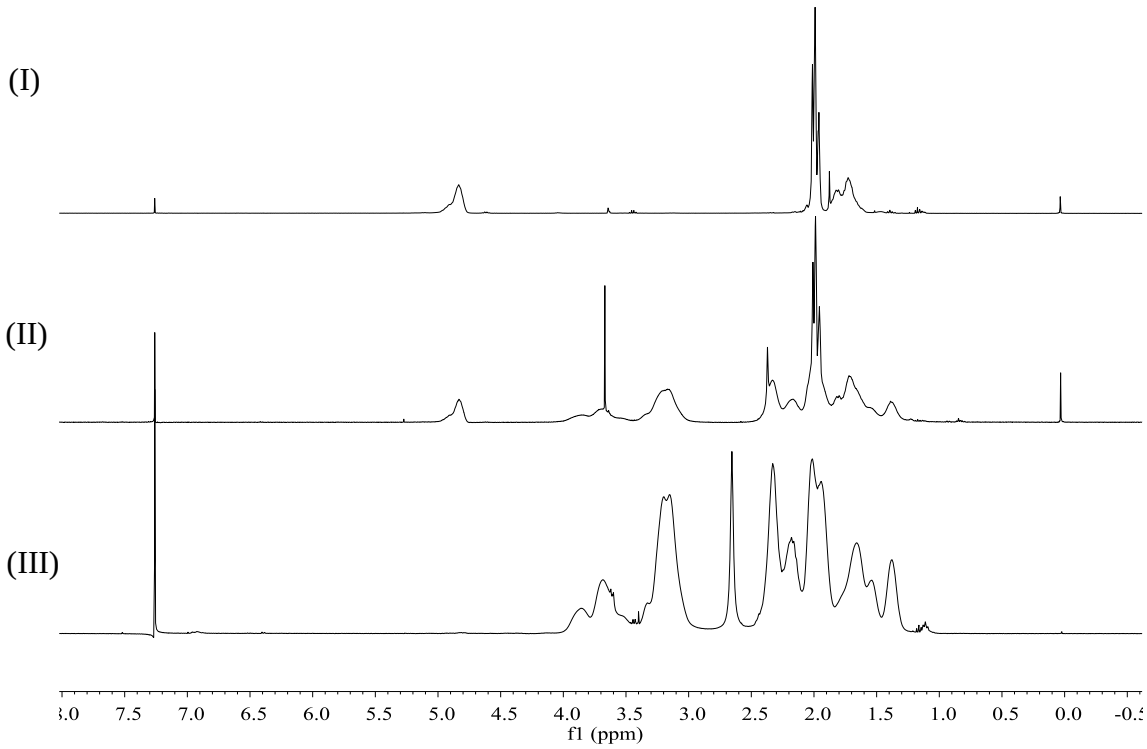

Figure 9. 400 MHz-^{1}H NMR spectra of (I) PVAc macroCTA 16, (II) copolymer product (Table 4.3; Entry 2) and (III) PNVP in $CDCl_3$

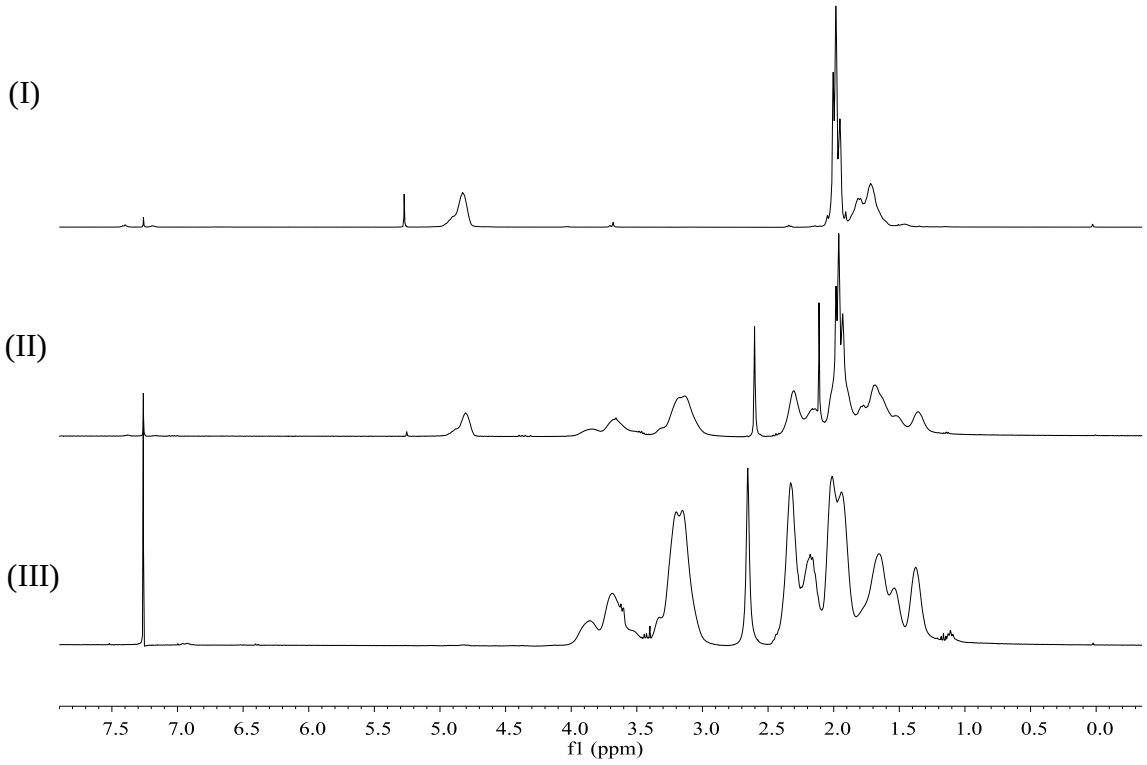

Figure 10. 400 MHz-^{1}H NMR spectra of (I) PVAc macroCTA 17, (II) copolymer product (Table 4.3; Entry 3) and (III) PNVP in $CDCl_3$

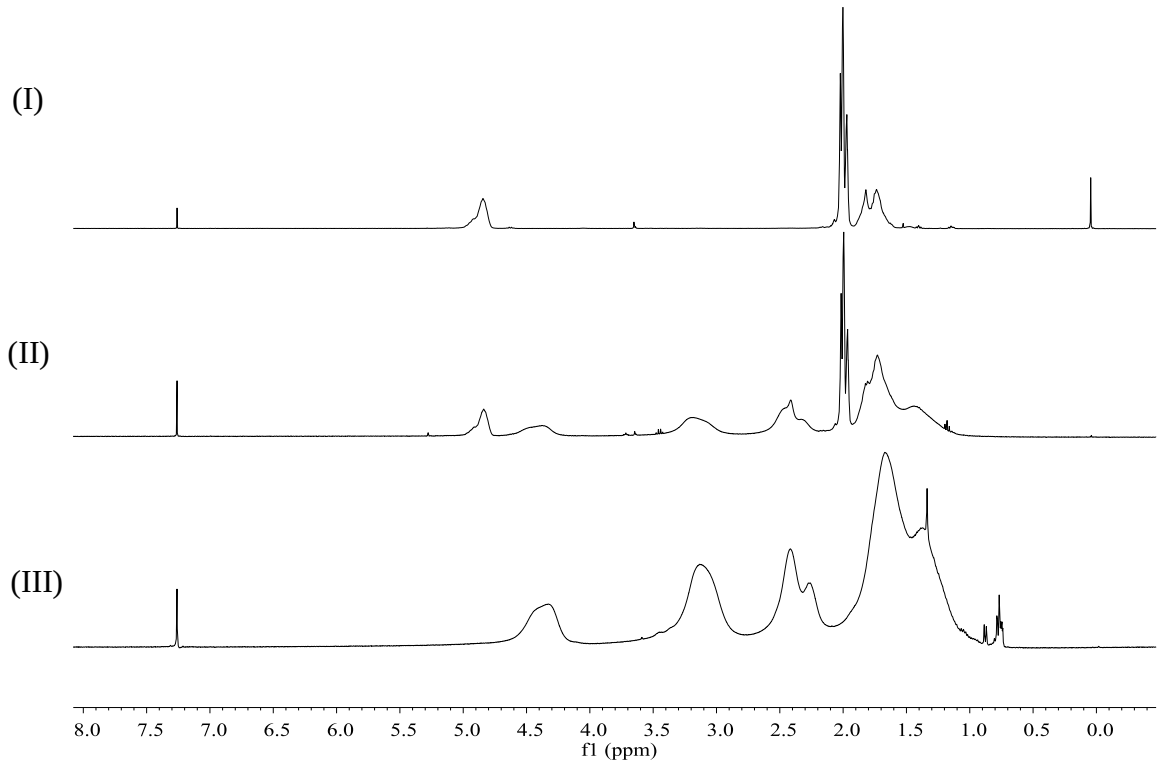

Figure 11. 400 MHz-^{1}H NMR spectra of (I) PVAc macroCTA 16, (II) copolymer product (Table 4.4; Entry 1) and (III) PNVCL in $CDCl_3$

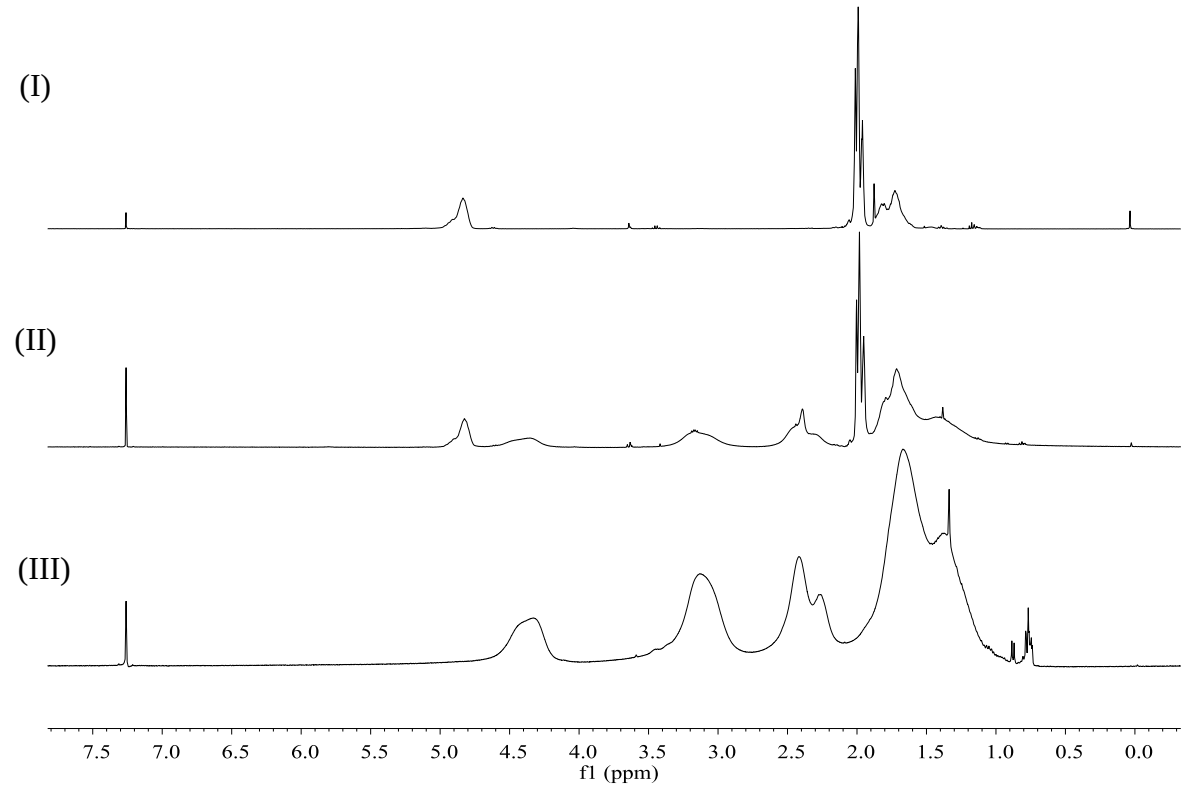

Figure 12. 400 MHz-^{1}H NMR spectra of (I) PVAc macroCTA 16, (II) copolymer product (Table 4.4; Entry 2) and (III) PNVCL in $CDCl_3$

Appendix 2

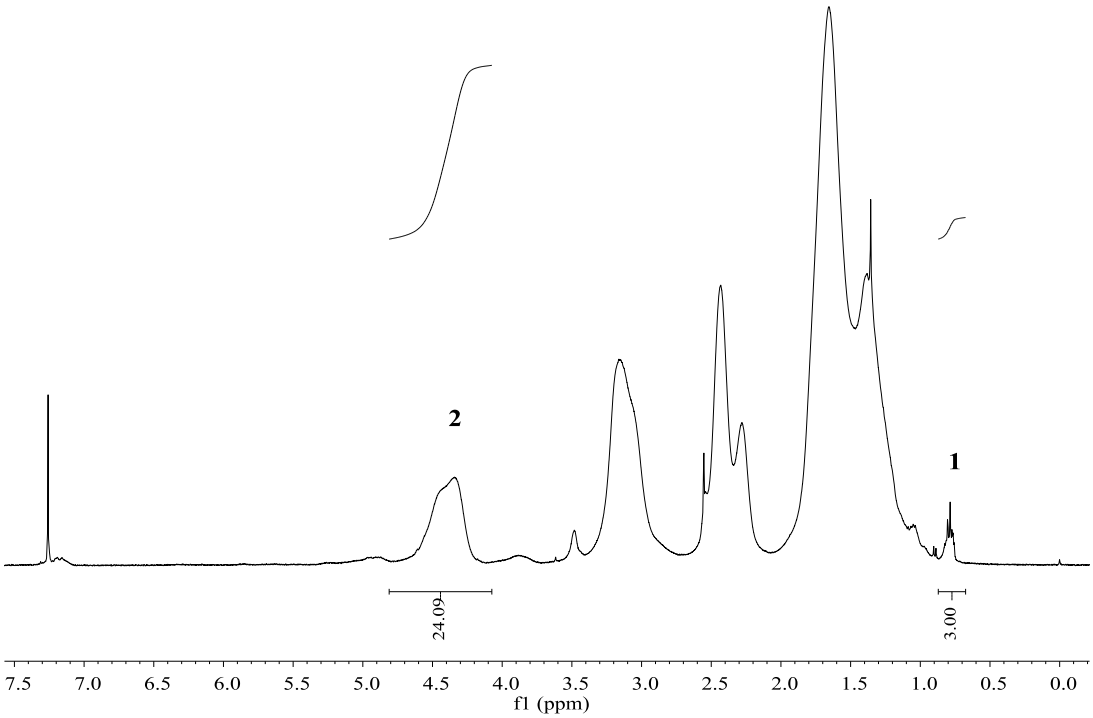

Figure 1. 400 MHz-^{1}H NMR spectrum of Star 5 in $CDCl_3$

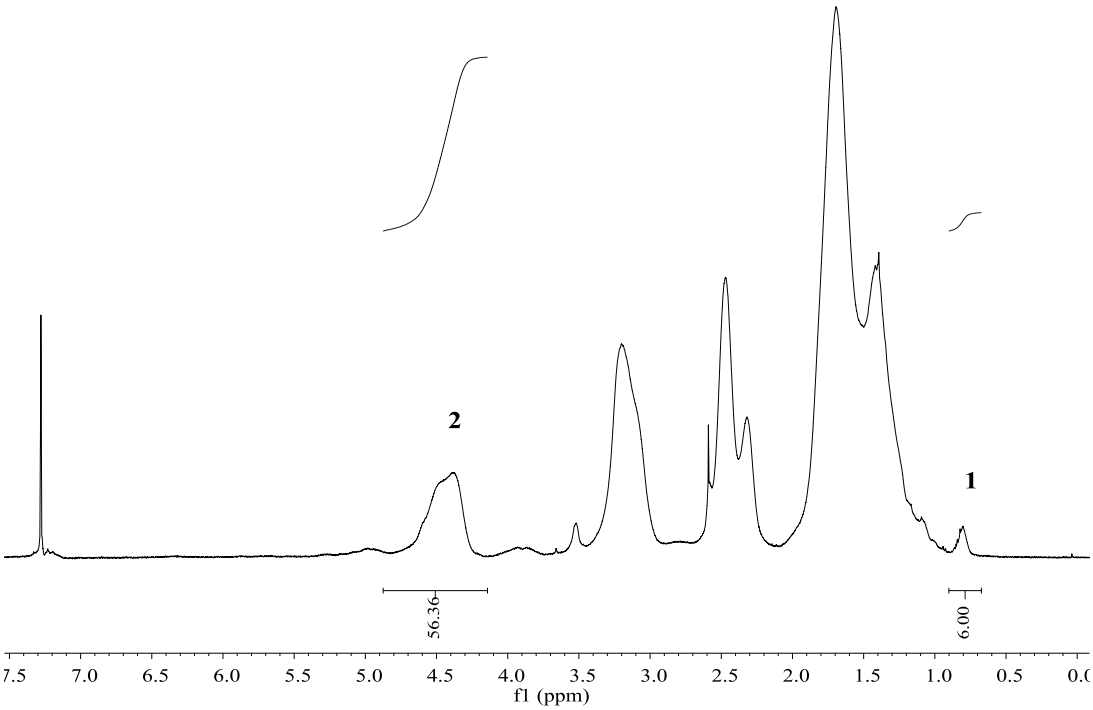

Figure 2. 400 MHz-^{1}H NMR spectrum of Star 6 in $CDCl_3$

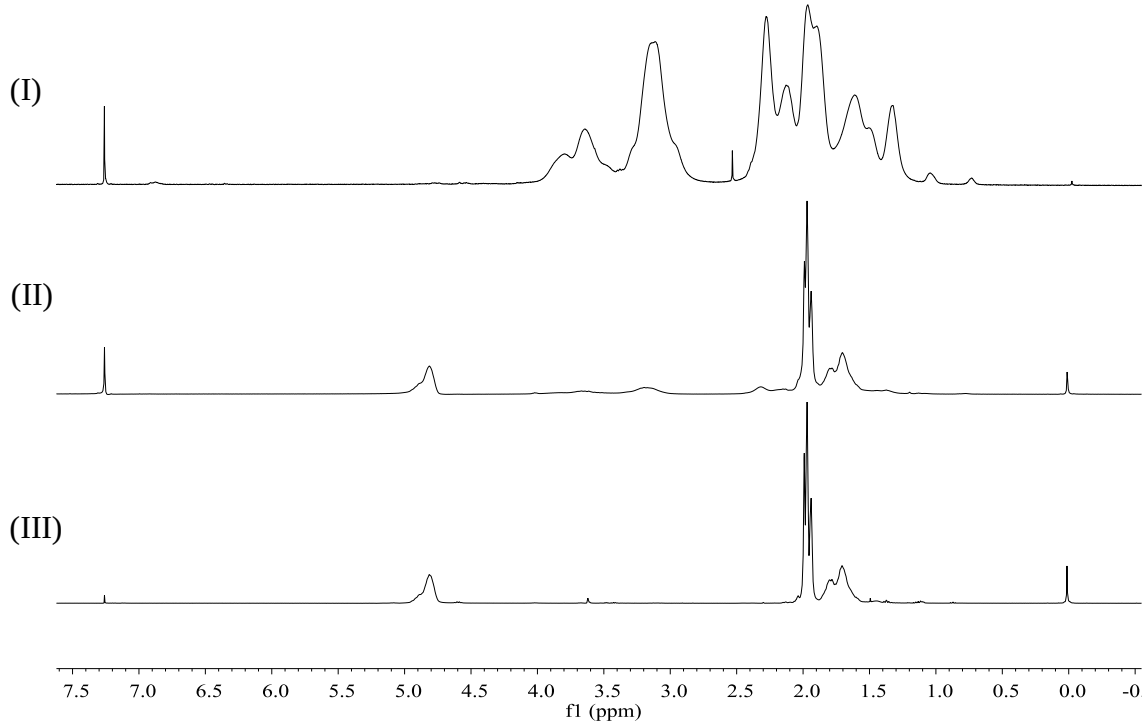

Figure 3. 400 MHz-^{1}H NMR spectra of (I) Star 3, (II) Star-block 1 and (III) PVAc in $CDCl_3$.

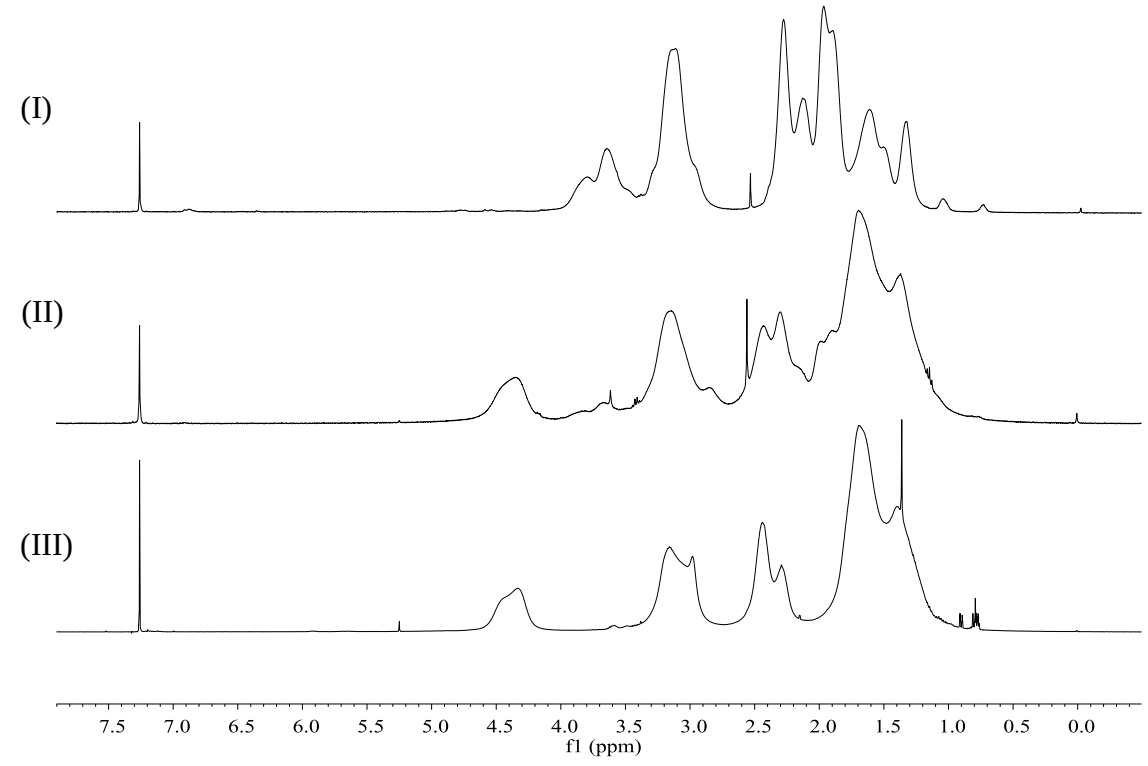

Figure 4. 400 MHz-^{1}H NMR spectra of (I) Star 3, (II) Star-block 2 and (III) PNVCL in $CDCl_3$.

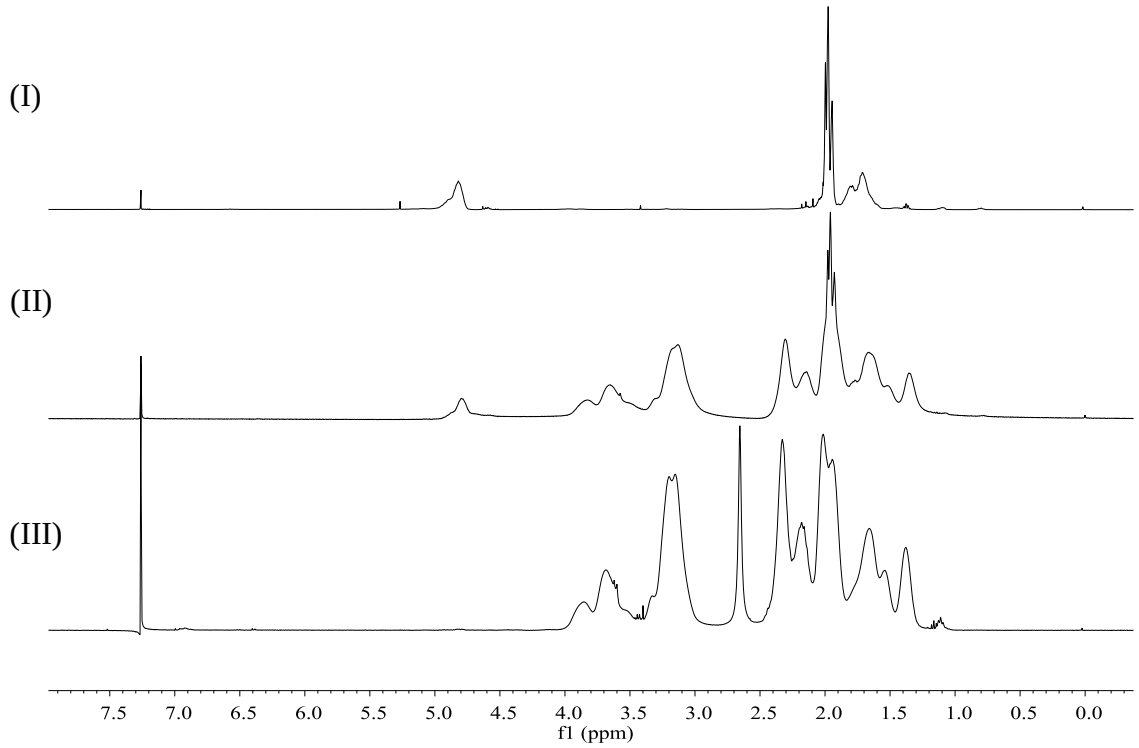

Figure 5. 400 MHz-^{1}H NMR spectra of (I) Star 4, (II) Star-block 3 and (III) PNVP in $CDCl_3$.

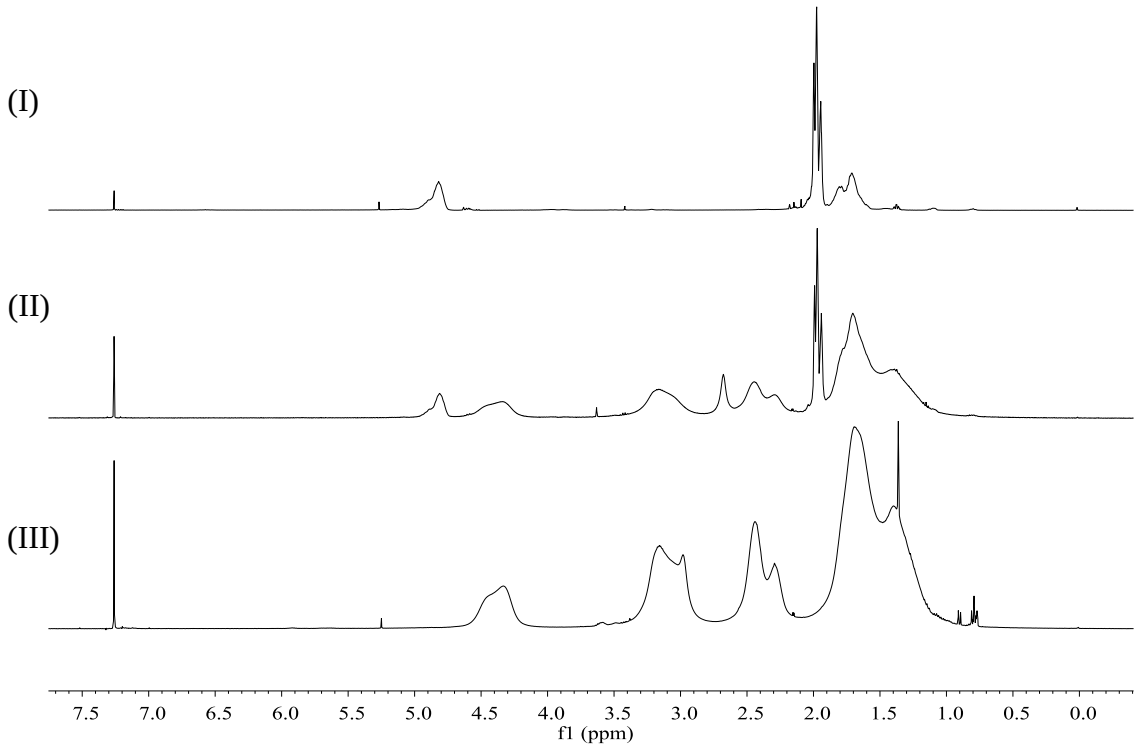

Figure 6. 400 MHz -1H NMR spectra of (I) Star 4, (II) Star-block 4 and (III) PNVCL in $CDCl_3$.

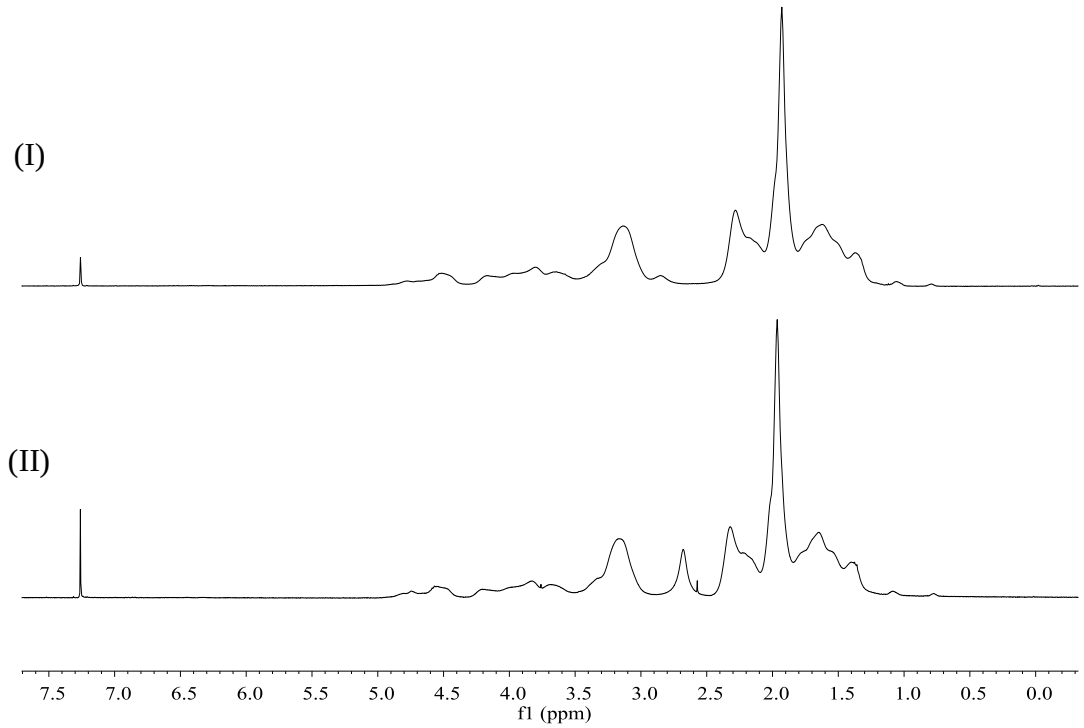

Figure 7. 400 MHz-^{1}H NMR comparison of (I) Star-random 1 and (II) Star-random 4 in $CDCl_3$.

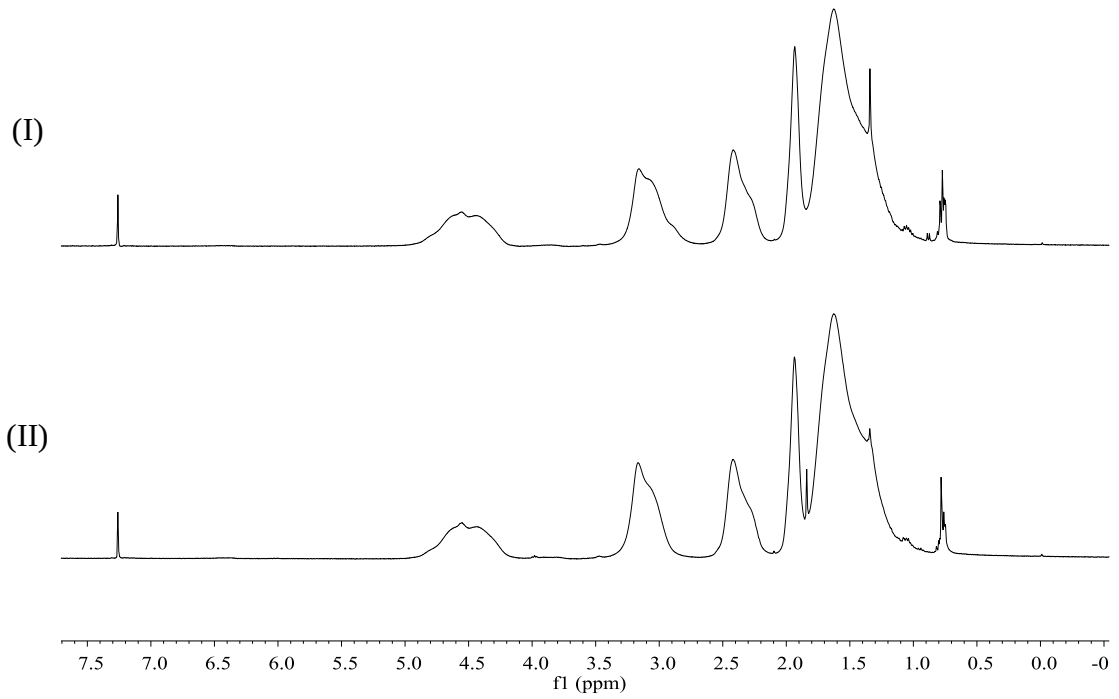

Figure 8. 400 MHz-^{1}H NMR comparison (I) Star-random 2 and (II) Star-random 5 in $CDCl_3$

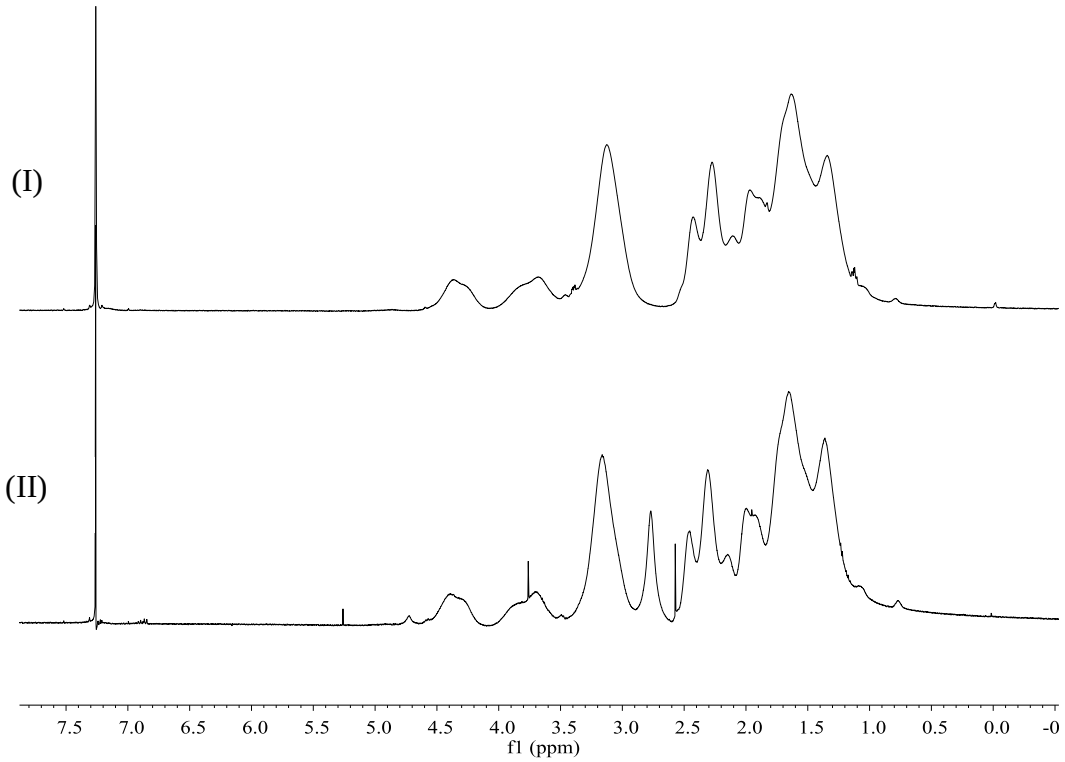

Figure 9. 400 MHz-1H NMR comparison of (I) Star-random 3 and (II) Star-random 6 in $CDCl_3$

Appendix 3

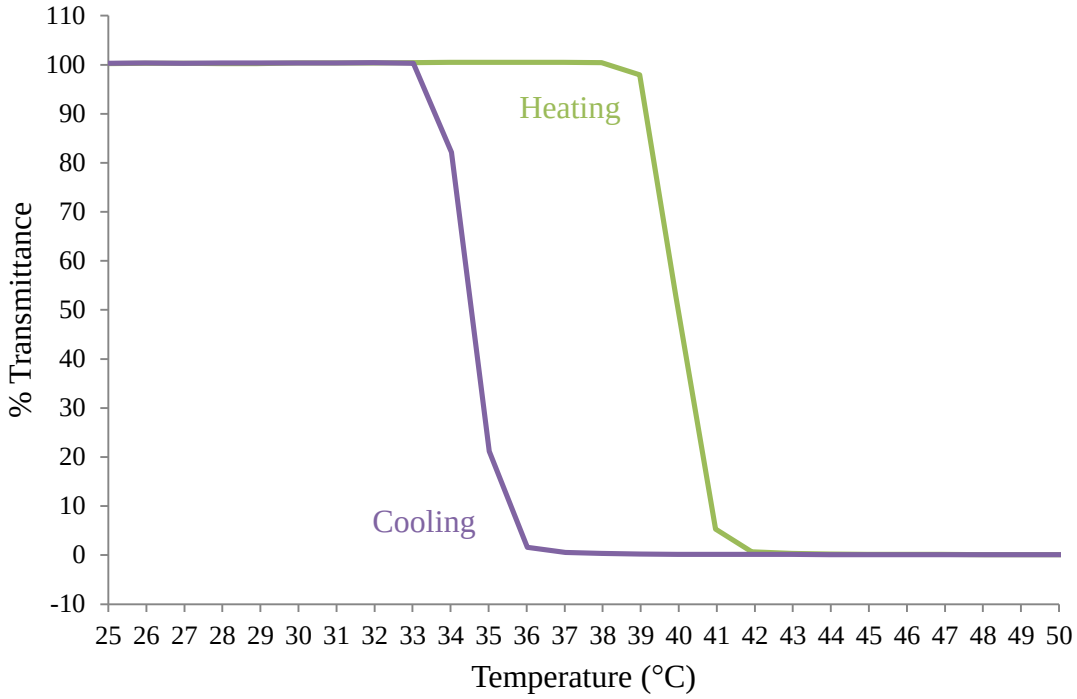

Figure 1. Plot showing % transmittance against temperature (°C) for PNVCL synthesised in the presence of RAFT agent 3 in bulk

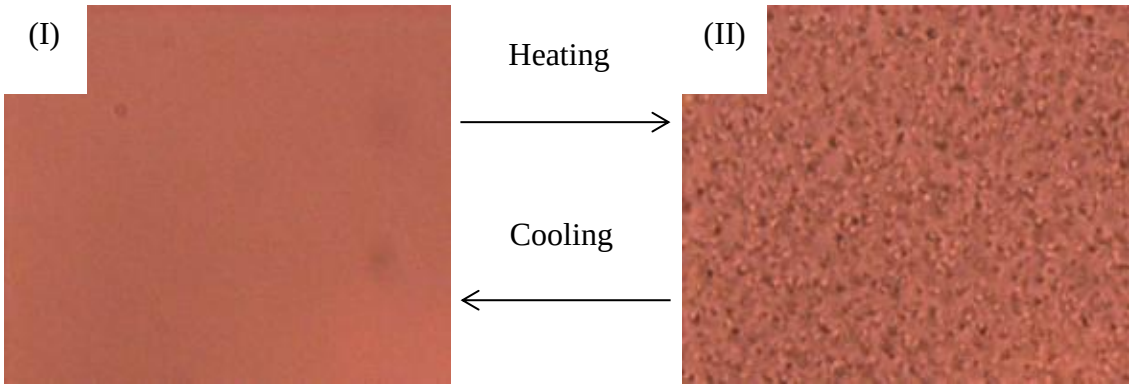

Figure 2. Comparison of optical microscope images (I) above and (II) below the LCST for PNVCL synthesised in the presence of RAFT agent 3 in bulk

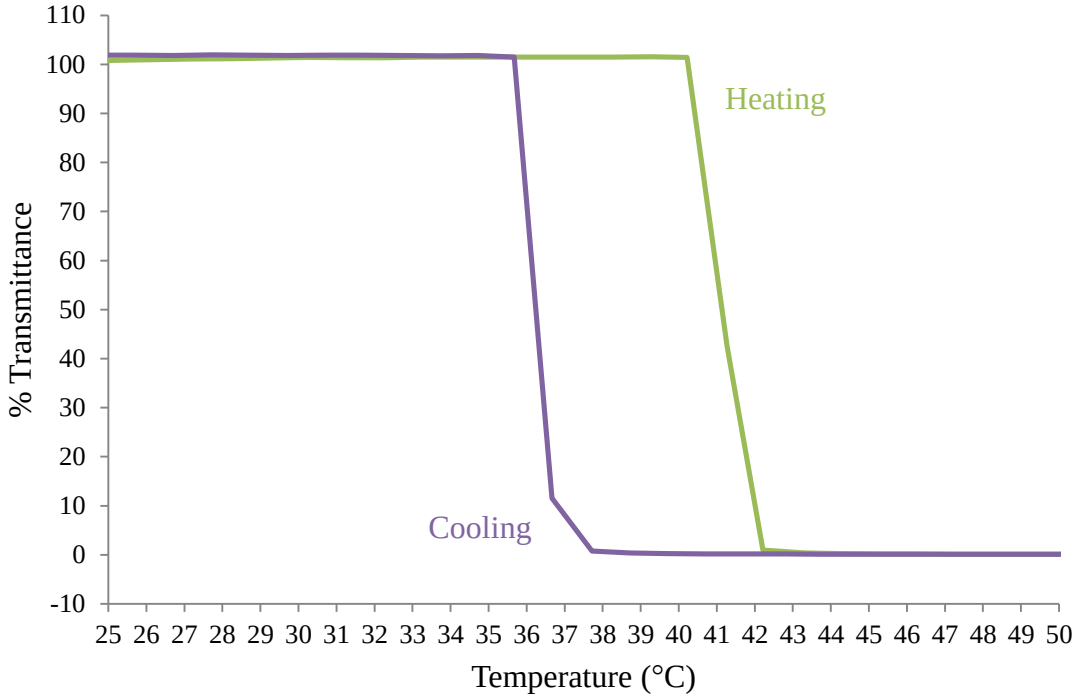

Figure 3. Plot showing % transmittance against temperature (°C) for PNVCL synthesised in the presence of RAFT agent 3 in bulk in 1, 4 dioxane

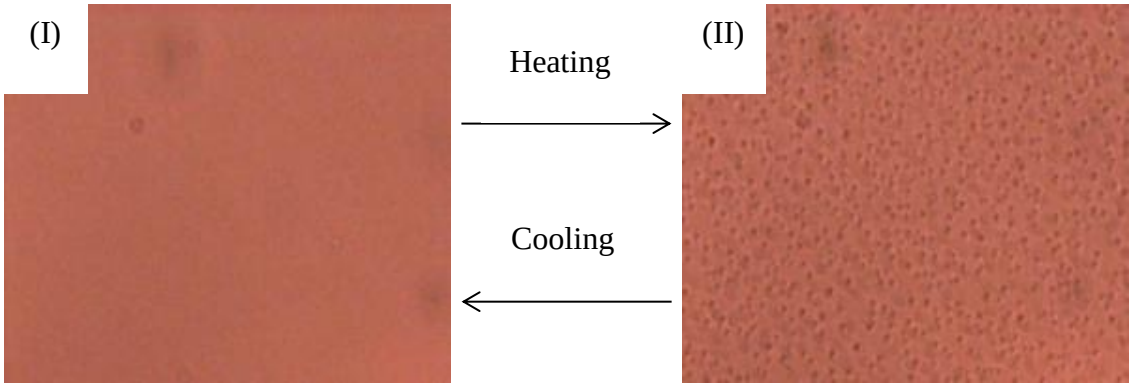

Figure 4. Comparison of optical microscope images (I) above and (II) below the LCST for PNVCL synthesised in the presence of RAFT agent 3 in 1, 4 dioxane

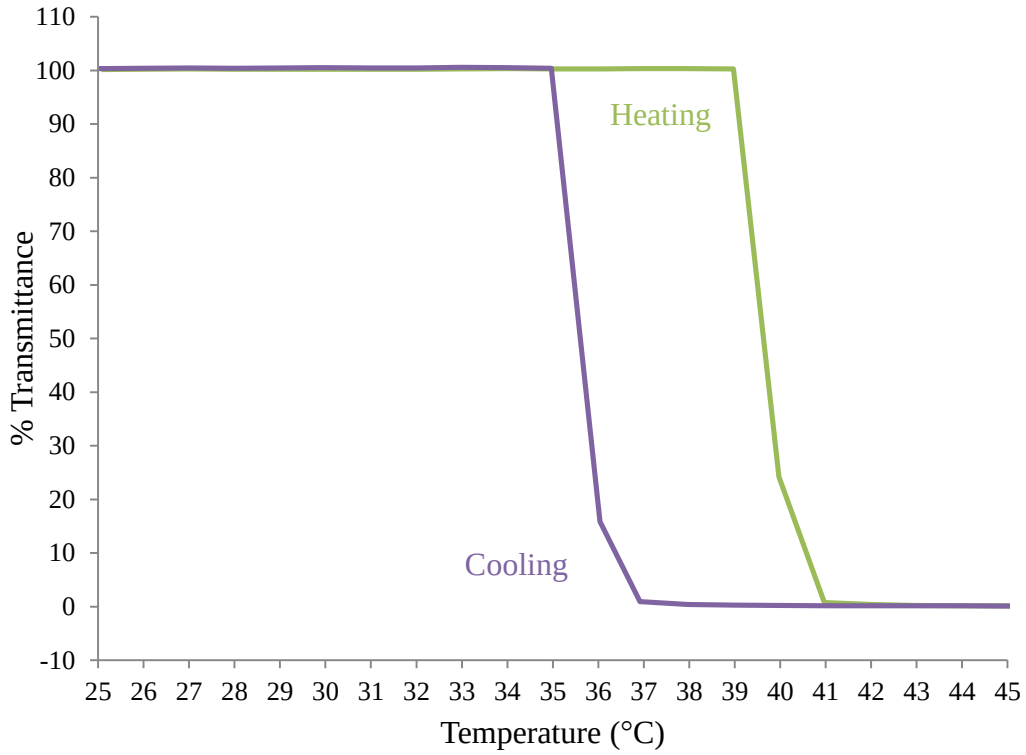

Figure 5. Plot showing % transmittance against temperature (°C) for PNVCL synthesised in the presence of RAFT agent 5

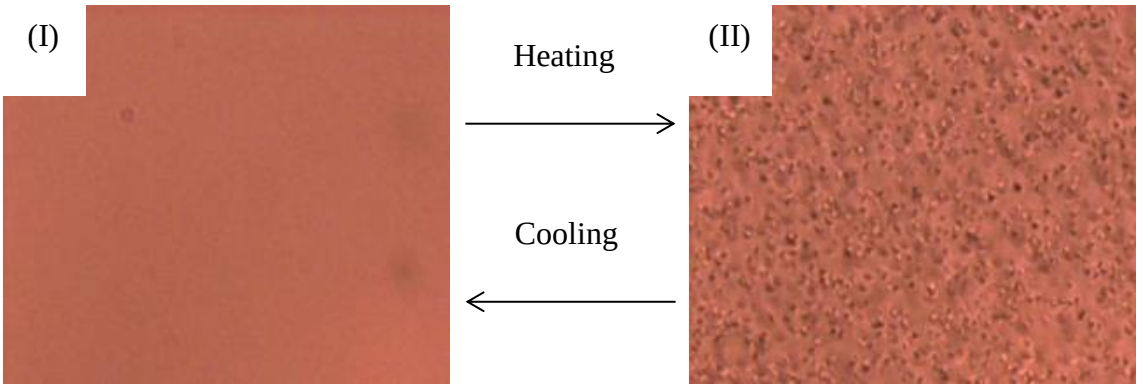

Figure 6. Comparison of optical microscope images (I) above and (II) below the LCST for PNVCL synthesised in the presence of RAFT agent 5

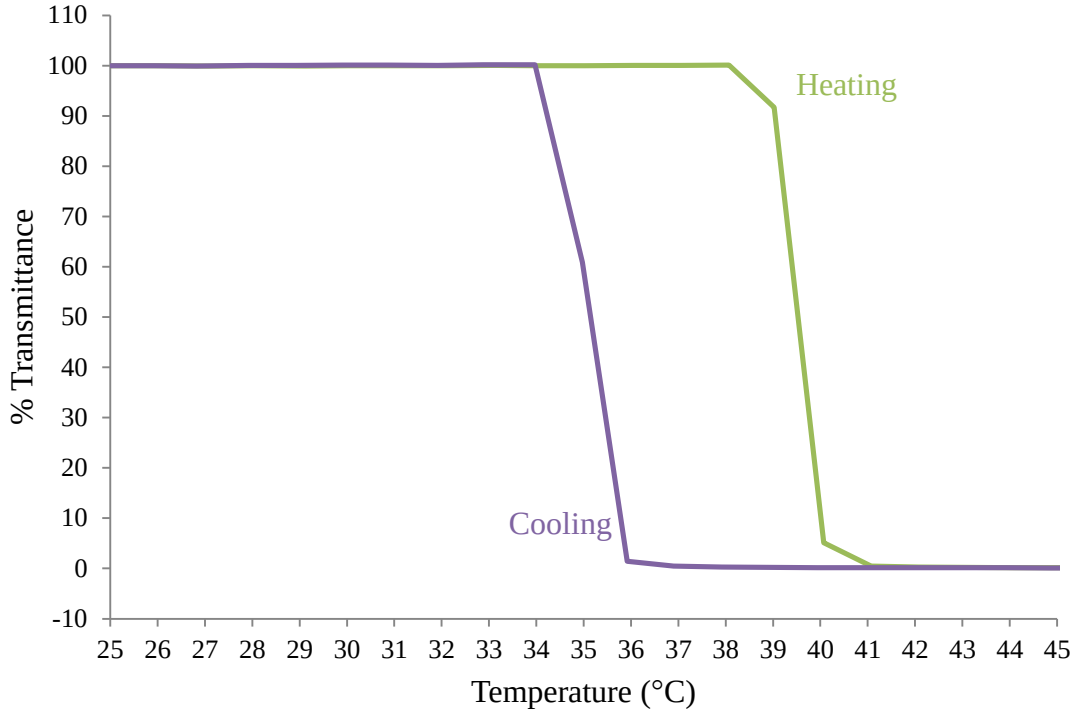

Figure 7. Plot showing % transmittance against temperature (°C) for PNVCL synthesised in the presence of RAFT agent 7

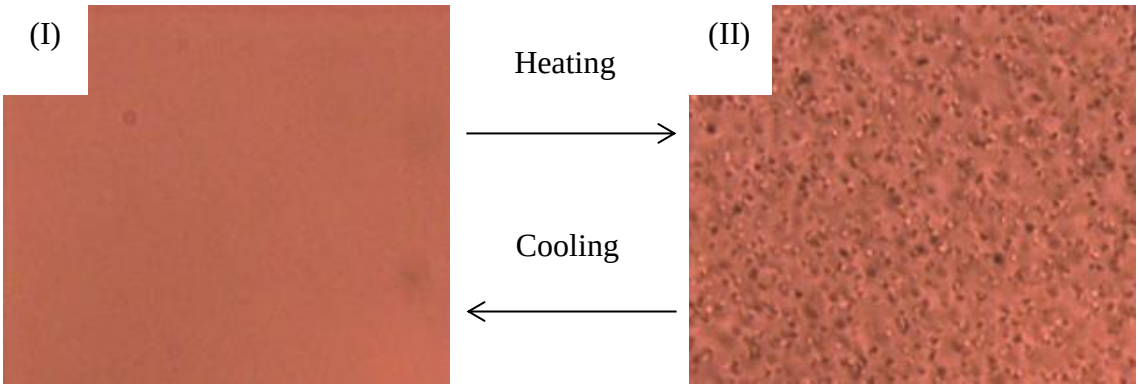

Figure 8. Comparison of optical microscope images (I) above and (II) below the LCST for PNVCL synthesised in the presence of RAFT agent 7

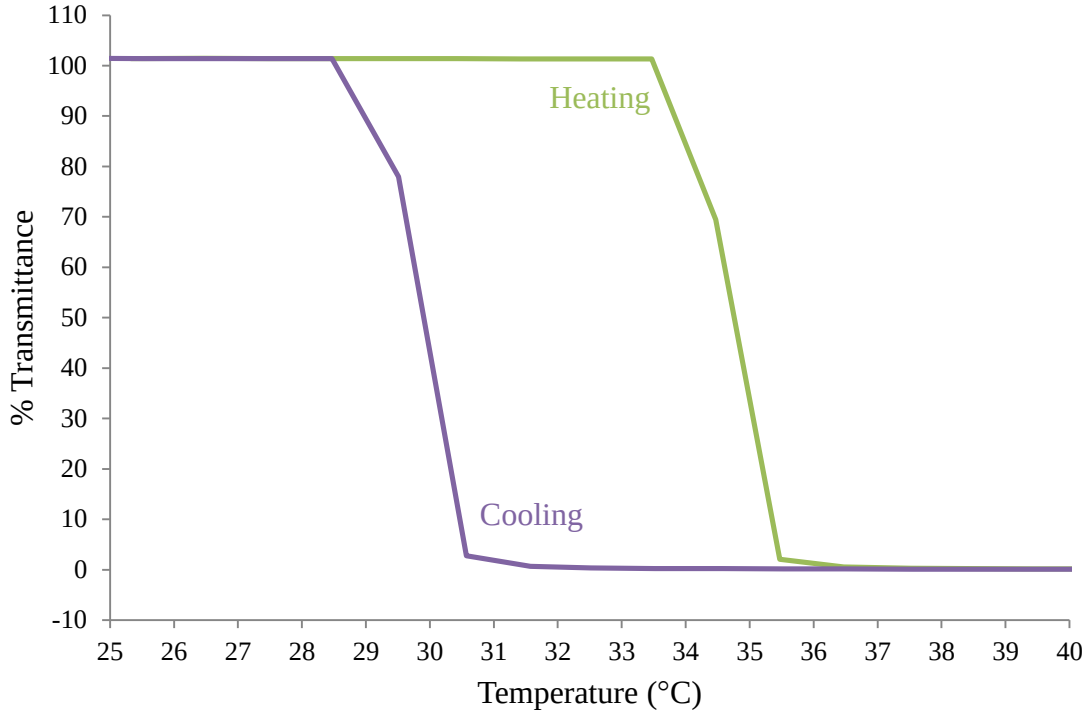

Figure 9. Plot showing % transmittance against temperature (°C) for conventional PNVCL

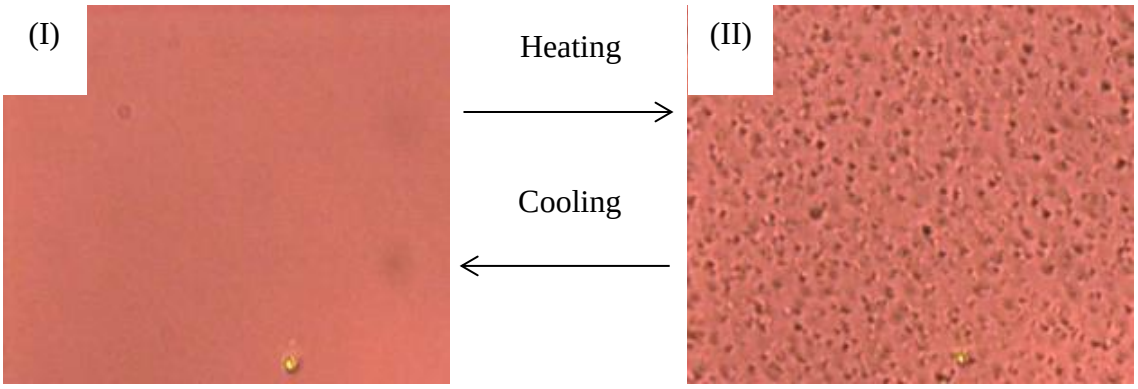

Figure 10. Comparison of optical microscope images (I) above and (II) below the LCST for PNVCL synthesised conventionally in 1,4 dioxane

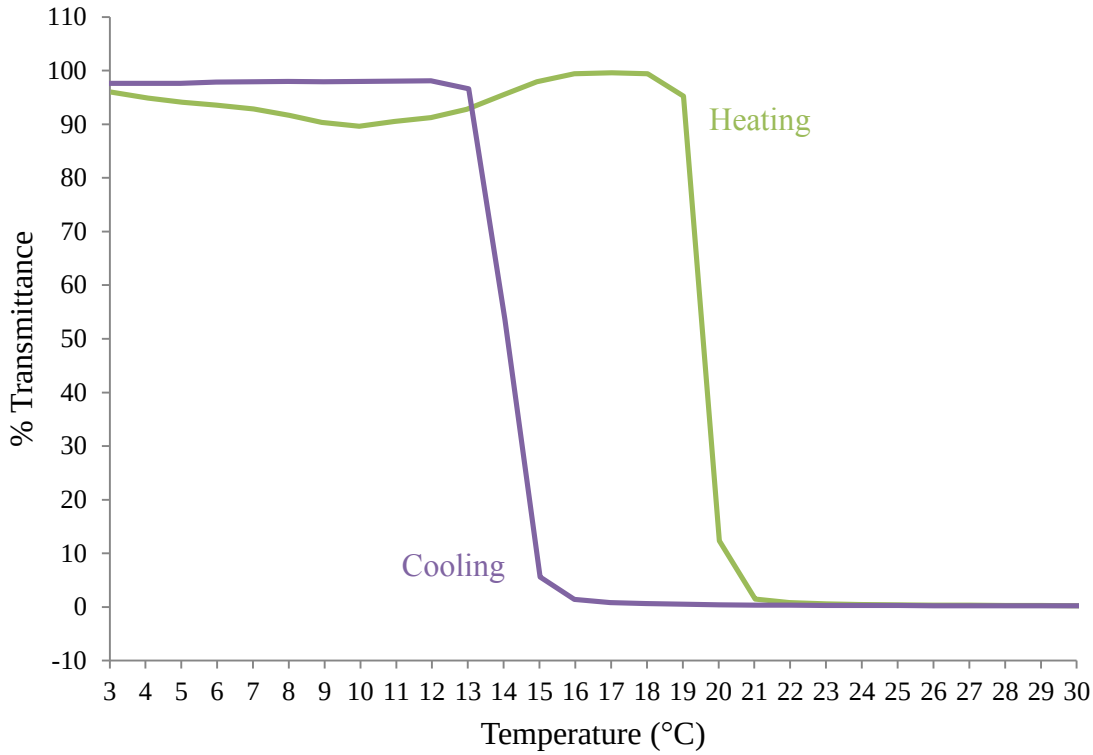

Figure 11. Plot showing % transmittance against temperature (°C) for PNVCL-*ran*-PVAC prepared in the presence of RAFT agent 9

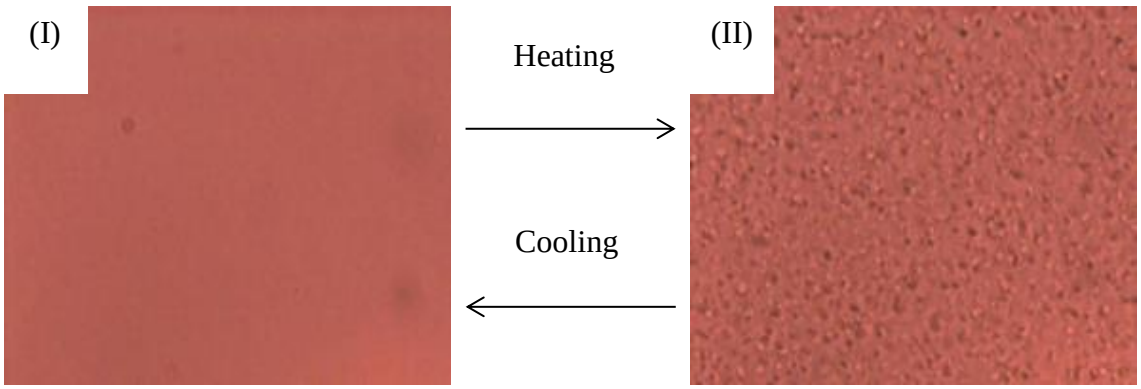

Figure 12. Comparison of optical microscope images above and below the LCST for PNVCL-*ran*-PVAc synthesised in presence of RAFT agent 9

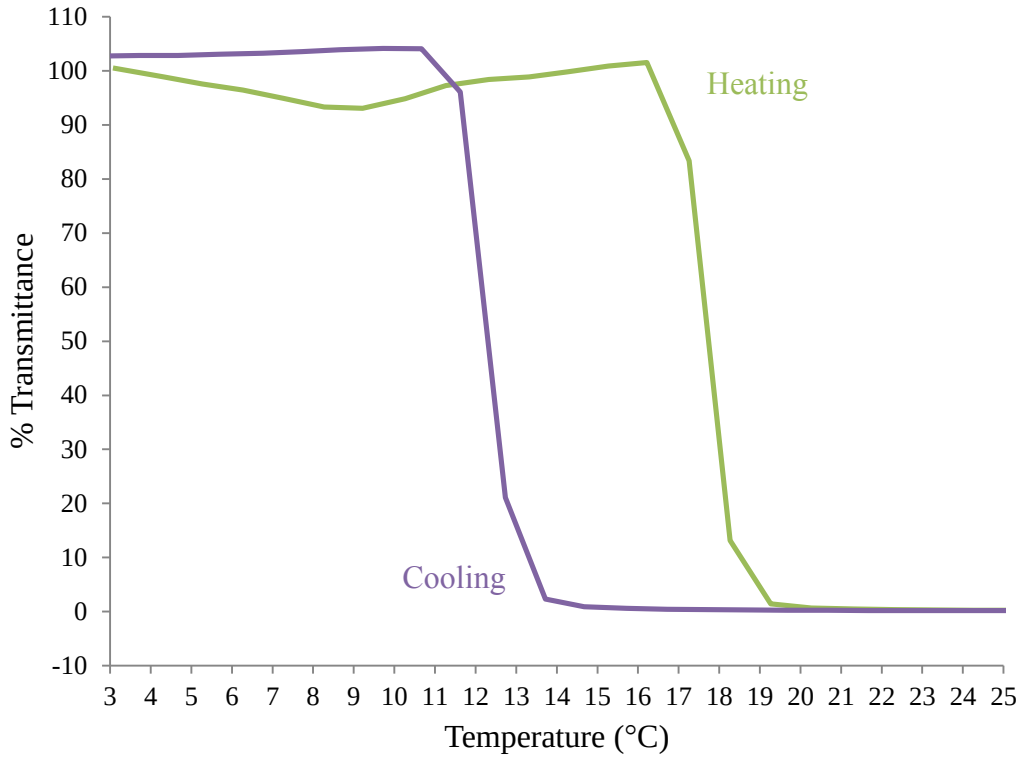

Figure 13. Plot showing % transmittance against temperature (°C) for PNVCL-*ran*-PVAc prepared in the presence of RAFT agent 11

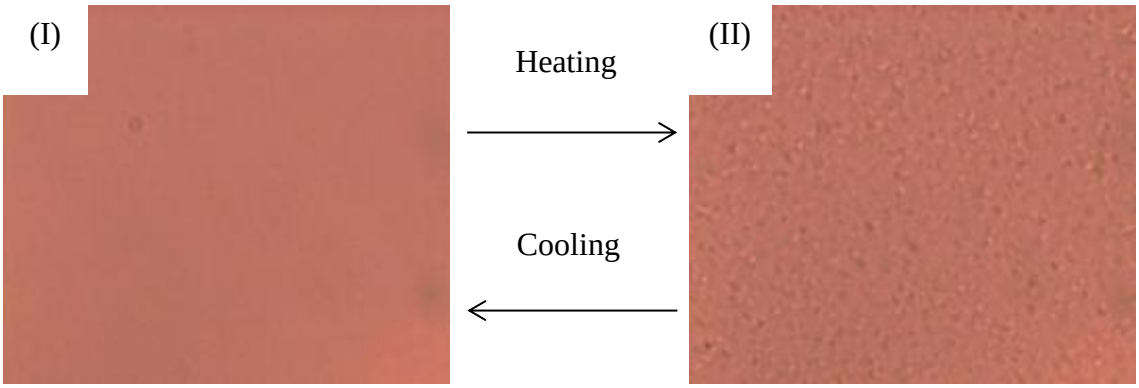

Figure 14. Comparison of optical microscope images above and below the LCST for PNVCL-*ran*-PVAc synthesised in presence of RAFT agent 11

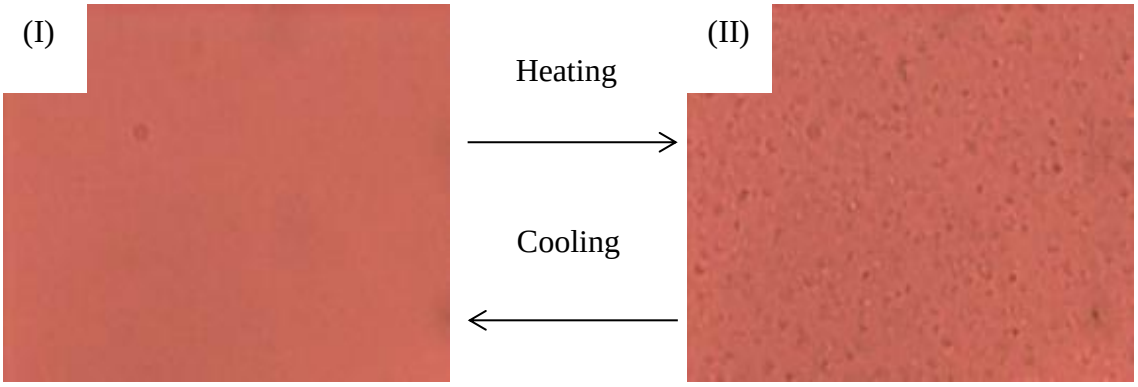

Figure 15. Comparison of optical microscope images above and below the LCST for conventional PNVCL-*ran*-PVAc

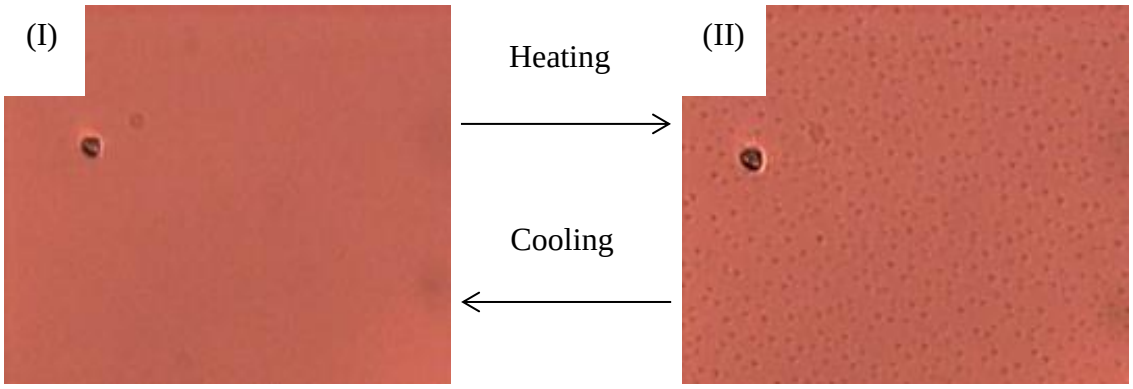

Figure 16. Comparison of optical microscope images above and below the LCST for PNVCL-*ran*-PNVP synthesised in presence of RAFT agent 5

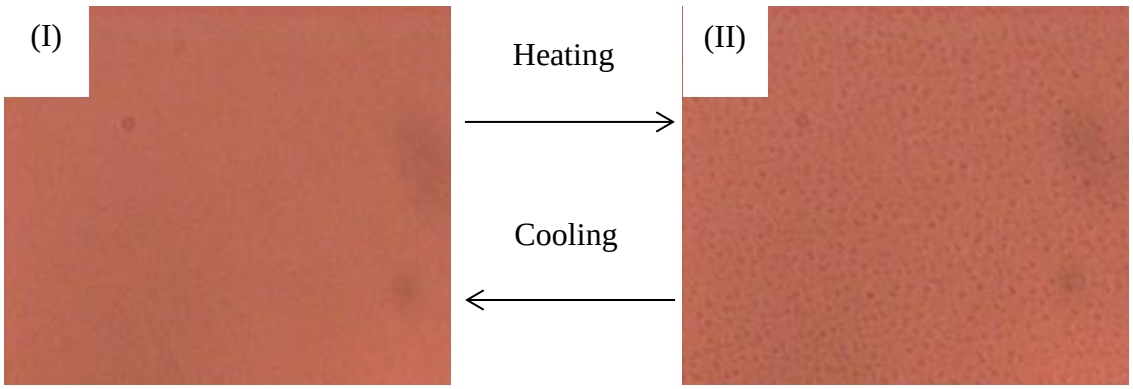

Figure 17. Comparison of optical microscope images above and below the LCST for PNVCL-*ran*-PVAc synthesised in presence of RAFT agent 9

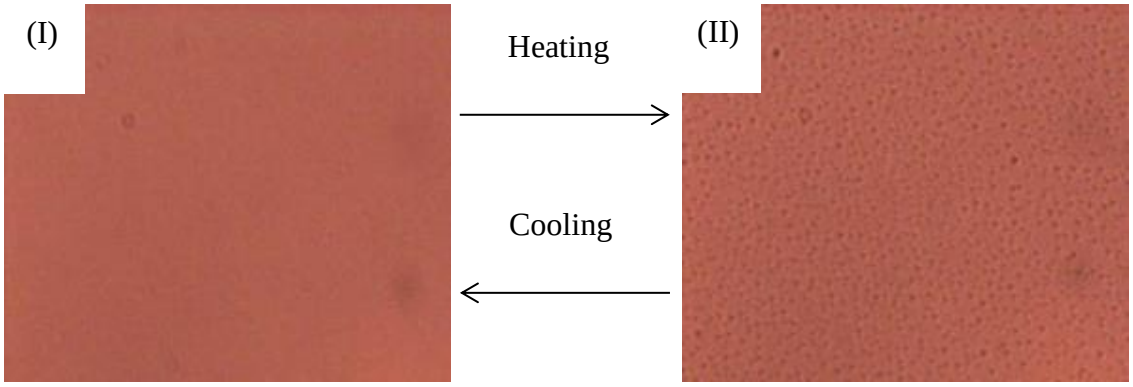

Figure 18. Comparison of optical microscope images above and below the LCST for PNVCL-*ran*-PVAc synthesised in presence of RAFT agent 11

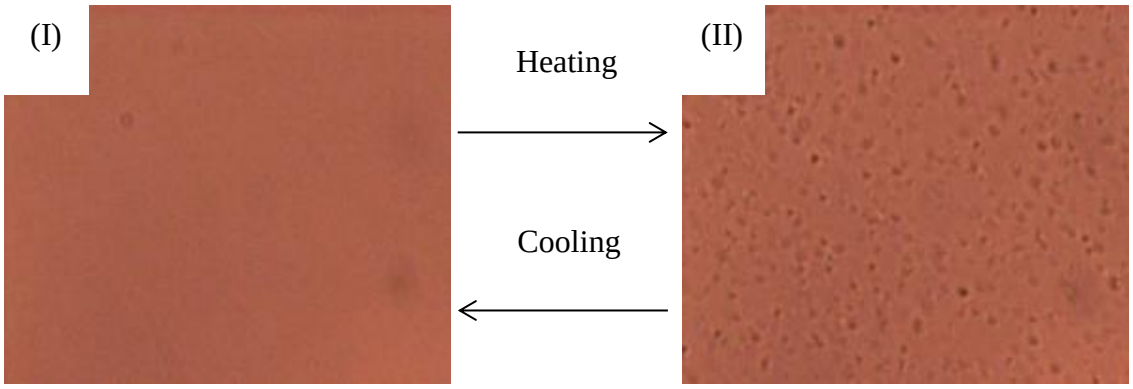

Figure 19. Comparison of optical microscope images above and below the LCST for conventional PNVCL–*ran*-PNVP